**UNIVERSIDAD COMPLUTENSE DE MADRID**
FACULTAD DE FARMACIA


# TESIS DOCTORAL

## Compuestos multidiana derivados de chalconas para el tratamiento y diagnóstico de enfermedades neurodegenerativas

## Chalcone-derived multitarget compounds for the treatment and diagnosis of neurodegenerative diseases

MEMORIA PARA OPTAR AL GRADO DE DOCTOR

PRESENTADA POR

**Jorge Gómez-Carpintero Jiménez**

Directores

**José Carlos Menéndez Ramos**
**Juan Francisco González Matilla**

Madrid

# UNIVERSIDAD COMPLUTENSE DE MADRID

FACULTAD DE FARMACIA


# TESIS DOCTORAL

Compuestos multidiana derivados de chalconas para el tratamiento y diagnóstico de enfermedades neurodegenerativas//Chalcone-derived multitarget compounds for the treatment and diagnosis of neurodegenerative diseases

MEMORIA PARA OPTAR AL GRADO DE DOCTOR

PRESENTADA POR

Jorge Gómez-Carpintero Jiménez

DIRECTORES

José Carlos Menéndez Ramos
Juan Francisco González Matilla

# UNIVERSIDAD COMPLUTENSE DE MADRID

FACULTAD DE FARMACIA



# TESIS DOCTORAL

Chalcone-derived multitarget compounds for the treatment and diagnosis of neurodegenerative diseases

MEMORIA PARA OPTAR AL GRADO DE DOCTOR

PRESENTADA POR


Jorge Gómez-Carpintero Jiménez


DIRECTORES


José Carlos Menéndez Ramos
Juan Francisco González Matilla

# Table of contents

## Glossary

**μM** Micromolar

**5HT** 5-hydroxytryptamine

**AA** Arachidonic acid

**AAT** Alanine aminotransferase

**ACh** Acetylcholine

**AChE** Acetylcholinesterase

**AChEI** Acetylcholinesterase Inhibitor

**AD** Alzheimer´s Disease

**AE** Atom economy

**AGEs** Advanced Glycation End-products

**AIBN** Azo-bisisobutyronitrile

**AICD** Amyloid intracellular domain

**AMP** Adenosyl Monophosphate

**AMPA** α-amino-3-hydroxy-5-methyl-4-isoxazolepropionic acid

**API** Active Pharmaceutical Ingredient

**APP** Amyloid Precursor Protein

**ATP** Adenosyl Triphosphate

**Aβ** Beta amyloid

**BACE-1** Beta-site APP cleaving enzyme 1

**BBB** Blood Brain Barrier

**Boc** *tert*-Butoxycarbonyl

**BOP** Benzotriazole-1-yl-oxy-tris-(dimethylamino)-phosphonium hexafluorophosphate

**BuChE** Butyrylchlolinesterase

**CA** Carbonic anhydrase

**CAS** Catalytic Anionic Site

**CDI** Carbonyldiimidazole

**ChE** Cholinesterase

**CNS** Central Nervous System

**CoA** Coenzyme A

**COX** Cyclooxygenase

**Cys** Cysteine

**DALY** Disability-adjusted life years

**DCFA-DA** Dichlorofluorescein-Diacetate

**DCM** Dichloromethane

**DDQ** 2,3-Dichloro-5,6-dicyano-1,4-benzoquinone

**DIPEA** Diisopropyl ethyl amine

**DLC** Delocalised lipophilic cation

**DMAP** Dimethyl amino pyridine

**DMF** Dimethylformamide

**DMSO** Dimethyl sulphate

**DPCK** Dephospho-CoA kinase

**DPPA** Diphenylphosphoryl azide

**DPT** Di(2-pyridyl) thionocarbonate

**EAAT** Excitatory amino acid transporter

**EDC·HCl** 1-Ethyl3(3dimethylaminopropyl)carbodiimide hydrochloride

**eq** Equivalent

**EtOAc** Ethyl acetate

**EtOH** Ethanol

**FRET** Förster Resonance energy transfer

**g** Gram

**GABA** Gamma aminobutyric acid

**GAT** Gamma-Aminobutyric acid transporters

**GDH** Glutamate dehydrogenase

**GDP** Gross domestic product

**GFP** Green Fluorescent Protein

**Glu** Glutamic acid

**GSK-3α** Glycogen Synthase Kinase-3 alpha

**GSK-3β** Glycogen synthase kinase-3 beta

**$H_2O$** Water

**HATU** Hexafluorophosphate Azabenzotriazole Tetramethyl Uronium

**His** Histidine

**HMBC** Heteronuclear multiple-bond correlation spectroscopy

**HMQC** Heteronuclear multiple-quantum correlation spectroscopy

**HOBt** Hydroxybenzotriazole

**HPLC** High Performance Liquid Chromatography

**HRMS** High Resolution Mass Spectrometry

**HSVM** High Speed Vibratory Milling

**Hz** Hertz

**$IC_{50}$** Inhibitory Concentration 50

**iGluR** Ionotropic glutamate receptor

**ILAE** International League Against Epilepsy

**IMM** Inner mitochondrial membrane

**IMS** Inner membrane space

**KA** Kainic acid

**KEAP-1** Kelch ECH associating protein 1

**LB** Lewy´s body

**LOX** Lipooxigenase

**Lys** Lysine

**M** Molar

**MAO** Monoamino oxidase

**MCR** Multicomponent reaction

**MDA** Malondialdehyde

**MeCN** Acetonitrile

**MeOH** Methanol

**mg** milligram

**mGluR** Metabotropic glutamate receptor

**MHC II** Major Histocompatibility Complex type II

**ml** Millilitre

**mm** Millimetre

**MPTP** 1-methyl-4-phenyl-1, 2, 3, 6-tetrahydropyridine

**MTDL** Multitarget Drug Ligand

**MtPanK** Mycobacterium tuberculosis Pantothenate Kinase

**NADP** Nicotinamide adenine dinucleotide phosphate

**NFT** Neurofibrillary tangles

**NF-κB** Nuclear factor kappa-light-chain-enhancer of activated B cells

**nm** Nanometre

**NMDA** N-methyl-D aspartate

**NMR** Nuclear Magnetic Resonance

**Nrf-2** Nuclear factor erythroid 2-related factor 2

**NSAID** Non-steroid antiinflamatory drug

**OMM** Outer mitochondrial membrane

**ORAC** Oxygen Radical Absorption Capacity

**PAMP** Pathogen-associated Molecular Pattern

**PAMPA** Parallel Artificial Membrane Permeability Assay

**PanK** Panthotenate Kinase

**PAS** Peripheric Anionic Site

**PG** Prostaglandin

**PHL** Paired helical filaments

**PMI** Process Mass Intensity

**PNS** Peripheral Nervous System

**PPAT** Phosphopantetheine adenylyl transferase

**PPCDC** Phosphopantothenoylcysteine decarboxylase

**PPCS** Phosphopantothenoylcysteine synthase

**Ps-TsIm** *para*-Toluene sulphonic Imidazole

**p-tau** Tau protein

**RET** Resonance Energy Transfer

**RME** Reaction Mass Efficiency

**RNS** Reactive Nitrogen species

**ROS** Reactive Oxygen species

**RP-HPLC** Reverse phase High Performance Liquid Chromatography

**RT** Room temperature

**SAR** Structure-Activity Relationship

**Ser** Serine

**SLP** Self-labelling Protein

**SNIFIT** SNAP-tag-based indicators with a fluorescent intramolecular tether

**SNpc** Substantia nigra pars compacta

**TBAF** Tetrabutyl ammonium fluoride

**TCT** 2,4,6-trichloro 1,3,5-triazine

**TFA** Trifluoroacetic acid

**THF** Tetrahydro furane

**TIPS** Triisopropyl silyl

**TLR** Toll-like Receptor

**TMR** Tetramethyl rhodamine

**TPP** Triphenylphosponium

**TSTU** N,N,N',N'-Tetramethyl-O-(N-succinimidyl)uronium tetrafluoroborate

**VGSC** Voltage gated sodium channel

**VGCC** Voltage-gated Calcium Channel

## Summary

### Introduction

Neurological disorders are a great burden for health systems worldwide. These diseases are characterized by a disfunction in neurons and the type of neuron affected and the way it is affected will depend on the disorder. Among these disorders, Alzheimer´s disease, Parkinson´s disease and epilepsy stand out as they affect a great number of patients and there is an increasing tendency in their incidence and prevalence. The ethology of these diseases is complex, as there are numerous factors involved in their establishment and progression. In the cases of Alzheimer´s and Parkinson's disease, these factors involve protein misfolding, an increase in oxidative stress, different types of neuronal dysfunction (cholinergic neurons in Alzheimer´s disease and dopaminergic neurons in Parkinson´s disease) and a deregulated immune response. In the case of epilepsy, the cause underlies in an unbalance between excitatory and inhibitory neurotransmission, with predomination of the former.

### Objectives

1. The synthesis and characterisation of a family of multitarget drug ligands against Alzheimer´s disease. These ligands are based on a flavonoid scaffold (naringenin and hesperetin) to which the pharmacophores of molecules such as tacrine and donepezil (two well-known cholinesterase inhibitors) and different tryptamines (which possess pleiotropic neuroprotective activities) have been tethered. The compounds are to be tested to verify their potential as multitarget drug ligands.

2. The synthesis and characterization of theragnostic systems for oxidative stress in mitochondria. The synthesis of these compounds will be carried out using a multicomponent reaction in which a chalcone, a beta ketoester and an amine possessing a triphenylphosphonium functional group are combined to form a dihydroanthranilate. The triphenylphosphonium group is positively charged and this will direct the dihydroanthranilate structure towards the mitochondrial matrix, as the latter is negatively charged. There, it will capture a reactive oxygen species or a reactive nitrogen species and will convert into its fully aromatised form, which is fluorescent. This way, it will reduce oxidative stress by acting as a free radical scavenger, but also, by turning fluorescent in the process, it will diagnose free radical presence, converting these molecules in potential theragnostic systems for oxidative stress.

3. The synthesis and characterization of dihydroanthranilate derived structures synthesized through the multicomponent reaction. These scaffolds have been derived towards the synthesis of acridones, which are privileged structures, possessing multiple pharmacological activities, and *m*-terphenylamines. The latter have demonstrated are able to selectively inhibit COX-1, which is important in neuroinflammation processes. Additionally, tacrine has been tethered to these structures, managing this way to achieve molecules with multitarget capability.

4. The development of a mechanochemical synthetic method for primary amides. The primary amide group is widely distributed in biology and in APIs, and therefore a sustainable synthesis without the use of solvents or gaseous reagents would be a considerable advance towards a more environmentally friendly chemistry.

5. The application of the primary amide synthesis to the development of a sequential one-pot mechanochemical synthesis of rufinamide, an antiepileptic drug used for the treatment of the Lennox-Gasteaut syndrome.

6. The chemical synthesis of a sensor that allows the quantification of the activity and real time visualization of the enzyme pantothenate kinase. This is the limiting enzyme in the biosynthesis of coenzyme A and it has been recently related to diverse diseases, neurological disorders among them. The ligand will bind in vivo to a fusion protein containing pantothenate kinase expressed in cells and this way, through FRET effect, the visualization and quantification of the activity of pantothenate kinase will be achieved.

**Results and discussion**

Objective number 1 was achieved by the formation of an oxime that having a carboxylic acid at its side chain. Using peptide chemistry conditions, this group was bound to different moieties such as tacrine, N-benzylpiperidine and tryptamines to form several families of hybrid molecules based on naringenin and hespertin.

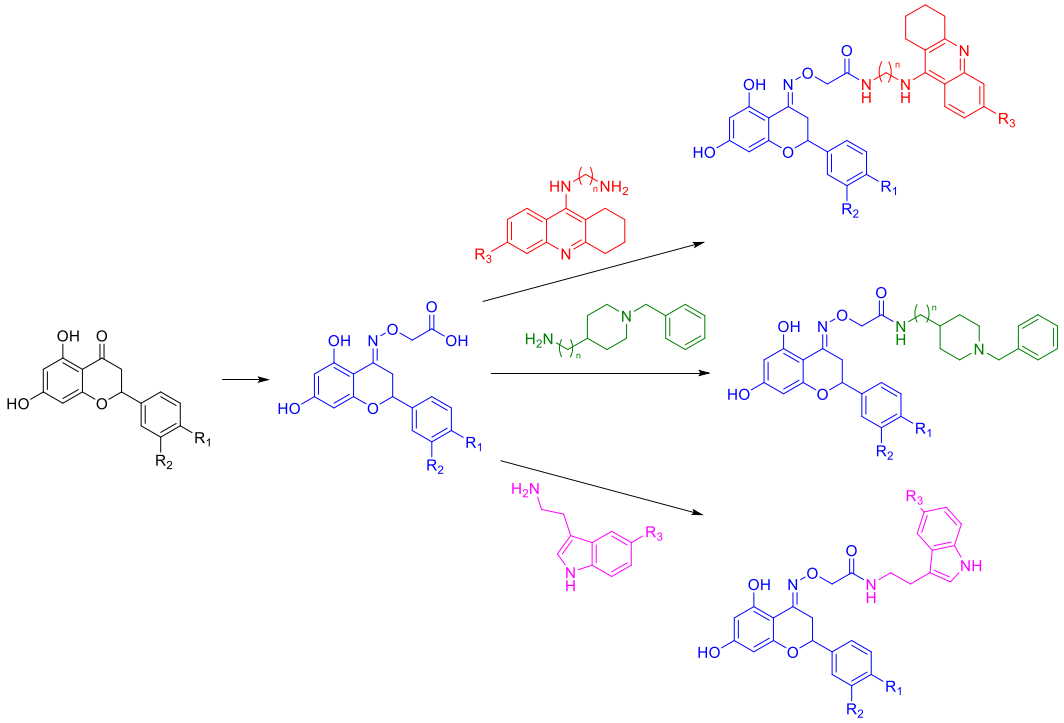

These molecules were pharmacologically tested by Professor Javier del Pino from the department of toxicology at the veterinary faculty of Universidad Complutense and Professors Sagrario Martín-Aragón and Paloma Bermejo from the department of pharmacology at the Faculty of Pharmacy of Universidad Complutense. Some of these compounds displayed good pharmacological activities against multiple disease targets and are interesting hits towards the development of a molecule against Alzheimer´s disease.

Through a multicomponent reaction between a chalcone, a beta-ketoester and an amine a large family of highly functionalised dihydroanthranilates was synthesised. Using an amine bearing a triphenylphosphonium group, a family of tripehylphosphonium-bearing dihydroanthranilates with potential as theragnostic systems for mitochondrial oxidative stress was synthesised. These

compounds were oxidised to their aromatic derivatives using DDQ and their optical properties were measured.

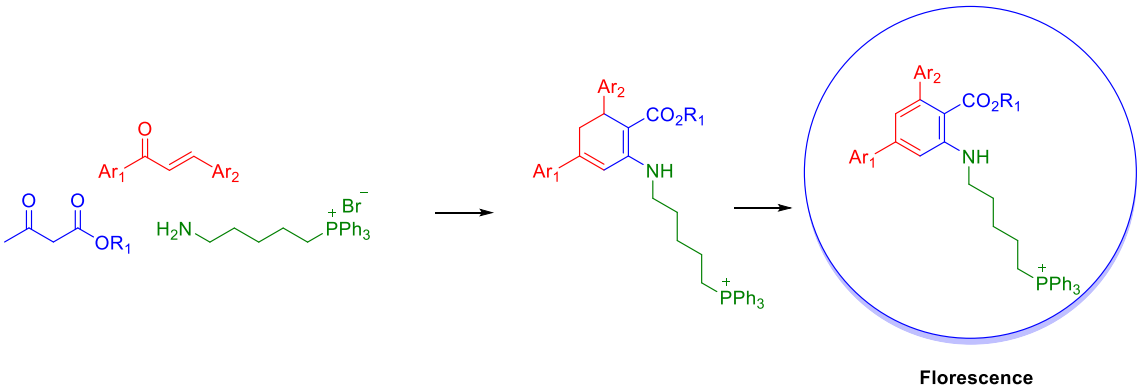


Additionally, for the achievement of objective 3, some dihydroanthranilate scaffolds were derived to other structures such as acridones or *m*-terphenyl amines, the latter being selective COX-1 inhibitors. To these last structures, tacrine was tethered to achieve potential multitarget drug ligands. The pharmacological activity of these molecules against acetylcholinesterase and butyrylcholinesterase was tested and it was found that all of them possesses good inhibitory activity against both enzymes.

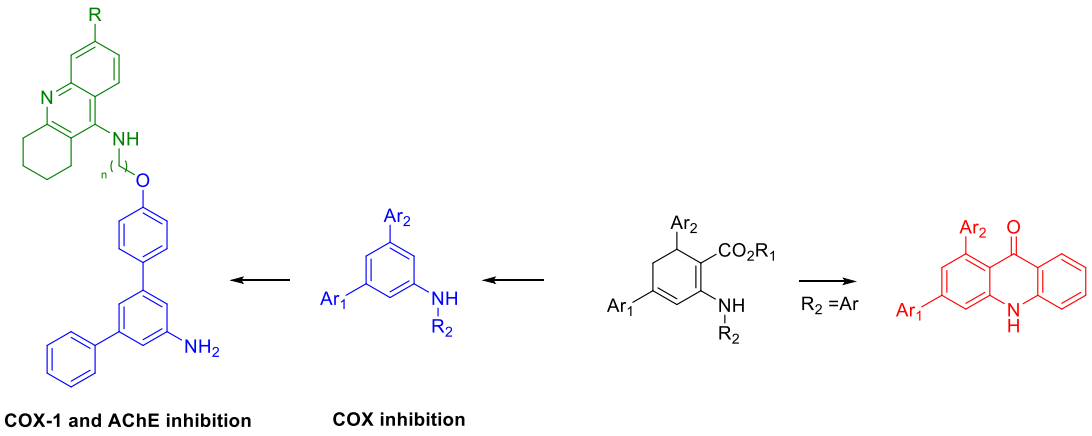


As there were no previously described mechanochemical synthesis of primary amides,a method was devised based on ester amidation with ammonia generated in situ from calcium nitride and ethanol. The optimal conditions involved the use of 0.1 equivalents of indium trichloride, 0.1 ml of ethanol, 3 equivalents of calcium nitride, a milling frequency of 30 Hz and a milling time of 90 minutes. This way, structurally diverse primary amides were synthesised from their ester precursors, generally in good yields.

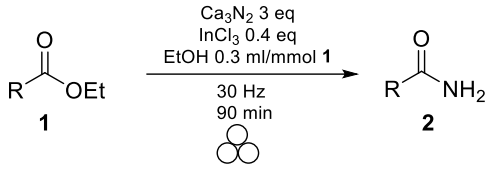


Taking advantage of this result, a mechanochemical, one-pot synthesis of rufinamide, an antiepileptic drug used against Lennox-Gasteaut syndrome, was developed. The process was

carried out without the use of solvents nor the need for chromatographic purification and is a clear improvement in the green parameters of previously described syntheses.

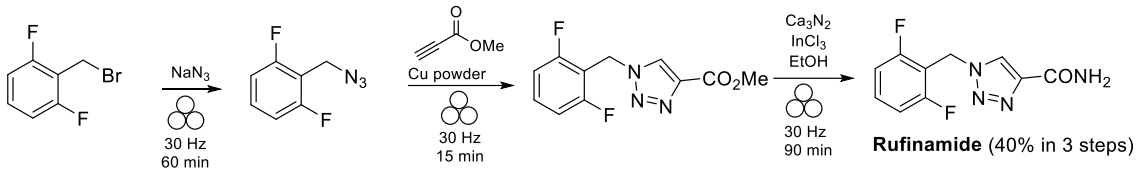


Finally, during an internship carried out in the group led by Kai Johnsson at Max Planck centre for medical research, the synthesis of two chemical ligands for a fusion protein containing pantothenate kinase, the rate-limiting enzyme for the biosynthesis of coenzyme A, a green fluorescent protein and a tag protein, in this case Halo-tag, was carried out. The ligands bear a moiety that can specifically bind Halo-tag, and this way, by a conformational change that takes place when a specific inhibitor of pantothenate kinase that is included in the ligand´s structure, the activity of the enzyme can be measured. Additionally, the ligand carries a rhodamine moiety that allows, by FRET with the green fluorescence protein within the fusion protein, to determine the activity of the enzyme. This is done by the ratio between the intensity of the emission caused by the FRET effect and the green fluorescent protein.

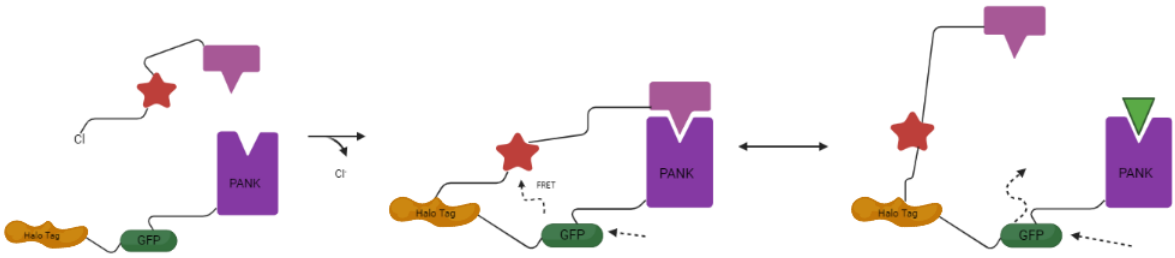


The synthesis of the ligand was carried out by a sequential reaction scheme starting from methyl (6-hydroxymethyl)nicotinate, a simple starting material, which was transformed into two chemical ligands through linear sequences comprising xx steps. These ligands were assayed in cell cultures, and it was determined that they could bind to the fusion proteins and that the desired FRET effect occurred between them and the green fluorescent proteins.

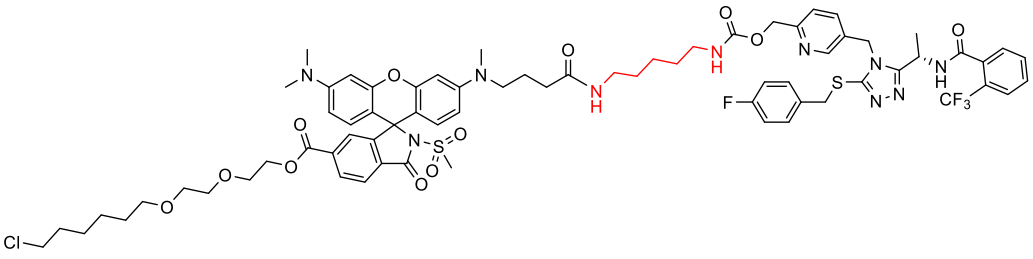

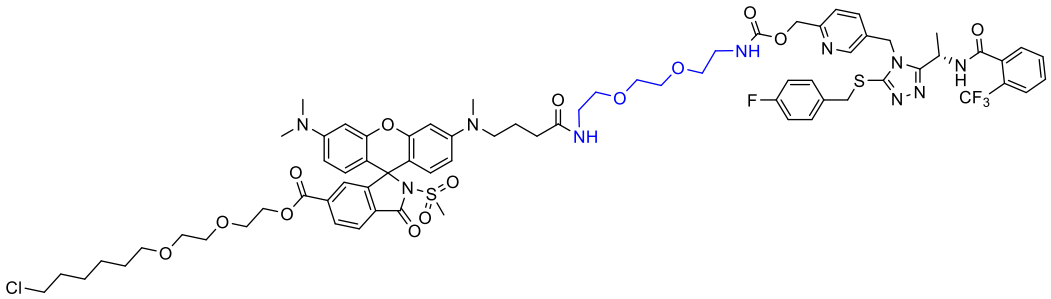

**Conclusions**

The chemical synthesis of different molecules with potential against different neurological disorders has been carried out. Hybrid molecules based on flavonoids have been synthesised and pharmacologically assayed. Potential theragnostic systems against mitochondrial oxidative stress were also synthesised with a multicomponent reaction. Using this same reaction, different scaffolds with potential use against neurological disorders have been achieved, such as acridones or m-terphenylamines, and from the latter structure, a small group of potential multitarget drug ligands has been tailored. Additionally, the mechanochemical one-pot synthesis of a commercialised antiepileptic drug, rufinamide has been achieved, together with a general mechanochemical method for the synthesis of primary amides. Finally, two different chemical ligands for a fusion protein containing pantothenate kinase to determine its activity and behaviour in real time have been synthesised. Assays in cell cultures have determined that both ligands bind to the fusion protein and that there is FRET effect between them and the fusion protein.

## Resumen

### Introducción

Los trastornos neurológicos suponen una gran carga para los sistemas sanitarios mundiales. Estas enfermedades se caracterizan por una disfunción de las neuronas y el modo de afectación de éstas depende de la enfermedad en cuestión. Entre ellas, destacan la enfermedad del Alzheimer, la enfermedad de Parkinson y la epilepsia ya que afectan a un gran número de personas en el mundo y hay una tendencia creciente en cuanto a su incidencia y prevalencia. La etiología de estas enfermedades suele ser compleja al haber múltiples factores involucrados en su establecimiento y progresión. En el caso de la enfermedad de Alzheimer y de Parkinson se produce un mal plegamiento proteico, un aumento del estrés oxidativo, una disfunción de distintos tipos de neuronas (colinérgicas en caso del Alzheimer y dopaminérgicas en caso del Parkinson) y una respuesta inmune exacerbada. En el caso de la epilepsia, la causa suele ser un desbalance en el equilibrio excitatorio-inhibitorio del cerebro, a favor de la excitación.

### Objetivos

1. La síntesis y caracterización farmacológica de una familia de ligandos multidiana frente a la enfermedad del Alzheimer. Estos ligandos están basados en un esqueleto de flavonoide (naringenina y hesperitina) a los cuales se les han unido los farmacóforos de otras moléculas como la tacrina y el donepezilo, conocidos inhibidores de acetilcolinesterasa, y diferentes triptaminas, las cuales poseen múltiples capacidades neuroprotectoras.

2. La síntesis y caracterización de sistemas teragnósticos para estrés oxidativo en mitocondrias. La síntesis de estos sistemas se basa en una reacción multicomponente en la que participan una chalcona, un beta-cetoéster y una amina que posee un grupo trifenilfosfonio, para formar un dihidroantranilato. El grupo trifenilfosfonio, al estar cargado positivamente, hará que los compuestos se dirijan al interior de la mitocondria al poseer la matriz mitocondrial una carga neta negativa. Allí captará un radical libre de oxígeno o de nitrógeno, se oxidará y adquirirá la capacidad de emitir fluorescencia. De esta manera, al captar el radical libre, mitigará en parte el estrés oxidativo y al volverse fluorescente solo en su presencia servirá para el diagnóstico de estrés oxidativo.

3. La síntesis y caracterización de estructuras derivadas de los dihidroantranilatos sintetizados a través de la reacción multicomponente. Estos esqueletos se han derivado hacia la síntesis de acridonas, las cuales son estructuras privilegiadas que poseen multitud de actividades farmacológicas y hacia la síntesis de m-terfenilaminas. Estas últimas han mostrado tener actividad inhibitoria selectiva frente a COX-1, la cual es importante en el desarrollo de procesos neuroinflamatorios. Asimismo, estas estructuras se han unido a tacrina, que como se ha mencionado previamente es un conocido inhibidor de colinesterasas, logrando así potenciales compuestos multidiana frente a la enfermedad del Alzheimer.

4. El desarrollo de una síntesis mecanoquímica para la formación de amidas primarias. El grupo amida primaria está ampliamente distribuido en la naturaleza y en el mundo farmacológico y por tanto, una síntesis sostenible sin necesidad de disolventes o de bombeo de amoniaco sería una mejora considerable para su obtención.

5. La aplicación del método anterior al desarrollo de una secuencia de reacción mecanoquímica *one-pot* para la síntesis de rufinamida, un fármaco antiepiléptico usado para el síndrome de Lennox-Gasteaut. La secuencia se llevará a cabo mediante una secuencia de tres pasos de reacción en el molino de bolas vibratorio.

6. La síntesis química de un sensor que permita cuantificar y visualizar a tiempo real la actividad de la enzima pantotenato kinasa (PanK). Esta enzima es limitante en la biosíntesis de la coenzima A y recientemente se ha demostrado su importancia en diversas patologías, incluyendo enfermedades neurodegenerativas. El ligando sintetizado se unirá in vivo a una proteína de fusión expresada en células y de esta manera, mediante efecto FRET se podrá visualizar y cuantificar la actividad de PanK.

**Resultados y discusión**

El objetivo 1 se llevó a cabo mediante la formación de una oxima en el grupo carbonilo de los flavonoides, el cual a su vez dejaba libre un resto de ácido carboxílico que se usó para unir tacrina N-bencilpieridina y distintas triptaminas y formar distintas moléculas híbridas basadas en naringenina y hesperitina mediante química de péptidos.

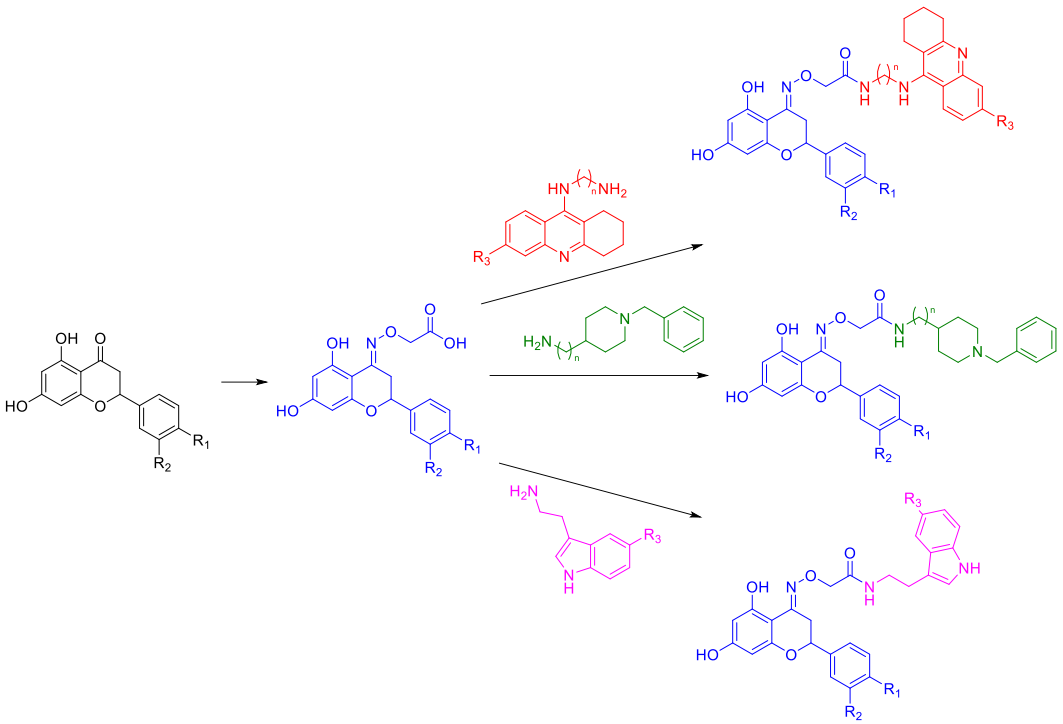

Estas moléculas fueron ensayadas farmacológicamente por el profesor Javier del Pino y las profesoras Sagrario Martín-Aragón y Paloma Bermejo. Se determinó que algunos de estos compuestos pueden considerase un buen punto de partida para el futuro desarrollo de ligandos multidiana frente a la enfermedad del Alzheimer.

Mediante una reacción multicomponente entre una chalcona, un beta cetoéster y una amina se sintetizaron una amplia familia de dihidroantranilatos altamente funcionalizados para la realización del objetivo 2. Usando una amina que lleva un grupo funcional trifenilfosfonio se logró sintetizar una familia de compuestos con potencial uso como sistemas teragnósticos. Estos

compuestos se aromatizaron por tratamiento con DDQ para determinar sus propiedades ópticas.

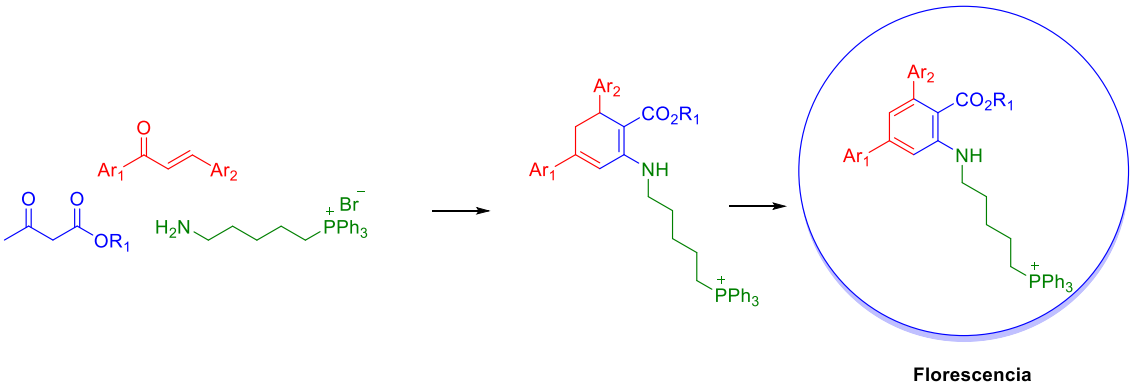


Asimismo, para la consecución del objetivo 3, algunos esqueletos de dihidroantranilato fueron derivados a otras estructuras como acridonas o meta-terfenilaminas, las cuales son inhibidores selectivos de COX-1. A estas últimas estructuras se les unió tacrina para sintetizar potenciales ligandos multidiana frente a la enfermedad del Alzheimer. Se probó la actividad de estas moléculas híbridas frente a acetil y butiril colinesterasa y se determinó que todas poseían una buena capacidad inhibitoria frente a ambas enzimas.

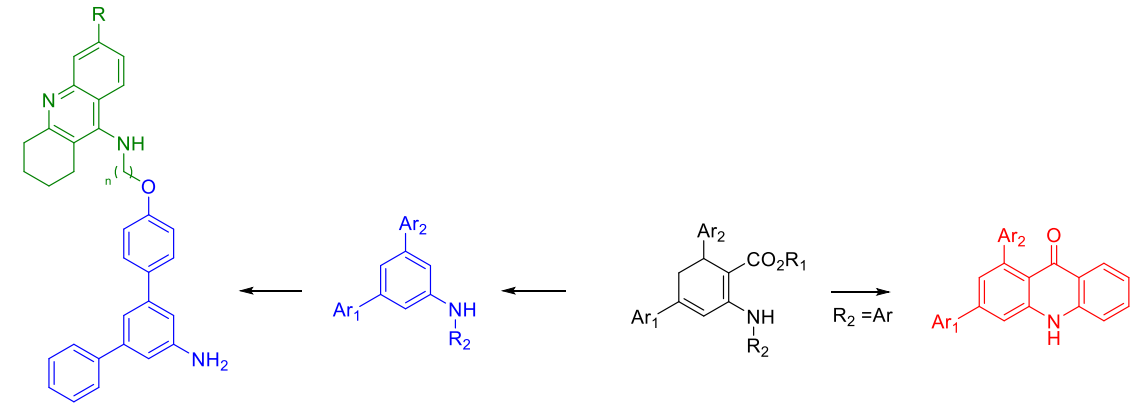


Puesto que que no había antecedentes previos de la síntesis de amidas primarias en mecanoquímica, se desarrolló un método basado en la amidación de ésteres utilizando nitruro de calcio y etanol para generar amoníaco *in situ*. Se determinó que las condiciones de reacción óptimas eran 0.4 equivalentes de tricloruro de indio, 0.1 ml de etanol, 3 equivalentes de nitruro de calcio, una frecuencia de 30 hercios y un tiempo de molienda de 90 minutos. De esta manera se lograron obtener diversas amidas primarias a partir de sus correspondientes ésteres con buenos rendimientos.

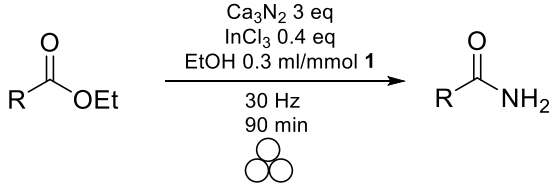

Aprovechando este resultado, se se realizó una síntesis mecanoquímica *one-pot* de la rufinamida, un antiepiléptico utilizado para el tratamiento del síndrome de Lennox-Gasteaut. El proceso se llevó a cabo sin etapas de purificación cromatográfica ni uso de disolventes y supone una clara mejora en los parámetros verdes del proceso con respecto a otras rutas sintéticas previamente descritas.

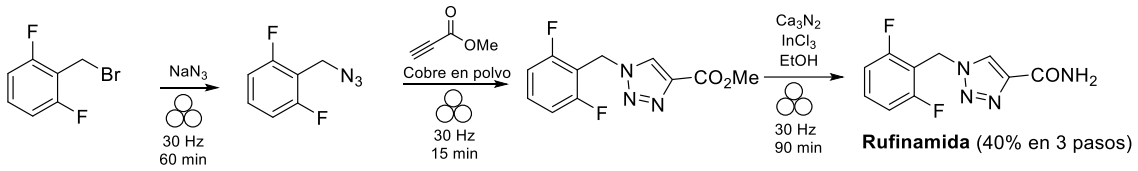


Por último, durante una estancia en el instituto Max Planck para la investigación médica, el grupo del profesor Kai Johnsson, se procedió a la síntesis química de un ligando para una proteína de fusión que incluye a la enzima pantotenato kinasa, la cual es limitante en la biosíntesis de coenzima A, junto con una proteína verde fluorescente y una proteína tag, en este caso Halo-tag. El ligando lleva una parte que específicamente es capaz de unirse a Halo-tag, quedando la proteína de fusión permanentemente marcada, y de esta manera mediante un cambio de conformación ocasionado por la unión de un inhibidor específico de la enzima pantotenato kinasa, el cual está incluido en la estructura del ligando. El ligando además incluye una rodamina que mediante efecto FRET con la proteína verde fluorescente será capaz de emitir fluorescencia. De esta manera, mediante cuantificación de efecto FRET a tiempo real, se puede determinar la concentración de sustrato endógeno unido a la enzima.

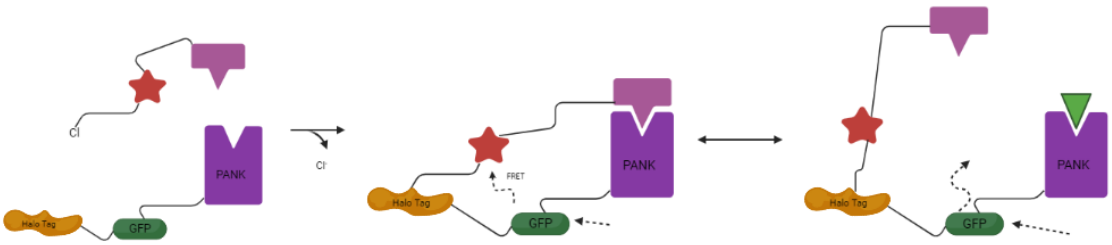


La síntesis del ligando se llevó a cabo mediante un esquema de reacción secuencial, con un material de partida simple y asequible, el 6-(hidroximetil)nicotinato de metilo, al cual se le fueron agregando distintos fragmentos hasta sintetizar dos ligandos químicos de elevado peso molecular distintos en una ruta lineal de 17 pasos. Estos ligandos se estudiaron en cultivos celulares y se determinó que eran capaces de unirse a las proteínas de fusión y que se producía efecto FRET entre la proteína verde fluorescente y la parte de la rodamina del ligando.

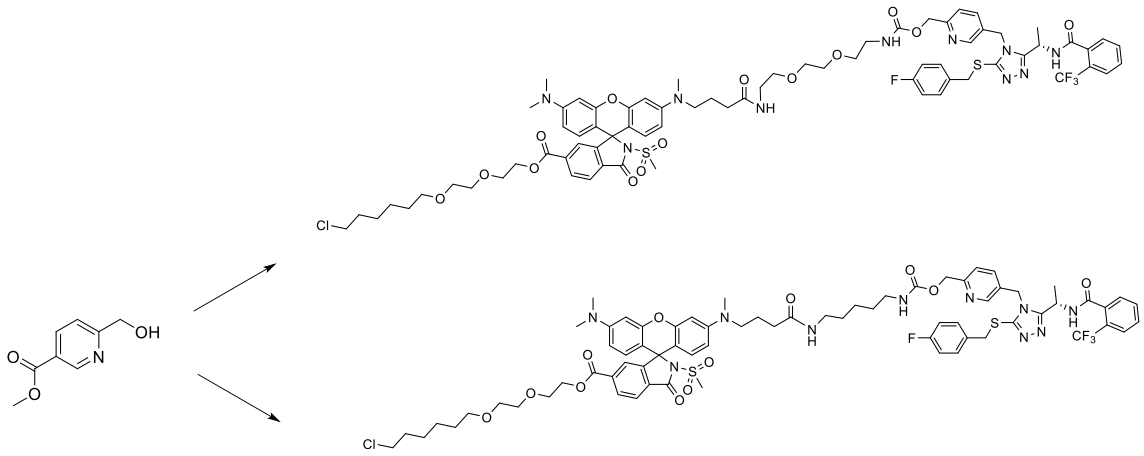

**Conclusiones**

Se ha realizado la síntesis de diversas moléculas con potencial acción frente a distintos desordenes neurológicos con distintas aproximaciones. Se han sintetizado y ensayado farmacológicamente ligandos multidiana basados en esqueletos de flavonoides. Se ha sintetizado mediante una rección multicomponente, potenciales sistemas teragnósticos frente a estrés oxidativo mitocondrial. También se ha utilizado la misma reacción multicomponente para la posterior obtención de estructuras químicas con potencial acción frente a enfermedades neurodegenerativas, e incluso para la obtención de un pequeño grupo de ligandos multidiana también destinados frente a la enfermedad del Alzheimer. Asimismo, se ha logrado la síntesis mecanoquímica *one-pot* de un antiepiléptico comercializado, la rufinamida, gracias a un método general para la síntesis mecanoquímica de amidas primarias previamente desarrollado. Por último, se han sintetizado dos ligandos para una proteína de fusión que incluye a pantotenato kinasa para lograr determinar su funcionamiento a tiempo real mediante microscopía confocal, y se determinó mediante experimentos en cultivos celulares que ambos ligandos son capaces de unirse a la proteína de fusión y son capaces de realizar con la parte de la proteína verde fluorescente un efecto FRET.

# Chapter 1. Introduction

## Introduction

### 1.0 Neurological disorders

With an increasing global life expectancy, neurological disorders are becoming the major causes of death and disability worldwide. A study published by *The Lancet* in 2019 found that neurological disorders, including Alzheimer´s disease, Parkinson´s disease and epileptic disorders, were the leading cause of disability-adjusted life years (DALYs) with a total number of 276 million, and the second leading cause of deaths, with a total number of 9 million, in 2016. This study also found that between 1990 and 2016 the absolute number of DALYs and deaths caused by neurological disorders increased (deaths by a 39% and DALYs by a 15%). The interpretation that can be extrapolated from this data is that globally, the burden that neurological disorders follow an increasing tendency, which can be attributed to the ageing and increasing life expectancy of the world´s population. This poses a serious challenge to world health systems worldwide, which are facing an increasing demand for treatment, daily care and support related to neurological disorders.[1]

Neurological disorders comprise a great variety of diseases in which the common factor is the malfunction or deterioration of neurons. Among this great hotchpotch of diseases we can find neurodegenerative diseases such as Alzheimer's or Parkinson´s disease, all the different types of epilepsy, infections caused by microorganisms that cause encephalitis or meningitis, migraines or brain stroke.[2] However, concerning the matter of this work, its central point will be neurodegenerative disorders and epilepsy.

### 2.0 Alzheimer´s disease

Alzheimer´s disease (named after the German physician Alois Alzheimer) is the most common class of dementia, and it is histologically characterized by the occurrence of extracellular neuritic plaques and intracellular neurofibrillary tangles. When Alzheimer first characterized the disease, he noted the presence of this plaques along with a great loss of neurons. This patient suffered from personality change together with a significant loss in cognitive abilities before dying and the disease was classified as serious disease of the cerebral cortex.

More than 100 years after it was firstly described, Alzheimer´s disease stands out as one of the greatest challenges for health systems worldwide. It has been estimated that in 2015 the total number of people suffering from dementia is 46.8 million and that this number will almost double every 20 years. If this tendency is to continue, in 2030, the total number of people with dementia will reach 74.7 million people and by 2050, this number will rise up to 131.5 million. It has also been estimated that there are 9.9 million cases of dementia each year, with the regional distribution of the incidence of dementia is 4.9 million in Asia, 2.5 million in Europe, 1.7 million in the Americas and 0.8 million in Africa. It has also been estimated that the total costs attributed to dementia are US $ 818 billion, which represent a 1.09% of the global GDP. These statistics clearly describe the importance of AD globally. Figures 1, 2 and 3 graphically represent this information[3].

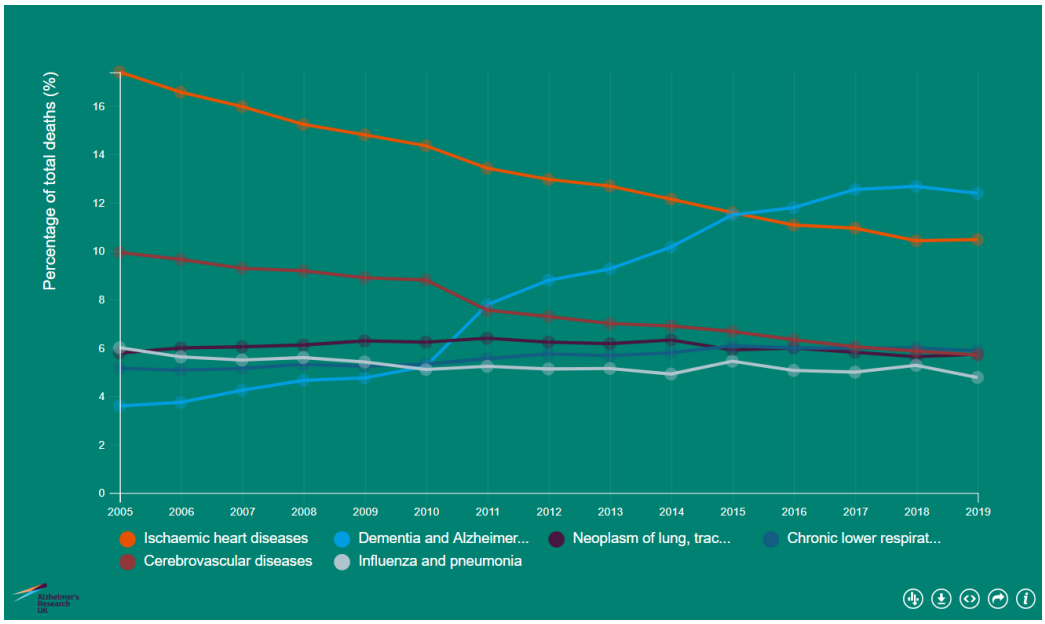


Figure 1. Percentage of total deaths caused by AD. Extracted from https://www.dementiastatistics.org/statistics/deaths-due-to-dementia/

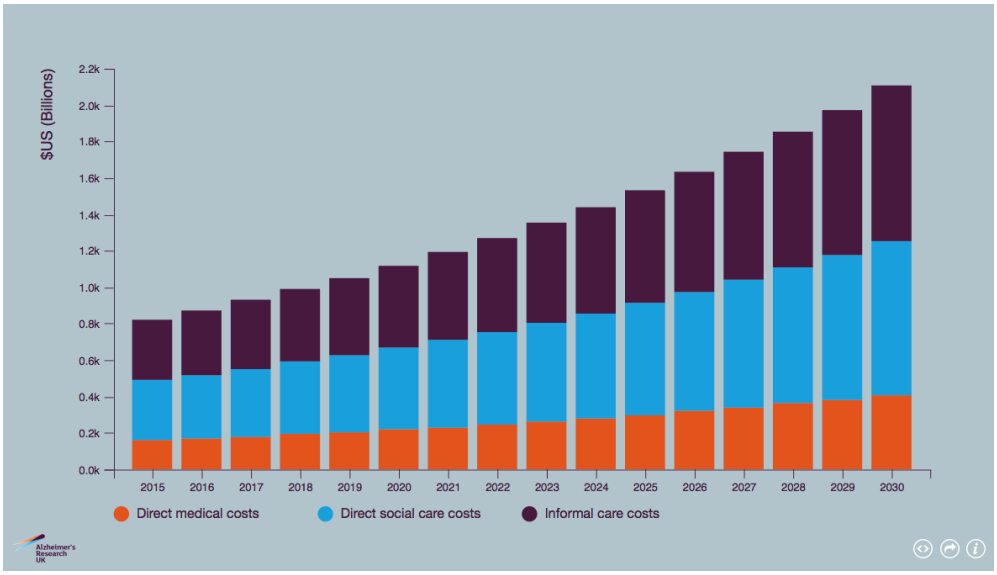


Figure 2. Medical costs associated with AD and its projection in the upcoming years. Extracted from https://www.dementiastatistics.org/statistics-about-dementia/human-and-financial-impact/

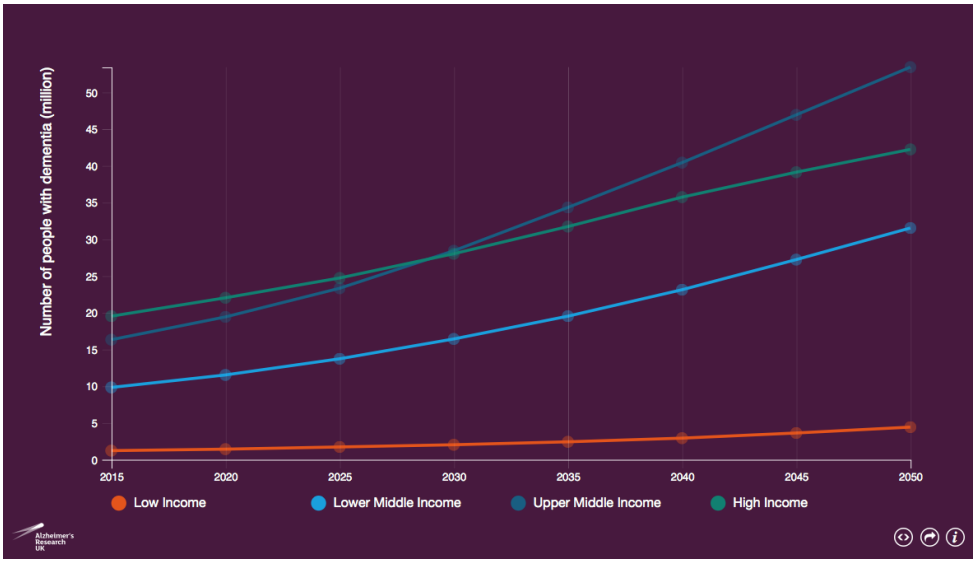


Figure 3. Number of people with dementia in different country incomes. Extracted from https://www.dementiastatistics.org/statistics/global-prevalence/

All these data, together with the lack of an effective treatment, convert AD in a major worldwide health concern and a better insight of it is necessary in order to stop the current tendency of increasing incidence, prevalence and costs.

### 2.1 AD´s physiopathology

With respect to AD´s physiopathology, its multifactorial nature is widely accepted by the scientific community. Although there are still many questions regarding the pathogenic mechanisms of the disease, there are some factors that are believed to play an important role in its development. Among these factors we can cite the formation of beta amyloid (Aβ) plaques, neurofibrillary tangles formed by a hyperphosphorylated tau protein, high concentrations of reactive oxygen species (ROS) and reactive nitrogen species (RNS), a general decrease in cholinergic neurotransmission, caused by cellular death of this type of neurons, a high concentration of neurotoxic metals and an out-of-control immune response in the brain[4,5].

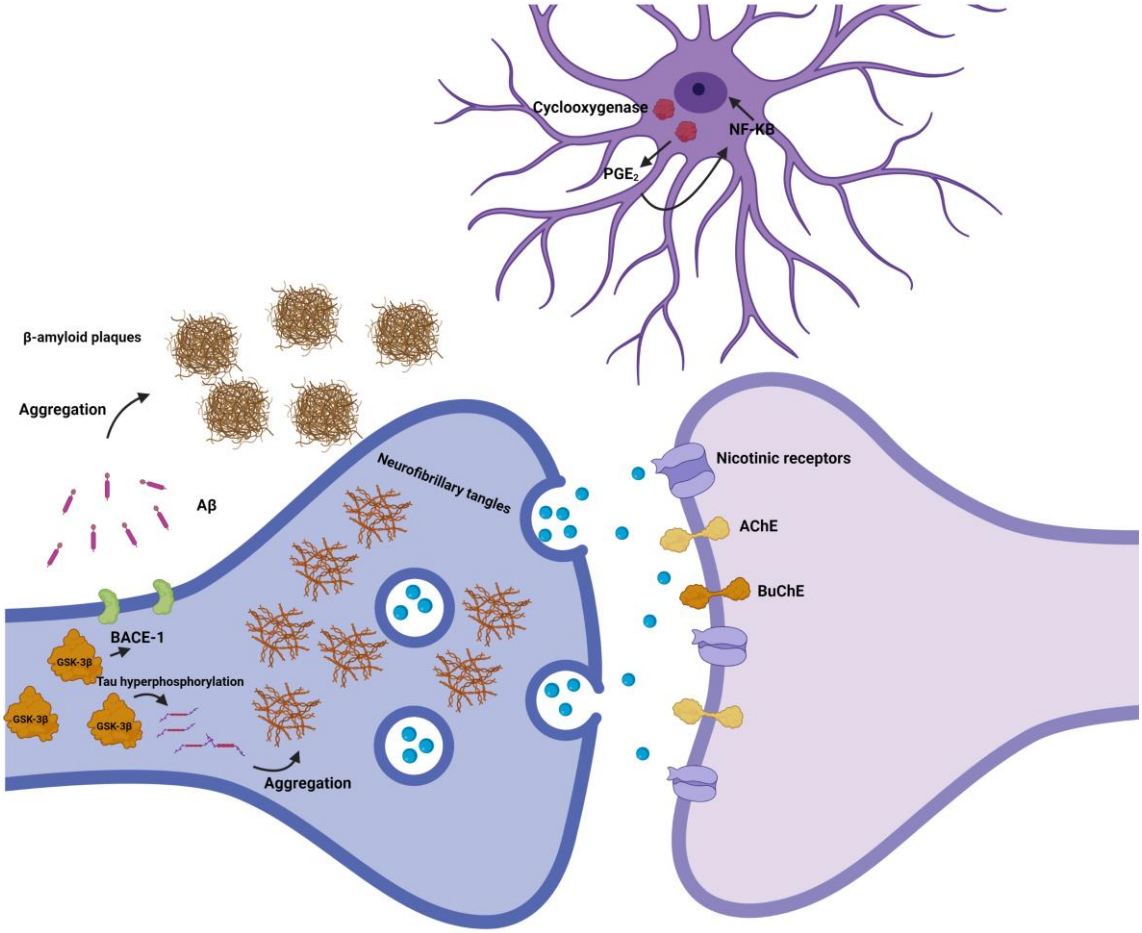


Figure 4. Scheme representing pathways for the development and establishment of AD

### 2.1.1 Aβ plaques

One of AD´s classical hallmarks is the extracellular presence of protein aggregates formed by filaments of amyloid β peptides. The origin of these peptide aggregates is the proteolytic cleavage of amyloid precursor protein (APP) by two different enzymes, namely β-secretase (BACE-1) and γ-secretase, which catalyse the first and second steps of APP respectively. APP is cleaved in the first place by BACE-1 into soluble APP-β and a 99 amino acid transmembrane peptide C-99, which is further cleaved by γ-secretase to extracellularly release peptides of a length between 38 to 43 amino acids, being the major products Aβ 40 and Aβ 42, both of which play a critical role in the development of the disease (figure 1). Aβ 42 is more insoluble and tends to aggregate in a greater degree than Aβ 40, and indeed there is an increased Aβ 42: Aβ 40 ratio in the familial version of the disease[6,7]. Taking all this into consideration, many efforts have been made to reduce the formation of these aggregates as a way to treat the disease. Among all of the ways to act on this pathological pathway, research groups have attempted to inhibit the aggregation of Aβ by using planar structures that disrupt the interaction between fibrils[8], to modulate or inhibit the activity of γ-secretase[9] and to inhibit BACE-1[10]. Although there are advanced clinical trials with molecules that act on each of these points, none of them has still reached the market.

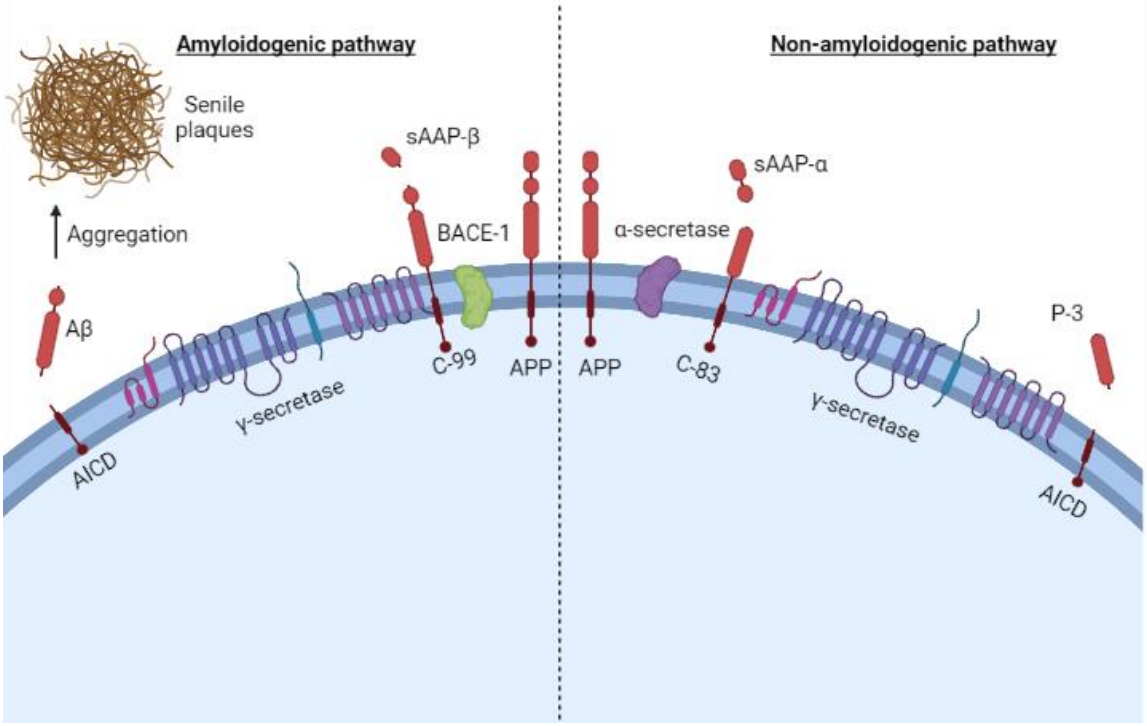


Figure 5. Pathological and non-pathological processing of APP.

### 2.1.2 Neurofibrillary tangles

Tau protein is one of the major neuronal microtubular associated protein (MAP) which has a simple B-sheet helicoidal structure. Its major role is to enhance the microtubular assembling process and to stabilise its structure, and this function is regulated by its degree of phosphorylation. In a physiological state, tau is phosphorylated in two or three sites, and its hyperphosphorylation, one of the trademarks of AD, causes a dysfunction on its microtubular assembly properties. Additionally, in its hyperphosphorylated state, tau is the major subunit that composes paired helical filaments (PHLs) and straight filaments, that conform neurofibrillary tangles (NFTs)[11]. Abnormally hyperphosphorylated tau not only loses its physiological function, but also recruits normally phosphorylated tau and other MAPs and disrupts microtubular function[12]. NFTs are inert and have no effect on the correct assembly of microtubules, but they cause cellular injuries by occupying abnormal portions of intracellular space[13]. The occurrence of NFTs is a necessary requirement for the appearance of the clinical symptoms observed in AD and its number is correlated with the degree of dementia[14].

In AD, there are multiple causes for an abnormal phosphorylation of tau, such as a dysregulation of neuronal biochemical pathways which cause a phosphorylation/dephosphorylation imbalance or alterations in glucose metabolism. In this spite, there are many therapeutical targets that can be tackled to alter the course of the disease. One of the possible paths to revert the formation of NFTs is the inhibition of tau hyperphosphorylation, which can be achieved by inhibiting kinase enzymes that have tau as its substrate, being glycogen synthase kinase-3β (GSK-3β) the major role actor[15,16]. Other possible paths to impede NFT formation is the inhibition of tau misfolding[17] or increasing the clearance of already abnormally hyperphosphorylated tau protein[18].

### 2.1.3. Oxidative stress

The brain is the organ in the human body that requires the greatest oxygen supply, and therefore high concentrations of reactive oxygen species (ROS) and reactive nitrogen species (ROS) form inside neurons. This fact, together with the high amounts of peroxidazible fatty acids present in brain tissue can lead to vital macromolecular damage and hence, to neuronal dysfunction and subsequent death[19]. However, in a physiological state, the pro-oxidant and antioxidant mechanisms inside neurons balance out and no damage is bestowed to neurons. Moreover, during normal metabolism, superoxide ($O_2^{\cdot-}$) hydrogen peroxide ($H_2O_2$) and hypochlorous acid (HClO) are produced. In AD, this balance is disrupted, causing ROS and RNS to proliferate and damage vital cellular structures[20].

There are many sources from which this imbalance can happen. Recently, it has been determined that Aβ can induce the formation of harmful free radicals indirectly, by attraction and hyperactivation of microglial cells, which in turn generate pro-inflammatory molecules and free radical species that result in neuronal death[21,22]. Other possible mechanism for ROS and RNS generation is the metal-catalysed Fenton reaction, which from $H_2O_2$ generates hydroxyl radical ($OH^{\cdot}$), a highly reactive species that alters severely the structure of vital macromolecules[23]. Additionally, there are binding sites for biometals such as Cu and Zn in Aβ plaques, which enhance the toxicity of these structures by converting them directly in primary sites of ROS and RNS generation[24].

To restore the pro-oxidant and antioxidant equilibrium diverse strategies have been devised. In the first place, using direct free radical scavengers that can stabilise free radicals and stop the damage caused by highly reactive species such as superoxide[25]. Other possibility is to activate the cellular antioxidant defensive mechanisms, which translates into the nuclear translocation of the nuclear erythroid related factor 2 (Nrf-2). Nrf-2 is a protein sequestered in the cytoplasm by kelch ECH associating protein 1 (KEAP-1), which is polyubiquitinated and degraded under normal conditions. However, under an oxidant or electrophilic environment, these molecules disrupt the interaction between KEAP-1 and Nrf-2 and the latter translocases to the nucleus, activating a diverse number of antioxidant and detoxifying genes. Nrf-2 activators are also receiving wide attention for their great antioxidant potential and their use in AD[26]. Finally, metal ion chelators are also being used with the purpose of sequestering toxic metal ions and preventing their potential harmful effect via the Fenton reaction[23].

### 2.1.4 Cholinergic dysfunction

The cholinergic hypothesis was presented more than 20 years ago, and it postulates that the decline in the cognitive function of patients is directly related to the decay and dysfunction of cholinergic neurons. It was found that the severity of AD was positively correlated to the degree of cholinergic loss, and in fact most commercialised treatments increase the levels of acetylcholine (ACh), producing a symptomatic improvement[27]. ACh is a widely distributed neurotransmitter released in vesicles and binds to post-synaptic nicotinic receptors in the case of brain tissue. It is mainly degraded by the enzyme acetylcholinesterase (AChE) in the synaptic cleft but butyrylcholinesterase (BuChE) can also perform the same function and hydrolyse bigger choline esters[28, 29]. In recent years, these enzymes have also been related to the aggregation of Aβ, increasing their significance as potential therapeutic targets for AD. These enzymes perform this fact due the presence of residues in the peripheric anionic site (PAS), a site in both enzymes situated at the entrance of the gorge that bears the catalytic active site[30]. Inhibition of these

enzymes can therefore be beneficial in a double sense: raising acetylcholine levels that partially revert cognitive deterioration and inhibition of the aggregation of Aβ, stopping this way the formation of senile plaques.

### 2.1.5 Neuroinflammation

In recent years, there has been increasing evidence that the behaviour of the immune response conditions the development of AD. As previously stated, Aβ is recognised by microglial and astroglial cells, causing the production and release of ROS and proinflammatory molecules, contributing to the progression and severity of AD[31]. Aβ oligomers and fibrils are recognisable pathogen-associated molecular patterns (PAMPs), which bind to diverse membrane bound proteins of microglia and astroglia such as CD36, CD14, α6β1 integrin, CD47 or different Toll-like receptors (TLRs)[32–35]. In a physiological way, microglia interact with these aggregates and phagocytise them, clearing them from the extracellular medium. However, in some cases of AD this clearance is inefficient, causing exacerbated proinflammatory cytokine and ROS release, and ending consequently in neuronal death[36].

An interesting approach to modulate microglial cell response is to inhibit cyclooxygenase (COX) enzymes. There are two existing isoforms of COX, COX-1 and COX-2, the former being constituently expressed in tissues and the latter inducible. These enzymes are responsible for prostaglandin (PG) synthesis from arachidonic acid (AA), being prostaglandins potent inflammatory mediators[37]. The well-known non-steroid anti-inflammatory drugs (NSAIDs) inhibit COX enzymes and have gained wide attention in recent years as a mode to control an exacerbated immune response in AD and have been tested as potential therapeutic agents for AD[38].

## 3.0 Parkinson´s disease

Parkinson´s disease (PD) was firstly described by James Parkinson in 1817 in his "Essay on the shaking Palsy". Resting tremor, stiffness and the typical station and gait were the symptoms he detailed in his workpiece and more than 200 years after, Parkinson´s disease is still a burden for worldwide health systems[39]. PD affects around 0.3% of the general population and 1 to 3% of the population older than 65 years. As it can be extracted from this data, we can observe that due to the rise in global life expectancy and being a disease especially prevalent on the elderly, all indicates that is projection is going to be ascending in the next years. Its numbers are expected to rise up to 8.7 to 9.3 million patients in 2030[40,41].

PD is a progressive neurodegenerative disease has two different groups of symptoms: motor and non-motor. The former express themselves as the ones Parkinson´s described (rigidity, bradykinesia, postural instability, gait dysfunction and tremor), while the latter manifest as dementia, hyposmia and gastrointestinal dysfunction[42]. These symptoms are due to the progressive degeneration of the nigrostriatal dopaminergic neurons and loss of the substantia nigra pars compacta brain region.

### 3.1 PD´s physiopathology

Being another neurological progressive neuropathy, PDs classical hallmark are Lewy´s bodies (LB), which are conformed by a 140 amino acid protein, whose exact function is still to be determined, α-synuclein. α-synuclein's phosphorylation and fibrillization lead to LB formation and subsequent cell death. In PD, LBs can be found in parts of the central nervous system: basal ganglia, the dorsal motor neurons of the vagus, the olfactory bulb and the intermediolateral nucleus of the spinal cord; and also, in some parts of the peripheric nervous system, such as the celiac ganglia and the enteric nervous system. The appearance of these protein aggregates in different parts of the nervous system correspond to the clinical manifestations of the disease. However, the most damaged brain section in PD is the substantia nigra pars compacta (SNpc), which experiments a significant loss of dopaminergic neurons. In fact, treatment with levodopa a prodrug metabolised in the organism to dopamine causes a symptomatic improvement of patients. Although LBs and dopaminergic neuron loss are the classical physiopathological hallmarks of PD, other dysfunctions accompany and contribute to the progress of the disease, such as mitochondrial oxidative dysfunctions, dopaminergic dysregulations, alteration of calcium channel activity or neuroinflammation (figure 3) [42].

Figure 6. Schematic representation of PD's physiopathology

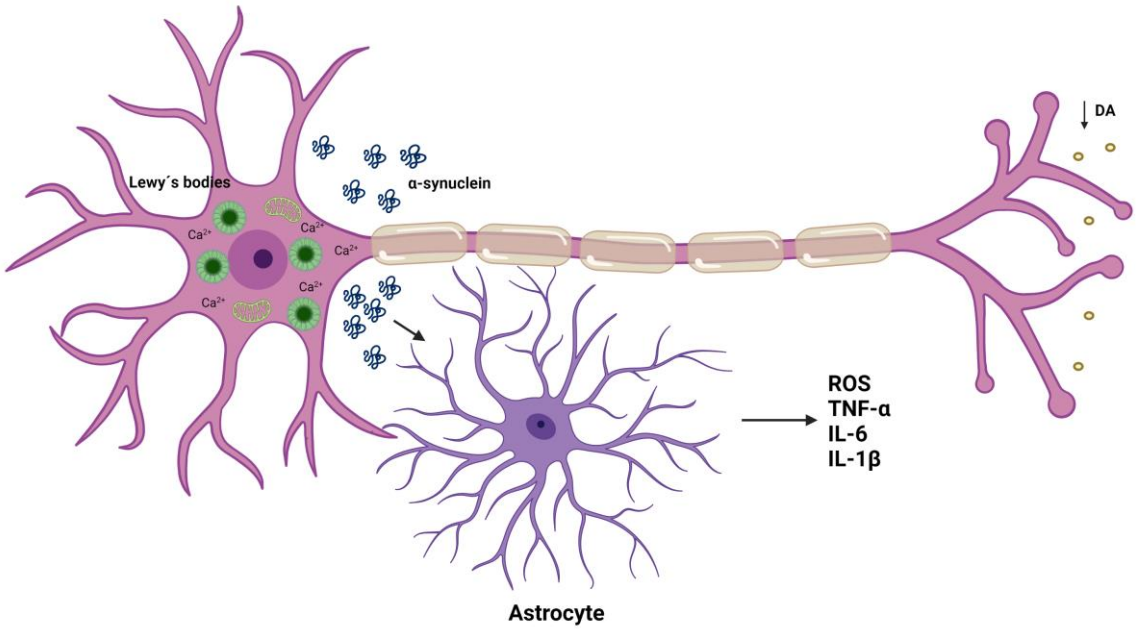


### 3.1.1 α-Synuclein aggregation

α-Synuclein is an abundant brain protein found both extracellularly and membrane bound in neurons. It composes almost 1% of the total protein in soluble cytosolic brain fractions. Although its role is still not fully understood, it has been suggested to have different roles in synaptic vesicle transport and release, fatty acid binding, physiological regulation of certain enzymes, transporters and neurotransmitter vesicles, and in neuronal survival. Knockout mice of all synucleins (α, β and γ) led to age-dependant neuronal dysfunction. Its relatively unfolded nature is determined by its high hydrophilicity and high net charge. However, when the mechanisms in charge of detecting and solving protein misfolding are impaired, or the structure of the protein mutated, aggregation tends to occur[43,44].

Once LB formation has occurred, misfolding surveillance mechanisms in neurons become more readily inactivated as the chaperones heat shock proteins 70 and 40, get sequestered in the aggregates and therefore, functionally unavailable for the neurons. When aggregated, α-synuclein is believed to be toxic in many different ways: inhibition of Golgi transport, membrane permeabilization and alteration of vesicle docking, impairing the proteasome system or altering the morphology and correct functioning of mitochondria[44].

In this spite many efforts have been directed towards reducing the toxicity of α-synuclein aggregates. In the first place, trying to increase protein clearance, mainly by the autophagy-lysosome pathway, but also stopping its aggregation, or even by immunising against LBs[45].

### 3.1.2. Mitochondrial dysfunction

Mitochondrial dysfunction is closely related to the development of PD. Experiments performed with complex I of the mitochondrial respiration electron chain inhibitors such as rotenone or 1-methyl-4-phenyl-1, 2, 3, 6-tetrahydropyridine (MPTP), demonstrated to induce dopaminergic neurodegeneration in flies, humans and rodents. As a matter of fact, the activity of complex I in PD patients is impaired in substantia nigra, musculoskeletal tissue and platelets. The inhibition of complex I causes an increase in mitochondrial permeability, an increase in the generation of ROS and an increase in the activity of nitric oxide synthase. There is post-mortem evidence of damage caused by oxidative stress in PD patients. Moreover, it was found that mice overexpressing α-synuclein were more sensitive to the neurotoxic effects of MPTP, whereas mice with a normal expression of α-synuclein, were not susceptible to the toxic effects of 3-nitropropionic acid, malonate and MPTP. This suggests a relationship between the toxic effects caused by α-synuclein and mitochondrial dysfunction. Additionally, mitochondria present in their outer membrane monoaminoxidase (MAO) enzymes that oxidise dopamine to its quinone forms and free radicals. Further oxidation products may cyclise to aminochromes, which are reactive enough to produce superoxide radicals[46,47].

There are emerging therapeutic options to mitigate the oxidative stress present in PD. In the first place by administration of free radical scavengers to capture and stabilise ROS produced in PD. Additionally, activation of Nrf-2 pathway is another viable option to reduce oxidative stress levels as activation and translocation of Nrf-2 induces powerful mechanisms to defend the cell against oxidative stress. Finally, inhibition of MAO enzymes may as well restore the physiological dopaminergic levels as well to reduce oxidative stress generated by its activity.

### 3.1.3 Calcium channel alteration

Calcium plays an important role in the correct functioning of neurons and is closely related to cellar processed that can lead to neuronal death in PD, such as oxidative stress, mitochondrial impairment, proteasomal dysfunction or neuroinflammation. The *substantia nigra* neurons are autonomous pacemakers generating action potentials at a slow rate (2-10 Hz), and this self-generated action potentials cause $Ca^{2+}$ release into the cell, and excess of intracellular calcium levels during prolonged periods of time is highly neurotoxic. In this connection, voltage-gated calcium channels (VGCCs) and especially L-type (long lasting) are crucial in calcium homeostasis in neurons, as they are the main regulators of calcium homeostasis inside neurons. It has been determined that the expression of these channels is increased in PD, causing a dysfunction in

$Ca^{2+}$ homeostasis and cell death throughout the brain. Therefore, by blocking these channels a neuroprotective effect could be afforded and numerous VGCC blockers have been through clinical trials[48–50].

### 3.1.4. Neuroinflammation

There is increasing evidence that a considerable portion of the oxidative stress present in patients of PD is caused by microglia. Recent studies suggest that microglial cells phagocytise extracellular aggregated α-synuclein as an effort to clear it, either as a consequence of neuronal apoptotic death or as extracellularly released. This in consequence, activates microglia which produces and releases numerous proinflammatory cytokines and ROS which in turn, provoke a greater degree of neuronal death. As a means of controlling immune response in the brain and ameliorate oxidative stress damage, NSAIDs have been proposed as a therapeutic as like it was previously mentioned inhibit the production of proinflammatory prostaglandins and reduce the impact of an exacerbated immune response[51–53].

## 4.0 Epilepsy

Epilepsy is a neurological disorder characterized by recurrent seizures that can be accompanied by loss of consciousness, consequence of an abnormally high neuronal activity. The diagnose of the disease requires that the patient has presented at least two different events of unprovoked seizure. This disorder approximately affects 50 million people worldwide. The term 'epilepsy' englobes a whole range of different neurological disorders that have different ethology manifestations and severity, with all of them sharing the common trait of uncontrolled seizures. IN order to standardise the disease, the international league against epilepsy (ILAE) described a procedure to improve the diagnosis and treatment of epilepsy patients. This model presents three levels: the first corresponds to the type of seizure (focal, generalised, or unknown), the second to the type of epilepsy (focal epilepsy, generalised epilepsy or a combination of both) and the third is the specific diagnosis of the epileptic syndrome[54].

This disease accounts for more than 13 million DALYs and is responsible for the 0.5% of the global burden of disease. It has been estimated than 7.6 over 1000 people have or will have epilepsy during their lifetime and affects people from all ages, sexes, races or income groups. The people that present the disease usually present a lower standard of living in comparison to healthy individuals due to an increased risk of injury during a seizure and also a higher risk of death for the same cause. Although the great majority of epilepsy cases are treatable and can be controlled, the higher risk of injury and death due to a seizure in lower income countries due to a more difficult access to antiepileptic drugs together with all of these figures convert epilepsy into a worldwide health problem[55].

### 4.1 Epilepsy pathophysiology

Being epilepsy a wide range of syndromes, the mechanisms underlying the disease are also complex. In the brain there is a tight equilibrium between excitatory and inhibitory neurotransmitters and disruption of this balance is essential to understand the cause of the specific epileptic syndrome. In the case of epilepsy, the balance is turned towards a heavier

weight of the excitation, and therefore the treatment of the disease is focused on reverting back the equilibrium by mainly three pathways: increasing inhibitory transmission (championed by GABAergic transmission), decreasing excitatory transmission (championed by glutamatergic transmission), the blockage of voltage-gated channels and decreasing the PH in brain tissue[56].

### 4.1.1 GABAergic transmission

Gamma amino butyric acid (GABA) is the main inhibitory neurotransmitter in the brain and interacts with three different types of GABA receptors, A, B and C. $GABA_A$ receptors are the main passage of chloride ion, which is negatively charged, inside cells, increasing their negative potential and thus hyperpolarising them. $GABA_B$ is a G-protein coupled metabotropic receptor linked to a potassium channel, whose role is to decrease the frequency of neurotransmission release and $GABA_C$ receptors are also chloride channels situated in the retina, and their role is not yet fully understood[57–59].

The action of the GABA system can be enhanced in numerous ways, such as direct binding of the GABA receptors, enhancement of the GABA channel activity by modulation at allosteric sites, reducing the GABA uptake by presynaptic neurons and the increase of GABA concentration, mainly by the inhibition of GABA degradation (catalysed by GABA-aminotransferase). In fact, there are numerous commercialised drugs that act at GABAergic transmission such as phenobarbital, ganaxolone, a wide range of benzodiazepines, vigabatrin or valproic acid.

### 4.1.2 Glutamatergic transmission

Glutamate plays a double role in epilepsy, as excitatory neurotransmitter and also as a precursor of GABA (glutamate is decarboxylated by glutamate decarboxylase to form GABA). Glutamate carries out its physiological function by binding to 2 different kinds of receptors: ionotropic glutamate receptors (iGluRs) and metabotropic glutamate receptors (mGluRs). The former are associated with rapid transmission of action potentials associated with ions and the latter with slow secondary messenger responses[60].

Among iGluRs, three different kinds of receptors can be distinguished, according to agonist molecules that they bind: NMDA receptors (N-methyl-D aspartate), AMPA receptors (α-amino-3-hydroxy-5-methyl-4-isoxazolepropionic acid) and kainite receptors (kainic acid). NMDA and AMPA receptors can be found in post synaptic neurons, while kainite receptors can be found in either in pre and post synaptic neurons[61].

Both glycine and aspartate bind to NMDA receptors, causing an opening of sodium and calcium channels inside the neuron, and its overstimulation causes an overload of calcium ions, generating excitotoxicity, not only associated with epilepsy, but also with neurodegenerative diseases such as AD or PD. In this spite, blocking NMDA receptors is a good strategy for the treatment of epilepsy; some examples of drugs used for this purpose are felbamate or ketamine (non-competitive inhibitor)[61].

AMPA receptors are permeable mainly to sodium and potassium ions and are responsible for fast response due to glutamate release. Inhibition of these channels reduces neuronal excitation and therefore controls seizures. This converts AMPA receptors in good targets for the treatment

of epilepsy and many molecules have been designed to act on them such as talampanel or perampanel[61].

Kainate receptors are also permeable to sodium and potassium ions, having a direct excitatory effect in post synaptic neurons and an indirect excitatory effect in presynaptic neurons by the inhibition of GABA release. Kainate inhibitors such as topiramate have also been designed to reduce sodium and potassium-mediated action potentials and by enhancing the release of GABA[62].

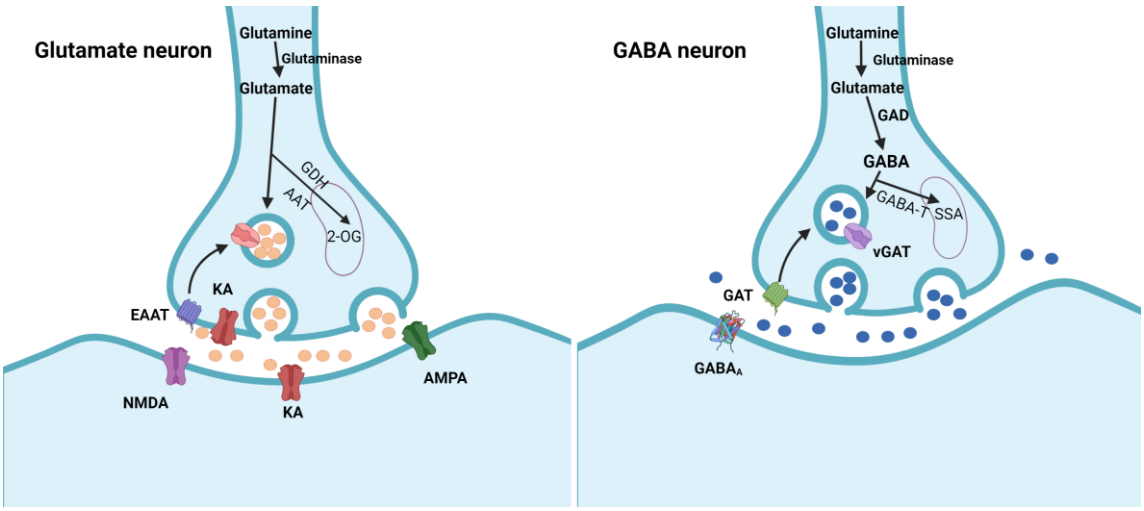


Figure 7. Scheme comparing a glutamate neuron from a GABA neuron.

### 4.1.3 Voltage-gated channels

Ion channels are a diverse family of transmembrane proteins and are activated only by differences in membrane potential, without the binding of endogenous ligands. Depending on the ion channel, different ions flow inside and outside of cells and with this in mind, modulation of the activity of these channels could be an interesting option for the treatment of epilepsy.

Sodium channels mainly transport sodium inside the cells by concentration difference. Sodium has a greater concentration outside than inside neurons, which causes that when an action potential reaches the neuron, sodium enters inside the neuron, causing depolarisation and transmission of the action potential. These channels present three main states: activated (the channel is open by an action potential), closed (the resting and basal conformation) and inactive (after the transmission of the action potential, the channel closes by hyperpolarizarion and requires time to reach closed conformation). With this in mind, many voltage-gated sodium channel blockers have been designed to control seizures such as lamotrigine, zonisamide, rufinamide or carbamazepine[63,64].

Voltage-gated calcium channels are typically starters of action potentials and also mediate neurotransmitter vesicle release among other functions. These channels are widely recognized therapeutic targets and many molecules acting on them have been designed to treat hypertension, pain and other cardiovascular disorders. Having also an important role in epilepsy, many voltage-gated calcium channel blockers have been designed such as clobazam, lamotrigine, rufinamide or levetiracetam[65,66].

Due to the cardiovascular side effects of sodium and calcium-gated channel blockers, voltage-gated potassium channels are emerging as an interesting therapeutic target. These channels are responsible for the repolarisation of neurons after an action potential and for regulating the balance between the outside and the inside membrane potential. Due to its role in regulating action potentials, some molecules have been designed inn order to enhance the function of voltage-gated potassium channels, such as retigabine[67,68].

#### 4.1.4 Brain pH

It is well known that brain pH plays a crucial role in the brain´s excitatory/inhibitory activity and that minor variations can induce paroxysomal responses, being basic media promotors of seizures, while acid media seizure blockers. In this spite carbonic anhydrases (CA), a widely distributed family of metalloenzymes, which catalyse the hydration of carbon dioxide to form the bicarbonate ion, are key actors in the brain´s pH regulation. This has led to the development of CA inhibitors that acidify brain tissue and control seizure activity. Some carbonic anhydrase inhibitors are zonisamide, topiramate and sulthiame, all of them presenting a sulphonamide functional group that displaces an $OH^-$ ligand present in the enzyme and thus, blocking their action[69–72].

(1) Feigin, V. L.; Nichols, E.; Alam, T.; Bannick, M. S.; Beghi, E.; Blake, N.; Culpepper, W. J.; Dorsey, E. R.; Elbaz, A.; Ellenbogen, R. G.; Fisher, J. L.; Fitzmaurice, C.; Giussani, G.; Glennie, L.; James, S. L.; Johnson, C. O.; Kassebaum, N. J.; Logroscino, G.; Marin, B.; Mountjoy-Venning, W. C.; Nguyen, M.; Ofori-Asenso, R.; Patel, A. P.; Piccininni, M.; Roth, G. A.; Steiner, T. J.; Stovner, L. J.; Szoeke, C. E. I.; Theadom, A.; Vollset, S. E.; Wallin, M. T.; Wright, C.; Zunt, J. R.; Abbasi, N.; Abd-Allah, F.; Abdelalim, A.; Abdollahpour, I.; Aboyans, V.; Abraha, H. N.; Acharya, D.; Adamu, A. A.; Adebayo, O. M.; Adeoye, A. M.; Adsuar, J. C.; Afarideh, M.; Agrawal, S.; Ahmadi, A.; Ahmed, M. B.; Aichour, A. N.; Aichour, I.; Aichour, M. T. E.; Akinyemi, R. O.; Akseer, N.; Al-Eyadhy, A.; Al-Shahi Salman, R.; Alahdab, F.; Alene, K. A.; Aljunid, S. M.; Altirkawi, K.; Alvis-Guzman, N.; Anber, N. H.; Antonio, C. A. T.; Arabloo, J.; Aremu, O.; Ärnlöv, J.; Asayesh, H.; Asghar, R. J.; Atalay, H. T.; Awasthi, A.; Ayala Quintanilla, B. P.; Ayuk, T. B.; Badawi, A.; Banach, M.; Banoub, J. A. M.; Barboza, M. A.; Barker-Collo, S. L.; Bärnighausen, T. W.; Baune, B. T.; Bedi, N.; Behzadifar, M.; Behzadifar, M.; Béjot, Y.; Bekele, B. B.; Belachew, A. B.; Bennett, D. A.; Bensenor, I. M.; Berhane, A.; Beuran, M.; Bhattacharyya, K.; Bhutta, Z. A.; Biadgo, B.; Bijani, A.; Bililign, N.; Bin Sayeed, M. S.; Blazes, C. K.; Brayne, C.; Butt, Z. A.; Campos-Nonato, I. R.; Cantu-Brito, C.; Car, M.; Cárdenas, R.; Carrero, J. J.; Carvalho, F.; Castañeda-Orjuela, C. A.; Castro, F.; Catalá-López, F.; Cerin, E.; Chaiah, Y.; Chang, J. C.; Chatziralli, I.; Chiang, P. P. C.; Christensen, H.; Christopher, D. J.; Cooper, C.; Cortesi, P. A.; Costa, V. M.; Criqui, M. H.; Crowe, C. S.; Damasceno, A. A. M.; Daryani, A.; De la Cruz-Góngora, V.; De La Hoz, F. P.; De Leo, D.; Degefa, M. G.; Demoz, G. T.; Deribe, K.; Dharmaratne, S. D.; Diaz, D.; Dinberu, M. T.; Djalalinia, S.; Doku, D. T.; Dubey, M.; Dubljanin, E.; Duken, E. E.; Edvardsson, D.; El-Khatib, Z.; Endres, M.; Endries, A. Y.; Eskandarieh, S.; Esteghamati, A.; Esteghamati, S.; Farhadi, F.; Faro, A.; Farzadfar, F.; Farzaei, M. H.; Fatima, B.; Fereshtehnejad, S. M.; Fernandes, E.; Feyissa, G. T.; Filip, I.; Fischer, F.; Fukumoto, T.; Ganji, M.; Gankpe, F. G.; Garcia-Gordillo, M. A.; Gebre, A. K.; Gebremichael, T. G.; Gelaw, B. K.; Geleijnse, J. M.; Geremew, D.; Gezae, K. E.; Ghasemi-Kasman, M.; Gidey, M. Y.; Gill, P. S.; Gill, T. K.; Gnedovskaya, E. V.; Goulart, A. C.; Grada, A.; Grosso, G.; Guo, Y.; Gupta, R.; Gupta, R.; Haagsma, J. A.; Hagos, T. B.; Haj-Mirzaian,

A.; Haj-Mirzaian, A.; Hamadeh, R. R.; Hamidi, S.; Hankey, G. J.; Hao, Y.; Haro, J. M.; Hassankhani, H.; Hassen, H. Y.; Havmoeller, R.; Hay, S. I.; Hegazy, M. I.; Heidari, B.; Henok, A.; Heydarpour, F.; Hoang, C. L.; Hole, M. K.; Homaie Rad, E.; Hosseini, S. M.; Hu, G.; Igumbor, E. U.; Ilesanmi, O. S.; Irvani, S. S. N.; Islam, S. M. S.; Jakovljevic, M.; Javanbakht, M.; Jha, R. P.; Jobanputra, Y. B.; Jonas, J. B.; Józwiak, J. J.; Jürisson, M.; Kahsay, A.; Kalani, R.; Kalkonde, Y.; Kamil, T. A.; Kanchan, T.; Karami, M.; Karch, A.; Karimi, N.; Kasaeian, A.; Kassa, T. D.; Kassa, Z. Y.; Kaul, A.; Kefale, A. T.; Keiyoro, P. N.; Khader, Y. S.; Khafaie, M. A.; Khalil, I. A.; Khan, E. A.; Khang, Y. H.; Khazaie, H.; Kiadaliri, A. A.; Kiirithio, D. N.; Kim, A. S.; Kim, D.; Kim, Y. E.; Kim, Y. J.; Kisa, A.; Kokubo, Y.; Koyanagi, A.; Krishnamurthi, R. V.; Kuate Defo, B.; Kucuk Bicer, B.; Kumar, M.; Lacey, B.; Lafranconi, A.; Lansingh, V. C.; Latifi, A.; Leshargie, C. T.; Li, S.; Liao, Y.; Linn, S.; Lo, W. D.; Lopez, J. C. F.; Lorkowski, S.; Lotufo, P. A.; Lucas, R. M.; Lunevicius, R.; Mackay, M. T.; Mahotra, N. B.; Majdan, M.; Majdzadeh, R.; Majeed, A.; Malekzadeh, R.; Malta, D. C.; Manafi, N.; Mansournia, M. A.; Mantovani, L. G.; März, W.; Mashamba-Thompson, T. P.; Massenburg, B. B.; Mate, K. K. V.; McAlinden, C.; McGrath, J. J.; Mehta, V.; Meier, T.; Meles, H. G.; Melese, A.; Memiah, P. T. N.; Memish, Z. A.; Mendoza, W.; Mengistu, D. T.; Mengistu, G.; Meretoja, A.; Meretoja, T. J.; Mestrovic, T.; Miazgowski, B.; Miazgowski, T.; Miller, T. R.; Mini, G. K.; Mirrakhimov, E. M.; Moazen, B.; Mohajer, B.; Mohammad Gholi Mezerji, N.; Mohammadi, M.; Mohammadi-Khanaposhtani, M.; Mohammadibakhsh, R.; Mohammadnia-Afrouzi, M.; Mohammed, S.; Mohebi, F.; Mokdad, A. H.; Monasta, L.; Mondello, S.; Moodley, Y.; Moosazadeh, M.; Moradi, G.; Moradi-Lakeh, M.; Moradinazar, M.; Moraga, P.; Moreno Velásquez, I.; Morrison, S. D.; Mousavi, S. M.; Muhammed, O. S.; Muruet, W.; Musa, K. I.; Mustafa, G.; Naderi, M.; Nagel, G.; Naheed, A.; Naik, G.; Najafi, F.; Nangia, V.; Negoi, I.; Negoi, R. I.; Newton, C. R. J.; Ngunjiri, J. W.; Nguyen, C. T.; Nguyen, L. H.; Ningrum, D. N. A.; Nirayo, Y. L.; Nixon, M. R.; Norrving, B.; Noubiap, J. J.; Nourollahpour Shiadeh, M.; Nyasulu, P. S.; Ogbo, F. A.; Oh, I. H.; Olagunju, A. T.; Olagunju, T. O.; Olivares, P. R.; Onwujekwe, O. E.; Oren, E.; Owolabi, M. O.; A, M. P.; Pakpour, A. H.; Pan, W. H.; Panda-Jonas, S.; Pandian, J. D.; Patel, S. K.; Pereira, D. M.; Petzold, M.; Pillay, J. D.; Piradov, M. A.; Polanczyk, G. V.; Polinder, S.; Postma, M. J.; Poulton, R.; Poustchi, H.; Prakash, S.; Prakash, V.; Qorbani, M.; Radfar, A.; Rafay, A.; Rafiei, A.; Rahim, F.; Rahimi-Movaghar, V.; Rahman, M.; Rahman, M. H. U.; Rahman, M. A.; Rajati, F.; Ram, U.; Ranta, A.; Rawaf, D. L.; Rawaf, S.; Reinig, N.; Reis, C.; Renzaho, A. M. N.; Resnikoff, S.; Rezaeian, S.; Rezai, M. S.; Rios González, C. M.; Roberts, N. L. S.; Roever, L.; Ronfani, L.; Roro, E. M.; Roshandel, G.; Rostami, A.; Sabbagh, P.; Sacco, R. L.; Sachdev, P. S.; Saddik, B.; Safari, H.; Safari-Faramani, R.; Safi, S.; Safiri, S.; Sagar, R.; Sahathevan, R.; Sahebkar, A.; Sahraian, M. A.; Salamati, P.; Salehi Zahabi, S.; Salimi, Y.; Samy, A. M.; Sanabria, J.; Santos, I. S.; Santric Milicevic, M. M.; Sarrafzadegan, N.; Sartorius, B.; Sarvi, S.; Sathian, B.; Satpathy, M.; Sawant, A. R.; Sawhney, M.; Schneider, I. J. C.; Schöttker, B.; Schwebel, D. C.; Seedat, S.; Sepanlou, S. G.; Shabaninejad, H.; Shafieesabet, A.; Shaikh, M. A.; Shakir, R. A.; Shams-Beyranvand, M.; Shamsizadeh, M.; Sharif, M.; Sharif-Alhoseini, M.; She, J.; Sheikh, A.; Sheth, K. N.; Shigematsu, M.; Shiri, R.; Shirkoohi, R.; Shiue, I.; Siabani, S.; Siddiqi, T. J.; Sigfusdottir, I. D.; Sigurvinsdottir, R.; Silberberg, D. H.; Silva, J. P.; Silveira, D. G. A.; Singh, J. A.; Sinha, D. N.; Skiadaresi, E.; Smith, M.; Sobaih, B. H.; Sobhani, S.; Soofi, M.; Soyiri, I. N.; Sposato, L. A.; Stein, D. J.; Stein, M. B.; Stokes, M. A.; Sufiyan, M. B.; Sykes, B. L.; Sylaja, P.; Tabarés-Seisdedos, R.; Te Ao, B. J.; Tehrani-Banihashemi, A.; Temsah, M. H.; Temsah, O.; Thakur, J. S.; Thrift, A. G.; Topor-Madry, R.; Tortajada-Girbés, M.; Tovani-Palone, M. R.; Tran, B. X.; Tran, K. B.; Truelsen, T. C.; Tsadik, A. G.; Tudor Car, L.; Ukwaja, K. N.; Ullah, I.; Usman, M. S.; Uthman, O. A.; Valdez, P. R.; Vasankari, T. J.; Vasanthan, R.; Veisani, Y.; Venketasubramanian, N.; Violante, F. S.; Vlassov, V.; Vosoughi, K.; Vu, G. T.; Vujcic, I. S.; Wagnew, F. S.; Waheed, Y.; Wang, Y. P.; Weiderpass, E.; Weiss, J.; Whiteford, H. A.; Wijeratne, T.; Winkler, A. S.; Wiysonge, C. S.; Wolfe, C. D.

A.; Xu, G.; Yadollahpour, A.; Yamada, T.; Yano, Y.; Yaseri, M.; Yatsuya, H.; Yimer, E. M.; Yip, P.; Yisma, E.; Yonemoto, N.; Yousefifard, M.; Yu, C.; Zaidi, Z.; Zaman, S. Bin; Zamani, M.; Zandian, H.; Zare, Z.; Zhang, Y.; Zodpey, S.; Naghavi, M.; Murray, C. J. L.; Vos, T. Global, Regional, and National Burden of Neurological Disorders, 1990–2016: A Systematic Analysis for the Global Burden of Disease Study 2016. *Lancet Neurol.* **2019**, *18* (5), 459–480. https://doi.org/10.1016/S1474-4422(18)30499-X.

(2) Borumandnia, N.; Majd, H. A.; Doosti, H.; Olazadeh, K. The Trend Analysis of Neurological Disorders as Major Causes of Death and Disability According to Human Development, 1990-2019. *Environ. Sci. Pollut. Res.* **2022**, *29* (10), 14348–14354. https://doi.org/10.1007/s11356-021-16604-5.

(3) prince, martin. World Alzheimer Report. **2015**.

(4) Abeysinghe, A. A. D. T.; Deshapriya, R. D. U. S.; Udawatte, C. Alzheimer's Disease; a Review of the Pathophysiological Basis and Therapeutic Interventions. *Life Sci.* **2020**, *256* (April), 117996. https://doi.org/10.1016/j.lfs.2020.117996.

(5) Anwal, L. A Comprehensive Review on Alzheimer'S Disease. *World J. Pharm. Pharm. Sci.* **2021**, *10* (7), 1170. https://doi.org/10.20959/wjpps20217-19427.

(6) Hur, J.-Y. γ-Secretase in Alzheimer's Disease. *Exp. Mol. Med.* **2022**, No. July 2021, 1–14. https://doi.org/10.1038/s12276-022-00754-8.

(7) Luo, J. E.; Li, Y. M. Turning the Tide on Alzheimer's Disease: Modulation of γ-Secretase. *Cell Biosci.* **2022**, *12* (1), 1–12. https://doi.org/10.1186/s13578-021-00738-7.

(8) Belluti, F.; Rampa, A.; Gobbi, S.; Bisi, A. Small-Molecule Inhibitors/Modulators of Amyloid-β Peptide Aggregation and Toxicity for the Treatment of Alzheimer's Disease: A Patent Review (2010-2012). *Expert Opin. Ther. Pat.* **2013**, *23* (5), 581–596. https://doi.org/10.1517/13543776.2013.772983.

(9) Maia, M. A.; Sousa, E. BACE-1 and γ-Secretase as Therapeutic Targets for Alzheimer's Disease. *Pharmaceuticals* **2019**, *12* (1). https://doi.org/10.3390/ph12010041.

(10) Moussa-Pacha, N. M.; Abdin, S. M.; Omar, H. A.; Alniss, H.; Al-Tel, T. H. BACE1 Inhibitors: Current Status and Future Directions in Treating Alzheimer's Disease. *Med. Res. Rev.* **2020**, *40* (1), 339–384. https://doi.org/10.1002/med.21622.

(11) Rafii, M. S. Targeting Tau Protein in Alzheimer's Disease. *Lancet* **2016**, *388* (10062), 2842–2844. https://doi.org/10.1016/S0140-6736(16)32107-9.

(12) Li, B.; Chohan, M. O.; Grundke-Iqbal, I.; Iqbal, K. Disruption of Microtubule Network by Alzheimer Abnormally Hyperphosphorylated Tau. *Acta Neuropathol.* **2007**, *113* (5), 501–511. https://doi.org/10.1007/s00401-007-0207-8.

(13) Wang, J. Z.; Gong, C. X.; Zaidi, T.; Grundke-Iqbal, I.; Iqbal, K. Dephosphorylation of Alzheimer Paired Helical Filaments by Protein Phosphatase-2A and -2B. *J. Biol. Chem.* **1995**, *270* (9), 4854–4860. https://doi.org/10.1074/jbc.270.9.4854.

(14) Oddo, S.; Vasilevko, V.; Caccamo, A.; Kitazawa, M.; Cribbs, D. H.; LaFerla, F. M. Reduction of Soluble Aβ and Tau, but Not Soluble Aβ Alone, Ameliorates Cognitive Decline in Transgenic Mice with Plaques and Tangles. *J. Biol. Chem.* **2006**, *281* (51), 39413–39423. https://doi.org/10.1074/jbc.M608485200.

(15) Ly, P. T. T.; Wu, Y.; Zou, H.; Wang, R.; Zhou, W.; Kinoshita, A.; Zhang, M.; Yang, Y.; Cai, F.; Woodgett, J.; Song, W. Inhibition of GSK3β-Mediated BACE1 Expression Reduces

Alzheimer-Associated Phenotypes. *J. Clin. Invest.* **2013**, *123* (1), 224–235. https://doi.org/10.1172/JCI64516.

(16) Engel, T.; Goñi-Oliver, P.; Lucas, J. J.; Avila, J.; Hernández, F. Chronic Lithium Administration to FTDP-17 Tau and GSK-3β Overexpressing Mice Prevents Tau Hyperphosphorylation and Neurofibrillary Tangle Formation, but Pre-Formed Neurofibrillary Tangles Do Not Revert. *J. Neurochem.* **2006**, *99* (6), 1445–1455. https://doi.org/10.1111/j.1471-4159.2006.04139.x.

(17) Crowe, A.; Huang, W.; Ballatore, C.; Johnson, R. L.; Hogan, A. M. L.; Huang, R.; Wichterman, J.; McCoy, J.; Huryn, D.; Auld, D. S.; Smith, A. B.; Inglese, J.; Trojanowski, J. Q.; Austin, C. P.; Brunden, K. R.; Lee, V. M. Y. Identification of Aminothienopyridazine Inhibitors of Tau Assembly by Quantitative High-Throughput Screening. *Biochemistry* **2009**, *48* (32), 7732–7745. https://doi.org/10.1021/bi9006435.

(18) Berger, Z.; Ravikumar, B.; Menzies, F. M.; Oroz, L. G.; Underwood, B. R.; Pangalos, M. N.; Schmitt, I.; Wullner, U.; Evert, B. O.; O'Kane, C. J.; Rubinsztein, D. C. Rapamycin Alleviates Toxicity of Different Aggregate-Prone Proteins. *Hum. Mol. Genet.* **2006**, *15* (3), 433–442. https://doi.org/10.1093/hmg/ddi458.

(19) Nunomura, A.; Perry, G.; Aliev, G.; Hirai, K.; Takeda, A.; Balraj, E. K.; Jones, P. K.; Ghanbari, H.; Wataya, T.; Shimohama, S.; Chiba, S.; Atwood, C. S.; Petersen, R. B.; Smith, M. A. Oxidative Damage Is the Earliest Event in Alzheimer Disease. *J. Neuropathol. Exp. Neurol.* **2001**, *60* (8), 759–767. https://doi.org/10.1093/jnen/60.8.759.

(20) Huang, W. J.; Zhang, X.; Chen, W. W. Role of Oxidative Stress in Alzheimer's Disease (Review). *Biomed. Reports* **2016**, *4* (5), 519–522. https://doi.org/10.3892/br.2016.630.

(21) Huang, X.; Atwood, C. S.; Hartshorn, M. A.; Multhaup, G.; Goldstein, L. E.; Scarpa, R. C.; Cuajungco, M. P.; Gray, D. N.; Lim, J.; Moir, R. D.; Tanzi, R. E.; Bush, A. I. The Aβ Peptide of Alzheimer's Disease Directly Produces Hydrogen Peroxide through Metal Ion Reduction. *Biochemistry* **1999**, *38* (24), 7609–7616. https://doi.org/10.1021/bi990438f.

(22) Butterfield, D. A.; Drake, J.; Pocernich, C.; Castegna, A. Evidence of Oxidative Damage in Alzheimer's Disease Brain: Central Role for Amyloid β-Peptide. *Trends Mol. Med.* **2001**, *7* (12), 548–554. https://doi.org/10.1016/S1471-4914(01)02173-6.

(23) Castellani, R. J.; Moreira, P. I.; Perry, G.; Zhu, X. The Role of Iron as a Mediator of Oxidative Stress in Alzheimer Disease. *BioFactors* **2012**, *38* (2), 133–138. https://doi.org/10.1002/biof.1010.

(24) M. Valko, H. Morris, M. T. D. C. Metals, Toxicity and Oxidative Stress. *Curr. Med. Chem.* **2005**, *12*, 1161–1208.

(25) Pietta, P. G. Flavonoids as Antioxidants. *J. Nat. Prod.* **2000**, *63* (7), 1035–1042. https://doi.org/10.1021/np9904509.

(26) Bahn, G.; Jo, D. G. Therapeutic Approaches to Alzheimer's Disease Through Modulation of NRF2. *NeuroMolecular Med.* **2019**, *21* (1), 1–11. https://doi.org/10.1007/s12017-018-08523-5.

(27) Sims, N. R.; Bowen, D. M.; Allen, S. J.; Smith, C. C. T.; Neary, D.; Thomas, D. J.; Davison, A. N. Presynaptic Cholinergic Dysfunction in Patients with Dementia. *J. Neurochem.* **1983**, *40* (2), 503–509. https://doi.org/10.1111/j.1471-4159.1983.tb11311.x.

(28) Bajda, M.; Więckowska, A.; Hebda, M.; Guzior, N.; Sotriffer, C. A.; Malawska, B.

Structure-Based Search for New Inhibitors of Cholinesterases. *Int. J. Mol. Sci.* **2013**, *14* (3), 5608–5632. https://doi.org/10.3390/ijms14035608.

(29) Snyder, P. J.; Ph, D.; Giacobini, E.; Ph, D.; Foix, L. A. P. C.; Hayden, K.; System, C.; Group, W.; Hampel, H.; Mesulam, M. M.; Cuello, C.; Khachaturian, A. S.; Farlow, M. R.; Snyder, P. J.; Khachaturian, Z. S.; Hampel, H. Alzheimer's & Dementia : The Journal of the Alzheimer's Association Revisiting the Cholinergic Hypothesis in Alzheimer's Disease : Emerging Evidence from Translational and Clinical Research. *J. Prev. Alzheimer's Dis.* **2020**, *6* (1), 2–15.

(30) Inestrosa, N. C.; Alvarez, A.; Pérez, C. A.; Moreno, R. D.; Vicente, M.; Linker, C.; Casanueva, O. I.; Soto, C.; Garrido, J. Acetylcholinesterase Accelerates Assembly of Amyloid-β-Peptides into Alzheimer's Fibrils: Possible Role of the Peripheral Site of the Enzyme. *Neuron* **1996**, *16* (4), 881–891. https://doi.org/10.1016/S0896-6273(00)80108-7.

(31) Jevtic, S.; Sengar, A. S.; Salter, M. W.; McLaurin, J. A. The Role of the Immune System in Alzheimer Disease: Etiology and Treatment. *Ageing Res. Rev.* **2017**, *40* (September), 84–94. https://doi.org/10.1016/j.arr.2017.08.005.

(32) Richard, K. L.; Filali, M.; Préfontaine, P.; Rivest, S. Toll-like Receptor 2 Acts as a Natural Innate Immune Receptor to Clear Amyloid B1-42 and Delay the Cognitive Decline in a Mouse Model of Alzheimer's Disease. *J. Neurosci.* **2008**, *28* (22), 5784–5793. https://doi.org/10.1523/JNEUROSCI.1146-08.2008.

(33) Walter, S.; Letiembre, M.; Liu, Y.; Heine, H.; Penke, B.; Hao, W.; Bode, B.; Manietta, N.; Walter, J.; Schulz-Schüffer, W.; Faßbender, K. Role of the Toll-like Receptor 4 in Neuroinflammation in Alzheimer's Disease. *Cell. Physiol. Biochem.* **2007**, *20* (6), 947–956. https://doi.org/10.1159/000110455.

(34) Song, M.; Jin, J. J.; Lim, J. E.; Kou, J.; Pattanayak, A.; Rehman, J. A.; Kim, H. D.; Tahara, K.; Lalonde, R.; Fukuchi, K. I. TLR4 Mutation Reduces Microglial Activation, Increases Aβ Deposits and Exacerbates Cognitive Deficits in a Mouse Model of Alzheimer's Disease. *J. Neuroinflammation* **2011**, *8*, 1–14. https://doi.org/10.1186/1742-2094-8-92.

(35) Tuppo, E. E.; Arias, H. R. The Role of Inflammation in Alzheimer's Disease. *Int. J. Biochem. Cell Biol.* **2005**, *37* (2), 289–305. https://doi.org/10.1016/j.biocel.2004.07.009.

(36) Chen, Y.; Colonna, M. Two-Faced Behavior of Microglia in Alzheimer's Disease. *Nat. Neurosci.* **2022**, *25* (1), 3–4. https://doi.org/10.1038/s41593-021-00963-w.

(37) Hoozemans, J. J. M.; Veerhuis, R.; Janssen, I.; Van Elk, E. J.; Rozemuller, A. J. M.; Eikelenboom, P. The Role of Cyclo-Oxygenase 1 and 2 Activity in Prostaglandin E2 Secretion by Cultured Human Adult Microglia: Implications for Alzheimer's Disease. *Brain Res.* **2002**, *951* (2), 218–226. https://doi.org/10.1016/S0006-8993(02)03164-5.

(38) Hoozemans, J.; Rozemuller, J.; van Haastert, E.; Veerhuis, R.; Eikelenboom, P. Cyclooxygenase-1 and -2 in the Different Stages of Alzheimers Disease Pathology. *Curr. Pharm. Des.* **2008**, *14* (14), 1419–1427. https://doi.org/10.2174/138161208784480171.

(39) York, G. K. The History of James Parkinson and His Disease. *J. Neurol. Sci.* **2017**, *381* (2017), 35. https://doi.org/10.1016/j.jns.2017.08.147.

(40) Ou, Z.; Pan, J.; Tang, S.; Duan, D.; Yu, D.; Nong, H.; Wang, Z. Global Trends in the Incidence, Prevalence, and Years Lived With Disability of Parkinson's Disease in 204 Countries/Territories From 1990 to 2019. *Front. Public Heal.* **2021**, *9* (December).

https://doi.org/10.3389/fpubh.2021.776847.

(41) Tysnes, O. B.; Storstein, A. Epidemiology of Parkinson's Disease. *J. Neural Transm.* **2017**, *124* (8), 901–905. https://doi.org/10.1007/s00702-017-1686-y.

(42) Simon, D. K.; Tanner, C. M.; Brundin, P. Parkinson Disease Epidemiology, Pathology, Genetics, and Pathophysiology. *Clin. Geriatr. Med.* **2020**, *36* (1), 1–12. https://doi.org/10.1016/j.cger.2019.08.002.

(43) Mullin, S.; Schapira, A. α-Synuclein and Mitochondrial Dysfunction in Parkinson's Disease. *Mol. Neurobiol.* **2013**, *47* (2), 587–597. https://doi.org/10.1007/s12035-013-8394-x.

(44) Breydo, L.; Wu, J. W.; Uversky, V. N. α-Synuclein Misfolding and Parkinson's Disease. *Biochim. Biophys. Acta - Mol. Basis Dis.* **2012**, *1822* (2), 261–285. https://doi.org/10.1016/j.bbadis.2011.10.002.

(45) Dehay, B.; Bourdenx, M.; Gorry, P.; Przedborski, S.; Vila, M.; Hunot, S.; Singleton, A.; Olanow, C. W.; Merchant, K. M.; Bezard, E.; Petsko, G. A.; Meissner, W. G. Targeting α-Synuclein for Treatment of Parkinson's Disease: Mechanistic and Therapeutic Considerations. *Lancet Neurol.* **2015**, *14* (8), 855–866. https://doi.org/10.1016/S1474-4422(15)00006-X.

(46) Raza, C.; Anjum, R.; Shakeel, N. ul A. Parkinson's Disease: Mechanisms, Translational Models and Management Strategies. *Life Sci.* **2019**, *226* (January), 77–90. https://doi.org/10.1016/j.lfs.2019.03.057.

(47) Bose, A.; Beal, M. F. Mitochondrial Dysfunction in Parkinson's Disease. *J. Neurochem.* **2016**, *139*, 216–231. https://doi.org/10.1111/jnc.13731.

(48) Surmeier, D. J.; Schumacker, P. T.; Guzman, J. D.; Ilijic, E.; Yang, B.; Zampese, E. Calcium and Parkinson's Disease. *Biochem. Biophys. Res. Commun.* **2017**, *483* (4), 1013–1019. https://doi.org/10.1016/j.bbrc.2016.08.168.

(49) Hurley, M. J.; Brandon, B.; Gentleman, S. M.; Dexter, D. T. Parkinson's Disease Is Associated with Altered Expression of Ca V1 Channels and Calcium-Binding Proteins. *Brain* **2013**, *136* (7), 2077–2097. https://doi.org/10.1093/brain/awt134.

(50) Swart, T.; Hurley, M. J. Calcium Channel Antagonists as Disease-Modifying Therapy for Parkinson's Disease: Therapeutic Rationale and Current Status. *CNS Drugs* **2016**, *30* (12), 1127–1135. https://doi.org/10.1007/s40263-016-0393-9.

(51) Cuadrado, A.; Pajares, M.; Rojo I., A.; Manda, G.; Boscá, L. Inflammation in Parkinson ' s Disease : Mechanisms and Therapeutic Implications. *Cells* **2020**, 1–32.

(52) Gelders, G.; Baekelandt, V.; Van der Perren, A. Linking Neuroinflammation and Neurodegeneration in Parkinson's Disease. *J. Immunol. Res.* **2018**, *2018*. https://doi.org/10.1155/2018/4784268.

(53) Poly, T. N.; Islam, M. M. (Rubel); Yang, H. C.; Li, Y. C. J. Non-Steroidal Anti-Inflammatory Drugs and Risk of Parkinson's Disease in the Elderly Population: A Meta-Analysis. *Eur. J. Clin. Pharmacol.* **2019**, *75* (1), 99–108. https://doi.org/10.1007/s00228-018-2561-y.

(54) Vote, C. E. Report By the Numbers. *Development* **2016**, *1* (May), 1–41.

(55) Organization, W. H. A Public Health Imperative. **2019**, *1*.

(56) Sills, G. J.; Rogawski, M. A. Mechanisms of Action of Currently Used Antiseizure Drugs.

*Neuropharmacology* **2020**, *168* (September 2019), 107966. https://doi.org/10.1016/j.neuropharm.2020.107966.

(57) Kaila, K.; Ruusuvuori, E.; Seja, P.; Voipio, J.; Puskarjov, M. GABA Actions and Ionic Plasticity in Epilepsy. *Curr. Opin. Neurobiol.* **2014**, *26* (Figure 1), 34–41. https://doi.org/10.1016/j.conb.2013.11.004.

(58) Sperk, G.; Furtinger, S.; Schwarzer, C.; Pirker, S. GABA and Its Receptors in Epilepsy. *Adv. Exp. Med. Biol.* **2004**, *548*, 92–103. https://doi.org/10.1007/978-1-4757-6376-8_7.

(59) Sarlo, G. L.; Holton, K. F. Brain Concentrations of Glutamate and GABA in Human Epilepsy: A Review. *Seizure* **2021**, *91* (January), 213–227. https://doi.org/10.1016/j.seizure.2021.06.028.

(60) Celli, R.; Santolini, I.; Van Luijtelaar, G.; Ngomba, R. T.; Bruno, V.; Nicoletti, F. Targeting Metabotropic Glutamate Receptors in the Treatment of Epilepsy: Rationale and Current Status. *Expert Opin. Ther. Targets* **2019**, *0* (0), 1. https://doi.org/10.1080/14728222.2019.1586885.

(61) Hanada, T. Ionotropic Glutamate Receptors in Epilepsy: A Review Focusing on Ampa and Nmda Receptors. *Biomolecules* **2020**, *10* (3). https://doi.org/10.3390/biom10030464.

(62) Vincent, P.; Mulle, C. Kainate Receptors in Epilepsy and Excitotoxicity. *Neuroscience* **2009**, *158* (1), 309–323. https://doi.org/10.1016/j.neuroscience.2008.02.066.

(63) Mantegazza, M.; Curia, G.; Biagini, G.; Ragsdale, D. S.; Avoli, M. Voltage-Gated Sodium Channels as Therapeutic Targets in Epilepsy and Other Neurological Disorders. *Lancet Neurol.* **2010**, *9* (4), 413–424. https://doi.org/10.1016/S1474-4422(10)70059-4.

(64) Brodie, M. J. Sodium Channel Blockers in the Treatment of Epilepsy. *CNS Drugs* **2017**, *31* (7), 527–534. https://doi.org/10.1007/s40263-017-0441-0.

(65) Zamponi, G. W. Targeting Voltage-Gated Calcium Channels in Neurological and Psychiatric Diseases. *Nat. Rev. Drug Discov.* **2016**, *15* (1), 19–34. https://doi.org/10.1038/nrd.2015.5.

(66) Simms, B. A.; Zamponi, G. W. Neuronal Voltage-Gated Calcium Channels: Structure, Function, and Dysfunction. *Neuron* **2014**, *82* (1), 24–45. https://doi.org/10.1016/j.neuron.2014.03.016.

(67) D'Adamo, M. C.; Catacuzzeno, L.; di Giovanni, G.; Franciolini, F.; Pessia, M. K+ Channelepsy: Progress in the Neurobiology of Potassium Channels and Epilepsy. *Front. Cell. Neurosci.* **2013**, *7* (SEP), 1–21. https://doi.org/10.3389/fncel.2013.00134.

(68) Köhling, R.; Wolfart, J. Potassium Channels in Epilepsy. *Cold Spring Harb. Perspect. Med.* **2016**, *6* (5), 24. https://doi.org/10.1101/cshperspect.a022871.

(69) Supuran, C. T. Carbonic Anhydrase Inhibitors. *Bioorganic Med. Chem. Lett.* **2010**, *20* (12), 3467–3474. https://doi.org/10.1016/j.bmcl.2010.05.009.

(70) Villalba, M. L.; Palestro, P.; Ceruso, M.; Gonzalez Funes, J. L.; Talevi, A.; Bruno Blanch, L.; Supuran, C. T.; Gavernet, L. Sulfamide Derivatives with Selective Carbonic Anhydrase VII Inhibitory Action. *Bioorganic Med. Chem.* **2016**, *24* (4), 894–901. https://doi.org/10.1016/j.bmc.2016.01.012.

(71) Ciccone, L.; Cerri, C.; Nencetti, S.; Orlandini, E. Carbonic Anhydrase Inhibitors and Epilepsy: State of the Art and Future Perspectives. *Molecules* **2021**, *26* (21).

https://doi.org/10.3390/molecules26216380.

(72) Ruusuvuori, E.; Kaila, K. Carbonic Anhydrases and Brain PH in the Control of Neuronal Excitability. *Subcell. Biochem.* **2014**, *75*, 271–1290. https://doi.org/10.1007/978-94-007-7359-2_14.

# Chapter 2. Objectives

**Objectives**

1. To develop a series of multitarget ligands against Alzheimer´s disease (AD). The multifactorial nature of AD renders the multitarget strategy a useful approach to its treatment. To this end, we selected a flavonoid core, as these polyphenolic natural structures present multiple pharmacological activities that are potentially useful for the treatment of Alzheimer´s disease, such as antioxidant, acetylcholinesterase and butyrylcholinesterase inhibition, Aβ aggregation inhibition and metal chelation. We decided to tether to these molecules to different molecules which can be also potentially useful for the treatment of AD, such as tacrine or donepezil, two well-known AChE / BuChE inhibitors and different tryptamines such as melatonin or serotonin, which have been reported to possess multiple beneficial pharmacological activities against neurodegenerative diseases. These hybrids have been tested against several pharmacological targets to verify their potential for the development of multitarget drug ligands.

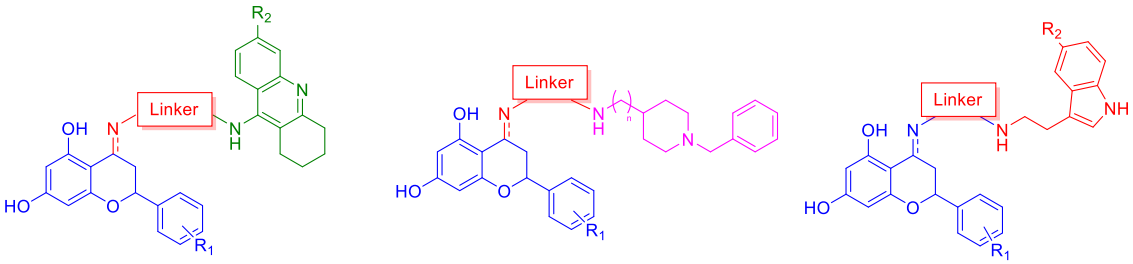


2. To develop a multicomponent reaction leading to derivatives of the dihydroanthranilate scaffold tethered to a triphenyl phosphonium moiety to grant these molecules a positive charge that allows their targeting to the mitochondrial matrix, as the latter possesses an overall negative charge. Mitochondrial oxidative stress is a hallmark of many neurodegenerative diseases such as AD or Parkinson´s disease (PD). These dihydroanthranilates should accumulate inside the mitochondrial matrix and scavenge ROS or RNS, while being dehydrogenated to yield the corresponding aromatic derivatives, which are fluorescent.

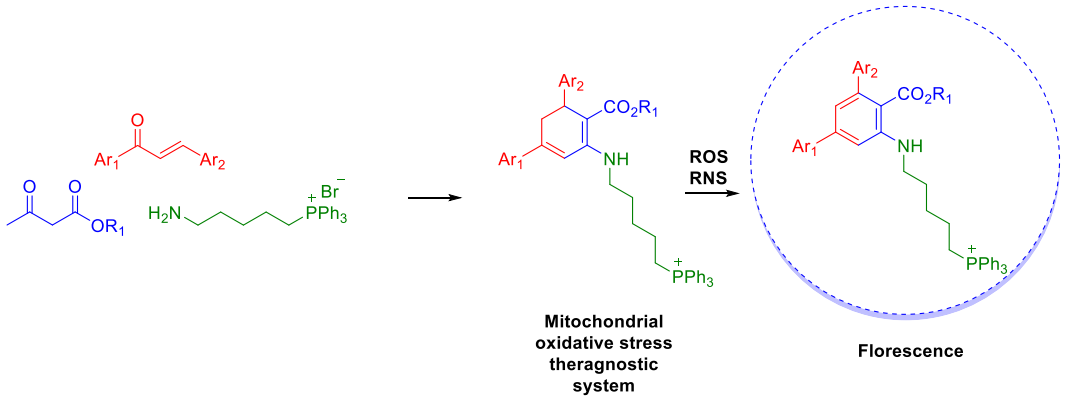


3. The derivatization of dihydroanthranilates to other structures with potential use in neurological disorders, in particular diarylacridones and *m*-terphenyl amines. The latter compounds possess COX-1 selective inhibition capacity and can therefore be useful in the treatment of neurological disorders such as AD or PD, which also show a heavy component of neuroinflammation. In order to develop multitarget drug ligands for AD, the binding of tacrine to m-terphenylamines via suitable linkers was also planned.

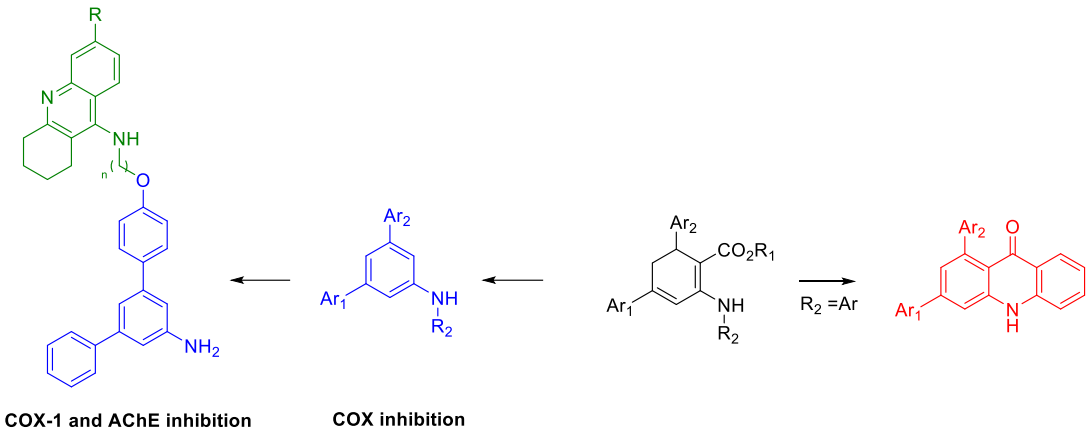


These objectives can be viewed as connected by the fact that both the flavanones and the m-terphenyl derivatives are originated from chalcones.

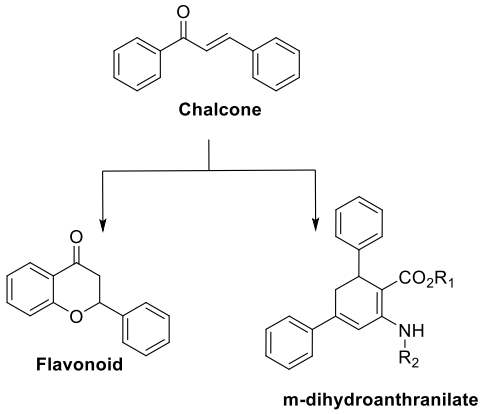


4. Voltage-gated sodium channel (VGSC) blockers, besides their use in epilepsy, have neuroprotective properties against ischemic damage. In this context, one of the objectives of this thesis is the development of a simple, sustainable synthetic route to rufinamide, a VGSC blocker in therapeutic use against the Lennox-Gasteaut syndrome, that is amenable to the future synthesis of analogues. The chosen approach aims at a one-pot, solid-state protocol based on the use of mechanical energy derived from ball milling. The final step requires the prior development of mechanochemical conditions for the synthesis of primary amides from esters.

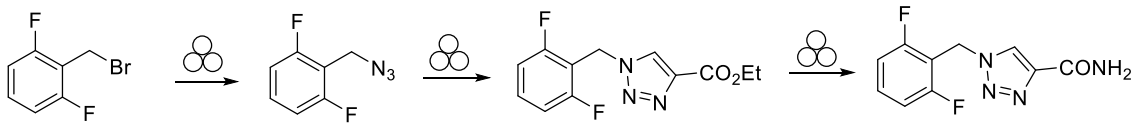


5. The chemical synthesis of the chemical ligand of a SNIFIT (SNAP-tag based indicator with an intramolecular tether) for pantothenate kinase (PanK). PanK is the key regulatory enzyme for the synthesis of coenzyme A, a key biomolecule for different biochemical processes such as the Krebs cycle or palmitic acid biosynthesis. Additionally, PanK has been recently found to be important in many pathologies, such as tuberculosis, type II diabetes or neurodegenerative processes. Therefore, a better insight of the activity of PanK in real time under different

situations could be useful to acquire a greater knowledge of the role this enzyme in these disorders

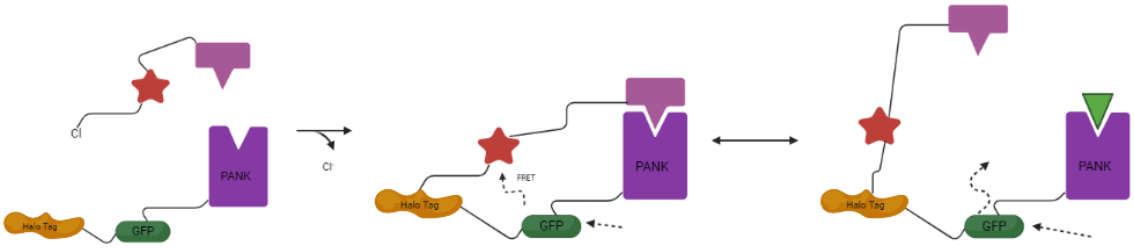

# Chapter 3. Design, synthesis and study of a family of flavonoid-based multitarget drug ligands against Alzheimer's disease

# Design, synthesis and study of a family of flavonoid-based multitarget drug ligands against Alzheimer's disease

## 1. Introduction

### 1.1 Flavonoids, a readily available source of biological active compounds

Natural products have been an important source of chemically diverse active molecules with a wide range of biological activities that make them interesting therapeutical options for a wide range of diseases. In particular, in recent decades many studies describe natural compounds as a promising source of therapeutic molecules for the treatment of neurodegenerative diseases.[1,2,3,4]

Among natural products, flavonoids have generated interest due to their plethora of pharmacological activities, rendering them interesting options to develop new therapeutic agents. Flavonoids are secondary metabolites present in many plants, and are usually classified into flavanones, dihydroflavonols, flavan-3-ols, flavones, flavan-3-ols, anthocyanidins, isoflavones, neoflavones and chalcones (figure 1), with over 8000 compounds known. They all share a polyphenolic structure, and they perform different function as antioxidants, antimicrobials or as light screening agents.[5,6].

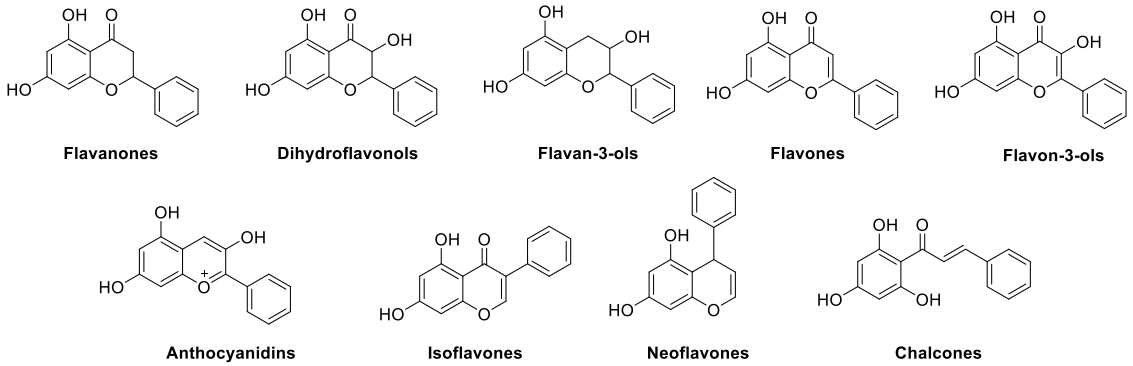


Figure 1. Chemical structure of some relevant flavonoid families to MTDLs Design

The antioxidant ability of flavonoids to reduce free radical formation and to scavenge free radicals depends on the generation of an aryloxy radical that can react with a second radical, generating an electrophilic cyclohexadienone species which still have the potential to react with nucleophiles species with potential to generate cellular toxicity (scheme 2)[7] but also to activate cellular antioxidant mechanisms such as the translocation of Nrf-2 to the nucleus. In fact, flavonoids such as naringenin[8] and galangin[9] have reported to activate it and mitigate oxidative stress.

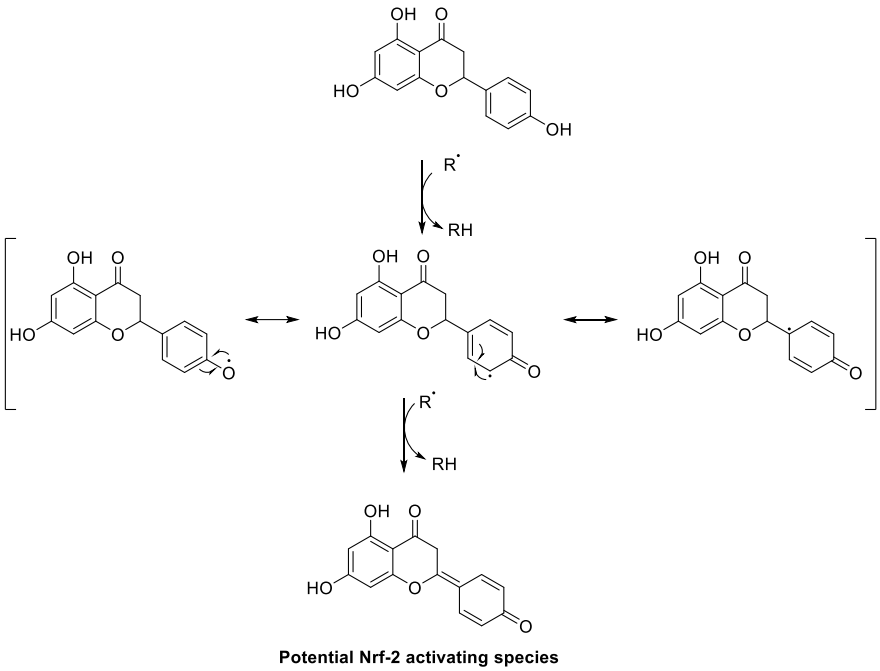


Scheme 2. Free radical scavenging and stabilization by a flavonoid core.

The antioxidant activity of flavonoids is not exclusively driven by their redox potential, and there are other different mechanisms that support their antioxidant capabilities, such as: the induction of the Nrf-2 transcription factor[8], which activates the cellular response to oxidative stress, metal chelation, [10] which prevents the Fenton reaction, and the capacity to mitigate oxidative stress induced by nitric oxide[11].

In addition to their antioxidant capacity, flavonoids are privileged structures in drug discovery, due to their wide range of pharmacological targets, including several of special relevance for the treatment of neurological disorders. For example, the flavanone naringenin has proved to inhibit acetylcholinesterase (AChE) and butyrylcholinesterase (BuChE) [12], to have estrogenic receptor affinity[13], to inhibit the cyclooxygenase and lipooxigenase pathways[13] and β amyloid (Aβ) aggregation [13]. Hesperitin has demonstrated to inhibit the NF-κB pathway[14], which results in anti-inflammatory activity and has proven to possesses the capacity to inhibit the aggregation of $A\beta_{25-35}$. Quercetin can also inhibit the aggregation of Aβ and beta-secretase BACE-1, which is responsible for the cleavage of Amyloid precursor protein (APP)[15]. Luteolin is another flavonoid that has generated interest in neurological disease therapies, due to its ability to inhibit Glycogen Synthase Kinase-3 GSK-3α, which decreases BACE1-mediated cleavage of APP and Aβ expression by decreasing gene transcription and production of the BACE1[16,17]. Finally, galangin has been one of the latest compounds of the flavonoid family that have attracted attention for the treatment of neurodegenerative diseases. Galangin has been reported to inhibit BuChE at micromolar concentrations, and to decrease B-secretase, Aβ 42 and p-tau levels [18,19] (Figure 2). These biological activities of flavonoids have a pleiotropic effect of neurodegenerative diseases such as Alzheimer´s disease or Parkinson´s disease, and therefore they stand out as interesting scaffolds for the design of Multitarget drug ligands[20].

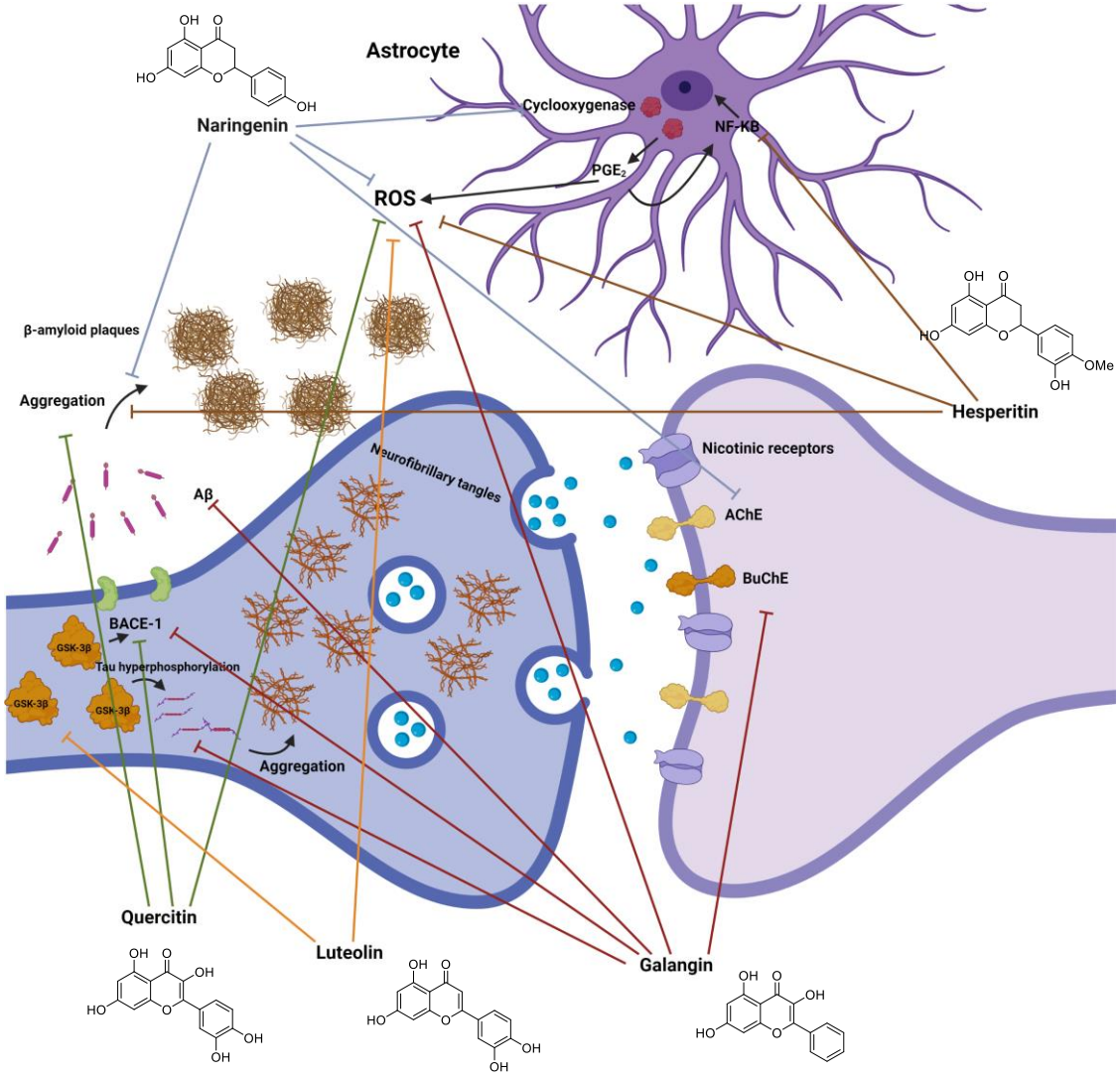


Figure 2. Representative example of flavonoids of interest against several targets in AD

## 1.2 Multitarget drug ligands containing a flavonoid scaffold

The multifactorial nature of neurodegenerative diseases is the key cause of the absence of effective treatments since a single molecule with a specific therapeutic target and effect is insufficient to treat the disease. Multitarget drug ligands (MTDLs) are emerging as an interesting option for the treatment of neurodegenerative processes. MTDLs are molecular entities that designed to act in various pharmacological targets by combining several pharmacophores into a single molecule. They potentially present some advantages over conventional single-targeted molecules such as single dose administration; a simplified pharmacokinetic and pharmacodynamic profile; decrease in the possibility of drug-drug interactions; simpler clinical trial and drug approval processes and therefore a potential cost reductions for national health systems; also, sometimes they show a synergistic effect between their pharmacophores, even at low doses [21].

For the development of MTDLs there are currently three main approaches (figure 4). The "**fusion"** strategy consists in partially overlap the pharmacophore of targeted molecules to generate a single molecular entity. The "**merging"** strategy implies a higher degree of pharmacophore overlapping, identifying the "tolerant region" for each pharmacological target, and fusing the common frameworks present in the ligands. This approach has the considerable

advantage of a reduced molecular weight, implying a greater adherence to Lipinski´s rules. The last approach is the "**linking"** strategy which typically attaches two different pharmacophores with linkers of different nature and size. In some cases, the linker itself can act as a pharmacophore and bind to the desired pharmacological target. Linkers in this type of hybrid molecules can either be cleavable or non-cleavable, the former being when the linker is cleaved under a biological environment and pharmacophores act independently. This last approach would convert these ligands in prodrugs, as they would require cellular metabolism to be released and act as drugs separately instead as if they were a singular entity. The goal of the linking strategy is a greater retention of the pharmacodynamic profile of the original pharmacophores, while its disadvantage is the high molecular weight of the new entity, which difficult its distribution and its entry in cells[22].

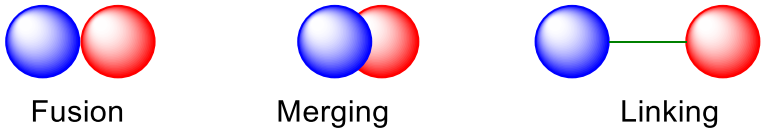


Figure 4. Main approaches to design MTDLs

The high functionalisation of flavonoids provides synthetic handles allowing to link a variety of fragments. This, combined with their versatile biological activity, has caused flavonoids to become a popular scaffold on which to design MTDLs[20]. A commentary of the most relevant ones is given below.

Singh et al designed and synthesised a new family of MTDLs based on the chromen-4-one moiety, which were designed to target acetylcholinesterase (AChE), advanced glycation end products (AGEs) and oxidative stress. AGEs are the products from Maillard´s reaction between carbohydrates and proteins. The glycation of Aβ has been associated to a greater aggregation and also, the interaction of AGEs with their receptors (RAGEs) provoke a greater production of ROS, which could contribute to the development of AD[23]. Thus, a benzene ring containing methoxy groups was attached to the chromene template to evaluate the impact of these groups on radical scavenging. Moreover, a tertiary amino group was assembled, as it had proved to be critical in good AChE inhibition results in previous studies. The amines studied were linked to the chromene structure via alkylation of hydroxyl group at position C7 of the heterocyclic system, combining different lengths of the alkyl side chain (scheme 3). The alkylation of **I** with the corresponding dibromoalkanes yielded compounds **II**, which were transformed to **III** via nucleophilic substitution using commercially available secondary amines and $K_2CO_3$ as a base (scheme 3). Most of these compounds inhibited AChE in the nanomolar range and bound dually to the catalytic active site (CAS) and to the peripheric anionic site (PAS), and therefore they could potentially inhibit Aβ fibril formation. Additionally, these compounds present notable free radical scavenging capacities, converting these hybrids in interesting multi-target agents for the treatment of AD [24]. The SAR analysis carried out for the synthesised compounds revealed that AChE inhibition is dependent on the $R_1$ substituents of the benzene ring, and the best results are observed for cyclic amines and for 2 and 3-carbon side chain lengths. In addition, the compounds containing various methoxy groups on the side ring proved to have a good inhibitory effect on AGE formation. The compound chosen as a hit for future optimization efforts is shown in scheme 3.

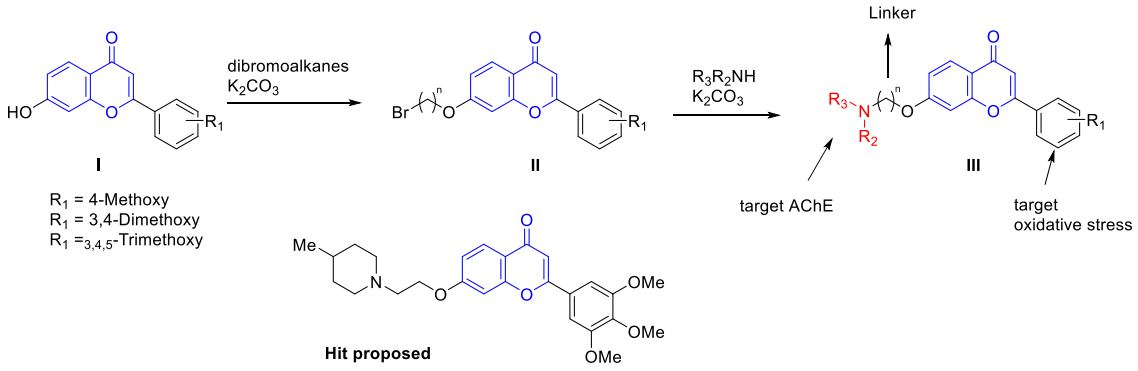


Scheme 3. Examples of chromene hybrid structures developed by Singh et al.

In work carried out by Rodríguez-Franco and co-workers[25], a family of structurally varied tacrine-4-oxo-4H-chromene hybrid compounds were synthesised and evaluated against different targets for Alzheimer´s disease. The synthesis of these compounds started by tethering different diamine chains to 1,2,3,4-tetrahydroacridine, or to the corresponding 6-chloro or 6,8-dichloro derivatives, providing intermediates **I**. Unsubstituted 4-oxo-4H-chromene-2-carboxylic acid **III** was commercially available and the corresponding methoxy derivatives **II** were synthesised from the suitable methoxyphenol, by Michael addition to dimethyl acetylenedicarboxylate to give the intermediate **I**, which was hydrolysed under acid conditions and then cycled by an intramolecular Friedel-Crafts acylation, to obtain the 4-oxochromene-2-carboxylic acids **III**. The coupling of both fragments was carried with the activating agent BOP (benzotriazol-1-yloxytris(dimethylamino)phosphonium hexafluorophosphate) to obtain compounds **IV**, and finally the methoxy groups were demethylated to give the corresponding phenols **V** (scheme 4).

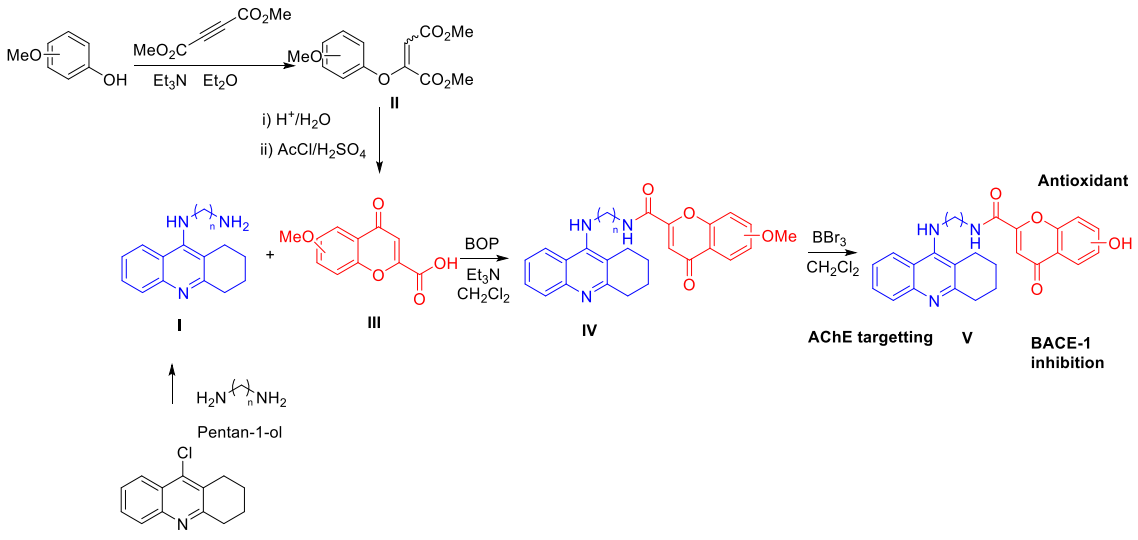


Scheme 4. Synthesis of chromene-derived MTDLs

The compounds synthesised showed potent AChE and BuChE inhibitory activities in the micromolar and nanomolar range. SAR studies determined that chlorine at C6 improved the inhibitory activity of the hybrid compounds, while an additional chlorine at C8 decreased it. The antioxidant activity of synthetised compounds was *assessed by* the kinetic ORAC *test* using fluorescein (ORAC-FL). Thus, all compounds tested showed moderate antioxidant activities,

inferior to the reference apigenin. The blood brain barrier (BBB) permeability was tested using the PAMPA method, which predicted that most compounds would successfully reach brain tissue by passive diffusion. Finally, a selection of all compounds tested was screened for BACE-1 inhibition, showing moderate to good inhibitory activities. According to these preliminary results, compound **X**, having the most balanced profile, is an interesting hit for MTDL development (figure 6).

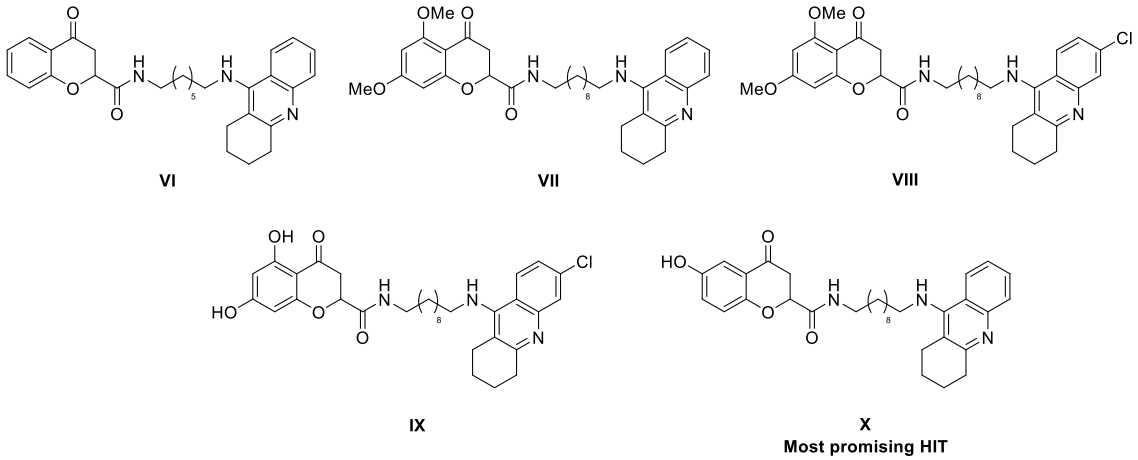


Figure 6. Selection of most promising chromene-derived MTDLs

In additional work, the same group designed a series of donepezil-flavonoid hybrids. Thus, they selected the flavonoid scaffold contained the 4-oxo-4H-chromene fragment, common to all flavones and the benzyl piperidine moiety, which is considered the pharmacophore framework of donepezil. Compounds **I** were obtained using the same synthetic approach described above, and replacement of phenols by aniline allowed the preparation of the 4-oxoquinoline-2-carboxylate frameworks **II**. Then, the N-benzyl piperidine moiety was attached via peptide coupling conditions using either CDI (carbonyl diimidazole) or BOP (Benzotriazole-1-yl-oxy-tris-(dimethylamino)-phosphonium hexafluorophosphate) for **I** and $Al(CH_3)_3$ for **II,** to obtain the corresponding compounds **III** and **IV**. Finally, the compounds bearing methoxy groups were demethylated using $BBr_3$, to yield compounds **V** and **VI,** amplifying this way the compound library (Scheme 5).

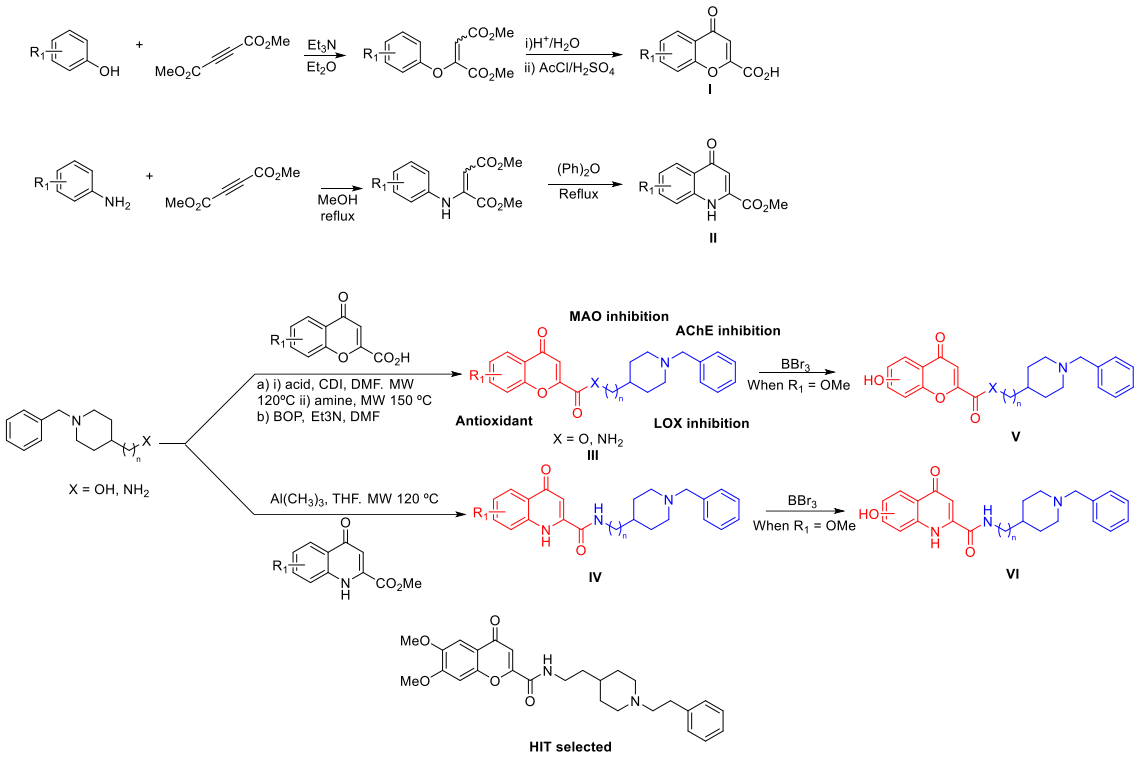


Scheme 5. Synthetic scheme of the chromone/quinolone – donepezil hybrids designed by Rodríguez-Franco and co-workers.

The results of biological studies showed that hybrid compounds containing a chromene scaffold were more potent human AChE inhibitors than quinolones, being the majority of chromene compounds in the nanomolar range, while quinolones were in the upper micromolar one. The synthesized hybrid compounds were BBB permeable, except the ones than contain a phenol group, according to PAMPA predictions. Complementary biological studies of compounds that had shown most promise in the preliminary studies showed lipooxigenase (LOX), MAO-A and MAO-B inhibition, blockade of sigma-1 and -2 receptors (important in the maintenance of physiological antioxidant proteins and mitochondrial function) protection against mitochondrial oxidative damage. Among all hybrids designed, N-(2-(1-benzylpiperidin-4-yl)ethyl)-6,7-dimethoxy-4-oxo-4H-chromene-2-carboxamide presented the best-balanced profile in all biological assays and was chosen as hit for further development[26].

Cruz and co-workers synthesised a family of xanthone and flavone derivatives with dual acetylcholinesterase and antioxidant activity. The synthetic pathway involved an initial Grover Shah and Shah (GSS) reaction using phloroglucinol and 2,6 dihydroxy benzoic acid in the presence of Eaton´s reagent ($P_2O_5$-$MeSO_3H$) to generate the xanthone framework. Then, the dimethylaminomethyl group required for was introduced via a Mannich reaction in order to obtain AChE inhibitory activity and metal chelating ability to improve the antioxidant capacity in both flavonoid and xanthone frameworks. Flavanone derivative (**II**) showed the best biological result of both families of compounds, showing moderate activity as radical scavenger (similar to the parent compound bacailein), while xanthone derivatives (**I**) did not present significant activity as radical scavengers. Concerning metal chelating capacities, a number of xanthone derivatives exhibited Fe and Cu chelating properties, which was associated to the presence of the dimethylamine group, while for flavone compounds the chelating capacity was related to the existence of catechol (1,2-dihydroxybenzene) functional group. The AChE inhibition assays showed the best results for bacailein derivative containing the dimethyl amino group, while

xanthone derivatives showed a low inhibition capacity. Thus the authors of the study found that bacailein derivatives containing the dimethyl amino group exhibited improved properties compared to xanthone derivatives to be developed as MTDLs. [27] (figure 6).

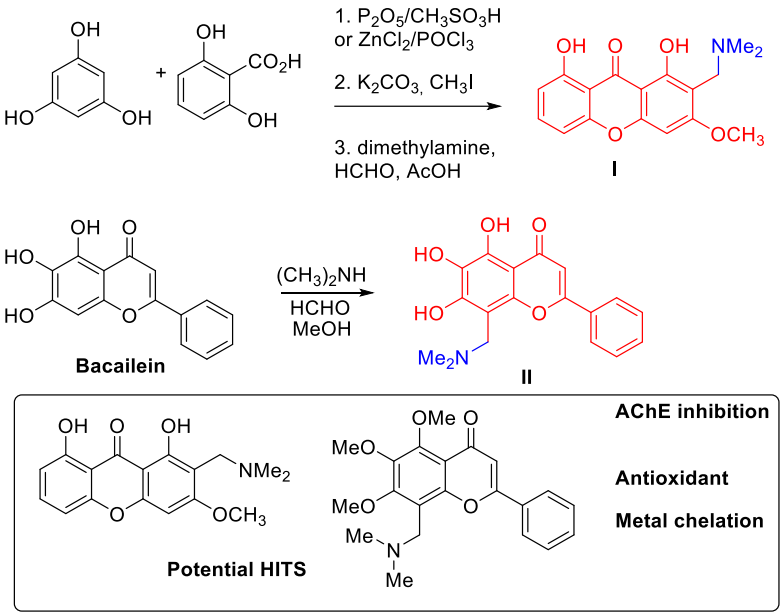


Figure 6. Synthetic scheme followed and selected HITs by Cruz and co-workers.

Finally, Li and collaborators developed a series of homoisoflavonoid (3-benzylidene-4-chromanone)-based hybrid compounds containing tertiary amine moieties as MTDLs for Alzheimer´s disease. The compounds were synthesised by aldol condensation of aldehyde **I** and chromanone **II**, which were obtained from hydroxybenzaldehyde and 3,4 dimethoxyphenol respectively. These compounds presented excellent AChE and MAO-B inhibitory activities, and other relevant characteristics for the design of MTDLs against neurodegenerative disorders such as inhibition of Aβ aggregation, antioxidant capacity and metal chelation were observed. Additionally, these compounds showed the capacity of crossing the blood brain barrier (BBB). Thus, these studies identified two MTDL hits, which presented the best multitarget balance activities and pharmacokinetic profile.[28] (figure 7).

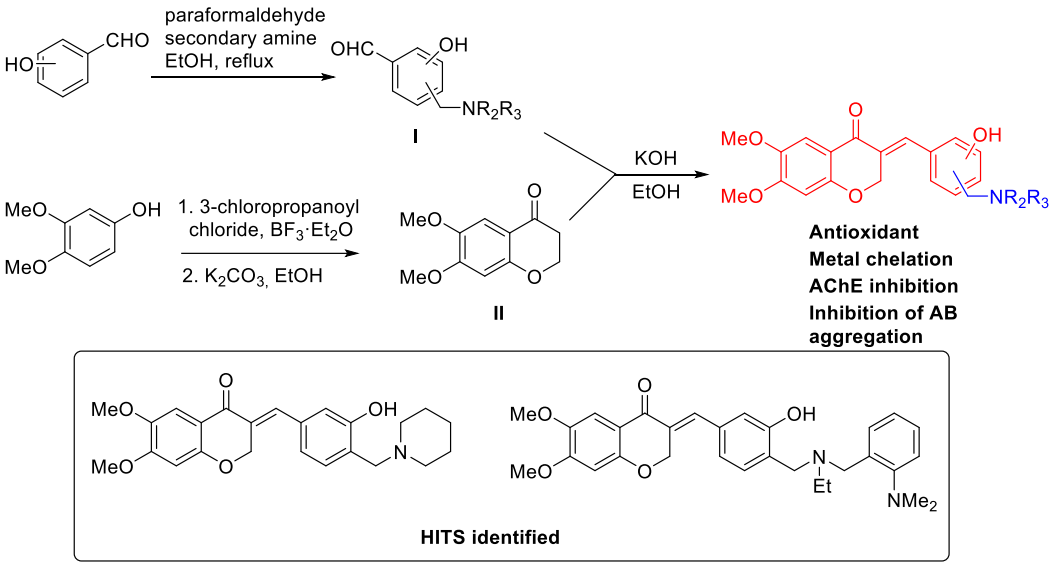


Figure 7. Synthetic scheme followed and hits selected by Li and co-workers.

## 1.3 Cholinergic hypothesis in Alzheimer´s disease and Acetylcholinesterase inhibitors for multi-target drug ligands development

Alzheimer´s disease multifactorial ethology is widely accepted by the scientific community. The first scientific evidence in Alzheimer's disease revealed, the loss of cholinergic transmission, which stands out as one of the most important hallmarks of the disease.[29] The consequent dysfunction of the brain´s cholinergic system contributes heavily to the cognitive decline and behavioural abnormalities observed in AD patients. This evidence led to the "cholinergic hypothesis of AD" and the search for cholinesterase inhibitors[30].

The currently approved therapy for Alzheimer's disease consists of four small molecules (donepezil, rivastigmine, galantamine and memantine)[21] (Figure 8) and a monoclonal antibody (aducanumab),[31] which are unable to halt the progress of the disease and return the brain to its original functional state.[32]. Three of these treatments for AD, namely donepezil, rivastigmine and galantamine, plus tacrine, which was withdrawn from the market due to hepatic toxicity, are based on increasing the levels of acetylcholine in the brain, which is expected to provide a symptomatic improvement in patients. These drugs are used to treat moderate to severe cases of AD, acting as inhibitors of the cholinesterase enzymes. Cholinesterases (ChE) are members of the family of serine hydrolases and catalyse the hydrolysis and degradation of choline esters. There are two forms of ChE, namely acetylcholinesterase (AChE) and butyrylcholinesterase (BuChE). The main function of AChE is to hydrolyse and inactivate acetylcholine (ACh), the main neurotransmitter of the central nervous system, while BuChE acts on esters with a large acyl group, such as butyrylcholine or benzoylcholine. This function is performed by the enzyme with the aid of three residues (His440, Ser200 and Glu327 in AChE, and His438, Ser198, Glu325 in BuChE)[33] in the catalytic active site (CAS) situated in the gorge of both enzymes.

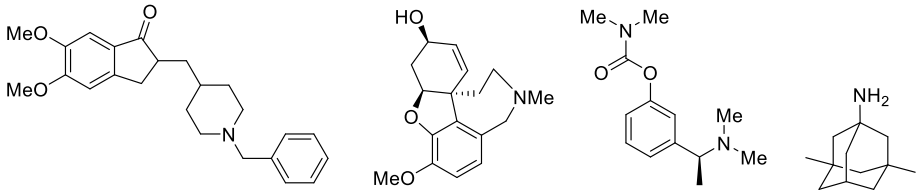


Figure 8. small molecules approved for the treatment of Alzheimer´s disease.

Recent studies indicated that the long-term use of these AChE inhibitors drugs has further benefits on the disease, since acetylcholinesterase and butyrylcholinesterase contribute to a further extent to the progress of brain atrophy. Inhibition of AChE causes a decrease in the levels of Aβ, due to the role of peripheric anionic site (PAS) to catalyse the formation of Aβ fibrils. Therefore, the inhibition of AChE and BuChE, could be beneficial in a double sense: it could increase the levels of acetylcholine, which produce a symptomatic improvement and alternatively, decrease the toxicity associated to Aβ[34, 35].

Thus, reported multitarget ligands mainly provide cholinesterase inhibition together with additional biological activities to avoid the side effects of classical AChEIs and/or to simultaneously control other pathological pathways of AD.

### 1.3.1 Tacrine-based multitarget ligands

The number of hybrid compounds, containing tacrine, is wide and several combinations of pharmacophore compounds have been designed, tackling a wide range of targets. Tacrine was the first cholinesterase inhibitor drug approved against AD, which was withdrawn from the drug market, due to its potential to cause hepatic toxicity[34]. However, this toxicity seems to be associated to an oxidized metabolite whose formation can be avoided by substitution of the tacrine benzene ring. Thus, because of its high potency and synthetic accessibility, tacrine has been extensively used in the design of multi-target compounds[36]. In this way, early hybrid molecules based on the tacrine heterocyclic framework were the tacrine homodimers developed by Pang et al. which targeted the CAS and the PAS sites in a dual fashion[37]. Later studies conducted by the Bolognesi group have shown that the incorporation of planar aromatic linkers provides increased activity as well as inhibition of amyloid aggregation[38]. Additional examples can be found in studies carried out by Sun et al, who synthesised a series of MTDLs based on tacrine and ferulic acid, which showed cholinesterase and Aβ aggregation inhibition, and a neuroprotective effect against oxidative stress generated by hydrogen peroxide[39]. Spilovska et al. described the synthesis of a family of hybrid compounds containing 6-chlorotacrine and an analogue of scutellarin, linked by carbon chains, which demonstrated good AChE and BChE inhibition. However, the scutellarin fragment did not provide the expected antioxidant capacity to the hybrid compounds[40]. As mentioned above (Scheme 4), Rodríguez-Franco et al. designed a family of hybrid compounds based on tacrine and 4-oxo-4H-chromene which target β-secretase 1 (BACE-1) and AChE inhibitory and antioxidant capacities[41]. Chen et al. designed hybrid structures based on tacrine and silibinin, with the purpose of decreasing tacrine toxicity, since the flavonoid silibinin is a known hepatoprotective substance. The compounds synthesised achieved this objective, inhibiting ChE and with low toxicity levels and they proved to possess neuroprotective effects against oxidative stress[42]. Li et al. described a multifunctional family of tacrine-flavonoid compounds, which exhibited cholinergic activity, β-

amyloid level reduction and metal chelating properties. Computational studies revealed that these compounds simultaneously bind to the CAS and the PAS regions of AChE[43]. Sun et al developed a series of hybrid compounds containing homoisoflavonoids in order to achieve MAO inhibition, together with tacrine and a carbon chain linker, which exhibited potent ChE and MAO-B inhibition, as well as good blood-brain barrier permeability[44]. Liao an co-workers reported a good inhibition of AChE and Aβ aggregation, together with a neuroprotective effect against oxidative stress, for a number of multifunctional compounds containing 6-chlorotacrine and 5,6,7-trimethoxyflavone structural fragments[45] (figure 9).

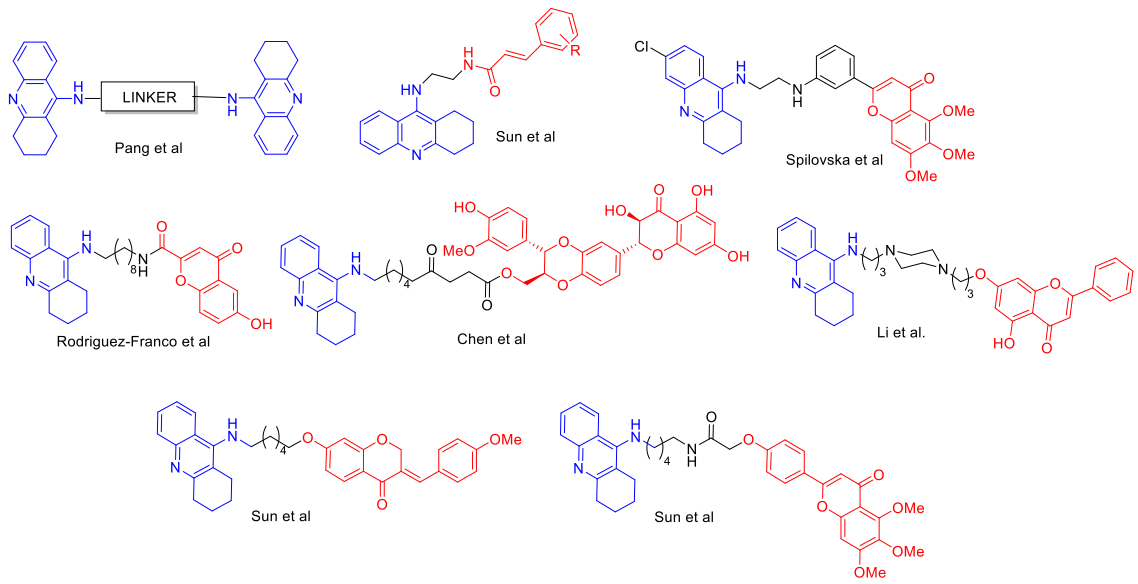


Figure 9. Chemical structure of MTDLs based on tacrine of relevance to this work. The tacrine moiety is shown in blue, the linker in black and the second pharmacophore in red.

## 1.4 Tryptamines in neurodegenerative diseases

Receptors modulated by melatonin and serotonin are implicated in several physiological pathways, such as the regulation of sleep and seasonal cycles, and also have a role in the immune system and regulation of antioxidant species in the brain. Melatonin (N-(2-(5-methoxy-1H-indol-3-yl)ethyl)acetamide) is a hormone synthesised in the pineal gland that controls circadian rhythm and other physiological activities such as regulation of the immune function, blood pressure homeostasis, free radical scavenging, and antioxidant capacity. Especially important for AD are the two latter, due to the consistent relationship between oxidative stress and the development of AD[46].

Concerning its free radical scavenging capacity, melatonin supresses lipid peroxidation, counteracts Fenton reaction-mediated oxidative stress and directly scavenge harmful ROS and RNS such as $^{\cdot}OH$, or $^{\cdot}NO_2$[46]. It also enhances the antioxidant power of various endogenous antioxidant molecules, such as α-tocopherol or ascorbic acid[47]. Indirectly, melatonin can also downregulate the expression of COX-2, thus reducing oxidative damage caused by the immune system[48]. Moreover, melatonin is capable of inducing the powerful Nrf-2 cellular antioxidant system[48], operating this way as an antioxidant molecule directly and indirectly. Besides its antioxidant capabilities, melatonin has other pleiotropic therapeutic effects in AD, because it can inhibit the formation of amyloid fibrils from peptides $A\beta_{1-40}$ and $A\beta_{1-42}$[49]. Additionally, melatonin can attenuate the hyperphosphorylation of Tau, stopping the formation of

neurofibrillary tangles[50]. These features make melatonin an excellent scaffold to develop new molecules for the therapeutic treatment of AD.

Serotonin, or 5-hydroxy tryptamine (5-HT), is a neurotransmitter that plays an important role in depression and other mood related disorders[51]. Serotonin binds to a large family of different 5HT receptors and there is increasing evidence that their modulation can be important for the development and treatment of AD[52]. A study showed that the administration of selective serotonin reuptake inhibitors reduced the production of Aβ proteins and the toxicity associated with them[53]. It has also been demonstrated that activation of $5HT_4$ receptors slows down amyloid pathology and brain inflammation[54]. These features convert serotonin in an interesting scaffold for the development of multitarget drugs for the treatment of AD.

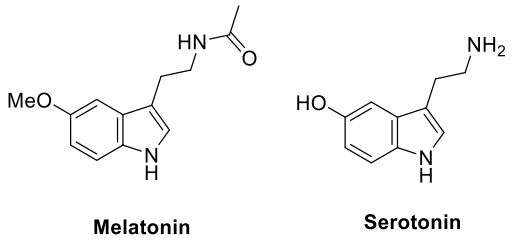


Figure 10. Chemical structures of melatonin and serotonin.

### 1.4.1 Melatonin-based hybrids

The number of multifunctional compounds, that combine melatonin together to other pharmacophores against neurodegenerative diseases is wide. Here we will discuss a few examples, which we consider of relevance to this thesis.

Rodrúguez-Franco et al. reported the design of hybrid compounds containing melatonin and a tertiary amine fragment derived from AP2238, a well-known dual binding site acetylcholinesterase inhibitor. The synthesis of these compounds started with a nucleophilic substitution reaction between the amine group of **I** and 4-(bromomethyl)-benzonitrile **II** to yield intermediate **III**. Then, the cyano group was hydrolyzed under basic conditions to give compound **IV**, which was coupled with different commercially available tryptamines to yield a family of tryptamine N-dibenzylamine hybrid compounds **V**.

Biological assays revealed potent ChE inhibition, through interaction of the hybrids with the residues in PAS region of AChE. PAMPA assays also revealed that all hybrids would be able to successfully permeate BBB. Antioxidant capacity was tested by ORAC assay, and it revealed that all compounds are good peroxyl radical scavengers and compounds containing a methoxy group at C6 or C5 exhibited the best results, especially the latter, which can be attributed to a radical stabilization role. Additionally, all compounds were neuroprotective and compounds A, B and C (Figure 11) were able to stimulate neurogenesis.[55]

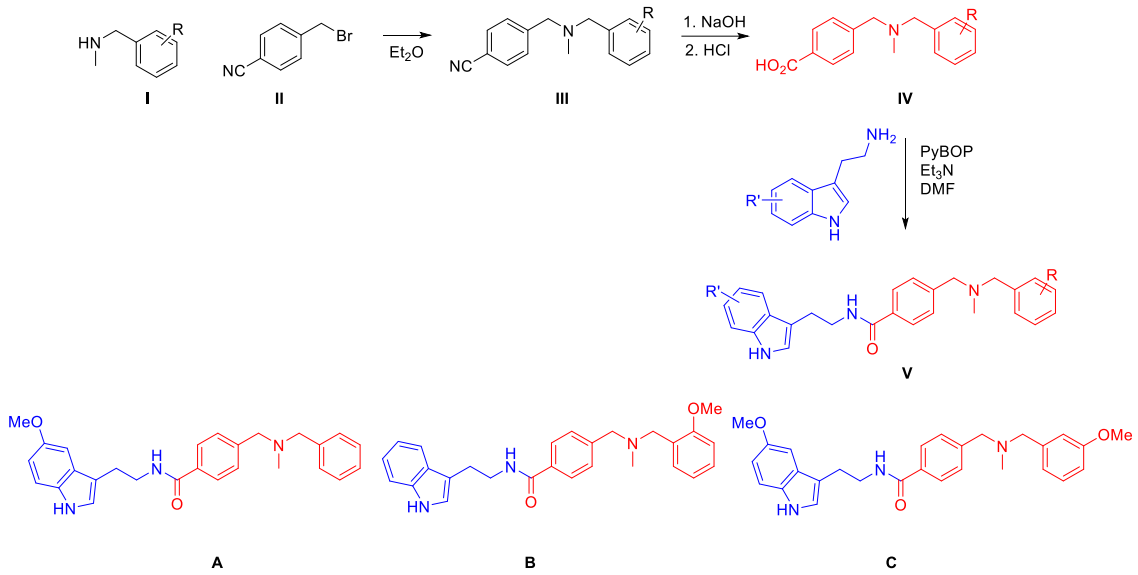


Scheme 6. Synthetic route followed by Rodríguez Franco to synthesise a family of melatonin-derived hybrids.

Chojnacki et al. reported the design of multifunctional compounds, formed from curcumin and melatonin as essential pharmacophores. The synthesis started from ethyl 4-chloro-3-oxobutanoate that was converted via a nucleophilic substitution into the ylide **I**, which was then tethered to 5-methoxytriptamine by reaction with the ester group to produce intermediate **II**. This compound was converted into **III** by a Wittig reaction with substituted benzaldehydes. In order to test the role of the Michael acceptor fragment, the series of compounds **III** was reduced to corresponding saturated compound **IV**. The neuroprotective capacity of these compounds was tested in M-65 cells, using a cellular model for toxicity caused by Aβ and oxidative stress. The results showed that the hydroxyl position is essential for neuroprotection, while the conjugated double bond and methoxy group in the heterocyclic did not influence on the neuroprotective capacities. Furthermore, compounds **V** and **VI** showed a dose-dependent ability to inhibit Aβ oligomer aggregation and **VI** also showed significant antioxidant capacity, while also halting the intracellular formation of Aβ oligomers. However, the PAMPA assay of these compounds predicted some difficulty to cross BBB, probably due to the hydroxy groups present in their structure. The penetration in brain tissue was tested *in vivo* model which revealed that compound **VI** was able to successfully cross BBB. All these features convert compounds **V** and **VI** into potential hits for the development of MTDLs against AD.[56]

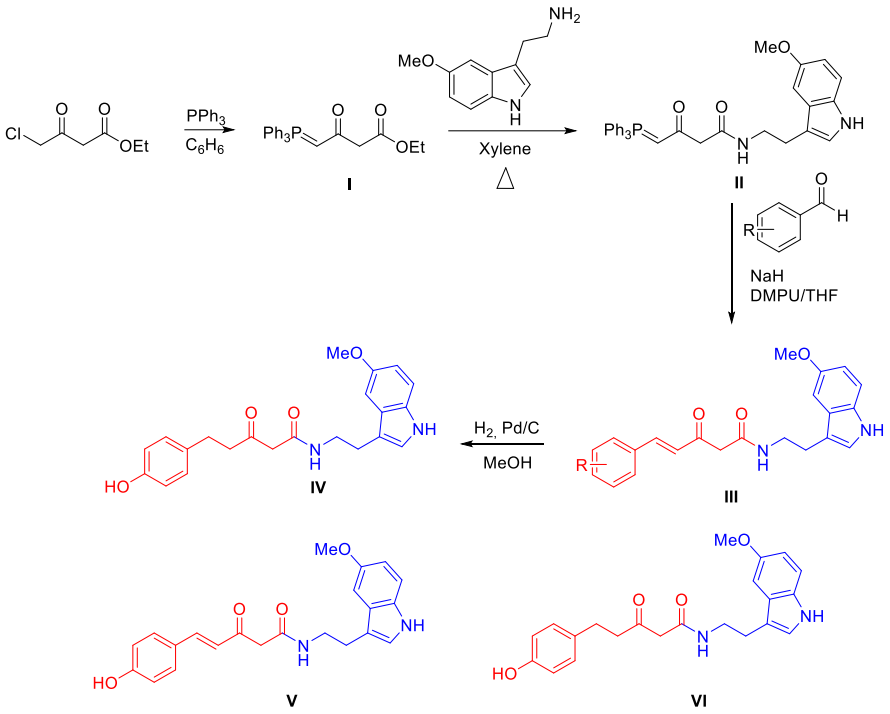

Scheme 7. Synthetic scheme followed by Chojnacki and co-workers to produce melatonin/curcumin hybrids.

Jiang et al. described a new series of MTDLs based on the alkaloid berberine with melatonin. Their synthesis started with the demethylation of one of the methoxy groups of berberine under thermal and pressure conditions to provide intermediate **I**. Alternatively, tryptamines and their 5-methoxy and 5-methyl analogues reacted with 3-bromopropyl chloride to provide compound **II**. Finally, the nucleophilic substitution of **II** with **I** yielded hybrid compounds **III**. Biological studies showed a moderate AChE inhibitory capacity for tryptamine-berberine hybrids, although they exhibited excellent free radical scavenging capacity in an ORAC assay. Finally, these compounds also exhibited notable capacity to inhibit Aβ aggregation, higher than that of the parent compounds berberine and melatonin. [57]

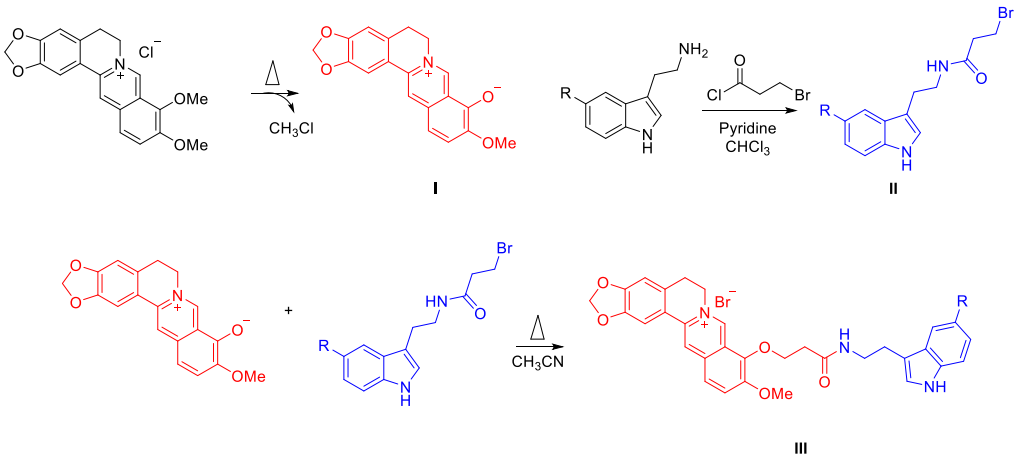

Scheme 8. Synthetic route followed by Jiang and collaborators to synthesize berberine-tryptamine hybrids.

## 2.0 Objectives

As part of our research into new therapeutic entities to treat Alzheimer's disease, one of the aims of this work was to design and synthesise a new family of MTDLs that target several factors involved in the development of the disease, such as amyloid and tau aggregation, cholinesterase inhibition or antioxidant protection. Thus, we selected the well-known flavonoid pharmacophore, which has been studied previously by several authors, based on the use of different attachment positions, as previously reported in this section. Thus, Rodríguez Franco used the C2 position of the chromene framework and Li and co-authors the position C3, while Cruz and Singh employed the fused benzene ring of the heterocyclic system to attach the linker. In this work, we decided to explore the carbonyl group of the flavonoid framework to attach other pharmacophores and develop new MTDLs for AD (figure 1).

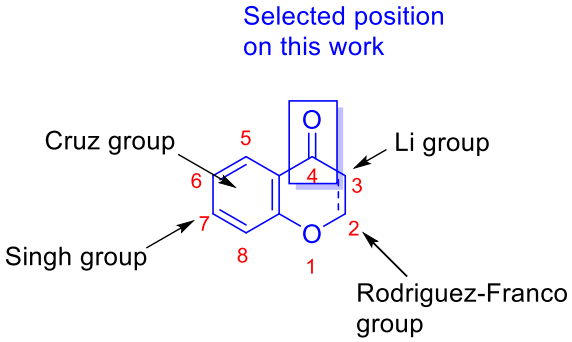


Figure 1. Positions used for flavonoids in previous works and in this work.

Although limited studies have been carried out in order to fully reveal the mechanism by which many flavonoids inhibit the aggregation of AB amyloid, there are evidences that the presence of 3',4'-dihydroxy groups of the B-ring and their H-bonding to the amide groups of the peptide plays a crucial role and leads to the formation of adducts with Aβ-42 through specific binding to the lysine residues Lys16 and Lys28[58]. Additionally, it has been reported that polyphenolic compounds such as myricetin and morin, are more efficient to destabilise the β-sheet structures of the peptide due to additional hydrogen-bond interactions with carbonyl groups, besides normally being more potent antioxidants. Consequently, we decided that the phenolic groups should be free in the flavonoid-based multitarget structures, and we studied the attachment to the carbonyl carbon of the heterocyclic skeleton.

Thus, we designed **flavonoids-tacrine hybrids I**, which contain the flavonoid system selected (naringenin and hesperetin), conserving their phenolic groups, and the tacrine core. In this way, we expected to retain the Aβ aggregation inhibition effect and the antioxidant capacity of flavonoids, as well as the AChE inhibitory capacity. Additionally, the size and class of linkers may play a key role in the design of bivalent AChE inhibitors that bind to both CAS and PAS of AChE since the linker has also been documented to decrease the hepatotoxicity associated to tacrine metabolites[59]. In a similar fashion, **flavonoid-donepezil hybrids II** were designed by linking naringenin and hesperetin to the N-amino-benzyl piperidine moiety of donepezil, which is considered its pharmacophore. These hybrids are also expected to be inhibitors of AChE and BuChE, as well as to retain the Aβ aggregation inhibition and antioxidant capacities of the flavonoid frameworks. Finally, we also devised a family of **flavonoid-tryptamine hybrids III** with the same purpose of evaluating them as potential MTDLs. The multiple pharmacological activities of melatonin or serotonin combined with the previously cited activities of flavonoids

should provide a boosted antioxidant effect, together with increased neuroprotection against different neurotoxic agents (figure 2).

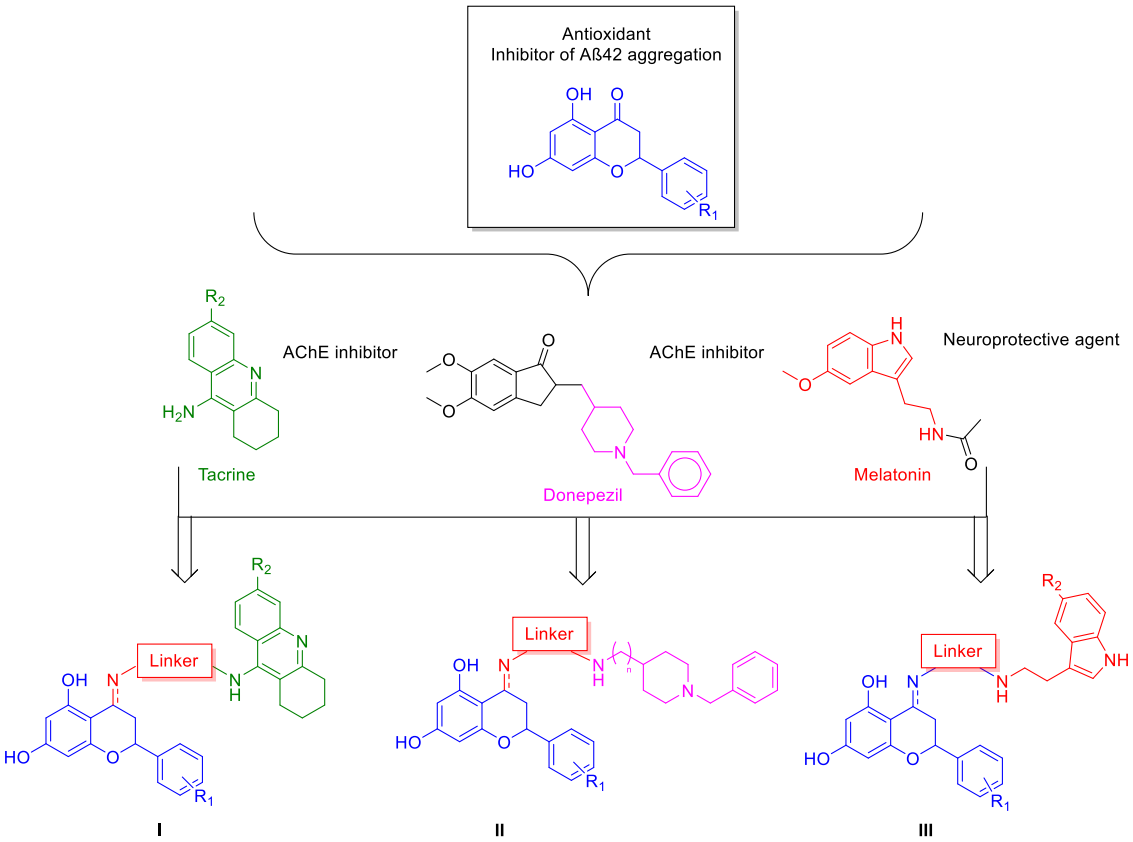


Figure 2. Structures of the MTDLs designed.

## 3.0 Results

## 3.1 Synthesis

### 3.1.1 Synthesis of flavonoid-tacrine hybrids

We planned a synthetic route starting from anthranilic acid derivatives, which would be treated with in the presence of phosphorus oxychloride to yield the chloro derivatives **1.1**. From these compounds, we planned the use of diamine linkers that would yield compounds **1.2**, containing a terminal primary amine residue. Finally, the flavanone-tacrine hybrids would be obtained by a reductive amination reaction of compounds **1.2** with the chosen flavanone (scheme 1).

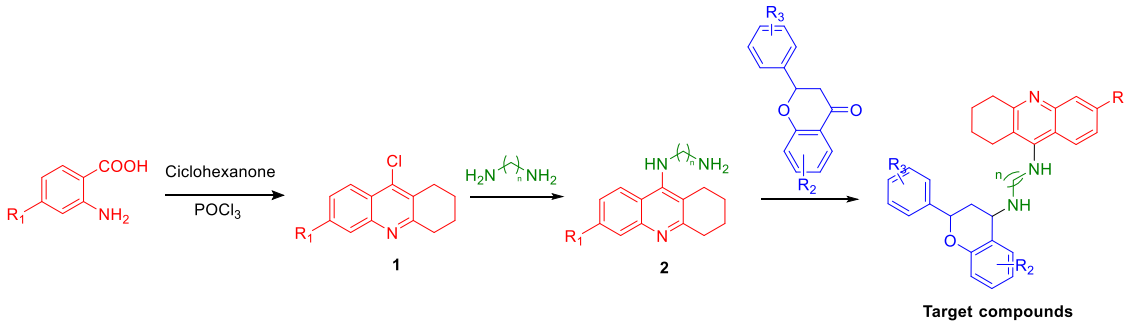


Scheme 1. Initial synthetic scheme proposed for the development of flavonoid-tacrine hybrids.

Thus, the first step was the synthesis of 9-chloroacridine **1.1a** and 6,9 dichloroacridine **1.1b** that was performed via a Niementowsky quinoline synthesis. Thus, heating anthranilic acid or 4-chloroanthranilic acid with cyclohexanone, in the presence of an excess of phosphorus oxychloride, led to compounds **1.1a** and **1.1b** in excellent yields of 99% in both cases and without the need for purification. Compounds **1.1** were heated with an excess of several diamines in phenol to achieve compounds **1.2a**-**1.2f** in excellent yields (83-96%) via aromatic nucleophilic substitution reactions (Scheme 2).

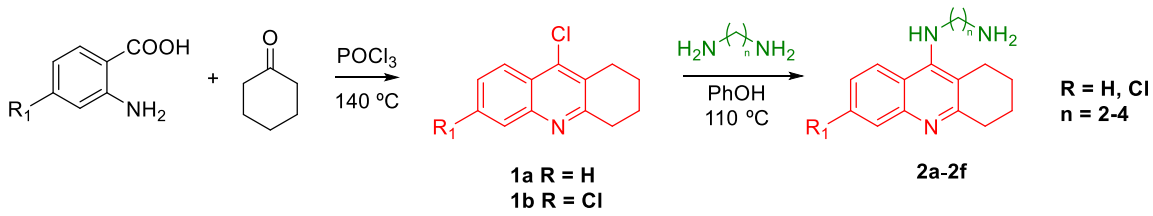


Scheme 2. Synthetic scheme followed to obtain diamine-tethered tacrine intermediates.

Regarding the flavonoid component **1.5**, both naringenin and hesperetin are commercially available. Related compounds were obtained by cyclization of the suitable *o*-hydroxychalcone. Thus, compound **1.5c** was prepared by aldol condensation of 3,5-dimethoxyacetophenone with benzaldehyde, followed by selective O-demethylation in the presence of $BBr_3$ and an intramolecular acid-promoted Michael addition (Scheme 3).

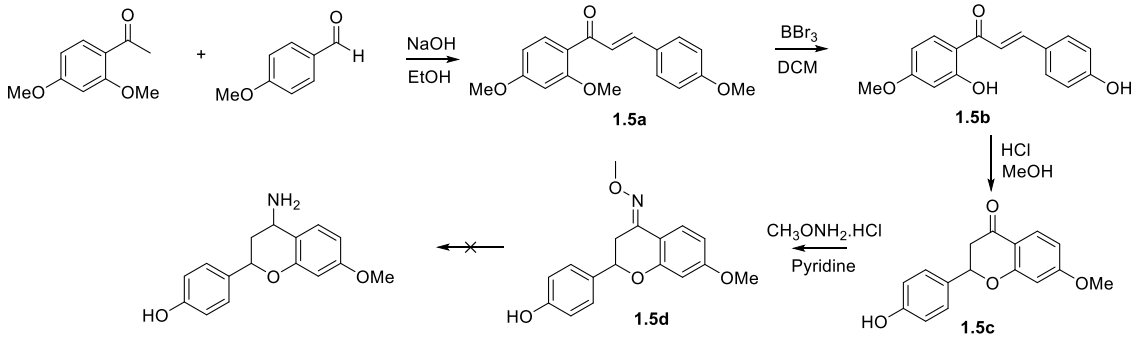


Scheme 3. Preparation of synthetic flavanone **1.5c**.

The 2D-NMR-assisted assignments of chalcone **1.5b**, which were useful for the assignment of our flavanone derivatives after chalcone **1.5a** demethylation which left one methoxy group, are shown in Table 1.

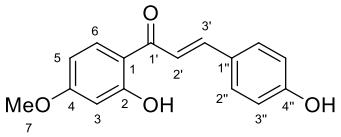

Table 1. Assignments for compound **1.5b**.

| δ (ppm) $^{13}$C | HMQC (δ (ppm) $^{1}$H) | HMBC (δ (ppm) $^{1}$H) | Assignment |
|---|---|---|---|
| **55.7** | 3.87 | - | 7 |
| **101.2** | 6.47 | 13.55 | 3 |
| **108.2** | 6.51 | - | 5 |
| **114.3** | - | 13.55 | 1 |
| **116.1** | 6.90 | - | 3'' |
| **118.1** | 7.47 | - | 2' |
| **127.9** | - | 6.90, 7.47 | 1'' |
| **130.7** | 7.60 | 7.60, 7.86 | 2'' |
| **131.5** | 7.84 | - | 6 |
| **144.1** | 7.87 | 7.60 | 3' |
| **158.0** | - | 7.58 | 4'' |
| **166.2** | - | 3.87 | 4 |
| **166.8** | - | 7.84, 13.55 | 2 |
| **192.1** | - | 7.47, 7.83 | 1' |

Prior to attempting to tether the flavonoid compounds to the tacrine structural fragments through a reductive amination, and because there was very little literature precedent of the reaction of flavanones with N-nucleophiles, we studied the reaction of butylamine and naringenin. Imine formation was observed within 30 minutes of reaction and this compound (**1.3**) was easily isolated, but attempts to reduce the C=N bond with different reducing agents, namely $NaBH_4$, $Na(CN)BH_3$, $Na(AcO)_3BH$, $LiAlH_4$ and $H_2$ over Pd/C under different conditions were unsuccessful. Moreover, imine formation with compound **1.2a** yielded a highly impure crude material that was also impossible to reduce.

We ascribed the low reactivity of the imino group to intramolecular hydrogen bonding stabilisation by the neighbouring hydroxyl group, and for this reason we treated naringenin with dimethyl sulphate as a methylating agent to yield compound **1.4a**, having all hydroxyl groups methylated. Its treatment with butylamine led to imine **1.4b** formation, but its attempted reduction with the previously mentioned reducing agents failed (scheme 4). A similar result was

obtained for the O-methyloxime[60] **1.5d**, which lacked an oxygen function adjacent to the imine (Scheme 3). Attempts at the reduction of the carbonyl group of compound **1.5c** with different reducing agents such as hydride donors or $H_2$ and Pd/C, even at high $H_2$ pressures, also failed (Scheme 5).

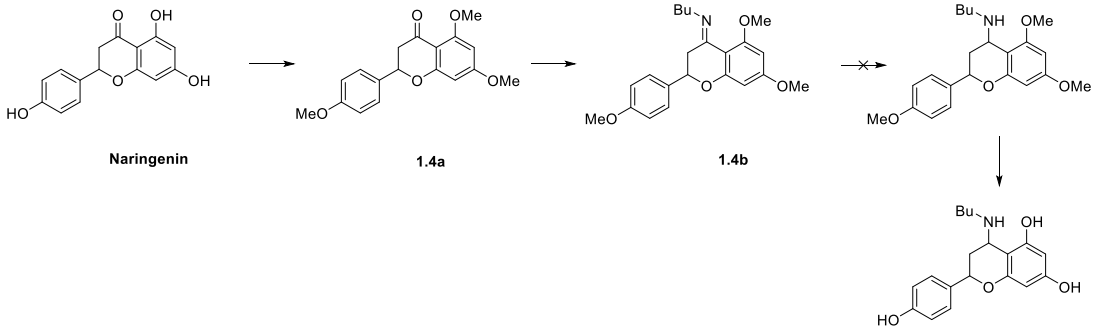


Scheme 4. Synthetic scheme of methylated naringenin analogue.

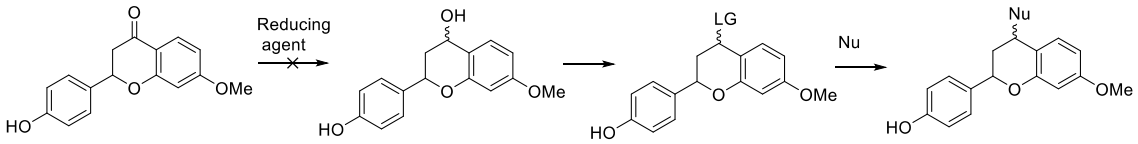


Scheme 5. Synthetic scheme planned for the tethering of different pharmacophores to -(4-hydroxyphenyl)-7-methoxychroman-4-one.

Realising that the oxime was resistant to several washes with HCl to remove pyridine from the reaction medium, and also bearing in mind the presence of metabolically stable O-alkyl oximes in some drugs, cephalosporin in particular, we deduced that this stability could be used to design a family of MTDLs by using O-carboxymethyl hydroxylamine hydrochloride, which has a free carboxylic acid group that can be used to tether diamine-tacrine compounds using peptide synthesis techniques. Thus, the corresponding oximes of the flavanones naringenin and hesperetin were prepared by reaction with O-carboxymethyl hydroxylamine hemichloride in pyridine under reflux conditions, obtaining the flavanone oximes **1.6a** and **1.6b** in quantitative yield (scheme 6).

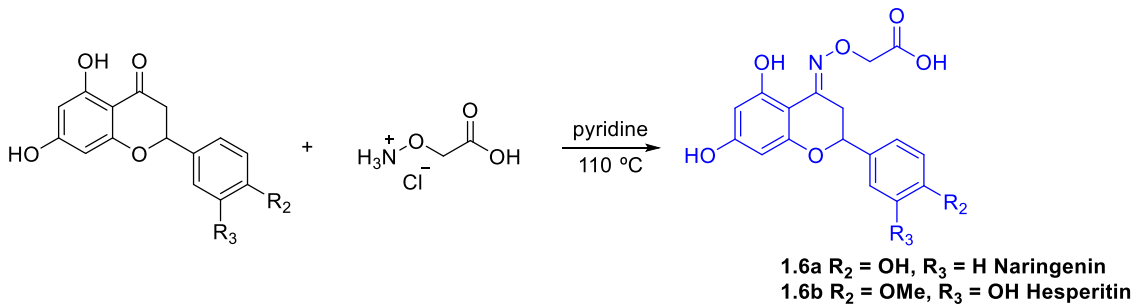


Scheme 6. Scheme followed for the synthesis of flavanone oxime acids.

Finally, the flavonoid oxime intermediates **1.6a** and **1.6b** and the tacrine-linker intermediates **1.2a**-**1.2f** were linked by an amide bond formation, using EDCI and HOBt, in a mixture of DCM/MeOH to provide hybrid compounds **1.7a**-**1.7l** in moderate yields (scheme 7).

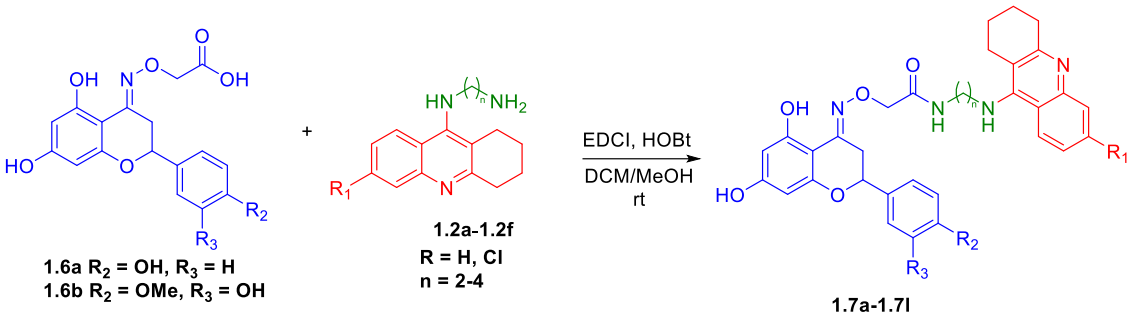


Scheme 7. Scheme followed for the synthesis of flavanone-tacrine hybrids.

Table 2. Hybrid flavonoid-tacrine compounds synthesised.

| Compound | $R_1$ | $R_2$ | $R_3$ | n | Yield (%) |
|---|---|---|---|---|---|
| **1.7a** | H | OH | H | 2 | 27 |
| **1.7b** | H | OH | H | 3 | 22 |
| **1.7c** | H | OH | H | 4 | 29 |
| **1.7d** | Cl | OH | H | 2 | 25 |
| **1.7e** | Cl | OH | H | 3 | 32 |
| **1.7f** | Cl | OH | H | 4 | 29 |
| **1.7g** | H | OMe | OH | 2 | 25 |
| **1.7h** | H | OMe | OH | 3 | 31 |
| **1.7i** | H | OMe | OH | 4 | 17 |
| **1.7j** | Cl | OMe | OH | 2 | 18 |
| **1.7k** | Cl | OMe | OH | 3 | 17 |
| **1.7l** | Cl | OMe | OH | 4 | 22 |

### 3.1.2 Synthesis of flavonoid-donepezil hybrids

As previously explained, the N-benzyl piperidine fragment is essential in the AChE and BuChE inhibitory activity of donepezil. This has caused that multiple research groups have used this fragment in order to develop MTDLs with this pharmacological activity. For this reason, oximes **1.6a** and **1.6b** were treated under the same conditions with 1-benzylpiperidin-4-amine and 2-(1-benzylpiperidin-4-yl) ethan-1-amine to yield hybrids **1.8a**-**1.8d**, again in moderate yields (scheme 8).

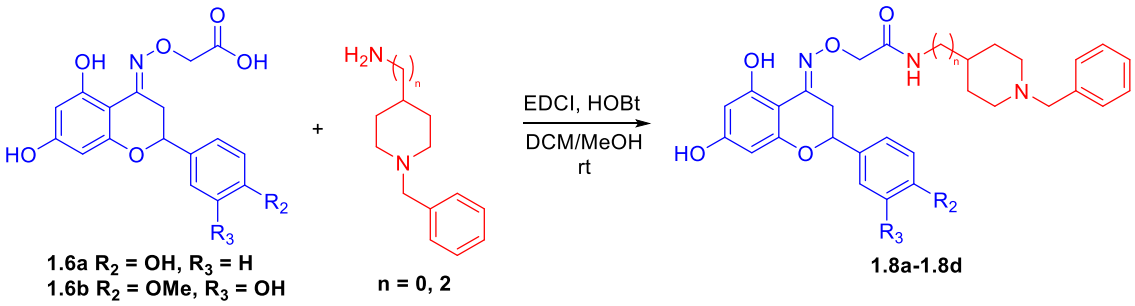


Scheme 8. Scheme followed for the synthesis of flavanone-N-benzyl piperidine hybrids.

Table 3. Flavonoid-N-benzyl piperidine hybrid compounds synthesised.

| Compound | $R_2$ | $R_3$ | n | Yield (%) |
|---|---|---|---|---|
| **1.8a** | OH | H | 0 | 32 |
| **1.8b** | OH | H | 2 | 22 |
| **1.8c** | OMe | OH | 0 | 26 |
| **1.8d** | OMe | OH | 2 | 20 |

### 3.1.3 Synthesis of flavonoid-tryptamine hybrids

Finally, in order to expand the family of MTDL hybrids based on flavonoids, we decided to bind several tryptamine derivatives to oximes **1.6a** and **1.6b**. Tryptamines, and especially melatonin, are known to have pleiotropic neuroprotective effects so attaching them to flavonoids could afford compounds with enhanced neuroprotective capacity. This way, we reacted oximes **1.6a** and **1.6b** with tryptamines derivatives bearing -OMe, -OH (serotonin) and H substituents at $R_1$ using the same conditions previously described to yield compounds **1.9a**-**1.9f** (scheme 9).

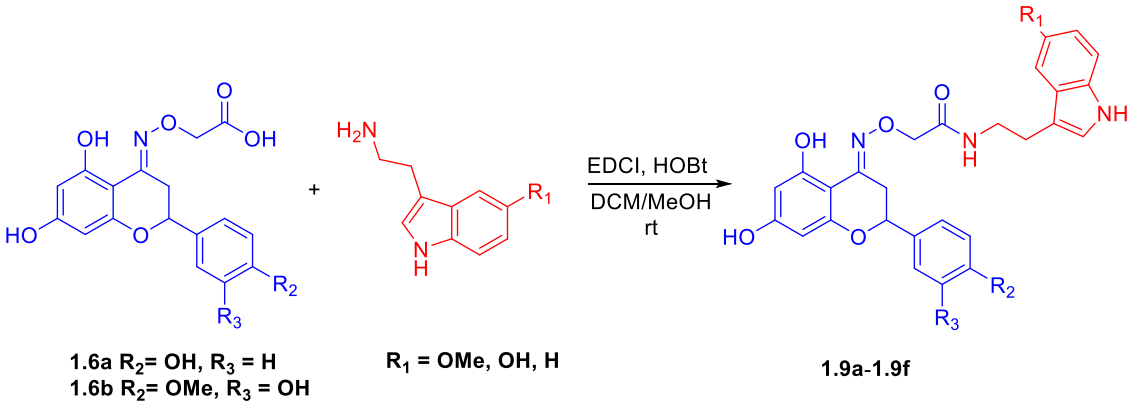


Scheme 9. Scheme followed for the synthesis of flavanone-tryptamine hybrids.

Table 4. Flavanone-tryptamine hybrids synthesized

| Compound | $R_1$ | $R_2$ | $R_3$ | Yield (%) |
|---|---|---|---|---|
| **9a** | OMe | OH | H | 22 |
| **9b** | OH | OH | H | 28 |
| **9c** | H | OH | H | 33 |
| **9d** | OMe | OMe | OH | 27 |
| **9e** | OH | OMe | OH | 24 |
| **9f** | H | OMe | OH | 31 |

## 3.2 Pharmacological characterization of flavonoid hybrid compounds

Once all compounds were synthesised, we assayed them against different pharmacological targets in order to verify their potential as MTDLs. Cell viability and MDA and Aβ protection studies were carried out by Professor Javier del Pino in the Department of Toxicology of the Faculty of Veterinary from Universidad Complutense de Madrid. DCFA-DA antioxidant assay and AChE and BuChE inhibition studies were performed by Professors Sagrario Martín-Aragón

and Paloma Bermejo from the Department of Pharmacology of the Faculty of Pharmacy of Universidad Complutense de Madrid. Further characterization is in progress.

### 3.2.1 Cell viability

Prior to the pharmacological study, all hybrid compounds were assayed for their toxicity against neuronal SN56 cells, which were treated with increasing concentrations of the compounds (1, 20, 40, 80 and 100 μM). Following incubation for 24 h, cell viability was tested by the 3-(4,5-dimethylthiazol-2-yl)-2,5-diphenyltetrazolium (MTT) assay. As shown in Figures 1 and 2, none of the flavonoid-tacrine hybrids modified cell viability at concentrations up to 40 μM. At concentrations of 60 μM and greater, some compounds like **1.7a**, **1.7b** or **1.7c** started to show toxicity and at concentrations of 80 μM and 100 μM this toxicity increased. In general compounds that possess the naringenin moiety seem to be worse tolerated that the ones derived from hesperetin. However, this toxicity only is significant at high concentrations.

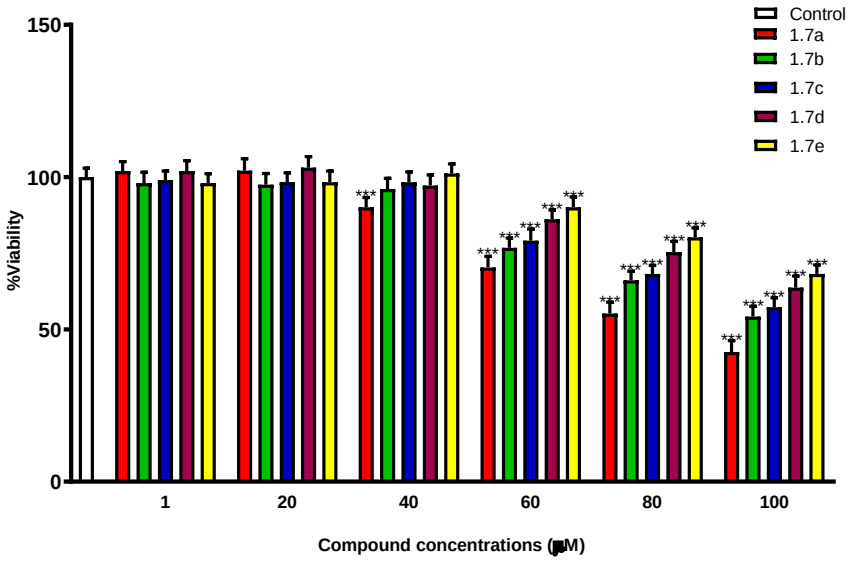


Figure 1. Percentage of cell viability at different concentrations of compounds **1.7a**-**1.7e**. *** $p<0.001$ indicates significant statistical differences with the control.

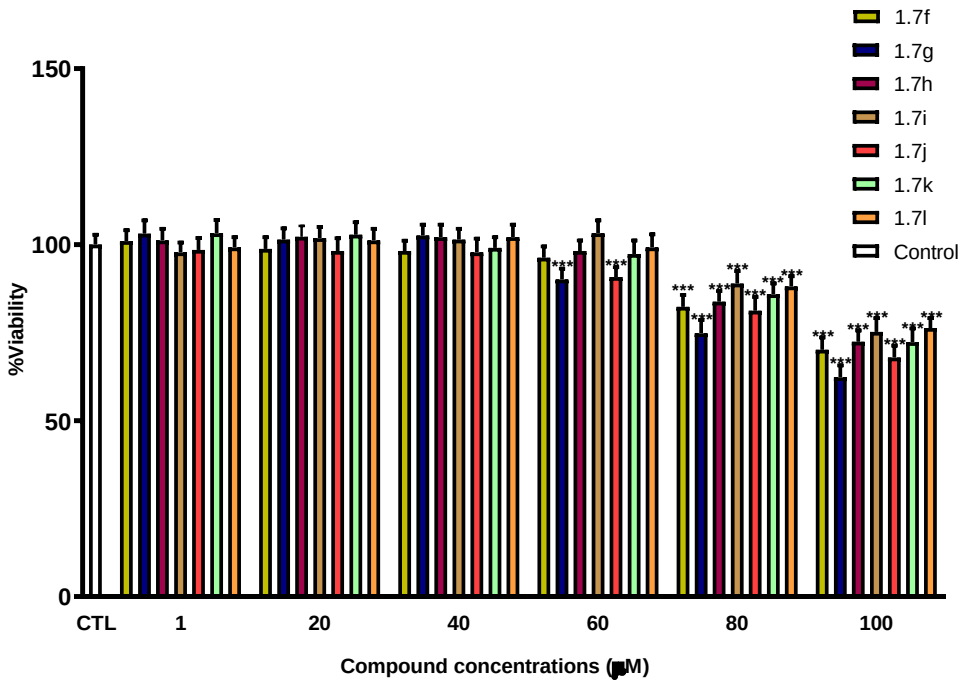


Figure 2. Percentage of cell viability at different concentrations of compounds **1.7f**-**1.7l**. *** p<0.001 indicates significant statistical differences with the control.

Cellular toxicity studies indicated that flavonoid-donepezil hybrids were less toxic than the flavonoid-tacrine homologues, presenting a good toxic profile, as it is shown in figure 3. Thus, these compounds showed moderate toxicity at concentrations up to 80 µM. At 100 µM, **1.8a**-**1.8d** showed a moderate toxicity.

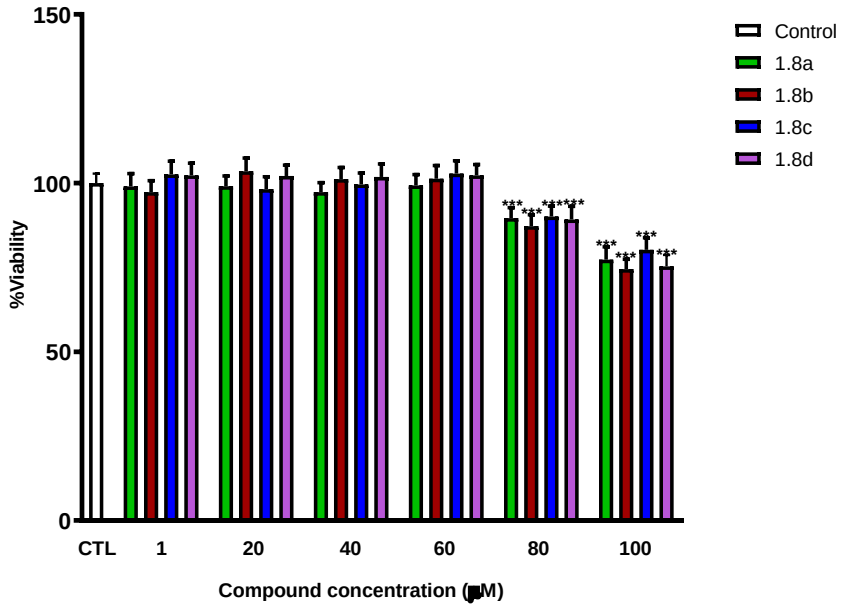


Figure 3. Percentage of cell viability at different concentrations of compounds **1.8a**-**1.8d**. *** p<0.001 indicates significant statistical differences with the control.

Cell viability studies revealed that flavonoid-tryptamine hybrids have a wide safety range, being well tolerated at all concentrations assayed, even at 100 µM, where all flavonoid-tacrine and flavonoid-N-benzyl piperidine hybrids showed toxicity. Thus, flavonoid-tryptamine hybrids presented the best safety profile.

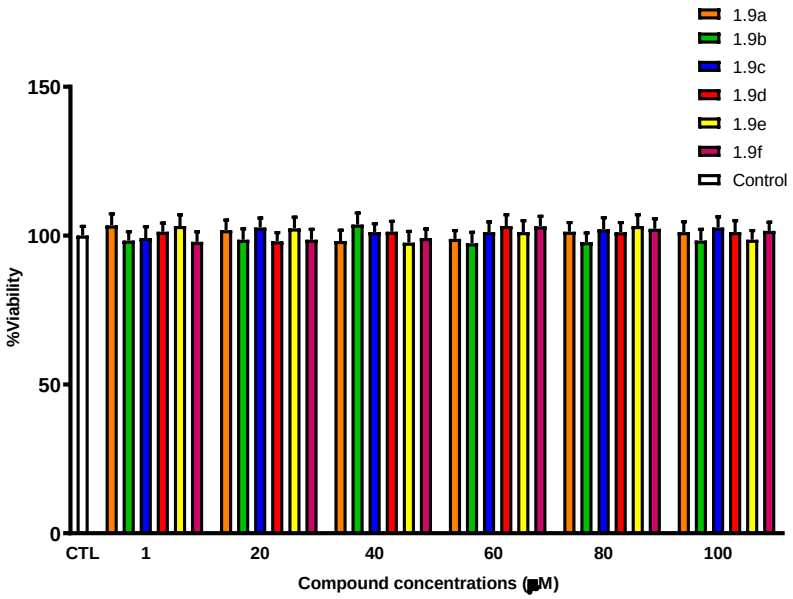


Figure 4. Percentage of cell viability at different concentrations of compounds **1.9a**-**1.9f**.

### 3.2.2 Neuroprotection against oxidative stress

Due to the antioxidant properties expected to be associated to the flavonoid, we carried out several experiments in order to examine the effect of our compounds against oxidative stress, which is key to several neurological diseases.

### 3.2.21 MDA antioxidant assay

The concentration of malondialdehyde (MDA) increases with raised levels of oxidative stress due to an augmented lipid peroxidation. To assess the antioxidant properties of all hybrids an MDA assay was carried on, based on the reaction of MDA with thiobarbituric acid (TBA) forming the MDA-TBA adduct (scheme 7). This is a stable chromophore that has a maximum of absorption at 532 nm and is the species detected in the assay. Thus, reductions in the concentration of this adduct will translate in less lipid peroxidation, and therefore in a greater antioxidant capacity of the compounds[61]. In the case of the assay we performed, we used Trolox, an analogue of vitamin E with a high antioxidant capacity due to the polyphenolic structure embedded in its structure, which is susceptible to being oxidised to the correspondent quinone (scheme 7). In this assay, it was used at a concentration of 100 µM.

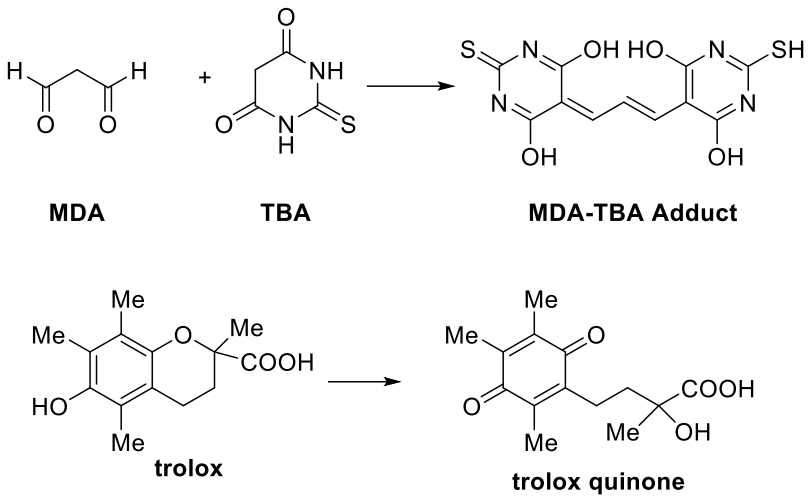


Scheme 10. Condensation of MDA with two molecules of TBA and oxidation of Trolox to its quinone form.

After exposure of SN56 cells to $H_2O_2$ (140 mM), MDA concentration increased to 230% of the basal value ($p < 0.001$ vs control), which proves the high sensitivity of these cells to ROS-induced lipid peroxidation. When the experiment was performed in the presence of flavonoid-tacrine hybrids (**1.7a**-**1.7l**), all compounds showed a moderate antioxidant activity, which manifested itself only at concentrations above 60 µM for the hesperetin derivatives and was higher for the compounds containing the hesperetin framework **1.7j**, **1.7k**, **1.7l**, which exhibited antioxidant activity at concentration of 40 µM. Compounds bearing a chlorine atom in position 6 of the tacrine moiety such as **1.7d**, **1.7e**, **1.7j**, **1.7k** and **1.7l** seem to have an increased antioxidant capacity than the non-chlorine bearing derivatives and also 3 carbon atom linker compounds seem to possess an slightly greater antioxidant capacity than 2 or 4 carbon linker compounds (table 5). Compound **1.7k**, which contains a 6-chlorotacrine moiety and a 3-carbon atom linker, showed the best protective effects against $H_2O_2$-induced lipid peroxidation of this MTDL family, having a better antioxidant capacity than the reference compound, trolox. Additionally, compounds **1.7d**-**1.7i** have moderate antioxidant properties with a similar antioxidant capacity to trolox at the same concentration (100 µM). Compounds **1.7j**-**1.7l** have a superior antioxidant capacity than trolox, having at concentrations of 60 µM a considerable antioxidant capacity, however not superior to the standard. At concentrations of 80 µM, compounds **1.7j** and **1.7l** show a similar antioxidant power to trolox at 100 µM and compound **1.7k** a superior capacity than the standard. At 100 µM, these compounds show greater antioxidant power than the standard.

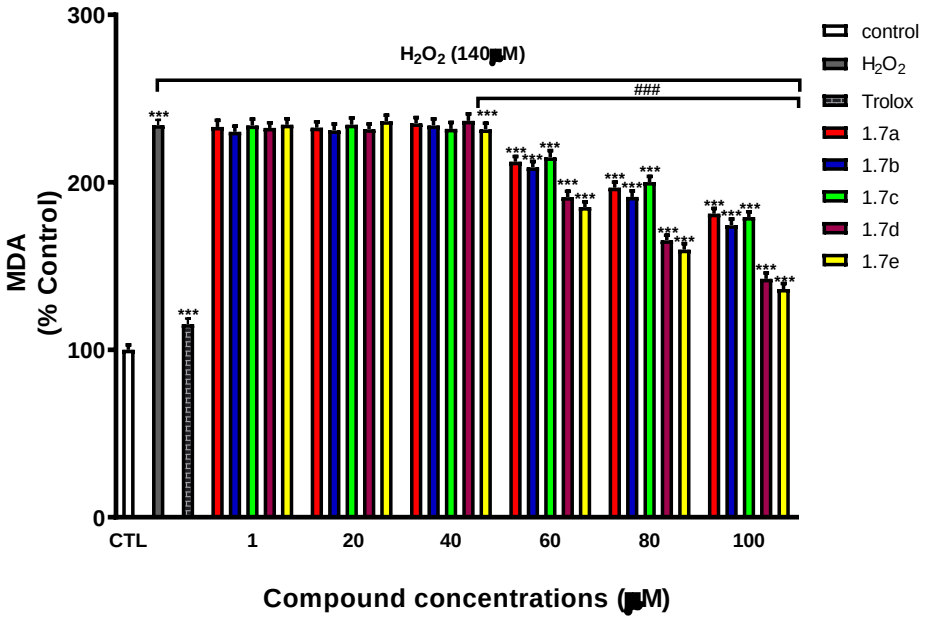


Figure 5. Percentage of MDA compared with control at different concentrations of compounds **1.7a**-**1.7e**. *** p<0.001 indicates significant statistical differences with the control after one way ANOVA followed by Barlett´s post-hoc test. ### p<0.001 indicates significant differences compared to $H_2O_2$ after one way ANOVA followed by Barlett´s post-hoc test.

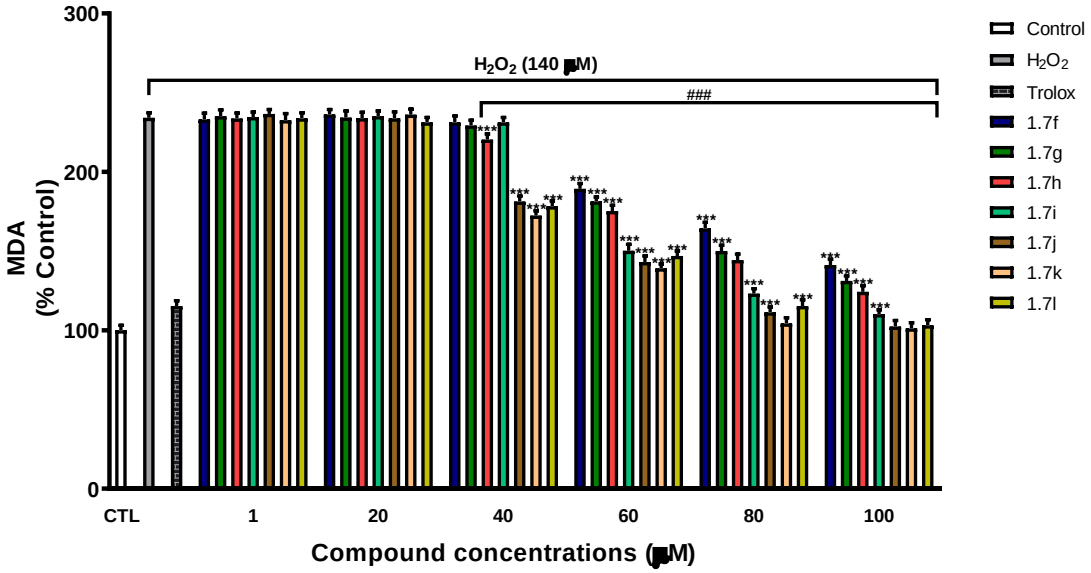


Figure 6. Percentage of MDA compared with control at different concentrations of compounds **1.7f**-**1.7l**. *** p<0.001 indicates significant statistical differences with the control after one way ANOVA followed by Barlett´s post-hoc test. ### p<0.001 indicates significant differences compared to $H_2O_2$ after one way ANOVA followed by Barlett´s post-hoc test.

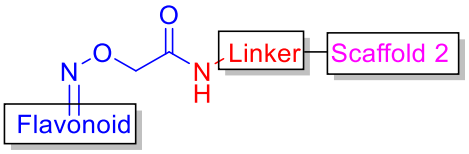


Table 5. Table illustrating the % of MDA with respect to control at 100 µM concentration and the substituents of all flavonoid tacrine-derivatives.

| Compound | Flavonoid | Number of carbon atoms in linker | Scaffold 2 | % MDA (100 µM) |
|---|---|---|---|---|
| **7a** | Naringenin | 2 | tacrine | 181.2 |
| **7b** | Naringenin | 3 | tacrine | 174.3 |
| **7c** | Naringenin | 4 | tacrine | 179.2 |
| **7d** | Naringenin | 2 | 6-chlorotacrine | 142.3 |
| **7e** | Naringenin | 3 | 6-chlorotacrine | 136.3 |
| **7f** | Naringenin | 4 | 6-chlorotacrine | 141.2 |
| **7g** | Hesperitin | 2 | tacrine | 131.2 |
| **7h** | Hesperitin | 3 | tacrine | 124.3 |
| **7i** | Hesperitin | 4 | tacrine | 110.1 |
| **7j** | Hesperitin | 2 | 6-chlorotacrine | 102.3 |
| **7k** | Hesperitin | 3 | 6-chlorotacrine | 101.2 |
| **7l** | Hesperitin | 4 | 6-chlorotacrine | 103.1 |
| **trolox** | - | - | - | 115.3 |

When the protective capacity against $H_2O_2$-induced lipid peroxidation of the flavonoid-donepezil hybrids compounds were tested in the MDA assay, we again observed that the compounds **1.8c** and **1.8d** bearing a hesperetin flavonoid moiety present a higher antioxidant capacity than compounds **1.8a** and **1.8b**, which present a naringenin flavonoid moiety. Thus, compounds **1.8c** and **1.8d** started to show antioxidant activity at a concentration of 40 µM, while **1.8a** and **1.8b** started at concentrations of 60 µM, and compound **1.8c** showed a similar antioxidant capacity to the reference at the same concentration.

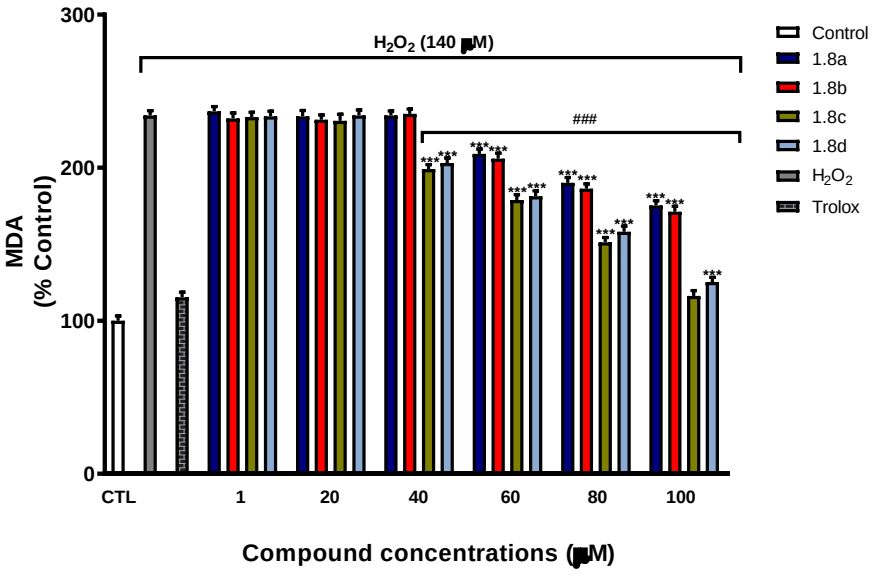

Figure 7. Percentage of MDA compared with control at different concentrations of compounds **8a**-**8d**. *** p<0.001 indicates significant statistical differences with the control after one way ANOVA followed by Barlett´s post-hoc test. ### p<0.001 indicates significant differences compared to $H_2O_2$ after one way ANOVA followed by Barlett´s post-hoc test.

When we studied the cell protecting capacity of flavonoid-tryptamine hybrid compounds in the SN56 cell line, we found the best antioxidant profile, as was expected from compound design. This effect is probably due to the synergic effect of the two moieties of the molecule, which are well-known antioxidants. At a concentration of 20 µM, compounds **1.9a** and **1.9d**, which bear both a melatonin moiety, started to show a moderate antioxidant activity as expected due to the powerful antioxidant effect of melatonin. At a concentration of 40 µM, compounds **1.9d**, **1.9e** and **1.9f**, which derive from hesperitin instead of naringenin, presented a better antioxidant activity than **1.9a**, **1.9b** and **1.9c**. This is consistent with the previous result, as all the other hybrids presented a better activity for the hesperitin rather than for the naringenin moiety. At a concentration of 100 µM all compounds apart from **1.9c** present a better antioxidant activity than the reference trolox at the same concentration, making them also promising agents for the development of MTDLs.

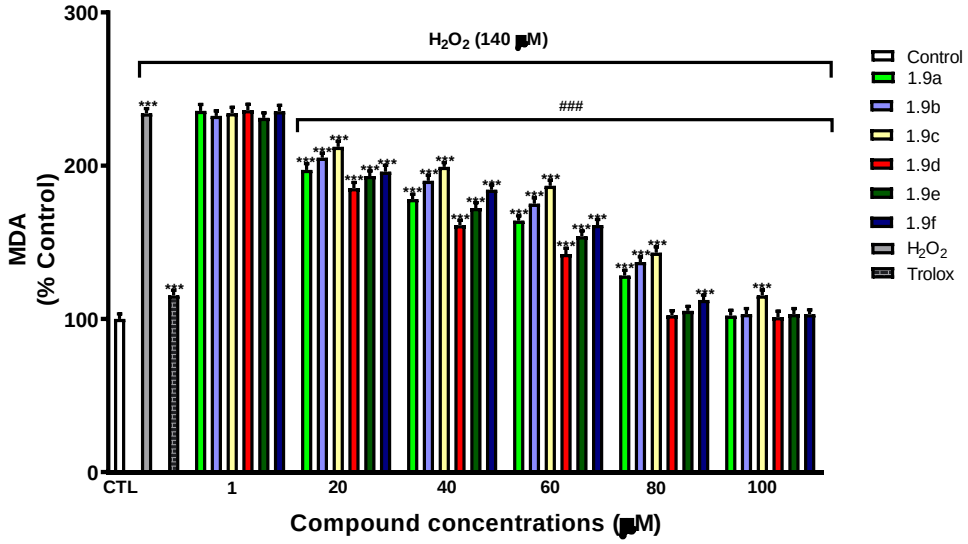


Figure 8. Percentage of MDA compared with control at different concentrations of compounds **1.9a**-**1.9f**. *** p<0.001 indicates significant statistical differences with the control after one way ANOVA followed by Barlett´s post-hoc test. ### p<0.001 indicates significant differences compared to $H_2O_2$ after one way ANOVA followed by Barlett´s post-hoc test.

### 3.2.22 Intracellular reactive oxygen species scavenging activity by the DCFA-DA antioxidant assay

To investigate the effect of our compounds on intracellular levels of ROS, radical oxygen scavenging was tested in human neuroblastoma (SH-SY5Y) cells using the cell-permeable probe 2,7-dichlorofluorescin diacetate (DFCH-DA). Non-fluorescent DCFH-DA, hydrolyzed to DCFH inside the cells by cellular estearases, is still non-fluorescent but is retained inside the cell and yields the highly fluorescent DCF in the presence of intracellular hydrogen peroxide and related peroxides. Thus, the fluorescence observed in the assay is in an inverse relationship with the scavenging ability of the compounds under assay (Scheme 8).

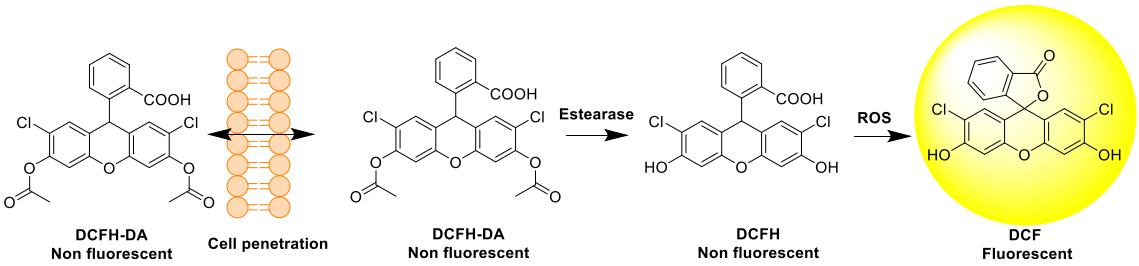


Scheme 8. Illustration of DCFA-DA antioxidant assay.

So, in order to further assess the antioxidant capacity of the hybrids, a DCFA-DA assay was performed. The results show that all hybrid compounds show a better ROS scavenging activity than the precursor compound tacrine. However, compounds that present a hesperetin moiety (**1.7g**-**1.7l**) show a greater ROS scavenging activity than the ones thar present a naringenin moiety (**1.7c**, **1.7d**). With the previous MDA assay results also taken into consideration, we can conclude that hesperetin is a more antioxidant flavone than naringenin, being these results coherent with the literature[62]. Despite the good results shown by the hesperetin hybrids, none of them show a superior activity to quercetin, a well-known antioxidant flavone.

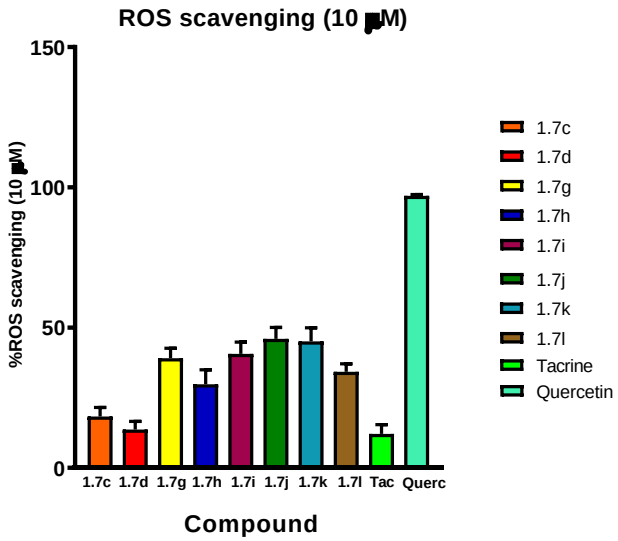


Figure 9. Percentage of ROS scavenging by 10 µM concentrations of selected compounds.

### 3.2.3 Cholinesterase inhibitory activity

### 3.2.31 AChE *in vitro* inhibitory activity

As has previously been stated, excess hydrolysis and degradation of ACh by AChE and BuChE are a classical hallmark of AD, and the inhibition of both enzymes improves the symptoms of the disease. Therefore, the development of multitarget drug ligands that included this pharmacological action would be interesting in this spite. To test this premise, we carried out AChE and BuChE inhibition assays.

In recent years, a wide number of methods have been developed to quantify AChE and BuChE activities. However, the most popular and commonly used is the Ellman method[63]. This method uses the substrate acetylthiocholine iodide (ACTI) and 5,5'-dithio-bis-2-nitrobenzoic acid (DTNB). AChE and BuChE hydrolyse acetylthiocholine and the thiocholine generated then reacts with DTNB, and the reaction results in 5-thio-2-nitro benzoic acid (TNB) which possesses a yellow colour. The colour intensity of the product is measured at 405 nm and is dependent on the enzyme activity (scheme 9).

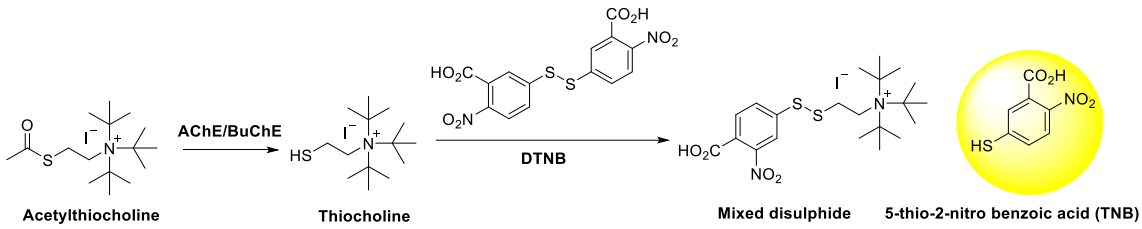


Scheme 9. Scheme showing the basis of the Ellman assay.

The results obtained with the Ellman method show that compounds **1.7c**, **1.7d** and **1.7g**-**1.7l** inhibit acetylcholinesterase in the micromolar or even the nanomolar range. Compound **1.7d** even shows a superior activity than the reference compound, tacrine. All the tested compounds show inhibition activity within the micromolar or the nanomolar range, converting them into good or excellent AChE inhibitors.

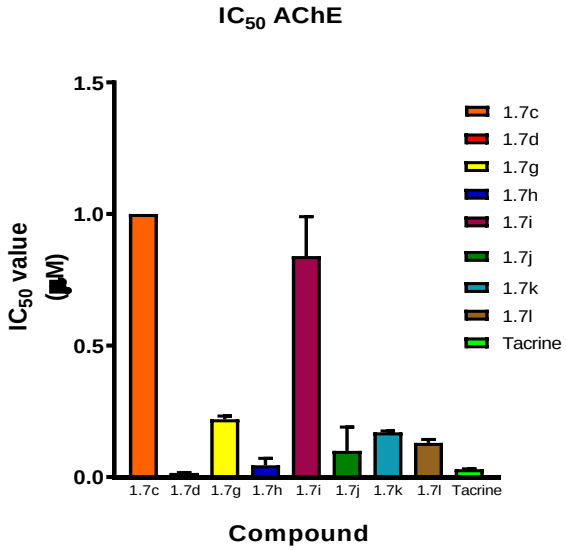


Figure 10. $IC_{50}$ values for AChE inhibition of selected flavonoid-tacrine hybrids.

### 3.2.32 BuChE in vitro inhibitory activity

As previously mentioned, BuChE also has an important role in the development of AD. It hydrolyses AChE, reducing its brain concentration and also is partially responsible for the aggregation of Aβ. Therefore, it stands out as a therapeutic target in AD and its inhibition is also important for the development of MTDLs against it.

In this connection, a BuChE inhibition assay was also performed with the previous compounds, also using the Ellman method. The results show that all the compounds are inhibitors in the micromolar range, being the most potent compounds **1.7c**, **1.7d**, **1.7g** and **1.7h**, with $IC_{50}$ below 0.1 µM. Although none of the tested compounds show activities superior to the reference compound, tacrine, that inhibits in the nanomolar range, all show good inhibitory activity against BuChE.

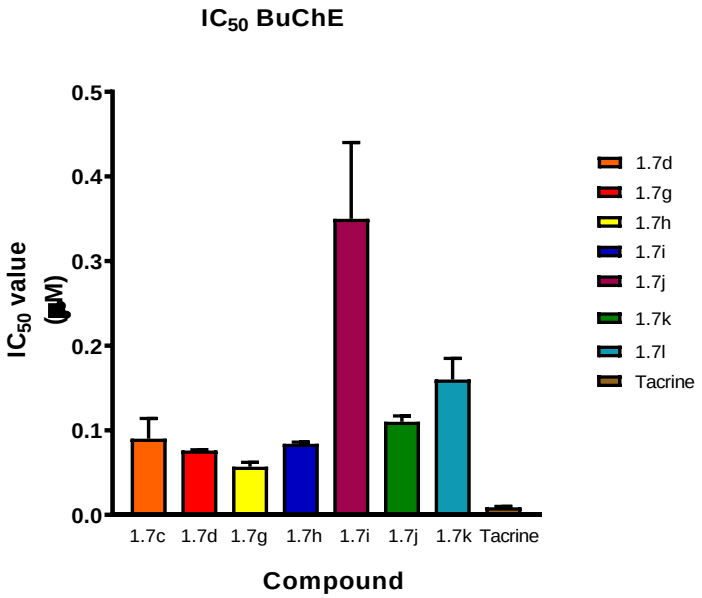


Figure 11. $IC_{50}$ values for BuChE inhibition of different flavonoid-tacrine hybrids.

### 3.2.33 AChE inhibition in a human neuroblastoma cell line (SH-SY5Y) of compounds 1.7

In order to further test the inhibitory activity of the compounds against AChE, we studied the AChE inhibition potency in a human neuroblastoma cell line (SH-SY5Y). This assay provides a more accurate profile of the pharmacokinetic and activity and toxicity properties of the tested compounds than enzyme inhibition assays, since the compounds are in a cellular context. The cell line used for the assay was human neuroblastoma (SH-SY5Y) and the method used for the determination of the inhibitory activity was the Ellman method previously mentioned. The experiment was performed at concentrations of 10, 1, 0.1 and 0.01 µM, and the results are shown in table 5.

| Compound | AChE inhibition (%) in SH-SY5Y | | | |
|---|---|---|---|---|
| | 10 µM | 1 µM | 0.1 µM | 0.01 µM |
| **7c** | 52.56 ± 5.09** | 5.13 ± 6.85 | - | - |
| **7d** | 90.09 ± 2.69** | 52.05 ± 3.41** | 31.45 ± 5.51** | - |
| **7g** | 13.68 ± 6.87** | - | - | - |
| **7h** | 79.49 ± 2.91** | 46.50 ± 2.61** | 23.94 ± 7.26* | - |
| **7i** | 13.68 ± 6.85** | - | - | - |
| **7j** | 70.17 ± 5.95** | 19.83 ± 2.30* | 2.56 ± 4.73 | - |
| **7k** | 92.44 ± 1.47** | 77.61 ± 4.68** | 46.84 ± 4.43** | 30.17 ± 2.84 |
| **7l** | 86.92 ± 1.69** | 34.27 ± 6.35** | 14.53 ± 5.60 | - |
| **Tacrine** | 58.63 ± 3.21** | 16.07 ± 9.15 | - | - |

Table 5. Percentage inhibition of AChE in cells by flavonoid-tacrine hybrids. **p<0.01, *p<0.05 indicates significant difference when compared to control according to one way ANOVA followed by Newman-Keuls post-hoc test.

All the compounds show inhibitory activity against AChE at a concentration of 10 µM, and **1.7d**, **1.7h**, **1.7k** and **1.7l** were the best AChEIs, all of them showing inhibition values up to 80%. Furthermore, these compounds are more active than tacrine, which was the standard used in the assays, at the same concentration. At a concentration of 1 µM, the tendency consolidates with compounds **1.7d**, **1.7h**, **1.7k** and **1.7l** presenting greater % inhibition that tacrine. Compounds **7g** and **7i**, which were the least active ones at 10 µM, no longer show activity at 1 µM. At 0.1 µM compound **1.7c** no longer presents activity and the reference compound, tacrine, is also no longer active. Compounds **1.7d**, **1.7h**, **1.7k** and **1.7l** have the best inhibitory activities and compound **7k** still presents an excellent 46% inhibition at this concentration. At a concentration of 0.01 µM no compound inhibits AChE except for hybrid **1.7k**, that still shows a 30% inhibition.

These results show that compound **1.7k** presents the best AChE inhibitor profile, being highly active in the in vitro assay and the most active compound in the neuroblastoma cell line (SH-SY5Y) assay. **1.7k** was also active against BuChE and presents good antioxidant profiles, converting it into a promising lead compound for the development of an MTDL against Alzheimer´s disease.

To throw some light about how compound **1.7k** binds to AChE, a docking study was performed using Autodock Vina, with *Torpedo californica´*s AChE crystal structure, co-crystalysed with a polymethylene-linked bis-tacrine dimer (7 carbon linker) (5EI5 in PDB). This enzyme was chosen as a model for the docking study due to its similarity with the human enzyme. The docking study shows that compound **1.7k** (light blue) has polar contacts (orange) with aspartic acid 71 and

tyrosine 120, while having nonpolar (blue) contacts with tyrosine 333, phenylalanine 329, tryptophan 83 and tyrosine 69, in a similar fashion to the bistacrine ligand co-crystallized with the enzyme (grey). Aspartic acid 71, tyrosine 120, tyrosine 333, tyrosine 69 and phenylalanine 329 are residues present in the peripheric anionic site of AChE, which means that a strong interaction of compound **7k** with this site of the enzyme could block the catalytic activity associated with the misfolding of Aβ and add another potential activity to the compound against AD and prompted us to carry out the next experiment.

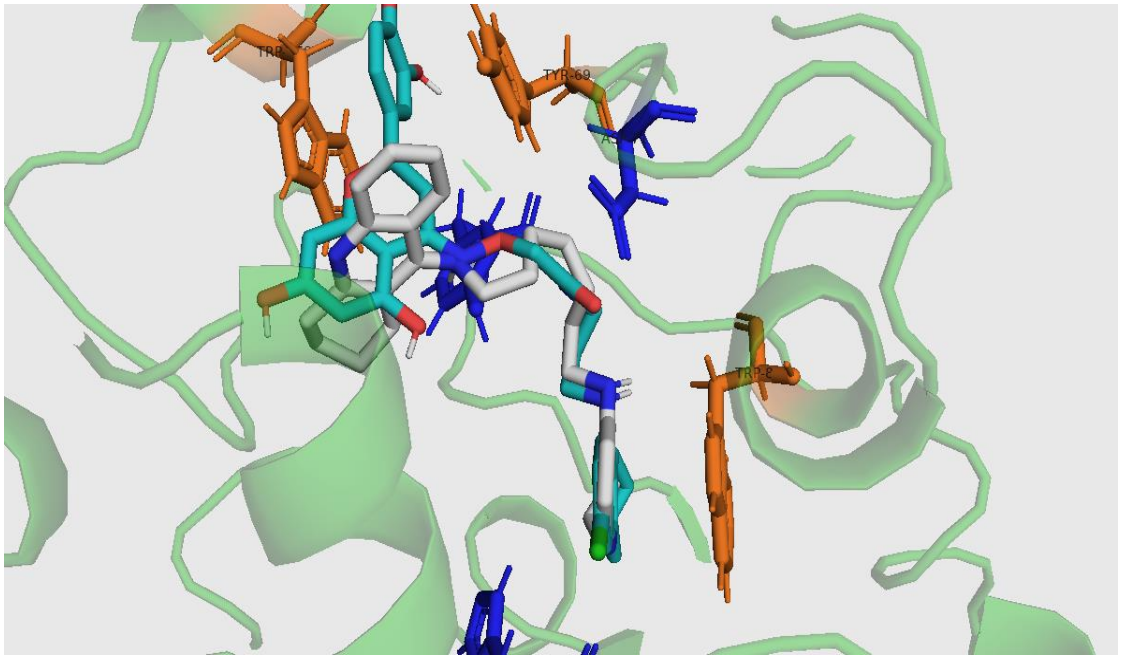

Figure 12. Docking showing the interaction of **1.7k** and bis-tacrine with AChE from *Torpedo californica*. Model generated with Pymol.

### 3.3.4 Protection against Aβ toxicity

Formation, accumulation, and aggregation of toxic proteins, like amyloid-proteins (Aβ), leads to neurodegeneration. Taking into consideration the fact that compounds **1.7** displayed good activities against oxidative stress and AChE and BuChE inhibition, probably associated to occupation of the peripheric anionic site, we decided to study their protecting capacity against Aβ aggregation.

In order to determine the neuroprotective effects against Aβ proteins of these compounds, SN56 cholinergic neurons from basal forebrain[64], the main brain cholinergic region where selective damage on cholinergic neurons is observed in AD, were pre-treated with or without the selected compounds (20-100 µM), and then treated with Aβ proteins (1 µM). Cell viability was determined following 24 h Aβ1-42 protein treatment of SN56 cells, by MTT assay. The assay is based on the cleavage of the yellow tetrazolium MTT salt to purple formazan crystals by mitochondrial dehydrogenase. Cells were incubated in yellow MTT solution at a final concentration of 0.5 mg/mL for 4 h after treatment with the Aβ1-42 protein. Following incubation at 37 °C, the resulting formazan product obtained after medium removal was dissolved in 250 µL DMSO. The formation of solubilized formazan product was measured

spectrophotometrically at 570 nm. Control cells treated with vehicle were taken as 100% viability (scheme 10).

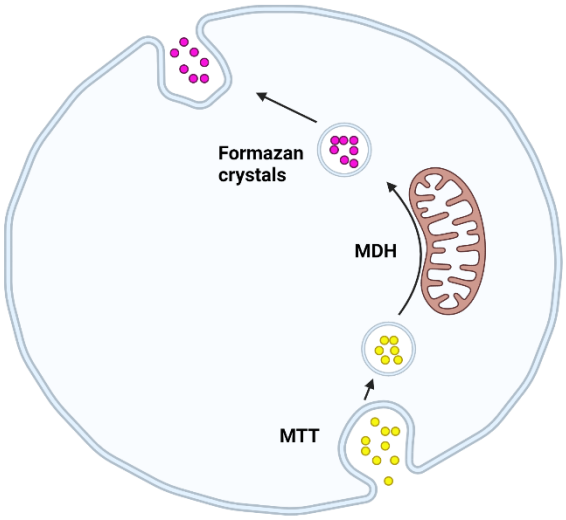


Scheme 10. Diagram illustrating the biological principles of the MTT assay.

In figure 13 the viability of cells at a fixed concentration of Aβ (1 µM) with different concentrations of compounds **1.7d**, **1.7g** and **1.7i**-**1.7l** can be observed.

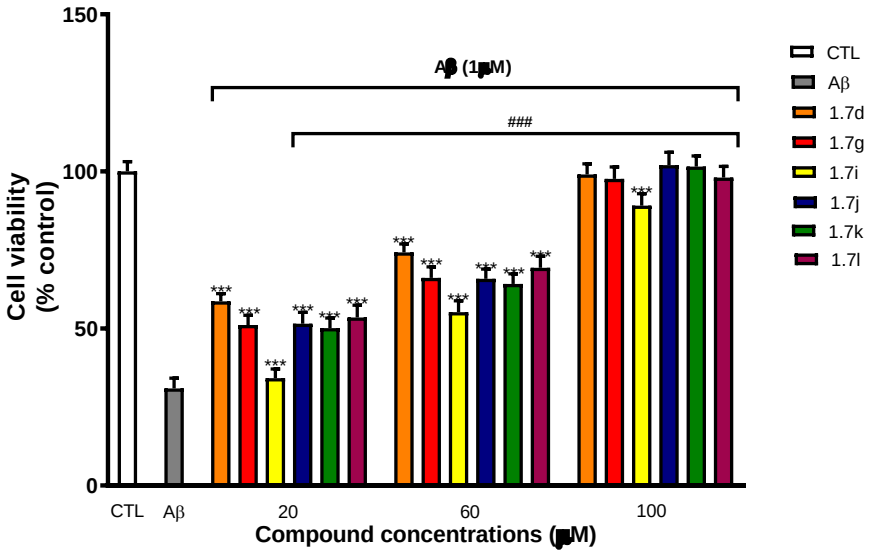


Figure 13. Percentage of cell viability after being exposed to 1µM concentration of Aβ and then to flavonoid-tacrine hybrids. *** $p<0.001$ indicates significant statistical differences with the control after one way ANOVA followed by Barlett´s post-hoc test. ### $p<0.001$ indicates significant differences compared to Aβ after one way ANOVA followed by Barlett´s post-hoc test.

After 24 h treatment with the Aβ1-42 proteins, a decrease in cell viability was observed. Pre-treatment with **1.7d** and **1.7g** reverted, in a concentration-dependent way, partially for **1.7i** and completely for **1.7d**, **1.7g**, **1.7j**, **1.7k** and **1.7l**, the reduction of cell viability induced after Aβ1-42

proteins treatment alone. This reversion started at 20 µM for all compounds except **1.7i**, which showed moderately protective against Aβ. At concentrations of 60 µM, all compounds show considerable protective capability against Aβ, the best being **1.7d** and the least protective again **1.7i**. At a concentration of 100 µM all compounds show a very high protecting capacity against Aβ being a cell viability of 100% and no significant differences were found between with the control cells data in almost all cases. The antioxidant activity of these compounds is in the same order of magnitude (micromolar) as the Aβ protective capacity, which is positive for the development of a potential MTDL, as all activities should be in a concentration of a similar order of magnitude. On the other hand, their potency inhibiting AChE and BuChE is in the nanomolar range.

The protective activity of the flavonoid-tryptamine compounds **1.9a**-**1.9f** against Aβ was also measured. As in the previous case with the flavonoid-tacrine hybrids, the concentration of Aβ is fixed at 1 µM in all cases and there are three different concentrations of compounds, 20 µM, 60 µM and 100 µM.

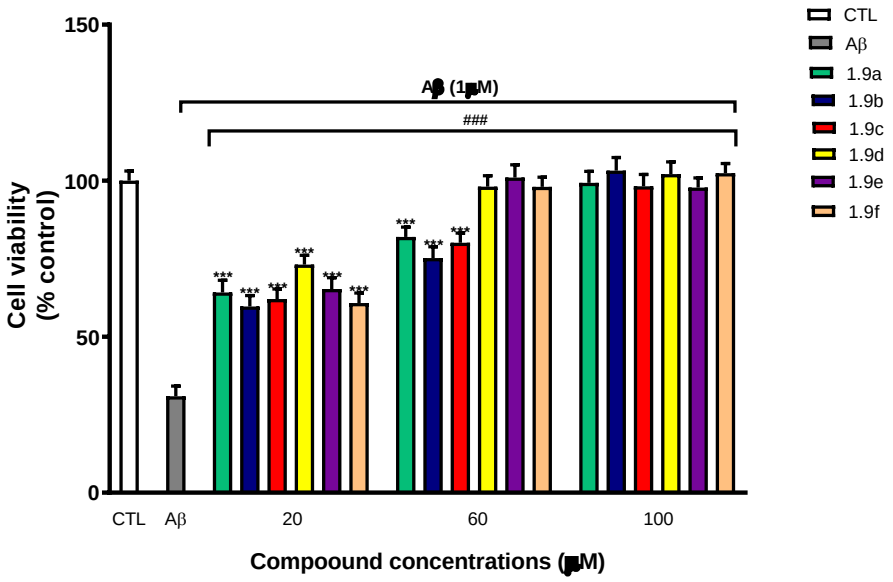


Figure 13. Percentage of cell viability after being exposed to 1µM concentration of Aβ and then to flavonoid-tryptamine hybrids. *** $p<0.001$ indicates significant statistical differences with the control after one way ANOVA followed by Barlett´s post-hoc test. ### $p<0.001$ indicates significant differences compared to Aβ after one way ANOVA followed by Barlett´s post-hoc test.

At a concentration of 20 µM, all compounds show a potent protective capacity against Aβ, being compound **1.9d** the most potent one. At a concentration of 60 µM, all compounds show an increased protecting capacity against Aβ, with compounds bearing hesperetin **1.9d**-**1.9e** showing a better protecting capacity than the naringenin derivatives **1.9a**-**1.9c**. At a concentration of 100 µM all compounds show a very high protecting activity, being the cell viability approximately 100% in all cases. This can be correlated with the antioxidant capacity exhibited by these compounds in the MDA antioxidant assay, with the hesperetin-based compounds having a greater antioxidant activity than the naringenin derivatives. In the case of

these hybrids, their activities show a more equilibrated profile, with all activities ranging in micromolar concentrations. However, structural modifications should be made to enhance these activities, perhaps by replacing the flavonoid core for a more antioxidant one, such as quercetin.

## 4.0 Experimental

### 4.01 General procedure for the synthesis of compounds 1.1a and 1.1b.

Anthranilic acid or 4-chloro anthranilic acid (1 equivalent) was dissolved in cyclohexanone (1.1 equivalents) and $POCl_3$ (10 ml) was added to the mixture, which was stirred for 3 hours at 140 °C. Subsequently, the reaction was cooled down at room temperature and quenched with a saturated solution of $K_2CO_3$ and extracted 3 times with DCM (20 ml). The organic extracts were combined, dried with $Na_2SO_4$, and concentrated in vacuo. The residue was washed with hexane to yield the corresponding 9-chloro-1,2,3,4-tetrahydroacridine.

**1.1a. 9-Chloro-1,2,3,4-tetrahydroacridine.** Prepared from anthranilic acid (1.5 g, 6.9 mmol). Brown solid (99% yield).

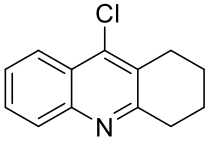


**$^1$H NMR** (250 MHz, $CDCl_3$) δ 8.14 (dd, J = 8.4, 1.5 Hz, 1H), 8.00 (dd, J = 8.5, 1.3 Hz, 1H), 7.65 (ddd, J = 8.4, 6.9, 1.6 Hz, 1H), 7.59 – 7.46 (m, 1H), 3.13 (ddd, J = 6.8, 4.9, 1.8 Hz, 2H), 3.07 – 2.91 (m, 2H), 1.94 (m, 4H). (NMR data consistent with values found in literature)[65].

**1.1b. 6,9-Dichloro-1,2,3,4-tetrahydroacridine.** Prepared from 4-chloroanthranilic acid (1.5 g, 6 mmol). Brown solid (99% yield).

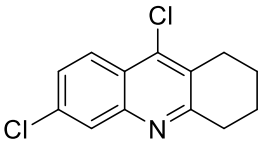


**$^1$H NMR** (250 MHz, MeOD) δ 8.18 (d, J = 9.0 Hz, 1H), 7.91 (d, J = 2.1 Hz, 1H), 7.59 (dd, J = 9.0, 2.1 Hz, 1H), 3.08 (m, 2H), 3.02 (m, 2H), 1.97 (m, 4H). NMR data consistent with values found in literature)[66].

### 4.02 General procedure for the synthesis of compounds 1.2a to 1.2f

To the corresponding 9-chloro-1,2,3,4-tetrahydroacrinine or 6,9-dichloro-1,2,3,4-tetrahydroacrinine (1 equivalent), the suitable diamine (6 equivalents) and phenol (6 equivalents) were added. The mixture was heated up to 110 °C and was stirred for 4 hours. The reaction mixture was subsequently cooled down to room temperature and diluted with dichloromethane. The mixture was then washed 3 times with 1M NaOH and once with brine. The organic phase was dried with $Na_2SO_4$ and concentrated in vacuum to yield compounds **2a**-**2f**.

**1.2a. N1-(1,2,3,4-tetrahydroacridin-9-yl)ethane-1,2-diamine.** Prepared from 9-chloro-1,2,3,4-tetrahydroacridine **1.1a** (0.60 g, 2.76 mmol) and 1,2-ethanediamine (0.99 g, 16.53 mmol). Brown oil (84% yield).

**IR** ($cm^{-1}$): 3290, 2931, 2113, 1561.

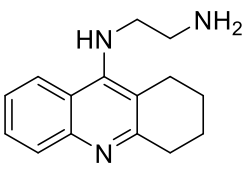


**$^1$H NMR** (250 MHz, $CDCl_3$) δ 7.95 (dd, J = 8.5, 1.7 Hz, 1H), 7.87 (dd, J = 8.5, 1.3 Hz, 1H), 7.48 (ddd, J = 8.4, 6.8, 1.4 Hz, 1H), 7.28 (ddd, J = 8.3, 6.8, 1.3 Hz, 1H), 3.45 (t, J = 5.7 Hz, 2H), 3.01 (m, 2H), 2.93 – 2.86 (t, J = 5.7, 2H), 2.75 – 2.66 (m, 2H), 1.85 (m, 4H).

**$^{13}$C NMR** (63 MHz, $CDCl_3$) δ 158.7, 151.5, 147.5, 128.9, 128.8, 124.1, 123.3, 120.7, 116.7, 51.4, 42.8, 34.2, 25.2, 23.4, 23.2.

**Elemental analysis**. Anal. Calc. for $C_{15}H_{19}N_3$ C, 74.65; H, 7.94; N, 17.41. Found: C, 63.95; H, 7.21; N, 12.78.

**1.2b N1-(1,2,3,4-tetrahydroacridin-9-yl)propane-1,3-diamine.** Prepared from 9-chloro-1,2,3,4-tetrahydroacridine **1.1a** (0.60 g, 2.76 mmol) and 1,3-propanediamine (1.23 g, 16.53 mmol). Brown oil (87% yield).

**IR** ($cm^{-1}$): 3240, 2927, 2856, 2373, 1560.

**$^1$H NMR** (250 MHz, MeOD) δ 7.88 (d, J = 8.5 Hz, 1H), 7.62 (d, J = 8.5 Hz, 1H), 7.34 (t, J = 7.5 Hz, 1H), 7.14 (t, J = 7.7 Hz, 1H), 3.32 (t, J = 7.0 Hz, 2H), 2.76 (t, J = 5.9 Hz, 2H), 2.47 (t, J = 6.7 Hz, 4H), 1.70 – 1.48 (m, 6H).

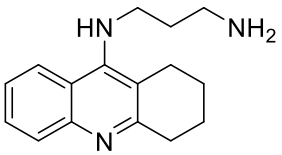


**$^{13}$C NMR** (63 MHz, MeOD) δ 156.6, 150.2, 145.5, 127.0, 125.6, 122.1, 121.7, 118.8, 114.2, 44.8, 37.7, 32.5, 31.7, 23.6, 21.5, 21.1.

**Elemental analysis**. Anal. Calc. for $C_{16}H_{21}N_3$ C, 75.26; H, 8.29; N, 16.46. Found: C, 67.35; H, 9.16; N, 12.84.

**1.2c. N1-(1,2,3,4-tetrahydroacridin-9-yl)butane-1,4-diamine.** Prepared from 9-chloro-1,2,3,4-tetrahydroacridine **1.1a** (0.60 g, 2.76 mmol) and 1,4-butanediamine (1.46 g, 16.53 mmol). Brown oil (87% yield).

**IR** ($cm^{-1}$): 3050, 2923, 2853, 2105, 1559.

**$^1$H NMR** (250 MHz, $CDCl_3$) δ 7.99 – 7.84 (m, 2H), 7.52 (ddd, J = 8.3, 6.8, 1.4 Hz, 1H), 7.35 – 7.26 (m, 1H), 3.51 (t, J = 7.0 Hz, 2H), 3.04 (d, J = 4.9 Hz, 2H), 2.72 (t, J = 6.8 Hz, 1H), 2.65 (s, 2H), 1.87 (p, J = 3.4 Hz, 4H), 1.75 – 1.63 (m, 2H), 1.60 – 1.47 (m, 2H).

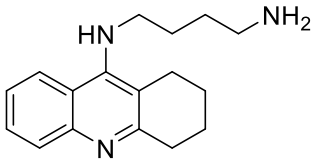


**$^{13}$C NMR** (63 MHz, $CDCl_3$) δ 156.4, 151.7, 146.8, 129.2, 128.2, 124.2, 123.4, 120.1, 116.1, 115.8, 49.7, 42.1, 33.7, 31.3, 25.2, 23.3, 22.9.

**Elemental analysis**. Anal. Calc. for $C_{17}H_{23}N_3$ C, 75.80; H, 8.61; N, 15.60. Found: C, 68.85; H, 7.55; N, 10.87.

**1.2d. N-(6-chloro-1,2,3,4-tetrahydroacridin-9-yl)ethanediamine.** Prepared from 6,9-dichloro-1,2,3,4-tetrahydroacridine **1.1b** (0.6 g, 2.38 mmol) and 1,2-ethanediamine (0.86 g, 14.28 mmol). Brown oil (92% yield).

**IR** ($cm^{-1}$): 3205, 2926, 2857, 2115, 1554.

**$^1$H NMR** (250 MHz, MeOD) δ 8.14 (d, *J* = 9.1 Hz, 1H), 7.77 (d, *J* = 2.2 Hz, 1H), 7.37 (dd, *J* = 9.1, 2.2 Hz, 1H), 3.60 (t, *J* = 6.5 Hz, 2H), 3.00 (m, 2H), 2.91 (t, *J* = 6.5 Hz, 2H), 2.81 (m, 2H), 1.94 (m, 4H).

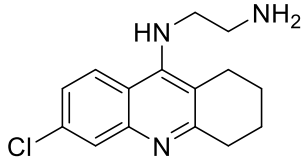


**$^{13}$C NMR** (63 MHz, MeOD) δ 161.2, 149.1, 143.9, 135.9, 127.2, 126.8, 125.7, 120.3, 118.1, 52.3, 43.6, 34.8, 26.5, 24.4, 24.0.

**Elemental analysis**. Anal. Calc. for $C_{15}H_{18}ClN_3$ C, 65.33; H, 6.58; N, 15.24. Found: C, 61.67; H, 6.13; N, 12.97.

**1.2e. N-(6-chloro-1,2,3,4-tetrahydroacridin-9-yl)propane-1,3-diamine.** Prepared from 6,9-dichloro-1,2,3,4-tetrahydroacridine **1.1b** (0.6 g, 2.38 mmol) and 1,3-propanediamine (1.06 g, 14.28 mmol). Brown oil (78% yield).

**IR** ($cm^{-1}$): 3309, 2925, 2855, 2103, 1554.

**$^1$H NMR** (250 MHz, MeOD) δ 8.12 (d, *J* = 9.1 Hz, 1H), 7.74 (d, *J* = 2.2 Hz, 1H), 7.33 (dd, *J* = 9.1, 2.2 Hz, 1H), 3.62 (t, *J* = 7.1 Hz, 2H), 2.97 (m, 2H), 2.73 (m 4H), 1.96 – 1.89 (m, 4H), 1.83 (m, 2H).

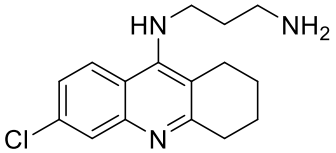


**$^{13}$C NMR** (63 MHz, MeOD) δ 159.4, 125.6, 125.3, 124.1, 118.5, 116.1, 47.2, 46.8, 46.1, 38.8, 33.2, 25.0, 22.9, 22.4.

**Elemental analysis**. Anal. Calc. for $C_{16}H_{20}ClN_3$ C, 66.31; H, 6.96; N, 14.50. Found C, 59.60; H, 6.44; N, 10.96.

**1.2f. N-(6-chloro-1,2,3,4-tetrahydroacridin-9-yl)butane-1,4-diamine.** Prepared from 6,9-dichloro-1,2,3,4-tetrahydroacridine **1.1b** (0.6 g, 2.38 mmol) and 1,4-butanediamine (1.26 g, 14.28 mmol). Brown oil (82% yield).

**IR** ($cm^{-1}$): 3288, 2925, 2855, 2118, 1555.

**$^1$H NMR** (250 MHz, MeOD) δ 7.95 (d, *J* = 9.1 Hz, 1H), 7.68 (d, *J* = 2.2 Hz, 1H), 7.18 (dd, *J* = 9.1, 2.2 Hz, 1H), 3.45 (t, *J* = 7.1 Hz, 2H), 2.88 (m, 2H), 2.62 (m, 4H), 1.82 (m, 4H), 1.63 (m, 2H), 1.58 – 1.40 (m, 2H).

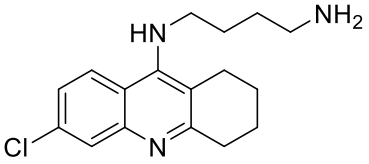


**$^{13}$C NMR** (63 MHz, MeOD) δ 160.7, 153.3, 149.1, 135.7, 127.2, 126.9, 125.3, 119.8, 117.0, 50.0, 42.7, 34.8, 31.4, 30.2, 26.4, 24.4, 24.0.

**Elemental analysis**. Anal. Calc. for $C_{17}H_{22}ClN_3$ C, 67.20, H, 7.30; N, 13.83. Found: C, 64.18; H, 6.85; N, 10.51.

**4.03 Procedure for the synthesis of compound 1.3**

Naringenin (0.5 g, 1.8 mmol) was dissolved in ethanol (30 ml) and butylamine 0.144 g, 2.0 mmol) was added to the mixture, which was stirred for 30 minutes. Subsequently, the solvent was evaporated and (E)-4-(butylimino)-2-(4-hydroxyphenyl)chromane-5,7-diol was isolated as a brown oil (0.59 g, 99% yield).

**$^1$H NMR** (250 MHz, MeOD) δ 7.28 (d, J = 8.6 Hz, 2H), 6.83 (d, J = 8.6 Hz, 2H), 5.73 – 5.62 (m, 1H), 5.20 (dd, J = 12.6, 3.0 Hz, 1H), 3.07 – 2.89 (m, 1H), 2.80 (dd, J = 8.2, 6.7 Hz, 2H), 2.53 (s, 1H), 1.67 – 1.48 (m, 2H), 1.48 – 1.26 (m, 2H), 0.94 (t, J = 7.2 Hz, 3H).

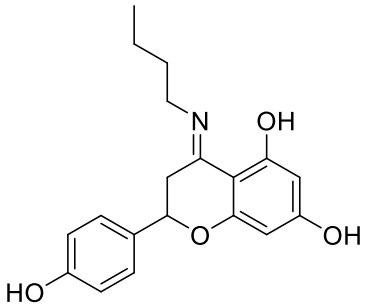


**$^{13}$C NMR** (63 MHz, MeOD) δ 193.9, 178.4, 178.4, 164.7, 164.7, 163.7, 158.3, 130.4, 128.0, 115.6, 99.9, 99.1, 98.5, 78.9, 42.9, 40.0, 31.3, 19.9, 13.2.

**4.04 Procedure for the synthesis of compound 1.4a**

Naringenin (0.5 g, 1.8 mmol) was dissolved in acetone (30 ml) and $K_2CO_3$ (1.0 g, 7.4 mmol) and dimethyl sulphate (0.92 g, 7.4 mmol) were added to the mixture, which was warmed to 50 °C and stirred overnight. The reaction was cooled down to room temperature, diluted with ethyl acetate (50 ml) and water (25 ml) was added to the mixture. The two phases were separated, and the organic phase was washed with water (25 ml) two more times and with brine (25 ml) once. The organic phase was dried with $Na_2SO_4$ and concentrated in vacuo to give a residue that was purified by column chromatography (20-70% ethyl acetate in petroleum ether) to yield trimethylnaringenin as an off-white solid (0.25 g, 43% yield)

**Mp**: 90 °C.

**IR** ($cm^{-1}$): 2960, 2300, 2104, 1662, 1601.

**$^1$H NMR** (250 MHz, $CDCl_3$) δ 7.39 – 7.27 (m, 2H), 6.96 – 6.81 (m, 2H), 6.07 (d, *J* = 2.2 Hz, 1H), 6.03 (q, *J* = 2.5 Hz, 1H), 5.29 (dd, *J* = 13.1, 3.0 Hz, 1H), 3.83 (d, *J* = 1.3 Hz, 3H), 3.76 (d, *J* = 1.1 Hz, 3H), 3.75 (d, *J* = 1.1 Hz, 3H), 2.98 (ddd, *J* = 16.5, 13.2, 1.2 Hz, 1H), 2.78 – 2.62 (m, 1H).

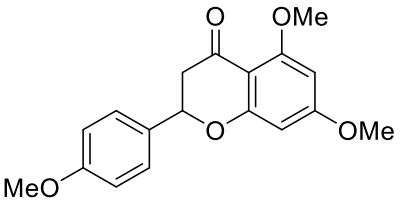


**$^{13}$C NMR** (63 MHz, $CDCl_3$) δ 190.0, 166.4, 165.5, 162.7, 160.3, 131.2, 128.1, 114.6, 106.4, 93.9, 93.5, 79.4, 56.6, 56.0, 55.8, 45.8.

**Elemental analysis**. Anal. Calc. for $C_{18}H_{18}O_5$ C, 68.78; H, 5.77; N, 0.00. Found: C, 68.04; H, 6.14; N, 0.13.

**4.05 Procedure for the synthesis compound 1.5a**

2,4 dimethoxy acetophenone (2.0 g, 11 mmol) and 4-methoxy benzaldehyde (1.5 g, 11 mmol) were dissolved in ethanol (40 ml) and 6 M NaOH (0.11 g, 2.7 mmol) was added to the mixture, which was stirred at room temperature for 2 hours. The reaction mixture was filtered and the solid washed with petroleum spirit and dried to yield 3-(4-methoxyphenyl)prop-2-en-1-one as a pale yellow solid (3.3 g, 99% yield).

**Mp**: 83 °C.

**IR** ($cm^{-1}$): 3175, 3004, 2968, 2841, 2096, 1643.

**$^1$H NMR** (250 MHz, $CDCl_3$) δ 7.65 (d, *J* = 8.6 Hz, 1H), 7.56 (d, *J* = 15.7 Hz, 1H), 7.51 – 7.41 (m, 2H), 7.30 (d, *J* = 15.8 Hz, 1H), 6.82 (d, *J* = 8.8 Hz, 2H), 6.46 (dd, *J* = 8.6, 2.3 Hz, 1H), 6.40 (d, *J* = 2.3 Hz, 1H), 3.80 (s, 3H), 3.76 (s, 3H), 3.74 (s, 3H).

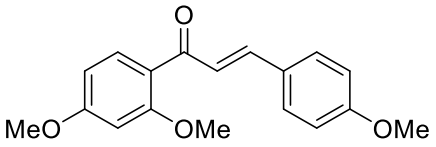


**$^{13}$C NMR** (63 MHz, $CDCl_3$) δ 191.1, 164.4, 161.7, 160.7, 142.5, 133.1, 130.4, 128.5, 125.4, 122.8, 114.7, 105.5, 99.0, 56.2, 56.0, 55.8.

**Elemental analysis**. Anal. Calc. for $C_{18}H_{18}O_4$ C, 72.47; H, 6.08; N, 0.00. Found: C, 71.84; H, 6.07; N, 0.04.

### 4.06 Procedure for the synthesis of compound 1.5b

(E)-1-(2,4-dimethoxyphenyl)-3-(4-methoxyphenyl)prop-2-en-1-one (1.5 g, 5.0 mmol) was dissolved in dry DCM (20 ml) under inert atmosphere and 10 ml of a 1M solution of $BBr_3$ in xxx was added dropwise at -78 °C. The solution was allowed to warm up at room temperature and was stirred for 3 hours. The reaction was quenched using a saturated solution of $K_2CO_3$ until pH 8 and then adjusted to a pH 5 using 0.5 M HCl. The aqueous phase was extracted three times using 15 ml of EtOAc and the extracts combined together, dried using $Na_2SO_4$ and concentrated in vacuo to yield (E)-1-(2-hydroxy-4-methoxyphenyl)-3-(4-hydroxyphenyl)prop-2-en-1-one as a yellow solid (1.34 g, 98% yield).

**Mp**: 107 °C.

**IR** ($cm^{-1}$): 3187, 2934, 2836, 1651,

**$^1$H NMR** (250 MHz, $CDCl_3$) δ 13.55 (s, 1H), 7.90 – 7.79 (m, 2H), 7.58 (d, *J* = 8.6 Hz, 2H), 7.46 (d, *J* = 15.4 Hz, 1H), 6.92 – 6.85 (m, 2H), 6.53 – 6.45 (m, 2H), 3.86 (s, 3H).

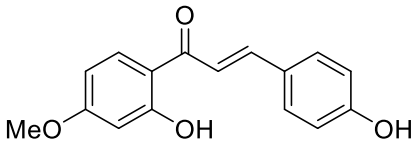


**$^{13}$C NMR** (63 MHz, $CDCl_3$) δ 192.1, 166.8, 166.2, 158.0, 144.1, 131.5, 130.7, 127.9, 118.1, 116.1, 114.3, 108.2, 101.2, 55.7.

**Elemental analysis**. Anal. Calc. for $C_{16}H_{14}O_4$ C, 71.10; H, 5.22; N, 0.00. Found: C, 70.23; H, 5.27; N, 0.31.

### 4.07 Procedure for the synthesis of compound 1.5c

Acetyl chloride (4.71 g, 60 mmol) was dissolved in 20 ml of methanol at a temperature of 0 °C under argon and stirred at room temperature for 30 minutes. (E)-1-(2-hydroxy-4-methoxyphenyl)-3-(4-hydroxyphenyl)prop-2-en-1-one (1g, 3.7 mmol) was dissolved in this mixture under argon and refluxed overnight. The reaction mixture was cooled down to room temperature and concentrated in vacuo to yield a residue that was redissolved in ethyl acetate (20 ml) and washed with water (10 ml) three times. The organic phase was dried with $Na_2SO_4$ and concentrated in vacuo to yield a solid residue that was purified by column chromatography (20-70% ethyl acetate in petroleum ether) to yield 2-(4-hydroxyphenyl)-7-methoxychroman-4-one as a yellow solid (0.51 g, 51% yield).

**Mp**: 142 °C.

**IR** ($cm^{-1}$): 3140, 2960, 2831, 1660, 1601.

**$^1$H NMR** (250 MHz, $CDCl_3$) δ 7.87 (d, *J* = 8.8 Hz, 1H), 7.40 – 7.32 (m, 2H), 6.94 – 6.83 (m, 2H), 6.61 (dd, *J* = 8.8, 2.4 Hz, 1H), 6.48 (d, *J* = 2.4 Hz, 1H), 5.41 (dd, *J* = 13.2, 3.0 Hz, 1H), 3.83 (s, 3H), 3.06 (dd, *J* = 16.9, 13.2 Hz, 1H), 2.80 (dd, *J* = 16.9, 3.0 Hz, 1H).

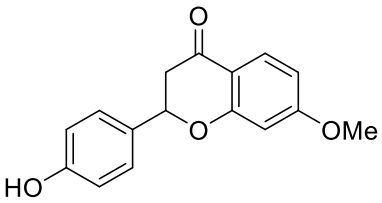


**$^{13}$C NMR** (63 MHz, $CDCl_3$) δ 191.2, 166.4, 163.8, 156.2, 131.0, 128.9, 128.1, 115.8, 114.9, 110.4, 101.0, 79.9, 55.8, 44.2.

**Elemental analysis**. Anal. Calc. for $C_{16}H_{14}O_4$ C, 71.10; H, 5.22; N, 0.00. Found: C, 70.08; H, 5.61; N, 0.12.

### 4.08 Procedure for the synthesis of compound 1.5d

2-(4-hydroxyphenyl)-7-methoxychroman-4-one (0.5g, 3.6 mmol) was dissolved in pyridine (10 ml) and O-methyl hydroxylamine hydrochloride was added to the mixture, which was heated to reflux for 2 hours. The mixture was cooled down to room temperature and diluted in ethyl acetate (30 ml). The mixture was washed with a 0.5 M solution of HCl (10 ml) three times, dried with $Na_2SO_4$ and concentrated in vacuo to yield (E)-2-(4-hydroxyphenyl)-7-methoxychroman-4-one O-methyl oxime as a brown solid (0.53 g, 97% yield)

**Mp**: 134 °C.

**IR** ($cm^{-1}$): 3374, 2930, 2506, 1603.

**$^1$H NMR** (250 MHz, MeOD) δ 7.76 (d, *J* = 8.8 Hz, 1H), 7.30 – 7.23 (m, 2H), 6.84 – 6.76 (m, 2H), 6.54 (dd, *J* = 8.8, 2.5 Hz, 1H), 6.44 (d, *J* = 2.5 Hz, 1H), 4.95 (dd, *J* =17.2, 3.1 Hz, 1H), 3.91 (s, 3H), 3.76 (s, 3H), 3.26 (dd, *J* = 12.2, 3.1 Hz, 1H), 2.62 (dd, *J* = 17.2, 12.2 Hz, 1H).

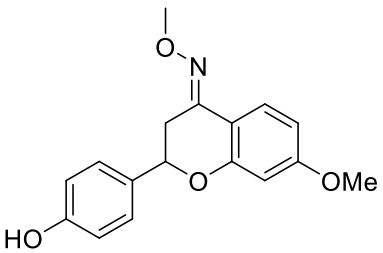


**$^{13}$C NMR** (63 MHz, MeOD) δ 162.7, 158.6, 157.7, 149.4, 131.2, 127.8, 127.7, 125.1, 115.2, 111.1, 109.3, 101.6, 77.6, 61.2, 54.8, 30.6.

**Elemental analysis**. Anal. Calc. for $C_{17}H_{17}NO_4$ C, 68.22; H, 5.72; N, 4.68. Found: C, 67.72; H, 6.10; N, 4.29.

### 4.09 General procedure for the synthesis of compound 1.6a and 1.6b

The suitable flavonoid (1 equivalent) and O-carboxymethyl hydroxylamine hydrochloride (2 equivalents) were dissolved in pyridine (5 ml) and the mixture was heated at 110 °C for 2h. The reaction mixture was cooled down to room temperature and diluted in ethyl acetate (20 ml). The organic mixture was extracted with 0.5 M hydrochloric acid (5 x 5 ml) and dried with $Na_2SO_4$. The organic extract was concentrated in vacuo to yield oximes **1.6a** and **1.6b**.

**1.6a. (*E*)-2-(((5,7-Dihydroxy-2-(4-hydroxyphenyl) chroman-4-ylidene)amino)oxy)acetic acid.**
Prepared from naringenin (0.5 g, 1.83 mmol). Off-white solid (99% yield).

**Mp**: 170 °C.

**IR** ($cm^{-1}$): 3442, 3122, 2929, 1698, 1604.

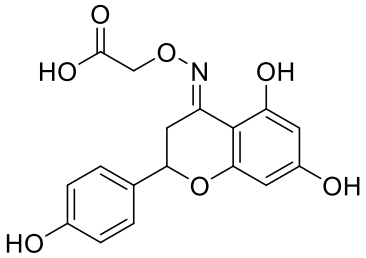

**$^1$H NMR** (250 MHz, MeOD) δ 7.29 (d, *J* = 7.9 Hz, 2H), 6.81 (d, *J* = 7.9 Hz, 2H), 5.92 (d, *J* = 3.2 Hz, 1H), 4.52 (s, 2H), 3.58 – 3.44 (m, 1H), 2.74 (dd, *J* = 17.2, 12.3 Hz, 1H).

**$^{13}$C NMR** (63 MHz, MeOD) δ 197.7, 161., 159.7, 159.2, 157.6, 155.0, 130.8, 127.7, 115.1, 97.0, 96.5, 95.4, 76.8, 30.5.

**Elemental analysis**. Anal. Calc. for $C_{17}H_{15}NO_7$ C, 59.13; H, 4.38; N, 4.06. Found: C, 59.57, H, 4.81; N, 6.02.

**1.6b. (*E*)-2-(((5,7-Dihydroxy-2-(3-hydroxy-4-methoxyphenyl)chroman-4-ylidene)amino)oxy)acetic acid.** Prepared from hesperetin (0.5 g, 1.65 mmol). Off-white solid (99% yield).

**Mp**: 109 °C.

**IR** ($cm^{-1}$): 3279, 2921, 2095, 1723, 1633, 1606.

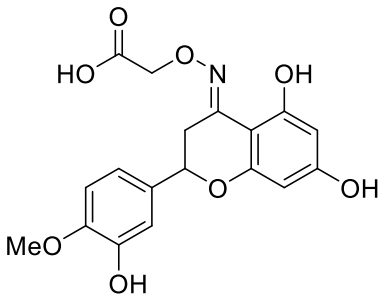

**$^1$H NMR** (250 MHz, MeOD) δ 6.95 (m, 3H), 6.01 – 5.91 (m, 2H), 4.65 (s, 2H), 3.88 (s, 3H), 3.52 (dd, *J* = 17.4, 2.8 Hz, 1H), 2.77 (dd, *J* = 17.2, 12.0 Hz, 1H).

**$^{13}$C NMR** (63 MHz, MeOD) δ 185.7, 163.0, 161.3, 160.7, 157.3, 149.5, 148.1, 134.3, 119.3, 114.8, 112.9, 98.4, 98.2, 97.1, 78.1, 72.8, 56.8, 50.3, 32.0.

**Elemental analysis**. Anal. Calc. for $C_{18}H_{17}N_3O_8$ C, 57.60; H, 4.57; N, 3.73. Found: C, 57.29; H, 4.85; N, 3.89.

**4.10 General procedure for the synthesis of compounds 1.7a to 1.7k**

The correspondent flavonoid oxime carboxylic acid (1 equivalent) and N-1(1,2,3,4-tetrahydroacrydin-9-yl) diamine (1 equivalent) were dissolved in a mixture of 4:1 dichloromethane/methanol mixture (5 ml) together with EDCI (1.5 equivalents) and HOBt (1.5 equivalents) and the mixture was stirred at room temperature overnight. The reaction was quenched with water (5 ml) and the mixture was extracted with ethyl acetate (10 ml) five times. The organic extract was dried with $Na_2SO_4$ and concentrated in vacuo to yield a solid that was then purified by column chromatography (9:1 dichloromethane/methanol) to yield compounds **1.7a**-**1.7k**.

**1.7a. (*E*)-2-(((5,7-Dihydroxy-2-(4-hydroxyphenyl)chroman-4-ylidene)amino)oxy)-N-(2-((1,2,3,4-tetrahydroacridin-9-yl)amino)ethyl)acetamide.** Prepared from compounds **1.2a** (60 mg, 0.24 mmol) and **1.6a** (85 mg, 0.24 mmol). Brown solid (27% yield).

**Mp**: 201 °C.

**IR** ($cm^{-1}$): 3249, 3097, 2926, 2107, 1628, 1577.

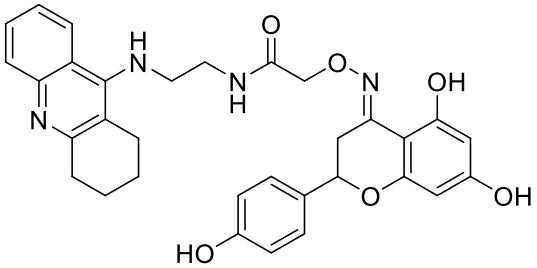

**$^1$H NMR** (500 MHz, MeOD) δ 8.42 (d, *J* = 8.8 Hz, 1H), 7.80 (m, 1H), 7.71 (d, *J* = 8.2 Hz, 1H), 7.59 – 7.52 (m, 1H), 7.30 – 7.25 (m, 2H), 6.87 – 6.81 (m, 2H), 5.86 (d, *J* = 1.7 Hz, 1H), 5.50 (d, *J* = 2.1 Hz, 1H), 4.82 (dd, *J* = 12.4, 3.0 Hz, 1H), 4.58 (s, 2H), 4.22 – 4.13 (m, 2H), 3.87 – 3.78 (m, 1H), 3.72 (dt, *J* = 14.5, 5.0 Hz, 1H), 3.42 (dd, *J* = 17.4, 3.2 Hz, 1H), 2.90 (d, *J* = 5.1 Hz, 2H), 2.73 – 2.64 (m, 3H), 1.88 (d, *J* = 5.8 Hz, 4H).

**$^{13}$C NMR** (126 MHz, MeOD) δ 172.4, 161.3, 159.2, 159.0, 157.5, 156.2, 156.1, 132.1, 130.2, 127.4, 124.8, 119.5, 116.2, 114.9, 111.6, 96.2, 96.1, 95.3, 76.3, 72.7, 53.4, 49.8, 38.5, 30.0, 28.4, 23.8, 21.7, 20.5.

**Elemental analysis**. Anal. Calc. for $C_{32}H_{32}N_4O_6$ C, 67.59; H, 5.67; N, 9.85. Found C 66.78; H, 5.59; N, 9.88.

**1.7b. (*E*)-2-(((5,7-Dihydroxy-2-(4-hydroxyphenyl)chroman-4-ylidene)amino)oxy)-N-(2-((1,2,3,4-tetrahydroacridin-9-yl)amino)propyl)acetamide.** Prepared from compounds **1.2b** (63 mg, 0.24 mmol) and **1.6a** (85 mg, 0.24 mmol). Brown solid (22% yield).

**Mp**: 194 °C.

**IR** ($cm^{-1}$): 3091, 2934, 2100, 1632, 1589.

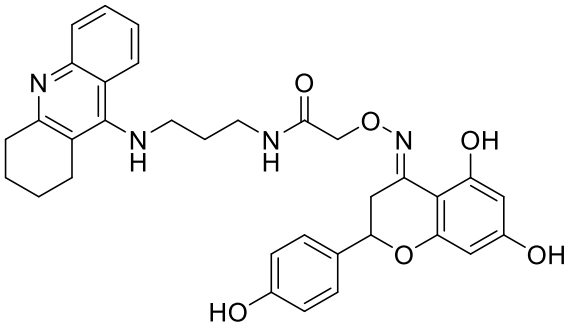

**$^1$H NMR** (250 MHz, MeOD) δ 8.41 – 8.21 (m, 1H), 7.83 – 7.64 (m, 2H), 7.57 – 7.44 (m, 1H), 7.33 – 7.19 (m, 2H), 6.89 – 6.75 (m, 2H), 5.78 (d, *J* = 2.3 Hz, 1H), 5.66 (d, *J* = 2.3 Hz, 1H), 4.81 (dd, *J* = 12.5, 3.0 Hz, 2H), 4.54 (s, 2H), 3.93 (t, *J* = 7.1 Hz, 2H), 3.50 – 3.37 (m, 3H), 2.96 (d, *J* = 5.2 Hz, 2H), 2.75 – 2.59 (m, 3H), 2.03 (q, *J* = 6.3 Hz, 2H), 1.93 (s, 4H).

**$^{13}$C NMR** (63 MHz, MeOD) δ 172.9, 163.1, 161.1, 160.8, 159.3, 158.3, 158.2, 151.9, 140.2, 134.3, 132.0, 129.2, 127.0, 126.7, 120.6, 117.5, 116.7, 113.4, 97.9, 97.1, 78.1, 74.6, 47.2, 37.5, 32.1, 31.8, 29.7, 25.2, 23.4, 22.2.

**Elemental analysis**. Anal. Calc. for $C_{33}H_{34}N_4O_6$ C, 68.03; H, 5.88; N, 9.62. Found: C, 67.58; H, 5.70; N, 9.46.

**1.7c. (*E*)-2-(((5,7-Dihydroxy-2-(4-hydroxyphenyl)chroman-4-ylidene)amino)oxy)-N-(4-((1,2,3,4-tetrahydroacridin-9-yl)amino)butyl)acetamide.** Prepared from compounds **1.2c** (66 mg, 0.24 mmol) and **1.6a** (85 mg, 0.24 mmol). Brown solid (29% yield).

**Mp**: 153 °C.

**IR** ($cm^{-1}$): 3081, 2927, 2863, 2106, 1632, 1591.

**$^1$H NMR** (500 MHz, MeOD) δ 8.36 – 8.28 (m, 1H), 7.89 – 7.80 (m, 1H), 7.74 (dd, *J* = 8.5, 1.3 Hz, 1H), 7.64 – 7.53 (m, 1H), 7.34 – 7.27 (m, 2H), 6.89 – 6.79 (m, 2H), 5.86 – 5.78 (m, 1H), 5.70 – 5.59 (m, 1H), 4.55 (d, *J* = 1.7 Hz, 2H), 3.92 (t, *J* = 7.5 Hz, 2H), 3.50 (dd, *J* = 17.3, 3.1 Hz, 1H), 3.42 – 3.37 (m, 2H), 3.00 (s, 2H), 2.79 (dd, *J* = 17.3, 12.3 Hz, 1H), 2.61 (s, 2H), 1.96 (d, *J* = 3.6 Hz, 4H), 1.87 (p, *J* = 7.7 Hz, 2H), 1.71 (q, *J* = 6.9 Hz, 2H).

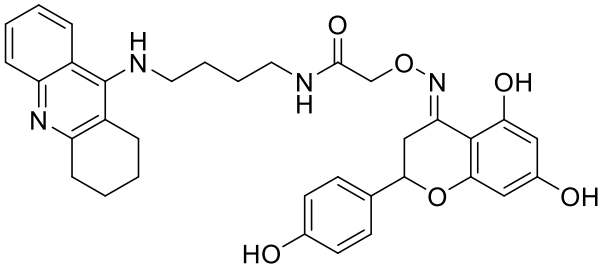

**$^{13}$C NMR** (126 MHz, MeOD) δ 170.6, 161.3, 161.2, 159.3, 159.0, 157.5, 156.5, 156.2, 150.1, 138.4, 132.6, 130.2, 127.4, 125.1, 124.9, 118.7, 115.5, 114.9, 111.3, 96.2, 96.2, 95.3, 76.3, 72.8, 38.1, 30.0, 27.9, 27.6, 26.2, 23.3, 21.5, 20.4.

**Elemental analysis**. Anal. Calc. for $C_{34}H_{36}N_4O_6$ C, 68.44; H, 6.08; N, 9.39. Found: C, 67.98; H, 5.85; N, 9.65.

**1.7d. (*E*)-N-(2-((6-Chloro-1,2,3,4-tetrahydroacridin-9-yl)amino)ethyl)-2-(((5,7-dihydroxy-2-(4-hydroxyphenyl)chroman-4-ylidene)amino)oxy)acetamide.** Prepared from compounds **1.2d** (68 mg, 0.24 mmol) and **1.6a** (85 mg, 0.24 mmol). Brown solid (25% yield).

**Mp**: 217 °C.

**IR** (cm$^{-1}$): 3203, 3082, 2922, 2853, 2101, 1630, 1576.

**$^1$H NMR** (250 MHz, MeOD) δ 8.42 (d, *J* = 9.3 Hz, 1H), 7.69 (d, *J* = 2.2 Hz, 1H), 7.54 (dd, *J* = 9.3, 2.1 Hz, 1H), 7.36 – 7.24 (m, 2H), 6.91 – 6.79 (m, 2H), 5.86 (d, *J* = 2.3 Hz, 1H), 5.42 (d, *J* = 2.3 Hz, 1H), 4.90 – 4.76 (m, 1H), 4.59 (s, 2H), 4.17 (s, 2H), 3.93 – 3.64 (m, 3H), 2.88 (s, 2H), 2.76 – 2.57 (m, 4H), 1.88 (s, 4H).

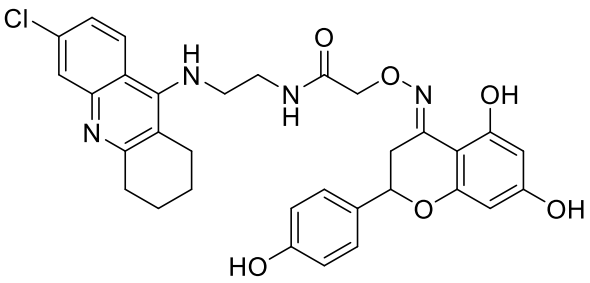

**$^{13}$C NMR** (63 MHz, MeOD) δ 174.4, 163.1, 160.9, 159.8, 157.9, 140.1, 131.9, 129.2, 127.1, 116.7, 113.7, 97.8, 97.1, 78.1, 74.5, 67.2, 51.9, 40.2, 31.9, 30.1, 25.6, 23.4, 22.1, 20.2.

**Elemental analysis**. Anal. Calc. for $C_{32}H_{31}ClN_4O_6$ C, 63.73; H, 5.18; N, 9.29. Found: C, 62.24; H, 5.16; N, 8.98.

**1.7e. (*E*)-N-(3-((6-Chloro-1,2,3,4-tetrahydroacridin-9-yl)amino)propyl)-2-(((5,7-dihydroxy-2-(4-hydroxyphenyl)chroman-4-ylidene)amino)oxy)acetamide.** Prepared from compounds **1.2d** (71 mg, 0.24 mmol) and **1.6**a (85 mg, 0.24 mmol). Brown solid (32% yield).

**Mp**: 191 °C.

**IR** (cm$^{-1}$): 3309, 2931, 2109, 1630, 1601.

**$^1$H NMR** (250 MHz, MeOD) δ 8.38 (d, *J* = 9.3 Hz, 1H), 7.74 (d, *J* = 2.2 Hz, 1H), 7.47 (dd, *J* = 9.3, 2.2 Hz, 1H), 7.34 – 7.28 (m, 2H), 6.88 – 6.81 (m, 2H), 5.75 (d, *J* = 2.3 Hz, 1H), 5.57 (d, *J* = 2.4 Hz, 1H), 4.56 (s, 2H), 3.94 (t, *J* = 7.5 Hz, 2H), 3.57 – 3.42 (m, 3H), 3.00 (d, *J* = 5.9 Hz, 2H), 2.79 – 2.59 (m, 3H), 2.09 (s, 2H), 2.02 – 1.92 (m, 4H).

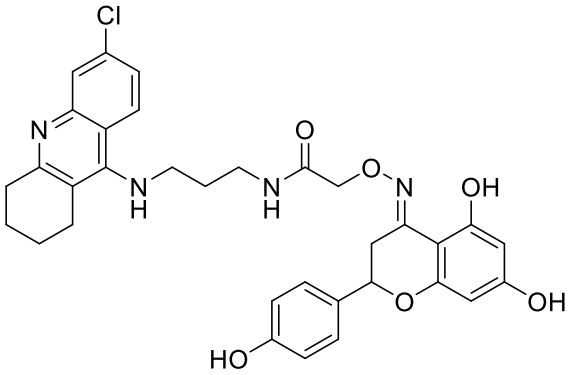


**$^{13}$C NMR** (63 MHz, MeOD) δ 172.9, 162.9, 160.9, 160.7, 159.2, 158.2, 157.7, 152.3, 141.0, 140.2, 132.1, 129.3, 127.1, 119.7, 116.7, 115.8, 113.7, 97.9, 97.1, 78.1, 74.7, 50.5, 47.9, 37.6, 31.9, 31.8, 29.8, 25.0, 23.2, 22.2.

**Elemental analysis**. Anal. Calc. for $C_{33}H_{33}ClN_4O_6$ C, 64.23; H, 5.39; N, 9.08. Found: C, 63.89; H, 5.22; N, 8.68.

**1.7f. (*E*)-N-(4-((6-Chloro-1,2,3,4-tetrahydroacridin-9-yl)amino)butyl)-2-(((5,7-dihydroxy-2-(4-hydroxyphenyl)chroman-4-ylidene)amino)oxy)acetamide.** Prepared from compounds **1.2e** (75 mg, 0.24 mmol) and **1.6a** (85 mg, 0.24 mmol). Brown solid (29% yield).

**Mp**: 208 °C.

**IR** (cm$^{-1}$): 3223, 3085, 2930, 2108, 1630, 1573.

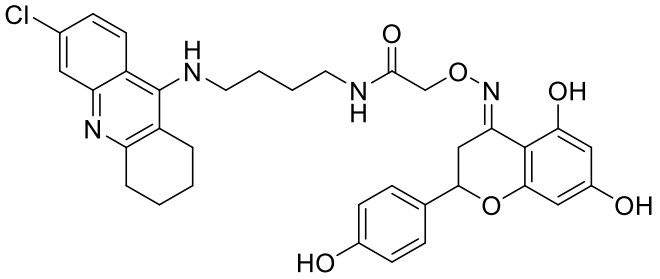


**$^1$H NMR** (250 MHz, MeOD) δ 8.23 (d, *J* = 9.3 Hz, 1H), 7.72 (d, *J* = 2.2 Hz, 1H), 7.53 (dd, *J* = 9.2, 2.2 Hz, 1H), 7.35 – 7.24 (m, 2H), 6.89 – 6.78 (m, 2H), 5.77 (d, *J* = 2.3 Hz, 1H), 5.57 (d, *J* = 2.3 Hz, 1H), 4.55 (s, 2H), 3.86 (t, *J* = 7.5 Hz, 2H), 3.50 (dd, *J* = 17.3, 3.1 Hz, 1H), 3.42 (d, *J* = 6.1 Hz, 3H), 2.97 (s, 2H), 2.76 (dd, *J* = 17.3, 12.4 Hz, 1H), 2.57 (s, 2H), 2.00 – 1.91 (m, 4H), 1.86 (d, *J* = 7.8 Hz, 2H), 1.73 (d, *J* = 7.1 Hz, 2H).

**$^{13}$C NMR** (63 MHz, MeOD) δ 172.5, 163.0, 161.0, 160.8, 159.3, 158.3, 157.5, 140.1, 132.0, 129.3, 127.1, 120.0, 116.7, 115.8, 113.7, 98.0, 97.9, 97.0, 78.2, 74.7, 50.4, 39.9, 31.8, 30.0, 29.4, 27.9, 25.0, 23.3, 23.1, 22.2.

**Elemental analysis**. Anal. Calc. for $C_{34}H_{35}ClN_4O_6$ C, 64.71; H, 5.59; N, 8.88. Found: C, 64.36; H, 5.49; N, 8.59.

**1.7g. (*E*)-2-(((5,7-Dihydroxy-2-(3-hydroxy-4-methoxyphenyl)chroman-4-ylidene)amino)oxy)-N-(2-((1,2,3,4-tetrahydroacridin-9-yl)amino)ethyl)acetamide.** Prepared from compounds **1.2a** (55 mg, 2.26 mmol)and **1.6b** (85 mg, 2.26 mmol). Pale brown solid (25% yield).

**Mp**: 191 °C.

**IR** (cm$^{-1}$): 3193, 3070, 2931, 2109, 1631, 1576.

**$^1$H NMR** (250 MHz, MeOD) δ 8.43 (d, *J* = 8.6 Hz, 1H), 7.81 (ddd, *J* = 7.9, 6.8, 1.0 Hz, 1H), 7.71 (dd, *J* = 8.5, 1.4 Hz, 1H), 7.55 (ddd, *J* = 8.5, 6.8, 1.4 Hz, 1H), 6.98 – 6.82 (m, 3H), 5.84 (d, *J* = 2.3 Hz, 1H), 5.43 (d, *J* = 2.3 Hz, 1H), 4.76 (dd, *J* = 12.2, 3.0 Hz, 1H), 4.59 (s, 2H), 4.17 (m, 2H), 3.87 (s, 4H), 3.85 – 3.65 (m, 2H), 2.88 (s, 2H), 2.69 – 2.54 (m, 3H), 1.85 (m, 4H).

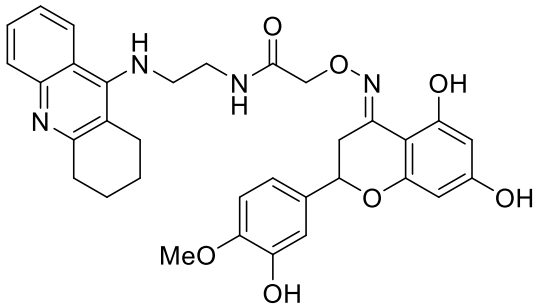


**$^{13}$C NMR** (63 MHz, MeOD) δ 174.3, 163.0, 160.9, 160.6, 158.2, 157.8, 152.1, 149.6, 148.1, 140.0, 134.3, 134.0, 126.8, 126.7, 120.6, 119.2, 117.6, 114.8, 113.0, 112.9, 98.0, 97.9, 97.1, 77.9, 74.5, 56.8, 51.7, 40.3, 31.9, 29.7, 25.5, 23.4, 22.1.

**Elemental analysis**. Anal. Calc. for $C_{33}H_{34}N_4O_7$ C, 66.21; H, 5.72; N, 9.36. Found: C, 65.84; H, 5.62; N, 9.06.

**1.7h. (*E*)-2-(((5,7-Dihydroxy-2-(3-hydroxy-4-methoxyphenyl)chroman-4-ylidene)amino)oxy)-N-(3-((1,2,3,4-tetrahydroacridin-9-yl)amino)propyl)acetamide.** Prepared from compounds **1.2b** (58 mg, 2.26 mmol) and **1.6b** (85 mg, 2.26 mmol). Pale brown solid (31% yield).

**Mp**: 180 °C.

**IR** (cm$^{-1}$): 3069, 2925, 2113, 1632, 1587.

**$^1$H NMR** (250 MHz, MeOD) δ 8.35 (d, *J* = 8.7 Hz, 1H), 7.83 – 7.69 (m, 2H), 7.52 (ddd, *J* = 8.4, 6.6, 1.6 Hz, 1H), 6.97 – 6.82 (m, 3H), 5.80 (d, *J* = 2.3 Hz, 1H), 5.67 (d, *J* = 2.3 Hz, 1H), 4.79 (dd, *J* = 12.1, 3.0 Hz, 2H), 4.56 (s, 2H), 3.94 (t, *J* = 7.2 Hz, 2H), 3.87 (s, 3H), 3.54 – 3.45 (m, 2H), 3.00 (d, *J* = 6.4 Hz, 2H), 2.74 – 2.58 (m, 3H), 2.08 (m, 2H), 2.03 – 1.88 (m, 4H).

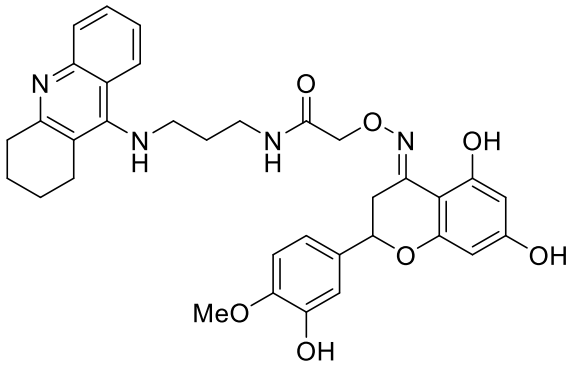


**$^{13}$C NMR** (63 MHz, MeOD) δ 172.9, 163.1, 161.0, 160.6, 158.1, 151.9, 149.6, 148.1, 140.2, 134.3, 134.1, 127.0, 126.7, 120.6, 119.2, 117.5, 114.8, 113.3, 112.9, 98.0, 97.9, 97.1, 77.9, 74.6, 56.8, 47.3, 37.5, 32.1, 31.8, 29.7, 25.2, 23.4, 22.2.

**Elemental analysis**. Anal. Calc. for $C_{34}H_{36}N_4O_7$ C, 66.65; H, 5.92; N, 9.14. Found: C, 65.87; H, 5.52; N, 9.45.

**1.7i. (*E*)-2-(((5,7-Dihydroxy-2-(3-hydroxy-4-methoxyphenyl)chroman-4-ylidene)amino)oxy)-N-(4-((1,2,3,4-tetrahydroacridin-9-yl)amino)butyl)acetamide.** Prepared from compounds **1.2c** (61 mg, 2.26 mmol) and **1.6b** (85 mg, 2.26 mmol). Brown solid (17% yield).

**Mp**: 172 °C.

**IR** (cm$^{-1}$): 3069, 2925, 2102, 1631, 1586.

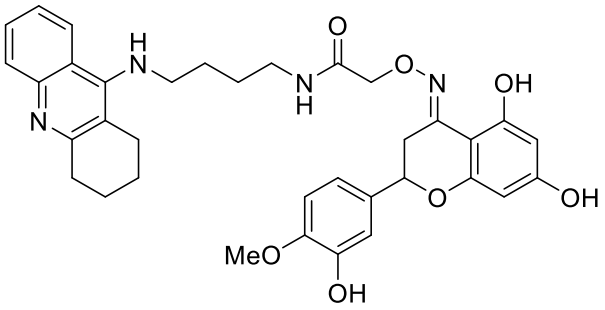

**$^1$H NMR** (250 MHz, MeOD) δ 8.31 (d, *J* = 8.6 Hz, 1H), 7.88 – 7.79 (m, 1H), 7.74 (dd, *J* = 8.6, 1.5 Hz, 1H), 7.61 – 7.53 (m, 1H), 7.02 – 6.82 (m, 3H), 5.80 (d, *J* = 2.3 Hz, 1H), 5.62 (d, *J* = 2.3 Hz, 1H), 4.90 – 4.82 (m, 2H), 4.55 (s, 2H), 3.94 – 3.85 (m, 5H), 3.49 (dd, *J* = 17.3, 3.2 Hz, 1H), 3.40 (t, *J* = 5.5 Hz, 2H), 3.00 (m, 2H), 2.76 (dd, *J* = 17.3, 12.0 Hz, 1H), 2.59 (m, 2H), 2.03 – 1.91 (m, 4H), 1.86 (m, 2H), 1.71 (m, 2H).

**$^{13}$C NMR** (63 MHz, MeOD) δ 172.5, 163.1, 161.1, 160.6, 158.1, 158.0, 151.9, 149.6, 148.2, 140.3, 134.4, 134.1, 127.0, 126.7, 120.6, 119.2, 117.3, 114.8, 113.1, 112.9, 98.0, 97.1, 77.9, 74.7, 56.8, 39.9, 31.8, 29.7, 29.5, 28.0, 25.1, 23.3, 22.2.

**Elemental analysis**. Anal. Calc. for $C_{35}H_{38}N_4O_7$ C, 67.08; H, 6.11; N, 8.94. Found: C, 68.12; H, 5.86; N, 8.47.

**1.7j. (*E*)-N-(2-((6-Chloro-1,2,3,4-tetrahydroacridin-9-yl)amino)ethyl)-2-(((5,7-dihydroxy-2-(3-hydroxy-4-methoxyphenyl)chroman-4-ylidene)amino)oxy)acetamide.** Prepared from compounds **1.2d** (62 mg, 2.26 mmol) and **1.6b** (85 mg, 2.26 mmol). Pale brown solid (12% yield).

**Mp**: 198 °C.

**IR** ($cm^{-1}$): 3066, 2927, 2119, 1630, 1579.

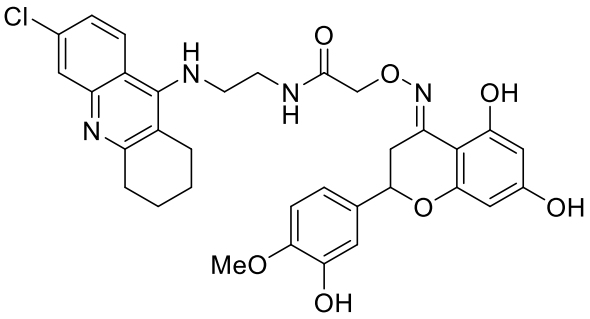

**$^1$H NMR** (250 MHz, MeOD) δ 8.41 (d, *J* = 9.2 Hz, 1H), 7.69 (d, *J* = 2.1 Hz, 1H), 7.51 (dd, *J* = 9.2, 2.1 Hz, 1H), 7.00 – 6.85 (m, 3H), 5.87 (d, *J* = 2.3 Hz, 1H), 5.41 (d, *J* = 2.3 Hz, 1H), 4.82 (d, *J* = 11.9 Hz, 1H), 4.59 (s, 2H), 4.15 (m, 2H), 3.89 (s, 3H), 3.85 – 3.66 (m, 2H), 2.88 (m, 2H), 2.70 (m, 3H), 1.87 (m, 4H).

**$^{13}$C NMR** (63 MHz, MeOD) δ 174.3, 163.1, 160.8, 160.6, 157.9, 157.7, 153.2, 149.6, 148.2, 141.3, 134.0, 128.8, 127.1, 120.1, 119.2, 116.3, 114.8, 113.7, 112.9, 97.9, 97.1, 77.9, 74.5, 56.8, 51.8, 40.1, 31.9, 30.1, 25.5, 23.4, 22.2.

**Elemental analysis**. Anal. Calc. for $C_{33}H_{33}ClN_4O_7$ C, 62.61; H, 6.25; N, 8.85. Found: C, 62.73; H, 6.12; N, 8.58.

**1.7k. (*E*)-N-(3-((6-Chloro-1,2,3,4-tetrahydroacridin-9-yl)amino)propyl)-2-(((5,7-dihydroxy-2-(3-hydroxy-4-methoxyphenyl)chroman-4-ylidene)amino)oxy)acetamide.** Prepared from compounds **1.2e** (66 mg, 2.26 mmol) and **1.6b** (85 mg, 2.26 mmol). Pale brown solid (17% yield).

**Mp**: 189 °C.

**IR** ($cm^{-1}$): 3257 3067, 2926, 2100, 1630, 1573.

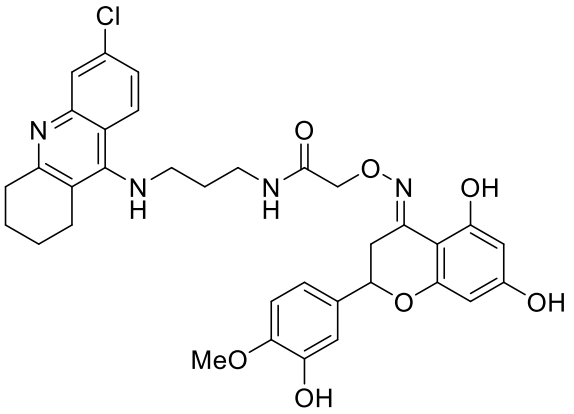

**$^1$H NMR** (250 MHz, MeOD) δ 8.31 (d, *J* = 9.3 Hz, 1H), 7.69 (d, *J* = 2.2 Hz, 1H), 7.46 (dd, *J* = 9.3, 2.2 Hz, 1H), 7.02 – 6.83 (m, 3H), 5.82 (d, *J* = 2.3 Hz, 1H), 5.62 (d, *J* = 2.3 Hz, 1H), 4.84 (dd, *J* = 12.0, 3.0 Hz, 3H), 4.56 (s, 2H), 3.89 (m, 5H), 3.54 – 3.41 (m, 3H), 2.99 (s, 2H), 2.78 – 2.63 (m, 3H), 2.07 (q, *J* = 6.6 Hz, 2H), 2.01 – 1.91 (m, 4H).

**$^{13}$C NMR** (63 MHz, MeOD) δ 172.9, 163.1, 161.0, 160.7, 158.1, 157.5, 149.6, 148.1, 134.0, 128.9, 126.9, 120.5, 119.2, 114.8, 114.2, 112.9, 97.9, 97.1, 96.4, 77.9, 74.6, 56.8, 47.6, 37.5, 32.0, 31.7, 30.3, 25.1, 23.4, 22.4.

**Elemental analysis**. Anal. Calc. for $C_{34}H_{35}ClN_4O_7$ C, 63.11; H, 5.45; N, 8.66. Found: C, 62.93; H, 5.67; N, 8.64.

**1.7l.** (***E***)**-N-(4-((6-Chloro-1,2,3,4-tetrahydroacridin-9-yl)amino)butyl)-2-(((5,7-dihydroxy-2-(3-hydroxy-4-methoxyphenyl)chroman-4-ylidene)amino)oxy)acetamide.** Prepared from compounds **1.2f** (69 mg, 2.26 mmol) and **1.6b** (85 mg, 2.26 mmol). Pale brown solid (22% yield).

**Mp**: 182 °C.

**IR** ($cm^{-1}$): 3238, 3070, 2972, 2116, 1630, 1575.

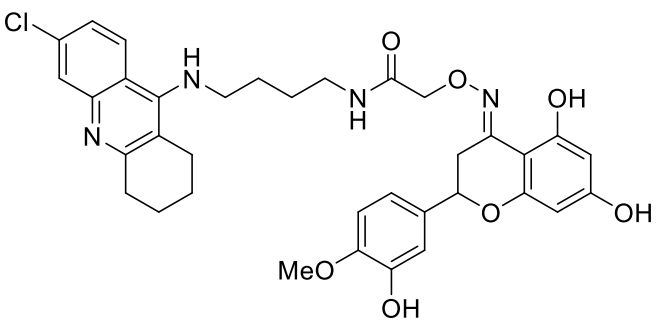

**$^1$H NMR** (250 MHz, MeOD) δ 8.22 (d, *J* = 9.3 Hz, 1H), 7.72 (d, *J* = 2.1 Hz, 1H), 7.52 (dd, *J* = 9.3, 2.2 Hz, 1H), 7.04 – 6.83 (m, 3H), 5.85 – 5.76 (d, *J* = 2.3 Hz, 1H), 5.58 (d, *J* = 2.3 Hz, 1H), 4.56 (s, 2H), 3.89 (s, 3H), 3.84 (t, *J* = 7.3 Hz, 2H), 3.50 (dd, *J* = 17.3, 3.2 Hz, 1H), 3.41 (t, *J* = 6.1 Hz, 1H), 2.98 (m, 2H), 2.76 (dd, *J* = 17.3, 12.1 Hz, 1H), 2.57 (m, 2H), 1.95 (m, 4H), 1.87 (m, 2H), 1.77 – 1.65 (m, 2H).

**$^{13}$C NMR** (63 MHz, MeOD) δ 172.5, 163.1, 161.0, 160.6, 158.1, 157.3, 149.6, 148.2, 139.9, 134.1, 128.9, 127.0, 123.6, 120.4, 119.2, 116.0, 114.8, 113.9, 112.9, 98.0, 97.8, 97.0, 78.0, 74.7, 56.8, 44.7, 39.9, 31.8, 30.2, 29.4, 27.9, 25.1, 23.3, 22.3.

**Elemental analysis**. Anal. Calc. for $C_{35}H_{37}ClN_4O_7$ C, 63.58; H, 5.64; N, 8.47. Found: C, 63.74; H, 5.53; N, 8.45.

**4.11 General procedure for the synthesis of compounds 1.8a to 1.8d**

The suitable flavonoid oxime carboxylic acid (1 equivalent) and aminobenzyl piperidine (1 equivalent) were dissolved in a mixture of 4:1 dichloromethane/methanol mixture (5 ml) together with EDCI (1.5 equivalents) and HOBt (1.5 equivalents) and the mixture was stirred at room temperature overnight. The reaction was quenched with water (5 ml) and the mixture was extracted with ethyl acetate (10 ml) five times. The organic extract was dried with $Na_2SO_4$ and concentrated in vacuo to yield a solid that was then purified by column chromatography (9:1 dichloromethane/methanol) to yield compounds **1.8a**-**1.8d**.

**1.8a. (*E*)-N-(1-benzylpiperidin-4-yl)-2-(((5,7-dihydroxy-2-(4-hydroxyphenyl)chroman-4-ylidene)amino)oxy)acetamide.** Prepared from compound **1.6a** (60 mg, 1.74 mmol) and 1-benzylpiperidin-4-amine (33 mg, 1.74 mmol). Pale yellow solid (32% yield).

**Mp**: 173 °C.

**IR** ($cm^{-1}$): 3178, 2923, 2097, 1632, 1603.

**$^1$H NMR** (250 MHz, MeOD) δ 7.16 – 7.05 (m, 7H), 6.62 (d, *J* = 8.6 Hz, 2H), 5.75 (d, *J* = 2.4 Hz, 1H), 5.73 (d, *J* = 2.4 Hz, 1H), 4.34 (s, 2H), 3.62 (tt, *J* = 10.6, 4.3 Hz, 1H), 3.42 (s, 2H), 3.31 (dd, *J* = 17.3, 3.1 Hz, 1H), 2.73 (d, *J* = 12.0 Hz, 2H), 2.61 (dd, *J* = 17.3, 12.3 Hz, 1H), 2.10 (td, *J* = 11.8, 2.7 Hz, 2H), 1.68 (dd, *J* = 13.3, 3.8 Hz, 2H), 1.53 – 1.34 (m, 2H).

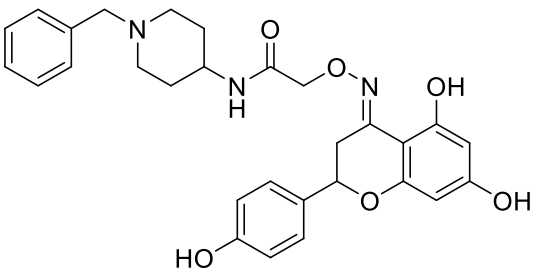


**$^{13}$C NMR** (63 MHz, MeOD) δ 171.6, 163.3, 161.4, 161.0, 159.3, 158.3, 137.5, 132.2, 131.5, 129.9, 129.3, 116.7, 98.2, 98.2, 97.2, 78.3, 74.4, 64.0, 53.4, 47.9, 32.1, 32.0.

**Elemental analysis**. Anal. Calc. for $C_{29}H_{31}N_3O_6$ C, 67.30; H, 6.04; N, 8.12. Found: C, 66.80; H, 6.08; N, 8.48.

**1.8b. (*E*)-N-(2-(1-Benzylpiperidin-4-yl)ethyl)-2-(((5,7-dihydroxy-2-(4-hydroxyphenyl)chroman-4-ylidene)amino)oxy)acetamide.** Prepared from compound **1.6a** (60 mg, 1.74 mmol) and 2-(1-benzylpiperidin-4-yl)ethan-1-amine (38 mg, 1.74 mmol). White solid (22% yield).

**Mp**: 194 °C.

**IR** ($cm^{-1}$): 3192, 2925, 2107, 1632, 1606.

**$^1$H NMR** (250 MHz, MeOD) δ 7.45 (s, 5H), 7.40 – 7.30 (m, 2H), 6.92 – 6.79 (m, 2H), 6.02 (s, 2H), 5.04 (dd, *J* = 11.9, 3.2 Hz, 2H), 4.58 (s, 2H), 3.96 (s, 2H), 3.55 (dd, *J* = 17.4, 3.2 Hz, 1H), 3.23 (m, 2H), 2.95 (dd, *J* = 17.4, 11.9 Hz, 1H), 2.46 (m, 2H), 1.89 (m, 2H), 1.44 (m, 5H).

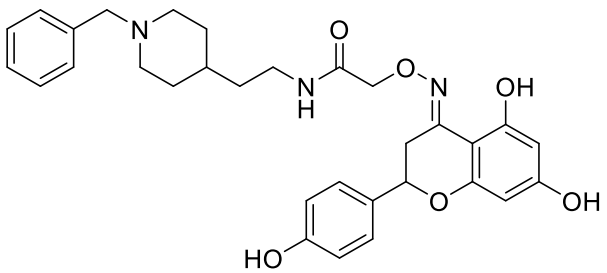

**$^{13}$C NMR** (63 MHz, MeOD) δ 172.3, 163.5, 161.3, 161.1, 159.3, 158.4, 132.8, 132.4, 132.0, 130.9, 130.5, 129.4, 116.7, 98.3, 97.4, 78.3, 74.6, 62.8, 37.3, 36.6, 32.5, 31.7, 31.1, 31.0.

**Elemental analysis**. Anal. Calc. for $C_{31}H_{35}N_3O_6$ C, 68.24; H, 6.47; N, 7.70. Found: C,67.93; H, 6.09, N, 6.46.

**1.8c. (*E*)-N-(1-Benzylpiperidin-4-yl)-2-(((5,7-dihydroxy-2-(3-hydroxy-4-methoxyphenyl)chroman-4-ylidene)amino)oxy)acetamide.** Prepared from compound **1.6b** (60 mg, 1.60 mmol) and 1-benzylpiperidin-4-amine (30 mg, 1.60 mmol). Pale yellow solid (26% yield).

**Mp**: 128 °C.

**IR** ($cm^{-1}$): 3057, 2928, 2808, 2106, 1630, 1603.

**$^1$H NMR** (250 MHz, MeOD) δ 7.33 (m, 5H), 6.98 – 6.89 (m, 3H), 5.96 (s, 2H), 4.55 (s, 2H), 3.87 (s, 3H), 3.82 (d, *J* = 4.3 Hz, 1H), 3.53 (d, *J* = 19.6 Hz, 3H), 2.98 – 2.72 (m, 3H), 2.33 – 2.15 (m, 2H), 1.88 (d, *J* = 12.6 Hz, 2H), 1.75 – 1.53 (m, 2H).

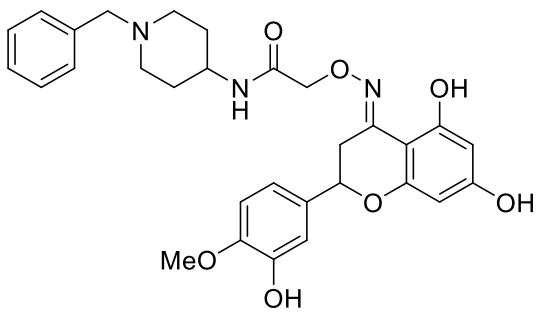


**$^{13}$C NMR** (63 MHz, MeOD) δ 171.5, 163.2, 161.3, 160.8, 158.0, 149.5, 148.1, 138.1, 134.2, 131.3, 129.8, 129.1, 119.2, 114.8, 112.9, 98.2, 97.1, 78.0, 74.3, 64.2, 56.8, 53.4, 48.0, 32.2, 31.9.

**Elemental analysis**. Anal. Calc. for $C_{30}H_{33}N_3O_7$ C, 65.80; H, 6.48; N, 7.30. Found: C, 66.32; H, 6.42; N, 7.40.

**1.8d. (*E*)-N-(2-(1-Benzylpiperidin-4-yl)ethyl)-2-(((5,7-dihydroxy-2-(3-hydroxy-4-methoxyphenyl)chroman-4-ylidene)amino)oxy)acetamide.** Prepared from compound **1.6b** (60 mg, 1.60 mmol) and 2-(1-benzylpiperidin-4-yl)ethan-1-amine (35 mg, 1.60 mmol). Orange solid (20% yield).

**Mp**: 154 °C.

**IR** ($cm^{-1}$): 3194, 3068, 2924, 2105, 1630, 1601.

**$^1$H NMR** (250 MHz, MeOD) δ 7.49 – 7.35 (m, 5H), 7.02 – 6.90 (m, 3H), 6.04 (d, *J* = 2.3 Hz, 1H), 6.01 (d, *J* = 2.3 Hz, 1H), 5.03 (dd, *J* = 11.5, 3.2 Hz, 1H), 4.58 (s, 2H), 3.88 (s, 5H), 3.53 (dd, *J* = 17.3, 3.3 Hz, 1H), 3.16 (t, *J* = 11.0 Hz, 2H), 2.94 (dd, *J* = 17.3, 11.5 Hz, 1H), 2.47 – 2.27 (m, 2H), 1.83 (d, *J* = 11.7 Hz, 2H), 1.49 (m, 2H), 1.46 – 1.23 (m, 3H).

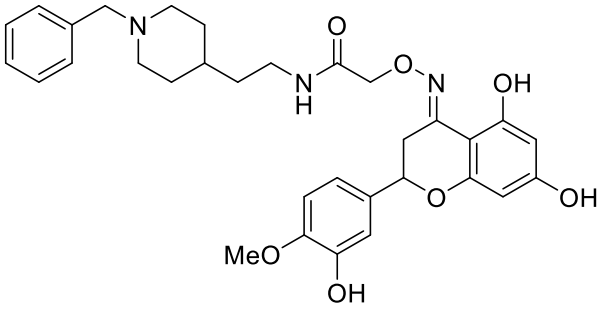

**$^{13}$C NMR** (63 MHz, MeOD) δ 172.2, 163.5, 161.2, 160.9, 158.1, 149.5, 148.1, 134.1, 133.5, 132.2, 130.6, 130.4, 119.3, 114.8, 112.9, 98.3, 97.4, 77.9, 74.6, 63.0, 56.8, 54.3, 37.3, 36.6, 32.7, 31.6, 31.3, 31.1.

**Elemental analysis**. Anal. Calc. for $C_{32}H_{37}N_3O_7$ C, 66.77; H, 6.07; N, 7.67. Found: C, 67.00; H, 6.30; N, 7.38.

### 4.12 General procedure for the synthesis of compounds 1.9a to 1.9f

The correspondent flavonoid oxime carboxylic acid (1 equivalent) and tryptamine (1 equivalent) were dissolved in a mixture of 4:1 dichloromethane/methanol mixture (5 ml) together with EDCI (1.5 equivalents) and HOBt (1.5 equivalents) and the mixture was left stirring at room temperature overnight. The reaction was quenched with water (5 ml) and the mixture was extracted with ethyl acetate (10 ml) five times. The organic extract was dried with $Na_2SO_4$ and concentrated in vacuo to yield a solid that was then purified by column chromatography (9:1 dichloromethane/methanol) to yield compounds **1.9a**-**1.9f**.

**1.9a. (*E*)-2-(((5,7-Dihydroxy-2-(4-hydroxyphenyl)chroman-4-ylidene)amino)oxy)-N-(2-(5-methoxy-1H-indol-3-yl)ethyl)acetamide.** Prepared from compound **1.6a** (60 mg, 1.74 mmol) and 5-methoxytriptamine (33 mg, 1.74 mmol). Off-white solid (22% yield).

**Mp**: 223 °C.

**IR** (cm$^{-1}$): 3379, 3174,2936, 2120, 1639, 1601.

**$^1$H NMR** (250 MHz, MeOD) δ 7.28 (d, *J* = 8.9, 2H), 7.17 (dd, *J* = 8.8, 0.6 Hz, 1H), 7.08 – 6.99 (m, 2H), 6.84 (d, *J* = 8.9, 2H), 6.72 (dd, *J* = 8.8, 2.4 Hz, 1H), 5.99 (d, *J* = 2.4 Hz, 1H), 5.95 (d, *J* = 2.3 Hz, 1H), 4.86 (dd, *J* = 12.5, 3.0 Hz, 1H), 4.55 (s, 2H), 3.80 (s, 3H), 3.58 (t, *J* = 7.2 Hz, 2H), 2.94 (t, *J* = 7.2 Hz, 2H), 2.66 (dd, *J* = 17.3, 12.5 Hz, 1H).

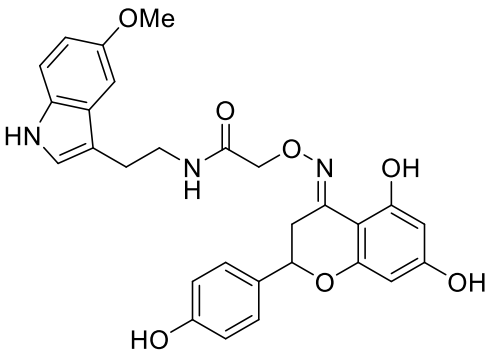


**$^{13}$C NMR** (63 MHz, MeOD) δ 172.0, 163.2, 161.3, 161.0, 159.2, 158.3, 155.3, 133.7, 132.2, 129.4, 124.7, 116.6, 113.4, 113.1, 113.0, 101.5, 98.2, 97.1, 78.2, 74.4, 56.6, 41.3, 31.8, 26.6.

**Elemental analysis**. Anal. Calc. for $C_{28}H_{27}O_7N_3$ C, 64.98; H, 5.26; N, 8.12. Found C, 64.55; H, 5.35; N, 8.12.

**1.9b. (*E*)-2-(((5,7-Dihydroxy-2-(4-hydroxyphenyl)chroman-4-ylidene)amino)oxy)-N-(2-(5-hydroxy-1H-indol-3-yl)ethyl)acetamide.** Prepared from compound **1.6a** (60 mg, 1.74 mmol) and 5-hydroxytriptamine (31 mg, 1.74 mmol). Grey solid (28% yield).

**Mp**: 165 °C.

**IR** ($cm^{-1}$): 3418, 3127, 2921, 2112, 1638, 1611.

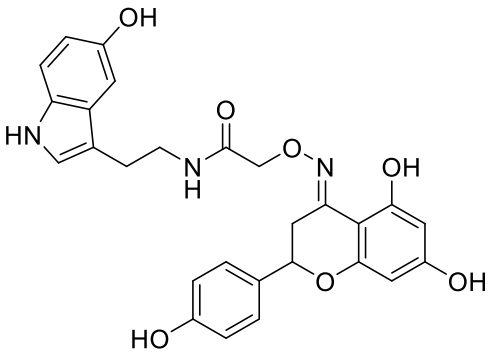

**$^1$H NMR** (250 MHz, MeOD) δ 7.20 – 7.11 (d, *J* = 8.8 Hz, 2H), 7.02 – 6.95 (dd, J=8.6, 0.5 Hz, 1H), 6.86 (s, 1H) 6.83 (dd, J= 2.3 Hz, 0.5 Hz, 2H), 6.71 (d, 8.8 Hz, 2H), 6.52 (d, J= 8.6, 2.3Hz, 2H) 5.87 (d, *J* = 2.3 Hz, 1H), 5.83 (d, *J* = 2.3 Hz, 1H), 4.44 (s, 2H), 3.43 (t, J= 7.2 Hz, 2H), 2.78 (t, *J* = 7.2 Hz, 2H), 2.58 (dd, *J* = 17.3, 12.5 Hz, 1H).

**$^{13}$C NMR** (63 MHz, MeOD) δ 172.0, 163.2, 161.3, 161.0, 159.2, 158.3, 151.5, 133.4, 132.2, 129.7, 129.4, 124.8, 116.6, 113.1, 112.8, 112.5, 103.8, 98.3, 98.2, 97.1, 78.2, 74.4, 41.2, 31.8, 26.6.

**Elemental analysis**. Anal. Calc. for $C_{27}H_{25}O_7N_3$ C, 64.41; H, 5.00; N, 8.35. Found C, 63.91; H, 5.08; N, 8.51.

**1.9c. (*E*)-N-(2-(1H-Indol-3-yl)ethyl)-2-(((5,7-dihydroxy-2-(4-hydroxyphenyl)chroman-4-ylidene)amino)oxy)acetamide.** Prepared from compound **1.6a** (60 mg, 1.74 mmol) and tryptamine (27 mg, 1.74 mmol). Off-white solid (33% yield).

**Mp**: 158 °C.

**IR** ($cm^{-1}$): 3414, 3068, 2935, 2102, 1628, 1609.

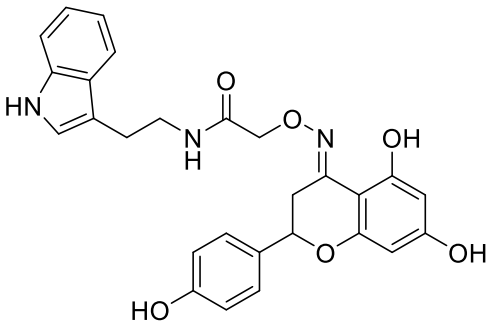

**$^1$H NMR** (250 MHz, MeOD) δ 7.56 (dt, *J* = 7.8, 1.1 Hz, 1H), 7.35 – 7.22 (m, 3H), 7.12 – 6.92 (m, 3H), 6.90 – 6.78 (d, J= 8.6 Hz, 2H), 6.00 (d, *J* = 2.3 Hz, 1H), 5.96 (d, *J* = 2.3 Hz, 1H), 4.91 – 4.82 (dd, J=12.5, 3.0 Hz, 1H), 4.56 (s, 2H), 3.59 (t, *J* = 7.2 Hz, 2H), 2.98 (t, *J* = 7.2 Hz, 2H), 2.68 (dd, *J* = 17.3, 12.5 Hz, 1H).

**$^{13}$C NMR** (63 MHz, MeOD) δ 172.0, 163.3, 161.3, 161.0, 159.2, 158.2, 138.5, 132.2, 129.3, 129.1, 123.9, 122.7, 120.1, 119.6, 116.6, 113.3, 112.6, 98.2, 98.2, 97.1, 78.2, 74.4, 41.4, 31.8, 26.6.

**Elemental analysis**. Anal. Calc. for $C_{27}H_{25}O_6N_3$ C, 66.52; H, 5.17; N, 8.62. Found C, 66.64; H, 5.23; N, 8.36.

**1.9d. (*E*)-2-(((5,7-dihydroxy-2-(3-hydroxy-4-methoxyphenyl)chroman-4-ylidene)amino)oxy)-N-(2-(5-methoxy-1H-indol-3-yl)ethyl)acetamide.** Prepared from compound **1.6b** (60 mg, 1.60 mmol) and 5-methoxytriptamine (30 mg, 1.60 mmol). Off-white solid (27% yield).

**Mp**: 215 °C.

**IR** ($cm^{-1}$): 3430, 3350, 2931, 2103, 1626, 1601.

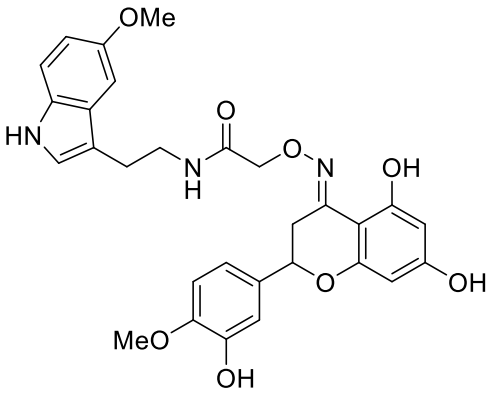


**$^{1}$H NMR** (250 MHz, MeOD) δ 7.15 (d, *J* = 8.8 Hz, 1H), 7.04 (d, *J* = 2.4 Hz, 1H), 7.01 (s, 1H), 6.96 – 6.83 (m, 3H), 6.70 (dd, *J* = 8.8, 2.4 Hz, 1H), 5.96 (d, *J* = 2.2 Hz, 1H), 5.94 (d, *J* = 2.3 Hz, 1H), 4.54 (s, 2H), 3.86 (s, 3H), 3.78 (s, 3H), 3.56 (t, *J* = 7.1 Hz, 2H), 2.93 (t, *J* = 7.2 Hz, 2H), 2.67 (dd, *J* = 17.3, 12.1 Hz, 1H).

**$^{13}$C NMR** (63 MHz, MeOD) δ 172.0, 163.2, 161.3, 160.8, 158.1, 155.3, 152.5, 149.5, 148.1, 134.2, 133.7, 129.4, 124.6, 119.3, 114.9, 113.3, 113.0, 112.8, 101.4, 98.2, 97.1, 95.6, 78.0, 74.4, 56.8, 56.6, 41.3, 31.8, 26.6.

**Elemental analysis**. Anal. Calc. for $C_{29}H_{29}O_8N_3$ C, 63.61; H, 5.34; N, 7.67. Found C, 62.02; H, 5.75; N, 7.40.

**1.9e. (*E*)-2-(((5,7-Dihydroxy-2-(3-hydroxy-4-methoxyphenyl)chroman-4-ylidene)amino)oxy)-N-(2-(5-hydroxy-1H-indol-3-yl)ethyl)acetamide.** Prepared from compound **1.6a** (60 mg, 1.60 mmol) and 5-hydroxytriptamine (28 mg, 1.60 mmol). Grey-red solid (24% yield).

**Mp**: 168 °C.

**IR** ($cm^{-1}$): 3412, 3289, 2932, 2106, 1616.

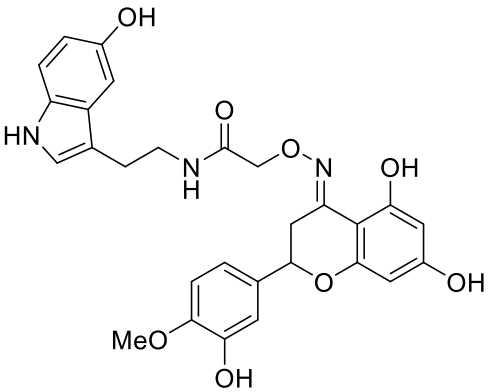


**$^{1}$H NMR** (250 MHz, MeOD) δ 7.10 (d, J = 8.7 Hz, 1H), 6.99 – 6.83 (m, 5H), 6.63 (dd, J = 8.7, 2.3 Hz, 1H), 5.98 – 5.95 (m, 1H), 5.95 – 5.93 (m, 1H), 4.55 (s, 2H), 3.86 (s, 3H), 3.54 (t, J = 7.2 Hz, 2H), 2.89 (t, J = 7.2 Hz, 2H), 2.69 (dd, J = 17.3, 12.1 Hz, 1H).

**$^{13}$C NMR** (63 MHz, MeOD) δ 171.5, 162.8, 162.7, 160.9, 160.4, 157.6, 151.1, 149.1, 147.6, 133.8, 133.0, 129.3, 124.3, 118.9, 114.4, 112.7, 112.4, 112.4, 112.1, 103.4, 97.8, 96.7, 77.6, 74.0, 56.3, 40.8, 31.4, 26.2.

**Elemental analysis**. Anal. Calc. for $C_{28}H_{27}O_8N_3$ C, 63.03; H, 5.10; N, 7.88. Found C, 63.32; H, 5.10; N, 7.88.

**1.9f. (*E*)-N-(2-(1H-Indol-3-yl)ethyl)-2-(((5,7-dihydroxy-2-(3-hydroxy-4-methoxyphenyl)chroman-4-ylidene)amino)oxy)acetamide.** Prepared from compound **1.6b** (60 mg, 1.60 mmol) and tryptamine (26 mg, 1.60 mmol). Orange solid (31% yield).

**Mp**: 148 °C.

**IR** ($cm^{-1}$): 2929, 2111, 1631, 1604.

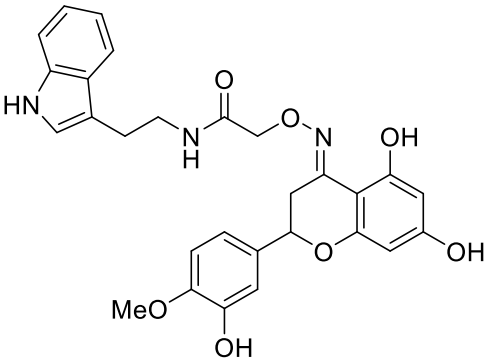


**$^{1}$H NMR** (250 MHz, MeOD) δ 7.53 (dt, *J* = 7.7, 1.1 Hz, 1H), 7.27 (dt, *J* = 8.1, 1.0 Hz, 1H), 7.08 – 6.81 (m, 6H), 5.97 (d, *J* = 2.3 Hz, 1H), 5.94 (d, *J* = 2.3 Hz, 1H), 4.85 (dd, *J* = 12.2, 3.0 Hz, 1H), 4.53 (s, 2H), 3.85 (s, 3H), 3.56 (t, *J* = 7.2 Hz, 2H), 3.37 (dd, *J* = 13.9, 3.6 Hz, 1H), 2.96 (t, *J* = 7.2 Hz, 2H), 2.65 (dd, *J* = 17.3, 12.2 Hz, 1H).

**$^{13}$C NMR** (63 MHz, MeOD) δ 172.0, 163.3, 161.3, 160.8, 158.1, 149.5, 148.0, 138.5, 134.2, 129.1, 123.9, 122.8, 120.1, 119.6, 119.3, 114.9, 113.3, 112.8, 112.6, 98.2, 98.2, 97.1, 78.0, 74.4, 56.8, 41.5, 31.8, 26.6.

**Elemental analysis**. Anal. Calc. for $C_{28}H_{27}O_7N_3$ C, 64.98; H, 5.26; N, 8.12. Found C, 65.02; H, 5.37; N, 8.24.

## 5.0 References


(1) Bui, T. T.; Nguyen, T. H. Natural Product for the Treatment of Alzheimer's Disease. *J. Basic Clin. Physiol. Pharmacol.* **2017**, *28* (5), 413–423. https://doi.org/10.1515/jbcpp-2016-0147.

(2) Zhang, H.; Bai, L.; He, J.; Zhong, L.; Duan, X.; Ouyang, L.; Zhu, Y.; Wang, T.; Zhang, Y.; Shi, J. Recent Advances in Discovery and Development of Natural Products as Source for Anti-Parkinson's Disease Lead Compounds. *Eur. J. Med. Chem.* **2017**, *141*, 257–272. https://doi.org/10.1016/j.ejmech.2017.09.068.

(3) Xu, L.; Li, Y.; Dai, Y.; Peng, J. Natural Products for the Treatment of Type 2 Diabetes Mellitus: Pharmacology and Mechanisms. *Pharmacol. Res.* **2018**, *130*, 451–465. https://doi.org/10.1016/j.phrs.2018.01.015.

(4) Cragg, G. M.; Grothaus, P. G.; Newman, D. J. Impact of Natural Products on Developing New Anti-Cancer Agents. *Chem. Rev.* **2009**, *109* (7), 3012–3043. https://doi.org/10.1021/cr900019j.

(5) Airoldi, C.; La Ferla, B.; D`Orazio, G.; Ciaramelli, C.; Palmioli, A. Flavonoids in the Treatment of Alzheimer's and Other Neurodegenerative Diseases. *Curr. Med. Chem.* **2018**, *25* (27), 3228–3246. https://doi.org/10.2174/0929867325666180209132125.

(6) Pietta, P. G. Flavonoids as Antioxidants. *J. Nat. Prod.* **2000**, *63* (7), 1035–1042. https://doi.org/10.1021/np9904509.

(7) Galati, G.; O'Brien, P. J. Potential Toxicity of Flavonoids and Other Dietary Phenolics: Significance for Their Chemopreventive and Anticancer Properties. *Free Radic. Biol. Med.* **2004**, *37* (3), 287–303. https://doi.org/10.1016/j.freeradbiomed.2004.04.034.

(8) Wang, K.; Chen, Z.; Huang, L.; Meng, B.; Zhou, X.; Wen, X.; Ren, D. Naringenin Reduces Oxidative Stress and Improves Mitochondrial Dysfunction via Activation of the Nrf2/ARE Signaling Pathway in Neurons. *Int. J. Mol. Med.* **2017**, *40* (5), 1582–1590. https://doi.org/10.3892/ijmm.2017.3134.

(9) Arredondo, F.; Echeverry, C.; Abin-Carriquiry, J. A.; Blasina, F.; Antúnez, K.; Jones, D. P.; Go, Y. M.; Liang, Y. L.; Dajas, F. After Cellular Internalization, Quercetin Causes Nrf2 Nuclear Translocation, Increases Glutathione Levels, and Prevents Neuronal Death against an Oxidative Insult. *Free Radic. Biol. Med.* **2010**, *49* (5), 738–747. https://doi.org/10.1016/j.freeradbiomed.2010.05.020.

(10) Fernandez, M. T.; Mira, M. L.; Florêncio, M. H.; Jennings, K. R. Iron and Copper Chelation by Flavonoids: An Electrospray Mass Spectrometry Study. *J. Inorg. Biochem.* **2002**, *92* (2), 105–111. https://doi.org/10.1016/S0162-0134(02)00511-1.

(11) Gutierrez-Merino, C.; Lopez-Sanchez, C.; Lagoa, R.; K. Samhan-Arias, A.; Bueno, C.; Garcia-Martinez, V. Neuroprotective Actions of Flavonoids. *Curr. Med. Chem.* **2011**, *18* (8), 1195–1212. https://doi.org/10.2174/092986711795029735.

(12) Heo, H. J.; Kim, M. J.; Lee, J. M.; Choi, S. J.; Cho, H. Y.; Hong, B.; Kim, H. K.; Kim, E.; Shin, D. H. Naringenin from Citrus Junos Has an Inhibitory Effect on Acetylcholinesterase and a Mitigating Effect on Amnesia. *Dement. Geriatr. Cogn. Disord.* **2004**, *17* (3), 151–157. https://doi.org/10.1159/000076349.

(13) Ghofrani, S.; Joghataei, M. T.; Mohseni, S.; Baluchnejadmojarad, T.; Bagheri, M.; Khamse, S.; Roghani, M. Naringenin Improves Learning and Memory in an Alzheimer's Disease Rat Model: Insights into the Underlying Mechanisms. *Eur. J. Pharmacol.* **2015**, *764*, 195–201. https://doi.org/10.1016/j.ejphar.2015.07.001.

(14) Ma, H.; Feng, X.; Ding, S. Hesperetin Attenuates Ventilator-Induced Acute Lung Injury through Inhibition of NF-KB-Mediated Inflammation. *Eur. J. Pharmacol.* **2015**, *769*, 333–341. https://doi.org/10.1016/j.ejphar.2015.11.038.

(15) Sabogal-Guáqueta, A. M.; Muñoz-Manco, J. I.; Ramírez-Pineda, J. R.; Lamprea-Rodriguez, M.; Osorio, E.; Cardona-Gómez, G. P. *The Flavonoid Quercetin Ameliorates Alzheimer's Disease Pathology and Protects Cognitive and Emotional Function in Aged Triple Transgenic Alzheimer's Disease Model Mice*; Elsevier Ltd, 2015; Vol. 93. https://doi.org/10.1016/j.neuropharm.2015.01.027.

(16) Wang, H.; Wang, H.; Cheng, H.; Che, Z. Ameliorating Effect of Luteolin on Memory Impairment in an Alzheimer's Disease Model. *Mol. Med. Rep.* **2016**, *13* (5), 4215–4220. https://doi.org/10.3892/mmr.2016.5052.

(17) Ly, P. T. T.; Wu, Y.; Zou, H.; Wang, R.; Zhou, W.; Kinoshita, A.; Zhang, M.; Yang, Y.; Cai, F.; Woodgett, J.; Song, W. Inhibition of GSK3β-Mediated BACE1 Expression Reduces Alzheimer-Associated Phenotypes. *J. Clin. Invest.* **2013**, *123* (1), 224–235. https://doi.org/10.1172/JCI64516.

(18) Guo, A. J. Y.; Xie, H. Q.; Choi, R. C. Y.; Zheng, K. Y. Z.; Bi, C. W. C.; Xu, S. L.; Dong, T. T. X.; Tsim, K. W. K. Galangin, a Flavonol Derived from Rhizoma Alpiniae Officinarum, Inhibits Acetylcholinesterase Activity in Vitro. *Chem. Biol. Interact.* **2010**, *187* (1–3), 246–248. https://doi.org/10.1016/j.cbi.2010.05.002.

(19) Huang, L.; Lin, M.; Zhong, X.; Yang, H.; Deng, M. Galangin Decreases P-Tau, Aβ 42 and β-Secretase Levels, and Suppresses Autophagy in Okadaic Acid-Induced PC12 Cells via an Akt/GSK3β/MTOR Signaling-Dependent Mechanism. *Mol. Med. Rep.* **2019**, *19* (3), 1767–1774. https://doi.org/10.3892/mmr.2019.9824.

(20) Jalili-Baleh, L.; Babaei, E.; Abdpour, S.; Nasir Abbas Bukhari, S.; Foroumadi, A.; Ramazani, A.; Sharifzadeh, M.; Abdollahi, M.; Khoobi, M. A Review on Flavonoid-Based Scaffolds as Multi-Target-Directed Ligands (MTDLs) for Alzheimer's Disease. *Eur. J. Med. Chem.* **2018**, *152*, 570–589. https://doi.org/10.1016/j.ejmech.2018.05.004.

(21) Benek, O.; Korabecny, J.; Soukup, O. A Perspective on Multi-Target Drugs for Alzheimer's Disease. *Trends Pharmacol. Sci.* **2020**, *41* (7), 434–445. https://doi.org/10.1016/j.tips.2020.04.008.

(22) Zhou, J.; Jiang, X.; He, S.; Jiang, H.; Feng, F.; Liu, W.; Qu, W.; Sun, H. Rational Design of Multitarget-Directed Ligands: Strategies and Emerging Paradigms. *J. Med. Chem.* **2019**, *62* (20), 8881–8914. https://doi.org/10.1021/acs.jmedchem.9b00017.

(23) Ko, S. Y.; Ko, H. A.; Chu, K. H.; Shieh, T. M.; Chi, T. C.; Chen, H. I.; Chang, W. C.; Chang, S. S. The Possible Mechanism of Advanced Glycation End Products (AGEs) for Alzheimer's Disease. *PLoS One* **2015**, *10* (11), 1–16. https://doi.org/10.1371/journal.pone.0143345.

(24) Singh, M.; Kaur, M.; Singh, N.; Silakari, O. Bioorganic & Medicinal Chemistry Exploration of Multi-Target Potential of Chromen-4-One Based Compounds in Alzheimer ' s Disease : Design , Synthesis and Biological Evaluations. *Bioorg. Med. Chem.* **2017**, *25* (24), 6273–6285. https://doi.org/10.1016/j.bmc.2017.09.012.

(25) Fernández-Bachiller, M. I.; Pérez, C.; Monjas, L.; Rademann, J.; Rodríguez-Franco, M. I. New Tacrine-4-Oxo-4H-Chromene Hybrids as Multifunctional Agents for the Treatment of Alzheimer's Disease, with Cholinergic, Antioxidant, and β-Amyloid-Reducing Properties. *J. Med. Chem.* **2012**, *55* (3), 1303–1317. https://doi.org/10.1021/jm201460y.

(26) Estrada Valencia, M.; Herrera-Arozamena, C.; de Andrés, L.; Pérez, C.; Morales-García, J. A.; Pérez-Castillo, A.; Ramos, E.; Romero, A.; Viña, D.; Yáñez, M.; Laurini, E.; Pricl, S.; Rodríguez-Franco, M. I. Neurogenic and Neuroprotective Donepezil-Flavonoid Hybrids with Sigma-1 Affinity and Inhibition of Key Enzymes in Alzheimer's Disease. *Eur. J. Med. Chem.* **2018**, *156*, 534–553. https://doi.org/10.1016/j.ejmech.2018.07.026.

(27) Cruz, I.; Puthongking, P.; Cravo, S.; Palmeira, A.; Cidade, H.; Pinto, M.; Sousa, E. Xanthone and Flavone Derivatives as Dual Agents with Acetylcholinesterase Inhibition and Antioxidant Activity as Potential Anti-Alzheimer Agents. **2017**, *2017*.

(28) Li, Y.; Qiang, X.; Luo, L.; Yang, X.; Xiao, G.; Zheng, Y.; Cao, Z. Bioorganic & Medicinal Chemistry Multitarget Drug Design Strategy against Alzheimer ' s Disease : Homoisoflavonoid Mannich Base Derivatives Serve as Acetylcholinesterase and Monoamine Oxidase B Dual Inhibitors with Multifunctional Properties. **2017**, *25*, 714–726. https://doi.org/10.1016/j.bmc.2016.11.048.

(29) Sims, N. R.; Bowen, D. M.; Allen, S. J.; Smith, C. C. T.; Neary, D.; Thomas, D. J.; Davison, A. N. Presynaptic Cholinergic Dysfunction in Patients with Dementia. *J. Neurochem.* **1983**, *40* (2), 503–509. https://doi.org/10.1111/j.1471-4159.1983.tb11311.x.

(30) Snyder, P. J.; Ph, D.; Giacobini, E.; Ph, D.; Foix, L. A. P. C.; Hayden, K.; System, C.; Group, W.; Hampel, H.; Mesulam, M. M.; Cuello, C.; Khachaturian, A. S.; Farlow, M. R.; Snyder, P. J.; Khachaturian, Z. S.; Hampel, H. Alzheimer's & Dementia : The Journal of the Alzheimer's Association Revisiting the Cholinergic Hypothesis in Alzheimer's Disease : Emerging Evidence from Translational and Clinical Research. *J. Prev. Alzheimer's Dis.* **2020**, *6* (1), 2–15.

(31) Yang, P.; Sun, F. Aducanumab : The First Targeted Alzheimer ' s Therapy. **2021**, *15* (March 2019), 166–168. https://doi.org/10.5582/ddt.2021.01061.

(32) Santos, M. A.; Chand, K.; Chaves, S. Recent Progress in Repositioning Alzheimer's Disease Drugs Based on a Multitarget Strategy. *Future Med. Chem.* **2016**, *8* (17), 2113–2142. https://doi.org/10.4155/fmc-2016-0103.

(33) Bajda, M.; Więckowska, A.; Hebda, M.; Guzior, N.; Sotriffer, C. A.; Malawska, B. Structure-Based Search for New Inhibitors of Cholinesterases. *Int. J. Mol. Sci.* **2013**, *14* (3), 5608–5632. https://doi.org/10.3390/ijms14035608.

(34) Sameem, B.; Saeedi, M.; Mahdavi, M.; Shafiee, A. A Review on Tacrine-Based Scaffolds as Multi-Target Drugs (MTDLs) for Alzheimer's Disease. *Eur. J. Med. Chem.* **2017**, *128*, 332–345. https://doi.org/10.1016/j.ejmech.2016.10.060.

(35) De Ferrari, G. V.; Canales, M. A.; Shin, I.; Weiner, L. M.; Silman, I.; Inestrosa, N. C. A Structural Motif of Acetylcholinesterase That Promotes Amyloid β-Peptide Fibril Formation. *Biochemistry* **2001**, *40* (35), 10447–10457. https://doi.org/10.1021/bi0101392.

(36) Mishra, P.; Kumar, A.; Panda, G. Anti-Cholinesterase Hybrids as Multi-Target-Directed Ligands against Alzheimer's Disease (1998–2018). *Bioorganic Med. Chem.* **2019**, *27* (6), 895–930. https://doi.org/10.1016/j.bmc.2019.01.025.

(37) Pang, Y. P.; Quiram, P.; Jelacic, T.; Hong, F.; Brimijoin, S. Highly Potent, Selective, and Low Cost Bis-Tetrahydroaminacrine Inhibitors of Acetylcholinesterase. Steps toward Novel Drugs for Treating Alzheimer's Disease. *J. Biol. Chem.* **1996**, *271* (39), 23646–23649. https://doi.org/10.1074/jbc.271.39.23646.

(38) Bolognesi, M. L.; Bartolini, M.; Mancini, F.; Chiriano, G.; Ceccarini, L.; Rosini, M.; Milelli, A.; Tumiatti, V.; Andrisano, V.; Melchiorre, C. Bis(7)-Tacrine Derivatives as Multitarget-Directed Ligands: Focus on Anticholinesterase and Antiamyloid Activities. *ChemMedChem* **2010**, *5* (8), 1215–1220. https://doi.org/10.1002/cmdc.201000086.

(39) Chen, Y.; Lin, H.; Zhu, J.; Gu, K.; Li, Q.; He, S.; Lu, X.; Tan, R.; Pei, Y.; Wu, L.; Bian, Y.; Sun, H. Design, Synthesis,: In Vitro and in Vivo Evaluation of Tacrine-Cinnamic Acid Hybrids as Multi-Target Acetyl- and Butyrylcholinesterase Inhibitors against Alzheimer's Disease. *RSC Adv.* **2017**, *7* (54), 33851–33867. https://doi.org/10.1039/c7ra04385f.

(40) Spilovska, K.; Korabecny, J.; Sepsova, V.; Jun, D.; Hrabinova, M.; Jost, P.; Muckova, L.; Soukup, O.; Janockova, J.; Kucera, T.; Dolezal, R.; Mezeiova, E.; Kaping, D.; Kuca, K. Novel Tacrine-Scutellarin Hybrids as Multipotent Anti-Alzheimer's Agents: Design, Synthesis and Biological Evaluation. *Molecules* **2017**, *22* (6). https://doi.org/10.3390/molecules22061006.

(41) Fernández-Bachiller, M. I.; Pérez, C.; González-Muñoz, G. C.; Conde, S.; López, M. G.; Villarroya, M.; García, A. G.; Rodríguez-Franco, M. I. Novel Tacrine-8-Hydroxyquinoline Hybrids as Multifunctional Agents for the Treatment of Alzheimers Disease, with Neuroprotective, Cholinergic, Antioxidant, and Copper-Complexing Properties. *J. Med. Chem.* **2010**, *53* (13), 4927–4937. https://doi.org/10.1021/jm100329q.

(42) Chen, X.; Zenger, K.; Lupp, A.; Kling, B.; Heilmann, J.; Fleck, C.; Kraus, B.; Decker, M.; Straße, D.; Jena, D.-. Tacrine-Silibinin Codrug Shows Neuro- and Hepatoprotective E Ff Ects in Vitro and Pro-Cognitive and Hepatoprotective E Ff Ects in Vivo. *J. Med. Chem.* **2012**, *55* (11), 1303–1317.

(43) Li, S. Y.; Wang, X. B.; Xie, S. S.; Jiang, N.; Wang, K. D. G.; Yao, H. Q.; Sun, H. Bin; Kong, L. Y. Multifunctional Tacrine-Flavonoid Hybrids with Cholinergic, β-Amyloid-Reducing, and Metal Chelating Properties for the Treatment of Alzheimer's Disease. *Eur. J. Med. Chem.* **2013**, *69*, 632–646. https://doi.org/10.1016/j.ejmech.2013.09.024.

(44) Sun, Y.; Chen, J.; Chen, X.; Huang, L.; Li, X. Inhibition of Cholinesterase and Monoamine Oxidase-B Activity by Tacrine-Homoisoflavonoid Hybrids. *Bioorganic Med. Chem.* **2013**, *21* (23), 7406–7417. https://doi.org/10.1016/j.bmc.2013.09.050.

(45) Liao, S.; Deng, H.; Huang, S.; Yang, J.; Wang, S.; Yin, B.; Zheng, T.; Zhang, D.; Liu, J.; Gao, G.; Ma, J.; Deng, Z. Design, Synthesis and Evaluation of Novel 5,6,7-Trimethoxyflavone-6-Chlorotacrine Hybrids as Potential Multifunctional Agents for the Treatment of Alzheimer's Disease. *Bioorganic Med. Chem. Lett.* **2015**, *25* (7), 1541–1545. https://doi.org/10.1016/j.bmcl.2015.02.015.

(46) Srinivasan, V.; Pandi-Perumal, S. R.; Cardinali, D. P.; Poeggeler, B.; Hardeland, R. Melatonin in Alzheimer's Disease and Other Neurodegenerative Disorders. *Behav. Brain Funct.* **2006**, *2*, 1–23. https://doi.org/10.1186/1744-9081-2-15.

(47) Hardeland R. Antioxidative Protection by Melatonin. *Endocrine* **2005**, *27* (2), 119–130.

(48) Dong, W.; Mei, Q.; Yu, J.; Xu, J.; Xiang, L.; Xu, Y. Effects of Melatonin on the Expression of INOS and COX-2 in Rat Models of Colitis. **2003**, *9* (6), 1307–1311.

(49) Pappolla, M. A.; Sos, M.; Omar, R. A.; Bick, R. J.; Hickson-bick, D. L. M.; Reiter, R. J.; Efthimiopoulos, S.; Robakis, N. K. Melatonin Prevents Death of Neuroblastoma Cells Exposed to the Alzheimer Amyloid Peptide. **1997**, *17* (5), 1683–1690.

(50) Deng, Y.; Xu, G.; Duan, P.; Zhang, Q.; Wang, J. Effects of Melatonin on Wortmannin-Induced Tau Hyperphosphorylation 1. **2005**, *26* (5), 519–526. https://doi.org/10.1111/j.1745-7254.2005.00102.x.

(51) Kupfer, D. J.; Reynolds, C. F. Serotonin in Aging , Late-Life Depression , and Alzheimer ' s Disease : The Emerging Role of Functional Imaging. **1998**, No. 97.

(52) Claeysen, S.; Giannoni, P. Serotonin: A New Hope in Alzheimer ' s Disease? **2015**. https://doi.org/10.1021/acschemneuro.5b00135.

(53) Cirrito, J. R.; Disabato, B. M.; Restivo, J. L.; Verges, D. K.; Goebel, W. D. Serotonin Signaling Is Associated with Lower Amyloid- β Levels and Plaques in Transgenic Mice and Humans. **2011**, *108* (36), 14968–14973. https://doi.org/10.1073/pnas.1107411108.

(54) Girard, D.; Girot, S.; Baranger, K.; Giannoni, P.; Gaven, F.; Stephan, D.; Migliorati, M.; Khrestchatisky, M.; Roman, F. S. Neuropharmacology Chronic Treatments with a 5-HT 4 Receptor Agonist Decrease Amyloid Pathology in the Entorhinal Cortex and Learning and Memory de Fi Cits in the 5xFAD Mouse Model of Alzheimer ' s Disease Jo E. **2017**, *126*, 128–141. https://doi.org/10.1016/j.neuropharm.2017.08.031.

(55) López-Iglesias, B.; Pérez, C.; Morales-García, J. A.; Alonso-Gil, S.; Pérez-Castillo, A.; Romero, A.; López, M. G.; Villarroya, M.; Conde, S.; Rodríguez-Franco, M. I. New Melatonin- N, N -Dibenzyl(N -Methyl)Amine Hybrids: Potent Neurogenic Agents with Antioxidant, Cholinergic, and Neuroprotective Properties as Innovative Drugs for Alzheimers Disease. *J. Med. Chem.* **2014**, *57* (9), 3773–3785. https://doi.org/10.1021/jm5000613.

(56) Chojnacki, J. E.; Liu, K.; Yan, X.; Toldo, S.; Selden, T.; Estrada, M.; Halquist, M. S.; Ye, D.; Zhang, S. Jeremy E. Chojnacki , Kai Liu, , Xing Yan, Stefano Toldo, Tyler Selden, Martin Estrada, María Isabel Rodríguez-Franco, Matthew S. Halquist, Dexian Ye, and Shijun Zhang. *ACS Chem. Neurosci.* **2014**, *5* (8), 690–699.

(57) Jiang, H.; Wang, X.; Huang, L.; Luo, Z.; Su, T.; Ding, K.; Li, X. Benzenediol-Berberine Hybrids: Multifunctional Agents for Alzheimer's Disease. *Bioorganic Med. Chem.* **2011**, *19* (23), 7228–7235. https://doi.org/10.1016/j.bmc.2011.09.040.

(58) Sato, M.; Murakami, K.; Uno, M.; Nakagawa, Y.; Katayama, S.; Akagi, K. I.; Masuda, Y.; Takegoshi, K.; Irie, K. Site-Specific Inhibitory Mechanism for Amyloid B42 Aggregation by Catechol-Type Flavonoids Targeting the Lys Residues. *J. Biol. Chem.* **2013**, *288* (32), 23212–23224. https://doi.org/10.1074/jbc.M113.464222.

(59) Wu, W. Y.; Dai, Y. C.; Li, N. G.; Dong, Z. X.; Gu, T.; Shi, Z. H.; Xue, X.; Tang, Y. P.; Duan, J. A. Novel Multitarget-Directed Tacrine Derivatives as Potential Candidates for the Treatment of Alzheimer's Disease. *J. Enzyme Inhib. Med. Chem.* **2016**, *32* (1), 572–587. https://doi.org/10.1080/14756366.2016.1210139.

(60) Chen, L.; Li, F. Q.; Hou, B. H.; Hong, G. F.; Yao, Z. J. Site-Specific Fluorescent Labeling Approaches for Naringenin, an Essential Flavonone in Plant Nitrogen-Fixation Signaling Pathways. *J. Org. Chem.* **2008**, *73* (21), 8279–8285. https://doi.org/10.1021/jo8014165.

(61) Siddique, Y. H.; Ara, G.; Afzal, M. Estimation of Lipid Peroxidation Induced by Hydrogen Peroxide in Cultured Human Lymphocytes. *Dose-Response* **2012**, *10* (1), 1–10.

https://doi.org/10.2203/dose-response.10-002.Siddique.

(62) Saija, A.; Scalese, M.; Lanza, M.; Marzullo, D.; Bonina, F.; Castelli, F. Flavonoids as Antioxidant Agents: Importance of Their Interaction with Biomembranes. *Free Radic. Biol. Med.* **1995**, *19* (4), 481–486. https://doi.org/10.1016/0891-5849(94)00240-K.

(63) Ellman, G. L.; Courtney, K. D.; Andres, V.; Featherstone, R. M. A New and Rapid Colorimetric Determination of Acetylcholinesterase Activity. *Biochem. Pharmacol.* **1961**, *7* (2), 88–95. https://doi.org/10.1016/0006-2952(61)90145-9.

(64) Do Carmo, S.; Kannel, B.; Cuello, A. C. The Nerve Growth Factor Metabolic Pathway Dysregulation as Cause of Alzheimer's Cholinergic Atrophy. *Cells* **2021**, *11* (1). https://doi.org/10.3390/cells11010016.

(65) Tang, H.; Zhao, L. Z.; Zhao, H. T.; Huang, S. L.; Zhong, S. M.; Qin, J. K.; Chen, Z. F.; Huang, Z. S.; Liang, H. Hybrids of Oxoisoaporphine-Tacrine Congeners: Novel Acetylcholinesterase and Acetylcholinesterase-Induced β-Amyloid Aggregation Inhibitors. *Eur. J. Med. Chem.* **2011**, *46* (10), 4970–4979. https://doi.org/10.1016/j.ejmech.2011.08.002.

(66) Hu, M. K.; Wu, L. J.; Hsiao, G.; Yen, M. H. Homodimeric Tacrine Congeners as Acetylcholinesterase Inhibitors. *J. Med. Chem.* **2002**, *45* (11), 2277–2282. https://doi.org/10.1021/jm010308g.

# Chapter 4. Design and synthesis of terphenyl derivatives: potential multitarget and theranostic compounds against oxidative stress and neuroinflammation

**Design and synthesis of terphenyl derivatives: potential multitarget and theranostic compounds against oxidative stress and neuroinflammation**

## 1.0 Introduction

### 1.1 Multicomponent reactions

**Chemical space** is a relatively new concept which tries to define a multidimensional space which englobes all possible molecules. This space can be defined by parameters such as molecular mass, hydrophobicity, or $sp^3$ character. This way, a potentially infinite space can be narrowed down to a defined region depending on the subject of research. In medicinal chemistry, this space is usually defined by drug-likeness parameters such as molecular mass below 500 kDa and a requisite for the molecules is to be formed by certain elements (C, H, N, S, O, P). Based on these premises, it has been estimated that this space is composed by $10^{60}$ different molecules [1,2].

**Multicomponent reactions** (MCRs) are defined as "a convergent reaction class, in which three or more commercially available or simple molecules react to contribute significantly, with all or many of their atoms, to the final reaction product"3. MCRs are generally one-pot processes that proceed either through a single synthetic operation or through sequential steps (without changes in the reaction medium). MCRs are a key tool in contemporary chemistry, due to their ability to provide sustainable processes with a high atom economy and reduced waste generation due to the absence of intermediate isolation and purification stages, compared to a stop and go synthetic methodology. Furthermore, MCRs are excellent tool to generate libraries of compounds following the build/couple/pair strategy, as they combine multiple scaffolds with small modifications or functional groups, this covering large regions of chemical space [4–6] (figure 1).

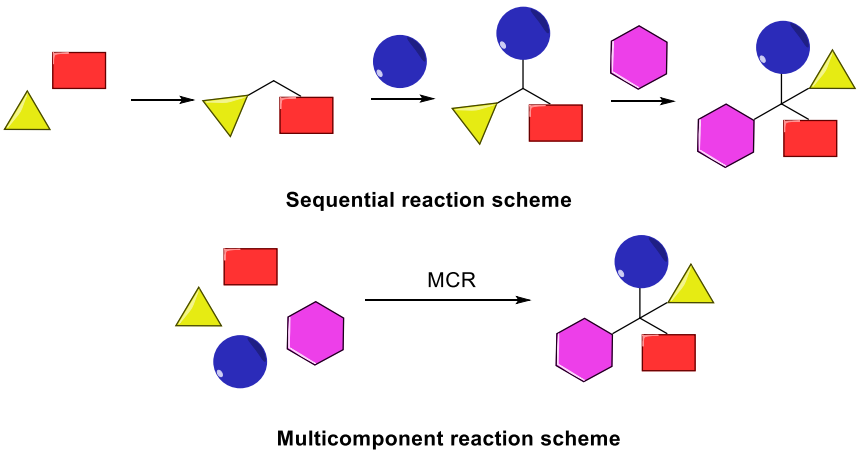


Figure 1. Comparison between multi-step sequential synthesis and a multicomponent reaction.

Multicomponent reactions have proved to have a wide number of applications in organic synthesis, and many examples have been described in the literature, such as: reactions involving

isocyanide use [7], radical-induced reactions [8], metal-catalysed syntheses [9] and photoinduced reactions [10] . Moreover, MCRs have been used for the synthesis of a variety of biologically relevant scaffolds such as: pyrroles, dihydropyrimidinones, pyrazoloquinolones, imidazopyridines, chromenopyridines, dihydropyridines, oxazoles and pyridines, among other heterocyclic systems [6]. In this context, we are interested in multicomponent reactions as tools for the discovery of molecules with potential as agents against neurodegenerative processes.

## 1.2 Mitochondria-targeted probes

Reactive oxygen species (ROS) have received much attention in recent years, as they have been found to be a key element of pathological and physiological states in living organisms. ROS have been associated with aging and diverse pathologies such as neurogenerative diseases like Alzheimer´s, Parkinson´s or Huntington´s diseases, together with other diseases like cancer. In recent years, the role of ROS in key physiological processes such as the immunological response to pathogens and cellular signalling has been elucidated[11] .

Mitochondria are the primary site of generation of ROS inside cells. They are a major source of the superoxide radical and hydrogen peroxide due to their role as the site of cell respiration. This also renders them particularly vulnerable to oxidative stress-associated damage. Chemical entities that allow to understand the dynamics of ROS inside mitochondria and that can simultaneously quench oxidative damage are particularly attractive in the biological/medicinal chemistry fields [12].

Mitochondria are comprised by 4 different compartments: the outer mitochondrial membrane (OMM), the inner membrane space (IMS), the inner mitochondria membrane (IMM) and the mitochondrial matrix. The combination of the small pore size of the OMM, the high protein concentration in the IMM and the strong negative membrane potential (-180 mV) make the mitochondrial matrix difficult to access by most organic molecules[13] (figure 2).

Due to the difficulties found by organic molecules for reaching the mitochondrial matrix, different methods have been designed for their delivery inside the mitochondria, acting either as probes or therapeutic agents. One of the approaches to the selective targeting of mitochondria takes advantage of the high electrochemical potential between the IMS and the matrix, maintained by the IMM. While all positively charged species are attracted to the mitochondrial matrix, delocalised lipophilic cations (DLCs) are particularly effective at crossing the IMM. DLCs are small molecules that possess a positive charge that can be delocalised through resonance. The transport of these molecules across the IMM is highly favoured due to the charge being spread through a larger area leading to a high ionic radius and allowing easier solvation in a lipidic environment [12,14,15].

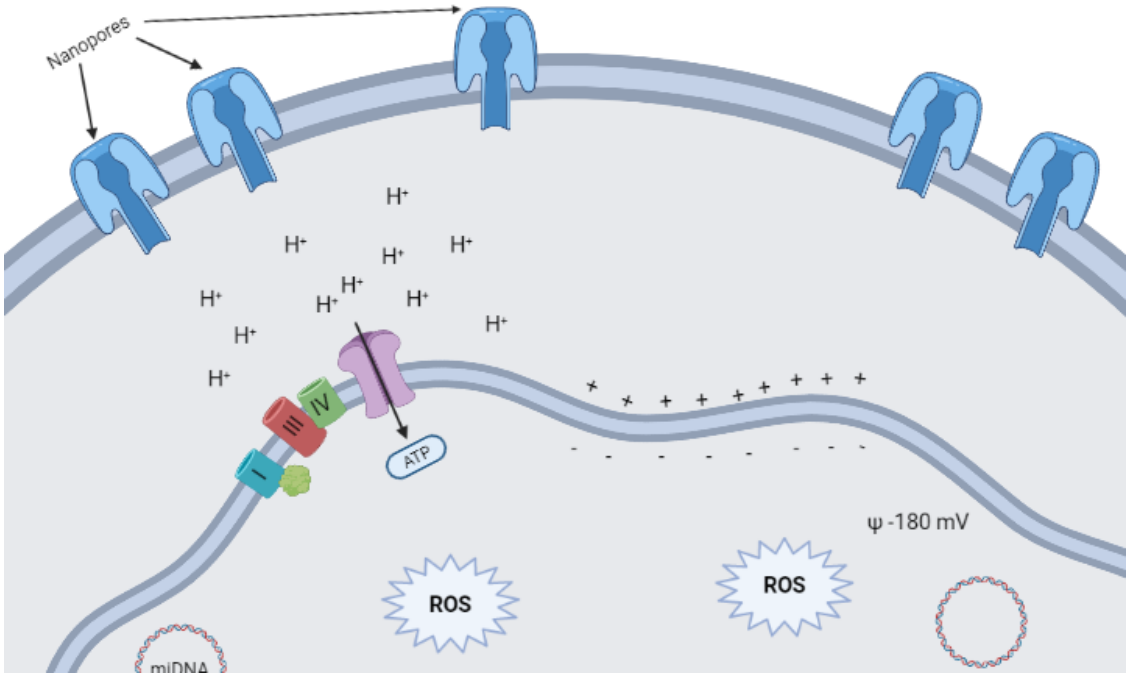


Figure 2. Scheme illustrating the different compartments and membranes in mitochondria.

The most widely used structural element used to generate DLCs is the triphenylphosphonium (TPP) cation. TPP has been used in the past for measuring the mitochondrial membrane potential and in recent times, has been attached to numerous molecules to deliver them to the mitochondrial matrix [16]. Through this strategy, molecules such as glutathione (GSH) [17], cysteine [18], peroxinitrite[19] and superoxide[20] have been detected *in vivo*. Additionally, many molecules with antioxidant potential such as ubiquinol [21], α-tocopherol [22], lipoic acid [23] and ebselen [24], as well as spin traps [25] , have been successfully bound to the TPP cation and directed towards the mitochondria, thus increasing their efficacy as free radical scavengers. Hence, incorporating a starting material bearing a TPP moiety in a multicomponent reaction could enrich the exploration of chemical space in search of a probes/antioxidants targeting mitochondrial oxidative stress, a cornerstone of neurodegenerative diseases.

## 1.3 Theranostic agents

Regarding neurodegenerative processes, the lack of an effective treatment is not the only challenge for effective disease handling. A robust, non-invasive diagnosis is also needed and, in this respect, theranostic systems have been receiving widespread attention in recent years.

Theranostic agents integrate both therapeutic and diagnostic properties in a single entity, offering an integrated solution for multifactorial pathological processes. These systems have been applied to the treatment and diagnosis of different types of cancer, and numerous reviews have been written describing the different strategies followed[26–30]. With respect to neurodegenerative diseases, a common hallmark is protein misfolding and many agents have been designed to exploit this feature for a simultaneous treatment and diagnosis. Typically, these are planar compounds that insert themselves between the misfolded protein sheets and

disrupt the formation of toxic aggregates while simultaneously changing their optical properties. Some examples of these molecules are shown in figure 3[31–34].

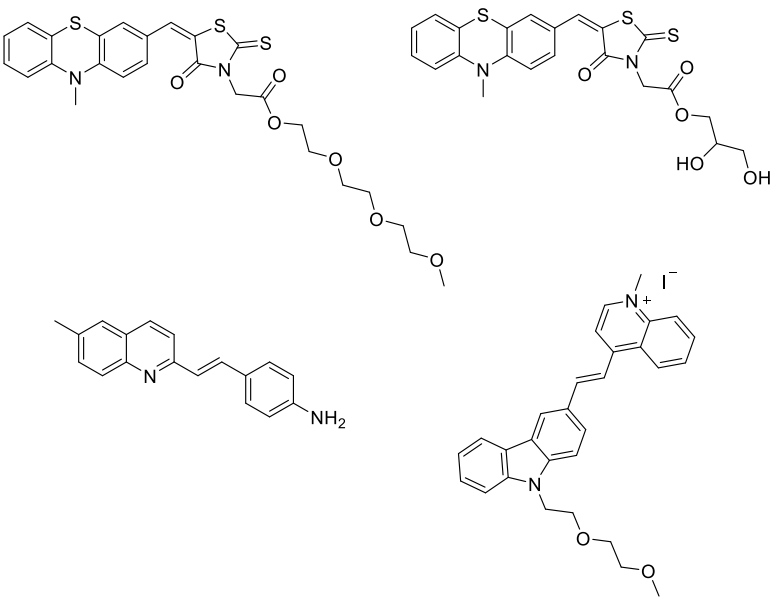

Figure 3. Some examples of Aβ targeted theragnostic systems

Another common hallmark shared by all neurodegenerative processes is the abundance of ROS and RNS, which saturate the capacity of the cell of counteracting the damage that they produce. In this regard, many ROS probes have also been designed that typically act by a change in the optical properties of the system following a direct ROS or RNS scavenging action. There is a good deal of literature describing the design and evaluation of probes for this purpose, but very often their therapeutic effectiveness has not been evaluated. Thus, there is a need for agents that can provide both therapeutic capacity and simultaneously diagnose exacerbated oxidative stress.

## 1.4 Cyclooxygenase and neurodegenerative diseases

Inflammation has been acknowledged as a pathological hallmark contributing to the development of neurodegenerative diseases such as AD [35]. Until recently, neuroinflammation was believed to be a consequence of senile plaques and neurofibrillary tangles. However, in recent years, it has been shown to play a major role in AD progress, as important as that of the previously named factors if not even more [36].

Microglial cells and astrocytes are the main actors involved in the inflammatory response in the brain [37]. Microglial cells are mesodermically-derived macrophages that possess all the features that characterise these cells such as being able to express the Major Histocompatibility Complex type II (MHC II), proinflammatory cytokines, chemokines, and ROS, as well as having phagocytic and scavenger capacities. Depending on the conditions, microglia can produce either neuroprotective or neurotoxic effects in the brain, depending on whether or not a physiological equilibrium exists in the brain [38]. On the other hand, astrocytes are immune system cells whose role is not completely understood, but it is hypothesised that they play a role as maintainers of connective tissue in the brain and skeletal function in the brain, maintaining a correct functioning and integrity of synapses. Their role in the immune response involves the production and secretion of proinflammatory cytokines, ROS, and also the clearance of strange bodies, such

as Aβ plaques. They also have a key role in production of complement proteins, whose abnormal functioning due to Aβ plaques has recently been related to a proinflammatory neurotoxic effect [35,39,40] (figure 2).

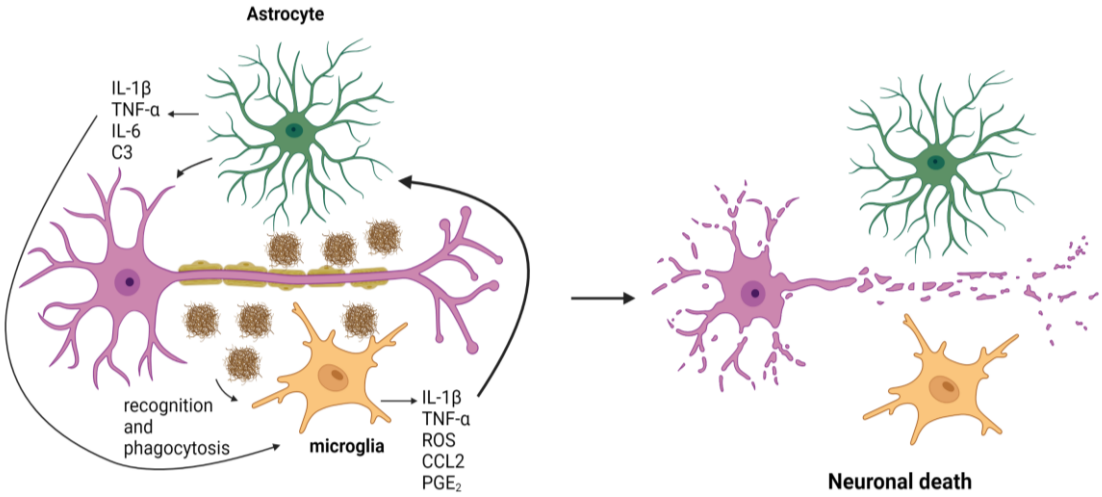


Figure 4. Scheme showing damage in neurons caused by an immune response positive feedback

Taking these factors into consideration, cyclooxygenase (COX) emerges as a cornerstone in inflammatory response as it coverts arachidonic acid into prostaglandins, which greatly contributes to its exacerbation [41]. There two different COX isoforms, COX-1 which is constituently expressed in most tissues and cells, including microglia, and COX-2 which is inducible under inflammatory stimuli. However, although COX-1 is related with the homeostasis of the immune response, recent studies have demonstrated an overexpression of this isoform in microglia surrounding Aβ plaques [42]. On the other hand, COX-2 is not expressed in AD patients' brains, except in the very early phases of the disease [43]. Additionally, selective inhibition of COX-1 has proven to be therapeutically beneficial in rodent models of AD by reducing Aβ and tau pathology and alteration of microglial phenotype [44]. Therefore, developing potent and selective inhibitors for COX-1 could be a viable therapeutic option for the treatment of AD. We became interested in the use of multicomponent reactions as a strategy for the synthesis of COX-1 selective inhibitors, as it should be readily translated into the fast preparation of a family of structurally varied compounds.

## 2.0 Objectives

The main objective of this work is the development of potential neuroprotective and diagnostic molecules for oxidative stress using a multicomponent reaction involving a chalcone, a beta ketoester and an amine. This reaction, previously developed by our group, combines these three elements using Ce (IV) as a catalyst and ethanol as a solvent, producing a highly substituted m-dihydroanthranilate skeleton [45,46]. The high degree of functionalization of these structures renders them easily convertible to more complex frameworks, potentially covering a broader region of chemical space. The scope of this reaction has been verified by altering the structure of the chalcones, beta ketoesters and amines, admitting a wide variety of substituents. The dihydroanthranilates were then subjected to different reactions to convert them into other structures such a posterior aromatization with either DDQ or AIBN/NBS or heating aromatic amine substituted derivatives under microwave conditions to obtain acridones, a highly privileged structure in drug discovery.

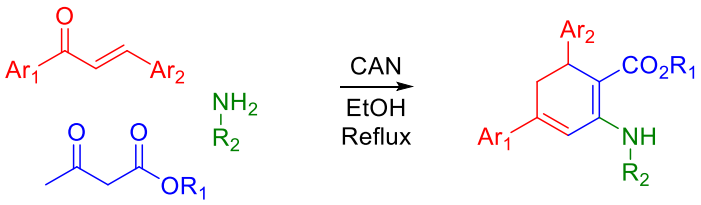


Scheme 1. Formation of dihydroanthranilates via a three-component reaction between chalcones, β-ketoesters and amines.

Among, the different amines used for the synthesis of these dihydroanthranilates, one bearing a triphenylphosphonium could be used for the development of mitochondrial probes. While dyhydroanthranilates are non-fluorescent, its aromatized derivatives are, so in response to an oxidative agent, dihydroanthranilates should react with it, thus becoming oxidized and therefore, fluorescent [48]. These derivatives should also act as free radical scavengers inside the mitochondria by the same mechanism, which could possibly convert these compounds in potential theragnostic molecules.

Finally, dihydroanthranilates can be transformed to *m*-amino terphenyl through a robust synthetic route. These structures have proven to be selective COX-1 inhibitors. However more potent and less lipophilic derivatives should be synthesised in order to produce a more drug-like molecule. Additionally, these structures could be furtherly derivatised to obtain multitarget drug ligands that not only act in COX-1, but also in other AD targets such as Acetylcholinesterase (AChE) or Butyrylcholinesterase (BuChE), thus obtaining potentially more efficient therapeutic agents.

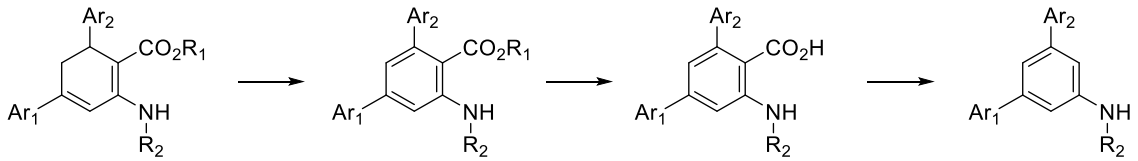


Scheme 2. Synthetic scheme followed to obtain *m*-terphenylamines

## 3.0 Results

### 3.1 Multicomponent synthesis and chiral characterization of *m*-terphenyls with an embedded dihydroanthranilate unit

As previously mentioned, dihydroantranilate skeletons were obtained by a multicomponent reaction using a chalcone, a beta ketoester and an amine. All beta ketoesters and amines were purchased from commercial sources. However, most chalcones had to be synthesised via an aldol condensation reaction between acetophenones and aromatic aldehydes in the presence of sodium hydroxide, generally followed by simple filtration as the products precipitated from ethanol.

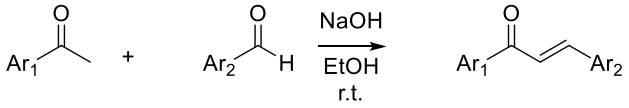


**2.01a-2.01q**

Scheme 1. Formation of chalcones via an aldol condensation reaction between aromatic ketones and aromatic aldehydes.

| Compound | $R_1$ | $R_2$ | Yield (%) |
|---|---|---|---|
| **2.01a** | 4-$NO_2$-$C_6H_4$ | Ph | 80 |
| **2.01b** | Ph | 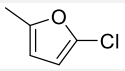 | 66 |
| **2.01c** | 4-OMe-$C_6H_4$ | Ph | 70 |
| **2.01d** | Ph | 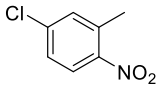 | 20 |
| **2.01e** | 4-Br-$C_6H_4$ | Ph | 68 |
| **2.01f** | Ph | 4-$NO_2$-$C_6H_4$ | 94 |
| **2.01g** | 4-Br-$C_6H_4$ | 4-Br-$C_6H_4$ | 99 |
| **2.01h** | 4-Me-$C_6H_4$ | 2-$NO_2$-$C_6H_4$ | 76 |
| **2.01i** | 2-$NO_2$-$C_6H_4$ | 4-Br-$C_6H_4$ | 64 |
| **2.01j** | Ph |  | 78 |
| **2.01k** | Ph | 4-Br-$C_6H_4$ | 79 |
| **2.01l** | Ph |  | 86 |
| **2.01m** | 2,4-MeO-$C_6H_3$ | 4-MeO-$C_6H_4$ | 79 |
| **2.01n** | 4-Cl-$C_6H_4$ | 4-Cl-$C_6H_4$ | 85 |
| **2.01o** | 4-MeO-$C_6H_4$ | 3-MeO-$C_6H_4$ | 84 |
| **2.01p** | 4-$NO_2$-$C_6H_4$ | 4-$NO_2$-$C_6H_4$ | 91 |
| **2.01q** | 4-Cl-$C_6H_4$ | 4-$NO_2$-$C_6H_4$ | 86 |

Table 1. Starting chalcones synthesised

With the starting chalcones in hand, the multicomponent reactions were performed. Although this was known chemistry,[46,47] we have extended the scope of the reaction and also proved the integrity of an stereocenter at the amine component. The reactions were performed by

dissolving the beta keto ester and amine in ethanol at room temperature, adding the cerium ammonium nitrate a catalyst and finally the the chalcone, followed by heating under reflux. The reaction is then easily purified through an aqueous extraction in the first place and a column chromatography afterwards to achieve the desired dihydroanthranilates in good yields in most cases (table 2). Many of the compounds had been previously synthesised in our group (compounds underlined in table 2),[47] but it was necessary to re-synthesise them again in order to complete their characterization. The reaction mechanism had been previously proposed to comprise the initial formation of an intermediate enaminoester, followed by its Michael addition to the chalcone, tautomerism to the less substituted enamine and intramolecular cyclocondensation (Scheme 4).

Since prior work from our group had shown that the use of ammonia as the amine component is not compatible with the formation of the **2.02** framework, giving rise to dihydropyridines instead[49], in order to obtain compounds bearing a primary amino group, ammonium formate was added as a source of ammonia to the reaction mixture derived from the use of butylamine to promote an *in situ* aza-Michael/retro-aza-Michael reaction sequence from the non-isolated butylamino-substituted dihydroanthranilate[46,47] (scheme 4).

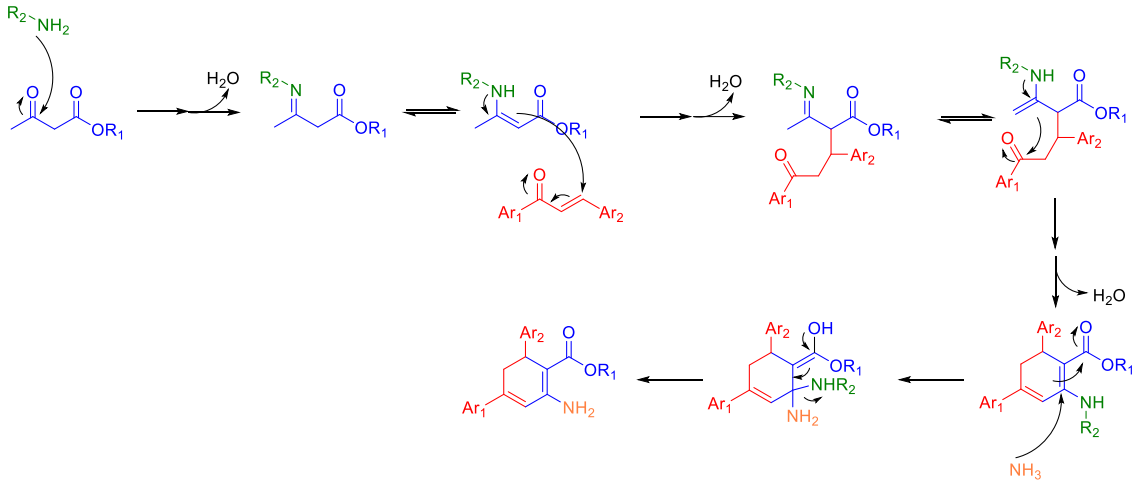

Scheme 2. Mechanism of the three-component reaction between chalcones, β-keto esters and amines.

| Compound | $Ar_1$ | $Ar_2$ | $R_1$ | $R_2$ | Yield (%) |
|---|---|---|---|---|---|
| **2.02a** | Ph | Ph | Et | H | 93 |
| **2.02b** | 4-$NO_2$-$C_6H_4$ | Ph | Et | H | 96 |
| **2.02c** | Ph | 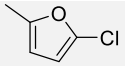 | Et | H | 67 |
| **2.02d** | 4-Me-$C_6H_4$ | Ph | Et | H | 69 |
| **2.02e** | 4-MeO-$C_6H_4$ | Ph | Et | H | 64 |
| **2.02f** | 4-Br-$C_6H_4$ | 4-Br-$C_6H_4$ | Et | H | 89 |
| **2.02g** | Ph |  | Et | H | 78 |
| **2.02h** | 4-$NO_2$-$C_6H_4$ | Ph | Et | $CH_2C_6H_5$ | 78 |
| **2.02i** | Ph | Ph | tBu | $CH_2C_6H_5$ | 84 |

| | | | | | |
|---|---|---|---|---|---|
| **2.02j** | Ph | Ph | Et | 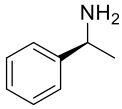 | 67 |
| **2.02k** | Ph | Ph | Et | 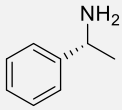 | 58 |
| **2.02l** | Ph | 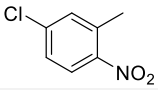 | Et | Bu | 58 |
| **2.02m** | 4-Br-$C_6H_4$ | Ph | Et | Bu | 59 |
| **2.02n** | Ph | 4-$NO_2$-$C_6H_4$ | Et | Bu | 78 |
| **2.02o** | 4-Me-$C_6H_4$ | 2-$NO_2$-$C_6H_4$ | Et | Bu | 74 |
| **2.02p** | 2-$NO_2$-$C_6H_4$ | 4-Br-$C_6H_4$ | Et | Bu | 62 |
| **2.02q** | Ph |  | Et | Bu | 62 |
| **2.02r** | Ph | Ph | Et | 3-Cl-$C_6H_4$ | 48 |
| **2.02s** | Ph | 4-$NO_2$-$C_6H_4$ | Et | Ph | 59 |
| **2.02t** | Ph | 4-Br- $C_6H_4$ | Et | Ph | 59 |
| **2.02u** | Ph | Ph | Et | 4-$NMe_2$-$C_6H_4$ | 84 |
| **2.02v** | Ph | Ph | Et | 4-Br-$C_6H_4$ | 53 |
| **2.02w** | Ph | Ph | Et | 3,5-$ClC_6H_3$ | 48 |
| **2.02x** | 4-MeO-$C_6H_4$ | Ph | Et | Ph | 41 |
| **2.02y** | 4-Cl-$C_6H_4$ | Ph | Et | Ph | 41 |
| **2.02z** | 2,4-MeO-$C_6H_3$ | 4-MeO-$C_6H_4$ | Et | Ph | 43 |
| **2.02aa** | 4-Cl-$C_6H_4$ | 4-Cl-$C_6H_4$ | Et | Ph | 39 |

Table 2. Compounds synthesised using the three-component reaction between chalcones, β-keto esters and amines

As can be observed from table 2, the results of the reaction depend on the amine used for the synthesis. In the case of aliphatic amines, yields are usually above 55% after column chromatography, while aromatic amines rarely afford a yield over 50% with the same purification process, with the exception of compound **2.02u**. This can be attributed to the reaction mechanism. The first step, involving the condensation of the amine with the beta ketoester to form an enaminoester, depends on the nucleophilicity of the amine used, being aliphatic amines more nucleophilic than their aromatic counterparts, even though the enamine system is less conjugated. The exception that can be observed for compound **2.02u** can be explained taking into consideration the increased electron density of 4-N-dimethylamino aniline.

As a way to expand the structural diversity of this library, the aromatization of these compounds was performed using DDQ as the oxidising agent (Scheme 4). The reaction was performed at room temperature and provided good yields, leading to a robust method for the obtention of the fully aromatic functionalized *m*-terphenyl derivatives (table 3). Similarly, to the case of **2.02**, some compounds **2.03** had been previously obtained by our group but had to be re-synthesised in order to obtain full characterization data (compounds underlined in table 3).

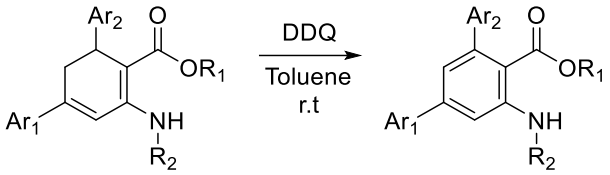


**2.03a-2.03l**

Scheme 3. Oxidation of dyhydroanthranilates obtained to their aromatic derivatives

| Compound | $Ar_1$ | $Ar_2$ | $R_1$ | $R_2$ | Yield (%) |
|---|---|---|---|---|---|
| **2.03a** | Ph | Ph | Et | H | 68 |
| **2.03b** | 4-$NO_2$-$C_6H_4$ | Ph | Et | H | 74 |
| **2.03c** | 4-Me-$C_6H_4$ | Ph | Et | H | 66 |
| **2.03d** | Ph | 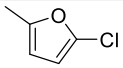 | Et | H | 72 |
| **2.03e** | 4-MeO-$C_6H_4$ | Ph | Et | H | 78 |
| **2.03f** | 4-$NO_2$-$C_6H_4$ | Ph | Et | $CH_2C_6H_5$ | 66 |
| **2.03g** | Ph | Ph | Et | 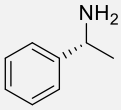 | 67 |
| **2.03h** | Ph | Ph | Et | 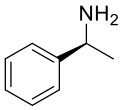 | 64 |
| **2.03i** | 4-Me-$C_6H_4$ | 2-$NO_2$-$C_6H_4$ | Et | Bu | 59 |
| **2.03j** | Ph | 4-Br-$C_6H_4$ | Et | Ph | 44 |
| **2.03k** | Ph | Ph | Et | 4-$NMe_2$-$C_6H_4$ | 62 |
| **2.03l** | Ph | Ph | Et | 4-Br-$C_6H_4$ | 46 |

Table 3. Compounds obtained through the oxidation of dyhydroanthranilates with DDQ.

Two chiral amines, namely (*S*)- and (*R*)-1-phenylethan-1-amine were used to investigate the possibility of racemization along the two-step sequence. The multicomponent reaction between ethyl acetoacetate, chalcone and either of these two amines provided the corresponding mixture of diastereoisomers, which were aromatised, and thus the stereogenic centre of the dihydroanthranilate fragment was lost, leaving only the $\alpha$-amino stereocenter. We had initially planned to verify the enantiopurity of the reaction products by reverse phase chiral HPLC, but their poor solubility in polar HPLC mobile phases prevented their study. However, by hydrolysing the ester groups to the correspondent carboxylic acids, their solubilities improved sufficiently, and this allowed verifying their enantiopurity, thus confirming the robustness of this method.

### 3.2.1 Synthesis of probes for mitochondrial oxidative stress

Previous work has shown that, while the dihydroanthranilate derivatives are non-fluorogenic, their aromatic derivatives are able to emit fluorescence[48]. This behaviour is interesting in the design of turn-on fluorescent probes for oxidative species, as dihydroanthranilates are easily oxidised in the presence of radical species. A major limitation of many known such probes is that they emit fluorescence themselves, leading to practical problems associated to the difficulty of

detecting a signal against a bright background. This inconvenience is bypassed by turn-on fluorescent probes, which present very little native fluorescence but become fluorescent upon reacting with the analyte.

As a way to direct the dihydroanthranilates to mitochondria, a positive charge was added to the molecules by the introduction of a triphenylphosphonium moiety in the $R_2$ position of the structure. As a route to reach these structures, we first carried out our multicomponent reaction starting from 5-amino-1-pentanol as the primary amine component, which provided the correspondent dihydroantranilate **I**. We then tosylated the hydroxyl group, which yielded compound **II**, but unfortunately all attempts to introduce the triphenylphosphinonium moiety via an $S_N2$ displacement reaction were unsuccesful (scheme 8).

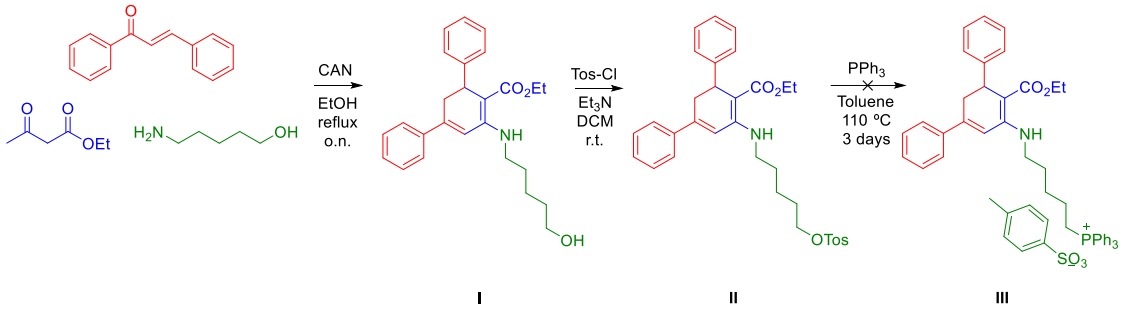


Scheme 4. Attempt to synthesise dyhydroanthranilate bearing phosphonium salt.

Due to these negative results, we attempted an alternative route that involved the acylation of the free amino group of compounds **2.02a** and **2.03a** with (4-chloro-4-oxobutyl)triphenylphosphonium bromide. This reaction worked well for compound **2.3a**, but not in the case of its dihydro derivative **2.02a**, where a very efficient conjugation with the ester group may have rendered the amino unreactive. No further attempts were made because the acylated product **2.08** was clearly much less fluorescent when revealed with the UV lamp than its predecessor, rendering the compound useless for the intended purpose (scheme 9).

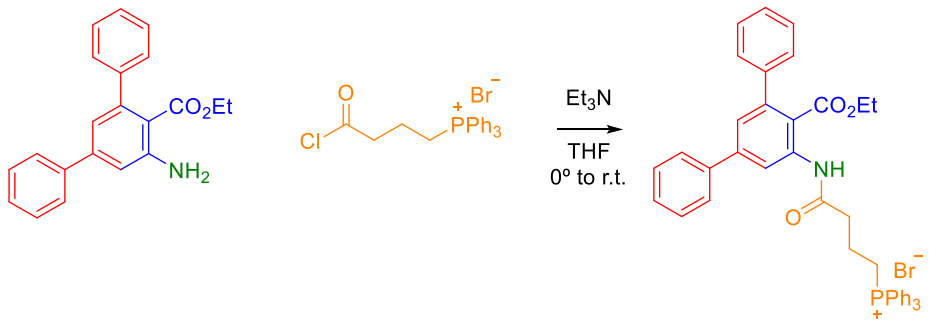


Scheme 5. Synthesis of compound 8 via amidation of compound **2.03a**.

At this point, we decided to explore the possibility of carrying out the initial multicomponent reaction leading to dihydroanthranylate derivatives from a derivative of pentylamine bearing a triphenylphosphonium group. To prepare the starting material, we first refluxed 5-amino-1-pentanol in 49% aqueous hydrobromic for 3 hours with the purpose to substitute the hydroxy group for a bromide and therefore obtain the hydrobromide of 5-bromopentanamine **2.04**. This compound was then heated in the confocal microwave reactor with triphenylphosphine at 140

°C for 2 hours in the absence of solvent to obtain (5-ammoniopentyl)triphenylphosphonium bromide **2.05,** for use as the primary amine in the multicomponent reaction (scheme 7).

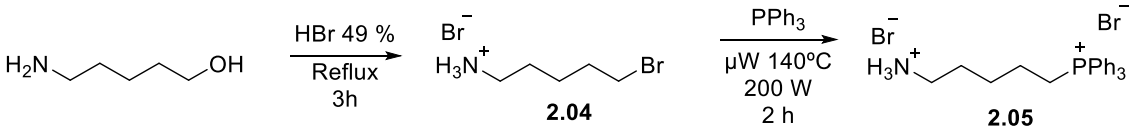


Scheme 6. Formation of amine **2.05**.

While, not unexpectedly, the direct reaction of **2.05** with chalcone and ethyl acetoacetate under the usual reaction conditions gave only traces of the target compound, the addition of triethylamine to release (5-aminopentyl)triphenylphosphonium bromide as a base allowed the preparation of a small library of 8 compounds **2.06** variously substituted at $Ar_1$ and $Ar_2$ with electron-donating and electron withdrawing groups to observe the effect on the optical properties of the compounds, as well as a *tert*-butyl ester specifically designed to be easily hydrolysed and obtain a better cellular retention. (Scheme 10) (Table 6).

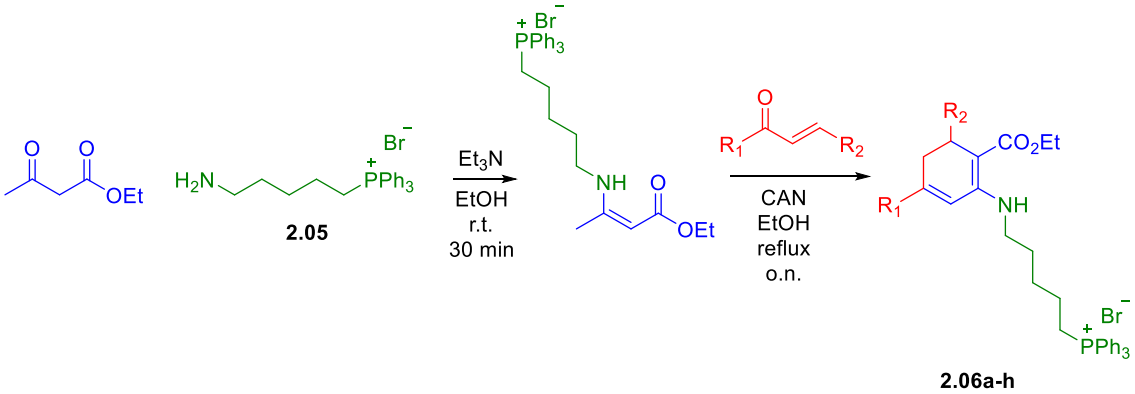


Scheme 7. Formation of compounds **2.06a**-**2.06h**.

| Compound | $Ar_1$ | $Ar_2$ | $R_1$ | Yield (%) |
|---|---|---|---|---|
| **2.06a** | Ph | Ph | Et | 65 |
| **2.06b** | Ph | 4-OMe-$C_6H_4$ | Et | 60 |
| **2.06c** | 4-OMe-$C_6H_4$ | 3-OMe-$C_6H_4$ | Et | 52 |
| **2.06d** | Ph |  | Et | 65 |
| **2.06e** | Ph | Ph | tBu | 64 |
| **2.06f** | Ph | 4-$NO_2$-$C_6H_4$ | Et | 65 |
| **2.06g** | 4-Cl-$C_6H_4$ | 4-$NO_2$-$C_6H_4$ | Et | 64 |
| **2.06h** | 4-$NO_2$-$C_6H_4$ | 4-$NO_2$-$C_6H_4$ | Et | 67 |

Table 4. Compounds obtained via multicomponent reaction of chalcones, β-ketoesters and amine **2.05**.

In order to study the fluorescent properties of the anthranilate derivatives, we attempted the dehydrogenation of compound **2.06a** to its aromatic derivative. However, since in this case chromatographic purification was not feasible, we tried alternative methods of oxidation such

as dissolving the compound in nitrobenzene and heating it up to 250 °C in the microwave reactor, which led only to decomposition. As an alternative, we decided to brominate the benzylic position of the starting material using N-bromosuccinimide in the presence of azo-bisisobutyronitrile (AIBN) as a free radical generator, which would be followed by a subsequent elimination of bromine with concomitant aromatization. This method yielded the desired compound in an excellent yield, and we proceeded to use it for the remaining compounds **2.06b**-**2.06h** (Scheme 11 and Table 7). In the case of **2.07a** and **2.07e**-**h**, the reaction was easily purified via a simple aqueous workup, providing the desired products in good purity and high yields. However, in the case of compounds **2.07b** and **2.07d**, a purification by column chromatography was needed. In the case of compound **2.07c**, the polarity of an unidentified side products was so similar that purification was not possible.

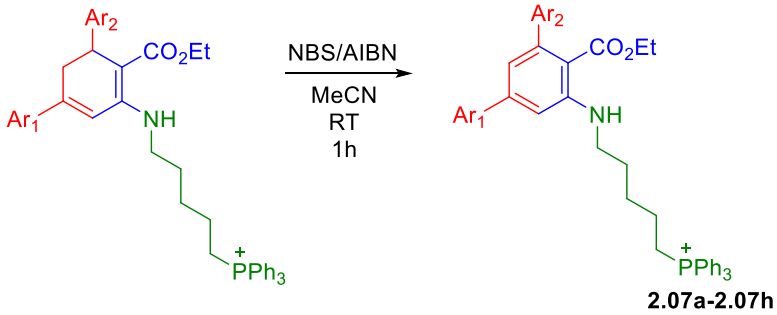


Scheme 8. Formation of aromatic compounds **2.07a**-**2.07h**.

| Compound | $Ar_1$ | $Ar_2$ | $R_1$ | Yield (%) |
|---|---|---|---|---|
| **2.07a** | Ph | Ph | Et | 96 |
| **2.07b** | Ph | 4-OMe-$C_6H_4$ | Et | 65 |
| **2.07c** | 4-OMe-$C_6H_4$ | 3-OMe-$C_6H_4$ | Et | - |
| **2.07d** | Ph |  | Et | 68 |
| **2.07e** | Ph | Ph | tBu | 94 |
| **2.07f** | Ph | 4-$NO_2$-$C_6H_4$ | Et | 99 |
| **2.07g** | 4-Cl-$C_6H_4$ | 4-$NO_2$-$C_6H_4$ | Et | 96 |
| **2.07h** | 4-$NO_2$-$C_6H_4$ | 4-$NO_2$-$C_6H_4$ | Et | 93 |

Table 5. Compounds formed through the oxidation of compounds **2.6a**-**2.6h** vias NBS and AIBN.

### 3.2.2 Optical characterization of mitochondrial oxidative stress probes

Once the aromatic compounds that would presumably result from the reaction of dihydroanthranilates with biological oxidants were available to us, we proceeded to characterise their spectral properties. We started by performing fluorescence measurements to determine the emission maxima of compounds **2.07a**-**2.07h** in ethanol. The results obtained (Figure 1) indicate that compounds **2.07f**-**h**, bearing aromatic nitro groups, do not emit fluorescence, and hence are not suitable candidates for the development of probes for mitochondrial oxidative stress. All the other compounds were fluorescent with emission maxima around 450 nm. Interestingly, compound **2.07d** presents an emission shift towards the red and has a maximum

of emission of 467 nm (Figure 1). Such emission red shifts are important for the development of biocompatible fluorescent probes, as light emissions closer to the red are less harmful for biological systems than ones closer to the blue as the former are less energetic. Moreover, interference from radiation absorption by the surrounding tissues is minimal in the red-near infrared region.

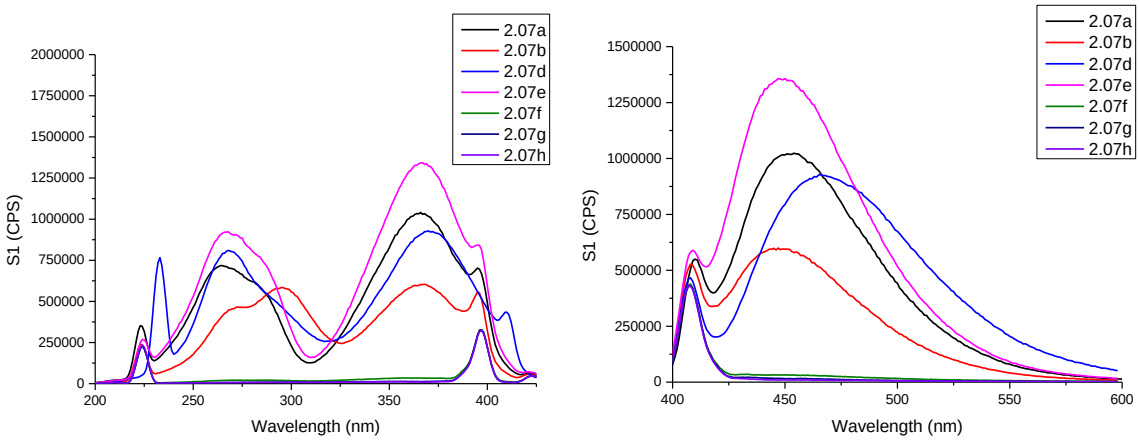


Figure 1. Excitation and emission spectra of compounds **2.07a**-**2.07f** in EtOH.

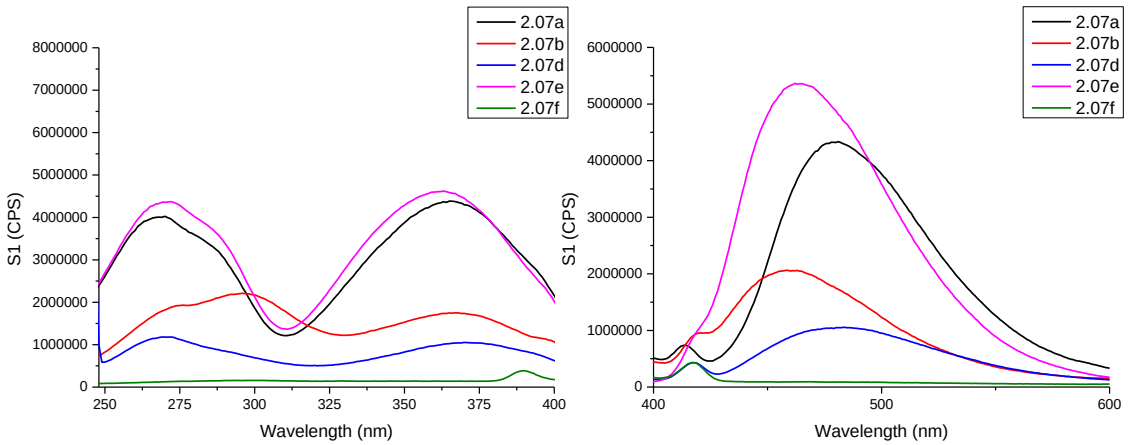


Figure 2. Excitation and emission spectra of compounds **2.07a**-**2.07f** in $H_2O$

It can be observed in figure 1 that compounds **2.07f**-**h** bearing a nitro group do not emit fluorescence, and hence are not suitable candidates for the development of probes for mitochondrial oxidative stress. This is due to the quenching of fluorescence by this functional group. All the other compounds were fluorescent with emission maxima around 450 nm. Interestingly, compound **2.07d** presents an emission shift towards the red and has a maximum

of emission of 467 nm. As these compounds are destined to be tested in an aqueous cellular medium, the excitation and emission spectra of these compounds were also recorded in water. The results are detailed in figure 2 and the emission and excitation maxima are collected in table 6 and show that the emission maxima of all compounds undergo a significant red shift (about 15 nm) in water in their emission spectra. Thus, a less energetic (and therefore less biologically harmful) wavelength could be used to obtain information about oxidative stress in cellular models.

| Compound | Excitation maxima (nm) | | Emission maxima (nm) | |
|---|---|---|---|---|
| | EtOH | $H_2O$ | EtOH | $H_2O$ |
| **2.07a** | 265, 365 | 269, 366 | 452 | 480 |
| **2.07b** | 295, 367 | 297, 368 | 447 | 460 |
| **2.07d** | 268, 370 | 271, 372 | 467 | 483 |
| **2.07e** | 267, 367 | 270, 363 | 450 | 464 |

Table 6. Maxima of excitation and emission of compounds **2.07a**, **2.07b**, **2.07d** and **2.07e** in EtOH and $H_2O$

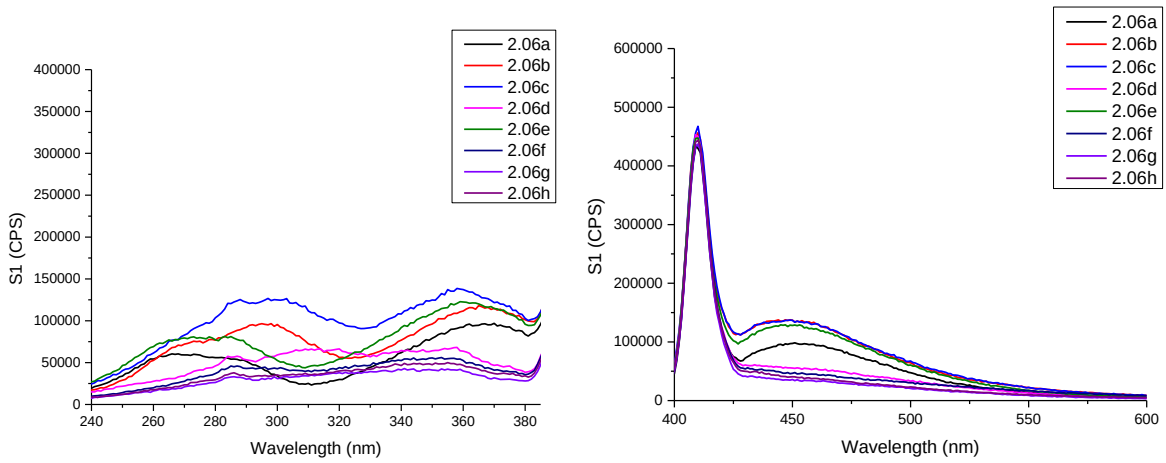


Figure 3. Excitation and emission spectra of compounds **2.06a**-**2.06h** in EtOH.

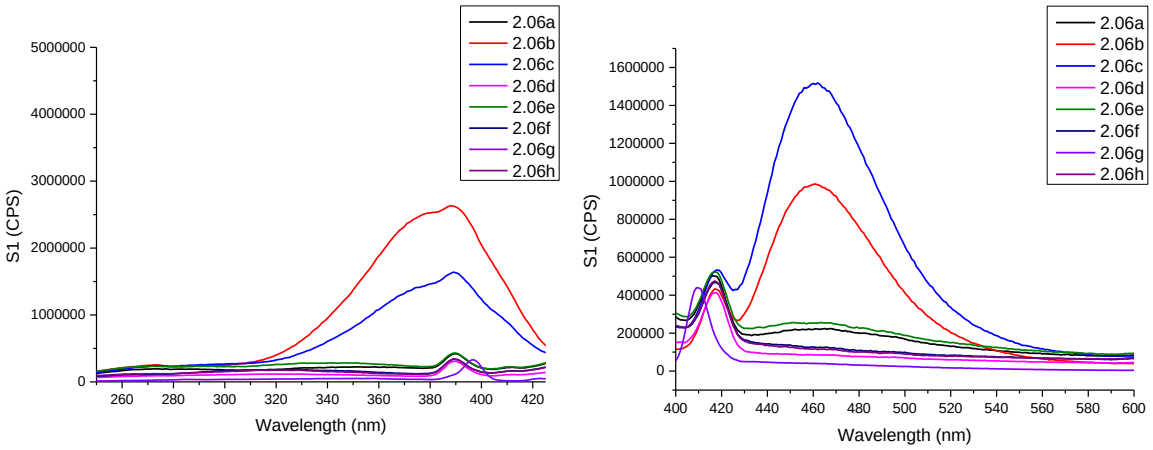


Figure 4. Excitation and emission spectra of compounds **2.06a**-**20.6h** in $H_2O$

The emission and excitation spectra of the dihydroanthranilate compounds **2.06a**-**2.06h** in ethanol (figure 3) and water (figure 4) were also recorded to examine their fluorescence in the absence of any oxidant agent. As originally hypothesised, no fluorescence was observed in ethanol, but when methoxy-bearing compounds **2.06b** and **2.06c** are dissolved in water, their excitation and emission spectra change, showing fluorescence at approximately the same wavelengths as their previously studied aromatic derivatives **2.07b** and **2.07c**. It is possible that these electron-rich compounds are aromatized in contact with oxygen dissolved in water and this way they acquire the capacity to emit fluorescence. This discovery seems to render compounds **2.06b** and **2.06c** unsuitable candidates for the development of fluorescent probes for mitochondrial oxidative stress.

| Entry | $\Phi_{ethanol}$ | $\Phi_{water}$ |
|---|---|---|
| **2.07a** | 0.169 ± 0.016 | 0.123 ± 0.036 |
| **2.07d** | 0.152 ± 0.036 | 0.047 ± 0.003 |
| **2.07e** | 0.337 ± 0.018 | 0.109 ± 0.017 |

Table 7. Quantum yields of compounds **2.07a**, **2.07d** and **2.07e** in EtOH and $H_2O$

To obtain numerical data of the fluorescence of compounds **2.07a**, **2.07d** and **2.07e**, their quantum yields were measured in ethanol and water (table 7). Quantum yield can be defined by the number of events occurring per photon absorbed by the system[50]. In fluorescence terms it can be translated into the number of photons emitted as fluorescence per photon absorbed by the system and is a numeric measure of the fluorescence of a compound. The compound that possesses the highest quantum yield is **2.07e**, with a value of 0.337, which represents a high fluorescence intensity. Both **2.07a** and **2.07e** also present good quantum yield values, about half of **2.07e**. In water, the quantum yield values decrease, being compound **2.07a** the least affected. Therefore, compounds **2.07a** and **2.07e** present the best optical properties for this purpose.

### 3.2 Synthesis of 1,3-diaryl-10-acridone derivatives from *m*-terphenyls

In order to further increase the structural diversity accessible from our *m*-terphenyls, a reaction allowing to transform the N-aryl derivatives of the dihydroanthranilate framework **2.02** into dihydroacridones was studied. Acridones are a privileged structure in medicinal chemistry as derivatives of this ring system possess a wide variety of biological activities such as antiviral [51], antitumoural [52,53], antifungal [54], antibacterial [55] and AChE and BuChE inhibition[56,57]. This last application is potentially interesting for the treatment of AD.

The most common way to synthesise these scaffolds is via a Jourdan-Ullman coupling of aryl halides and anthranilic acid derivatives followed by using strong acids or catalysis by metals to achieve the central ring formation[53,58]. Other ways to synthesise acridones involve coupling of anthranilates with benzynes, which are formed *in situ* from trimethylsilylphenyl triflate and cesium fluoride [59] or via a Heck coupling reaction between two equivalents of a substituted styryl and a quinolone, which is subsequently cyclized by an oxidative electrocyclization step (Scheme 5) [60].

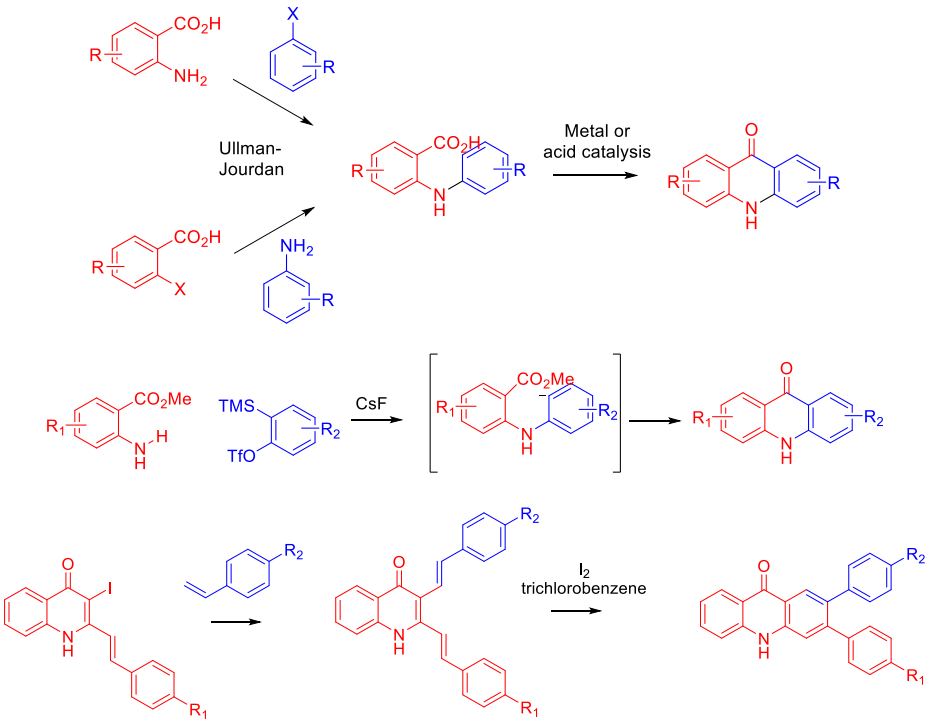


Scheme 9. Different described methodologies for the obtention of acridones.

For the synthesis of the dihydroacridones, we started from N-aryl substituted dihydroanthranilates which were cyclized under thermal conditions (250 °C, up to 200 W in the sealed tube reactor in DMF) for 90 minutes. This way, 4 dihydroacridones were obtained in good yields after purification by precipitation with petroleum ether [61] (Table 8).

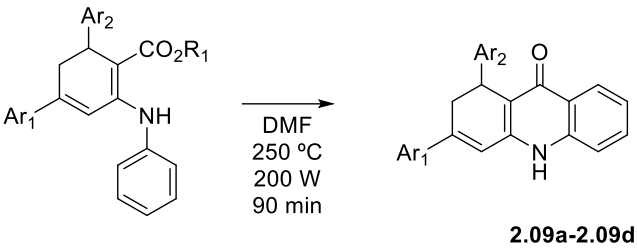


**2.09a-2.09d**

Scheme 10. Synthesis of dyhydroacridones **2.09a**-**2.09d** via heating in a sealed tube with N-aryl dihydroanthranilates as starting materials.

| Compound | $Ar_1$ | $Ar_2$ | Yield (%) |
|---|---|---|---|
| **2.09a** | 4-MeO-$C_6H_4$ | Ph | 43 |
| **2.09b** | 4-Cl-$C_6H_4$ | Ph | 52 |
| **2.09c** | 2,4-MeO-$C_6H_3$ | 4-MeO-$C_6H_4$ | 44 |
| **2.09d** | 4-Cl-$C_6H_4$ | 4-Cl-$C_6H_4$ | 27 |

Table 8. Dyhydroacridones obtained through reaction of N-aryl dyhydroanthranilates under sealed tube conditions

The reaction mechanism postulated in this case is similar to the one usually accepted for the Gould-Jacobs synthesis of 4-quinolones from anilines and ethyl ethoxymethylenemalonate, via the formation of an α-iminoketene intermediate with loss of ethanol, and its cyclization via a 6π electrocyclization reaction followed by a 1,3-hydrogen shift (scheme 6).

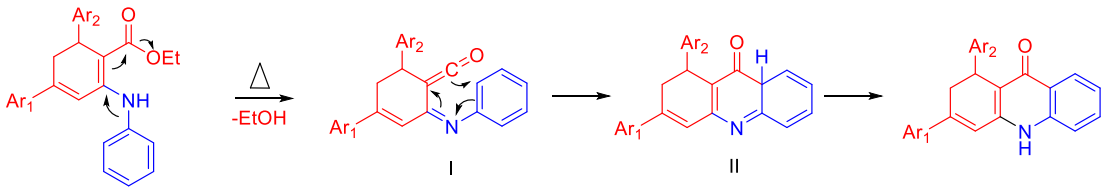


Scheme 11. Proposed reaction mechanism for the formation of dihydroacridones **2.09a**-**2.09d**.

To better exploit the full potential of this reaction to cover chemical space we decided to oxidise the dihydroacridones to their aromatic derivatives. We used for this purpose nitrobenzene both as a solvent and reagent, heating in the microwave reactor up to 250 °C for 90 minutes. The product was then easily isolated by crushing the reaction mixture with diethyl ether, yielding the desired acridones in good yields (table 9).

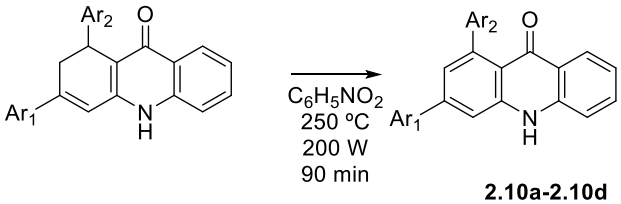


**2.10a-2.10d**

Scheme 12. Oxidation of compounds **2.09a**-**2.09d** to obtain acridones **2.10a**-**2.10d**.

| Entry | $Ar_1$ | $Ar_2$ | Yield (%) |
|---|---|---|---|
| **2.10a** | 4-MeO-$C_6H_4$ | Ph | 74 |
| **2.10b** | 4-Cl-$C_6H_4$ | Ph | 70 |
| **2.10c** | 2,4-MeO-$C_6H_3$ | 4-MeO-$C_6H_4$ | 77 |
| **2.10d** | 4-Cl-$C_6H_4$ | 4-Cl-$C_6H_4$ | 43 |

Table 9. Compounds **2.10a**-**2.10d** obtained through oxidation of compounds **2.09a**-**2.09d**.

## 3.3 Synthesis and characterization of COX-1 inhibitors

In previous work by our group, *m*-terphenyl amino compounds were identified as selective inhibitors of the COX-1 enzyme. In order to extend this library, the multicomponent reaction previously described was used as a starting point, followed by a subsequent aromatization. The next step involved the hydrolysis of the ester group that was carried out in basic conditions, using aqueous NaOH at 60 °C (Scheme 12). This reaction yielded the desired acids almost quantitatively in all cases, due to the easy workup of the reaction and the isolation of compounds **2.11a-g** without the need for chromatography.

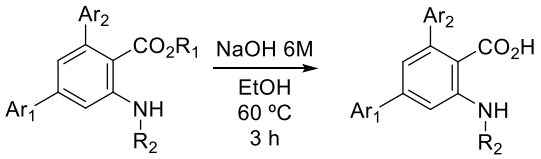


**2.11a-2.11g**

Scheme 13. Hydrolysis of anthranilic esters to the corresponding anthranilic acids.

| Entry | $Ar_1$ | $Ar_2$ | $R_1$ | $R_2$ | Yield (%) |
|---|---|---|---|---|---|
| **2.11a** | Ph | Ph | Et | H | 99 |
| **2.11b** | 4-$NO_2$-$C_6H_4$ | Ph | Et | H | 99 |
| **2.11c** | Ph | 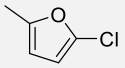 | Et | H | 99 |
| **2.11d** | 4-$NO_2$-$C_6H_4$ | Ph | Et | $CH_2C_6H_5$ | 97 |
| **2.11e** | 4-OMe-$C_6H_4$ | Ph | Et | H | 99 |
| **2.11f** | 4-Me-$C_6H_4$ | Ph | Et | H | 99 |
| **2.11g** | Ph | Ph | Et | 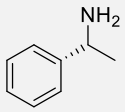 | 88 |

Table 10. Compounds obtained through the hydrolysis of different anthranilic esters

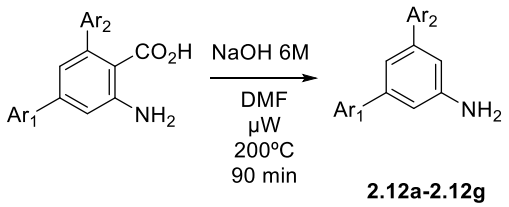


Scheme 13. Decarboxylation of anthranilic acids to obtain *m*-terphenyl amines **2.12a**-**2.12g**.

| Entry | $Ar_1$ | $Ar_2$ | $R_2$ | Yield (%) |
|---|---|---|---|---|
| **2.12a** | Ph | Ph | H | 68 |
| **2.12b*** | 4-$NH_2$-$C_6H_4$ | Ph | H | 37 |
| **2.12c** | Ph | 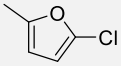 | H | 94 |
| **2.12d*** | 4-$NO_2$-$C_6H_4$ | Ph | $CH_2C_6H_5$ | 29 |
| **2.12e** | 4-OMe-$C_6H_4$ | Ph | H | 41 |
| **2.12f** | 4-Me-$C_6H_4$ | Ph | H | 50 |
| **2.12g** | 4-$NH_2$-$C_6H_4$ | Ph | $CH_2C_6H_5$ | 16 |

Table 11. *m*-Terphenylamines obtained through decarboxylation of anthranilic acids.

The final step involved the microwave-assisted decarboxylation of compounds **2.11**, with DMF as solvent and in the presence of 6M aqueous NaOH at 200 °C for 90 minutes (Scheme 13). This reaction provided varying yields depending on the substituents of the rings and did not demand chromatographic purification; pure compounds were obtained by precipitation with diethyl ether from crude product. With this methodology, we obtained 8 different derivatives to be tested against COX-1 and COX-2, in work still in progress.

In the case of compounds **2.09b** and **2.09d**, the aromatic nitro group was partially or totally reduced to amino in the course of the decarboxylation. Although this result is not easy to rationalize, there is some literature precedent pointing at the reducing properties of dimethylformamide at high temperatures[62,63].

In an effort to obtain molecules that could act as multitarget ligands we decided to combine in a single molecule, compounds **2.12** and tacrine, a well-known cholinesterase inhibitor. To this end, we demethylated the methoxy group of compound **2.12e** using $BBr_3$ as Lewis acid to obtain compound **2.13**. This hydroxy derivative was subsequently tethered to tacrine by way of a series of all-carbon linkers. These derivates were prepared in two steps, the first of which was a modified Friedländer reaction between 2-aminobenzonitrile or 4-chloro-2-aminobenzonitrile and cyclohexanone, to provide 9-aminoacridine **2.14a** or 6-chloro-9-aminoacridine **2.14b**. These intermediates were then bound to different dibromoalkanes to yield compounds **2.15a**-**2.15c** and finally to the hydroxy m-terphenylamine to yield the desired multitarget molecules **2.16a**-**2.16c** (scheme 14) (Table 12).

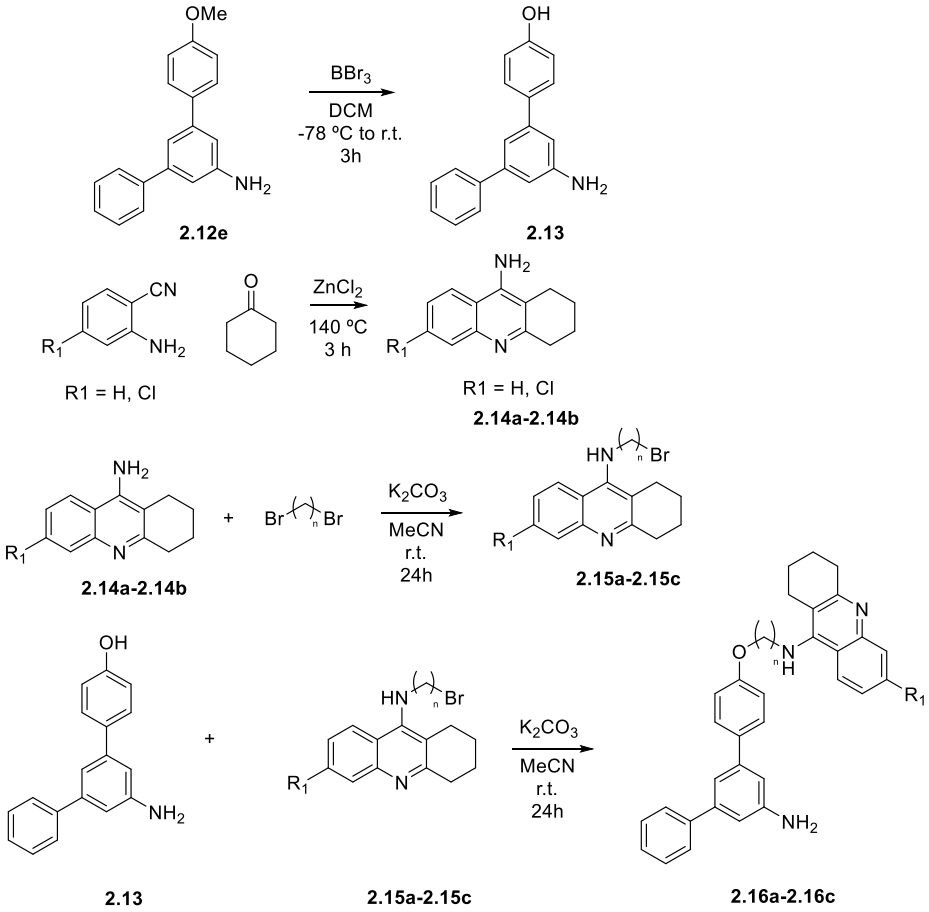


Scheme 14. Synthetic scheme used to obtain hybrid compounds **2.16a**-**2.16c**.

| Entry | $R_1$ | n | Yield (%) |
|---|---|---|---|
| **2.16a** | H | 7 | 30 |
| **2.16b** | H | 5 | 23 |
| **2.16c** | Cl | 7 | 32 |

Table 12. Hybrid compounds obtain by tethering compound **2.13** to compounds **2.15a**-**2.15c**.

These compounds were tested assayed against the enzymes acetylcholinesterase (AChE) and butyrylcholinesterase (BuChE). Their $IC_{50}$ concentrations are shown in table 13 and prove that all of these hybrid molecules inhibit both AChE and BuChE in the micromolar range. Compounds **2.16a** and **2.16b** are twice as selective for for BuChE with respect to AChE, however, they are 10 times less potent than than the tacrine reference at inhibiting AChE, and around 50 times less potent against BuChE. Nevertheless, **2.16a** and **2.16b** show good AChE and BuChE inhibitory activity. Compound **2.16c** presents a $IC_{50}$ against AChE higher than **2.16a** and **2.16b** (around double in both cases) and against BuChE (around an order of magnitude with respect to both). The main difference of this compound is the presence of a chlorine in the acridine moiety of the compound and both molecules only differ in this atom. The study of these compounds as COX-1 inhibitors is in progress.

| Entry | $IC_{50}$ (AChE) (μM) | $IC_{50}$ (BuChE) (μM) |
|---|---|---|
| **2.16a** | 0.353 | 0.181 |
| **2.16b** | 0.485 | 0.284 |
| **2.16c** | 0.881 | 1.831 |
| **Tacrine** | 0.035 | 0.0007 |

Table 13. $IC_{50}$ of hybrid compounds **2.16a**-**2.16c** against AChE and BuChE

## 4.0 Experimental

### 4.01 General procedure for the synthesis of compounds 2.01a to 2.01s

The correspondent acetophenone (1 equivalent) and benzaldehyde (1 equivalent) were dissolved in ethanol (50 ml) and 6M solution of NaOH (0.25 equivalents) were added to the reaction mixture. The reaction mixture was stirred at room temperature for 4 hours. The products were purified by filtration in case they precipitated in the reaction medium or by column chromatography (mobile phase 9:1 Hexane/Ethyl acetate).

**2.01a**. **(*E*)-1-(4-nitrophenyl)-3-phenylprop-2-en-1-one.** Prepared from 4-nitroacetophenone (24 mmol) and benzaldehyde (24 mmol). Off white solid (80% yield).

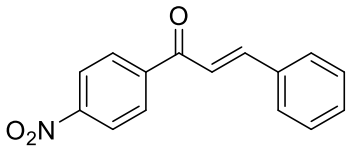

**$^1$H NMR** (250 MHz, $CDCl_3$) δ 8.44 – 8.36 (m, 2H), 8.22 – 8.16 (m, 2H), 7.89 (d, *J* = 15.7 Hz, 1H), 7.74 – 7.66 (m, 2H), 7.57 – 7.46 (m, 4H). (NMR data consistent with values described in literature)[64]

**2.01b**. **(*E*)-3-(5-chlorofuran-2-yl)-1-phenylprop-2-en-1-one.** Prepared from acetophenone (0.23 mmol) and 5-chlorofuran-2-carbaldehyde (0.23 mmol). Yellow solid (66% yield).

**IR** ($cm^{-1}$): 3420, 2987, 2321, 1729, 1679, 1595, 1448,

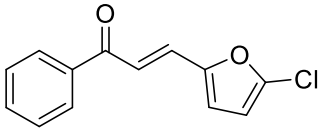

**$^1$H NMR** (250 MHz, $CDCl_3$) δ 8.13 – 8.01 (m, 2H), 7.66 – 7.44 (m, 5H), 6.72 (d, *J* = 3.5 Hz, 1H), 6.34 (d, *J* = 3.5 Hz, 1H).

**$^{13}$C NMR** (63 MHz, $CDCl_3$) δ 189.9, 151.6, 140.0, 138.3, 133.4, 129.9, 129.1, 128.9, 119.7, 118.5, 110.0.

**Elemental analysis**. Anal. Calc. for $C_{13}H_9ClO_2$ C, 67.11; H, 3.90; N, 0.00. Found: C, 65.17; H, 4.68; N, 0.72.

**2.01c. (*E*)-1-(4-methoxyphenyl)-3-phenylprop-2-en-1-one.** Prepared from 4-methoxyacetophenone (27 mmol) and benzaldehyde (27 mmol). Yellow solid (70% yield).

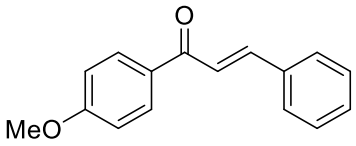

**$^1$H NMR** (250 MHz, $CDCl_3$) δ 8.11 – 7.99 (m, 2H), 7.81 (d, J = 15.7 Hz, 1H), 7.56 (d, *J* = 15.7 Hz, 1H), 7.42 (dd, J = 4.9, 1.9 Hz, 3H), 7.05 – 6.91 (m, 2H), 3.90 (s, 3H). (NMR data consistent with values described in literature).[64]

**2.01d. (*E*)-3-(5-chloro-2-nitrophenyl)-1-phenylprop-2-en-1-one.** Prepared from acetophenone (5.4 mmol) and 2-nitro-5-chloroacetophenone (5.4 mmol). Yellow solid (20% yield).

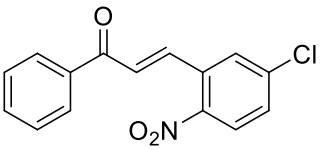

**$^1$H NMR** (250 MHz, $CDCl_3$) δ 8.16 – 8.00 (m, 4H), 7.70 (d, J = 2.3 Hz, 1H), 7.67 – 7.48 (m, 4H), 7.33 (d, *J* = 15.6 Hz, 1H). (NMR data consistent with values described in literature).[64]

**2.01e. (*E*)-1-(4-bromophenyl)-3-phenylprop-2-en-1-one.** Prepared from 4-bromoacetophenone (5 mmol) and benzaldehyde (5 mmol). Off white solid (68% yield).

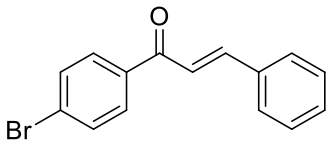


**$^1$H NMR** (250 MHz, $CDCl_3$) δ 7.93 – 7.87 (m, 2H), 7.83 (d, *J* = 15.7 Hz, 1H), 7.69 – 7.60 (m, 4H), 7.53 – 7.40 (m, 4H). (NMR data consistent with values described in literature).[64]

**2.01f. (*E*)-3-(4-nitrophenyl)-1-phenylprop-2-en-1-one.** Prepared from acetophenone (5 mmol) and 4-nitrobenzaldehyde (5 mmol). Off white solid (94% yield).

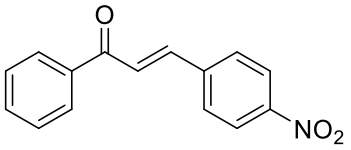


**$^1$H NMR** (250 MHz, $CDCl_3$) δ 8.32 – 8.25 (m, 2H), 8.08 – 8.01 (m, 2H), 7.87 – 7.76 (m, 3H), 7.70 – 7.49 (m, 4H). (NMR data consistent with values described in literature).[64]

**2.01g. (*E*)-1,3-bis(4-bromophenyl)prop-2-en-1-one.** Prepared from 4-bromoacetophenone (5 mmol) and 4-bromobenzaldehyde (5 mmol). Off white solid (99% yield).

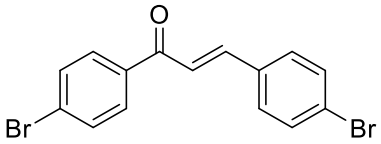


**$^1$H NMR** (250 MHz, $CDCl_3$) δ 7.92 – 7.84 (m, 2H), 7.75 (d, *J* = 15.7 Hz, 1H), 7.68 – 7.61 (m, 2H), 7.59 – 7.42 (m, 5H). (NMR data consistent with values described in literature).[64]

**2.01h. (*E*)-3-(2-nitrophenyl)-1-(p-tolyl)prop-2-en-1-one.** Prepared from 4-methylacetophenone (6.6 mmol) and 2-nitrobenzaldehyde (6.6 mmol). Off white solid (76% yield).

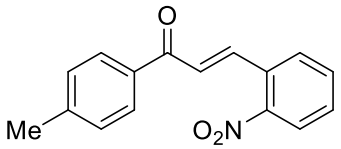


**$^1$H NMR** (250 MHz, $CDCl_3$) δ 8.18 – 8.04 (m, 2H), 7.99 – 7.90 (m, 2H), 7.78 – 7.64 (m, 2H), 7.57 (s, 1H), 7.32 (dd, J = 11.9, 3.8 Hz, 3H), 2.44 (s, 3H). (NMR data consistent with values described in literature).[64]

**2.01i. (*E*)-3-(4-bromophenyl)-1-(2-nitrophenyl)prop-2-en-1-one.** Prepared from 2-nitroacetophenone (6.6 mmol) and 4-bromobenzaldehyde (6.6 mmol). Off white solid (64% yield).

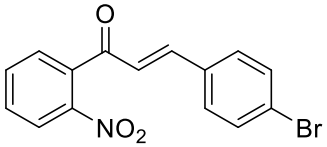


**$^1$H NMR** (250 MHz, $CDCl_3$) δ 8.24 – 8.14 (m, 1H), 7.78 (td, *J* = 7.5, 1.3 Hz, 1H), 7.67 (ddd, *J* = 8.2, 7.5, 1.6 Hz, 1H), 7.55 – 7.47 (m, 3H), 7.40 – 7.31 (m, 2H), 7.19 (d, J = 16.3 Hz, 1H), 6.98 (d, J = 16.3 Hz, 1H). (NMR data consistent with values described in literature).[64]

**2.01j**. **(*E*)-3-(furan-2-yl)-1-phenylprop-2-en-1-one.** Prepared from acetophenone and 2-furanocarboxaldyde. Brown oil (78% yield).

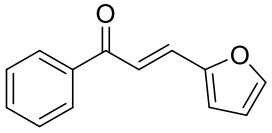

**$^1$H NMR** (250 MHz, $CDCl_3$) δ 8.07 – 7.99 (m, 2H), 7.66 – 7.40 (m, 6H), 6.73 (d, *J* = 3.4 Hz, 1H), 6.52 (dd, J = 3.4, 1.8 Hz, 1H). (NMR data consistent with values described in literature).[64]

**2.01k. (*E*)-3-(4-bromophenyl)-1-phenylprop-2-en-1-one.** Prepared from acetophenone and 4-bromobenzaldyde. Off white solid (79% yield).

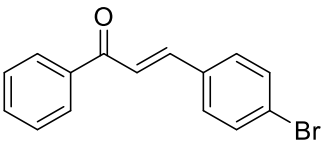

**$^1$H NMR** (250 MHz, $CDCl_3$) δ 8.02 (m, 2H), 7.74 (d, *J* = 15.7 Hz, 1H), 7.65 – 7.45 (m, 8H). (NMR data consistent with values described in literature).[64]

**2.01l. (*E*)-1-phenyl-3-(thiophen-2-yl)prop-2-en-1-one.** Prepared from acetophenone (8.3 mmol) and 2-tiophenocarboxaldehyde (8.3 mmol). Brown oil (86% yield).

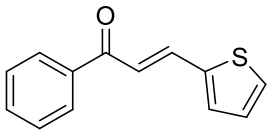

**$^1$H NMR** (250 MHz, $CDCl_3$) δ 8.07 – 7.91 (m, 3H), 7.63 – 7.46 (m, 4H), 7.46 – 7.30 (m, 3H), 7.10 (dd, J = 5.1, 3.7 Hz, 1H). (NMR data consistent with values described in literature).[64]

**2.01m. (*E*)-1-(2,4-dimethoxyphenyl)-3-(4-methoxyphenyl)prop-2-en-1-one.** Prepared from 2,4-dimethoxyacetophenone (3 mmol) and 4-methoxybenzaldehyde (3 mmol). Off white solid (79% yield).

**Mp**: 83 ºC.

**IR** ($cm^{-1}$): 3175, 3004, 2968, 2841, 2096, 1643.

**$^1$H NMR** (250 MHz, $CDCl_3$) δ 7.65 (d, *J* = 8.6 Hz, 1H), 7.56 (d, *J* = 15.7 Hz, 1H), 7.51 – 7.41 (m, 2H), 7.30 (d, *J* = 15.8 Hz, 1H), 6.82 (d, *J* = 8.8 Hz, 2H), 6.46 (dd, *J* = 8.6, 2.3 Hz, 1H), 6.40 (d, *J* = 2.3 Hz, 1H), 3.80 (s, 3H), 3.76 (s, 3H), 3.74 (s, 3H).

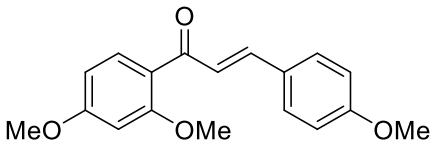

**$^{13}$C NMR** (63 MHz, $CDCl_3$) δ 191.1, 164.4, 161.7, 160.7, 142.5, 133.1, 130.4, 128.5, 125.4, 122.8, 114.7, 105.5, 99.0, 56.2, 56.0, 55.8.

**Elemental analysis**. Anal. Calc. for $C_{18}H_{18}O_4$ C, 72.47; H, 6.08; N, 0.00. Found: C, 71.84; H, 6.07; N, 0.04.

**2.01n. (*E*)-1,3-bis(4-chlorophenyl)prop-2-en-1-one.** Prepared from 4-Chloroacetophenone (4.5 mmol) and 4-chlorobenzaldehyde (4.5 mmol). Off white solid (85% yield).

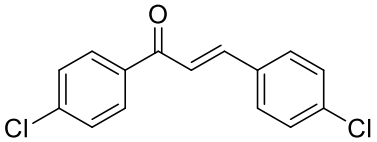

**$^1$H NMR** (250 MHz, $CDCl_3$) δ 8.04 – 7.95 (m, 2H), 7.80 (d, J = 15.7 Hz, 1H), 7.65 – 7.57 (m, 2H), 7.56 – 7.38 (m, 5H). (NMR data consistent with values described in literature).[64]

**2.01o**. **(*E*)-3-(3-methoxyphenyl)-1-(4-methoxyphenyl)prop-2-en-1-one.** Prepared from 4-methoxyacetphenone and 3-methoxybenzadehyde. Off-white solid (84% yield).

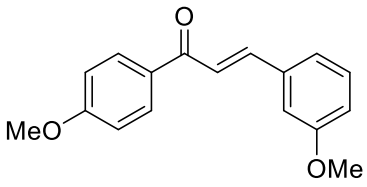


**$^1$H NMR** (250 MHz, $CDCl_3$) δ 8.11 – 8.03 (m, 2H), 7.80 (d, *J* = 15.6 Hz, 1H), 7.55 (d, *J* = 15.6 Hz, 1H), 7.42 – 7.24 (m, 2H), 7.18 (dd, *J* = 2.6, 1.6 Hz, 1H), 7.06 – 6.99 (m, 2H), 3.92 (s, 3H), 3.88 (s, 3H). (NMR data consistent with values described in literature).[65]

**2.01p. (*E*)-1,3-bis(4-nitrophenyl)prop-2-en-1-one.** Prepared from 4-nitroacetophenone and 4-nitrobenzaldehyde. Orange solid (91% yield).

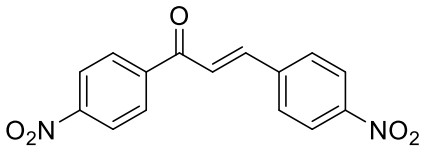


**$^1$H NMR** (250 MHz, $CDCl_3$) δ 8.47 – 8.38 (m, 2H), 8.34 (d, *J* = 8.8 Hz, 2H), 8.26 – 8.18 (m, 2H), 7.91 (d, *J* = 15.9 Hz, 1H), 7.85 (d, *J* = 8.7 Hz, 2H), 7.64 (d, *J* = 15.7 Hz, 1H). (NMR data consistent with values described in literature).[64]

**2.01q. (*E*)-3-(4-chlorophenyl)-1-(4-nitrophenyl)prop-2-en-1-one.** Prepared from 4-chloroacetphenone and 4-nitrobenzadehyde. Off-white solid (86% yield).

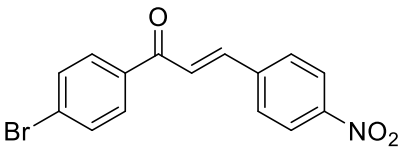


**$^1$H NMR** (250 MHz, $CDCl_3$) δ 8.28 (d, *J* = 8.8 Hz, 2H), 7.94 – 7.87 (m, 2H), 7.87 – 7.76 (m, 3H), 7.70 – 7.64 (m, 2H), 7.59 (d, *J* = 15.8 Hz, 1H). (NMR data consistent with values described in literature).[64]

**4.02 General procedure for the synthesis of compounds 2.02a to 2.02ab**

The suitable β-ketoester (1 equivalent) was stirred with the appropriate amine (1 equivalent) in ethanol (40 ml) at room temperature for 30 minutes and Cerium ammonium nitrate (10%) and the corresponding chalcone (1 equivalent) were added to the reaction mixture and it was heated to reflux overnight. In the case of compounds **2.02a**-**2.02g**, an excess of ammonium formate was added to the reaction mixture and furtherly stirred at reflux for 3 hours. Subsequently, all compounds were cooled down to room temperature and concentrated in vacuo. The residue was redissolved in ethyl acetate (40 ml) and washed twice with water (20 ml) and once with brine (20 ml). The organic phase was dried with $Na_2SO_4$ and concentrated in vacuo. The residue was purified by column chromatography to yield the corresponding dihydroanthranilates.

**2.02a. Ethyl 5'-amino-2',3'-dihydro-[1,1':3',1''-terphenyl]-4'-carboxylate.** Prepared from ethyl acetoacetate (9.6 mmol), butylamine (9.6 mmol) and (*E*)-1,3-diphenylpropenone (9.6 mmol). Excess ammonium formate was used to achieve primary amino residue. Purified by column chromatography (0-30% ethyl acetate/hexane). Yellow solid (93% yield).

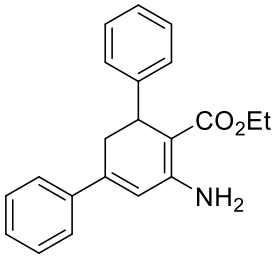

**$^1$H NMR** (250 MHz, $CDCl_3$) δ 7.46 – 7.09 (m, 10H), 6.23 (d, *J* = 2.9 Hz, 1H), 4.26 (d, *J* = 8.6 Hz, 1H), 4.20 – 3.98 (m, 2H), 3.23 (ddd, *J* = 17.0, 8.7, 2.9 Hz, 1H), 2.95 (dd, *J* = 17.0, 1.7 Hz, 1H), 1.19 (t, *J* = 7.1 Hz, 3H). (NMR data consistent with values described in literature).[46]

**2.02b. Ethyl 5'-amino-4''-nitro-2',3'-dihydro-[1,1':3',1''-terphenyl]-4'-carboxylate.** Prepared from ethyl acetoacetate (14.3 mmol), butylamine (14.3 mmol) and (*E*)-1-(4-nitrophenyl)-3-phenylprop-2-en-1-one (14.3 mmol). Excess ammonium formate was used to achieve primary amino residue. Purified by column chromatography (0-30% ethyl acetate/hexane). Yellow solid (96% yield).

**Mp**: 98-99 ºC

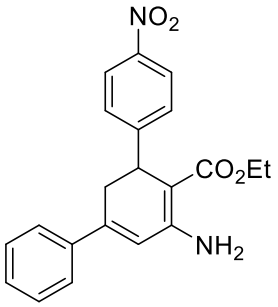


**IR** ($cm^{-1}$): 3402, 3301, 2982, 2895, 1645, 1509.

**$^1$H NMR** (300 MHz, $CDCl_3$) δ 8.08 – 8.01 (m, 2H), 7.46 – 7.38 (m, 2H), 7.38 – 7.26 (m, 5H), 6.27 (s, 1H), 4.32 (dd, *J* = 8.9, 1.7 Hz, 1H), 4.20 – 3.95 (m, 2H), 3.24 (ddd, *J* = 17.1, 8.8, 2.9 Hz, 1H), 2.94 – 2.82 (m, 1H), 1.14 (t, J = 7.1 Hz, 3H).

**$^{13}$C NMR** (75 MHz, $CDCl_3$) δ 169.5, 154.0, 153.2, 146.5, 144.9, 139.0, 129.0, 128.7, 128.1, 125.7, 123.5, 120.6, 90.1, 59.2, 37.0, 35.0, 14.5.

**Elemental analysis**: Anal. Calc. for $C_{21}H_{20}N_2O_4$ C, 69.22; H, 5.53; N, 7.69. Found: C, 68.91; H, 5.43; N, 7.58.

**2.02c. Ethyl 5-amino-3-(5-chlorofuran-2-yl)-2,3-dihydro-[1,1'-biphenyl]-4-carboxylate.** Prepared from ethyl acetoacetate (1.49 mmol), butylamine (1.49 mmol) and (*E*)-3-(5-chlorofuran-2-yl)-1-phenylprop-2-en-1-one (1.49 mmol). Excess ammonium formate was used to achieve primary amino residue. Purified by column chromatography (0-30% ethyl acetate/hexane). Orange solid (67% yield).

**Mp:** 116-117 ºC

**IR** ($cm^{-1}$): 3406, 3303, 2951, 2320, 1735, 1645.

**$^1$H NMR** (250 MHz, $CDCl_3$) δ 7.52 – 7.33 (m, 5H), 6.16 (d, *J* = 2.8 Hz, 1H), 5.99 – 5.87 (m, 2H), 4.29 (dt, *J* = 7.5, 1.5 Hz, 1H), 4.20 (q, *J* = 7.1 Hz, 2H), 3.17 (dd, *J* = 17.0, 1.9 Hz, 1H), 2.96 (ddd, *J* = 17.0, 7.6, 2.8 Hz, 1H), 1.27 (t, *J* = 7.1 Hz, 4H).

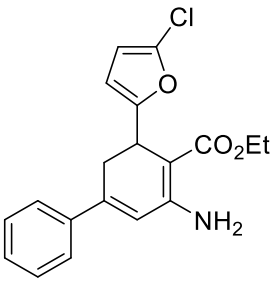


**$^{13}$C NMR** (63 MHz, $CDCl_3$) δ 170.0, 158.2, 153.7, 146.0, 139.6, 134.2, 129.2, 129.1, 126.2, 120.5, 107.9, 106.9, 88.6, 59.6, 32.3, 31.7, 15.0.

**Elemental analysis**: Anal. Calc. for $C_{19}H_{16}ClNO_3$ C, 66.77; H, 4.72; N, 4.10. Found: C, 64.38; H, 5.14; N, 3.95.

**2.02d. Ethyl 5'-amino-4-methyl-2',3'-dihydro-[1,1':3',1''-terphenyl]-4'-carboxylate.** Prepared from ethyl acetoacetate (17 mmol), butylamine (17 mmol) and (*E*)-1-phenyl-3-(p-tolyl)prop-2-en-1-one (17 mmol). Excess ammonium formate was used to achieve primary amino residue. Purified by column chromatography (0-30% ethyl acetate/hexane). Yellow solid (69% yield).

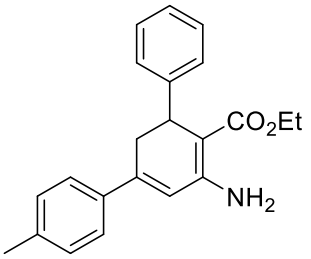


**$^1$H NMR** (250 MHz, $CDCl_3$) δ 7.33 (d, *J* = 8.1 Hz, 4H), 7.24 (t, *J* = 7.3 Hz, 2H), 7.20 – 7.12 (m, 3H), 6.23 (d, *J* = 2.7 Hz, 1H), 4.28 (d, *J* = 8.2 Hz, 1H), 4.23 – 4.02 (m, 2H), 3.21 (ddd, J = 17.0, 8.6, 2.7 Hz, 1H), 2.97 (dd, J = 16.9, 1.2 Hz, 1H), 2.37 (s, 3H), 1.21 (t, *J* = 7.1 Hz, 3H). (NMR data consistent with values described in literature).[46]

**2.02e. Ethyl 5'-amino-4-methoxy-2',3'-dihydro-[1,1':3',1''-terphenyl]-4'-carboxylate.** Prepared from ethyl acetoacetate (9.9 mmol), butylamine (9.9 mmol) and (*E*)-1-(4-methoxyphenyl)-3-phenylprop-2-en-1-one (9.9 mmol). Excess ammonium formate was used to achieve primary amino residue. Purified by column chromatography (0-30% ethyl acetate/hexane). Yellow solid (64% yield).

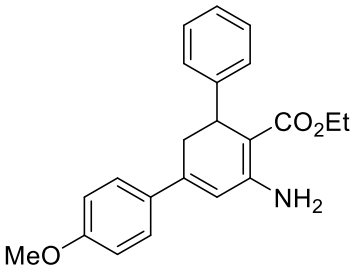


**$^1$H NMR** (250 MHz, $CDCl_3$) δ 7.45 – 7.31 (m, 2H), 7.18 (dd, *J* = 12.4, 8.8 Hz, 2H), 6.94 – 6.81 (m, 2H), 6.81 – 6.69 (m, 2H), 6.16 (d, *J* = 2.8 Hz, 1H), 4.24 – 4.17 (m, 1H), 4.09 (ddt, J = 9.4, 7.0, 3.0 Hz, 2H), 3.82 (s, 3H), 3.76 (s, 3H), 3.14 (ddd, *J* = 16.9, 8.4, 2.8 Hz, 1H), 2.91 (dd, *J* = 16.9, 1.7 Hz, 1H), 1.20 (t, *J* = 7.1 Hz, 3H). (NMR data consistent with values described in literature).[46]

**2.02f. Ethyl 5'-amino-4,4''-dibromo-2',3'-dihydro-[1,1':3',1''-terphenyl]-4'-carboxylate.** Prepared from ethyl acetoacetate (2.7 mmol), butylamine (2.7 mmol) and (E)-1,3-bis(4-bromophenyl)prop-2-en-1-one (2.7 mmol). Excess ammonium formate was used to achieve primary amino residue.Purified by column chromatography (0-30% ethyl acetate/hexane). Yellow solid (89% yield).

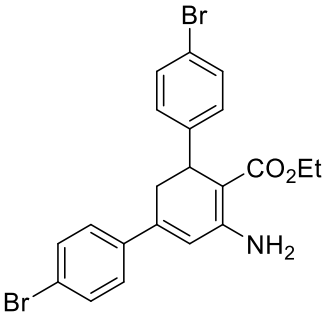


**$^1$H NMR** (250 MHz, $CDCl_3$) δ 7.50 – 7.43 (m, 2H), 7.37 – 7.31 (m, 2H), 7.26 – 7.20 (m, 2H), 7.18 – 7.11 (m, 2H), 6.21 (d, *J* = 2.9 Hz, 1H), 4.20 (dd, *J* = 9.1, 1.8 Hz, 1H), 4.17 – 3.98 (m, 2H), 3.18 (ddd, *J* = 16.9, 8.7, 3.0 Hz, 1H), 2.81 (dd, *J* = 17.0, 1.7 Hz, 1H), 1.18 (t, *J* = 7.1 Hz, 3H). (NMR data consistent with values described in literature).

**$^{13}$C NMR** (63 MHz, $CDCl_3$) δ 170.1, 152.9, 145.0, 144.2, 138.5, 132.2, 131.5, 130.2, 129.4, 127.6, 127.1, 123.3, 121.4, 120.2, 91.7, 59.6, 36.6, 35.7, 14.9. (NMR data consistent with values described in literature).[46]

**2.02g. Ethyl 5-amino-3-(thiophen-2-yl)-2,3-dihydro-[1,1'-biphenyl]-4-carboxylate.** Prepared from ethyl acetoacetate (17 mmol), butylamine (17 mmol) and (17 mmol). Excess ammonium formate was used to achieve primary amino residue. Purified by column chromatography (0-30% ethyl acetate/hexane). Yellow solid (78% yield).

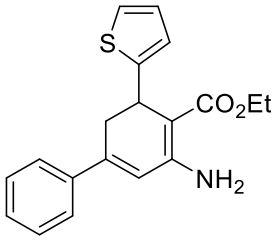


**$^1$H NMR** (250 MHz, $CDCl_3$) δ 7.53 – 7.32 (m, 5H), 7.04 – 6.99 (m, 1H), 6.87 – 6.81 (m, 2H), 6.22 (d, *J* = 2.2 Hz, 1H), 4.55 (ddd, J = 6.4, 3.0, 0.6 Hz, 1H), 4.22 (q, J = 7.1 Hz, 2H), 3.18 – 3.09 (m, 2H), 1.31 (t, *J* = 7.1 Hz, 3H). (NMR data consistent with values described in literature).

**$^{13}$C NMR** (63 MHz, $CDCl_3$) δ 170.0, 152.8, 150.4, 146.3, 139.8, 129.2, 129.1, 126.5, 126.3, 123.7, 122.9, 120.9, 93.1, 59.6, 35.8, 33.1, 15.0. (NMR data consistent with values described in literature).[46]

**2.02h. Ethyl 5'-(benzylamino)-4-nitro-2',3'-dihydro-[1,1':3',1''-terphenyl]-4'-carboxylate.** Prepared from ethyl acetoacetate (12.7 mmol), benzylamine (12.7 mmol) and (*E*)-1-(4-nitrophenyl)-3-phenylprop-2-en-1-one (12.7 mmol) (17 mmol). Purified by column chromatography (0-20% ethyl acetate/hexane).orange oil (78% yield).

**Mp**: 108 ºC.

**IR** ($cm^{-1}$): 3275, 2976, 2321, 1735, 1646.

**$^1$H NMR** (250 MHz, $CDCl_3$) δ 9.41 (t, *J* = 6.2 Hz, 1H), 8.18 – 8.08 (m, 2H), 7.51 – 7.11 (m, 15H), 6.67 (d, *J* = 2.9 Hz, 1H), 4.64 (d, *J* = 6.2 Hz, 2H), 4.32 (dd, *J* = 8.5, 1.7 Hz, 1H), 4.20 – 4.00 (m, 2H), 3.18 (ddd, *J* = 16.8, 8.4, 3.0 Hz, 1H), 2.89 (dd, *J* = 16.8, 1.8 Hz, 1H), 1.17 (t, *J* = 7.1 Hz, 3H).

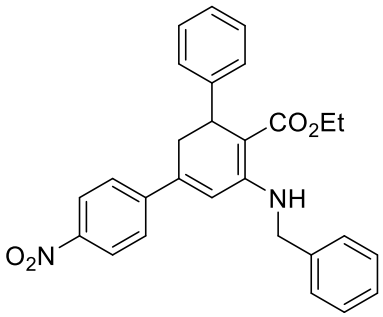


**$^{13}$C NMR** (63 MHz, $CDCl_3$) δ 170.7, 154.3, 146.9, 145.2, 143.8, 139.7, 129.3, 128.5, 127.9, 127.6, 127.2, 127.0, 126.6, 124.2, 120.1, 92.3, 59.6, 47.4, 37.1, 35.5, 14.8.

**Elemental analysis**: Anal. Calc. for $C_{28}H_{26}N_2O_4$ C, 73.99; H, 5.77; N, 6.16. Found: C, 72.98; H, 5.70; N, 6.01.

**2.02i. Tert-butyl 5'-(benzylamino)-2',3'-dihydro-[1,1':3',1''-terphenyl]-4'-carboxylate.** Prepared from tertbutyl acetoacetate (2.4 mmol), benzylamine (2.4 mmol) and (*E*)-1,3-diphenylpropenone (2.4 mmol). Purified by column chromatography (0-20% ethyl acetate/hexane). Yellow solid (84% yield).

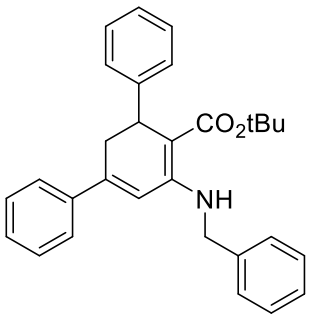


**$^1$H NMR** (250 MHz, $CDCl_3$) δ 9.38 (t, *J* = 6.2 Hz, 1H), 7.43 – 7.11 (m, 15H), 6.58 (d, *J* = 2.9 Hz, 1H), 4.62 (d, *J* = 6.2 Hz, 2H), 4.22 (dd, *J* = 8.8, 1.8 Hz, 1H), 3.15 (ddd, *J* = 16.9, 8.8, 2.9 Hz, 1H), 2.90 (dd, *J* = 16.9, 1.9 Hz, 1H), 1.36 (s, 9H). (NMR data consistent with values described in literature).

**$^{13}$C NMR** (63 MHz, $CDCl_3$) δ 170.9, 154.8, 146.5, 145.8, 140.7, 140.2, 129.2, 128.9, 128.8, 128.3, 127.7, 127.6, 127.3, 126.3, 126.1, 116.9, 93.0, 78.9, 47.2, 38.0, 35.4, 28.9. (NMR data consistent with values described in literature).[46]

**2.02j. Ethyl 5'-(((S)-1-phenylethyl)amino)-2',3'-dihydro-[1,1':3',1''-terphenyl]-4'-carboxylate** Prepared from ethyl acetoacetate (6.2 mmol), (S)-1-phenylethan-1-amine (6.2 mmol) and (*E*)-1,3-diphenylpropenone (6.2 mmol). Obtained as a mixture of diastereoisomers that was not purified any further. Yellow oil (67% yield).

**2.02k. Ethyl 5'-(((R)-1-phenylethyl)amino)-2',3'-dihydro-[1,1':3',1''-terphenyl]-4'-carboxylate** Prepared from ethyl acetoacetate (6.2 mmol), (R)-1-phenylethan-1-amine (6.2 mmol) and (*E*)-1,3-diphenylpropenone (6.2 mmol). Obtained as a mixture of diastereoisomers that was not purified any further. Yellow oil (58% yield).[46]

**2.02l. Ethyl 5'-(butylamino)-5''-chloro-2''-nitro-2',3'-dihydro-[1,1':3',1''-terphenyl]-4'-carboxylate.** Prepared from ethyl acetoacetate (1.7 mmol), butylamine (1.7 mmol) and (*E*)-3-(5-chloro-2-nitrophenyl)-1-phenylprop-2-en-1-one (1.7 mmol). Excess ammonium formate was used to achieve primary amino residue. Purified by column chromatography (0-20% ethyl acetate/hexane). Yellow oil (58% yield).

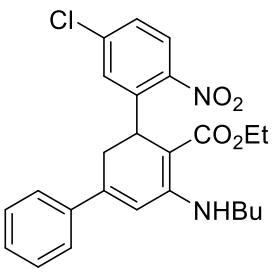


**$^{1}$H NMR** (250 MHz, $CDCl_3$) δ 8.97 (s, 1H), 7.63 (d, *J* = 8.6 Hz, 1H), 7.39 – 7.10 (m, 7H), 6.65 (d, *J* = 2.9 Hz, 1H), 4.64 (dd, *J* = 9.9, 1.5 Hz, 1H), 3.95 – 3.78 (m, 2H), 3.43 – 3.28 (m, 2H), 3.20 (ddd, *J* = 17.7, 9.9, 3.0 Hz, 2H), 2.92 (dd, *J* = 17.6, 1.6 Hz, 1H), 1.61 (m, 2H), 1.54 – 1.30 (m, 2H), 0.93 (dt, *J* = 9.5, 7.2 Hz, 6H). (NMR data consistent with values described in literature).

**$^{13}$C NMR** (63 MHz, $CDCl_3$) δ 170.1, 155.9, 148.0, 146.4, 143.5, 140.2, 139.0, 130.3, 129.4, 129.1, 127.5, 126.3, 125.7, 116.7, 88.3, 59.4, 43.1, 33.8, 33.1, 32.5, 20.6, 14.5, 14.3. (NMR data consistent with values described in literature).[46]

**2.02m. Ethyl 4-bromo-5'-(butylamino)-2',3'-dihydro-[1,1':3',1''-terphenyl]-4'-carboxylate.** Prepared from ethyl acetoacetate (1.7 mmol), butylamine (1.7 mmol) and ((*E*)-1-(4-bromophenyl)-3-phenylprop-2-en-1-one (1.7 mmol). Excess ammonium formate was used to achieve primary amino residue. Purified by column chromatography (0-20% ethyl acetate/hexane). Yellow oil (59% yield).

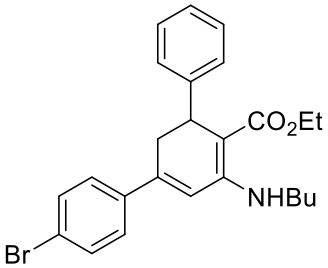


**$^{1}$H NMR** (250 MHz, $CDCl_3$) δ 9.05 (t, *J* = 5.5 Hz, 1H), 7.51 – 7.42 (m, 2H), 7.32 – 7.10 (m, 9H), 6.63 (d, *J* = 2.8 Hz, 1H), 4.28 (dd, *J* = 8.4, 1.8 Hz, 1H), 4.19 – 3.99 (m, 3H), 3.50 – 3.32 (m, 2H), 3.24 – 3.06 (m, 1H), 2.88 (dd, *J* = 16.8, 1.8 Hz, 1H), 1.77 – 1.62 (m, 3H), 1.59 – 1.41 (m, 3H), 1.18 (td, *J* = 8.3, 7.1, 2.5 Hz, 4H), 1.01 (dd, *J* = 8.1, 6.6 Hz, 4H). (NMR data consistent with values described in literature).

**$^{13}$C NMR** (63 MHz, $CDCl_3$) δ 170.8, 155.2, 148.0, 145.3, 139.6, 132.1, 128.4, 127.8, 127.6, 126.3, 117.1, 89.9, 59.2, 43.1, 37.1, 35.5, 33.1, 20.6, 15.0, 14.3. (NMR data consistent with values described in literature).[46]

**2.02n. Ethyl 5'-(butylamino)-4''-nitro-2',3'-dihydro-[1,1':3',1''-terphenyl]-4'-carboxylate.** Prepared from ethyl acetoacetate (6.3 mmol), butylamine (6.3 mmol) and (*E*)-3-(4-nitrophenyl)-1-phenylprop-2-en-1-one (6.3 mmol). Purified by column chromatography (0-20% ethyl acetate/hexane). Yellow oil (78% yield).

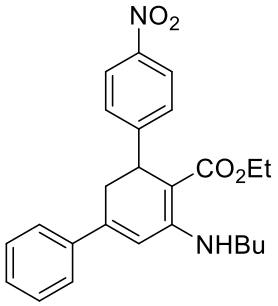


**$^{1}$H NMR** (250 MHz, $CDCl_3$) δ 8.99 (d, *J* = 5.3 Hz, 1H), 8.02 – 7.91 (m, 2H), 7.37 – 7.29 (m, 2H), 7.25 (s, 5H), 6.57 (d, *J* = 2.8 Hz, 1H), 4.26 (dd, *J* = 8.6, 1.6 Hz, 1H), 4.08 – 3.86 (m, 2H), 3.32 (dtd, *J* = 8.0, 7.0, 5.5 Hz, 2H), 3.13 (ddd, *J* = 16.9, 8.6, 2.9 Hz, 1H), 2.80 (dd, *J* = 16.9, 1.8 Hz, 1H), 1.67 – 1.50 (m, 2H), 1.48 – 1.31 (m, 2H), 1.05 (t, *J* = 7.1 Hz, 3H), 0.90 (t, *J* = 7.2 Hz, 3H). (NMR data consistent with values described in literature).

**$^{13}$C NMR** (63 MHz, $CDCl_3$) δ 169.0, 154.2, 153.0, 145.3, 144.9, 138.7, 127.9, 127.7, 127.1, 124.7, 122.3, 115.2, 86.8, 57.8, 41.7, 36.0, 33.7, 31.6, 19.1, 13.5, 12.8. (NMR data consistent with values described in literature).[46]

**2.02o. Ethyl 5'-(butylamino)-4-methyl-2''-nitro-2',3'-dihydro-[1,1':3',1''-terphenyl]-4'-carboxylate.** Prepared from ethyl acetoacetate (3.0 mmol), butylamine (3.0 mmol) and (*E*)-3-(2-nitrophenyl)-1-(p-tolyl)prop-2-en-1-one (3.0 mmol). Purified by column chromatography (0-20% ethyl acetate/hexane). Yellow oil (74% yield).

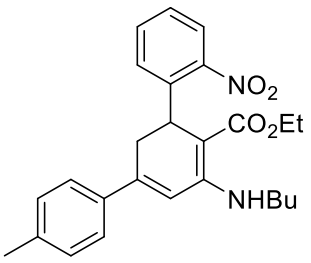


**$^{1}$H NMR** (250 MHz, $CDCl_3$) δ 7.74 (dd, *J* = 8.0, 1.4 Hz, 1H), 7.51 – 7.11 (m, 9H), 6.72 (d, *J* = 2.8 Hz, 1H), 4.72 (dd, *J* = 9.7, 1.6 Hz, 1H), 4.05 – 3.85 (m, 2H), 3.56 – 3.40 (m, 2H), 3.27 (ddd, *J* = 17.4, 9.6, 2.9 Hz, 1H), 3.05 (dd, *J* = 17.5, 1.7 Hz, 1H), 2.36 (s, 3H), 1.69 (m, 2H), 1.59 – 1.44 (m, 2H), 1.13 – 0.95 (m, 6H). (NMR data consistent with values described in literature).

**$^{13}$C NMR** (63 MHz, $CDCl_3$) δ 170.3, 156.0, 149.7, 146.5, 141.18, 139.50, 137.43, 132.63, 130.26, 129.77, 127.07, 126.16, 124.03, 115.43, 88.97, 59.21, 43.1, 34.0, 33.1, 32.3, 21.6, 20.6, 14.5, 14.3. (NMR data consistent with values described in literature).[46]

**2.02p. Ethyl 4''-bromo-5'-(butylamino)-2-nitro-2',3'-dihydro-[1,1':3',1''-terphenyl]-4'-carboxylate.** Prepared from ethyl acetoacetate (3.3 mmol), butylamine (3.3 mmol) and (*E*)-3-(2-nitrophenyl)-1-(p-tolyl)prop-2-en-1-one (3.3 mmol). Purified by column chromatography (0-20% ethyl acetate/hexane). Yellow oil (62% yield).

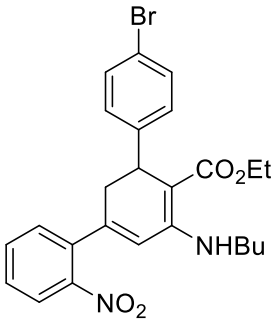


**$^1$H NMR** (250 MHz, $CDCl_3$) δ 9.01 (t, *J* = 5.7 Hz, 1H), 7.85 (dd, *J* = 8.0, 1.4 Hz, 1H), 7.53 – 7.33 (m, 4H), 7.16 – 7.07 (m, 2H), 6.83 (dd, *J* = 7.6, 1.5 Hz, 1H), 6.31 (d, *J* = 2.9 Hz, 1H), 4.25 – 4.14 (m, 1H), 4.16 – 3.94 (m, 2H), 3.30 (dddd, *J* = 13.9, 6.8, 5.1, 3.3 Hz, 3H), 2.45 (dd, *J* = 16.7, 1.7 Hz, 1H), 1.67 – 1.55 (m, 2H), 1.53 – 1.38 (m, 2H), 1.14 (t, *J* = 7.1 Hz, 3H), 0.97 (t, *J* = 7.2 Hz, 3H). (NMR data consistent with values described in literature).

**$^{13}$C NMR** (63 MHz, $CDCl_3$) δ 170.5, 154.7, 148.3, 144.7, 144.0, 137.1, 133.3, 131.4, 130.2, 129.6, 129.1, 124.6, 120.1, 119.5, 89.3, 59.3, 43.2, 37.2, 36.7, 33.1, 20.5, 14.9, 14.3. (NMR data consistent with values described in literature).[46]

**2.02q. Ethyl 5-(butylamino)-3-(furan-2-yl)-2,3-dihydro-[1,1'-biphenyl]-4-carboxylate.** Prepared from ethyl acetoacetate (5.0 mmol), butylamine (5.0 mmol) and (E)-3-(furan-2-yl)-1-phenylprop-2-en-1-one (5.0 mmol). Purified by column chromatography (0-20% ethyl acetate/hexane). Yellow oil (62% yield).

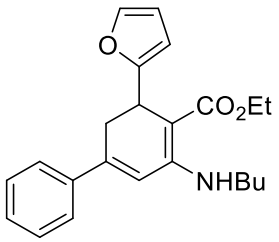


**$^1$H NMR** (250 MHz, $CDCl_3$) δ 9.06 (s, 1H), 7.51 – 7.26 (m, 6H), 6.58 (d, *J* = 2.8 Hz, 1H), 6.20 (dd, *J* = 3.2, 1.8 Hz, 1H), 5.92 (dt, *J* = 3.2, 1.0 Hz, 1H), 4.36 (dt, *J* = 7.3, 1.5 Hz, 1H), 4.19 (qd, *J* = 7.1, 0.7 Hz, 2H), 3.38 (qd, *J* = 6.9, 5.7 Hz, 2H), 3.28 – 3.17 (m, 1H), 2.94 (ddd, *J* = 16.8, 7.4, 2.9 Hz, 1H), 1.74 – 1.58 (m, 2H), 1.58 – 1.41 (m, 2H), 1.28 (td, *J* = 7.1, 4.5 Hz, 3H), 1.00 (t, *J* = 7.2 Hz, 3H). (NMR data consistent with values described in literature).

**$^{13}$C NMR** (63 MHz, $CDCl_3$) δ 170.6, 159.0, 155.6, 147.3, 141.2, 140.7, 129.0, 129.0, 126.5, 116.1, 110.3, 105.4, 87.5, 59.2, 43.1, 33.1, 32.1, 31.8, 20.6, 15.1, 14.3. (NMR data consistent with values described in literature).[46]

**2.02r. Ethyl 5'-((3-chlorophenyl)amino)-2',3'-dihydro-[1,1':3',1''-terphenyl]-4'-carboxylate.** Prepared from ethyl acetoacetate (4.8 mmol), 3-chloroaniline (4.8 mmol) and (*E*)-1,3-diphenylpropenone (4.8 mmol). Purified by column chromatography (0-20% ethyl acetate/hexane). Yellow oil (48% yield).

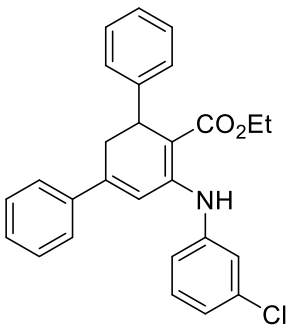


**$^1$H NMR** (250 MHz, $CDCl_3$) δ 10.76 (s, 1H), 7.56 – 6.96 (m, 15H), 6.64 (d, *J* = 2.8 Hz, 1H), 4.37 (dd, *J* = 8.5, 1.8 Hz, 1H), 4.27 – 4.04 (m, 3H), 3.25 (ddd, *J* = 16.8, 8.6, 2.9 Hz, 1H), 3.04 (dd, *J* = 16.8, 1.9 Hz, 1H), 1.20 (t, *J* = 7.1 Hz, 3H). (NMR data consistent with values described in literature).

**$^{13}$C NMR** (63 MHz, $CDCl_3$) δ 170.5, 150.8, 145.0, 144.8, 141.7, 140.1, 135.1, 130.5, 129.0, 128.5, 127.6, 126.6, 126.3, 123.9, 123.1, 121.2, 118.1, 97.1, 60.0, 37.1, 34.9, 14.8. (NMR data consistent with values described in literature).[46]

**2.02s. Ethyl 4''-nitro-5'-(phenylamino)-2',3'-dihydro-[1,1':3',1''-terphenyl]-4'-carboxylate.** Prepared from ethyl acetoacetate (3.9 mmol), aniline (3.9 mmol) and (E)-3-(4-nitrophenyl)-1-phenylprop-2-en-1-one (3.9 mmol). Purified by column chromatography (0-20% ethyl acetate/hexane). Yellow oil (59% yield).

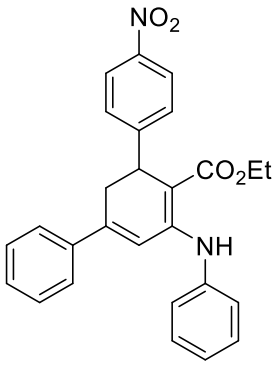


**$^{1}$H NMR** (250 MHz, $CDCl_3$) δ 10.82 (s, 1H), 8.14 – 8.06 (m, 2H), 7.49 – 7.24 (m, 9H), 7.18 (m, 3H), 6.69 (d, *J* = 2.9 Hz, 1H), 4.45 (d, *J* = 8.5 Hz, 1H), 4.25 – 4.02 (m, 2H), 3.31 (ddd, *J* = 16.7, 8.7, 2.9 Hz, 1H), 2.97 (dd, *J* = 16.8, 1.7 Hz, 1H), 1.18 (t, *J* = 7.1 Hz, 3H). (NMR data consistent with values described in literature).

**$^{13}$C NMR** (63 MHz, $CDCl_3$) δ 170.1, 153.6, 152.1, 146.6, 144.2, 139.7, 129.6, 129.3, 129.1, 128.5, 126.1, 124.7, 123.9, 123.9, 118.3, 95.7, 77.6, 59.9, 37.4, 34.5, 14.8. (NMR data consistent with values described in literature).[46]

**2.02t. Ethyl 4''-bromo-5'-(phenylamino)-2',3'-dihydro-[1,1':3',1''-terphenyl]-4'-carboxylate.** Prepared from ethyl acetoacetate (3.9 mmol), aniline (3.9 mmol) and (E)-3-(4-bromophenyl)-1-phenylprop-2-en-1-one (3.9 mmol). Purified by column chromatography (0-20% ethyl acetate/hexane). Yellow oil (59% yield).

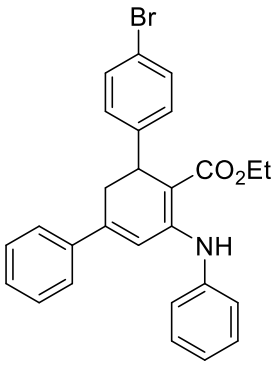


**$^{1}$H NMR** (300 MHz, $CDCl_3$) δ 10.75 (s, 1H), 7.40 – 7.26 (m, 10H), 7.20 – 7.08 (m, 5H), 6.66 (d, *J* = 2.9 Hz, 1H), 4.31 (d, J = 8.4 Hz, 1H), 4.23 – 4.05 (m, 3H), 3.23 (ddd, *J* = 16.7, 8.6, 2.9 Hz, 1H), 2.95 (dd, *J* = 16.7, 1.7 Hz, 1H), 1.19 (t, *J* = 7.1 Hz, 3H). (NMR data consistent with values described in literature).[46]

**2.02u. Ethyl 5'-((4-(dimethylamino)phenyl)amino)-2',3'-dihydro-[1,1':3',1''-terphenyl]-4'-carboxylate.** Prepared from ethyl acetoacetate (3.9 mmol), 4-dimethylaminoaniline (3.9 mmol) and (E)-1,3-diphenylpropenone (3.9 mmol). Purified by column chromatography (0-20% ethyl acetate/hexane). Yellow oil (81% yield).

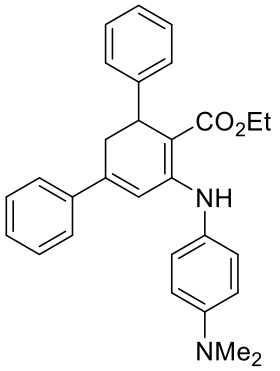


**$^1$H NMR** (250 MHz, $CDCl_3$) δ 10.62 (s, 1H), 7.49 – 7.44 (m, 1H), 7.41 – 7.36 (m, 1H), 7.36 – 7.22 (m, 10H), 7.22 – 7.13 (m, 2H), 7.07 (d, *J* = 8.8 Hz, 2H), 6.75 (d, *J* = 9.0 Hz, 2H), 6.60 (d, *J* = 2.9 Hz, 1H), 4.36 (dd, *J* = 8.4, 1.4 Hz, 1H), 4.23 – 4.05 (m, 3H), 3.24 (ddd, *J* = 16.7, 8.5, 2.9 Hz, 1H), 2.99 (s, 6H), 2.99 (dd, *J* = 16.7, 1.8 Hz, 1H), 1.20 (t, *J* = 7.1 Hz, 3H). (NMR data consistent with values described in literature).[46]

**2.02v. Ethyl 5'-((4-bromophenyl)amino)-2',3'-dihydro-[1,1':3',1''-terphenyl]-4'-carboxylate.** Prepared from ethyl acetoacetate (3.9 mmol), 4-bromoaniline (3.9 mmol) and (E)-1,3-diphenylpropenone (3.9 mmol). Purified by column chromatography (0-20% ethyl acetate/hexane). Yellow oil (53% yield).

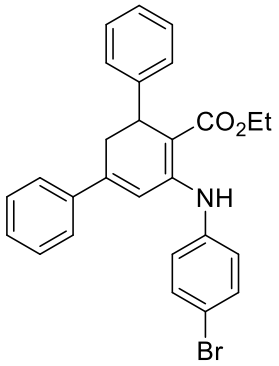


**$^1$H NMR** (250 MHz, $CDCl_3$) δ 10.84 (s, 1H), 7.51 (d, *J* = 8.7 Hz, 2H), 7.43 – 7.31 (m, 8H), 7.28 – 7.19 (m, 2H), 7.08 (d, *J* = 8.7 Hz, 2H), 6.69 (d, *J* = 2.8 Hz, 1H), 4.45 (dd, *J* = 8.4, 1.3 Hz, 1H), 4.30 – 4.11 (m, 2H), 3.32 (ddd, *J* = 16.7, 8.6, 2.8 Hz, 1H), 3.10 (dd, *J* = 16.7, 1.7 Hz, 1H), 1.26 (t, *J* = 7.1 Hz, 3H). (NMR data consistent with values described in literature).[46]

**2.02w. Ethyl 5'-((3,5-dichlorophenyl)amino)-2',3'-dihydro-[1,1':3',1''-terphenyl]-4'-carboxylate.** Prepared from ethyl acetoacetate (4.8 mmol), 3,5-chloroaniline (4.8 mmol) and (E)-1,3-diphenylpropenone (4.8 mmol). Purified by column chromatography (0-20% ethyl acetate/hexane). Yellow oil (48% yield).

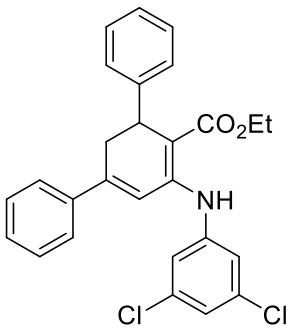


**$^1$H NMR** (250 MHz, $CDCl_3$) δ 10.73 (s, 1H), 7.37 – 7.15 (m, 12H), 7.10 (t, *J* = 1.8 Hz, 1H), 7.03 (d, *J* = 1.8 Hz, 2H), 6.58 (d, *J* = 2.8 Hz, 1H), 4.35 (dd, *J* = 8.4, 1.9 Hz, 1H), 4.24 – 4.05 (m, 2H), 3.23 (ddd, *J* = 16.9, 8.5, 2.9 Hz, 1H), 3.05 (dd, *J* = 16.9, 2.1 Hz, 1H), 1.19 (t, *J* = 7.1 Hz, 3H). (NMR data consistent with values described in literature).[46]

**$^{13}$C NMR** (63 MHz, $CDCl_3$) δ 170.3, 144.6, 139.9, 135.7, 129.2, 129.1, 128.6, 127.6, 126.7, 126.4, 123.5, 120.9, 117.7, 60.2, 37.1, 34.9, 14.7. (NMR data consistent with values described in literature).[46]

**2.02x. Ethyl 4-methoxy-5'-(phenylamino)-2',3'-dihydro-[1,1':3',1''-terphenyl]-4'-carboxylate.** Prepared from ethyl acetoacetate (6.5 mmol), aniline (6.5 mmol) and (E)-1-(4-methoxyphenyl)-3-phenylprop-2-en-1-one (6.5 mmol). Purified by column chromatography (0-20% ethyl acetate/hexane). Yellow solid (41% yield).

**Mp** 105 ºC.

**IR** ($cm^{-1}$): 3237, 3053, 2984, 2108, 1736, 1639.

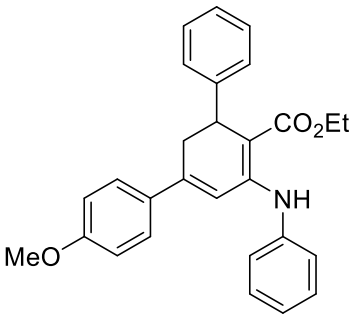


**$^1$H NMR** (250 MHz, $CDCl_3$) δ 10.64 (s, 1H), 7.27 – 7.15 (m, 6H), 7.12 – 7.07 (m, 2H), 7.06 – 6.99 (m, 3H), 6.70 – 6.62 (m, 2H), 6.56 (d, *J* = 2.8 Hz, 1H), 4.21 (dd, *J* = 8.5, 1.7 Hz, 1H), 4.03 (dddd, *J* = 17.9, 10.8, 7.1, 3.7 Hz, 2H), 3.64 (s, 3H), 3.11 (ddd, *J* = 16.6, 8.4, 2.9 Hz, 1H), 2.87 (dd, *J* = 16.6, 1.7 Hz, 1H), 1.10 (t, *J* = 7.1 Hz, 3H).

**$^{13}$C NMR** (63 MHz, $CDCl_3$) δ 170.6, 158.2, 151.3, 144.4, 140.3, 137.4, 129.5, 128.9, 128.8, 128.6, 126.2, 124.1, 123.5, 118.3, 113.8, 96.0, 59.8, 55.5, 36.3, 35.0, 14.8.

**Elemental analysis**: Anal. Calc. for $C_{28}H_{27}O_3N$ C, 79.03; H, 6.40; N, 3.29. Found C, 78.43; H, 6.18; N, 3.09.

**2.02y. Ethyl 4-chloro-5'-(phenylamino)-2',3'-dihydro-[1,1':3',1''-terphenyl]-4'-carboxylate.** Prepared from ethyl acetoacetate (5.4 mmol), aniline (5.4 mmol) and (E)-1-(4-chlorophenyl)-3-phenylprop-2-en-1-one (5.4 mmol). Purified by column chromatography (0-20% ethyl acetate/hexane). Yellow solid (41% yield).

**Mp**: 120ºC.

**IR** ($cm^{-1}$): 3224, 3038, 2974, 2098, 1734, 1640.

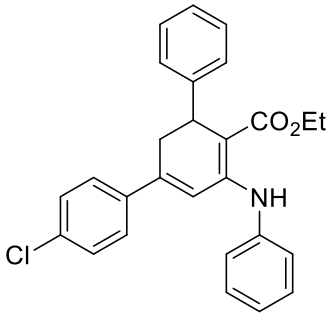


**$^1$H NMR** (250 MHz, $CDCl_3$) δ 10.76 (s, 1H), 7.38 – 7.06 (m, 14H), 6.64 (d, *J* = 2.8 Hz, 1H), 4.35 – 4.26 (m, 1H), 4.22 – 3.98 (m, 2H), 3.21 (ddd, *J* = 16.7, 8.6, 2.9 Hz, 1H), 2.92 (dd, *J* = 16.7, 1.7 Hz, 1H), 1.16 (t, *J* = 7.1 Hz, 3H).

**$^{13}$C NMR** (63 MHz, $CDCl_3$) δ 170.1, 151.4, 144.0, 143.7, 139.8, 131.8, 129.3, 128.8, 128.8, 128.7, 128.3, 125.9, 124.1, 123.4, 118.1, 94.7, 59.6, 36.4, 34.6, 14.6.

**Elemental analysis**: Anal. Calc. for $C_{28}H_{27}O_7N_3$ C, 64.98; H, 5.26; N, 8.12. Found C, 65.02; H, 5.47; N, 8.02 Anal. Calc. for $C_{27}H_{24}O_2NCl$ C, 75.43; H, 5.63; N, 3.26. Found C, 74.39; H, 5.54; N, 3.26.

**2.02z. Ethyl 2,4,4''-trimethoxy-5'-(phenylamino)-2',3'-dihydro-[1,1':3',1''-terphenyl]-4'-carboxylate.** Prepared from ethyl acetoacetate (6.1 mmol), aniline (6.1 mmol) and (E)-1-(2,4-dimethoxyphenyl)-3-(4-methoxyphenyl)prop-2-en-1-one (6.1 mmol). Purified by column chromatography (0-20% ethyl acetate/hexane). Pale yellow oil (39% yield).

**Mp**: 110 ºC.

**IR** ($cm^{-1}$): 3260, 2952, 2838, 2115, 1737, 1640.

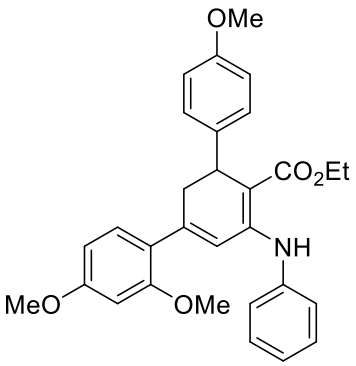


**$^1$H NMR** (250 MHz, $CDCl_3$) δ 10.82 (s, 1H), 7.35 (dd, *J* = 8.4, 7.2 Hz, 2H), 7.28 – 7.16 (m, 4H), 7.11 (d, *J* = 7.3 Hz, 1H), 6.92 (dd, *J* = 8.0, 0.7 Hz, 1H), 6.83 – 6.77 (m, 2H), 6.58 (d, *J* = 2.9 Hz, 1H), 6.39 (d, *J* = 8.2 Hz, 2H), 4.25 (dt, *J* = 8.0, 1.2 Hz, 1H), 4.22 – 4.04 (m, 2H), 3.79 (s, 6H), 3.70 (s, 3H), 3.21 (ddd, *J* = 16.6, 8.3, 2.9 Hz, 1H), 2.87 (dd, *J* = 16.7, 1.7 Hz, 1H), 1.22 (t, *J* = 7.1 Hz, 3H).

**$^{13}$C NMR** (63 MHz, $CDCl_3$) δ 170.7, 161.2, 158.6, 158.1, 151.8, 143.7, 140.4, 137.7, 129.9, 129.3, 128.8, 123.7, 123.5, 123.3, 119.8, 113.6, 104.6, 99.2, 95.3, 59.6, 55.7, 55.7, 55.5, 36.9, 36.5, 14.8.

**Elemental analysis**: Anal. Calc. for $C_{30}H_{31}O_5N$ C, 74.21; H, 6.44; N, 2.88. Found C, 73.49; H, 6.24; N, 2.90.

**2.02aa. Ethyl 4,4''-dichloro-5'-(phenylamino)-2',3'-dihydro-[1,1':3',1''-terphenyl]-4'-carboxylate.** Prepared from ethyl acetoacetate (5.8 mmol), aniline (5.8 mmol) and (E)-1,3-bis(4-chlorophenyl)prop-2-en-1-one (5.8 mmol). Purified by column chromatography (0-20% ethyl acetate/hexane). Yellow oil (31% yield).

**Mp**: 142 ºC.

**IR** ($cm^{-1}$): 3219, 3056, 2976, 1898, 2099, 1639.

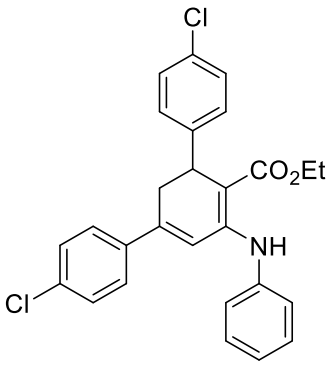


**$^1$H NMR** (250 MHz, $CDCl_3$) δ 10.83 (s, 1H), 7.49 – 7.15 (m, 13H), 6.70 (d, *J* = 2.8 Hz, 1H), 4.38 (dd, *J* = 8.5, 1.7 Hz, 1H), 4.30 – 4.10 (m, 2H), 3.28 (ddd, *J* = 16.6, 8.5, 2.9 Hz, 1H), 2.95 (dd, *J* = 16.6, 1.8 Hz, 1H), 1.26 (t, *J* = 7.1 Hz, 3H).

**$^{13}$C NMR** (63 MHz, $CDCl_3$) δ 170.2, 151.4, 143.6, 142.9, 139.9, 138.4, 134.9, 132.1, 129.6, 129.2, 129.0, 128.6, 127.4, 124.4, 123.6, 118.7, 59.9, 36.6, 34.8, 14.8.

**Elemental analysis**: Anal. Calc. for $C_{27}H_{23}O_2NCl_2$ C, 69.83; H, 4.99; N, 3.02. Found C, 69.11; H, 4.86; N, 3.02.

**4.03 General procedure for the synthesis of compounds 2.03a to 2.03l**

The corresponding dihydroanthranilate (1 equivalent) was dissolved in toluene (30 ml) and DDQ (1.1 equivalents) was added to the mixture, which was stirred at room temperature for 2 hours. The reaction mixture was concentrated in vacuo and redissolved in DCM (30 ml) and subsequently washed with water twice (20 ml) and brine (20 ml) once. The organic phase was dried with $Na_2SO_4$ and concentrated in vacuo. The residue was purified by column chromatography to yield the corresponding anthranilates.

**2.03a. Ethyl 5'-amino-[1,1':3',1''-terphenyl]-4'-carboxylate.** Prepared from compound **2.02a**. Purified by column chromatography (0-10% ethyl acetate/hexane). Brown solid (68% yield).

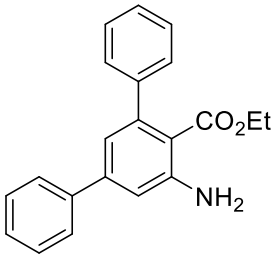


**$^1$H NMR** (250 MHz, $CDCl_3$) δ 7.67 – 7.33 (m, 10H), 6.95 (d, *J* = 1.4 Hz, 2H), 3.96 (q, *J* = 7.2 Hz, 2H), 0.77 (t, J = 7.2 Hz, 3H). (NMR data consistent with values described in literature).[46]

**2.03b. Ethyl 5'-amino-4-nitro-[1,1':3',1''-terphenyl]-4'-carboxylate.** Prepared from compound **2.02b**. Purified by column chromatography (0-30% ethyl acetate/hexane). Brown solid (74% yield).

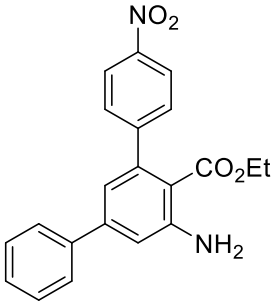


**Mp:** 215-216 ºC

**IR** ($cm^{-1}$): 3484, 3380, 3186, 2989, 2922, 1680.

**$^1$H NMR** (250 MHz, $CDCl_3$) δ 8.32 (d, *J* = 8.8 Hz, 2H), 7.78 (d, *J* = 8.8 Hz, 2H), 7.47 – 7.34 (m, 5H), 6.95 (m, 2H), 3.97 (q, *J* = 7.2 Hz, 2H), 0.77 (t, *J* = 7.1 Hz, 3H).

**Elemental analysis**: Anal. Calc. for $C_{21}H_{18}N_2O_4$ C, 69.60; H, 5.01; N, 7.73. Found: C, 68.19; H, 5.05; N, 7.08.

**2.03c. Ethyl 5'-amino-4-methyl-[1,1':3',1''-terphenyl]-4'-carboxylate.** Prepared from compound **2.02d**. Purified by column chromatography (0-30% ethyl acetate/hexane). Orange solid (66% yield).

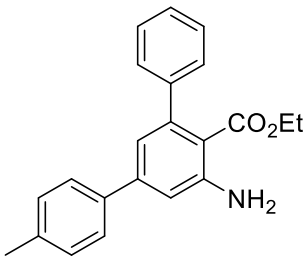


**$^1$H NMR** (250 MHz, $CDCl_3$) δ 7.50 (d, *J* = 8.1 Hz, 2H), 7.40 – 7.31 (m, 6H), 7.22 (d, *J* = 8.0 Hz, 2H), 7.12 (s, 1H), 7.02 (s, 1H), 3.93 (q, *J* = 7.1 Hz, 2H), 2.39 (s, 3H), 0.73 (t, J = 7.1 Hz, 3H). (NMR data consistent with values described in literature).[46]

**2.03d. Ethyl 3-amino-5-(5-chlorofuran-2-yl)-[1,1'-biphenyl]-4-carboxylate.** Prepared from compound **2.02c**. Purified by column chromatography (0-30% ethyl acetate/hexane). Yellow solid (72% yield).

**IR** ($cm^{-1}$): 3464, 2921, 2851, 2361, 1684.

**$^1$H NMR** (250 MHz, $CDCl_3$) δ 7.63 – 7.55 (m, 2H), 7.52 – 7.38 (m, 3H), 7.05 (d, *J* = 1.7 Hz, 1H), 6.93 (d, *J* = 1.7 Hz, 1H), 6.51 (d, *J* = 3.3 Hz, 1H), 6.28 (d, *J* = 3.3 Hz, 1H), 4.26 (q, *J* = 7.2 Hz, 2H), 1.19 (t, *J* = 7.2 Hz, 3H).

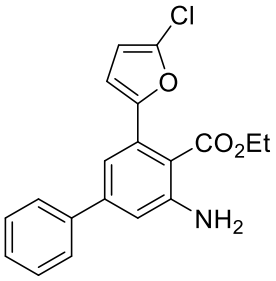


**$^{13}$C NMR** (63 MHz, $CDCl_3$) δ 169.3, 154.5, 148.9, 145.1, 140.2, 136.3, 131.9, 129.3, 128.6, 127.5, 118.0, 115.6, 112.1, 109.4, 108.3, 61.5, 14.3.

**Elemental analysis**: Anal. Calc. for $C_{19}H_{18}ClNO_3$ C, 66.38; H, 5.28; N, 4.07. Found: C, 64.38; H, 5.14; N, 3.95.

**2.03e. Ethyl 5'-amino-4-methoxy-[1,1':3',1''-terphenyl]-4'-carboxylate.** Prepared from compound **2.02e**. Purified by column chromatography (0-30% ethyl acetate/hexane). Brown oil (78% yield).

**IR** ($cm^{-1}$): 3475, 3373,2976, 2931, 2834, 1683.

**$^1$H NMR** (250 MHz, $CDCl_3$) δ 7.44 (d, *J* = 8.8 Hz, 2H), 7.28 – 7.22 (m, 5H), 6.90 – 6.79 (m, 4H), 3.83 (q, *J* = 7.2 Hz, 2H), 3.74 (s, 3H), 0.64 (t, *J* = 7.1 Hz, 3H).

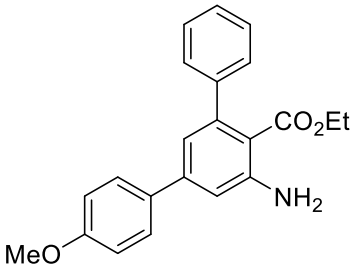


**$^{13}$C NMR** (63 MHz, $CDCl_3$) δ 169.5, 159.8, 148.1, 144.8, 144.0, 143.4, 132.6, 130.5, 129.4, 128.3, 128.1, 128.0, 126.9, 119.2, 114.3, 60.5, 55.4, 13.3.

**Elemental analysis**: Anal. Calc. for $C_{22}H_{21}NO_3$ C, 76.06; H, 6.09; N, 4.03. Found: C, 76.07; H, 6.05; N, 3.97.

**2.03f. Ethyl 5'-(benzylamino)-4-nitro-[1,1':3',1''-terphenyl]-4'-carboxylate.** Prepared from compound **2.02h**. Purified by column chromatography (0-30% ethyl acetate/hexane). Orange solid (66% yield).

**Mp:** 101-102 ºC

**IR** ($cm^{-1}$): 3275, 3063, 2977, 2893, 1646.

**$^1$H NMR** (250 MHz, $CDCl_3$) δ 8.18 – 8.10 (m, 2H), 7.57 – 7.48 (m, 2H), 7.38 – 7.17 (m, 10H), 6.92 (t, *J* = 5.6 Hz, 1H), 6.76 (d, *J* = 1.7 Hz, 1H), 6.73 (d, *J* = 1.7 Hz, 1H), 4.42 (d, *J* = 5.0 Hz, 2H), 3.83 (q, *J* = 7.1 Hz, 2H), 0.62 (t, *J* = 7.1 Hz, 3H).

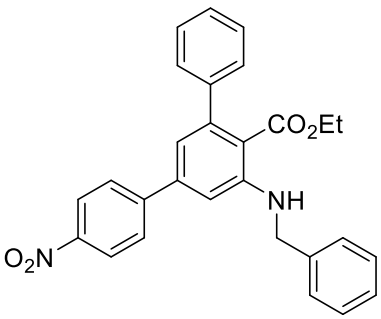


**$^{13}$C NMR** (63 MHz, $CDCl_3$) δ 170.0, 149.6, 147.8, 147.6, 145.7, 143.5, 142.4, 138.9, 129.3, 128.5, 128.4, 128.4, 127.8, 127.6, 127.5, 124.4, 118.1, 114.2, 109.8, 61.1, 48.1, 13.5.

**Elemental analysis**: Anal. Calc. for $C_{28}H_{24}N_2O_4$ C, 74.32; H, 5.35; N, 6.19. Found: C, 72.27; H, 5.35; N, 5.78.

**2.03g. Ethyl (R)-5'-((1-phenylethyl)amino)-[1,1':3',1''-terphenyl]-4'-carboxylate.** Prepared from the mixture of diastereoisomers of ethyl 5'-(((R)-1-phenylethyl)amino)-2',3'-dihydro-[1,1':3',1''-terphenyl]-4'-carboxylate. Purified by column chromatography (0-30% ethyl acetate/hexane). Brown oil (67% yield).

**IR** ($cm^{-1}$): 3377, 3025, 2974, 2339, 1676, 1561.

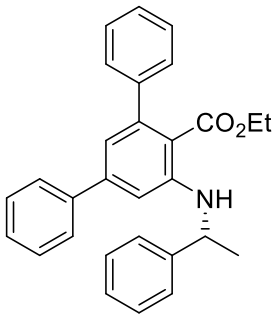


**$^1$H NMR** (250 MHz, $CDCl_3$) δ 7.33 – 7.03 (m, 18H), 6.91 (d, *J* = 4.2 Hz, 1H), 6.64 (d, *J* = 1.7 Hz, 1H), 6.51 (d, *J* = 1.7 Hz, 1H), 4.58 – 4.41 (m, 1H), 3.78 (q, *J* = 7.2 Hz, 2H), 1.46 (d, *J* = 6.7 Hz, 4H), 0.56 (t, *J* = 7.1 Hz, 3H).

**$^{13}$C NMR** (63 MHz, $CDCl_3$) δ 170.4, 148.9, 145.3, 144.7, 144.2, 141.1, 129.2, 129.1, 128.4, 128.3, 128.2, 127.5, 127.4, 127.1, 126.3, 118.1, 110.8, 60.83, 53.7, 25.5, 13.5.

**Elemental analysis**: Analysis calcd for $C_{29}H_{27}NO_2$ C, 82.63; H, 6.46; N, 3.32. Found: 82.49, 6.58, 3.37.

**2.03h. Ethyl (S)-5'-((1-phenylethyl)amino)-[1,1':3',1''-terphenyl]-4'-carboxylate.** Prepared from the mixture of diastereoisomers of ethyl 5'-(((S)-1-phenylethyl)amino)-2',3'-dihydro-[1,1':3',1''-terphenyl]-4'-carboxylate. Purified by column chromatography (0-30% ethyl acetate/hexane). Brown solid (64% yield).

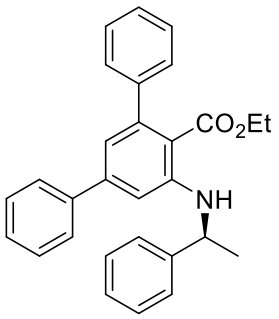


**$^1$H NMR** (250 MHz, $CDCl_3$) δ 7.34 – 7.11 (m, 20H), 6.69 – 6.64 (m, 1H), 6.60 (d, *J* = 1.8 Hz, 1H), 4.59 – 4.46 (m, 1H), 1.46 (d, *J* = 6.6 Hz, 3H).

**$^{13}$C NMR** (63 MHz, $CDCl_3$) δ 145.4, 141.0, 129.2, 129.1, 128.7, 128.4, 128.2, 127.5, 126.3, 118.5, 111.0, 111.0, 78.0, 53.8, 25.4.

**2.03i. Ethyl 5'-(butylamino)-4-methyl-2''-nitro-[1,1':3',1''-terphenyl]-4'-carboxylate.** Prepared from compound **2.02o**. Purified by column chromatography (0-20% ethyl acetate/hexane). Brown solid (59% yield).

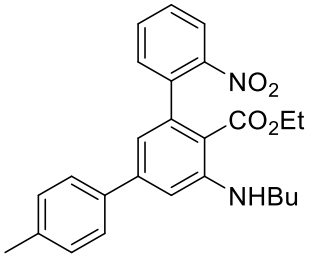


**$^1$H NMR** (250 MHz, $CDCl_3$) δ 7.95 (dd, *J* = 8.1, 1.3 Hz, 1H), 7.59 (s, 1H), 7.52 – 7.33 (m, 4H), 7.21 (dd, *J* = 7.6, 1.5 Hz, 2H), 7.17 – 7.12 (m, 2H), 6.82 (d, *J* = 1.7 Hz, 1H), 6.48 (d, *J* = 1.7 Hz, 1H), 3.80 (q, *J* = 7.1 Hz, 2H), 3.20 (td, *J* = 6.8, 4.2 Hz, 2H), 2.30 (s, 3H), 1.72 – 1.57 (m, 2H), 1.52 – 1.35 (m, 2H), 0.91 (t, *J* = 7.3 Hz, 3H), 0.61 (t, *J* = 7.2 Hz, 3H). (NMR data consistent with values described in literature).

**$^{13}$C NMR** (63 MHz, $CDCl_3$) δ 168.9, 152.0, 148.3, 145.6, 142.1, 140.6, 138.5, 137.9, 132.6, 131.5, 129.9, 127.7, 127.5, 124.2, 116.2, 109.7, 60.4, 43.5, 31.7, 21.6, 20.9, 14.4, 13.6. (NMR data consistent with values described in literature).[46]

**2.03j. Ethyl 4''-bromo-5'-(phenylamino)-[1,1':3',1''-terphenyl]-4'-carboxylate.** Prepared from compound **2.02t**. Purified by column chromatography (0-20% ethyl acetate/hexane). Brown oil (44% yield).

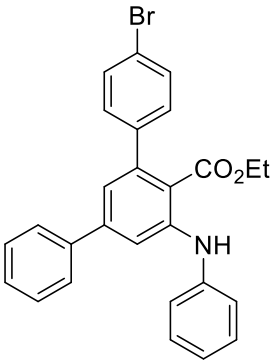


**$^1$H NMR** (300 MHz, $CDCl_3$) δ 8.16 (s, 1H), 7.50 – 7.41 (m, 5H), 7.37 – 7.22 (m, 5H), 7.22 – 7.13 (m, 4H), 7.02 – 6.93 (m, 1H), 6.90 (d, *J* = 1.7 Hz, 1H), 3.89 (q, *J* = 7.1 Hz, 2H), 0.75 (t, *J* = 7.2 Hz, 3H). (NMR data consistent with values described in literature).

**$^{13}$C NMR** (75 MHz, $CDCl_3$) δ 169.3, 145.5, 144.4, 143.4, 142.1, 141.5, 140.1, 131.2, 129.7, 129.5, 128.8, 128.2, 127.2, 121.1, 120.9, 120.2, 115.7, 113.2, 60.6. (NMR data consistent with values described in literature).[46]

**2.03k. Ethyl 5'-((4-(dimethylamino)phenyl)amino)-[1,1':3',1''-terphenyl]-4'-carboxylate.** Prepared from compound **2.02u**. Purified by column chromatography (0-20% ethyl acetate/hexane). Brown oil (62% yield).

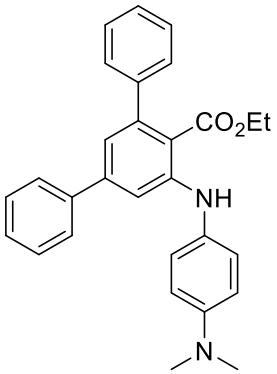


**$^1$H NMR** (250 MHz, $CDCl_3$) δ 7.97 (s, 1H), 7.47 – 7.40 (m, 2H), 7.34 – 7.21 (m, 9H), 7.18 – 7.14 (m, 1H), 7.13 – 7.06 (m, 2H), 6.84 (d, *J* = 1.7 Hz, 1H), 6.73 – 6.65 (m, 2H), 3.84 (q, *J* = 7.1 Hz, 2H), 2.87 (s, 6H), 0.65 (t, *J* = 7.2 Hz, 3H). (NMR data consistent with values described in literature).

**$^{13}$C NMR** (63 MHz, $CDCl_3$) δ 170.2, 148.3, 148.3, 145.1, 144.7, 143.9, 141.0, 129.1, 128.4, 128.4, 128.3, 127.7, 127.2, 125.4, 119.3, 114.2, 114.0, 111.8, 61.0, 41.5, 13.6. (NMR data consistent with values described in literature).[46]

**2.03l. Ethyl 5'-((4-bromophenyl)amino)-[1,1':3',1''-terphenyl]-4'-carboxylate.** Prepared from compound **2.02v**. Purified by column chromatography (0-20% ethyl acetate/hexane). Brown solid (62% yield).

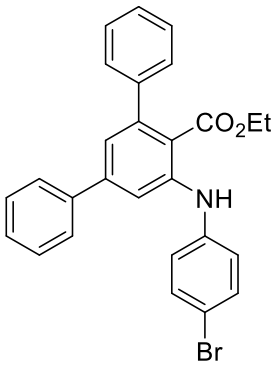


**$^1$H NMR** (250 MHz, $CDCl_3$) δ 8.15 (s, 1H), 7.61 – 7.52 (m, 3H), 7.49 – 7.36 (m, 10H), 7.20 – 7.14 (m, 2H), 7.13 (d, *J* = 1.7 Hz, 1H), 3.97 (q, *J* = 7.2 Hz, 2H), 0.77 (t, *J* = 7.2 Hz, 3H). (NMR data consistent with values described in literature).

**$^{13}$C NMR** (63 MHz, $CDCl_3$) δ 169.9, 145.1, 144.8, 144.6, 143.1, 141.3, 140.5, 132.8, 129.3, 128.6, 128.4, 127.6, 127.5, 122.3, 121.4, 117.2, 115.0, 113.5, 61.4, 13.5. (NMR data consistent with values described in literature).[46]

**4.04 General procedure for the synthesis of compound 2.04**

5-aminopentan-1-ol (1g, 9.7 mmol) was dissolved in 48% hydrobromic acid (10 ml) and heated to reflux for 2 hours. The mixture was concentrated in vacuo, yielding 5-bromopentan-1-aminium bromide as a brown solid (99% yield).

**$^1$H NMR** (250 MHz, MeOD) δ 3.48 (t, *J* = 6.6 Hz, 2H), 3.01 – 2.88 (m, 2H), 1.91 (dt, *J* = 13.6, 6.8 Hz, 2H), 1.70 (m, 2H), 1.62 – 1.48 (m, 2H). (NMR data consistent with values described in literature).[66]

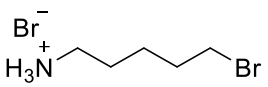


**4.05 General procedure for the synthesis of compound 2.05**

5-bromopentan-1-aminium bromide (1g, 4 mmol) and triphenyl phosphine (2.12 g, 8 mmol) were mixed in a microwave vial, and the vial placed in the cavity of an Anton-Paar microwave focused oven. The mixture was heated up to a maximum power of 200W and a temperature gradient programmed to reach 140 ºC in 5 minutes. The reaction mixture was stirred for 2 hours and then cooled down to room temperature. The mixture was then washed several times with diethyl ether, and the residue left, dissolved in methanol to extract it from the vial, and then concentrated in vacuo to yield (5-ammoniopentyl)triphenylphosphonium bromide as an orange solid (95% yield).

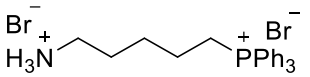


**$^1$H NMR** (250 MHz, MeOD) δ 8.01 – 7.66 (m, 15H), 3.56 – 3.44 (m, 2H), 2.93 (t, J = 6.7 Hz, 2H), 1.71 (m, 6H). (NMR data consistent with values described in literature).[67]

**4.06 General method for the synthesis of compounds 2.06a-2.06h**

The suitable β-ketoester (1 eq) and (5-ammoniopentyl)triphenylphosphonium bromide (1 eq) were dissolved in ethanol and triethylamine (1.1 eq) was added to the mixture and it was left stirring for 30 minutes. Subsequently, cerium ammonium nitrate (10%) and the corresponding chalcone (1 eq) were added to the mixture and it was heated up to reflux overnight. Afterwards, the reaction mixture was cooled down to room temperature and concentrated in vacuo. The residue was redissolved in ethyl acetate (40 ml) and washed twice with water (20 ml) and once with brine (20 ml). The organic phase was dried with $Na_2SO_4$ and concentrated in vacuo. The residue was purified by column chromatography to yield the desired TPP dihydroanthranilate.

**2.06a. (5-((6'-(ethoxycarbonyl)-1',2'-dihydro-[1,1':3',1''-terphenyl]-5'-yl)amino)pentyl)triphenylphosphonium bromide.** Prepared from (E)-1,3-diphenylpropenone (0.82 g, 4 mmol) and ethyl acetoacetate (0.52 g, 4 mmol). Purified by column chromatography (0-10% methanol in DCM). Yellow solid (65% yield).

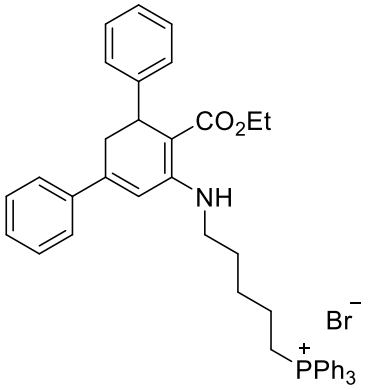


**Mp**: 71ºC.

**IR** ($cm^{-1}$): 3357, 3276, 3053, 2927, 2102, 1638, 1563.

**$^1$H NMR** (300 MHz, MeOD) δ 7.92 – 7.69 (m, 15H), 7.40 – 7.28 (m, 5H), 7.25 – 7.06 (m, 5H), 6.67 (d, *J* = 2.7 Hz, 1H), 4.23 (dd, *J* = 8.0, 2.1 Hz, 1H), 4.12 – 3.89 (m, 2H), 3.44 (d, *J* = 5.7 Hz, 4H), 3.08 (ddd, *J* = 16.7, 8.0, 2.8 Hz, 1H), 2.95 (dd, *J* = 16.9, 2.1 Hz, 1H), 1.74 (m, 6H), 1.12 (t, *J* = 7.1 Hz, 3H).

**$^{13}$C NMR** (63 MHz, MeOD) δ 171.9, 157.0, 148.1, 146.8, 136.3 (d, *J* = 3.0 Hz), 134.8 (d, *J* = 10.1 Hz), 131.5 (d, *J* = 12.7 Hz), 129.8, 129.7, 128.9, 128.3, 126.9, 126.9, 119.9 (d, *J* = 85.0 Hz), 116.9, 90.4, 59.8, 43.2, 38.0, 36.3, 30.7, 28.9 (d, *J* = 18.7 Hz), 23.2 (d, *J* = 6.8 Hz), 22.7 (d, *J* = 52.7 Hz), 14.8.

**Elemental analysis**: Anal. Calc. for $C_{44}H_{45}BrNO_2P$ C, 72.32; H, 6.21; N, 1.92. Found C, 71.84; H, 6.57; N, 2.14.

**2.06b. (5-((6'-(ethoxycarbonyl)-4-methoxy-1',2'-dihydro-[1,1':3',1''-terphenyl]-5'-yl)amino)pentyl)triphenylphosphonium bromide.** Prepared from (E)-3-(4-methoxyphenyl)-1-phenylprop-2-en-1-one (1.1 g, 4.6 mmol) and ethyl acetoacetate (0.6 g, 4.6 mmol). Purified by column chromatography (0-10% methanol in DCM). Yellow solid (60% yield).

**Mp** 78 ºC.

**IR** ($cm^{-1}$): 3366, 3275, 2928, 2096, 1635, 1561.

**$^1$H NMR** (300 MHz, MeOD) δ 7.98 – 7.69 (m, 15H), 7.36 (d, *J* = 8.4 Hz, 2H), 7.25 – 7.05 (m, 5H), 6.87 (d, *J* = 8.2 Hz, 2H), 6.62 (s, 1H), 4.25 – 4.17 (m, 1H), 4.07 – 3.93 (m, 2H), 3.78 (s, 3H), 3.55 – 3.37 (m, 4H), 2.97 (m, 2H), 1.73 (m, 6H), 1.11 (t, *J* = 7.1 Hz, 3H).

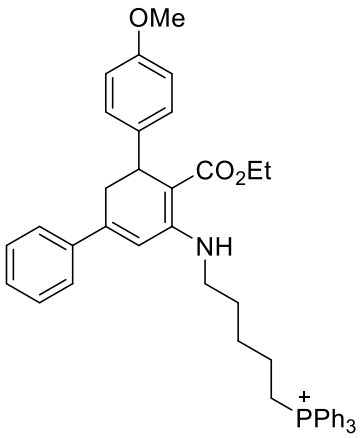


**$^{13}$C NMR** (75 MHz, MeOD) δ 170.5, 160.4, 156.0, 146.4, 145.7, 134.9 (d, *J* = 2.8 Hz), 133.4 (d, *J* = 10.4 Hz), 132.1 (d, *J* = 13.3 Hz), 130.1, 127.3 (d, *J* = 48.2 Hz), 126.9, 125.5, 119.1, 118.0, 113.7, 113.6, 88.6, 58.4, 54.4, 41.7, 36.6, 34.6, 29.3, 27.5 (d, *J* = 13.3 Hz), 21.8 (d, *J* =4.2 Hz), 21.4 (d, *J* = 50.9 Hz), 13.5.

**Elemental analysis**: Anal. Calc. for $C_{45}H_{47}BrNO_3P$ C, 71.05; H, 6.23; N, 1.84. Found C, 69.94; H, 6.51; N, 2.06.

**2.06c. (5-((6'-(ethoxycarbonyl)-3,4''-dimethoxy-1',2'-dihydro-[1,1':3',1''-terphenyl]-5'-yl)amino)pentyl)triphenylphosphonium bromide.** Prepared from (E)-3-(3-methoxyphenyl)-1-(4-methoxyphenyl)prop-2-en-1-one (1.4 g, 5.2 mmol) and ethyl acetoacetate (0.68 g, 5.2 mmol). Purified by column chromatography (0-10% methanol in DCM). Yellow solid (55% yield).

**Mp**: 73 ºC

**IR** ($cm^{-1}$): 3375, 3264, 2929, 2862, 2088, 1635, 1562.

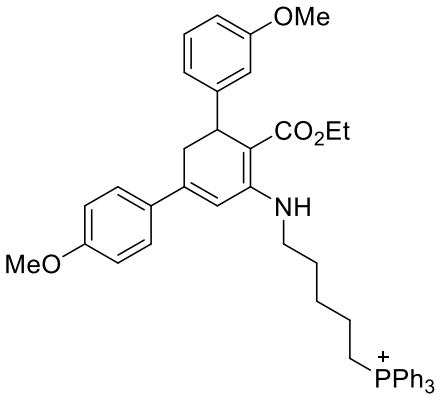


**$^1$H NMR** (250 MHz, MeOD) δ 7.76 – 7.52 (m, 16H), 7.26 – 7.18 (m, 2H), 6.92 (t, *J* = 7.9 Hz, 1H), 6.76 – 6.69 (m, 2H), 6.64 (d, *J* = 7.7 Hz, 1H), 6.58 (t, *J* = 2.1 Hz, 1H), 6.49 (dd, *J* = 8.1, 2.5 Hz, 1H), 6.44 (s, 1H), 4.02 (m, 1H), 3.92 – 3.75 (m, 2H), 3.63 (s, 3H), 3.51 (s, 3H), 3.26 (m, 4H), 2.81 (m,, 2H), 1.57 (m, 6H), 0.97 (t, *J* = 7.1 Hz, 3H).

**$^{13}$C NMR** (63 MHz, MeOD) δ 172.3, 162.3, 161.2, 157.9, 149.2, 148.5, 136.7 (d, J = 2.9 Hz), 135.2 (d, *J* = 10.0 Hz), 133.8, 132.0 (d, *J* = 12.8 Hz), 130.3, 128.8, 121.2, 120.4 (d, *J* = 86.4 Hz), 115.5, 115.2, 114.9, 112.1, 90.3, 60.2, 56.2, 55.9, 43.5, 38.4, 36.3, 31.1, 29.4 (d, *J* = 16.3 Hz), 23.5, 22.7, 15.3.

**Elemental analysis**: Anal. Calc. for $C_{46}H_{49}BrNO_4P$ C, 69.87; H, 6.25; N, 1.77. Found C, 68.73; H, 6.37; N, 2.18.

**2.06d. (5-((4-(ethoxycarbonyl)-5-(thiophen-2-yl)-5,6-dihydro-[1,1'-biphenyl]-3-yl)amino)pentyl)triphenylphosphonium.** Prepared from (E)-1-phenyl-3-(thiophen-2-yl)prop-2-en-1-one (940 mg, 4.4 mmol) and ethyl acetoacetate (0.57 g, 4.4 mmol). Purified by column chromatography (0-10% methanol in DCM). Brown solid (65% yield).

**Mp**: 65 ºC

**IR** ($cm^{-1}$): 3368, 3277, 3052, 2921, 2854, 2112, 1637, 1562.

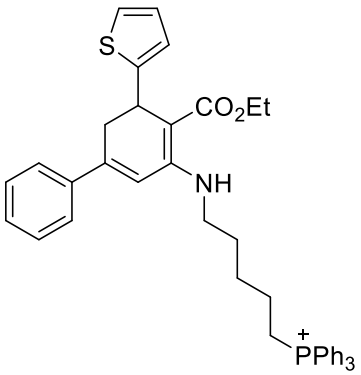


**$^1$H NMR** (300 MHz, MeOD) δ 7.93 – 7.68 (m, 15H), 7.54 – 7.46 (m, 2H), 7.43 – 7.31 (m, 3H), 7.00 (dd, *J* = 4.9, 1.4 Hz, 1H), 6.83 – 6.76 (m, 2H), 6.66 (d, *J* = 2.5 Hz, 1H), 4.50 (dd, *J* = 6.8, 2.3 Hz, 1H), 4.10 (q, *J* = 7.1 Hz, 2H), 3.49 – 3.36 (m, 4H), 3.10 (dd, *J* = 16.8, 2.3 Hz, 1H), 3.01 (ddd, *J* = 16.9, 6.9, 2.6 Hz, 1H), 1.72 (d, *J* = 12.1 Hz, 7H), 1.23 (t, *J* = 7.1 Hz, 3H).

**$^{13}$C NMR** (75 MHz, MeOD) δ 170.1, 155.0, 150.2, 147.5, 139.8, 134.9 (d, J = 3.3 Hz), 133.4 (d, *J* = 10.3 Hz), 130.1 (d, *J* = 12.6 Hz), 128.6, 128.4, 125.7, 125.6, 122.9, 122.0, 118.5 (d, *J* = 86.6 Hz), 115.3, 90.4, 58.6, 41.7, 32.7, 29.3, 27.5(d, J = 16. 6 Hz), 21.8 (d, *J* = 4.7 Hz), 21.3 (d, *J* = 51.5 Hz), 13.6.

**Elemental analysis**: Anal. Calc. for $C_{42}H_{43}BrNO_2PS$ C, 68.47; H, 5.88; N, 1.90; S, 4.35. Found C, 67.80; H, 6.24; N, 1.90; S, 4.22.

**2.06e. (5-((6'-(tert-butoxycarbonyl)-1',2'-dihydro-[1,1':3',1''-terphenyl]-5'-yl)amino)pentyl)triphenylphosphonium bromide.** Prepared from (E)-1,3-diphenylpropenone (1.3 g, 6.2 mmol) and tert-butyl acetoacetate (0.98 g, 6.2 mmol). Purified by column chromatography (0-10% methanol in DCM). Yellow solid (64% yield).

**Mp**: 74 ºC.

**IR** ($cm^{-1}$): 3365, 3278, 2925, 2861, 2112, 1638, 1563.

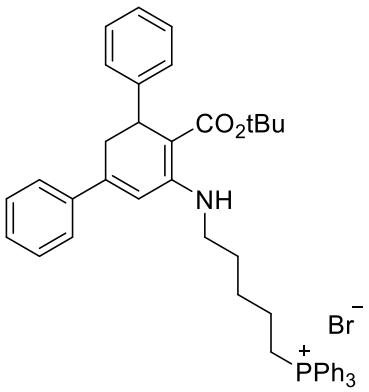


**$^{1}$H NMR** (250 MHz, MeOD) δ 7.96 – 7.70 (m, 15H), 7.47 – 7.28 (m, 5H), 7.26 – 7.08 (m, 5H), 6.67 (d, *J* = 2.8 Hz, 1H), 4.17 (dd, *J* = 8.3, 2.0 Hz, 1H), 3.54 – 3.38 (m, 4H), 3.07 (ddd, *J* = 16.8, 8.3, 2.9 Hz, 1H), 2.91 (dd, *J* = 16.8, 2.0 Hz, 1H), 1.75 (m, 6H), 1.31 (s, 9H).

**$^{13}$C NMR** (63 MHz, MeOD) δ 172.4, 156.7, 147.6, 141.9, 136.7 (d, *J* = 3.1 Hz), 135.2 (d, *J* = 10.7 Hz), 132.0 (d, *J* = 12.6 Hz), 130.1, 130.1, 129.3, 128.7, 127.3, 121.0, 119.7, 117.5, 92.8, 79.8, 55.3, 43.5, 39.2, 36.6, 31.2, 29.2, 23.5 (d, J = 14.3 Hz), 22.6 (d, *J* = 50.6 Hz).

**Elemental analysis**: Anal. Calc. for $C_{46}H_{49}BrNO_2P$ C, 72.81; H, 6.51; N, 1.85. Found C, 71.38; H, 6.69; N, 2.06.

**2.06f. (5-((6'-(ethoxycarbonyl)-4-nitro-1',2'-dihydro-[1,1':3',1''-terphenyl]-5'-yl)amino)pentyl)triphenylphosphonium bromide.** Prepared from (E)-3-(4-nitrophenyl)-1-phenylprop-2-en-1-one (1.2 g, 4.7 mmol) and ethyl acetoacetate (0.62 g, 4.7 mmol). Purified by column chromatography (0-10% methanol in DCM). Orange solid (64% yield).

**Mp**: 87 ºC.

**IR** ($cm^{-1}$): 3338, 3279, 2925, 2859, 2059, 1639, 1567.

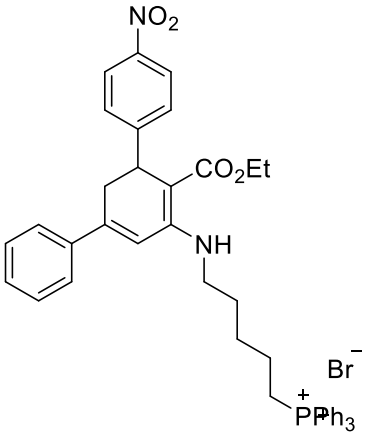


**$^{1}$H NMR** (250 MHz, MeOD) δ 8.16 – 8.03 (m, 2H), 7.95 – 7.71 (m, 15H), 7.51 – 7.29 (m, 7H), 6.76 (d, *J* = 2.7 Hz, 1H), 4.36 (d, *J* = 7.6 Hz, 1H), 4.11 – 3.91 (m, 2H), 3.57 – 3.41 (m, 4H), 3.13 (dd, *J* = 8.2, 2.8 Hz, 1H), 2.97 (dd, *J* = 17.0, 2.0 Hz, 1H), 1.75 (m, 6H), 1.11 (t, *J* = 7.1 Hz, 3H).

**$^{13}$C NMR** (63 MHz, MeOD) δ 171.8, 157.6, 155.7, 148.3, 141.3, 136.7 (d, *J* = 3.2 Hz), 135.2 (d, *J* = 10.3 Hz), 132.0 (d, *J* = 12.6 Hz), 130.5, 130.2, 129.8, 127.3, 124.6, 120.4 (d, J = 88.3 Hz), 117.4, 89.5, 60.4, 43.6, 38.7, 36.1, 31.2, 29.4 (d, *J* = 16.35 Hz), 23.7 (d, *J* = 4.4 Hz), 23.1 (d, *J* = 51.1 Hz), 15.3.

**Elemental analysis**: Anal. Calc. for $C_{44}H_{42}BrN_2O_4P$ C, 68.31; H, 5.47; N, 3.62. Found C, 65.40; H, 6.07; N, 4.23.

**2.06g. (5-((4''-chloro-6'-(ethoxycarbonyl)-4-nitro-1',2'-dihydro-[1,1':3',1''-terphenyl]-5'-yl)amino)pentyl)triphenylphosphonium bromide.** Prepared from (E)-1-(4-chlorophenyl)-3-(4-nitrophenyl)prop-2-en-1-one (1.05 g, 3.6 mmol) and ethyl acetoacetate (0.47 g, 3.6 mmol). Purified by column chromatography (0-10% methanol in DCM). Red solid (64% yield).

**Mp** 76 ºC

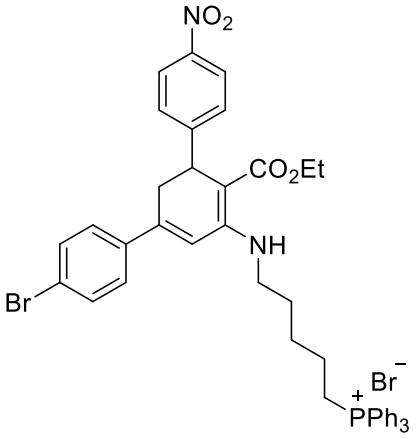

**IR** ($cm^{-1}$): 3281, 3054, 2930, 2863, 2447, 2058, 1639, 1510.

**$^1$H NMR** (250 MHz, MeOD) δ 8.01 – 7.90 (m, 2H), 7.82 – 7.58 (m, 15H), 7.40 – 7.34 (m, 2H), 7.34 – 7.29 (m, 2H), 7.27 – 7.18 (m, 2H), 6.66 (d, *J* = 2.8 Hz, 1H), 4.23 (d, *J* = 7.0 Hz, 1H), 3.99 – 3.79 (m, 2H), 3.34 (m, 4H), 3.03 (ddd, *J* = 17.0, 8.4, 2.8 Hz, 1H), 2.80 (dd, *J* = 17.0, 1.9 Hz, 1H), 1.62 (m, 6H), 0.98 (t, *J* = 7.1 Hz, 3H).

**$^{13}$C NMR** (63 MHz, MeOD) δ 171.8, 157.2, 155.5, 148.2, 146.8, 140.3, 136.7 (d, *J* = 3.1 Hz), 135.2 (d, *J* = 9.8 Hz), 133.3, 133.2 (d, *J* = 12.0 Hz), 129.8, 129.1, 124.6, 120.3 (d, *J* = 86.3 Hz), 118.0, 89.7, 60.4, 43.7, 38.7, 35.9, 31.2, 29.4 (d, *J* = 16.8 Hz), 23.7 (d, *J* = 4.6 Hz), 23.1 (d, *J* = 50.9 Hz), 15.25.

**Elemental analysis**: Anal. Calc. for $C_{44}H_{43}Br_2N_2O_4P$ C, 61.84; H, 5.07; N, 3.28. Found C, 60.77; H, 5.50; N, 3.36.

**2.06h. (5-((6'-(ethoxycarbonyl)-4,4''-dinitro-1',2'-dihydro-[1,1':3',1''-terphenyl]-5'-yl)amino)pentyl)triphenylphosphonium bromide.** Prepared from (E)-1,3-bis(4-nitrophenyl)prop-2-en-1-one (1.3 g, 4.4 mmol) and ethyl acetoacetate (0.57 g, 4.4 mmol). Purified by column chromatography (0-10% methanol in DCM). Red oil (64% yield).

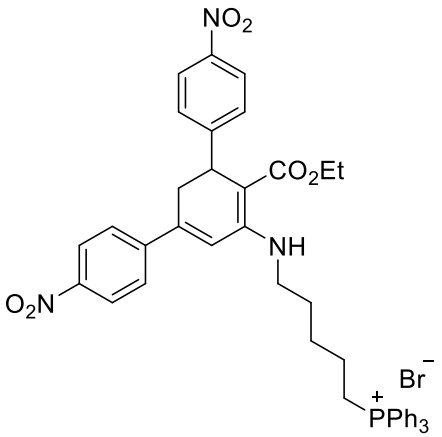

**IR** ($cm^{-1}$): 3279, 3056, 2925, 2858, 2060, 1641, 1589, 1509.

**$^1$H NMR** (250 MHz, MeOD) δ 9.11 (t, *J* = 5.7 Hz, 1H), 8.21 – 8.16 (m, 2H), 8.11 – 8.01 (m, 2H), 7.92 – 7.73 (m, 15H), 7.69 – 7.63 (m, 2H), 7.49 – 7.44 (m, 2H), 6.96 (d, *J* = 2.8 Hz, 1H), 4.40 (d, *J* = 8.1 Hz, 1H), 4.01 (m, 2H), 3.56 – 3.43 (m, 4H), 3.21 (dd, *J* = 8.4, 2.9 Hz, 1H), 2.99 (dd, *J* = 17.0, 1.8 Hz, 1H), 1.76 (m, 6H), 1.11 (t, *J* = 7.1 Hz, 3H).

**$^{13}$C NMR** (63 MHz, MeOD) δ 171.7, 156.6, 155.2, 149.5, 148.3, 147.5, 145.4, 136.7 (d, *J* = 3.0 Hz), 135.2 (d, *J* = 10.1 Hz), 132.0 (d, *J* = 12.1 Hz), 129.8, 128.4, 125.3, 124.7, 120.8, 120.3 (d, *J* = 86.0 Hz), 90.6, 60.6, 43.8, 38.6, 35.9, 23.8 (d, *J* = 4.9 Hz), 23.1 (d, *J* = 51.2 Hz) 15.2.

**Elemental analysis**: Anal. Calc. for $C_{44}H_{43}BrN_3O_6P$ C, 64.39; H, 5.28; N, 5.12. Found C, 63.51; H, 5.57; N, 5.17.

**4.07 General procedure for the synthesis of compounds 2.07a to 2.07h**

The corresponding TPP-dihydroanthranilate (1 eq), NBS (1.1 eq) and AIBN (0.05 eq) were dissolved in acetonitrile (10 ml) and the reaction mixture was stirred at room temperature for 30 minutes. The mixture was concentrated in vacuo, redissolved in ethyl acetate (20 ml) and washed twice with water (10 ml) and once with brine (10 ml). The reaction mixture was dried

with $Na_2SO_4$ and concentrated in vacuo to yield the TPP-anthranilate. Compounds **2.07b** and **2.07d** were purified by column chromatography (0-10% methanol in DCM).

**2.07a. (5-((4'-(ethoxycarbonyl)-[1,1':3',1''-terphenyl]-5'-yl)amino)pentyl)triphenylphosphonium bromide.** Prepared from compound **2.06a** (50 mg, 0.068 mmol). Brown solid (96% yield).

**Mp**: 75 ºC.

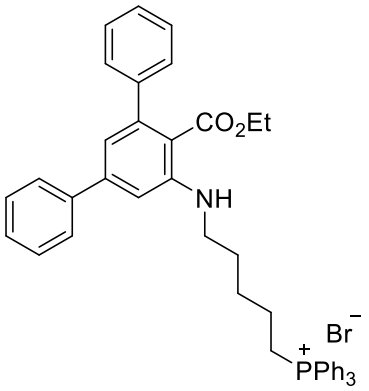


**IR** ($cm^{-1}$): 3363, 3052, 2926, 2859, 2104, 1672, 1561.

**$^1$H NMR** (250 MHz, MeOD) δ 7.78 – 7.53 (m, 15H), 7.52 – 7.46 (m, 2H), 7.35 – 7.20 (m, 6H), 7.14 (dd, *J* = 7.6, 1.9 Hz, 2H), 6.73 (d, *J* = 1.6 Hz, 1H), 6.65 (d, *J* = 1.6 Hz, 1H), 3.72 (q, *J* = 7.2 Hz, 2H), 3.29 (m, 2H), 3.10 (m, 2H), 1.60 (d, *J* = 3.7 Hz, 6H), 0.56 (t, *J* = 7.1 Hz, 3H).

**$^{13}$C NMR** (63 MHz, MeOD) δ 171.6, 151.0, 146.8, 146.4, 145.4, 136.7 (d, *J* = 3.0 Hz), 135.3 (d, *J* = 10.2 Hz), 132.0(d, *J* = 12.7 Hz), 130.4, 129.6, 129.5, 129.1 (d, *J* = 56.9 Hz), 128.4, 121.0, 119.6, 118.6, 114.0, 109.9, 61.9, 44.1, 29.6 (d, *J* = 2.4 Hz), 23.6 (d, J = 4.2 Hz), 23.1 (d, *J* = 51.5 Hz), 14.0.

**Elemental analysis**: Anal. Calc. for $C_{44}H_{43}BrNO_2P$ C, 72.52; H, 5.95; N, 1.92. Found C, 70.76; H, 6.07; N, 2.29.

**2.07b. (5-((6'-(ethoxycarbonyl)-4-methoxy-1',2'-dihydro-[1,1':3',1''-terphenyl]-5'-yl)amino)pentyl)triphenylphosphonium bromide.** Prepared from compound **2.06b** (50 mg, 0.066 mmol). Brown solid (65% yield).

**Mp** 66 ºC.

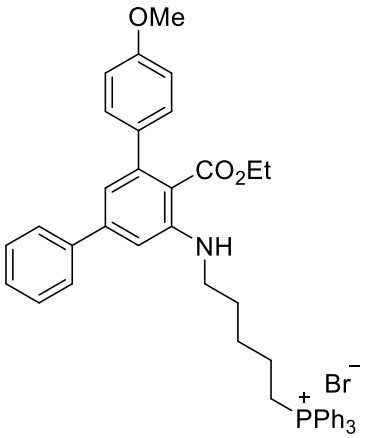


**IR** ($cm^{-1}$): 3366, 2923, 2853, 2095, 1672, 1560.

**$^1$H NMR** (250 MHz, MeOD) δ 7.80 – 7.55 (m, 15H), 7.50 – 7.39 (m, 2H), 7.24 (m, 3H), 7.14 (m, 2H), 6.91 – 6.82 (m, 2H), 6.71 (d, *J* = 1.7 Hz, 1H), 6.64 (d, *J* = 1.6 Hz, 1H), 3.77 – 3.64 (m, 5H), 3.28 (d, *J* = 13.7 Hz, 2H), 3.12 (d, *J* = 5.1 Hz, 2H), 1.62 (s, 6H), 0.56 (t, *J* = 7.1 Hz, 3H).

**$^{13}$C NMR** (63 MHz, MeOD) δ 171.7, 161.2, 151.1, 146.8, 146.0, 145.6, 136.7 (d, *J* = 3.0 Hz), 135.2 (d, *J* = 9.9 Hz), 132.0 (d, *J* = 11.8 Hz), 129.7, 129.5, 128.3, 120.3 (d, *J* = 86.8 Hz), 118.3, 115.7, 113.3, 109.3, 61.8, 56.2, 44.0, 29.5 (d, *J* = 11.5 Hz), 25.7, 23.6 (d, *J* = 3.4 Hz), 23.1 (d, *J* = 55.5 Hz), 14.0.

**Elemental analysis**: Anal. Calc. for $C_{45}H_{45}BrNO_3P$ C, 71.24; H, 5.98; N, 1.85. Found C, 70.77; H, 6.52; N, 3.04.

**2.07d. (5-((4-(ethoxycarbonyl)-5-(thiophen-2-yl)-[1,1'-biphenyl]-3-yl)amino)pentyl)triphenylphosphonium.** Prepared from compound **2.06d** (50 mg, 0.069 mmol). Brown oil (68% yield).

**IR** ($cm^{-1}$): 3374, 3055, 2927, 2861, 2100, 1674.

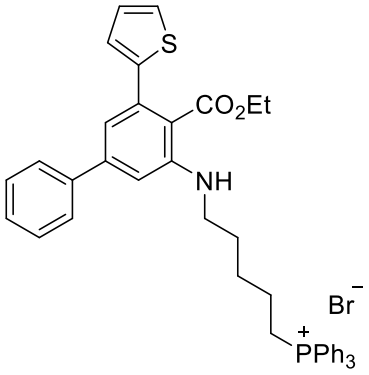


**$^{1}$H NMR** (250 MHz, MeOD) δ 7.71 – 7.48 (m, 15H), 7.43 – 7.37 (m, 2H), 7.29 – 7.18 (m, 4H), 6.87 (dd, *J* = 5.1, 3.5 Hz, 1H), 6.76 (dd, *J* = 3.5, 1.2 Hz, 1H), 6.68 (d, *J* = 1.6 Hz, 1H), 6.66 (d, *J* = 1.7 Hz, 1H), 3.80 (q, *J* = 7.1 Hz, 2H), 3.24 (d, *J* = 9.5 Hz, 2H), 3.01 (d, *J* = 6.0 Hz, 2H), 1.52 (s, 6H), 0.71 (t, *J* = 7.1 Hz, 3H).

**$^{13}$C NMR** (63 MHz, MeOD) δ 171.41, 150.51, 146.25, 146.00, 142.10, 138.19, 136.7 (d, J = 2.9 Hz), 135.2 (d, *J* = 10.3 Hz), 132.0 (d, *J* = 13.1 Hz), 130.46, 129.70, 128.62, 128.60, 127.01, 126.77, 120.2 (d, *J* = 86.0 Hz), 118.98, 110.61, 62.38, 44.09, 29.62, 23.6 (d, *J* = 4.3 Hz), 23.1 (d, *J* = 51.5 Hz), 14.33.

**Elemental analysis**: Anal. Calc. for $C_{42}H_{41}BrNO_2PS$ C, 68.66; H, 5.62; N, 1.91; S, 4.36. Found C, 68.67; H, 6.20; N, 2.37; S, 4.20.

**2.07e. (5-((4'-(tert-butoxycarbonyl)-[1,1':3',1''-terphenyl]-5'-yl)amino)pentyl)triphenylphosphonium bromide.** Prepared from compound **2.06e** (50 mg, 0.066 mmol). Brown solid (94% yield).

**Mp**: 76 ºC.

**IR** ($cm^{-1}$):3363, 2927, 2859, 2109, 1669, 1561.

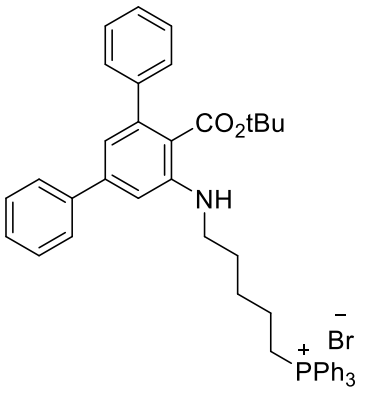


**$^{1}$H NMR** (250 MHz, MeOD) δ 7.93 – 7.69 (m, 15H), 7.68 – 7.59 (m, 2H), 7.45 – 7.28 (m, 8H), 6.86 (d, *J* = 1.7 Hz, 1H), 6.76 (d, *J* = 1.7 Hz, 1H), 3.46 (m, 2H), 3.26 (m, 2H), 1.77 (m, 6H), 1.13 (s, 9H).

**$^{13}$C NMR** (63 MHz, MeOD) δ 170.9, 150.9, 146.6, 145.7, 136.7, 136.7, 135.3, 135.2, 132.0, 131.8, 130.3, 129.9, 129.6, 128.6, 121.0, 119.7, 118.8, 109.9, 82.7, 55.3, 44.1, 29.6, 28.3, 23.6, 22.7.

**Elemental analysis**: Anal. Calc. for $C_{46}H_{47}BrNO_2P$ C, 73.01; H, 6.26; N, 1.85. Found C, 69.75; H, 6.25; N, 2.14.

**2.07f. (5-((6'-(ethoxycarbonyl)-4-nitro-[1,1':3',1''-terphenyl]-5'-yl)amino)pentyl)triphenylphosphonium bromide.** Prepared from compound **2.06f** (50 mg, 0.064 mmol). Orange solid (99% yield).

**Mp** 66 ºC.

**IR** ($cm^{-1}$): 3357, 2923, 2854, 2059, 1672, 1591.

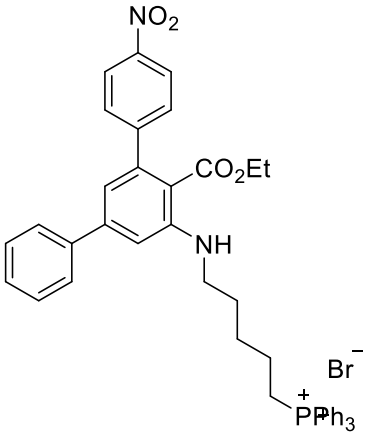

**$^1$H NMR** (250 MHz, MeOD) δ 8.33 – 8.22 (m, 2H), 7.98 – 7.71 (m, 15H), 7.68 – 7.60 (m, 2H), 7.57 – 7.37 (m, 6H), 6.95 (d, *J* = 1.7 Hz, 1H), 6.76 (d, *J* = 1.6 Hz, 1H), 3.88 (q, *J* = 7.1 Hz, 2H), 3.44 (m, 2H), 3.29 (m, 1H), 1.77 (m, 6H), 0.71 (t, *J* = 7.1 Hz, 3H).

**$^{13}$C NMR** (63 MHz, MeOD) δ 170. 7, 152.7, 151.9, 148.6, 147.0, 145.0, 142.0, 136.7 (d, *J* = 2.8 Hz), 135.2 (d, *J* = 9.5 Hz), 132.0 (d, *J* = 12.5 Hz), 130.7, 130.4, 129.9, 128.6, 124.6, 120.3 (d, *J* = 86.6 Hz), 118.3, 111.1, 62.0, 44.0, 29.7, 23.7, 23.1 (d, *J* = 50.0 Hz), 14.0.

**Elemental analysis**: Anal. Calc. for $C_{44}H_{44}BrN_2O_4P$ C, 68.13; H, 5.72; N, 3.61. Found C, 67.74; H, 6.01; N, 3.87.

**2.07g. (5-((4-chloro-4'-(ethoxycarbonyl)-4''-nitro-[1,1':3',1''-terphenyl]-5'-yl)amino)pentyl)triphenylphosphonium bromide.** Prepared from compound **2.06g** (50 mg, 0.062 mmol). Red solid (96% yield).

**Mp** 67 ºC.

**IR** ($cm^{-1}$): 3358, 3055, 2923, 2855, 2096, 1673, 1592.

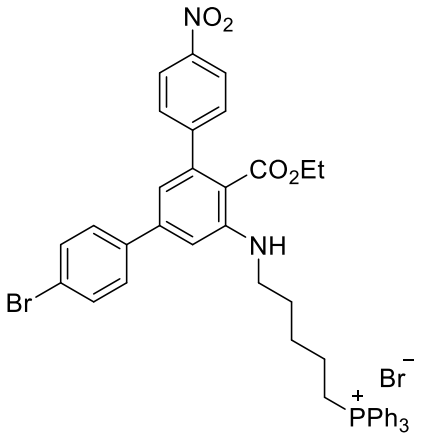

**$^1$H NMR** (250 MHz, MeOD) δ 8.15 (m, 2H), 7.81 – 7.57 (m, 15H), 7.47 (m, 4H), 7.40 – 7.33 (m, 2H), 6.81 (d, *J* = 1.7 Hz, 1H), 6.63 (d, *J* = 1.6 Hz, 1H), 3.76 (q, *J* = 7.1 Hz, 2H), 3.34 (m, 2H), 3.17 (m, 2H), 1.64 (s, 6H), 0.59 (t, *J* = 7.1 Hz, 3H).

**$^{13}$C NMR** (63 MHz, MeOD) δ 170.6, 152.5, 151.9, 148.6, 145.1, 141.0, 136.7 (d, *J* = 2.8 Hz), 135.2 (d, *J* = 9.9 Hz), 133.5, 132.0 (d, *J* = 12.5 Hz), 130.7, 130.5, 124.6, 120.5 (d, *J* = 84.6 Hz), 118.0, 112.5, 110.8, 62.0, 44.0, 29.7 (d, *J* = 4.6 Hz), 29.5, 23.7(d, *J* = 4.1 Hz), 23.5, 14.0.

**Elemental analysis**: Anal. Calc. for $C_{44}H_{41}Br_2N_2O_4P$ C, 61.98; H, 4.85; N, 3.29. Found C, 62.61; H, 5.70; N, 4.85.

**2.07h. (5-((4'-(ethoxycarbonyl)-4,4''-dinitro-[1,1':3',1''-terphenyl]-5'-yl)amino)pentyl)triphenylphosphonium bromide.** Prepared from compound **2.06h** (50 mg, 0.061 mmol). Red solid (93% yield).

**Mp**: 74 ºC.

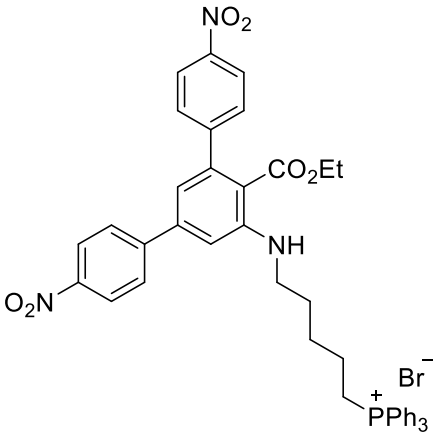

**IR** ($cm^{-1}$): 3356, 3056, 2923, 2855, 2446, 2102, 1677, 1585.

**$^1$H NMR** (250 MHz, MeOD) δ 8.21 – 8.12 (m, 4H), 7.81 – 7.59 (m, 15H), 7.43 – 7.30 (m, 2H), 6.90 (d, *J* = 1.7 Hz, 1H), 6.71 (d, *J* = 1.7 Hz, 1H), 3.78 (q, *J* = 7.2 Hz, 2H), 3.33 (d, *J* = 13.7 Hz, 2H), 1.65 (m, 6H), 0.60 (t, *J* = 7.1 Hz, 3H).

**$^{13}$C NMR** (63 MHz, MeOD) δ 170.4, 152.1, 151.8, 149.42, 148.7, 148.3, 145.12, 144.33, 136.7 (d, *J* = 3.0 Hz), 135.2 (d, *J* = 10.2 Hz), 132.0 (d, *J* = 12.8 Hz), 130.7, 129.8, 125.5, 124.7, 120.3 (d, *J* = 85.5 Hz), 118.3, 113.5, 111.4, 62.2, 44.1, 29.8, 29.6 (d, *J* = 11.0 Hz), 23.7 (d, *J* = 4.0 Hz), 23.1 (d, *J* = 50.8 Hz), 14.0.

**Elemental analysis**: Anal. Calc. for $C_{44}H_{41}BrN_3O_6P$ C, 64.55; H, 5.05; N, 5.13. Found C, 63.12; H, 5.79; N, 5.94.

**4.08 Procedure for the synthesis of compound 2.08**

ethyl 5'-amino-[1,1':3',1''-terphenyl]-4'-carboxylate (200 mg, 0.63 mmol) was dissolved in acetonitrile (15 ml) and triethylamine (95 mg, 0.95 mmol) and (4-chloro-4-oxobutyl)triphenylphosphonium bromide (330 mg, 0.76 mmol) were added to the mixture, which was stirred at room temperature overnight. The mixture was then concentrated in vacuo and purified by column chromatography (0-10% MeOH in DCM) to yield the desired product as a colourless solid (0.25 g, 55% yield).

**Mp**: 76-77 ºC

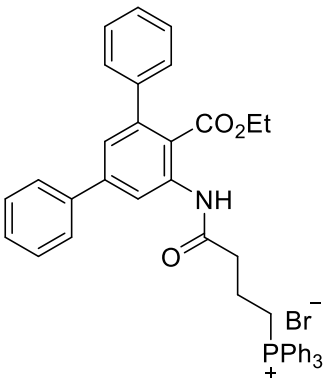

**IR** ($cm^{-1}$): 3370, 3054, 2977, 1674.

**$^1$H NMR** (250 MHz, MeOD) δ 7.79 – 7.45 (m, 19H), 7.36 – 7.10 (m, 10H), 3.64 (q, *J* = 7.2 Hz, 2H), 3.45 – 3.28 (m, 2H), 2.54 (t, *J* = 6.4 Hz, 2H), 1.87 (dt, *J* = 11.8, 6.8 Hz, 2H), 0.57 (t, *J* = 7.2 Hz, 3H).

**$^{13}$C NMR** (63 MHz, MeOD) δ 173.5, 170.2, 145.4, 144.9, 143.1, 141.0, 137.8, 137.3, 136.8, 136.8, 135.4, 135.2, 132.1, 131.9, 130.6, 129.9, 129.7, 129.1, 128.6, 127.4, 126.9, 123.8, 120.9, 119.5, 62.8, 23.1, 22.3, 20.1, 14.1.

**Elemental analysis**: Anal. Calc. for $C_{43}H_{39}BrNO_3P$ C, 70.88; H, 5.40; N, 1.92. Found C, 70.63; H, 5.88; N, 1.96.

**4.09 General procedure for the synthesis of compounds 2.09a to 2.06d**

A microwave vial containing a solution of the corresponding dihydroanthranilate in DMF (2 ml) was closed and placed in the cavity of an Anton-Paar focused microwave oven and heated up with a maximum power of 200 W and a temperature gradient programmed to reach up to 200 ºC in 5 minutes. The reaction mixture was stirred at this temperature for 90 minutes and then it was cooled down to room temperature. The solvent was removed under reduced pressure and the residue left, washed with chloroform to obtain the desired dihydroacridone.

**2.09a. 3-(4-methoxyphenyl)-1-phenyl-1,10-dihydroacridin-9(2H)-one.** Prepared from compound **2.02x** (220 mg, 0.47 mmol). Yellow solid (43% yield). yellow solid

**Mp**: 242 ºC.

**IR** ($cm^{-1}$): 3391, 2990, 2770, 2106, 1607.

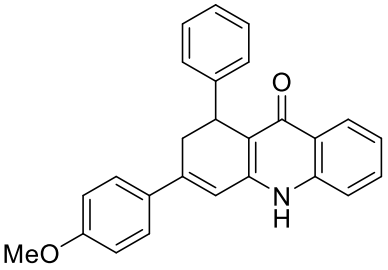


**$^{1}$H-NMR** (250 MHz, DMSO-$d_6$) 11.87 (s, 1H), 8.08 (dd, *J* = 8.1, 1.4 Hz, 1H), 7.68–7.53 (m, 4H), 7.48–7.37 (m, 3H), 7.29 (ddd, *J* = 8.1, 6.7, 1.3 Hz, 1H), 7.17–7.08 (m, 2H), 6.90 (d, *J* = 2.5 Hz, 1H), 6.78–6.65 (m, 2H), 4.57 (d, *J* = 7.8 Hz, 1H), 3.63 (s, 3H), 3.32–3.19 (ddd, *J* = 17.0, 8.3, 2.5 Hz, 1H), 3.10–3.01 (d, *J* = 17.0 Hz, 1H).

**$^{13}$C-NMR** (63 MHz, DMSO-$d_6$): 174.7, 157.9, 145.7, 143.8, 139.6, 139.1, 136.7, 131.7, 129.4, 129.3, 128.3, 125.8, 125.4, 123.1, 118.3, 117.4, 114.5, 113.7, 55.2, 34.4, 33.3.

**Elemental analysis**: Anal. Calc. for $C_{26}H_{21}O_2N$ C, 82.30; H, 5.58; N, 3.69. Found C, 81.91; H, 5.47; N, 3.85.

**2.09b. 3-(4-chlorophenyl)-1-phenyl-1,10-dihydroacridin-9(2H)-one.** Prepared from compound **2.02y** (300 mg, 0.7 mmol). Brown solid (52% yield).

**Mp**: 278 ºC.

**IR** ($cm^{-1}$): 3252, 3056, 2874, 2765, 2107, 1700, 1620.

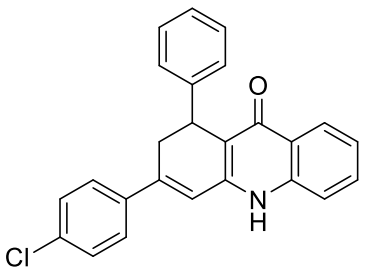


**$^{1}$H-NMR** (250 MHz, DMSO-$d_6$) 11.90 (s, 1H), 8.06 (dd, *J* = 8.1, 1.4 Hz, 1H), 7.69–7.51 (m, 5H), 7.50–7.37 (m, 3H), 7.29 (m, 2H), 7.20 (m, 2H), 6.90 (d, *J* = 2.5 Hz, 1H), 4.59 (d, *J* = 8.1 Hz, 1H), 3.24 (dd, J = 8.5, 2.3 Hz, 1H), 3.07 (dd, J = 17.6, 1.4 Hz, 1H).

**$^{13}$C-NMR** (63 MHz, DMSO-$d_6$) 174.6, 145.6, 144.0, 143.8, 139.6, 139.0, 131.8, 131.0, 129.5, 129.3, 129.3, 128.3, 125.9, 125.4, 123.2, 118.4, 117.5, 113.6, 34.0, 33.6.

**Elemental Analysis**: Anal. Calc. for $C_{25}H_{18}ONCl$ C, 78.22; H, 4.73; N, 3.65. Found C, 77.03; H, 4.85; N, 3.97.

**2.09c. 3-(2,4-dimethoxyphenyl)-1-(4-methoxyphenyl)-1,10-dihydroacridin-9(2H)-one.** Prepared from compound **2.02z** (150 mg, 0.3 mmol). Yellow solid (44% yield).

**Mp**: 168 ºC.

**IR** ($cm^{-1}$): 3214, 3066, 2932, 2829, 2118, 1603.

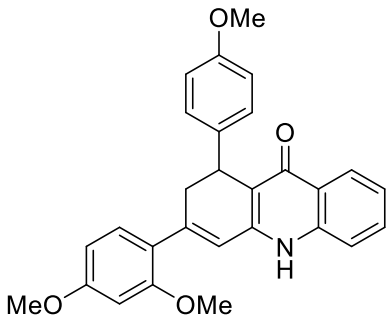


**$^1$H-NMR** (250MHz, DMSO-$d_6$): 12.14 (s, 1H), 8.15–8.07 (m, 1H), 7.65 (dd, *J* = 6.2, 1.5 Hz, 2H), 7.37–7.28 (m, 1H), 7.24 (dd, J = 8.5, 1.8 Hz, 1H), 7.20–7.11 (m, 2H), 6.86 (d, *J* = 2.4 Hz, 1H), 6.75 (dd, *J* = 8.9, 2.5 Hz, 2H), 6.66–6.60 (m, 1H), 6.57 (d, *J* = 2.4 Hz, 1H), 4.52 (d, J = 7.7 Hz, 1H), 3.81 (s, 3H), 3.79 (s, 3H), 3.66 (s, 3H), 3.28–3.17 (m, 1H), 2.92 (d, *J* = 17.3 Hz, 1H).

**$^{13}$C-NMR** (63MHz, DMSO-$d_6$): 161.4, 158.7, 157.9, 145.6, 144.7, 139.5, 136.6, 131.7, 129.6, 128.4, 125.2, 125.0, 121.8, 118.6, 118.4, 114.0, 113.6, 105.6, 99.3, 56.0, 55.7, 55.3, 36.3, 33.5.

**Elemental analysis**: Anal. Calc. for $C_{28}H_{25}O_4N$ C, 76.52; H, 5.73; N, 3.19. Found C, 75.31; H, 5.67; N, 3.38.

**2.09d. 1,3-bis(4-chlorophenyl)-1,10-dihydroacridin-9(2H)-one.** Prepared from compound **2.02aa** (173 mg, 0.3 mmol). Yellow solid (27% yield).

**Mp**: 287 ºC.

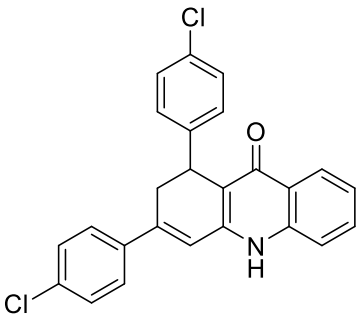


**IR** ($cm^{-1}$): 3252, 3059, 2749, 2681, 2113, 1624.

**$^1$H-NMR** (300 MHz, DMSO-$d_6$): 11.86 (s, 1H), 8.07 (dd, *J* = 8.1, 1.5 Hz, 1H), 7.68–7.56 (m, 3H), 7.53–7.47 (m, 2H), 7.30 (ddd, *J* = 8.1, 6.8, 1.1 Hz, 2H), 7.23 (s, 4H), 6.91 (d, *J* = 2.7 Hz, 1H), 4.60 (d, *J* = 8.3 Hz, 1H), 3.29–3.22 (m, 1H), 3.04 (dd, *J* = 17.6, 1.5 Hz, 1H).

**$^{13}$C-NMR** (75 MHz, DMSO-$d_6$): 174.7, 144.3, 143.8, 139.7, 138.0, 134.1, 132.0, 131.1, 129.4, 129.3, 128.5, 127.8, 125.5, 125.4, 124.5, 123.4, 118.5, 118.3, 113.8, 34.0, 33.7.

**Elemental analysis**: Anal. Calc. for $C_{25}H_{17}ONCl_2$ C, 71.78; H, 4.10; N, 3.35. Found C, 71.04; H, 4.20; N, 3.49.

### 4.10 General procedure for the synthesis of compounds 2.10a to 2.10d

A microwave vial containing a solution of the corresponding dihydroacridone in nitrobenzene was closed and placed in the cavity of an Anton-Paar focused microwave oven and heated up with a maximum power of 200 W and a temperature gradient programmed to reach up to 250 ºC in 5 minutes. The reaction mixture was stirred at this temperature for 90 minutes and then it was cooled down to room temperature. The solvent was removed under reduced pressure and the residue left, washed with chloroform, and crushed to obtain the desired dihydroacridone.

In the case of compound **2.10c**, the compound was purified by column chromatography with a mobile phase of 0-30% ethyl acetate.

**2.10a. 3-(4-methoxyphenyl)-1-phenylacridin-9(10H)-one**. Prepared from compound **2.09a** (50 mg, 0.13 mmol). Yellow solid (74% yield)

**Mp**: 296 ºC.

**IR** ($cm^{-1}$): 3264, 3107, 2929, 2106, 1889, 1617.

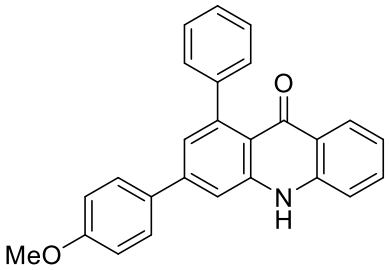


**$^{1}$H-NMR** (300 MHz, $CDCl_3$) 9.18 (s, 1H), 8.36 (dd, J = 8.2, 1.5 Hz, 1H), 7.69–7.59 (m, 3H), 7.55 (d, *J* = 1.8 Hz, 1H), 7.50–7.41 (m, 4H), 7.41–7.33 (m, 3H), 7.22 (ddd, *J* = 8.1, 7.0, 1.0 Hz, 1H), 6.99–6.92 (m, 2H), 3.83 (s, 3H).

**$^{13}$C-NMR** (75 MHz, CDCl3) 177.1, 158.8, 145.1, 144.9, 144.1, 140.2, 139.2, 134.8, 133.5, 129.7, 129.0, 128.6, 127.4, 127.1, 125.0, 122.1, 122.0, 117.0, 116.4, 114.2, 113.2, 55.2.

**Elemental analysis**: Anal. Calc. for $C_{26}H_{19}O_2N$ C, 82.74; H, 5.07; N, 3.71. Found C, 82.83; H, 5.18; N, 3.69.

**2.10b. 3-(4-chlorophenyl)-1-phenylacridin-9(10H)-one.** Prepared from compound **2.09b** (30 mg, 0.13 mmol). Yellow solid (74% yield).

**Mp**: 366 ºC.

**IR** ($cm^{-1}$): 3262, 3072, 2930, 2109, 1892, 1623.

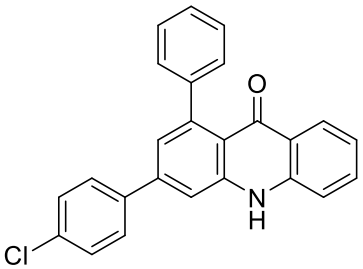


**$^{1}$H-NMR** (300 MHz, DMSO-$d_6$) 11.87 (s, 1H), 8.10 (dd, *J* = 8.1, 1.5 Hz, 1H), 7.86 (dd, *J* = 7.2, 1.8 Hz, 3H), 7.78 (ddd, *J* = 8.5, 6.9, 1.6 Hz, 1H), 7.61 (t, *J* = 7.2 Hz, 3H), 7.56–7.51 (m, 1H), 7.51–7.39 (m, 4H), 7.31–7.23 (m, 2H).

**$^{13}$C-NMR** (75 MHz, DMSO-$d_6$) 176.9, 144.0, 143.3, 143.1, 142.4, 140.9, 139.2, 133.8, 131.6, 130.9, 129.7, 129.2, 127.6, 127.5, 126.6, 123.5, 122.3, 121.6, 117.3, 116.9, 115.2.

**Elemental analysis**: Anal. Calc. for $C_{25}H_{16}ONCl$ C, 78.64; H, 4.22; N, 3.67. Found C, 77.90; H, 4.26; N, 3.67.

**2.10c. 3-(2,4-dimethoxyphenyl)-1-(4-methoxyphenyl)acridin-9(10H)-one.** Prepared from compound **2.09c** (30 mg, 0.07 mmol). Orange solid (77% yield).

**Mp**: 281 ºC.

**IR** ($cm^{-1}$): 3263, 3105, 2954, 2831, 2110, 1887, 1611.

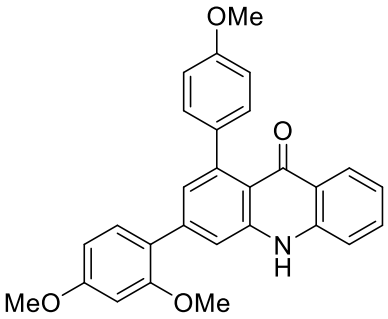


**$^1$H-NMR** (300 MHz, $CDCl_3$) 9.37 (s, 1H), 8.24 (dd, *J* = 8.2, 1.5 Hz, 1H), 7.57 (d, *J* = 1.7 Hz, 1H), 7.52 (ddd, *J* = 8.4, 6.9, 1.5 Hz, 1H), 7.36 (d, *J* = 8.3 Hz, 1H), 7.31–7.22 (m, 3H), 7.16–7.08 (m, 2H), 6.93–6.84 (m, 2H), 6.51–6.44 (m, 2H), 3.78 (s, 3H), 3.77 (s, 3H), 3.74 (s, 3H).

**$^{13}$C-NMR** (75 MHz, CDCl3) 176.8, 161.3, 158.8, 157.8, 142.9, 142.6,141.9, 140.0, 134.9, 133.3, 131.5, 129.9, 127.5, 127.0, 121.9, 121.8, 121.4, 116.7, 116.3, 113.2, 105.0, 99.1, 55.7, 55.5, 55.2.

**Elemental analysis**: Anal. Calc. for $C_{28}H_{23}O_4N$ C, 76.87; H, 5.30; N, 3.20. Found C, 76.15; H, 5.41; N, 3.15.

**2.10d. 1,3-bis(4-chlorophenyl)acridin-9(10H)-one.** Prepared from compound **2.09d** (30 mg, 0.07 mmol). Orange solid (43% yield).

**Mp** 298 ºC.

**IR** ($cm^{-1}$): 3264, 3114, 2922, 2105, 1619.

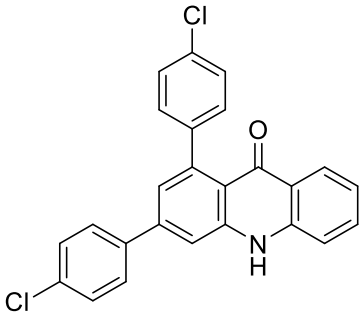


**$^1$H-NMR** (300 MHz, DMSO-$d_6$) 11.84 (s, 1H), 8.04 (dd, *J* = 8.2, 1.6 Hz, 1H), 7.87–7.81 (m, 2H), 7.78 (d, *J* = 1.8 Hz, 1H), 7.72 (ddd, *J* = 8.5, 6.9, 1.6 Hz, 1H), 7.63–7.58 (m, 2H), 7.54 (d, *J* = 8.3 Hz, 1H), 7.45–7.34 (m, 4H), 7.26–7.18 (m, 2H).

**$^{13}$C-NMR** (75 MHz, DMSO-$d_6$) 176.8, 143.3, 142.7, 142.4, 140.9, 137.9, 134.1, 133.9, 131.7, 131.6, 130.9, 130.1, 129.7, 129.4, 127.5, 126.7, 123.3, 122.4, 117.4, 117.0, 115.3.

**Elemental analysis**: Anal. Calc. for $C_{25}H_{15}ONCl_2$ C, 72.13; H, 3.63; N, 3.36. Found C, 71.23; H, 3.76; N, 3.53.

### 4.11 General procedure for the synthesis of compounds 2.11a to 2.11f

The corresponding anthranilic ester was dissolved in ethanol (30 ml) and a 6M solution of NaOH (10 ml) was added to the mixture. The reaction mixture was heated up to 60 ºC for 3 hours, and afterwards, it was quenched with concentrated HCl solution to PH 7. The mixture was extracted with ethyl acetate (30 ml) three times and all organic extracts combined, dried with $Na_2SO_4$, and concentrated in vacuo to yield the desired acids **2.11a**-**2.11f**.

**2.11a. 5'-amino-[1,1':3',1''-terphenyl]-4'-carboxylic acid.** Prepared from compound **2.03a** (500 mg, 1.6 mmol). Brown solid (99% yield).

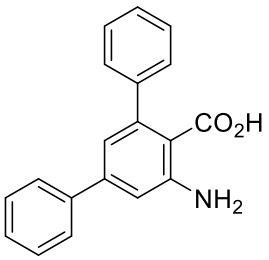


**$^1$H NMR** (250 MHz, MeOD) δ 7.59 (d, *J* = 6.9 Hz, 2H), 7.46 – 7.23 (m, 10H), 7.03 (d, *J* =1.7 Hz, 1H), 6.80 (d, *J* =1.7 Hz, 1H). (NMR data consistent with values described in literature). [47]

**2.11b. 5'-amino-4''-nitro-[1,1':3',1''-terphenyl]-4'-carboxylic acid.** Prepared from compound **2.03b** (700 mg, 1.9 mmol). Yellow solid (99% yield).

**Mp:** 180-181 ºC

**IR** (cm$^{-1}$): 3377, 3129, 3024, 2826, 1665, 1508.

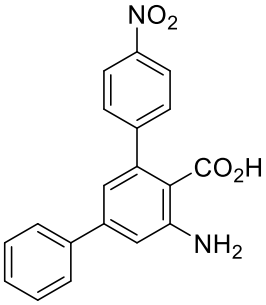


**$^1$H NMR** (300 MHz, MeOD) δ 8.26 – 8.19 (m, 2H), 7.75 – 7.67 (m, 2H), 7.64 – 7.57 (m, 2H), 7.46 – 7.27 (m, 3H), 7.07 (d, *J* = 1.7 Hz, 1H), 6.87 (d, *J* = 1.7 Hz, 1H).

**$^{13}$C NMR** (75 MHz, MeOD) δ 174.6, 150.3, 146.7, 146.3, 141.6, 140.6, 139.4, 129.2, 128.4, 127.2, 126.5, 122.7, 117.4, 114.2.

**Elemental analysis**: Anal. Calc. for $C_{19}H_{14}N_2O_4$ C, 68.26; H, 4.22; N, 8.38. Found: C, 68.30; H, 4.21; N, 8.39.

**2.11c. 3-amino-5-(5-chlorofuran-2-yl)-[1,1'-biphenyl]-4-carboxylic acid.** Prepared from compound **2.03d** (0.4 g, 0.1 mmol). Orange solid (99 % yield).

**Mp**: 119 º C.

**IR** (cm$^{-1}$): 3447, 3354, 2920, 2851, 2114, 1638.

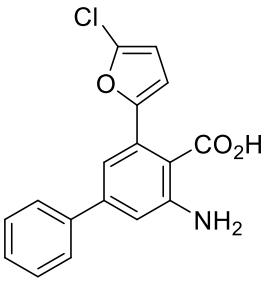


**$^1$H NMR** (250 MHz, MeOD) δ 7.69 – 7.58 (m, 2H), 7.48 – 7.32 (m, 4H), 7.13 (d, *J* = 1.6 Hz, 1H), 7.03 (d, *J* = 1.7 Hz, 1H), 6.76 (d, *J* = 3.4 Hz, 1H), 6.33 (d, *J* = 3.4 Hz, 1H).

**$^{13}$C NMR** (63 MHz, MeOD) δ 155.5, 148.2, 144.0, 142.3, 136.8, 130.5, 130.2, 129.1, 128.3, 116.6, 115.9, 111.0, 109.6.

**Elemental analysis**: Anal. Calc. for $C_{17}H_{12}ClNO_3$ C, 65.08; H, 3.68; N, 4.46. Found: C, 64.39; H, 3.98; N, 4.47.

**2.11d. 5'-(benzylamino)-4-nitro-[1,1':3',1''-terphenyl]-4'-carboxylic acid.** Prepared from compound **2.03e** (0.6 g, 0.1 mmol). Orange solid (97 % yield).

**Mp**: 113ºC.

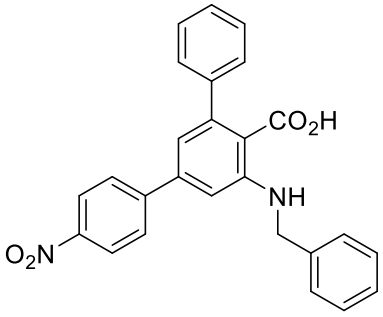


**IR** ($cm^{-1}$): 3366, 2920, 2849, 2112, 1718, 1647.

**$^1$H NMR** (250 MHz, MeOD) δ 8.04 (d, *J* = 8.8 Hz, 2H), 7.51 (d, *J* = 8.8 Hz, 2H), 7.37 – 7.03 (m, 15H), 6.70 (d, *J* = 1.6 Hz, 1H), 6.64 (d, *J* = 1.6 Hz, 1H), 4.28 (s, 2H).

**$^{13}$C NMR** (63 MHz, MeOD) δ 149.6, 148.8, 148.1, 144.3, 143.2, 141.4, 140.7, 130.1, 130.0, 129.5, 129.2, 128.9, 128.5, 128.3, 125.3, 119.0, 110.3, 55.3.

**Elemental analysis**: Anal. Calc. for $C_{26}H_{20}N_2O_4$ C, 73.57; H, 4.75; N, 6.60. Found: C, 72.64; H, 4.94; N, 6.28.

**2.11e. 5'-amino-4-methoxy-[1,1':3',1''-terphenyl]-4'-carboxylic acid.** Prepared from compound **2.03f** (0.74 g, 2.1 mmol). Yellow solid (99% yield).

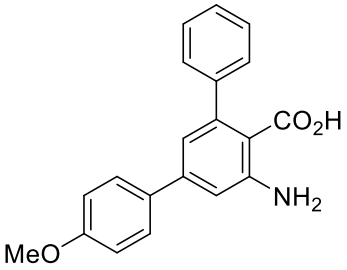


**Mp**: 161-162 ºC

**IR** ($cm^{-1}$): 3483, 3371, 2959, 1642, 1578.

**$^1$H NMR** (300 MHz, MeOD) δ 7.60 – 7.52 (m, 2H), 7.39 – 7.28 (m, 5H), 7.02 – 6.95 (m, 3H), 6.78 (d, *J* = 1.7 Hz, 1H), 3.82 (s, 3H).

**$^{13}$C NMR** (75 MHz, MeOD) δ 159.8, 148.8, 144.2, 143.4, 143.2, 132.5, 127.9, 127.7, 127.5, 126.4, 117.7, 113.8, 112.8, 54.4.

**Elemental analysis**: Anal. Calc. for $C_{20}H_{17}NO_3$ C, 75.22; H, 5.37; N, 4.39. Found: C, 74.59; H, 5.32; N, 4.93.

**2.11f. 5'-amino-4-methyl-[1,1':3',1''-terphenyl]-4'-carboxylic acid.** Prepared from compound **2.03c** (0.38 g, 2.1 mmol). Yellow solid (99% yield).

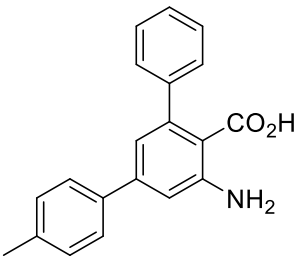


**$^1$H NMR** (250 MHz, DMSO-d6) δ 7.64 – 7.19 (m, 8H), 7.03 (d, J = 2.0 Hz, 1H), 6.70 (d, J = 2.0 Hz, 1H), 2.34 (s, 3H). (NMR data consistent with values described in literature). [47]

**2.11g. (R)-5'-((1-phenylethyl)amino)-[1,1':3',1''-terphenyl]-4'-carboxylic acid.** Prepared from compound **2.03g** (0.2 g, 0.47 mmol). Pale brown solid (88% yield).

**Mp**: 155-156 ºC.

**Specific optical rotation**, $[\alpha]^{25}_D$ = -165.6 º mL $dm^{-1}$ $g^{-1}$.

**IR** ($cm^{-1}$): 3389.11, 2857.47, 1888.11, 1650.40, 1560.06

**$^1$H NMR** (250 MHz, $CDCl_3$): δ 7.37-7.15 (m, 15H) 6.69 (d, *J* = 1.7 Hz, 1H), 6.61 (d, *J* = 1.7 Hz, 1H), 4.57 (q, *J* = 6.7 Hz, 1H), 1.52 (d, *J* = 6.7Hz, 3H).

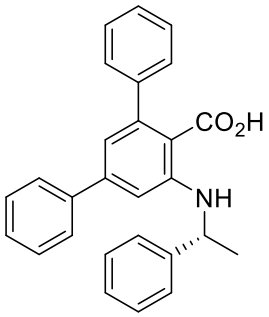


**$^{13}$C NMR** ($CDCl_3$, 63 MHz) δ: 173.7, 150.0, 146.1, 145.5, 145.2, 143.7, 140.8, 129.3, 129.1, 128.6, 128.5, 128.4, 128.4, 127.5, 127.5, 126.3, 118.6, 111.0, 109.9, 53.8, 25.6.

**Elemental analysis** Anal. Calc. for $C_{27}H_{22}NO_2$ C, 82.42; H, 5.89; N, 3.56; Found C, 82.37; H, 6.09; N, 3.41.

### 4.12 General procedure for the synthesis of compounds 2.12a to 2.12f

A microwave vial with a solution of the corresponding anthranilic acid in DMF (2 ml) and an aqueous 6M solution of NaOH was placed in the cavity of a CEM microwave focused oven at a maximum power of 200 W and a temperature gradient programmed to reach up to 180 ºC in 5 minutes. The reaction mixture was stirred at this temperature for 90 minutes and then it was cooled down to room temperature. The solution was diluted in DCM (20 ml) and washed 6 times with a saturated solution of LiCl. The organic phase was dried with $Na_2SO_4$ and concentrated in vacuo. The residue was washed with diethyl ether to yield the m-terphenylamines **2.12a**-**2.12f**. Compounds **2.12b** and **2.12d** were in part reduced to their amino derivatives in the microwave oven and were purified by column chromatography.

**2.12a. [1,1':3',1''-terphenyl]-5'-amine.** Prepared from compound 8a (200 mg, 0.69 mmol). Brown solid (68% yield).

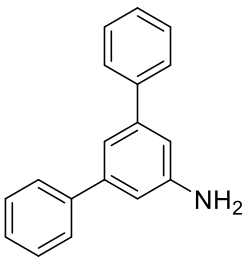


**$^1$H NMR** (250 MHz, DMSO) δ 7.64 (d, *J* = 7.1 Hz, 4H), 7.45 (t, *J* = 7.3 Hz, 4H), 7.35 (t, *J* = 7.2 Hz, 2H), 7.02 (s, 1H), 6.84 (d, *J* = 1.5 Hz, 2H), 5.32 (br s, 2H). (NMR data consistent with values described in literature). [47]

**2.12b. [1,1':3',1''-terphenyl]-4,5'-diamine.** Prepared from compound 8b (175 mg, 0.52 mmol). Dark brown solid (37% yield).

**Mp**: 78-79 ºC

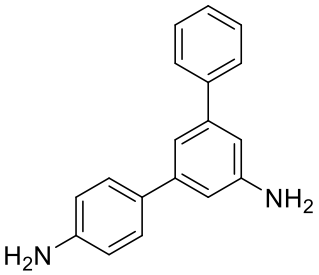


**IR** ($cm^{-1}$): 3332, 3209, 2919, 1850, 1591

**$^1$H NMR** (300 MHz, MeOD) δ 7.62 – 7.57 (m, 2H), 7.45 – 7.36 (m, 5H), 7.11 (d, *J* = 1.6 Hz, 1H), 6.95 – 6.88 (m, 2H), 6.84 – 6.77 (m, 2H).

**$^{13}$C NMR** (75 MHz, MeOD) δ 147.4, 146.4, 142.4, 141.7, 131.5, 128.3, 126.8, 126.6, 123.6 115.6, 115.4, 112.5, 112.2.

**Elemental analysis**: Anal. Calc. for $C_{16}H_{12}ClNO$ C, 71.25; H, 4.48; N, 5.19. Found: C, 71.08; H, 4,59; N, 5.27.

**2.12c. 5-(5-chlorofuran-2-yl)-[1,1'-biphenyl]-3-amine.** Prepared from compound 8c (175 mg, 0.52 mmol). yellow solid (94% yield).

**Mp**: 120 ºC

**IR** ($cm^{-1}$): 3054, 2920, 2851, 1683.

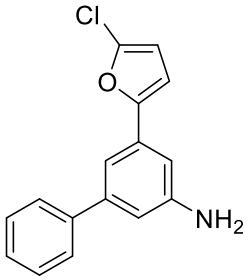


**$^1$H NMR** (250 MHz, MeOD) δ 7.67 – 7.58 (m, 2H), 7.50 – 7.31 (m, 3H), 7.21 (t, *J* = 1.5 Hz, 1H), 7.02 (t, *J* = 1.8 Hz, 1H), 6.93 (t, *J* = 1.9 Hz, 1H), 6.80 (d, *J* = 3.4 Hz, 1H), 6.37 (d, *J* = 3.4 Hz, 1H).

**$^{13}$C NMR** (63 MHz, MeOD) δ 155.9, 150.3, 144.5, 142.9, 136.9, 132.8, 130.2, 128.9, 128.4, 115.0, 113.4, 110.5, 109.9, 108.6.

**Elemental analysis**: Anal. Calc. for $C_{18}H_{16}N_2$ C, 83.04; H, 6.19; N, 10.76. Found: C, 82.56; H, 5.87; N, 9.67.

**2.12d. N-benzyl-4-nitro-[1,1':3',1''-terphenyl]-5'-amine.** Prepared from compound 8d. Orange oil (29% yield).

**IR** ($cm^{-1}$): 3405, 3026, 2922, 2850, 2447, 2114, 1558.

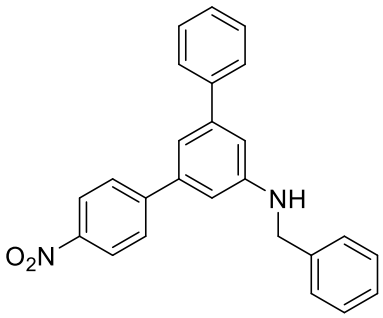


**$^1$H NMR** (250 MHz, $CDCl_3$) δ 8.21 (d, *J* = 8.8 Hz, 2H), 7.66 (d, *J* = 8.8 Hz, 2H), 7.52 (dd, *J* = 8.2, 1.5 Hz, 2H), 7.43 – 7.17 (m, 9H), 7.08 (d, *J* = 1.6 Hz, 1H), 6.84 (d, *J* = 1.9 Hz, 1H), 6.76 (t, *J* = 1.9 Hz, 1H), 4.39 (s, 2H).

**$^{13}$C NMR** (63 MHz, $CDCl_3$) δ 149.4, 148.6, 147.4, 143.8, 141.5, 140.8, 139.3, 129.2, 128.3, 128.1, 128.0, 127.9, 127.7, 124.5, 116.5, 112.6, 110.9, 48.8.

**Elemental analysis**: Anal. Calc. for $C_{25}H_{20}N_2O_2$ C, 78.93; H, 5.30; N, 7.36. Found: C, 78.59; H, 5.57; N, 7.01.

**2.12e. 4-methoxy-[1,1':3',1''-terphenyl]-5'-amine.** Prepared from compound 8e (180 mg, 0.52 mmol). Pale brown solid (41% yield).

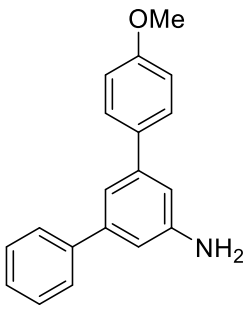


**$^1$H NMR** (250 MHz, DMSO) δ 7.70 – 7.36 (m, 7H), 7.10 – 6.94 (m, 3H), 6.91 – 6.74 (m, 2H), 5.27 (s, 2H), 3.90 – 3.71 (m, 3H). (NMR data consistent with values described in literature).[47]

**12f. 4-methyl-[1,1':3',1''-terphenyl]-5'-amine.** Prepared from compound 8f (0.170 g, 0.56 mmol). Pale brown solid (50% yield).

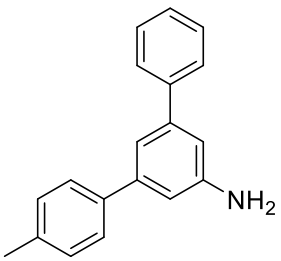


**$^1$H NMR** (250 MHz, $CDCl_3$) δ 7.62 (d, *J* = 6.0 Hz, 2H), 7.55 – 7.37 (m, 6H), 7.28 – 7.18 (m, 4H), 6.93 – 6.87 (m, 2H), 2.41 (s, 3H). (NMR data consistent with values described in literature).[47]

**2.12g. N5'-benzyl-[1,1':3',1''-terphenyl]-4,5'-diamine**. Prepared from compound 8d. Brown oil (16% yield).

**IR** ($cm^{-1}$): 3365, 3200, 3026, 2921, 2850, 1888.

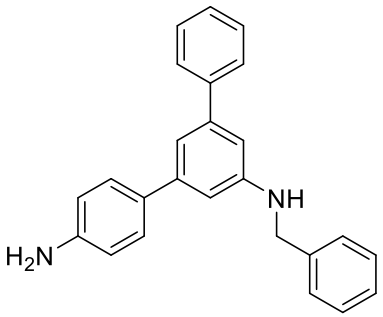


**$^1$H NMR** (250 MHz, $CDCl_3$) δ 7.69 – 7.61 (m, 2H), 7.53 – 7.30 (m, 11H), 7.18 (t, *J* = 1.6 Hz, 1H), 6.85 (dt, *J* = 5.4, 2.1 Hz, 2H), 6.83 – 6.76 (m, 2H), 4.49 (s, 2H).

**$^{13}$C NMR** (63 MHz, $CDCl_3$) δ 149.2, 146.3, 143.2, 143.2, 142.3, 139.8, 132.4, 129.1, 129.1, 128.6, 128.1, 127.8, 127.7, 127.6, 116.0, 115.7, 110.5, 110.3, 48.9.

**Elemental analysis**: Anal. Calc. for $C_{25}H_{22}N_2$ C, 85.68; H, 6.33; N, 7.99. Found: C, 84.78; H, 6.65; N, 8.89.

### 4.13. Procedure for the synthesis of compound 2.13

Compound **2.12e** (150 mg, 0.54 mmol) was dissolved in dry DCM (20 ml) in an argon atmosphere and 1M solution of $BBr_3$ in DCM (5 ml) was added to the solution at a temperature of -78 ºC. The reaction mixture was warmed up to room temperature and left stirring for 3 hours. Afterwards, the mixture was neutralized with a saturated solution of $K_2CO_3$ to PH 7 and the two layers separated. The organic phase was washed with water (10 ml) twice and brine (10 ml) once, dried with $Na_2SO_4$ and concentrated in vacuo to yield the desired phenol as an off-white solid (99% yield).

**Mp**: 193 ºC.

**IR** ($cm^{-1}$): 3307, 3191, 3028, 2921, 2342, 2893, 1514.

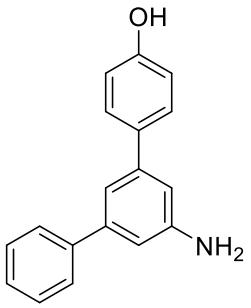


**$^1$H NMR** (250 MHz, MeOD) δ 7.54 – 7.46 (m, 2H), 7.41 – 7.15 (m, 5H), 7.03 (t, *J* = 1.6 Hz, 1H), 6.83 (m, 2H), 6.79 – 6.71 (m, 2H).

**$^{13}$C NMR** (63 MHz, MeOD) δ 158.61, 149.01, 144.35, 144.32, 143.38, 134.51, 130.14, 129.52, 128.67, 128.46, 117.61, 116.92, 114.61, 114.32.

**Elemental analysis**: Anal. Calc. for $C_{18}H_{15}NO$ C, 82.73; H, 5.79; N, 5.36. Found: C, 82.33; H, 5.34; N, 5.25.

### 4.14 General procedure for the synthesis of compounds 2.14a and 2.14b.

The corresponding 2-aminobenzonitrile (1 eq) was dissolved in cyclohexanone (10 ml) and zinc chloride (0.1 eq) was added to the mixture, which was stirred to 120 ºC for 5 hours. The mixture was allowed to cool down at room temperature and the precipitate formed was filtered and washed with hexane to yield the corresponding tetrahydroacridine.

**2.14a. 1,2,3,4-tetrahydroacridin-9-amine.** Prepared from 2-aminobenzonitrile (1.5 g, 8.5 mmol). Off white solid (99% yield).

**$^1$H NMR** (250 MHz, DMSO-d6) δ 8.14 (d, *J* = 8.5 Hz, 1H), 7.62 (d, *J* = 8.6 Hz, 1H), 7.52 – 7.41 (m, 1H), 7.33 – 7.19 (m, 1H), 6.42 (s, 2H), 2.79 (m, 2H), 1.88 – 1.70 (m, 4H). (NMR data consistent with values described in literature).[68]

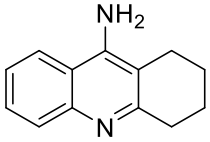


**2.14b. 6-chloro-1,2,3,4-tetrahydroacridin-9-amine.** Prepared from 4-chloro-2-aminobenzonitrile (2g, 13.1 mmol). Off-white solid (99% yield).

**$^1$H NMR** (250 MHz, DMSO-d6) δ 8.65 – 8.30 (m, 3H), 7.93 (s, 1H), 7.54 (d, *J* = 9.0 Hz, 1H), 2.94 (s, 2H), 1.81 (s, 4H). (NMR data consistent with values described in literature).[68]

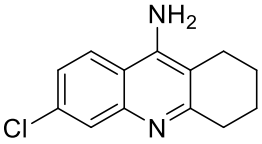


**4.15 General procedure for the synthesis of compounds 2.15a to 2.15c.**

The corresponding tetrahydroacridine (1 equivalent) and $K_2CO_3$ (2 equivalents) were suspended in acetonitrile (20 ml) and the required dibromoalkane was added to the mixture, which was allowed to stir at room temperature for 24 hours. The mixture was concentrated in vacuo and redissolved in ethyl acetate (20 ml) and washed with water twice (10 ml). The organic phase was dried with $Na_2SO_4$ and concentrated in vacuo, to yield a residue purified by column chromatography (0-10% methanol in DCM).

**2.15a. N-(7-bromoheptyl)-1,2,3,4-tetrahydroacridin-9-amine**. Prepared from 1,2,3,4-tetrahydroacridin-9-amine and 1,7-dibromoheptane. Brown oil (35% yield).

**IR** ($cm^{-1}$): 3228, 2921, 2851, 2099, 1521.

**$^1$H NMR** (250 MHz, $CDCl_3$) δ 7.86 (ddd, *J* = 10.0, 8.5, 1.3 Hz, 2H), 7.47 (ddd, *J* = 8.4, 6.8, 1.4 Hz, 1H), 7.27 (ddd, *J* = 8.3, 6.8, 1.3 Hz, 1H), 3.41 (d, *J* = 4.9 Hz, 2H), 3.34 – 3.25 (m, 2H), 2.99 (t, *J* = 3.2 Hz, 2H), 2.62 (d, *J* = 5.0 Hz, 2H), 1.84 (p, *J* = 3.4 Hz, 4H), 1.81 – 1.70 (m, 2H), 1.57 (d, *J* = 7.2 Hz, 2H), 1.42 – 1.15 (m, 14H). (NMR data consistent with values described in literature)[69]

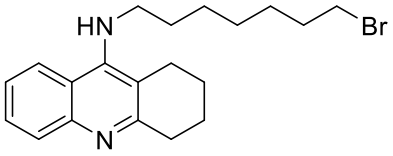


**$^{13}$C NMR** (63 MHz, $CDCl_3$) δ 158.7, 151.2, 147.7, 129.0, 128.8, 124.0, 123.3, 120.5, 116.2, 53.91 49.9, 34.4, 33.0, 32.1, 30.1, 28.9, 28.4, 28.4, 27.2, 25.2, 23.5, 23.2.

**2.15b. N-(5-bromopentyl)-1,2,3,4-tetrahydroacridin-9-amine**. Prepared from 1,2,3,4-tetrahydroacridin-9-amine and 1,5-dibromopentane. Brown oil (15% yield).

**IR** ($cm^{-1}$): 3233, 2851, 2106, 1721, 1567.

**$^1$H NMR** (250 MHz, $CDCl_3$) δ 7.98 (m, 2H), 7.59 (ddd, *J* = 8.4, 6.8, 1.4 Hz, 1H), 7.38 (ddd, *J* = 8.3, 6.8, 1.4 Hz, 1H), 4.17 – 4.01 (m, 1H), 3.55 (q, *J* = 7.0, 5.7 Hz, 2H), 3.44 (t, *J* = 6.6 Hz, 2H), 3.10 (td, *J* = 4.4, 2.2 Hz, 2H), 2.79 – 2.68 (m, 2H), 1.93 (dt, *J* = 10.6, 5.4 Hz, 6H), 1.79 – 1.66 (m, 2H), 1.66 – 1.51 (m, 2H). (NMR data consistent with values described in literature)[69]

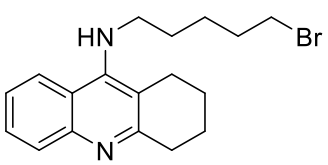

**$^{13}$C NMR** (63 MHz, $CDCl_3$) δ 158.5, 151.3, 147.3, 129.0, 128.7, 124.2, 123.3, 120.4, 116.3, 49.6, 34.1, 34.0, 32.7, 31.3, 25.9, 25.2, 23.4, 23.1.

**2.15c. N-(7-bromoheptyl)-6-chloro-1,2,3,4-tetrahydroacridin-9-amine.** Prepared from 6-chloro-1,2,3,4-tetrahydroacridin-9-amine and 1,7-dibromoheptane. Brown oil (31% yield).

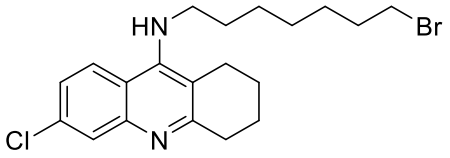


**$^{1}$H NMR** (250 MHz, $CDCl_3$) δ 7.92 (m, 2H), 7.30 (dd, *J* = 9.1, 2.2 Hz, 2H), 4.01 (t, *J* = 7.7 Hz, 1H), 3.67 (t, *J* = 6.5 Hz, 2H), 3.43 (td, *J* = 6.8, 2.0 Hz, 4H), 3.05 (d, *J* = 5.2 Hz, 2H), 2.68 (dd, *J* = 5.9, 2.7 Hz, 2H), 1.98 – 1.80 (m, 9H), 1.69 (t, *J* = 6.8 Hz, 2H), 1.65 – 1.56 (m, 2H), 1.50 – 1.32 (m, 13H). (NMR data consistent with values described in literature)

**$^{13}$C NMR** (63 MHz, $CDCl_3$) δ 159.8, 151.4, 134.5, 127.8, 125.0, 124.7, 118.7, 116.1, 63.3, 47.0, 34.3, 33.1, 33.0, 32.1, 29.0, 28.5, 27.1, 26.0, 25.0, 23.3. (NMR data consistent with values described in literature)[70]

**4.16 General procedure for the synthesis of compounds 2.16a to 2.16c**

5'-amino-[1,1':3',1''-terphenyl]-4-ol (1 equivalent) was dissolved in anhydrous acetone (5 ml) and $K_2CO_3$ was suspended in the solution which was left stirring for 30 minutes at room temperature. Subsequently, the corresponding N-alkylated-tacrine derivative (1 equivalent) was added to the mixture which was furtherly stirred for 24 hours. The mixture was concentrated in vacuo and purified by column chromatography (0-10% methanol in DCM) to yield the hybrid m-terphenylamine-tacrine hybrid compounds.

**2.16a. N-(7-((5'-amino-[1,1':3',1''-terphenyl]-4-yl)oxy)heptyl)-1,2,3,4-tetrahydroacridin-9-amine.** Prepared from N-(7-bromoheptyl)-1,2,3,4-tetrahydroacridin-9-amine (80 mg, 0.21 mmol). Brown oil (30% yield).

**IR** ($cm^{-1}$): 3337, 3143, 3047, 2888, 1810, 1684, 1598.

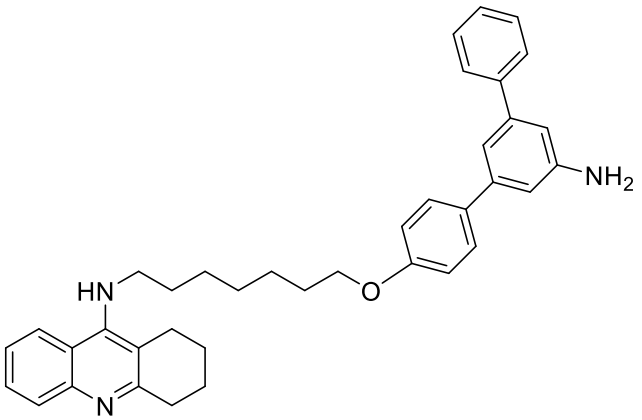


**$^{1}$H NMR** (250 MHz, $CDCl_3$) δ 8.16 (d, *J* = 8.6 Hz, 1H), 7.99 (d, *J* = 8.6 Hz, 1H), 7.60 – 7.51 (m, 3H), 7.51 – 7.24 (m, 7H), 7.09 (t, *J* = 1.6 Hz, 1H), 6.91 – 6.83 (m, 2H), 6.79 (d, *J* = 1.7 Hz, 2H), 3.93 (t, *J* = 6.3 Hz, 2H), 3.69 – 3.57 (m, 2H), 3.12 (s, 2H), 2.56 (m, 2H), 1.85 (d, *J* = 4.5 Hz, 4H), 1.71 (m, 5H), 1.39 (m, 8H).

**$^{13}$C NMR** (63 MHz, $CDCl_3$) δ 164.7, 159.0, 153.3, 147.5, 146.9, 143.3, 142.9, 141.9, 135.6, 134.2, 129.1, 128.6, 127.8, 127.6, 126.6, 124.8, 123.9, 121.6, 117.0, 115.0, 112.9, 112.9, 108.6, 105.4, 101.8, 68.2, 49.6, 31.9, 31.4, 29.6, 29.4, 27.2, 26.4, 24.5, 22.9, 22.2.

**Elemental analysis**: Anal. Calc. for $C_{38}H_{41}N_3O$ C, 82.12; H, 7.44; N, 7.56. Found: C, 84.10; H, 7.80; N, 7.42.

**2.16b. N-(5-((5'-amino-[1,1':3',1''-terphenyl]-4-yl)oxy)pentyl)-1,2,3,4-tetrahydroacridin-9-amine.** Prepared from N-(5-bromopentyl)-1,2,3,4-tetrahydroacridin-9-amine. Brown oil (23% yield).

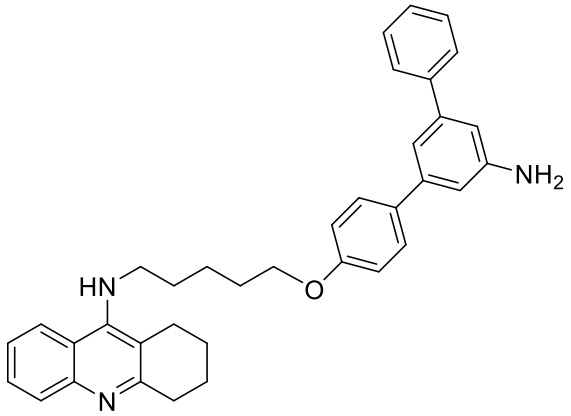


**IR** ($cm^{-1}$): 3206, 2920, 2851, 2106, 1573.

**$^1$H NMR** (500 MHz, $CDCl_3$) δ 8.28 (s, 1H), 8.08 (d, *J* = 8.6 Hz, 1H), 7.69 – 7.61 (m, 4H), 7.56 (d, *J* = 8.6 Hz, 2H), 7.49 – 7.35 (m, 6H), 7.18 (t, *J* = 1.5 Hz, 1H), 6.95 (d, *J* = 8.7 Hz, 2H), 6.89 (d, *J* = 1.6 Hz, 2H), 4.06 (t, *J* = 6.0 Hz, 2H), 3.77 (s, 2H), 3.23 (s, 2H), 2.67 (s, 2H), 1.91-1.81 (m, 10H).

**$^{13}$C NMR** (126 MHz, $CDCl_3$) δ 161.5, 158.9, 151.7, 147.5, 143.4, 142.8, 142.8, 141.9, 134.4, 129.1, 128.6, 127.8, 127.6, 117.0, 115.0, 112.9, 67.8, 49.5, 31.6, 30.1, 29.3, 26.0, 24.5, 23.9, 14.5.

**Elemental analysis**: Anal. Calc. for $C_{38}H_{41}N_3O$ C, 82.12; H, 7.44; N, 7.56. Found: C, 84.10; H, 7.70; N, 7.42.

**2.16c. N-(7-((5'-amino-[1,1':3',1''-terphenyl]-4-yl)oxy)heptyl)-6-chloro-1,2,3,4-tetrahydroacridin-9-amine.** Prepared from N-(7-bromoheptyl)-6-chloro-1,2,3,4-tetrahydroacridin-9-amine. Brown solid (32% yield).

**Mp**: 105ºC

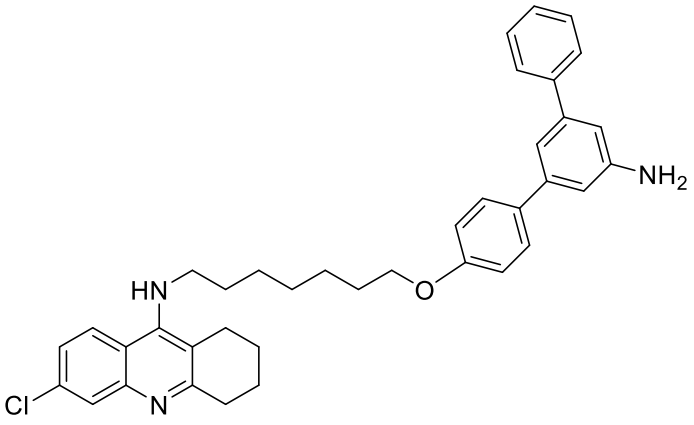


**IR** ($cm^{-1}$): 3330, 2921, 2852, 2104, 1669.

**$^1$H NMR** (500 MHz, MeOD) δ 8.32 (d, *J* = 9.3 Hz, 1H), 7.74 (d, *J* = 2.2 Hz, 1H), 7.63 (d, *J* = 7.7 Hz, 2H), 7.55 (d, *J* = 8.6 Hz, 2H), 7.51 (dd, *J* = 9.2, 2.2 Hz, 1H), 7.43 (t, *J* = 7.7 Hz, 2H), 7.34 (d, *J* = 7.3 Hz, 1H), 7.10 (d, *J* = 1.7 Hz, 1H), 6.98 – 6.92 (m, 3H), 4.02 (t, *J* = 6.3 Hz, 2H), 3.86 (t, *J* = 7.4 Hz, 2H), 2.98 (d, *J* = 6.4 Hz, 2H), 2.68 (d, *J* = 5.2 Hz, 2H), 2.00 – 1.92 (m, 5H), 1.86 – 1.77 (m, 4H), 1.53 (d, *J* = 7.0 Hz, 2H), 1.51 – 1.42 (m, 6H).

**$^{13}$C NMR** (126 MHz, MeOD) δ 160.5, 157.2, 156.3, 150.0, 144.3, 143.9, 143.4, 140.1, 138.7, 135.6, 130.1, 129.4, 128.6, 128.4, 126.8, 117.0, 116.9, 116.2, 114.6, 114.2, 114.1, 69.3, 35.0, 31.8, 31.1, 30.5, 30.2, 28.0, 27.3, 25.4, 24.1, 23.5, 22.6.

**HRMS**: m/z calc. for $C_{38}H_{40}ClN_3O$ 590.2, found 590.3.

## 5.0 References


(1) Dobson, C. M. Insight Chemical Space and Biology. *Nature* **2004**, *432* (December), 824–828.

(2) Peralta, D. Diversity in Medicinal Chemistry. *ChemMedChem* **2018**, *13* (1), 3–6. https://doi.org/10.1002/cmdc.201700803.

(3) Heravi, M.; Zadsirjan, V. *Synthesis of Heterocycles via MCRs, Using a Name Reaction in Combination with Another Reaction*; 2020. https://doi.org/10.1016/b978-0-12-818584-1.00003-3.

(4) Slobbe, P.; Ruijter, E.; Orru, R. V. A. Recent Applications of Multicomponent Reactions in Medicinal Chemistry. *Medchemcomm* **2012**, *3* (10), 1189–1218. https://doi.org/10.1039/c2md20089a.

(5) Insuasty, D.; Castillo, J.; Becerra, D.; Rojas, H.; Abonia, R. Synthesis of Biologically Active Molecules through Multicomponent Reactions. *Molecules* **2020**, *25* (3), 1–71. https://doi.org/10.3390/molecules25030505.

(6) Younus, H. A.; Al-Rashida, M.; Hameed, A.; Uroos, M.; Salar, U.; Rana, S.; Khan, K. M. Multicomponent Reactions (MCR) in Medicinal Chemistry: A Patent Review (2010-2020). *Expert Opin. Ther. Pat.* **2021**, *31* (3), 267–289. https://doi.org/10.1080/13543776.2021.1858797.

(7) El Kaim, L.; Gizolme, M.; Grimaud, L.; Oble, J. Direct Access to Heterocyclic Scaffolds by New Multicomponent Ugi-Smiles Couplings. *Org. Lett.* **2006**, *8* (18), 4019–4021. https://doi.org/10.1021/ol061605o.

(8) Liautard, V.; Landais, Y. Free-Radical Multicomponent Processes. *Multicomponent React. Org. Synth.* **2015**, *9783527332*, 401–438. https://doi.org/10.1002/9783527678174.ch14.

(9) Balme, G.; Bouyssi, D.; Monteiro, N. *Metal-Catalyzed Multicomponent Reactions*; 2005. https://doi.org/10.1002/3527605118.ch8.

(10) Garbarino, S.; Ravelli, D.; Protti, S.; Basso, A. Photoinduced Multicomponent Reactions. *Angew. Chemie - Int. Ed.* **2016**, *55* (50), 15476–15484. https://doi.org/10.1002/anie.201605288.

(11) Lane, R. K.; Hilsabeck, T.; Rea, S. L. The Role of Mitochondrial Dysfunction in Age-Related Diseases. *Biochim. Biophys. Acta - Bioenerg.* **2015**, *1847* (11), 1387–1400. https://doi.org/10.1016/j.bbabio.2015.05.021.

(12) Yousif, L. F.; Stewart, K. M.; Kelley, S. O. Targeting Mitochondria with Organelle-Specific Compounds: Strategies and Applications. *ChemBioChem* **2009**, *10* (12), 1939–1950. https://doi.org/10.1002/cbic.200900185.

(13) Zinovkin, R. A.; Zamyatnin, A. A. Mitochondria-Targeted Drugs. *Curr. Mol. Pharmacol.* **2018**, *12* (3), 202–214. https://doi.org/10.2174/1874467212666181127151059.

(14) Smith, R. A. J.; Hartley, R. C.; Murphy, M. P. Mitochondria-Targeted Small Molecule Therapeutics and Probes. *Antioxidants Redox Signal.* **2011**, *15* (12), 3021–3038. https://doi.org/10.1089/ars.2011.3969.

(15) Korshunova, G. A.; Shishkina, A. V.; Skulachev, M. V. Design, Synthesis, and Some Aspects of the Biological Activity of Mitochondria-Targeted Antioxidants. *Biochem.* **2017**, *82* (7), 760–777. https://doi.org/10.1134/S0006297917070021.

(16) Zielonka, J.; Joseph, J.; Sikora, A.; Hardy, M.; Ouari, O.; Vasquez-Vivar, J.; Cheng, G.; Lopez, M.; Kalyanaraman, B. Mitochondria-Targeted Triphenylphosphonium-Based Compounds: Syntheses, Mechanisms of Action, and Therapeutic and Diagnostic Applications. *Chem. Rev.* **2017**, *117* (15), 10043–10120. https://doi.org/10.1021/acs.chemrev.7b00042.

(17) Chen, J.; Jiang, X.; Zhang, C.; MacKenzie, K. R.; Stossi, F.; Palzkill, T.; Wang, M. C.; Wang, J. Reversible Reaction-Based Fluorescent Probe for Real-Time Imaging of Glutathione Dynamics in Mitochondria. *ACS Sensors* **2017**, *2* (9), 1257–1261. https://doi.org/10.1021/acssensors.7b00425.

(18) Niu, W.; Guo, L.; Li, Y.; Shuang, S.; Dong, C.; Wong, M. S. Highly Selective Two-Photon Fluorescent Probe for Ratiometric Sensing and Imaging Cysteine in Mitochondria. *Anal. Chem.* **2016**, *88* (3), 1908–1914. https://doi.org/10.1021/acs.analchem.5b04329.

(19) Cheng, D.; Pan, Y.; Wang, L.; Zeng, Z.; Yuan, L.; Zhang, X.; Chang, Y.-T. Selective Visualization of the Endogenous Peroxynitrite in an Inflamed Mouse Model by a Mitochondria-Targetable Two-Photon Ratiometric Fluorescent Probe. *J. Am. Chem. Soc.* **2017**, *139* (1), 285–292. https://doi.org/10.1021/jacs.6b10508.

(20) Han, X.; Wang, R.; Song, X.; Yu, F.; Lv, C.; Chen, L. A Mitochondrial-Targeting near-Infrared Fluorescent Probe for Bioimaging and Evaluating Endogenous Superoxide Anion Changes during Ischemia/Reperfusion Injury. *Biomaterials* **2018**, *156*, 134–146. https://doi.org/10.1016/j.biomaterials.2017.11.039.

(21) Escribano-Lopez, I.; Bañuls, C.; Diaz-Morales, N.; Iannantuoni, F.; Rovira-Llopis, S.; Gomis, R.; Rocha, M.; Hernandez-Mijares, A.; Murphy, M. P.; Victor, V. M. The Mitochondria-Targeted Antioxidant MitoQ Modulates Mitochondrial Function and Endoplasmic Reticulum Stress in Pancreatic β Cells Exposed to Hyperglycaemia. *Cell. Physiol. Biochem.* **2019**, *52* (2), 186–197. https://doi.org/10.33594/000000013.

(22) Smith, R. A. J.; Porteous, C. M.; Coulter, C. V.; Murphy, M. P. Selective Targeting of an Antioxidant to Mitochondria. *Eur. J. Biochem.* **1999**, *263* (3), 709–716. https://doi.org/10.1046/j.1432-1327.1999.00543.x.

(23) Brown, S. E.; Ross, M. F.; Sanjuan-Pla, A.; Manas, A. R. B.; Smith, R. A. J.; Murphy, M. P. Targeting Lipoic Acid to Mitochondria: Synthesis and Characterization of a Triphenylphosphonium-Conjugated α-Lipoyl Derivative. *Free Radic. Biol. Med.* **2007**, *42* (12), 1766–1780. https://doi.org/10.1016/j.freeradbiomed.2007.02.033.

(24) Filipovska, A.; Kelso, G. F.; Brown, S. E.; Beer, S. M.; Smith, R. A. J.; Murphy, M. P. Synthesis and Characterization of a Triphenylphosphonium-Conjugated Peroxidase Mimetic: Insights into the Interaction of Ebselen with Mitochondria. *J. Biol. Chem.* **2005**, *280* (25), 24113–24126. https://doi.org/10.1074/jbc.M501148200.

(25) Xu, Y.; Kalyanaraman, B. Synthesis and ESR Studies of a Novel Cyclic Nitrone Spin Trap Attached to a Phosphonium Group-a Suitable Trap for Mitochondria-Generated ROS? *Free Radic. Res.* **2007**, *41* (1), 1–7. https://doi.org/10.1080/10715760600911147.

(26) Ghalamfarsa, G.; Hojjat-Farsangi, M.; Mohammadnia-Afrouzi, M.; Anvari, E.; Farhadi, S.; Yousefi, M.; Jadidi-Niaragh, F. Application of Nanomedicine for Crossing the Blood–Brain Barrier: Theranostic Opportunities in Multiple Sclerosis. *J. Immunotoxicol.* **2016**, *13* (5), 603–619. https://doi.org/10.3109/1547691X.2016.1159264.

(27) Kojima, R.; Aubel, D.; Fussenegger, M. Novel Theranostic Agents for Next-Generation Personalized Medicine: Small Molecules, Nanoparticles, and Engineered Mammalian

Cells. *Curr. Opin. Chem. Biol.* **2015**, *28*, 29–38. https://doi.org/10.1016/j.cbpa.2015.05.021.

(28) Silva, F. R. O.; Lima, N. B.; Bellini, M. H.; Teixeira, L. F. S.; Du, E. Y.; Jamshidi, N.; Gooding, J.; Martin, A. D.; Macmillan, A.; Marquis, C. P.; Thordarson, P. Lanthanide-Based β-Tricalcium Phosphate Upconversion Nanoparticles as an Effective Theranostic Nonviral Vectors for Image-Guided Gene Therapy. *Nanotheranostics* **2022**, *6* (3), 306–321. https://doi.org/10.7150/ntno.68789.

(29) Yan, K. C.; Sedgwick, A. C.; Zang, Y.; Chen, G. R.; He, X. P.; Li, J.; Yoon, J.; James, T. D. Sensors, Imaging Agents, and Theranostics to Help Understand and Treat Reactive Oxygen Species Related Diseases. *Small Methods* **2019**, *3* (7). https://doi.org/10.1002/smtd.201900013.

(30) Lee, M. H.; Sharma, A.; Chang, M. J.; Lee, J.; Son, S.; Sessler, J. L.; Kang, C.; Kim, J. S. Fluorogenic Reaction-Based Prodrug Conjugates as Targeted Cancer Theranostics. *Chem. Soc. Rev.* **2018**, *47* (1), 28–52. https://doi.org/10.1039/c7cs00557a.

(31) Li, Y.; Yan, L.; Cai, J.; Zhang, W.; Li, L.; Du, Z.; Dong, C.; Meunier, B.; Chen, H. Development of Novel Theranostic Agents for in Vivo Amyloid Imaging and Protective Effects on Human Neuroblastoma Cells. *Eur. J. Med. Chem.* **2019**, *181*. https://doi.org/10.1016/j.ejmech.2019.111585.

(32) Li, Y. L.; Cai, J.; Yan, L.; Zhang, W.; Li, L.; Du, Z.; Fang, Y. X.; Dong, C. Z.; Meunier, B.; Chen, H. Phenothiazine-Based Theranostic Compounds for in Vivo near-Infared Fluorescence Imaging of β-Amyloid Plaques and Inhibition of Aβ Aggregation. *Dye. Pigment.* **2019**, *171* (July), 1–7. https://doi.org/10.1016/j.dyepig.2019.107744.

(33) Staderini, M.; Aulić, S.; Bartolini, M.; Tran, H. N. A.; González-Ruiz, V.; Pérez, D. I.; Cabezas, N.; Martínez, A.; Martín, M. A.; Andrisano, V.; Legname, G.; Menéndez, J. C.; Bolognesi, M. L. A Fluorescent Styrylquinoline with Combined Therapeutic and Diagnostic Activities against Alzheimer's and Prion Diseases. *ACS Med. Chem. Lett.* **2013**, *4* (2), 225–229. https://doi.org/10.1021/ml3003605.

(34) Li, Y.; Chen, C.; Xu, D.; Poon, C. Y.; Ho, S. L.; Zheng, R.; Liu, Q.; Song, G.; Li, H. W.; Wong, M. S. Effective Theranostic Cyanine for Imaging of Amyloid Species in Vivo and Cognitive Improvements in Mouse Model. *ACS Omega* **2018**, *3* (6), 6812–6819. https://doi.org/10.1021/acsomega.8b00475.

(35) Ardura-Fabregat, A.; Boddeke, E. W. G. M.; Boza-Serrano, A.; Brioschi, S.; Castro-Gomez, S.; Ceyzériat, K.; Dansokho, C.; Dierkes, T.; Gelders, G.; Heneka, M. T.; Hoeijmakers, L.; Hoffmann, A.; Iaccarino, L.; Jahnert, S.; Kuhbandner, K.; Landreth, G.; Lonnemann, N.; Löschmann, P. A.; McManus, R. M.; Paulus, A.; Reemst, K.; Sanchez-Caro, J. M.; Tiberi, A.; Van der Perren, A.; Vautheny, A.; Venegas, C.; Webers, A.; Weydt, P.; Wijasa, T. S.; Xiang, X.; Yang, Y. Targeting Neuroinflammation to Treat Alzheimer's Disease. *CNS Drugs* **2017**, *31* (12), 1057–1082. https://doi.org/10.1007/s40263-017-0483-3.

(36) Heneka, M. T.; Carson, M. J.; Khoury, J. El; Landreth, G. E.; Brosseron, F.; Feinstein, D. L.; Jacobs, A. H.; Wyss-Coray, T.; Vitorica, J.; Ransohoff, R. M.; Herrup, K.; Frautschy, S. A.; Finsen, B.; Brown, G. C.; Verkhratsky, A.; Yamanaka, K.; Koistinaho, J.; Latz, E.; Halle, A.; Petzold, G. C.; Town, T.; Morgan, D.; Shinohara, M. L.; Perry, V. H.; Holmes, C.; Bazan, N. G.; Brooks, D. J.; Hunot, S.; Joseph, B.; Deigendesch, N.; Garaschuk, O.; Boddeke, E.; Dinarello, C. A.; Breitner, J. C.; Cole, G. M.; Golenbock, D. T.; Kummer, M. P. Neuroinflammation in Alzheimer's Disease. *Lancet Neurol.* **2015**, *14* (4), 388–405.

https://doi.org/10.1016/S1474-4422(15)70016-5.

(37) Tuppo, E. E.; Arias, H. R. The Role of Inflammation in Alzheimer's Disease. *Int. J. Biochem. Cell Biol.* **2005**, *37* (2), 289–305. https://doi.org/10.1016/j.biocel.2004.07.009.

(38) Chen, Y.; Colonna, M. Two-Faced Behavior of Microglia in Alzheimer's Disease. *Nat. Neurosci.* **2022**, *25* (1), 3–4. https://doi.org/10.1038/s41593-021-00963-w.

(39) Jevtic, S.; Sengar, A. S.; Salter, M. W.; McLaurin, J. A. The Role of the Immune System in Alzheimer Disease: Etiology and Treatment. *Ageing Res. Rev.* **2017**, *40* (September), 84–94. https://doi.org/10.1016/j.arr.2017.08.005.

(40) Burgaletto, C.; Munafò, A.; Di Benedetto, G.; De Francisci, C.; Caraci, F.; Di Mauro, R.; Bucolo, C.; Bernardini, R.; Cantarella, G. The Immune System on the TRAIL of Alzheimer's Disease. *J. Neuroinflammation* **2020**, *17* (1), 1–11. https://doi.org/10.1186/s12974-020-01968-1.

(41) Yagami, T.; Koma, H.; Yamamoto, Y. Pathophysiological Roles of Cyclooxygenases and Prostaglandins in the Central Nervous System. *Mol. Neurobiol.* **2016**, *53* (7), 4754–4771. https://doi.org/10.1007/s12035-015-9355-3.

(42) Calvello, R.; Panaro, M. A.; Carbone, M. L.; Cianciulli, A.; Perrone, M. G.; Vitale, P.; Malerba, P.; Scilimati, A. Novel Selective COX-1 Inhibitors Suppress Neuroinflammatory Mediators in LPS-Stimulated N13 Microglial Cells. *Pharmacol. Res.* **2012**, *65* (1), 137–148. https://doi.org/10.1016/j.phrs.2011.09.009.

(43) Hoozemans, J. J. M.; Veerhuis, R.; Janssen, I.; Van Elk, E. J.; Rozemuller, A. J. M.; Eikelenboom, P. The Role of Cyclo-Oxygenase 1 and 2 Activity in Prostaglandin E2 Secretion by Cultured Human Adult Microglia: Implications for Alzheimer's Disease. *Brain Res.* **2002**, *951* (2), 218–226. https://doi.org/10.1016/S0006-8993(02)03164-5.

(44) Choi, S. H.; Aid, S.; Caracciolo, L.; Sakura Minami, S.; Niikura, T.; Matsuoka, Y.; Turner, R. S.; Mattson, M. P.; Bosetti, F. Cyclooxygenase-1 Inhibition Reduces Amyloid Pathology and Improves Memory Deficits in a Mouse Model of Alzheimer's Disease. *J. Neurochem.* **2013**, *124* (1), 59–68. https://doi.org/10.1111/jnc.12059.

(45) Sridharan, V.; Menéndez, J. C. Two-Step Stereocontrolled Synthesis of Densely Functionalized Cyclic β-Aminoesters Containing Four Stereocenters, Based on a New Cerium(IV) Ammonium Nitrate Catalyzed Sequential Three-Component Reaction. *Org. Lett.* **2008**, *10* (19), 4303–4306. https://doi.org/10.1021/ol801738d.

(46) Rocchi, D.; González, J. F.; Gómez-Carpintero, J.; González-Ruiz, V.; Martín, M. A.; Sridharan, V.; Menéndez, J. C. Three-Component Synthesis of a Library of m-Terphenyl Derivatives with Embedded β-Aminoester Moieties. *ACS Comb. Sci.* **2018**, *20* (12), 722–731. https://doi.org/10.1021/acscombsci.8b00137.

(47) Rocchi, D. Síntesis orientada a diversidad de heterociclos nitrogenados a partir de chalconas. Tesis doctoral, Universidad Complutense, **2015**.

(48) González-Ruiz, V.; Rajesh, J.; Olives, A. I.; Rocchi, D.; Gómez-Carpintero, J.; González, J. F.; Sridharan, V.; Martín, M. A.; Menéndez, J. C. Antioxidants as Molecular Probes: Structurally Novel Dihydro-m-Terphenyls as Turn-on Fluorescence Chemodosimeters for Biologically Relevant Oxidants. *Antioxidants* **2020**, *9* (7), 1–16. https://doi.org/10.3390/antiox9070605.

(49) Tenti, G.; Parada, E.; Leo, R.; Egea, J.; Mart, S.; Mar, A.; Sridharan, V.; Lo, M. G. New 5-Unsubstituted Dihydropyridines with Improved CaV1.3 Selectivity as Potential

Neuroprotective Agents against Ischemic Injury. *J. Med. Chem.* **2014**, *57*, 4313–4323.

(50) Braslavsky, S. E. Glossary of Terms Used in Photochemistry 3rd Edition: (IUPAC Recommendations 2006). *Pure Appl. Chem.* **2007**, *79* (3), 293–465. https://doi.org/10.1351/pac200779030293.

(51) Goodell, J. R.; Madhok, A. A.; Hiasa, H.; Ferguson, D. M. Synthesis and Evaluation of Acridine- and Acridone-Based Anti-Herpes Agents with Topoisomerase Activity. *Bioorganic Med. Chem.* **2006**, *14* (16), 5467–5480. https://doi.org/10.1016/j.bmc.2006.04.044.

(52) Cholewiński, G.; Dzierzbicka, K.; Kołodziejczyk, A. M. Natural and Synthetic Acridines/Acridones as Antitumor Agents: Their Biological Activities and Methods of Synthesis. *Pharmacol. Reports* **2011**, *63* (2), 305–336. https://doi.org/10.1016/S1734-1140(11)70499-6.

(53) Dzierzbicka, K.; Kołodziejczyk, A. M. Synthesis and Antitumor Activity of Conjugates of Muramyldipeptide or Normuramyldipeptide with Hydroxyacridine/Acridone Derivatives. *J. Med. Chem.* **2003**, *46* (1), 183–189. https://doi.org/10.1021/jm020991m.

(54) Ahua, K. M.; Ioset, J. R.; Ransijn, A.; Mauël, J.; Mavi, S.; Hostettmann, K. Antileishmanial and Antifungal Acridone Derivatives from the Roots of Thamnosma Rhodesica. *Phytochemistry* **2004**, *65* (7), 963–968. https://doi.org/10.1016/j.phytochem.2003.12.020.

(55) Aarjane, M.; Slassi, S.; Tazi, B.; Maouloua, M.; Amine, A. Novel Series of Acridone-1 , 2 , 3-Triazole Derivatives : Microwave-Assisted Synthesis , DFT Study and Antibacterial. *J. Chem. Sci.* **2019**, *0123456789*, 1–11. https://doi.org/10.1007/s12039-019-1653-2.

(56) Parveen, M.; Aslam, A.; Nami, S. A. A.; Malla, A. M.; Alam, M.; Lee, D. U.; Rehman, S.; Silva, P. S. P.; Silva, M. R. Potent Acetylcholinesterase Inhibitors: Synthesis, Biological Assay and Docking Study of Nitro Acridone Derivatives. *J. Photochem. Photobiol. B Biol.* **2016**, *161*, 304–311. https://doi.org/10.1016/j.jphotobiol.2016.05.028.

(57) Ma, W.; Bi, J.; Zhao, C.; Gao, Y.; Zhang, G. Design, Synthesis and Biological Evaluation of Acridone Glycosides as Selective BChE Inhibitors. *Carbohydr. Res.* **2020**, *491* (February), 107977. https://doi.org/10.1016/j.carres.2020.107977.

(58) Nishio, R.; Wessely, S.; Sugiura, M.; Kobayashi, S. Synthesis of Acridone Derivatives Using Polymer-Supported Palladium and Scandium Catalysts. *J. Comb. Chem.* **2006**, *8* (4), 459–461. https://doi.org/10.1021/cc060011+.

(59) Zhao, J.; Larock, R. C. Synthesis of Xanthones, Thioxanthones, and Acridones by the Coupling of Arynes and Substituted Benzoates. *J. Org. Chem.* **2007**, *72* (2), 583–588. https://doi.org/10.1021/jo0620718.

(60) Silva, V. L. M.; Silva, A. M. S. New Synthetic Methods for 2,3-Diarylacridin-9(10H)-One and (E)-2-Aryl-4-Styrylfuro[3,2-c]Quinoline Derivatives. *Tetrahedron* **2014**, *70* (34), 5310–5320. https://doi.org/10.1016/j.tet.2014.05.040.

(61) Rocchi, D.; Gómez-Carpintero, J.; González, J. F.; Menéndez, J. C. Sustainable Access to Acridin-9-(10H)Ones with an Embedded m-Terphenyl Moiety Based on a Three-Component Reaction. *Molecules* **2020**, *25* (23). https://doi.org/10.3390/molecules25235565.

(62) Prasanna, P.; Gunasekaran, P.; Perumal, S.; Menéndez, J. C. A Catalyst-Free Multicomponent Domino Sequence for the Diastereoselective Synthesis of (E)-3-[2-

Arylcarbonyl-3-(Arylamino)Allyl]Chromen-4-Ones. *Beilstein J. Org. Chem.* **2014**, *10*, 459–465. https://doi.org/10.3762/bjoc.10.43.

(63) Heravi, M. M.; Ghavidel, M.; Mohammadkhani, L. Beyond a Solvent: Triple Roles of Dimethylformamide in Organic Chemistry. *RSC Adv.* **2018**, *8* (49), 27832–27862. https://doi.org/10.1039/c8ra04985h.

(64) Rocchi, D.; González, J. F.; Menéndez, J. C. Montmorillonite Clay-Promoted, Solvent-Free Cross-Aldol Condensations under Focused Microwave Irradiation. *Molecules* **2014**, *19* (6), 7317–7326. https://doi.org/10.3390/molecules19067317.

(65) Jiang, R.; Miyamoto, A.; Martz, A.; Specht, A.; Ishibashi, H.; Kueny-Stotz, M.; Chassaing, S.; Brouillard, R.; De Carvalho, L. P.; Goeldner, M.; Nabekura, J.; Nielsen, M.; Grutter, T. Retrochalcone Derivatives Are Positive Allosteric Modulators at Synaptic and Extrasynaptic GABA A Receptors in Vitro. *Br. J. Pharmacol.* **2011**, *162* (6), 1326–1339. https://doi.org/10.1111/j.1476-5381.2010.01142.x.

(66) Li, R.; Yan, L.; Sun, X.; Zheng, W. A Bicyclic Pentapeptide-Based Highly Potent and Selective Pan-SIRT1/2/3 Inhibitor Harboring Nε-Thioacetyl-Lysine. *Bioorganic Med. Chem.* **2020**, *28* (7), 115356. https://doi.org/10.1016/j.bmc.2020.115356.

(67) Murphy, M. E; Salvino, J.; George, D. L. WO 2021/202540 A1. **2021**.

(68) Mao, F.; Li, J.; Wei, H.; Huang, L.; Li, X. Tacrine-Propargylamine Derivatives with Improved Acetylcholinesterase Inhibitory Activity and Lower Hepatotoxicity as a Potential Lead Compound for the Treatment of Alzheimers Disease. *J. Enzyme Inhib. Med. Chem.* **2015**, *30* (6), 995–1001. https://doi.org/10.3109/14756366.2014.1003212.

(69) Savini, L.; Gaeta, A.; Fattorusso, C.; Catalanotti, B.; Campiani, G.; Chiasserini, L.; Pellerano, C.; Novellino, E.; McKissic, D.; Saxena, A. Specific Targeting of Acetylcholinesterase and Butyrylcholinesterase Recognition Sites. Rational Design of Novel, Selective, and Highly Potent Cholinesterase Inhibitors. *J. Med. Chem.* **2003**, *46* (1), 1–4. https://doi.org/10.1021/jm0255668.

(70) Camps, P.; Formosa, X.; Muñoz-Torrero, D.; Petrignet, J.; Badia, A.; Clos, M. V. Synthesis and Pharmacological Evaluation of Huprine-Tacrine Heterodimers: Subnanomolar Dual Binding Site Acetylcholinesterase Inhibitors. *J. Med. Chem.* **2005**, *48* (6), 1701–1704. https://doi.org/10.1021/jm0496741.

# Chapter 5: Mechanochemical synthesis of rufinamide and primary amides

## 1.0 Introduction

### 1.1 Neuroglial sodium channels: A target for neurodegenerative diseases

Under pathological conditions, the CNS activates glial cells, particularly microglia, and triggers a complex neuroinflammatory pathway, which leads to the formation and release of various pro-inflammatory factors (chemokines and cytokines), increased oxidative stress and induced apoptosis of neurons. In this spite, sodium channels have been shown to play an essential role in the physiological and pathological function of glial cells. Due to the fact that glial cells are sensitive to ion flux, particularly $Ca^{2+}$ ions (although glial cells do not produce AP under physiological conditions), whose concentration is involved in microglial activation and in the regulation of their functions. In addition, the concentration of $Ca^{2+}$ ions is regulated by the sodium-calcium exchanger (NCX), which transfers three $Na^{+}$ ions for each $Ca^{2+}$ ion in opposite direction, which generates a total flow of one positive charge in each cycle, supporting intracellular $Ca^{2+}$ homeostasis. Furthermore, some experimental data suggest that NCX activation contributes to neuronal cell death in the ischaemic brain; to control the formation and residence time of $Ca^{2+}$ concentration in response to the neurotransmitters; to neurotransmitter release and to the generation of free radicals and NO in the mitochondria. Thus, sodium channel activation has the ability to increase $Ca^{2+}$ ion concentration through the reverse mode of NCX and sodium channel dysfunction can lead to neurological diseases[1]. Consequently, NCX was suggested to be implicated in the pathophysiology of cerebral ischaemia, epilepsy, and the main neurodegenerative diseases such as AD[2] . Therefore, voltage-gated sodium channels (VGSCs) are a potential pharmacological target for the development of neuroprotective drugs due to their ability to indirectly reduce intracellular calcium concentration.

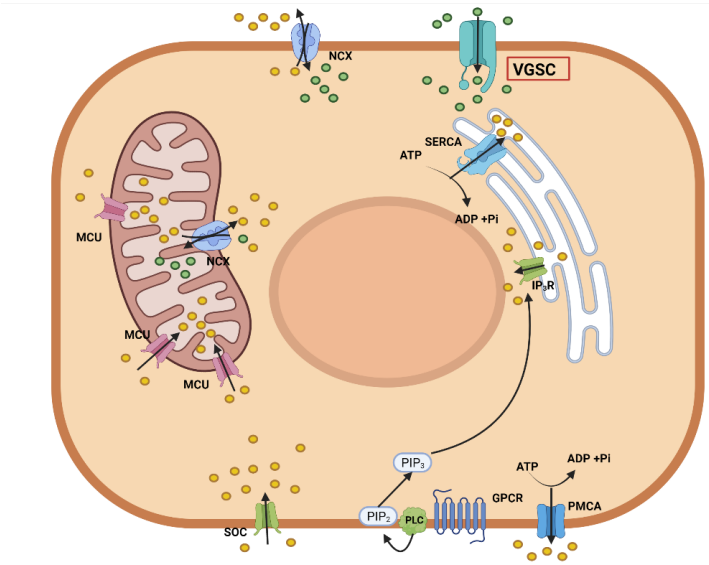


Figure 1. Scheme representing intracellular calcium homeostasis. As it can be observed, sodium metabolism plays a crucial role in the intracellular calcium concentration due to its role in NCX antiportation (calcium is represented with yellow circles, sodium with green circles).

Numerous drugs act as sodium channel blockers have shown a wide therapeutic range such as: antiarrhythmics, local anesthetics, anticonvulsants and to treat pain. Particularly relevant for us, are the neuronal sodium channel blockers, which have been found to have analgesic, anticonvulsant or neuroprotective activity, such as lamotrigine, zonisamide, Lubeluzole or rufinamide (figure 2).

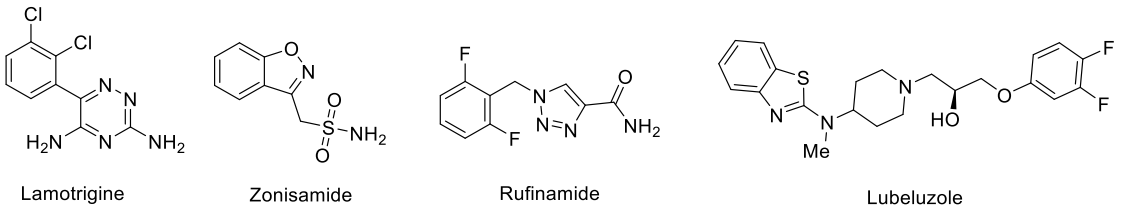


Figure 2. chemical structure of some sodium channel blockers.

**1.2. An overview of mechanochemical synthesis**

Mechanochemistry is defined by those reactions that are carried out with the input of mechanical energy, for example by grinding or with the use of ball milling.[3] Its use is attracting great attention in recent years as it presents numerous advantages in comparison with traditional organic synthesis. In the first place, mechanochemical synthesis has demonstrated to be effective and, in some cases, to have a superior efficacy in a growing spectrum of organic reactions. Secondly, the use of organic solvents is well known to be environmentally unfriendly and the absence or residual use in mechanochemical reactions helps to reduce the ecological impact of chemical reactions. Finally, the energy input to induce reactions is significantly inferior to conventional heating, contributing also to the reduction of the environmental impact of chemical reactions[4,5].

The first knowledge of mechanochemical reaction, using a mortar and a pestle dating from more than two thousand years ago[6]. However, this method has been outdated by more modern equipment due to its low reproducibility of the reaction conditions. In the recent years, ball mills have been used for mechanochemical reactions at laboratory level. The reactions are carried out in these equipment in a closed-up vessel, improving this way the safety of the reaction, and time and frequency of milling can also be programmed, allowing mechanochemical reactions to be highly reproducible[7].

There are different types of ball milling equipment. Planetary ball mills are devices where balls and reactants experience friction due to the centrifugal movement of the vessel and impact due to the collision of balls and reagents with its walls. Mixer horizontal mills produce a backwards and forwards movement that cause the balls and reagents inside the vessel to collide with its walls. This last technique has received the name of High-Speed Vibratory Milling (HSVM)[7] (Figure 3)

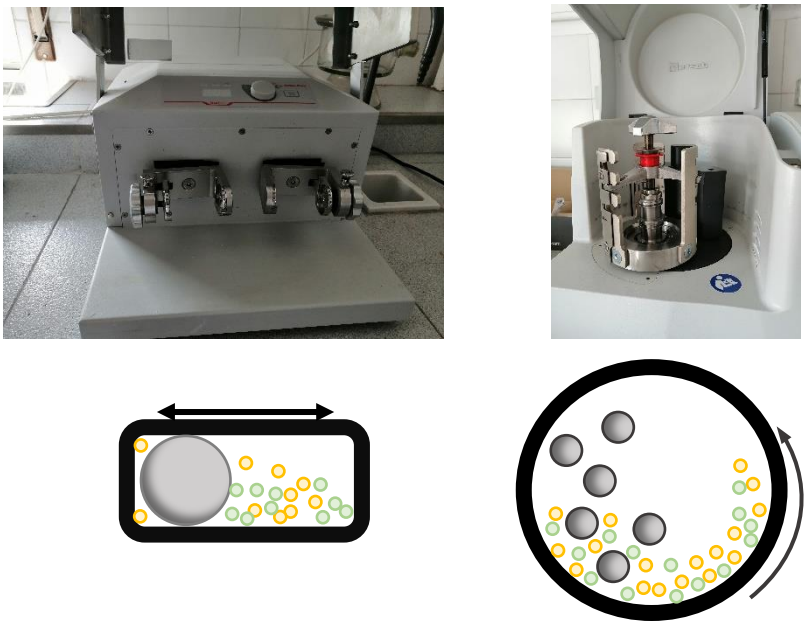

Figure 3. Image and scheme of vibratory ball mill (left) and planetary ball mill (right).

In the recent years, mechanochemical organic synthesis has received increasing attention and many classical organic syntheses have been extrapolated to mechanochemistry. These include aldol condensation[8], Wittig reaction[9], Michael addition[10], halogenation reactions[11] or even cross couplings such as Suzuki-Miyaura coupling[12] or Heck reaction[13]. Even multicomponent reactions such as the Strecker reaction[14], Ugi reaction[15] or Hantzsch pyrrole synthesis[16] have been successfully translated to mechanochemical conditions.

### 1.3 Rufinamide: Synthesis and pharmacological relevance

Rufinamide (1-(2,6-difuoro-phenyl) methyl-1H-1,2,3-triazole-4-carboxamide) is a triazole derived commercialised antiepileptic drug used for the treatment of Lennox-Gasteaut syndrome, a childhood type of epilepsy. Its mechanism of action is not fully understood but it is known to modulate sodium channel activity in neurons and limit neuronal action potential firing, contributing this way to membrane potential stabilization, and hence diminishing and controlling seizures[17,18].

Additionally, this compound has shown neuroprotective properties in several contexts, and thus it has been shown to protect pyramidal neurons in the hippocampus after transient global cerebral ischemia[19]. Moreover, in a model of brain damage induced by kainic acid, rufinamide was shown to inhibit the overactivation of microglia, suppressing the neuroinflammatory response, and also reduced the destruction of blood–brain barrier[20]. Rufinamide also improves cognition and increases neurogenesis in the aged gerbil by increasing the expression of the transcription factors IGF-1, IGF-1R and *p*-CREB that have well-documented roles in neuronal plasticity and long-term memory[21].

In the past years, several research papers and patents have proposed different synthetic pathways[18,22–24], which the key step is the formation of the triazole ring, being the formation of

2-(azidomethyl)-1,3-difluorobenzene (**II**) the previous requirement to perform this step. 2-(azidomethyl)-1,3-difluorobenzene (**II**) has been described using different azides and 2,6 difluorobenzyl halides (**I**). The formation of triazole ring has been achieved with propiolate derivatives, acrylate derivatives and enol ethers. The final synthetic step is the obtention of the primary amide moiety, which dependent on the reagent employed in the cycloaddition reaction. Additionally, industrial synthetic processes such as flow chemistry have been applied to the synthesis of rufinamide[25] (scheme 1).

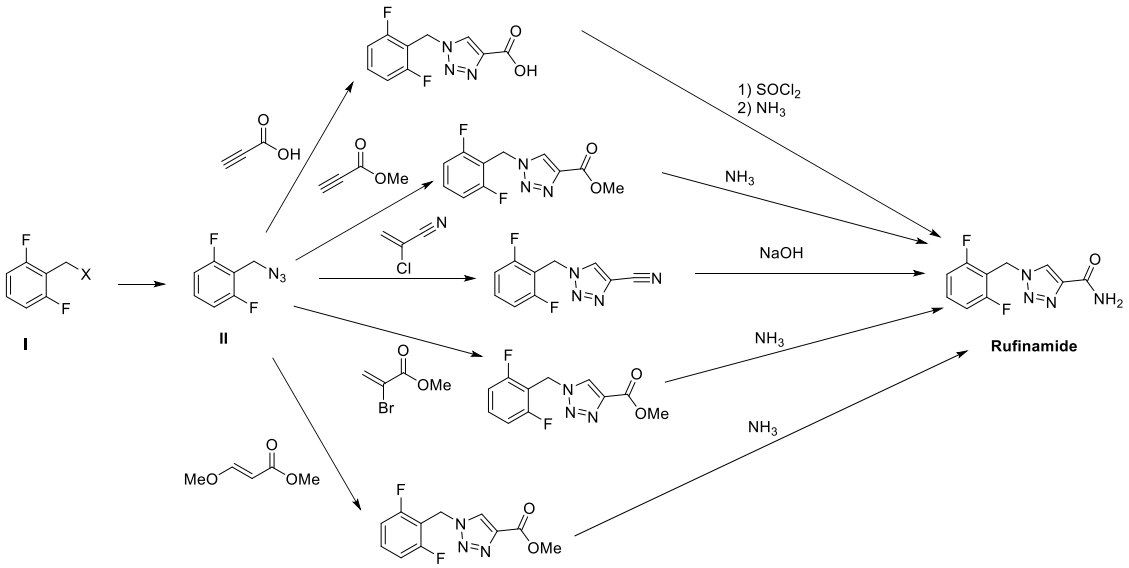


Scheme 1. Proposed synthetic routes for rufinamide.

### 1.4 Primary amides

The amide group is a relevant and widespread functional group in organic molecules, which is present in essential molecules as proteins and peptides and other relevant molecules, such as polymers, agrochemicals, and drugs. Consequently, amide synthesis is a common chemical reaction in the manufacture of drugs, comprising about 25% of all reactions carried out in medicinal chemistry projects[26]. Regarding primary amide distribution in drugs, it is a group with a major presence in antiepileptic drugs and biomolecules, such as levetiracetam or nicotinamide (Figure 4). This converts the synthesis of the primary amide group in a key step of the drug discovery and drug manufacture process.

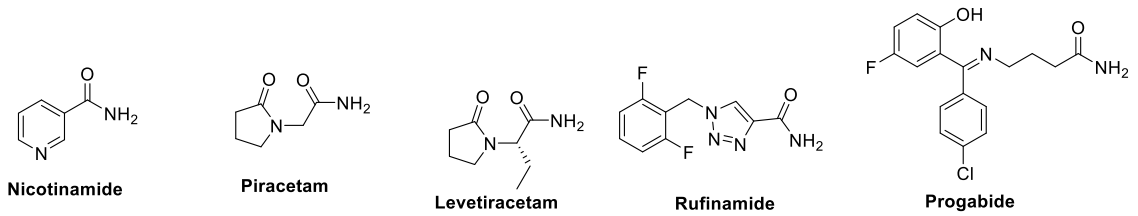


Figure 4. Different important biomolecules and drugs that possess a primary amide group.

Thus, many mechanochemical synthesis of amides have been developed by several authors (scheme 2); Margetić and co-workers developed a one-pot synthesis of aromatic amides and dipeptides structura by amide bond formation from carboxylic acid and primary amines, using EDC as a coupling agent and nitromethane as a Liquid Grinding Assistant (LGA). They managed to couple different substrates including aromatic and aliphatic acids, aromatic and aliphatic amines and amino acids to yield a total number of 28 examples in good to excellent yields[27].

in similar work Lamaty and co-workers proposed the use of CDI as a coupling agent. In this work, a sequential synthesis was employed, which corresponding carboxylic acid compound and CDI was carried out and an amine was added sequentially, after short times of milling to obtain the desired amide and finally the water addition removed the undesired by products. The scope of the process was supported by aromatic and aliphatic carboxylic acids, aromatic and aliphatic amines, oximes and hydrazines[28].

Other example of mechanochemical amide synthesis was reported by Pattawarapan and co-workers, whichproposed to employ 2,4,6-trichloro 1,3,5-triazine and an inorganic base as ammonium source. In this work, 30 examples were described in moderate to excellent yields and variety of substrates was tolerated, even amino acids to yield dipeptides[29] (scheme 6).

Delogu and co-workers developed a mechanochemical version of the Beckmann rearrangement to obtain a different variety of amides from a corresponding ketone, using hydroxylamine hydrochloride, imidazole and para-toluene sulphonic imidazole (ps-TsIm) in a sequential step (reporting a total of 34 examples). In some cases, where the ketone substrate was asymmetric, two different products were formed with different selectivity depending on the substituents present in the ketone. Furthermore, this method was also tested on aldehyde substrates yielding nitriles, which were partially hydrolysed to primary amides[30] (scheme 7).

A mechanoenzymatic approach was reported by Bolm and co-workers to form amide bonds and peptides synthesis used enzyme papain and L-cystein to catalyse the formation of peptide bonds), water to improve the yield of the reaction and an inorganic base. Impressively, the enzyme did not degrade under mechanochemical stress and produced the dipeptides in moderate to excellent yields[31].

Pattawarapan and colleagues also developed a method to synthesise primary amides using $NH_4SCN$ as a source of ammonia, 2,4,6-trichloro 1,3,5-triazine (TCT) to activate carboxylic acid and $K_2CO_3$ as base. The method employed for the synthesis is not HSVM, is grinding with a mortar and a pestle, which is a method not as reproducible as the former. Nevertheless, theymanaged to obtain a total number of 18 examples including aromatic, aliphatic and vinyl amides[32] (scheme 9).

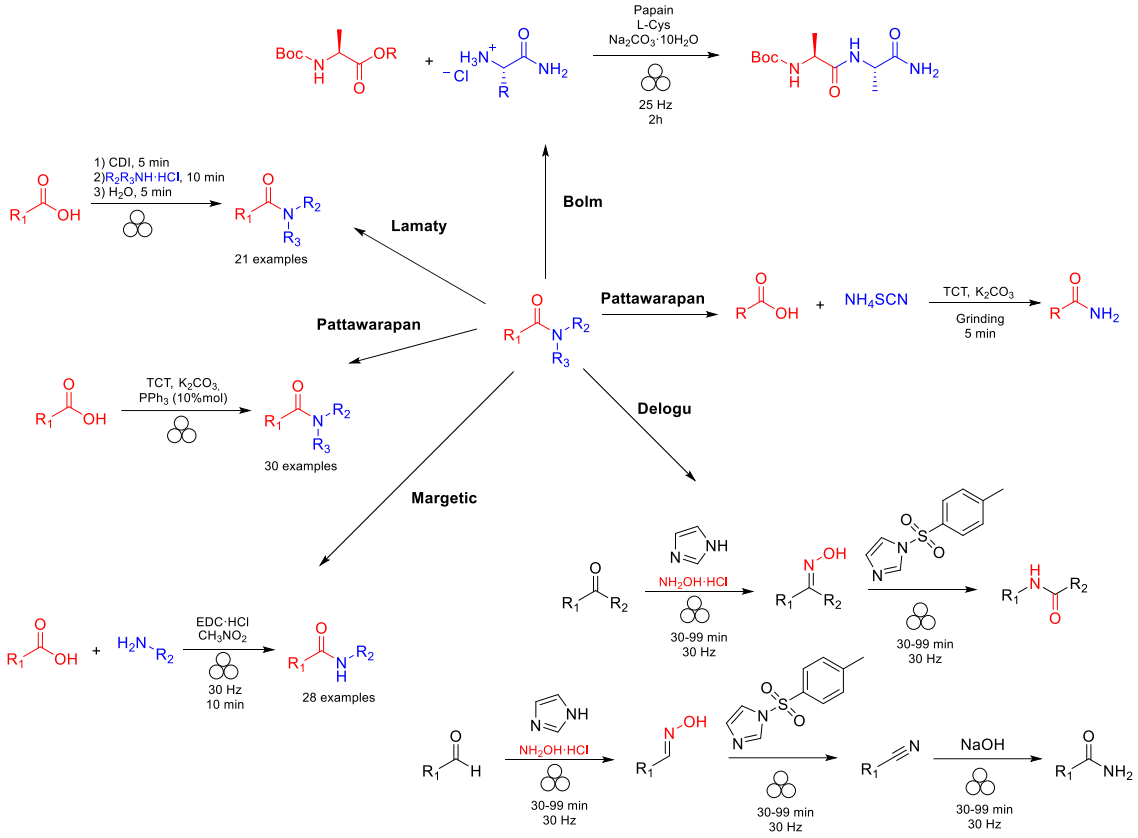


Scheme 2. Mechanochemical synthetic routes used by different authors to obtain primary amides.

## 2.0 Objectives

The need of develop eco-friendly processes in the synthesis of APIs is a great challenge to the pharmaceutical industry. In this work, we propose a synthetic sequence of three reactions to achieve rufinamide (scheme 1), starting with a nucleophilic substitution reaction of the 2-(bromomethyl)-1,3-difluorobenzene with sodium azide to obtain compound **3.3a**. A click chemistry reaction between intermediate **3.3a** and methyl propiolate was then devised in order to obtain triazole intermediate **3.3b**. This synthesis could be a starting point for the further development of specific brain VGSCs that can act not only in epilepsy, but also in other neurological disorders such as AD or PD.

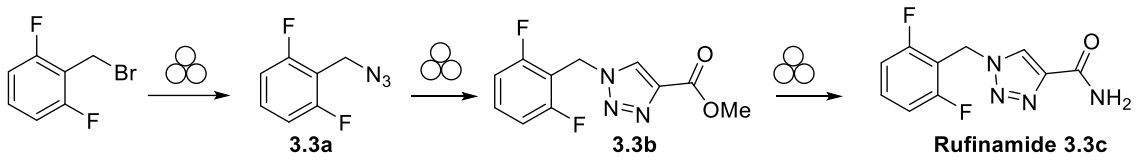


Scheme 1. Proposed mechanochemical synthetic route for rufinamide

The last part of the proposed sequence was the transformation of ester **3.3b** into the correspondent primary amide **3.3c**. As this reaction requires gaseous ammonia or liquid solutions that contain it, and this are hardly compatible with mechanochemistry, we searched agents that would allow to perform this transformation (Scheme 2).

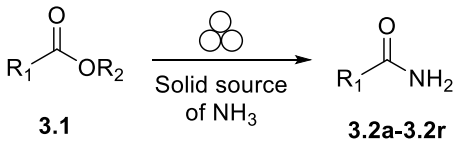


Scheme 2. Mechanochemical synthesis of primary amides.

## 3.0 Results

## 3.1 Synthesis of primary amides

The final step of the proposed synthesis involved the transformation of ester group to a primary amide starting. Thus, to develop the mechanochemical conditions we chose the ethyl 3-fluoro benzoate as a model (scheme 1). We select alkaline nitride as ammonia source since it reacts with water or alcohols to generate ammonia and the corresponding alkoxide (scheme 1)[33]. This reagent has been previously used for the synthesis of primary amides, under heavy reaction conditions, in which the reaction was carried out in a sealed tube, heating to 80 ºC and for 24 h [34]. Therefore, we performed our study for the reaction of model ethyl 3-fluoro benzoate, and magnesium nitride-ethanol system as ammonia source, but no reaction was observed when it was carried out in stainless steel milling jar, containing a single stainless steel ball, at 30 Hz during times up to 90 minutes (entry 1, table 1). Then, we explored $AlCl_3$ and $Yb(OTf)_3$ as Lewis acids to catalyse the reaction, to provide the 3-fluorobenzamide **3.2a** in a moderate yield (entries 2 and 3, table 3), the catalytic ability of copper as a Lewis acid was explored using $CuSO_4$ and CuBr as Cu (II) and Cu (I) species, which lead to the primary amine with a poor and good efficiency respectively (entries 4 and 5, table 1). Finally, we used $ZnCl_2$ and $InCl_3$ as lewis acids to catalyse the reaction, which leads to the best results of transformation, thus when the reaction was loaded with 20 % of catalyst and carried out at a 30 Hz for 90 min, lead to 85% and 91% of conversion respectively (entries 6 and 10, table 1). In order to optimize the reaction settings, the reaction time was reduced to 60 min, which led to a decrease in yield, particularly when zinc was used as a catalyst (entries 7 and 11, table 3); also, when the frequency was decreased to 25 Hz, this led to a decrease in the yield (entries 9 and 12, table 1). Finally, we decreased the catalyst loading to 10%, which resulted in a substantial decrease in the yield for $InCl_3$ (entries 8 and 13, table 1). Thus, Indium trichloride was identified as a better catalyst, allowing 91% conversion.

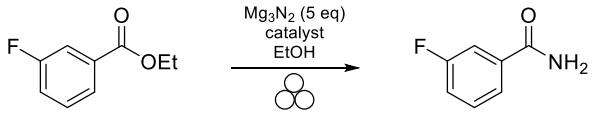


$$Mg_3N_2 + 6\ EtOH \longrightarrow 2\ NH_3 + 3\ Mg(OEt)_2$$

Scheme 1. Formation of compound 3.2a from 3.1a and $NH_3$ formation equation

| Entry | Catalyst (eqs.) | Time | Frequency (Hz)[a] | Conversion (%) [b, c] |
|---|---|---|---|---|
| **1** | - | 90 | 30 | 0 |
| **2** | $AlCl_3$ (0.2) | 90 | 30 | 37 |
| **3** | $Yb(OTf)_3$ (0.2) | 90 | 30 | 28 |
| **4** | $CuSO_4$ (0.1) | 90 | 30 | 12 |
| **5** | CuBr (0.2) | 90 | 30 | 67 |
| **6** | $ZnCl_2$ (0.2) | 90 | 30 | 85 |
| **7** | $ZnCl_2$ (0.2) | 60 | 30 | 52 |
| **8** | $ZnCl_2$ (0.1) | 90 | 30 | 43 |
| **9** | $ZnCl_2$ (0.1) | 90 | 25 | 37 |
| **10** | $InCl_3$ (0.2) | 90 | 30 | 91 |
| **11** | $InCl_3$ (0.2) | 60 | 30 | 87 |
| **12** | $InCl_3$ (0.2) | 60 | 25 | 83 |

| | | | | |
|---|---|---|---|---|
| **13** | $InCl_3$ (0.1) | 60 | 25 | 23 |

Table 1. Catalyst Optimization in the Synthesis of ethyl 3-fluoroacetate into 3-fluorobenzamide. [a] In a 25 mL stainless steel 2 milling jar containing a single stainless steel ball of 15 mm in diameter. [b]Estimated by 1H-NMR analysis of the reaction crude. [c]5 equivalents of magnesium nitride and 1 mL of ethanol were employed in all cases

Based on these optimised conditions, we then optimised the other reaction parameters. In an attempt to purify the crude reaction products by extraction and to avoid column chromatography purification, we tried to purify the reaction mixture by an ethyl acetate/water extraction, which despite excellent conversion, however, we only achieved a 23% isolated yield (entry 1, table 2). We hypothesised that these could be due to the interference of magnesium salts present in the reaction medium, which remain as a suspension during the workup, and this pushed us to use alternative sources of ammonia, such as ammonium chloride or ammonium formate, but these attempts were unsuccessful (entries 2 and 3, table 2).

In an effort to improve the isolation protocol, we performed the extraction of magnesium salts using Rochelle´s salt (Potassium sodium tartrate tetrahydrate), which often prevents the formation of emulsions in reactions involving aluminum-based reagents, but in our case, also proved ineffective. Lowering the amount of magnesium nitride to 2 equivalents proved also to be ineffective (entries 4 and 5, table 2) however the use of 3 equivalents of magnesium nitride together with increasing the catalyst load to 0.3 equivalents gave good, isolated yield of 73%. Finally, calcium nitride was then tried as a source of ammonia and results were slightly improved. A final improvement was also observed lowering the amount of ethanol used for the reaction (entries 7 to 9, table 2). In order to prove the beneficial effect of the mechanochemical conditions, a control experiment was carried out in solution, at room temperature, gave 49% isolated yield of compound **3.2a**.

| Entry | Catalyst (eqs) | Source of ammonia (eqs) | Proton source | Yield (%) |
|---|---|---|---|---|
| 1 | $InCl_3$ (0.2) | $Mg_3N_2$ (5) | EtOH (1ml) | 23 |
| 2 | $InCl_3$ (0.2) | $NH_4Cl$ | - | - |
| 3 | $InCl_3$ (0.2) | $NH_4COO$ | - | - |
| 4 | $InCl_3$ (0.2) | $Mg_3N_2$ (2) | EtOH (1ml) | traces |
| 5 | $InCl_3$ (0.3) | $Mg_3N_2$ (2) | EtOH (1ml) | traces |
| 6 | $InCl_3$ (0.4) | $Mg_3N_2$ (3) | EtOH (1ml) | 73 |
| 7 | $InCl_3$ (0.4) | $Ca_3N_2$ (3) | EtOH (1ml) | 79 |
| 8 | $InCl_3$ (0.4) | $Ca_3N_2$ (3) | EtOH (0.5ml) | 83 |
| 9 | $InCl_3$ (0.4) | $Ca_3N_2$ (3) | EtOH (0.3ml) | 88 |

Table 2. Optimization of Additional Reaction Parameters in the Synthesis of compound **2a**. All reactions were performed at 1 mmol scale by ball milling (stainless steel jar and ball) at 30 Hz for 90 min

With these optimised conditions, we decided to explore the scope of the mechanochemical protocol, and the reaction was carried with, aromatic, heteroaromatic, aliphatic and vinylic esters to achieve their correspondent primary amides. Additionally, functional groups such as amino, acetal, halogen or thioether groups were well tolerated. Interestingly, stereocenters

present in the substrates maintained their integrity as shown by the optical rotation of compounds **3.2l** and **3.2m**, which were identical to published values. The Yields oscillated in the range of 60-90% and were comparable to those obtained by sealed tube heating in 3 examples. We additionally proceeded to open the lactone chroman-2-one with the same procedure, and we obtained the correspondent amide **3.2r** in excellent yield, showing the great versatility of this method, even working on peptides (**3.2o**-**3.2q**) and therefore showing an applicability in peptide chemistry. (Scheme 2).

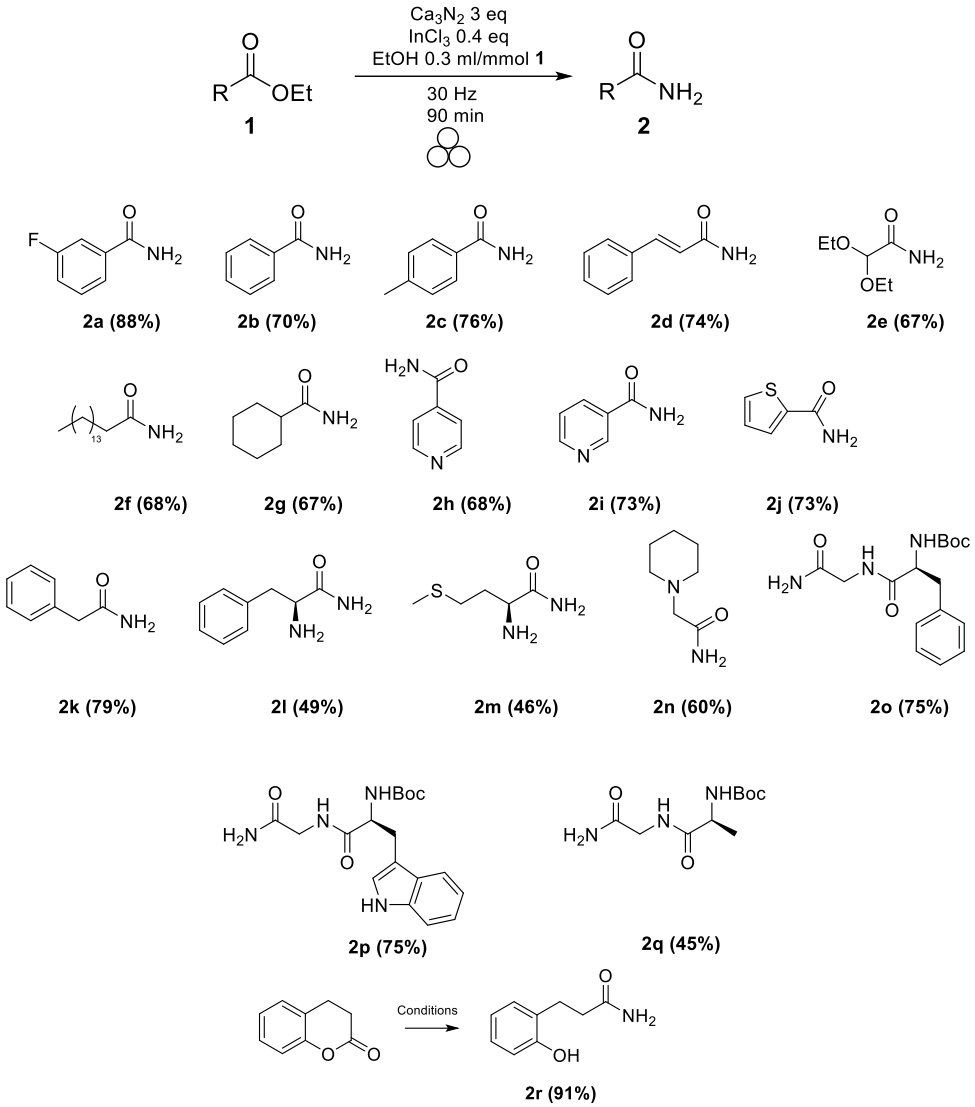


Scheme 2. Different primary amides synthesised

In order to show the applicability of this method for the synthesis of rufinamide, we first synthesised the ester precursor synthesised by the method described previously and we isolated it. Then we submitted this ester as a substrate for our synthetic method for the obtention of primary amides and we obtained rufinamide in a 61% yield (scheme 13).

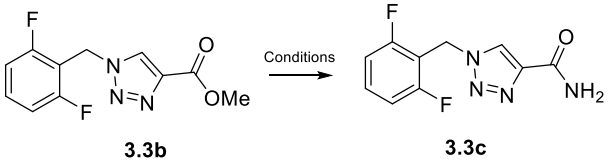

Scheme 3. Synthesis of rufinamide **3.3c** from isolated ester **3.3b**

## 3.2 Preparation of 2-(azidomethyl)-1,3-difluorobenzene

With the development of a mechanochemical method to transform the esters to the corresponding primary amides, we studied the first step on the synthetic sequence to obtain rufinamide and analogues. Thus, we studied the milling parameters that lead to perform the nucleophilic substitution of 2-(bromomethyl)-1,3-difluorobenzene with sodium azide. We tested the vibratory ball mill and the planetary ball mill under different reaction conditions of time, frequency, and number and size of balls. The results are displayed in table 1.

We started our work by determining the optimal reaction conditions of the first individual step to obtain azide **3.3a** from 2-(bromomethyl)-1,3-difluorobenzene. To explore the effects of the grinding parameters such as mass (number and size) of balls and rotational or oscillation speed, we first employed a planetary mill using a steel jar containing a powdered mixture of the benzyl halide derivate and sodium azide under several conditions (table 3, entries 1 to 3), but we recovered exclusively starting material in all cases, even in the presence of sodium chloride as abrasive grinding additive (table 3, entry 4). Due to these results, we moved to explore vibratory milling and the same mixture of benzyl halide/azide was set to 25 Hz, over 30 min as standard parameters. We first studied the effect of the number of balls and the model reaction was assayed in a steel jar containing 1, 3, 5, 6, 7, or 9 steel balls 5 mm in diameter; in this case, NMR analysis of the crude reaction mixtures showed the formation of azide **3.3a** and we found the best result when the reaction was performed with 6 balls, to obtain a 30 % conversion (table 3, entries 5 to 10), a representative example of the NMR study is illustrated in the figure 1. To improve conversion, we increased the reaction time to 60 minutes under optimal reaction conditions previously found, to give a conversion of 89 % (table 3, entry 11). Stimulated by these results, we decided to explore the vibration frequently parameter, which was increased up to 30 Hz, to give an excellent 97% of conversion (table 3, entry 12). When we scaled up the reaction to 0.5 g of benzyl bromide, under the same conditions, conversion decreased slightly to 88% (table 3, entry 13). Ball number optimization showed 6 balls of 5 mm diameter as optimal, while 7 and 9 balls were less effective. On the other hand, when the reaction was carried out with a single stainless-steel ball 15 mm in diameter, complete conversion was observed both at 30 and 25 Hz (table 3, entries 14 and 15).

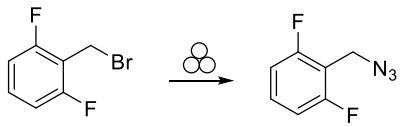


**3.3a**

Scheme 4. Synthesis of azide intermediate **3.3a**

| Entry | Mills | Number and size of balls | Rotation/oscillation frequency | milling time | Conversion |
|---|---|---|---|---|---|
| 1 | Planetary | 13 (5 mm) | 200rpm | 30m | 0 |
| 2 | | 26 (5 mm) | 200rpm | | 0 |
| 3 | | 26(5 mm) | 400 rpm | | 0 |

| | | | | | |
|---|---|---|---|---|---|
| 4 | | 13(5 mm) | 200 rpm | | 0* |
| 5 | vibratory | 1 (5 mm) | 25 Hz | 30m | traces |
| 6 | | 3 (5 mm) | | | 7.5 |
| 7 | | 5 (5 mm) | | | 22.4 |
| 8 | | 6 (5 mm) | | | 29.8 |
| 9 | | 7 (5 mm) | | | 25.2 |
| 10 | | 9 (5 mm) | | | 18.0 |
| 11 | | 6 (5 mm) | 25 Hz | 60m | 89.3 |
| 12 | | 6 (5 mm) | 30 Hz | | 97 |
| 13 | | 6 (5 mm) | 30 Hz | | 88** |
| 14 | | 1 (30 mm) | 30 Hz | | 100*** |

Table 3. Optimizing the mechanochemical reaction conditions to obtain azide **3.3a**. Table. The reaction was carried out for 100 mg (0.5 mmol) of 2-(bromomethyl)-1,3-difluorobenzene and 80 mg (1.2 mmol) of sodium azide, on a stainless-steel jar and balls. *The reaction was performed using sand as brass milling additive; ** The reaction was carried out for 500 mg of 2-(bromomethyl)-1,3-difluorobenzene and 400 mg of sodium azide. *** No starting material was observed

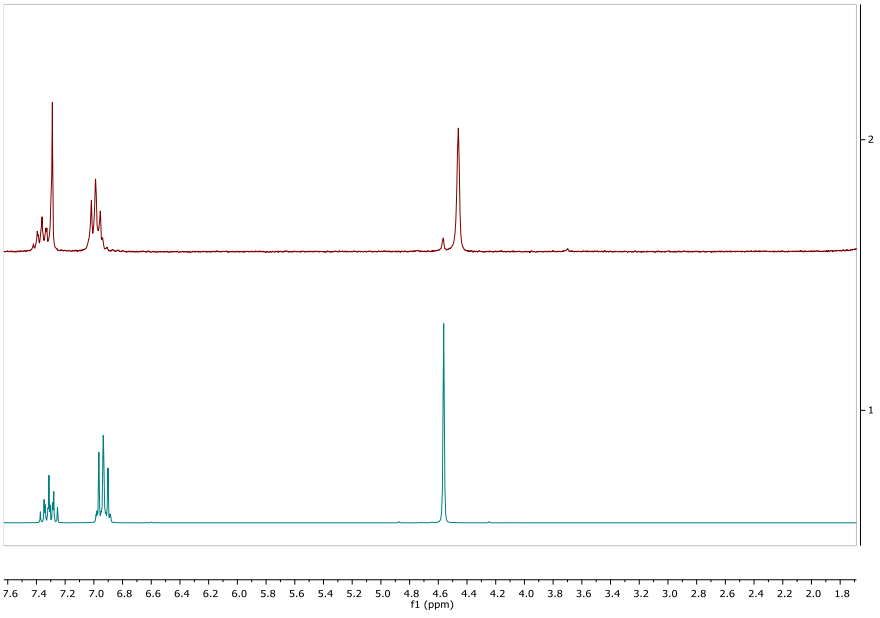


Figure 1. $^{1}$H-NMR spectrum of 2-(bromomethyl)-1,3-difluorobenzene (green) and a crude reaction mixture corresponding to entry 12 of table 1 (red).

### 3.3 Optimization of the tandem azidination-Huisgen cycloaddition sequential process

With the reaction conditions optimized for the first step of the reaction, our next goal was the optimization of the formation of the triazole compound **3.3b**. The Huisgen cycloaddition between the benzyl amide and methyl propiolate is a key step in this sequential synthesis, as

byproducts from the previous reaction as well as unreacted starting materials could alter the regioselectivity of the reaction. In order to exclusively obtain the 1,4 disubstituted 1,2,3 triazole ring, copper salts are used as catalyst of the reaction. Salts of copper I are the chemical species responsible for the catalysis of this reaction, however, copper II salts have been also used together with a reducing agent such as ascorbic acid to generate copper I species in situ. In table 2, we can observe the different conditions used and the results obtained.

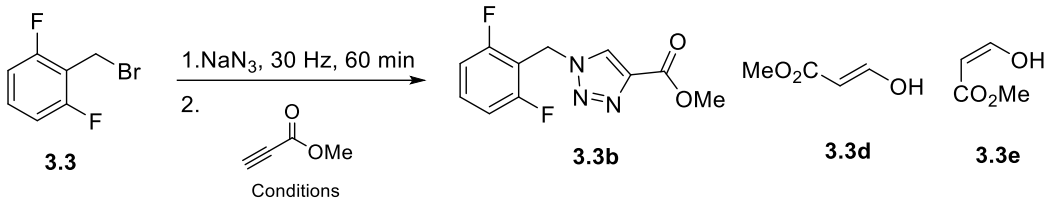


Scheme 5. One pot synthesis of triazole ester intermediate **3.3b**

| Entry | Copper Source | Reaction time | Ratio | Conversion* |
|---|---|---|---|---|
| | | | 3.3:3.3b:3.3d:3.3e | |
| 1 | Free catalyst | 60 min | | - |
| 2 | $CuSO_4$ (0.04 mmol) Ascorbic acid (0.05 mmol) | 60 min | | 85% |
| 3 | Catalyst Cu (I) A (0.05 mmol) | 60 min | 0:20:1:1 | 95% |
| 4 | Catalyst Cu (I) B 0.05 mmol) | 60 min | 0:10:1:1 | 90% |
| 5 | Cu powder (0.31 mmol) | 60 min | | 87% |
| 6 | Catalyst Cu (I) A (0.05 mmol) | 30 min | 1:23:2.2:1.5 | 96% |
| 7 | $CuSO_4$ (0.04 mmol) | 30 min | 0:2:6.1:1 | 60% |
| 8 | Cu powder (0.31 mmol) | 30 min | 0:25:1:1.2 | 100% |
| 9 | Catalyst Cu (I) A, 0.05 mmol | 15 min | 0:2:28:1:1 | 93% |
| 10 | Cu powder (0.31 mmol) | 15 min | 0:25:1:1.2 | 100% |
| 11 | Cu powder (0.15 mmol) | 15 min | 0:16.2:1:1.2 | 100% |
| 12 | Cu powder (0.08 mmol) | 15 min | 4.5:14.2:1:1.2 | 73% |

Table 2. different reaction conditions employed for the optimization of the triazole ring-A mixture of 100 mg (0.5 mmol) of 2-(bromomethyl)-1,3-difluorobenzene and 80 mg (1.2 mmol) of sodium azide, was subjected to ball-milling at 30 Hz using stainless one ball (size 15 mm) for 60 min. Then 05 ml (0.6 mmol) of methyl propiolate and the corresponding catalyst were added to the mixture and the mixture was further submitted to ball milling at the same parameter. Catalyst Cu (I) A: Tetrakis(Acetonitrile)Copper(I) Hexafluorophosphate. Catalyst Cu (I) B: Phenanthroline)bis(triphenylphosphine)copper(I) nitrate dichloromethane

We initially studied the formation of the triazole moiety in the absence of catalyst, but a poor conversion of 40% and the null regioselectivity encouraged us to add it. We then focused our attention on the addition of different copper catalysts on different oxidation states. Taking as a starting point the optimised conditions for the azide **3.3a** formation in the previous step, we then proceeded to add 1.2 equivalents of methyl propiolate and $CuSO_4$ in catalytic amount, together with sodium ascorbate to generate and regenerate the active Cu(I) catalytic species. The mixture was milled for 60 minutes, and we found to obtain an excellent regioselectivity and

an 85% conversion. However, $^{1}$H NMR analysis showed the formation of side products **3.3d** and **3.3e**, which were obtained by the Michael addition between methyl propiolate and water. With the idea in mind to improve the results obtained, we studied tetrakis(acetonitrile)copper(I) hexafluorophosphate, (phenanthroline)bis(triphenylphosphine)copper(I) nitrate dichloromethane and copper powder under the same reaction conditions. The use of Cu (I) and copper metal resulted in a greater product conversion (95%, 90% and 87% respectively) (entries 3-5). With this in hand, we studied different milling times and in the first place, we used tetrakis(acetonitrile)copper(I) hexafluorophosphate, copper sulphate/sodium ascorbate system and powder copper as catalyst, and the reaction was carried out by additional milling time of 30 and 15 min (entries 6-10). The proton NMR spectra of the reactions revealed in the first place that when using $CuSO_4$ as a catalyst and milling time was reduced from 60 to 30 minutes caused the yield decreased to 60% (entry 7). When using copper (I) as a catalyst, a small improvement in yield was observed. However full conversion of the azide **3.3a** to the triazole **3.3b** was not achieved in less than 60 minutes (entries 6 and 9). Finally, copper powder catalyst led to full conversion of the azide into the triazole. Additionally, the use of copper powder gave the best relationship between the desired products and side products (entries 8 and 10). Comparison between the crude obtained and 1-(2,6-difluorobenzyl)-1H-1,2,3-triazole-4-carboxylate can be observed in figure 2. Encouraged with the results obtained, we chose Cu powder as a catalyst due its easy removal and designed two additional experiments in which we decreased the load of the catalyst to 32% and 16 %. When the reaction was performed using a 16% load, lower conversion was observed (entry 12), and when the reaction was performed using a 32% load, a full conversion was observed, with also a slight increase of side products.

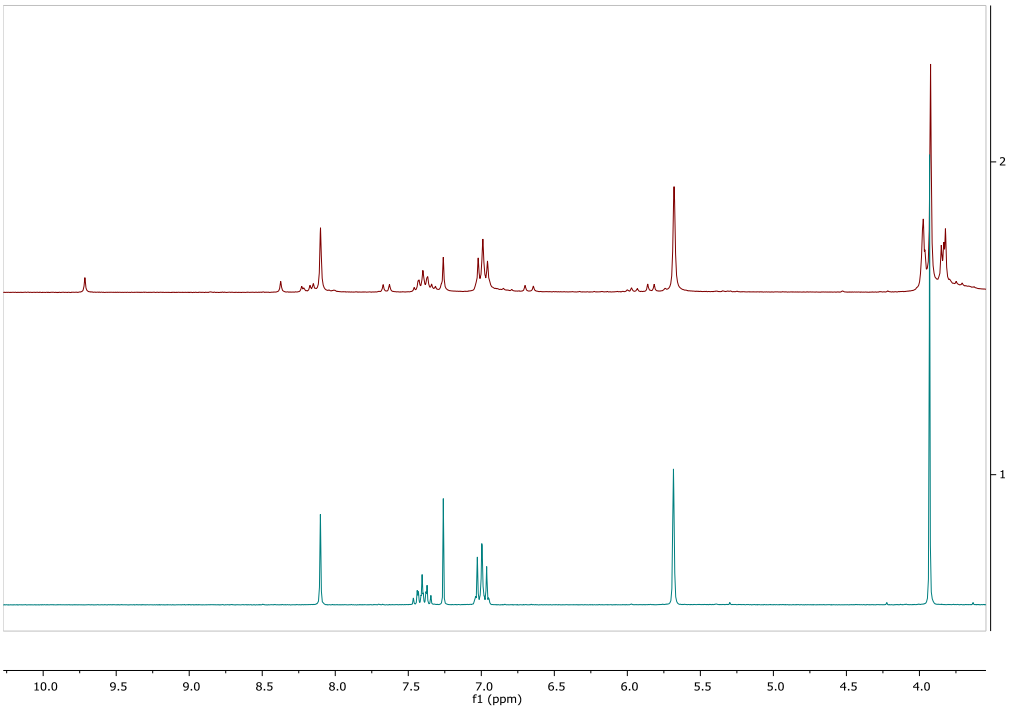


Figure 2. 1H-NMR spectrum of methyl 1-(2,6-difluorobenzyl)-1H-1,2,3-triazole-4-carboxylate (green) and a crude reaction mixture corresponding to entry 10 of table 2 (red).

## 3.4 Mechanochemical one-pot synthesis of rufinamide

The final step for the one pot synthesis of rufinamide was testing our optimized amide mechanochemical reaction sequentially with the azide **3.3a** and the triazole **3.3b** formation. Using the methodology previously described, we then proceeded to test the one pot mechanochemical synthesis of rufinamide **3.3c** and we managed to isolate a 40% yield in 3 steps, which implies more than a 70% yield in each individual step as a mean value (scheme 14).

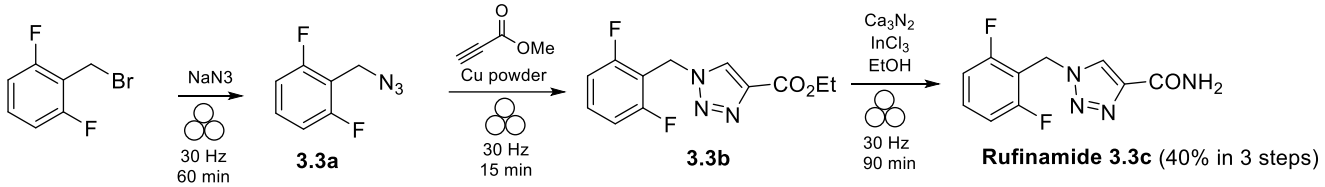


Scheme 14. Mechanochemical one-pot synthesis of rufinamide

## 3.5 Green metrics of the one pot synthesis of rufinamide

In recent years. In order to address the eco-efficiency of synthetic processes, several parameters have been taken into consideration besides yield. Some of these parameters are atom economy (AE), Reaction mass efficiency (RME), the environmental factor (E-factor) and process mass intensity (PMI). Atom economy can be defined as the molecular weight of desired product relative to the sum of all the molecular weights of all substances produced in a stoichiometric equation[35]. RME is defined as the total mass of isolated products relative to the total mass of reactants and incorporates stoichiometry and mass to the metrics, providing a bigger picture than AE[36]. Additionally, E-factor can be calculated as a total mass of waste generated in a technological or industrial process per unit of product. This means that low E-factor values are desired as they imply low quantities of waste produced in a process. However, one of the main limitations of E-factor is that it does not take into consideration the hazards or the environmental risk of the potential waste[37]. Finally PMI can be defined as the total input mass in a process relative to the mass of isolated product[38]. These parameters are complementary and evaluate the global efficiency of the process and are calculated as the ration of mass of waste per mass of product[39,40].

$$AE = \frac{Molecular\ weight\ of\ desired\ products}{Molecular\ weights\ of\ all\ product\ produced\ stoichiometrically} \times 100$$

$$RME = \frac{mass\ of\ isolated\ products}{mass\ of\ reactants} \times 100$$

$$E - factor = \frac{mass\ of\ total\ waste}{mass\ of\ isolated\ product}$$

$$PMI = \frac{total\ mass\ in\ process}{mass\ of\ isolated\ product}$$

Figure 3. Equations used to calculate E-factor and PMI.

To address the sustainability of this process, we calculated the values for these two parameters and compared them with the two most efficient solution synthesis described to date[41,42] (table

5). Our calculated value for the 3-step mechanochemical process for the synthesis of rufinamide was 18 for the overall process, which is significantly less than the industrial synthetic processes (25-100). In addition, PMI is an important mass-based metric for evaluating an individual or sequence of reactions, that can be used to study how much mass is used to synthesise a molecule. This process exhibited an excellent PMI value of 10, which supports than the mechanochemical synthetic approach for APIs is environmentally beneficial. It is also worth taking into consideration that the mechanochemical method developed did not require column chromatography since the product is easily purified by recrystallisation.

With regard to other environmental and economic factors such as external heating or reaction times, in selected patents, almost all processes required from external heating, and all of them required the use of solvents, while our process did not. This also represents a significant advance in the environmental sustainability of the synthesis of rufinamide.

| Route | Overall yield (%) | Atom economy (%) | RME (%) | E factor | PMI (g/g) | Reaction time (h) | Heating time (h) |
|---|---|---|---|---|---|---|---|
| Mechanochemistry | 40 | 34 | 9.5 | 18 | 10 | 2.2 | 0 |
| Batch synthesis in solution WO2014121383A1 | 64 | 35 | 22 | 67 | 33 | 35.1 | 15 |
| Batch synthesis in solution WO2010/043849 | 32 | 67 | 15 | a | 72 | 40 | 30 |

Table 5. Green metrics comparison between the mechanochemical one pot synthesis and two different industrial patents. E factor= Total waste (kg) / Total product (kg). PMI = process mass intensity. Green metrics was calculated employing the ACS tool. [a] Cannot be calculated with the available data.

## 4.0 Experimental

### 4.1 General procedure for the synthesis of primary amides

The suitable ester (1 mmol), calcium nitride (3 mmol), Indium trichloride (0.4 mmol) and EtOH (0.3 ml) were milled at a frequency of 30 Hz for 90 minutes using a 20 ml stainless steel jar with a 15 mm stainless steel ball. Subsequently, the reaction mixture was suspended in ethyl acetate (10 ml) and water (5 ml) was added. The aqueous layer was extracted with ethyl acetate (10 ml) three times, and the organic extracts combined together, dried with $Na_2SO_4$ and concentrated in vacuo. The correspondent solid was washed with petroleum ether (5 ml) to yield their correspondent amide.

**3-Fluorobenzamide (3.2a)**

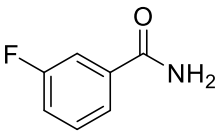


**$^1$H NMR** (250 MHz, DMSO-$d_6$) δ 8.07 (s, 1H), 7.77 – 7.61 (m, 2H), 7.56-7.46 (m, 2H), 7.44 – 7.32 (m, 1H). (NMR data consistent with values in literature)[43]

**$^{13}$C NMR** (63 MHz, DMSO-$d_6$) δ 166.5 (d, J = 2.5 Hz), 162.0 (d, J = 245.3 Hz), 136.7 (d, J = 6.9 Hz), 130.4 (d, J = 7.7 Hz), 123.6 (d, J = 2.8 Hz), 118.2 (d, J = 21.4 Hz), 114.2 (d, J = 22.8 Hz). (NMR data consistent with values in literature)[43]

**Benzamide (3.2b)**

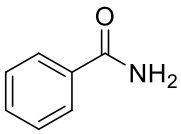


**$^1$H NMR** (250 MHz, DMSO-$d_6$) δ 8.00 (s, 1H), 7.96 – 7.81 (m, 2H), 7.61 – 7.33 (m, 4H). (NMR data consistent with values in literature)[43]

**$^{13}$C NMR** (63 MHz, DMSO-$d_6$) δ 168.3, 134.6, 131.6, 128.6, 127.8. (NMR data consistent with values in literature)[43]

**4-Methyl benzamide (3.2c)**

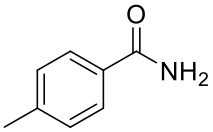


**$^1$H NMR** (300 MHz, $CDCl_3$) δ 7.84 – 7.65 (m, 2H), 7.35 – 7.21 (m, 2H), 6.04 (s, 2H), 2.43 (s, 3H). (NMR data consistent with values in literature)[43]

**$^{13}$C NMR** (75 MHz, $CDCl_3$) δ 169.5, 142.6, 130.5, 129.3, 127.4, 21.5. (NMR data consistent with values in literature)[43]

**Cinnamide (3.2d)**

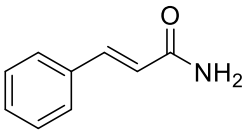


**$^1$H NMR** (300 MHz, DMSO-$d_6$) δ 7.62 – 7.51 (m, 3H), 7.48 – 7.32 (m, 4H), 7.13 (s, 1H), 6.62 (d, *J* = 15.9 Hz, 1H). (NMR data consistent with values in literature)[34]

**$^{13}$C NMR** (75 MHz, DMSO-$d_6$) δ 167.2, 139.7, 135.4, 129.9, 129.4, 128.0, 122.8. (NMR data consistent with values in literature)[34]

**2,2-Diethoxyacetamide (3.2e)**

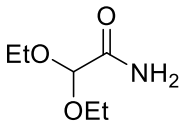


**$^1$H NMR** (300 MHz, $CDCl_3$) δ 6.48 (s, 1H), 6.15 (s, 1H), 4.75 (s, 1H), 3.71 – 3.47 (m, 4H), 1.19 (t, *J* = 7.1 Hz, 6H). (NMR data consistent with values in literature)[44]

**$^{13}$C NMR** (75 MHz, $CDCl_3$) δ 170.7, 98.3, 62.4, 15.1. (NMR data consistent with values in literature)[44]

**Palmitamide (3.2f)**

**$^1$H NMR** (300 MHz, $CDCl_3$) δ 5.47 (s, 2H), 2.22(t, J = 7.6 Hz, 2H), 1.63 (p, *J* = 7.4 Hz, 2H), 1.25 (s, 24H), 0.94 – 0.82 (m, 3H). (NMR data consistent with values in literature)[45]

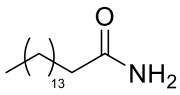


**$^{13}$C NMR** (75 MHz, $CDCl_3$) δ 175.7, 36.0, 31.9, 29.7, 29.7, 29.7, 29.7, 29.5, 29.4, 29.3, 25.6, 22.7, 14.1. (NMR data consistent with values in literature)[45]

**Ciclohexane carboxamide (3.2g)**

**$^1$H NMR** (250 MHz, $CDCl_3$) δ 5.56 (s, 2H), 2.19 (tt, *J* = 11.5, 3.5 Hz, 1H), 1.89 – 1.56 (m, 5H), 1.48 – 1.04 (m, 5H). (NMR data consistent with values in literature)[43]

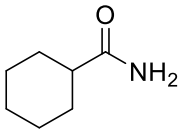


**$^{13}$C NMR** (75 MHz, $CDCl_3$) δ 179.0, 44.9, 29.8, 25.8, 25.8. (NMR data consistent with values in literature)[34]

**Isonicotinamide (3.2h)**

**$^1$H NMR** (300 MHz, $CDCl_3$) δ 8.72 (s, 2H), 8.25 (s, 1H), 7.81 – 7.75 (m, 2H), 7.73 (s, 1H). (NMR data consistent with values in literature)[43]

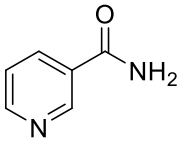


**$^{13}$C NMR** (75 MHz, $CDCl_3$) δ 166.3, 150.2, 141.3, 121.5. (NMR data consistent with values in literature)[46]

**Nicotinamide (3.2i)**

**$^1$H NMR** (300 MHz, DMSO-$d_6$) δ 9.09 (dd, *J* = 2.4, 0.9 Hz, 1H), 8.75 (dd, *J* = 4.8, 1.7 Hz, 1H), 8.26 (ddd, *J* = 7.9, 2.3, 1.7 Hz, 1H), 8.23 – 8.15 (m, 1H), 7.66 (s, 1H), 7.55 (ddd, *J* = 7.9, 4.8, 0.9 Hz, 1H). (NMR data consistent with values in literature)[43]

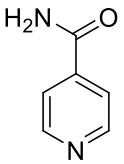


**$^{13}$C NMR** (75 MHz, DMSO-$d_6$) δ 166.9, 152.4, 149.2, 135.6, 130.1, 123.9. (NMR data consistent with values in literature)[43]

**Thiophene-2-carboxamide (3.2j)**

**$^1$H NMR** (250 MHz, DMSO-$d_6$) δ 7.99 (s, 1H), 7.81 – 7.70 (m, 2H), 7.41 (s, 1H), 7.14 (dd, *J* = 4.9, 3.7 Hz, 1H). (NMR data consistent with values in literature)[43]

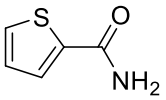


**$^{13}$C NMR** (63 MHz, DMSO-$d_6$) δ 163.3, 140.7, 131.4, 129.0, 128.3. (NMR data consistent with values in literature)[43]

**Phenylacetamide (3.2k)**

**$^1$H NMR** (300 MHz, $CDCl_3$) δ 7.35 – 7.14 (m, 5H), 5.90 (s, 1H), 5.39 (s, 1H), 3.50 (s, 2H). (NMR data consistent with values in literature)[34]

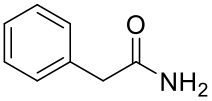

**$^{13}$C NMR** (75 MHz, $CDCl_3$) δ 173.8, 134.9, 129.4, 129.1, 127.4, 43.3. (NMR data consistent with values in literature)[34]

**Phenylalaninamide (3.2l)**

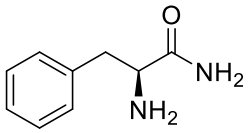

**$^{1}$H NMR** (300 MHz, MeOD) δ 7.35 – 7.19 (m, 5H), 3.63 – 3.53 (m, 1H), 3.04 (dd, *J* = 13.4, 5.9 Hz, 1H), 2.81 (dd, *J* = 13.4, 7.6 Hz, 1H).

**$^{13}$C NMR** (75 MHz, MeOD) δ 178.1, 137.5, 129.1, 128.2, 126.4, 56.0, 41.1.

**$[\alpha]_D^{25}$** (0.2 g/100 mL, $H_2O$ + 3 drops of 35% HCl) + 22.4. Lit.+ 20.0 (for the hydrochloride salt, 2 g/100 mL, $H_2O$).

**Methionamide (3.2m)**

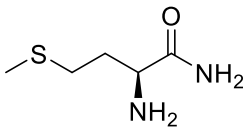

**$^{1}$H NMR** (300 MHz, MeOD) δ 3.46 (dd, *J* = 7.5, 5.6 Hz, 1H), 2.59 (dd, *J* = 8.2, 7.1 Hz, 2H), 2.11 (s, 3H), 2.02 – 1.92 (m, 1H), 1.89 – 1.77 (m, 1H). . (NMR data consistent with values in literature)[47]

**$^{13}$C NMR** (75 MHz, MeOD) δ 178.7, 53.6, 34.4, 29.8, 13.8. (NMR data consistent with values in literature)[47]

**$[\alpha]_D^{25}$** (0.005 g/100 mL, H2O + 3 drops of 35% HCl) = +6.6

**2-(Piperidin-1-yl)acetamide (3.2n)**

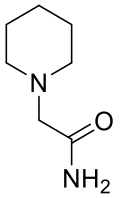

**$^{1}$H NMR** (250 MHz, $CDCl_3$) δ 7.13 (br s, 1H), 6.02 (br s, 1H), 2.93 (t, J = 1.1 Hz, 2H), 2.45 (t, J = 5.2 Hz, 4H), 1.57 (p, J = 5.5 Hz, 4H), 1.43 (q, J = 5.8 Hz, 2H). (NMR data consistent with values in literature)[48]

**$^{13}$C NMR** (63 MHz, $CDCl_3$) δ 174.28, 62.40, 55.10, 26.28, 23.79. (NMR data consistent with values in literature)[48]

**Tert-butyl (S)-(1-((2-amino-2-oxoethyl)amino)-1-oxo-3-phenylpropan-2-yl)carbamate (3.2o)**

**IR** ($cm^{-1}$): 3298, 3072, 2977, 1664.

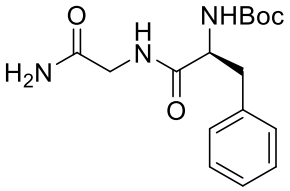

**$^{1}$H NMR** (250 MHz, $CDCl_3$, major conformer) δ 7.36–7.21 (m, 5H), 7.07 (br s, 1H, NH), 6.53 (br s, 1H), 5.90 (br s, 1H), 5.31 (br s, 1H), 4.37 (q, 1H, J = 7.0 Hz), 3.88 (m, 2H), 3.08 (m, 2H), 1.37 (s, 9H) ppm.

**$^{13}$C NMR** (62.5 MHz, $CDCl_3$) δ 172.6, 1721, 156.3, 136.8, 129.6, 129.2, 127.5, 81.1, 56.7, 43.1, 38.4, 28.6 ppm.

**$[\alpha]^{D}_{25}$** = +1.37 (c = 0.006 g/100 mL, $CHCl_3$).

**Elemental analysis**: Anal. Calcd. for $C_{16}H_{23}N_3O_4$, C, 59.80; H, 7.21; N, 13.08. Found: C, 59.45; H, 7.02; N, 12.79.

**Tert-butyl (S)-(1-((2-amino-2-oxoethyl)amino)-3-(1H-indol-3-yl)-1-oxopropan-2-yl)carbamate (3.2p).**

**IR** ($cm^{-1}$): 3296, 3066, 2976, 1655**.**

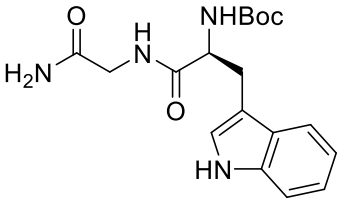

**$^1$H NMR** (250 MHz, $CDCl_3$) δ 9.00 (br s, 1H), 7.57 (d, J = 7.7 Hz, 1H), 7.31 (d, J = 8.6 Hz, 1H), 7.19−7.03 (m, 3H), 6.99 (s, 1H), 6.42 (br s, 1H), 6.25 (br s, 1H), 5.58 (br s, 1H), 4.44 (q, J = 6.5 Hz, 1H), 3.62 (br s, 2H), 1.39 (s, 9H).

**$^{13}$C NMR** (62.5 MHz, $CDCl_3$) δ 173.4, 172.8, 156.4, 136.7, 127.7, 124.1, 122.5, 119.94, 118.9, 112.0, 110.1, 81.0, 56.1, 43.0, 28.7 ppm.

**$[\alpha]_D^{25}$** = +6.16 (c = 0.006 g/100mL, $CHCl_3$).

**Elemental analysis**: Anal. Calcd. for $C_{18}H_{24}N_4O_4$, C, 59.99; H, 6.71; N, 15.55. Found: C, 59.72; H, 6.59; N, 15.31**.**

**Tert-butyl (S)-(1-((2-amino-2-oxoethyl)amino)-1-oxopropan-2-yl)carbamate (3.2q)**

**IR** ($cm^{-1}$): 3297, 2977, 1656.

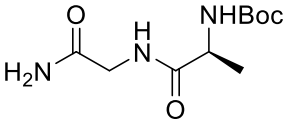

**$^1$H NMR** (250 MHz, $CDCl_3$ major conformer) δ 7.48 (br t, J = 5.0 Hz, 1H), 6.95 (br s, 1H), 6.26 (br s, 1H), 5.55 (br d, J = 5.0 Hz, 1H), 4.18 (m, 1H), 4.00 (dd, 2H, J = 17.0 and 5.5 Hz), 1.44 (s, 9H), 1.38 (d, 3H, J = 7.0 Hz).

**$^{13}$C NMR** (62.5 MHz, $CDCl_3$) δ 174.2, 172.6, 156.4, 80.9, 51.1, 43.1, 28.7, and 18.3.

**$[\alpha]^D_{25}$** = −11.25 (c = 0.004 g/ 100 mL, $CHCl_3$).

**Elemental analysis**: Anal. Calcd for $C_{10}H_{19}N_3O_4$: C, 48.97; H, 7.81; N, 17.13. Found: C, 48.68; H, 7.62; N, 16.97.

**3-(2-Hydroxyphenyl) propenamide (3.2r)**

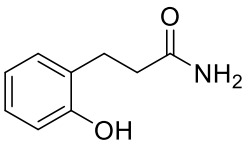

**$^1$H NMR** (250 MHz, DMSO-$d_6$) δ 9.36 (s, 1H), 7.33 (s, 1H), 7.11 – 6.92 (m, 2H), 6.85 – 6.64 (m, 3H), 2.72 (t, *J* = 7.3 Hz, 2H), 2.33 (t, *J* = 7.3 Hz, 2H). (NMR data consistent with values in literature) [34]

**$^{13}$C NMR** (63 MHz, DMSO-$d_6$) δ 174.5, 155.4, 130.0, 128.0, 127.3, 119.2, 115.3, 35.5, 25.9. (NMR data consistent with values in literature)[34]

**4.2 Procedure for the synthesis of azide 3.3a**

A 25 mL stainless steel jar was charged with a powdered mixture of 100 mg (0.5 mmol) of 2-(bromomethyl)-1,3-difluorobenzene and 80 mg (1.2 mmol) of sodium azide (in a 1:2 stoichiometric ratio) and the content was milled for 60 minutes at 30 Hz with a single 15 mm diameter stainless-steel ball. The product was recovered from the jar with a small amount of DCM, which was concentrated to dryness.

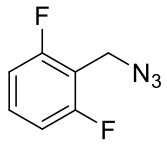


**$^1$H NMR** (250 MHz, $CDCl_3$) δ 7.32 (m, 1H), 6.96 (t, J = 7.8 Hz, 2H), 4.43 (s, 2H). (NMR data consistent with values in literature)[49]

**4.3 Procedure for the synthesis of methyl 1-(2,6-difluorobenzyl)-1H-1,2,3-triazole-4-carboxylate 3.3b**

A cylindrical 25 mL stainless steel jar was charged with a powdered mixture of 100 mg (0.5 mmol) of 2-(bromomethyl)-1,3-difluorobenzene and 80 mg (1.2 mmol) of sodium azide (in a 1:2 stoichiometric ratio) and the content was milled in a cylindrical 25 mL stainless steel jar with a single 15 mm diameter stainless-steel ball. Milling was performed at 30 Hz for 60 min, the jar was opened and 0.6 mmol (0.5 ml) of methyl propiolate and powdered copper (10 mg) was added to the crude mixture and ball milling was continued at 30 Hz for 15 minutes. The reaction mixture was removed from the jar with a small amount of methanol and concentrated to dryness.

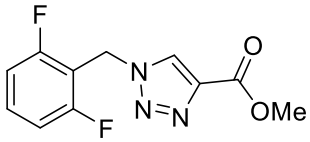


**$^1$H NMR** (250 MHz, $CDCl_3$) δ 8.10 (s, 1H), 7.50 – 7.32 (m, 1H), 7.00 (t, J = 7.9 Hz, 2H), 5.68 (s, 2H), 3.93 (s, 3H). (NMR data consistent with values in literature)[50]

**4.4 Procedure for the one pot synthesis of rufinamide 3.3c**

A mixture of 0.05 mmol (100 mg) of 2-(bromomethyl)-1,3-difluorobenzene and 1.2 mmol (80 mg) of sodium azide were milled at a frequency of 30 Hz for 60 minutes using a 20 ml stainless steel jar with a 15 mm stainless steel ball. Subsequently, 0.6 mmol (0.05 ml) of methyl propiolate and 0.08 mmol (10 mg) of copper powder were added to the mixture and milled at 30 Hz for 15 minutes. Afterwards, 1.4 mmol (215 mg) of calcium nitride, 0.24 mmol (53 mg) of Indium trichloride an 0.3 ml of ethanol were added to the jar and milled at 30 Hz for 90 minutes. The reaction mixture was suspended in ethyl acetate 10 ml and water (5 ml) was added. The two layers were separated, and the aqueous phase was extracted with ethyl acetate (10 ml) 3 times. All organic extracts were combined, dried with $Na_2SO_4$ and concentrated in vacuo to yield rufinamide as a white solid (40% yield).

**IR** ($cm^{-1}$): 3391 ($NH_2$), 3135, 2307, 1652 ($CONH_2$), 1624, 1470, 1233, 1031, 793.

**$^1$H NMR** (500 MHz, DMSO-d6) δ 8.56 (s, 1H), 7.87 (s, 1H), 7.61 – 7.46 (m, 2H), 7.20 (t, J = 8.1 Hz, 2H), 5.73 (s, 2H). (NMR data consistent with values in literature)[24].

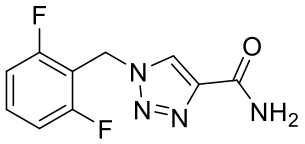

**$^{13}$C NMR** (126 MHz, DMSO-d6) δ, 161.34, 160.8 (dd, J1 = 249.9 Hz, J2 = 8.1 Hz), 142.83, 131.9 (t. J = 10.3 Hz), 126.84, 112.0 (d, J = 19.6 Hz), 111.08 (t, J = 20.1 Hz), 41.2 (t, J = 4.4 Hz). (NMR data consistent with values in literature)[24].

### 4.5 Green metrics for mechanochemistry one pot synthesis of rufinamide

Calculations were performed with The ACS Green Chemistry research tools. They can be found under https://www.acs.org/content/acs/en/greenchemistry/research-innovation/tools-for-green-chemistry.html

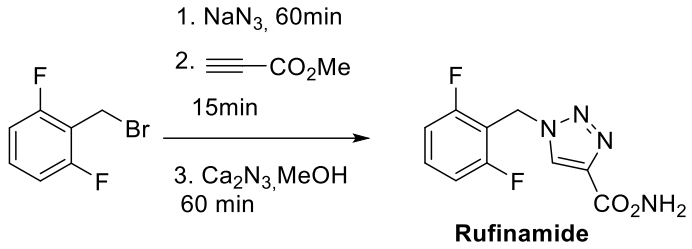


**Rufinamide**

Reaction stoichiometry:

$$C_7H_5BrF_2 + NaN_3 + C_4H_4O_2 + Cu + Ca_3N_2 + 6\,CH_3OH \longrightarrow C_{10}H_8F_2N_4O + 3\,Ca(MeO)_2 + H_3N + CH_3OH + NaBr$$

207,02 65,01 84,02 62 148 32 238 306 17 32 102

| Reagents and reactants | Calculated stoichiometric factor | Experimental stoichiometric factor | MW | Calculated stoichiometric factor x MW | Experimental coefficient x MW |
|---|---|---|---|---|---|
| $C_7H_5BrF_2$ | -1 | -1 | 207 | -207 | -207 |
| $NaN_3$ | -1 | -2.4 | 65 | -65 | -156 |
| $C_4H_4O_2$ | -1 | -1.2 | 84 | -84 | 100.8 |
| Cu | 0 | | 62 | 0 | |
| $Ca_3N_2$ | -1 | -3 | 148 | -148 | -444 |
| $CH_3OH$ | -6 | -3 | 32 | -192 | -96 |
| $C_{10}H_8F_2N_4O$ | 1 | 0.4 | 238 | 238 | 95.4 |
| $Ca(MeO)_2$ | 3 | 9 | 102 | 306 | 918 |
| $NH_3$ | 1 | 3 | 17 | 17 | 51 |
| $CH_3OH$ | 1 | 0.5 | 32 | 32 | 16 |
| NaBr | 1 | 1 | 102 | 102 | 102 |

**Green metrics for mecanochemical synthesis**

- **Atom economy** = 238/696 = 34%
- **RME**= 95.4/1000 = 9.5 %
- **E factor** (mass of waste/ mass of product) = = 1071/ 95.4 = 11.2 (Assuming 90% solvent recovery and excluding water).

**Green metrics for WO2014/121383 A1 patent**

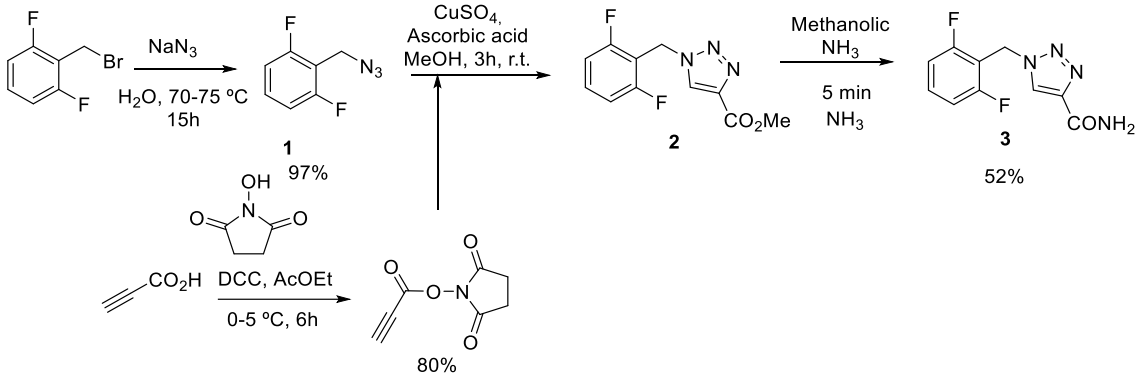


Reaction stoichiometry:

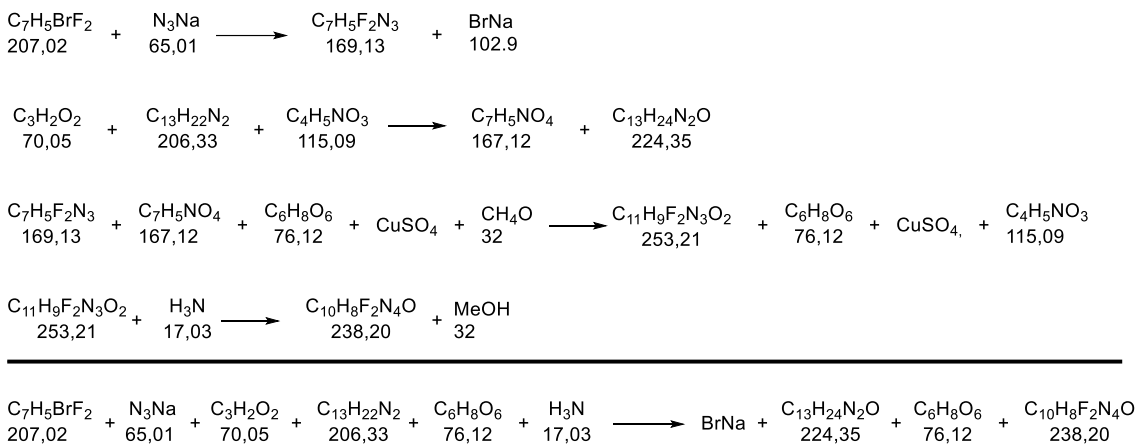


| Reagents and reactants | Calculated stoichiometric factor | Experimental stoichiometric factor | MW | Calculated Stoichiometric factor x MW | Experimental coefficient x MW |
|---|---|---|---|---|---|
| $C_7H_5BrF_2$ | -1 | -1 | 207 | -207 | -207 |
| $N_3Na$ | -1 | -1.2 | 65 | -65 | -78 |
| $C_7H_5F_2N_3$ | 0 | | 169 | 0 | |
| NaBr | +1 | +1 | 103 | 103 | 103 |
| $C_3H_2O_2$ | -1 | -1 | 70 | -70 | -70 |
| $C_{13}H_{22}N_2$ | -1 | -1 | 206 | -206 | -206 |

| | | | | | |
|---|---|---|---|---|---|
| $C_4H_9NO_3$ | -1 | -1.5 | 115 | -115 | 172 |
| $C_7H_5NO_4$ | 0 | | 167 | 0 | 167 |
| $C_{13}H_{24}N_2O$ | +1 | +1 | 224 | 224 | 224 |
| $C_6H_8O_6$ | 0 | 0.1 | 76 | 0 | |
| $CuSO_4$ | 0 | 0.1 | | 0 | |
| $CH_4O$ | 0 | | 32 | 0 | |
| $C_{11}H_9F_2N_3O_2$ | 0 | 0 | 253 | 253 | |
| $NH_3$ | -1 | -1.5 | 17 | -17 | 25.5 |
| $C_{10}H_8F_2N_4O$ | +1 | 0.73 | 238 | 238 | 152 |
| Reactión solvents | Reaction 1 | Reaction 2 | Reaction 3 | Reaction 4 | Total |
| $H_2O$ | 20.3 x 207 | | | | |
| AcOEt | | 8.7 x 70 | | | |
| MeOH | | | 5 x 169 | 10 x 253 | |
| Mass waste | 5481 | 609 | 845 | 2530 | 9465 |

Data have been calculated for examples 1, 3, 4 and 8 of the reference patent. 20.3 g $H_2O$/g; 8.7 g ACOEt/g of propiolic acid 5 g MeOH/g of **1**; 10 g MeOH/g of **2**

**Green metrics for WO2014/121383 A1 patent**

- Atom economy = 238/680 = 35 %
- RME = 152/673 = 22 %
- E factor (mass of waste /mass of product) = 9465 /152 = 62

**Green metrics for WO 2010/043849 A1 patent**

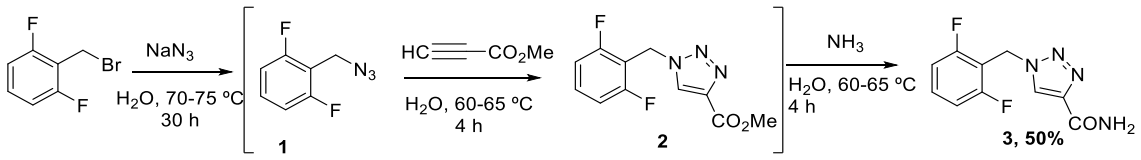


Reaction stoichiometry:

$$C_7H_5BrF_2 + NaN_3 + C_4H_4O_2 + NH_3 \longrightarrow C_{10}H_8F_2N_4O + CH_3OH + NaBr$$

| Reagents and Reactants | Calculated stoichiometric factor | Experimental stoichiometric factor | MW | Calculated Stoichiometric factor x MW | Experimental Coeficiente experimental x MW |
|---|---|---|---|---|---|

| | | | | | |
|---|---|---|---|---|---|
| $C_7H_5BrF_2$ | -1 | | 207 | -207 | -207 |
| $NaN_3$ | -1 | -1.2 | 65 | -65 | -78 |
| $C_4H_4O_2$ | -1 | -1.2 | 84 | -84 | -100 |
| $NH_3$ | 1 | 25 | 17 | 17 | 425 |
| $C_{10}H_8F_2N_4O$ | 1 | | 238 | 238 | 119 |
| $NH_3$ | 1 | 24 | 17 | 17 | 408 |
| $CH_3OH$ | 1 | 1.2 | 32 | 32 | 38 |
| NaBr | 1 | 1 | 102 | 102 | 102 |
| $H_2O$ | | 16 g / g | 18 | 288 | 288 |

Data have been calculated for one-pot preparation examples 1 of the reference patent[2]. 16 g $H_2O$ for g of 2,6-difluorobenzylbromide.

**Green metrics for WO 2010/043849 A1 patent**

- Atom economy = 238/373 = 63 %
- RME = 119/810 = 15 %

## 5.0 References


(1) Pappalardo, L. W.; Black, J. A.; Waxman, S. G. Sodium Channels in Astroglia and Microglia Graphical Abstract. *Glia* **2016**, *64* (10), 1628–1645. https://doi.org/10.1002/glia.22967.Sodium.

(2) Bagheri, S.; Haddadi, R.; Saki, S.; Kourosh-Arami, M.; Komaki, A. The Effect of Sodium Channels on Neurological/Neuronal Disorders: A Systematic Review. *Int. J. Dev. Neurosci.* **2021**, *81* (8), 669–685. https://doi.org/10.1002/jdn.10153.

(3) Mechano-Chemical Reaction. *IUPAC Compend. Chem. Terminol.* **2008**, *889*, 7141. https://doi.org/10.1351/goldbook.mt07141.

(4) Tan, D.; Friščić, T. Mechanochemistry for Organic Chemists: An Update. *European J. Org. Chem.* **2018**, *2018* (1), 18–33. https://doi.org/10.1002/ejoc.201700961.

(5) James, S. L.; Adams, C. J.; Bolm, C.; Braga, D.; Collier, P.; Friščic, T.; Grepioni, F.; Harris, K. D. M.; Hyett, G.; Jones, W.; Krebs, A.; Mack, J.; Maini, L.; Orpen, A. G.; Parkin, I. P.; Shearouse, W. C.; Steed, J. W.; Waddell, D. C. Playing with Organic Radicals as Building Blocks for Functional Molecular Materials. *Chem. Soc. Rev.* **2012**, *41* (1), 413–447. https://doi.org/10.1039/c1cs15171a.

(6) Takacs, L. The Historical Development of Mechanochemistry. *Chem. Soc. Rev.* **2013**, *42* (18), 7649–7659. https://doi.org/10.1039/c2cs35442j.

(7) Leonardi, M.; Villacampa, M.; Menéndez, J. C. Multicomponent Mechanochemical Synthesis. *Chem. Sci.* **2018**, *9* (8), 2042–2064. https://doi.org/10.1039/c7sc05370c.

(8) Raston, C. L.; Scott, J. L. Chemoselective , Solvent-Free Aldol Condensation Reaction. **2000**, No. April, 49–52. https://doi.org/10.1039/a907688c.

(9) Balema, V. P.; Wiench, J. W.; Pruski, M.; Pecharsky, V. K. Mechanically Induced Solid-State Generation of Phosphorus Ylides and the Solvent-Free Wittig Reaction. **2002**, 6244–6245.

(10) Jörres, M.; Mersmann, S.; Raabe, G.; Bolm, C. Organocatalytic Solvent-Free Hydrogen Bonding-Mediated Asymmetric Michael Additions under Ball Milling Conditions. *Green Chem.* **2013**, *15* (3), 612–616. https://doi.org/10.1039/c2gc36906k.

(11) Schmidt, R.; Stolle, A.; Ondruschka, B. Aromatic Substitution in Ball Mills: Formation of Aryl Chlorides and Bromides Using Potassium Peroxomonosulfate and NaX. *Green Chem.* **2012**, *14* (6), 1673–1679. https://doi.org/10.1039/c2gc16508b.

(12) Jiang, Z.; Li, Z.; Yu, J.; Su, W. Liquid-Assisted Grinding Accelerating: Suzuki − Miyaura Reaction of Aryl Chlorides under High-Speed Ball-Milling Conditions. **2016**, *3* (Table 1), 9–15. https://doi.org/10.1021/acs.joc.6b01938.

(13) Zhu, X.; Liu, J.; Chen, T.; Su, W. Mechanically Activated Synthesis of (E)-Stilbene Derivatives by High-Speed Ball Milling. *Appl. Organomet. Chem.* **2012**, *26* (3), 145–147. https://doi.org/10.1002/aoc.2827.

(14) Hernández, J. G.; Turberg, M.; Schiffers, I.; Bolm, C. Mechanochemical Strecker Reaction: Access to α-Aminonitriles and Tetrahydroisoquinolines under Ball-Milling Conditions. *Chem. - A Eur. J.* **2016**, *22* (41), 14513–14517.

https://doi.org/10.1002/chem.201603057.

(15) Polindara-García, L. A.; Juaristi, E. Synthesis of Ugi 4-CR and Passerini 3-CR Adducts under Mechanochemical Activation. *European J. Org. Chem.* **2016**, *2016* (6), 1095–1102. https://doi.org/10.1002/ejoc.201501371.

(16) Estévez, V.; Villacampa, M.; Menéndez, J. C. Three-Component Access to Pyrroles Promoted by the CAN–Silver Nitrate System under High-Speed Vibration Milling Conditions: A Generalization of the Hantzsch Pyrrole Synthesis. *Chem. Commun.* **2013**, *49* (6), 591–593. https://doi.org/10.1039/c2cc38099d.

(17) Arroyo, S. Rufinamide. *Neurotherapeutics* **2007**, *4* (1), 155–162. https://doi.org/10.1016/j.nurt.2006.11.006.

(18) Padmaja, R. D.; Chanda, K. A Short Review on Synthetic Advances toward the Synthesis of Rufinamide, an Antiepileptic Drug. *Org. Process Res. Dev.* **2018**, *22* (4), 457–466. https://doi.org/10.1021/acs.oprd.7b00373.

(19) Cho, J. H.; Park, C. W.; Ohk, T. G.; Moon, J. B.; Shin, M. C.; Won, M. H. Rufinamide Pretreatment Attenuates Ischemia–Reperfusion Injury in the Gerbil Hippocampus. *Neurol. Res.* **2017**, *39* (11), 941–952. https://doi.org/10.1016/j.resuscitation.2017.08.215.

(20) Yu, H.; He, B.; Han, X.; Yan, T. Rufinamide (RUF) Suppresses Inflammation and Maintains the Integrity of the Blood-Brain Barrier during Kainic Acid-Induced Brain Damage. *Open Life Sci.* **2021**, *16* (1), 845–855. https://doi.org/10.1515/biol-2021-0090.

(21) Chen, B. H.; Ahn, J. H.; Park, J. H.; Song, M.; Kim, H.; Lee, T. K.; Lee, J. C.; Kim, Y. M.; Hwang, I. K.; Kim, D. W.; Lee, C. H.; Yan, B. C.; Kang, I. J.; Won, M. H. Rufinamide, an Antiepileptic Drug, Improves Cognition and Increases Neurogenesis in the Aged Gerbil Hippocampal Dentate Gyrus via Increasing Expressions of IGF-1, IGF-1R and p-CREB. *Chem. Biol. Interact.* **2018**, *286* (January), 71–77. https://doi.org/10.1016/j.cbi.2018.03.007.

(22) Bureau, I. PCT. **2012**, No. 12.

(23) Borukhova, S.; Noël, T.; Metten, B.; Devos, E.; Hessel, V. Solvent- and Catalyst-Free Huisgen Cycloaddition to Rufinamide in Flow with a Greener, Less Expensive Dipolarophile. *ChemSusChem* **2013**, *6* (12), 2220–2225. https://doi.org/10.1002/cssc.201300684.

(24) Meena, D. R.; Rao, R. N.; Maiti, B.; Chanda, K. Novel Cu(I)-Catalyzed One-Pot Multicomponent Synthesis of the Antiepileptic Drug Rufinamide. *Res. Chem. Intermed.* **2017**, *43* (8), 4711–4717. https://doi.org/10.1007/s11164-017-2906-7.

(25) Zhang, P.; Russell, M. G.; Jamison, T. F. Continuous Flow Total Synthesis of Rufinamide. *Org. Process Res. Dev.* **2014**, *18* (11), 1567–1570. https://doi.org/10.1021/op500166n.

(26) Boström, J.; Brown, D. G.; Young, R. J.; Keserü, G. M. Expanding the Medicinal Chemistry Synthetic Toolbox. *Nat. Rev. Drug Discov.* **2018**, *17* (10), 709–727. https://doi.org/10.1038/nrd.2018.116.

(27) Štrukil, V.; Bartolec, B.; Portada, T.; Đilović, I.; Halasz, I.; Margetić, D. One-Pot Mechanosynthesis of Aromatic Amides and Dipeptides from Carboxylic Acids and Amines. *Chem. Commun.* **2012**, *48* (99), 12100–12102. https://doi.org/10.1039/c2cc36613d.

(28) Métro, T. X.; Bonnamour, J.; Reidon, T.; Sarpoulet, J.; Martinez, J.; Lamaty, F. Mechanosynthesis of Amides in the Total Absence of Organic Solvent from Reaction to Product Recovery. *Chem. Commun.* **2012**, *48* (96), 11781–11783. https://doi.org/10.1039/c2cc36352f.

(29) Duangkamol, C.; Jaita, S.; Wangngae, S.; Phakhodee, W.; Pattarawarapan, M. An Efficient Mechanochemical Synthesis of Amides and Dipeptides Using 2,4,6-Trichloro-1,3,5-Triazine and PPh3. *RSC Adv.* **2015**, *5* (65), 52624–52628. https://doi.org/10.1039/c5ra10127a.

(30) Mocci, R.; Colacino, E.; Luca, L. De; Fattuoni, C.; Porcheddu, A.; Delogu, F. The Mechanochemical Beckmann Rearrangement: An Eco-Efficient "Cut-and-Paste" Strategy to Design the "Good Old Amide Bond." *ACS Sustain. Chem. Eng.* **2021**, *9* (5), 2100–2114. https://doi.org/10.1021/acssuschemeng.0c07254.

(31) Hernández, J. G.; Ardila-Fierro, K. J.; Crawford, D.; James, S. L.; Bolm, C. Mechanoenzymatic Peptide and Amide Bond Formation. *Green Chem.* **2017**, *19* (11), 2620–2625. https://doi.org/10.1039/c7gc00615b.

(32) Jaita, S.; Phakhodee, W.; Chairungsi, N.; Pattarawarapan, M. Mechanochemical Synthesis of Primary Amides from Carboxylic Acids Using TCT/NH4SCN. *Tetrahedron Lett.* **2018**, *59* (39), 3571–3573. https://doi.org/10.1016/j.tetlet.2018.08.035.

(33) Veitch, G. E.; Bridgwood, K. L.; Rands-Trevor, K.; Ley, S. V. Magnesium Nitride as a Convenient Source of Ammonia: Preparation of Pyrroles. *Synlett* **2008**, No. 17, 2597–2600. https://doi.org/10.1055/s-0028-1083504.

(34) Veitch, G. E.; Bridgwood, K. L.; Ley, S. V. Magnesium Nitride as a Convenient Source of Ammonia: Preparation of Primary Amides. *Org. Lett.* **2008**, *10* (16), 3623–3625. https://doi.org/10.1021/ol801398z.

(35) Sheldon, R. A. Atom Efficiency and Catalysis in Organic Synthesis. *Pure Appl. Chem.* **2000**, *72* (7), 1233–1246. https://doi.org/10.1351/pac200072071233.

(36) McElroy, C. R.; Constantinou, A.; Jones, L. C.; Summerton, L.; Clark, J. H. Towards a Holistic Approach to Metrics for the 21st Century Pharmaceutical Industry. *Green Chem.* **2015**, *17* (5), 3111–3121. https://doi.org/10.1039/c5gc00340g.

(37) Tobiszewski, M.; Marć, M.; Gałuszka, A.; Namieśnik, J. Green Chemistry Metrics with Special Reference to Green Analytical Chemistry. *Molecules* **2015**, *20* (6), 10928–10946. https://doi.org/10.3390/molecules200610928.

(38) Monteith, E. R.; Mampuys, P.; Summerton, L.; Clark, J. H.; Maes, B. U. W.; McElroy, C. R. Why We Might Be Misusing Process Mass Intensity (PMI) and a Methodology to Apply It Effectively as a Discovery Level Metric. *Green Chem.* **2020**, *22* (1), 123–135. https://doi.org/10.1039/c9gc01537j.

(39) Constable, D. J. C.; Curzons, A. D.; Cunningham, V. L. Metrics to "green" Chemistry - Which Are the Best? *Green Chem.* **2002**, *4* (6), 521–527. https://doi.org/10.1039/b206169b.

(40) Sheldon, R. A. Metrics of Green Chemistry and Sustainability: Past, Present, and Future. *ACS Sustain. Chem. Eng.* **2018**, *6* (1), 32–48. https://doi.org/10.1021/acssuschemeng.7b03505.

(41) P. Bodhuri, P. Green Stuart, A. Karadeolian, E. G. C. WO 2014/121383 A1.

(42) Kankan, R.N; Rao, D.R; Birari, D. R. WO 2010/043849 A1.

(43) Xu, F.; Song, Y. Y.; Li, Y. J.; Li, E. L.; Wang, X. R.; Li, W. Y.; Liu, C. Sen. An Efficient Protocol for the Synthesis of Primary Amides via Rh-Catalyzed Rearrangement of Aldoximes. *ChemistrySelect* **2018**, *3* (12), 3474–3478. https://doi.org/10.1002/slct.201800265.

(44) Chiacchio, U.; Rescifina, A.; Saita, M. G.; Iannazzo, D.; Romeo, G.; Mates, J. A.; Tejero, T.; Merino, P. Zinc(II) Triflate-Controlled 1,3-Dipolar Cycloadditions of C-(2-Thiazolyl)Nitrones: Application to the Synthesis of a Novel Isoxazolidinyl Analogue of Tiazofurin. *J. Org. Chem.* **2005**, *70* (22), 8991–9001. https://doi.org/10.1021/jo051572a.

(45) Lambert, D. M.; Vandevoorde, S.; Diependaele, G.; Govaerts, S. J.; Robert, A. R. Anticonvulsant Activity of N-Palmitoylethanolamide, a Putative Endocannabinoid, in Mice. *Epilepsia* **2001**, *42* (3), 321–327. https://doi.org/10.1046/j.1528-1157.2001.41499.x.

(46) Ray, R.; Hazari, A. S.; Chandra, S.; Maiti, D.; Lahiri, G. K. Highly Selective Ruthenium-Catalyzed Direct Oxygenation of Amines to Amides. *Chem. - A Eur. J.* **2018**, *24* (5), 1067–1071. https://doi.org/10.1002/chem.201705601.

(47) Aguiar, R. M.; Leão, R. A. C.; Mata, A.; Cantillo, D.; Kappe, C. O.; Miranda, L. S. M.; De Souza, R. O. M. A. Continuous-Flow Protocol for the Synthesis of Enantiomerically Pure Intermediates of Anti Epilepsy and Anti Tuberculosis Active Pharmaceutical Ingredients. *Org. Biomol. Chem.* **2019**, *17* (6), 1552–1557. https://doi.org/10.1039/C8OB03088J.

(48) Khalil, A.; Elsayed, G. A.; Mohamed, H. A.; Raafat, A. Utility of Chloroacetonitrile in Construction of Some Hitherto Novel Pyrazole and Thiazole Derivatives. *J. Iran. Chem. Soc.* **2018**, *15* (1), 191–199. https://doi.org/10.1007/s13738-017-1223-9.

(49) Bodhuri, P; Green, S. P.; Karadeolian, A.; Cammisa, E. G. . WO 2014/121383 A1. **2014**.

(50) Li, W.; Zhou, X.; Luan, Y.; Wang, J. Direct Access to 1,4-Disubstituted 1,2,3-Triazoles through Organocatalytic 1,3-Dipolar Cycloaddition Reaction of α,β-Unsaturated Esters with Azides. *RSC Adv.* **2015**, *5* (108), 88816–88820. https://doi.org/10.1039/c5ra19038j.

# Chapter 6. Chemical synthesis of a probe for the study of Coenzyme A biosynthesis

## Chemical synthesis of a probe for the study of Coenzyme A biosynthesis

The work described in this chapter was performed during a stay at Max Planck institute for chemical research in Professor´s Kai Johnsson´s group, as part of the International Thesis requirements.

## 1. Introduction

### 1.1 Biosynthesis and biological role of coenzyme A

Coenzyme A (CoA) is a ubiquitous enzyme cofactor present in all living organisms. Its main role is to act as a carrier of acyl groups and as a carboxy activating group. It has an important role in vital biochemical pathways, such as the Krebs cycle and fatty acid biosynthesis, converting CoA into a cornerstone of cell metabolism[1].

Coenzyme A is endogenously synthesised by all living organisms in five steps in a highly evolutionary conserved biochemical pathway (figure 1). Pantothenate or vitamin $B_5$ is the substrate for pantothenate kinase (PanK), the first enzyme of the route. It converts pantothenate into 4-phosphopantothenate, which is subsequently coupled with cysteine in a step catalyzed by phosphopantothenoylcysteine synthase (PPCS) and decarboxylated by phosphopantothenoylcysteine decarboxylase (PPCDC), forming 4-phosphopantetethine. 4-phosphopantetheine is coupled to AMP by the enzyme phosphopantetheine adenylyl transferase (PPAT) to form dephospho-CoA, which is finally phosphorylated to CoA by the enzyme dephospho-CoA kinase (figure 1)[2].

Pantothenate kinase is the key regulatory enzyme in the biosynthesis of CoA because it catalyses the rate-limiting step, namely the phosphorylation of pantothenate into phospopantothenate, which is then rapidly converted into CoA[2].

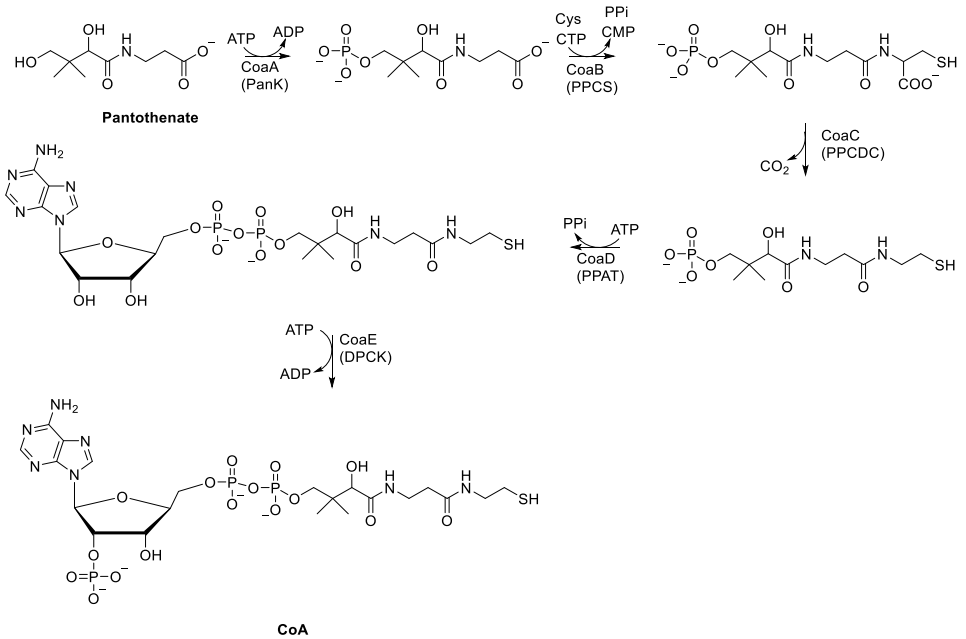


Figure 1. Biosynthesis of CoA.

Recently, some studies have identified PanK as a potential drug target for diverse diseases such as tuberculosis[3], type II diabetes[4] or neurodegeneration[5]. Hence, a deeper study of the activity and compartmentalization of CoA could provide a deeper insight of the role of CoA in diverse pathological situations.

## 1.2 Protein sensors

In order to assess the biological activity and compartmentalization of proteins and their role in cellular signalling networks, more than 750 protein sensors have been developed. Protein sensors are fusion proteins that are synthesised within cells and allow the space-temporal study of different cellular analytes by real time fluorescence signals, achieving great specificity[6].

Protein sensors consist of a sensing unit, being this the part of the protein that binds the analyte, and a reporter unit which is responsible for the fluorescence signal. Sensors having a single reporting unit are concentration-dependent and give an intentiometric readout, while sensors with two sensing units are concentration-independent and based on the resonance energy transfer (RET) effect, making them highly suitable for *in vivo* applications. Once the sensing unit binds its analyte, it undergoes a conformational change that modifies the optical properties of the reporting unit, allowing space-temporal resolution of the signals[7].

## 1.3 SNIFITs

In 2009 the Johnsson group described the first SNAP-tag-based indicators with a fluorescent intramolecular tether (SNIFIT), consisting of a trimeric protein sensor with a protein able to bind the analyte of interest, a RET donor protein and a self-labelling protein (SLP).[8] The self-labelling protein binds a chemically synthesized molecule, exogenous to the cell. This molecule contains a ligand for the protein of interest, a fluorophore, and the substrate for the SLP. When the ligand is not present, the ligand moiety of the probe binds the protein of interest, thus forcing a conformational change in which a Förster Resonance energy transfer (FRET) effect is observed between the fluorophore and the RET donor protein (closed conformation). When the analyte of interest is present, it displaces the ligand attached to the protein of interest changing the conformation of the biosensor to an open form and decreasing the efficiency of the FRET effect [9–12] (figure 2).

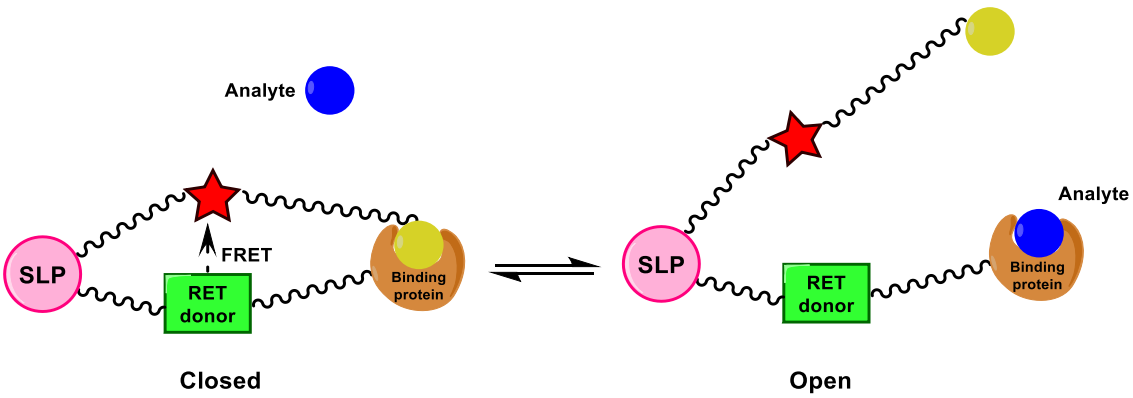


Figure 2. Schematic representation of the principles of SNIFITs.

The RET donor of the biosensor is typically either a genetically encoded fluorescent protein such as the green fluorescent protein (GFP), a genetically encoded chemoluminescent protein like luciferase or an organic fluorophore bound to a second self-labelling protein. GFP is usually preferred due to the better quantum yields obtained [11].

Among the different types of self-labelling proteins, SNAP-tag, CLIP-tag and Halo tag stand out as the most important. SNAP tag is a mutated suicide human O6 alkylguanine-DNA alkyl-transferase engineered by Johnsson et al that covalently reacts with O6-benzylguanine derivatives or the more permeable chloropyrimidine derivatives[13]. CLIP tag, a second mutant also developed by Johnsson and co-workers reacts with O2 benzylcytosine derivatives and binds them covalently [14]. Finally, Halo tag is an engineered protein derived from a haloalkane dehalogenase that specifically and covalently binds a 2-[2-[(6-chlorohexyl)oxy]ethoxy]ethane ligand[15]. The difference between these tags resides on their binding kinetics, being Halo tag several orders of magnitude faster than SNAP tag or CLIP tag[16]. However, the smaller size of SNAP and CLIP produces a smaller perturbation of the dynamics and functioning of the protein of interest to which they bind[17]. Therefore, the choice of one or another will depend on the different parameters that are to be taken into consideration when designing the SNIFIT.

In order to determine the sensor´s response to the analyte of interest, the intensity of fluorescence emitted at bot FRET partners is measured at different concentrations of the analyte of interest. A plot of the concentration of the analyte versus fluorescent intensity is drawn, and thus a titration curve is obtained. To obtain the dynamic range of the sensor ($RC_{max}$), the maximum ratio (corresponding to the fully open conformation, $R_{max}$) is divided by the minimal ratio (corresponding to fully closed conformation, $R_{min}$), giving $RC_{max}=R_{max}/R_{min}$. The concentration at which half of the maximum signal is obtained is $c_{50}$. While designing the biosensor, a $c_{50}$ that equals the intracellular concentration is required.[11, 18].

There are many literature examples of different SNIFITs created to assess the activity of many proteins of interest, including the $GABA_B$ receptor[12], a NADP reductase[10], carbonic anhydrase II[19], the glutamate receptor[20] and dihydrofolate reductase[9]. Amplifying the scope of analytes determined in this fashion is a, important challenge in order to acquire a better insight of biochemical pathways and the start and progress of many pathological processes.

## 2.0 Objectives

The aim of this work is the design and synthesis of a chemical sensor that allows a better insight of the dynamics and compartmentalization of PanK. The first part of this sensor consists of a 1,3,4 triazole moiety that specifically binds PanK. These molecules were originally designed to bind the *Mycobacterium tuberculosis* PanK (MtPanK), although they were not effective for their initial purpose [21]. The triazole unit was connected by two different linkers to the fluorophore responsible for the FRET effect, in this case a sulphonamide rhodamine (MAP rhodamines). MAP rhodamines have been reported to shift the equilibrium between their open and closed forms towards their closed spirocyclic forms, thus enhancing cellular permeability[22]. Finally the sulphonamide rhodamine is also bound to Halo tag substrate, 2-[2-[(6-chlorohexyl)oxy]ethoxy]ethanamine, a covalent probe of Halo tag (Figure 3).

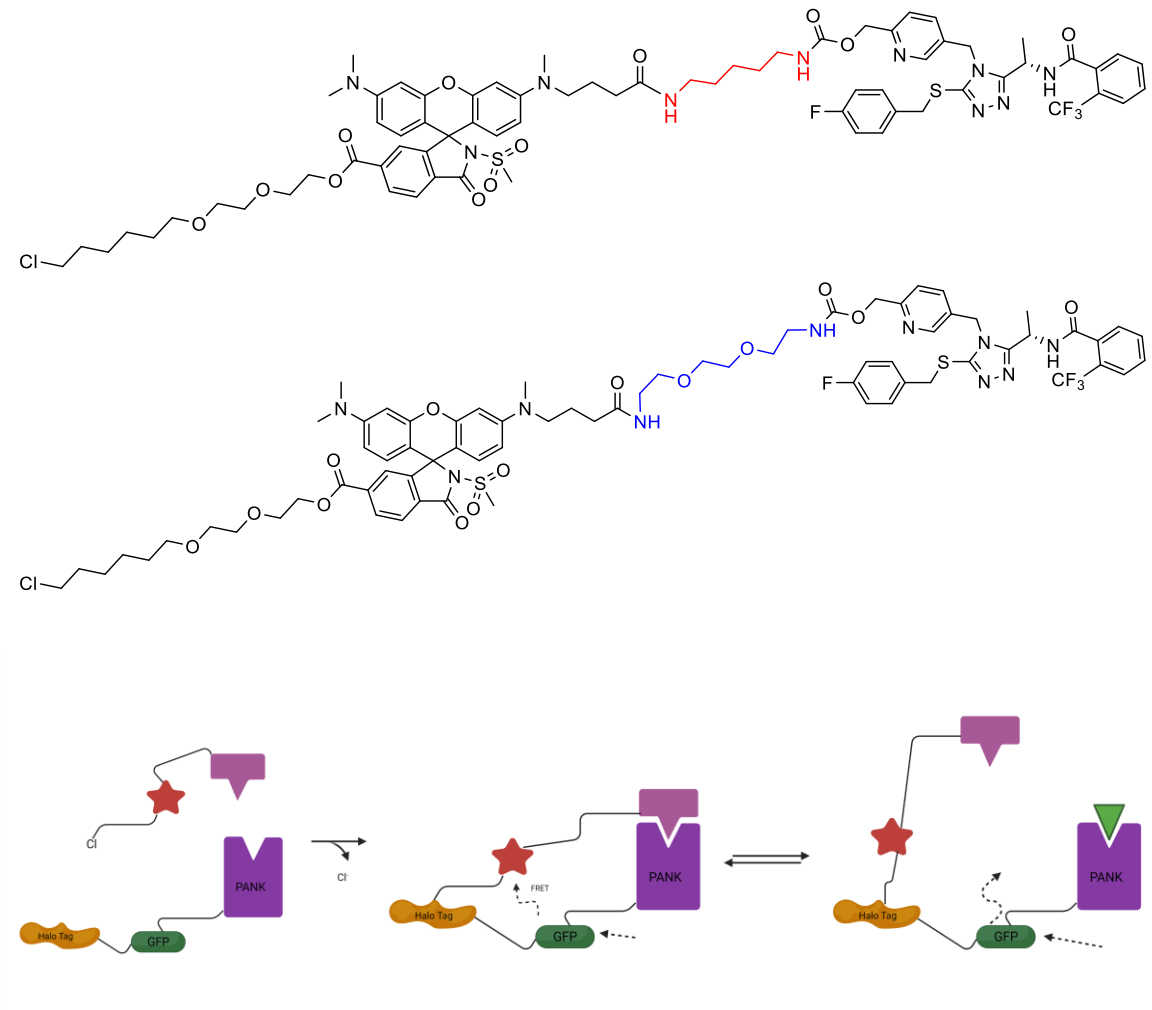


Figure 3. On the top: Chemical structure of the two chemical ligands designed to bind to the fusion protein PanK-GFP-Halo tag. ON the bottom: schematic representation of designed SNIFIT for PanK.

## 3.0 Results and discussion

### 3.1 Synthesis of the triazole moiety

The synthesis of the target chemical sensor started with methyl 6-(hydroxymethyl)nicotinate as a starting material due to ready its availability and low cost. The first step of the synthesis was the protection of the hydroxyl group with triisopropyl silyl chloride, in the presence of imidazole as a catalyst. Triisopropylsilyl (TIPS) is a highly stable protecting group, resistant to different reaction conditions, including mildly acidic ones, and therefore it was optimal for a long multi-step synthesis such as the one planned. The reaction proceeded with a 62% yield after purification, providing intermediate **4.01**. The ester group of **4.02** needed to be subsequently reduced to the corresponding alcohol. In the first place, we employed two equivalents in moles of $LiAlH_4$, which afforded the desired compound **4.02** but only in 8% yield. In an effort to improve this result, $LiBH_4$ was used as a reducing agent and the yield was raised to 44%. The next step was the substitution of the primary alcohol group thus generated by an azide to obtain intermediate **4.03**. This was first attempted through an Appel reaction with $CCl_4$ and triphenylphosphine, substituting the hydroxy group for a chloride, followed by $NaN_3$ to yield the azide, achieving only a 9% yield, which was improved to 89% using diphenyl phosphoryl azide (DPPA) as a source of azide. Intermediate **4.03** was converted into **4.05** in a two-step sequence using in first place palladium over carbon under a hydrogen atmosphere to reduce the azide to amine to the corresponding primary amine **4.04**. This intermediate was converted into **4.05** using Di(2-pyridyl) thionocarbonate (DPT) affording a global 7% yield over the two steps. This result was improved by using a Staudinger reaction to reduce the azide and obtain **4.04**, which was subsequently converted without purification to intermediate **4.05** using thiophosgene, achieving an overall yield of 33%. Intermediate **4.06** was obtained in full conversion by reacting intermediate **4.05** with hydrazine and was coupled in the presence of Hexafluorophosphate Azabenzotriazole Tetramethyl Uronium (HATU) with Boc-L alanine again in full conversion, leading to intermediate **4.07**. This compound was cyclised with a 20% solution of NaOH to obtain **4.08** with a 43% yield. **4.08** was S-alkylated with 4-fluorobenzyl bromide, providing **4.09** in 97% yield. The next step of the synthesis was Boc deprotection, which was carried out using trifluoroacetic acid (TFA) and yielded **4.10** in 94% yield. Once the amino group was free, **4.10** was reacted with 2-trifluoromethyl benzoic acid, again using HATU as a coupling agent, giving **4.11** in full conversion. The final steps involved the deprotection of the TIPS group, which was achieved with tetrabutylammonium fluoride (TBAF) as a source of fluoride ions, which proceeded in 41% yield. The resulting primary hydroxy group was coupled in the first place with 4-nitrophenyl chloroformate and, in the same pot, with either 1,8-diamino-3,6-dioxaoctane or 1,6 hexanediamine to afford **4.13a** in 79% yield or **4.13b** in 67% yield, respectively (figure 4).

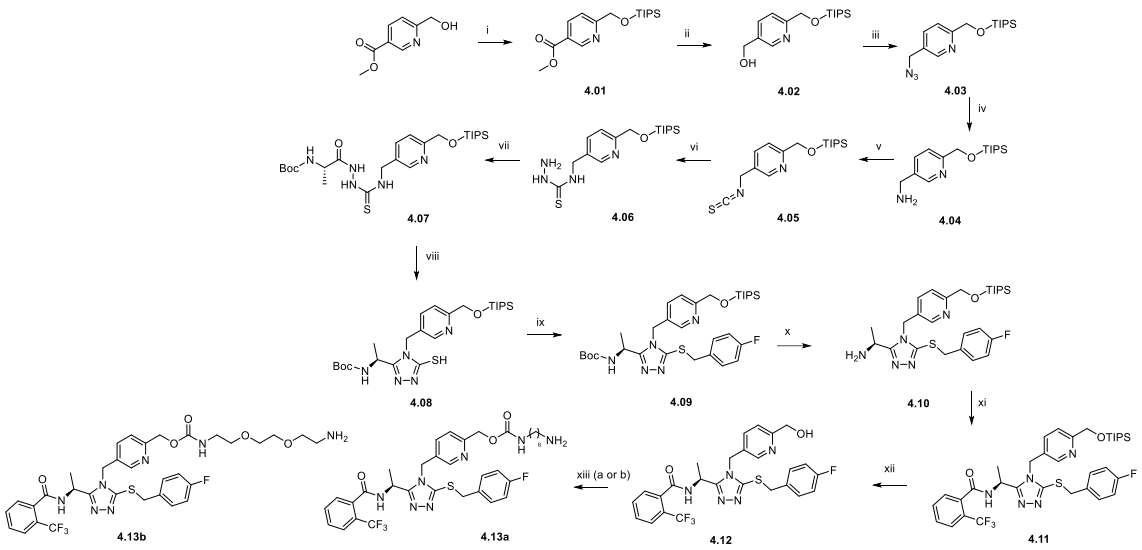

Figure 4. Reaction scheme used for the synthesis of 12a and 12b. Reaction conditions: **i**: TIPSCl, imidazole, DCM 0ºC to rt; **ii**: $LiBH_4$, THF 0ºC to rt; **iii**: DPPA, DBU, Toluene/THF; **iv**: $P(Bu)_3$, $H_2O$, THF, rt; **v**: $CSCl_2$ DIPEA, DCM 0º to rt; **vi**: $NH_2NH_2$ EtOH rt; **vii**: Boc L-alanine, HATU, DIPEA, DMF, rt; **viii**: 20% NaOH, MeOH, rt; **ix**: 4-fluoro benzyl bromide, $K_2CO_3$, DMF, rt; **x**: TFA, DCM, rt;; **xi**: 2-trifluoromethyl benzoic acid, HATU, DIPEA, **xii**: DMF; TBAF, DCM, rt; **xiii a**: 4-nitrophenyl chloroformate, DCM, DIPEA, rt; 1,6 hexanediamine, rt; **xii b**: : 4-nitrophenyl chloroformate, DCM, DIPEA, rt; 1,8-diamino-3,6-dioxaoctane, rt.

## 3.2 Synthesis of the MaP-rhodamine moiety

With the triazole derivatives **4.13a** and **4.13b** in hand, the MAP-rhodamine synthesis was performed. In this case, the commercial starting material was TMR (tetramethyl rhodamine) COOH (**4.14**), which possesses three free carboxylic acid groups, one of which is less reactive due to its equilibrium with a spirocyclic lactone (figure 5). The first step of the synthesis was the protection of the two additional carboxylic acids using allyl bromide to achieve **4.15** in full conversion. Intermediate **4.15** was transformed into the corresponding methane sulphonamide using EDCI as a coupling agent to obtain **4.16** in 53% yield. The final step was the deprotection of the allyl esters using palladium tetrakis and 1,3 dimethyl barbituric acid to obtain **4.17** in 98% yield (figure 6).

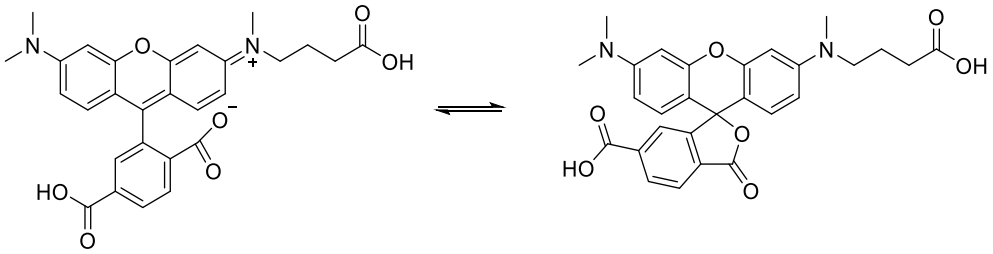

Figure 5. Equilibrium between the open and closed forms of TMR.

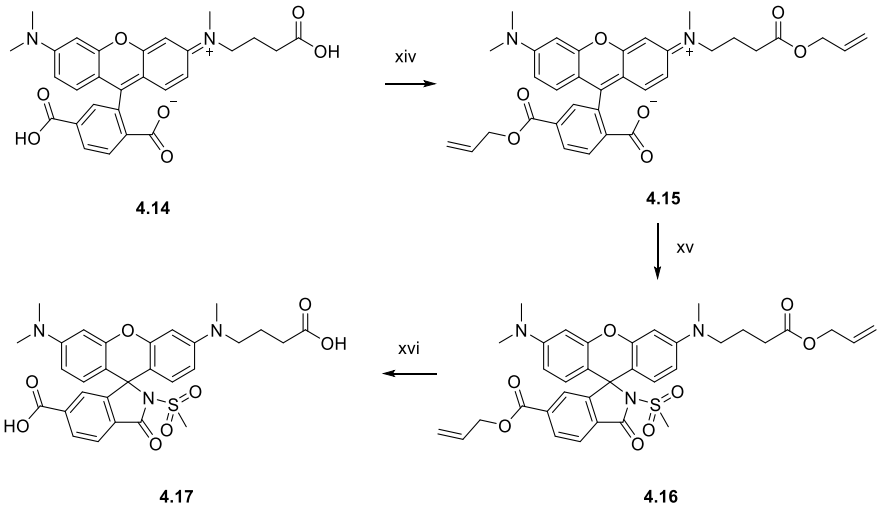


Figure 6. Reaction scheme followed for the synthesis of **4.17**. Reagents and conditions: xiv: allyl bromide, $Et_3N$, DMF, rt; xv: methanesulfonamide, EDCI, DMAP, DCM, rt; xvi: $Pd(PPh_3)_4$, 1,3 dimethyl barbituric acid, MeCN, rt.

## 3.3 Synthesis of the protein sensors

To finally obtain the target protein sensors, the first step was to join **4.13a** and **4.13b** to **4.17** using N,N,N',N'-Tetramethyl-O-(N-succinimidyl)uronium tetrafluoroborate (TSTU) as a coupling agent. This reaction was specific due to the higher reactivity of the aliphatic carboxylic acid with respect to its aromatic counterpart. Once starting material was no longer found in the reaction medium, in the same pot, another equivalent of TSTU and 2-[2-[(6-chlorohexyl)oxy]ethoxy]ethanamine were added to the mixture to furnish protein sensors **4.18a** and **4.18b** in 44% and a 27% yields, respectively.

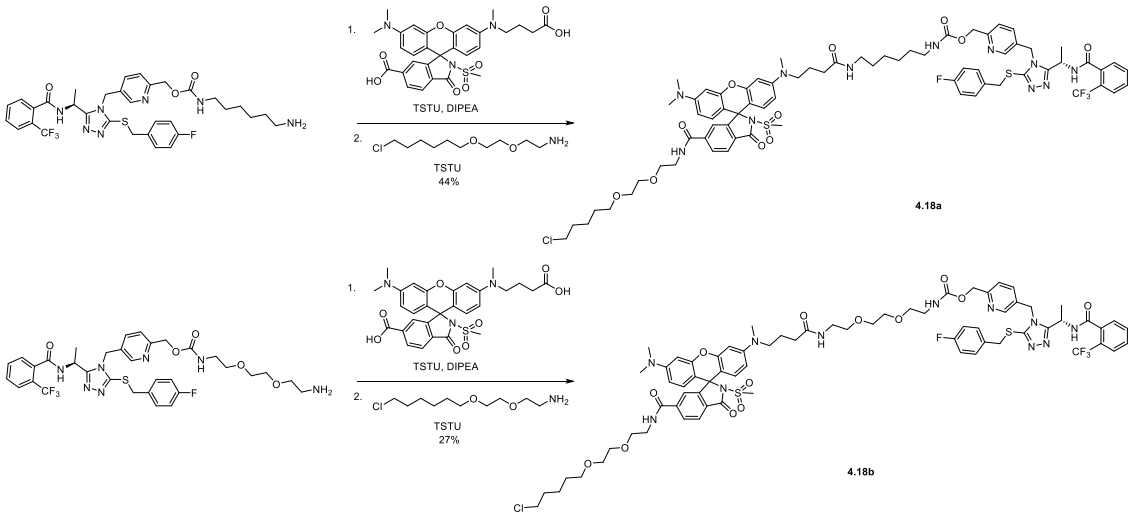


Figure 8. Reaction sequence for the synthesis of compounds **4.18a** and **4.18b**.

### 3.4 Verification of 4.18a and 4.18b behaving as SNIFITs in cells

Once the compounds were synthesised and characterised, we decided to test them in vivo inside HEK293 transfected cells. To observe whether the compounds attached to the fusion protein, 500 µM solution of compounds **4.18a** and **4.18b** were added to cell cultures, while in others, no compound was added. Results can be observed in figure 9.

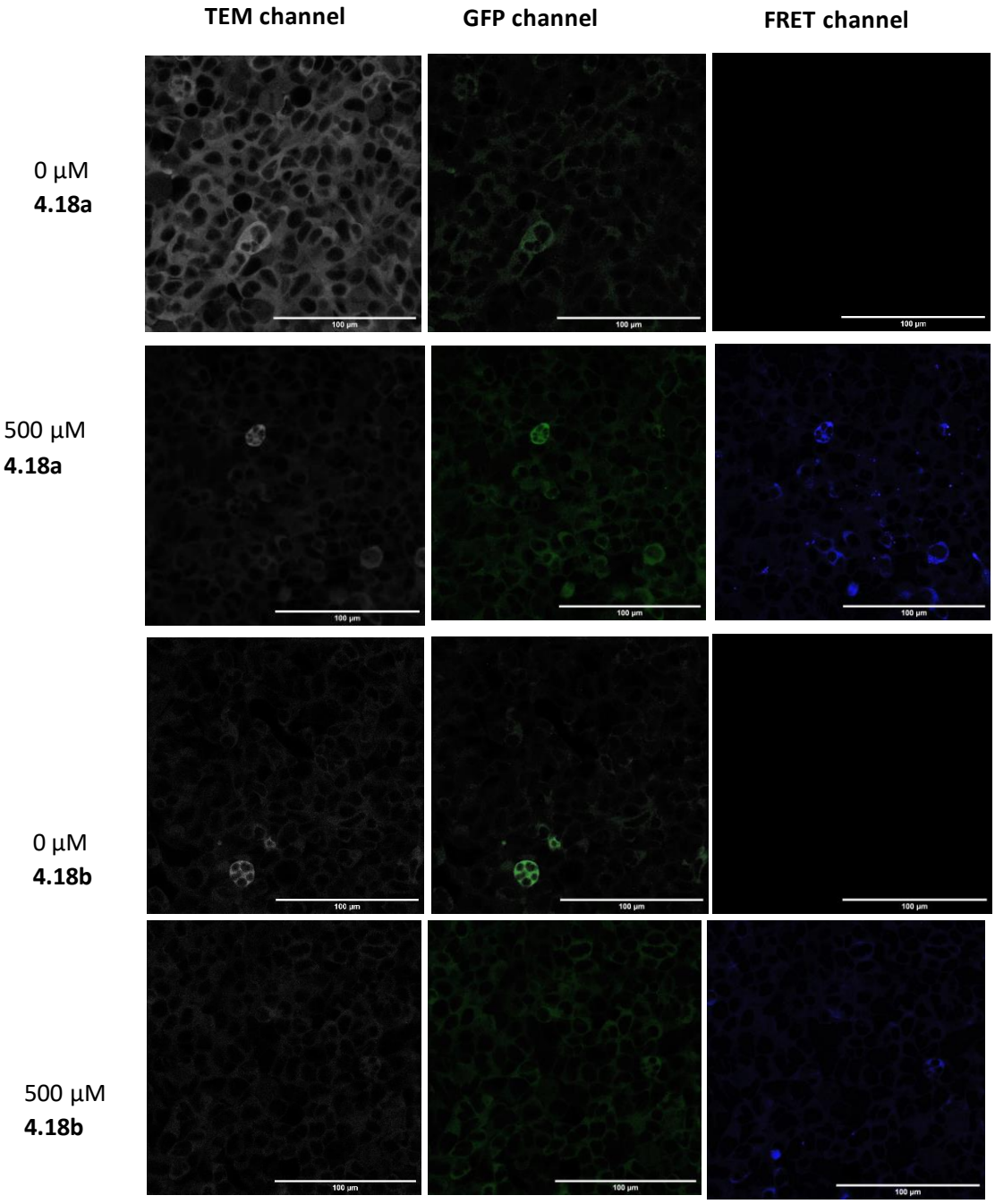


Figure 9. Microscopy images from cell cultures with compounds **4.18a** and **4.18b**.

It can be observed from figure 9 that when no compound is added to the cell cultures cell can be observed in the TEM channel and in the GFP channel, while nothing can be observed in the

FRET channel. When both compounds **4.18a** and **4.18b** are added, cells can be observed in the TEM and GFP channels, but also in the FRET channel, as the compounds have been attached to the fusion protein and is able to produce FRET with the GFP. In order to acquire a better insight of the dynamic range and the rest of the parameters of both sensors, more studies are required to be performed.

## 4.0 Experimental

### Synthesis of 4.01

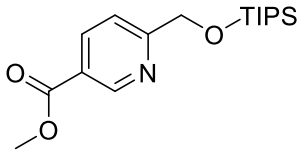


Methyl 6-(hydroxymethyl)nicotinate (5 g, 29.9 mmol) and imidazole (6.1 g, 89.7 mmol) were dissolved in dry DCM (80 ml). Chlorotriisopropylsilane (6.34 g, 32.9 mmol) was added dropwise at 0°C and the mixture was stirred at room temperature overnight. The reaction mixture was diluted with DCM and water (20 ml) was added. The two layers were separated, and the organic layer was washed with brine (15 ml) twice, dried with $Na_2SO_4$ and concentrated *in vacuo*. The residue was purified by flash column chromatography (Hexane/ 5-100% EtOAc) to give a colorless oil (5.97 g, 62% yield). Identity of compound was confirmed by LC-MS.

### Synthesis of 4.02

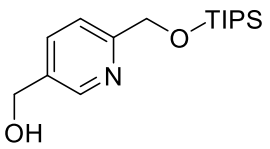


methyl 6-(((Triisopropylsilyl)oxy)methyl)nicotinate **4.01** (50 mg, 0.15 mmol) was dissolved in dry THF (10 ml) in an ice cool water bath and a 3M solution of $LiBH_4$ (0.51 ml, 1.5 mmol) was added dropwise. The solution was allowed to warm to room temperature and stirred for 24 hours. Subsequently, water (10 ml) and ethyl acetate (10 ml) were carefully added to the mixture and the two layers separated. The aqueous layer was extracted with ethyl acetate (10 ml) twice and the combined organic extracts were dried with $Na_2SO_4$ and concentrated *in vacuo*. The residue was purified by flash column chromatography (Hexane/ 10-100% EtOAc) to give a white solid (10 mg, 44% yield). Identity of compound was confirmed by LC-MS.

### Synthesis of 4.03

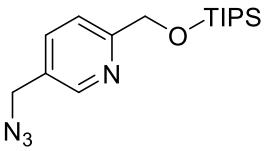


(6-(((Triisopropylsilyl)oxy)methyl)pyridin-3-yl)methanol **4.02** (0.2 g, 0.68 mmol) was dissolved in a 1:1 THF/Toluene mixture (20 ml) and diphenyl phosphoryl azide (0.28 g, 1.02 mmol) was added. Subsequently, DBU was added, and the mixture was stirred overnight at room temperature. Ethyl acetate (20 ml) was used to dilute the reaction mixture and water (20 ml) was used to quench the reaction. The two layers were separated, and the aqueous layer was extracted twice with ethyl acetate (20 ml). The combined organic extracts were dried with $Na_2SO_4$ and concentrated *in vacuo*. The residue was purified by flash column chromatography (Hexane/ 10-100% EtOAc) to give a colourless oil (0.19 g, 89% yield). Identity of compound was confirmed by LC-MS.

### Synthesis of 4.05

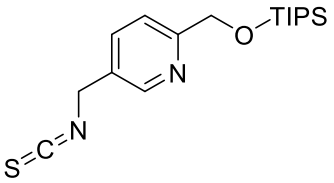


5-(Azidomethyl)-2-(((triisopropylsilyl)oxy)methyl)pyridine **4.03** (0.045 g, 0.14 mmol) was dissolved in THF (15 ml) and tributylphosphine (0.056 g, 0.28 mmol) was added to the reaction mixture, which was stirred at room temperature for 1 hour. Water (2 ml) was added, and the reaction mixture was

further stirred overnight. The reaction mixture was concentrated *in vacuo* and the colourless oil obtained was used for the next step without any further purification. Identity of compound was confirmed by HPLC-MS.

The crude oil was dissolved in DCM (10 ml) and DIPEA (0.036 g, 0.28 mmol) and thiophosgene (0.017g, 1.55 mmol) were added to the mixture at 0 °C. The mixture was stirred at room temperature for 1 hour and then water (3 ml) was added. The two layers were separated and the organic phase was washed with water (5 ml) twice and the with brine (5 ml). The organic phase was then dried with $Na_2SO_4$ and concentrated *in vacuo*. The residue was purified by column chromatography (hexane/ethyl acetate (0-100%)) to yield a brown oil (0.016 g, 33% yield). Identity of compound was confirmed by LC-MS.

**Synthesis of 4.06**

5-(Isothiocyanatomethyl)-2-(((triisopropylsilyl)oxy)methyl)pyridine **4.05** (0.153 g, 0.45 mmol) was dissolved in ethanol (10 ml). Separately, hydrazine (0.02 mg, 0.68 mmol) was also dissolved in ethanol and added to the first solution. The reaction mixture was stirred at room temperature for 30 minutes and afterwards, concentrated *in vacuo* to yield a white solid (0.167 g, 99% yield). Identity of compound was confirmed by LC-MS.

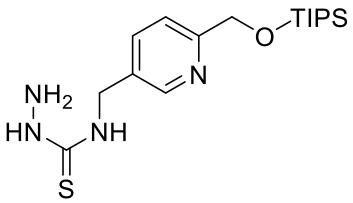


**Synthesis of 4.07**

Boc-L-alanine (67 mg, 0.36 mmol) was dissolved in DMF and DIPEA (0.195 g, 1.51 mmol) was added. Separately HATU (0.19 g, 0.503 mmol) was dissolved in DMF (1 ml), added to the first solution and stirred for 30 minutes. N-((6-(((triisopropylsilyl)oxy)methyl)pyridin-3-yl)methyl)hydrazinecarbothioamide **4.06** (0.17 g, 0.45 mmol) was dissolved in DMF (2 ml) and added to the first solution. The reaction mixture was stirred overnight and concentrated *in vacuo*. The residue was dissolved in DCM (30 ml) and washed with brine (10 ml) twice. The organic layer was dried with $Na_2SO_4$ and concentrated *in vacuo*. The residue was purified by flash column chromatography (5-100% EtOAc) to yield a white solid (0.19 g, 98% yield). Identity of compound was confirmed by LC-MS.

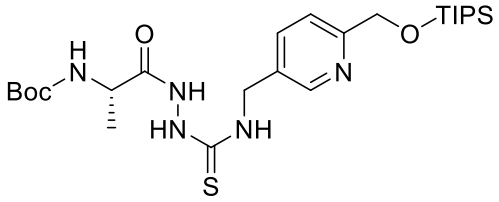


**Synthesis of 4.08**

*Tert*-Butyl (*S*)-(1-oxo-1-(2-(((6-(((triisopropylsilyl)oxy)methyl)pyridin-3-yl)methyl)carbamothioyl)hydrazyl)propan-2-yl)carbamate (0.18 g, 0.34 mmol) was dissolved in methanol (20 ml) and 20% NaOH (10 ml) was added carefully and the reaction mixture was stirred overnight at room temperature. The reaction mixture was then neutralised to pH 7 and concentrated *in vacuo*. The residue was purified by flash column chromatography (hexane/EtOAc 5-100%) to yield compound **4.08** as a white solid (76 mg, 43% yield). Identity of compound was confirmed by LC-MS.

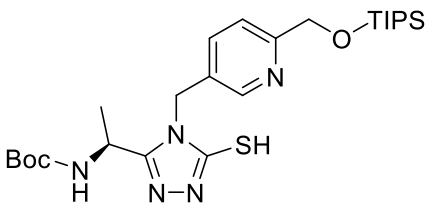


**Synthesis of 4.09**

*Tert*-Butyl (S)-(1-(5-mercapto-4-((6-(((triisopropylsilyl)oxy)methyl)pyridin-3-yl)methyl)-4H-1,2,4-triazol-3-yl)ethyl)carbamate **4.08** (77 mg, 0.15 mmol) and potassium carbonate (40 mg, 0.30 mmol) were dissolved in DMF (5 ml) and stirred at room temperature for 30 minutes. Subsequently, a solution of 4-fluorobenzyl bromide (31 mg, 0.16 mmol) in DMF (3 ml) was added dropwise and the reaction mixture was stirred at room temperature for 2 hours. The reaction mixture was concentrated *in vacuo* and the residue was purified by flash column chromatography (ethyl acetate/methanol 0-10%) to yield a white solid (90 mg, 97% yield). Identity of compound was confirmed by LC-MS.

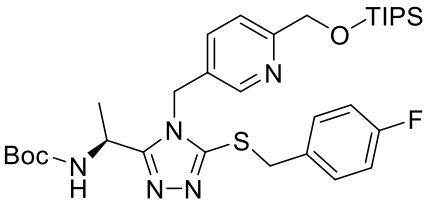


**Synthesis of 4.11**

*Tert*-Butyl (S)-(1-(5-((4-fluorobenzyl)thio)-4-((6-(((triisopropylsilyl)oxy)methyl)pyridin-3-yl)methyl)-4H-1,2,4-triazol-3-yl)ethyl)carbamate **4.09** (90 mg, 0.14 mmol) was dissolved in DCM (4 ml) and TFA (1 ml) was added to the solution, which was stirred at room temperature for 1 hour. After no starting material was left, the reaction mixture was concentrated *in vacuo*. Separately, 2-(trifluoromethyl) benzoic acid was dissolved in DMF (2ml) and DIPEA (54 mg, 0.42 mmol) was added to the solution. Alternatively, HATU (69 mg, 0.18 mmol) was dissolved in DMF (2 ml) and was added to the previous solution and stirred at room temperature for 30 minutes. The residue left from the Boc-deprotection was dissolved in DMF (2 ml) and added to the reaction mixture and the resulting solution was stirred overnight. The reaction mixture was concentrated *in vacuo* and the crude residue purified by flash column chromatography (ethyl acetate/methanol 0-10%) to yield a white solid (98 mg, 94% yield). Identity of compound was confirmed by LC-MS.

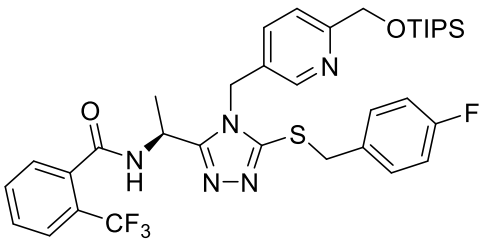


**Synthesis of 4.12**

(*S*)-N-(1-(5-((4-fluorobenzyl)thio)-4-((6-(((triisopropylsilyl)oxy)methyl)pyridin-3-yl)methyl)-4H-1,2,4-triazol-3-yl)ethyl)-2-(trifluoromethyl)benzamide **4.11** (96 mg, 0.136 mmol) was dissolved in THF (10 ml) and 1M solution of TBAF in THF (53 mg, 0.21 mmol, 21 µl) was added. The solution was stirred at room temperature for 1 hour and subsequently, the reaction mixture was concentrated under reduced pressure. The residue was purified by flash column chromatography (EtOAc/MeOH 1-10%) to give a white solid (31 mg, 42% yield). Identity of compound was confirmed by LC-MS.

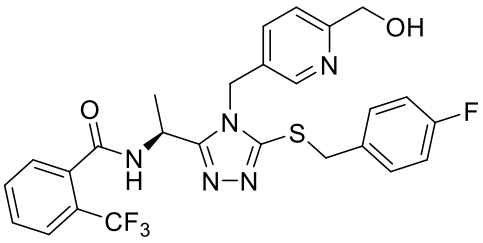


**Synthesis of 4.13a**

(S)-N-(1-(5-((4-fluorobenzyl)thio)-4-((6-(hydroxymethyl)pyridin-3-yl)methyl)-4H-1,2,4-triazol-3-yl)ethyl)-2-(trifluoromethyl)benzamide **4.12** (0.10 g, 0.19 mmol) and 4-nitrophenyl chloroformate (0.114 g, 0.57 mmol) were dissolved in DCM (20 ml) and DIPEA (73 mg, 0.57 mmol) was added to the solution. The reaction mixture was stirred at room temperature for 3 hours and alternatively 1,8-diamino-3,6-dioxaoctane (0.56 g, 3.78 mmol) was dissolved in DMSO (1 ml) and was added dropwise to the reaction mixture, which was stirred at room temperature for further 15 minutes. The reaction mixture was concentrated at reduced pressure and purified by RP-HPLC ($H_2O$ (0.1% TFA) 10-90% MeCN) to achieve a colourless oil (0.11 g, 79% yield).

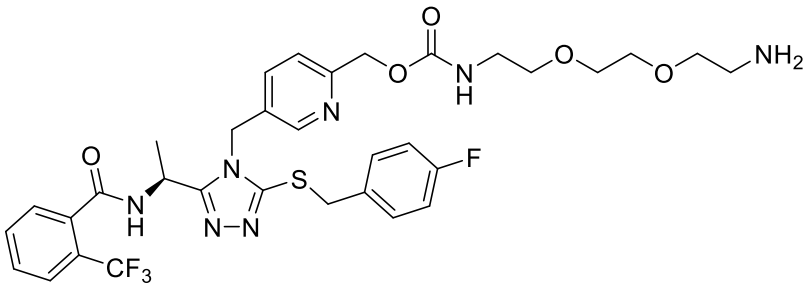


**$^1$H NMR** (400 MHz, MeOD) δ 8.43 (d, *J* = 2.6 Hz, 1H), 7.78 – 7.72 (m, 1H), 7.67 – 7.56 (m, 3H), 7.53 – 7.47 (m, 1H), 7.31 – 7.24 (m, 2H), 7.17 (dd, *J* = 5.3, 3.4 Hz, 1H), 7.04 – 6.96 (m, 2H), 5.38 (m, 3H), 5.22 (s, 2H), 4.36 (s, 2H), 3.71 (t, *J* = 5.4, 2H), 3.66 (m, 4H), 3.58 (t, *J* = 5.6 Hz, 2H), 3.36 (m, 2H), 3.14 (t, *J* = 5.0 Hz, 2H), 1.65 (d, *J* = 7.0 Hz, 3H).

**$^{13}$C NMR** (101 MHz, MeOD) δ 168.6, 163.6, 161.1, 160.7 (q, J = 37.0 Hz), 156.9, 156.9, 156.2, 151.1, 146.1, 137.0, 134.7 (q, J = 2.1 Hz), 132.7 (d, J = 3.1 Hz), 132.0, 131.0, 130.6 (d, J = 8.5 Hz), 130.0, 128.0, 126.8 (q, J = 32. 0 Hz), 126.2 (q, J = 5.1 Hz), 125.1, 122.4, 122.1, 117.8, 115.1 (d, J = 21.9 Hz), 69.9, 69.9, 69.6, 66.5, 65.1, 44.2, 40.8, 40.4, 39.3, 37.3, 17.4.

**HRMS** (ESI, pos. mode) m/z calc. for $C_{33}H_{37}N_7O_5F_4S^+$ 720.2586, found 720.2588 [M+H]

**Synthesis of 4.13b**

(S)-N-(1-(5-((4-fluorobenzyl)thio)-4-((6-(hydroxymethyl)pyridin-3-yl)methyl)-4H-1,2,4-triazol-3-yl)ethyl)-2-(trifluoromethyl)benzamide **4.12** (31 mg, 0.06 mmol) and 4-nitrophenyl chloroformate (34 mg, 0.17 mmol) were dissolved in DCM (5 ml) and DIPEA (22 mg, 0.17 mmol) was added to the solution. The reaction mixture was stirred at room temperature for 3 hours and alternatively 1,6 hexane diamine (0.13 g, 1.13 mmol) was dissolved in DMSO (1 ml) and was added dropwise to the reaction mixture, which was furtherly stirred at room temperature for

15 minutes. The reaction mixture was concentrated at reduced pressure and purified by RP-HPLC ($H_2O$ (0.1% TFA) 10-90% MeCN) to achieve a colourless oil (26 mg, 67% yield).

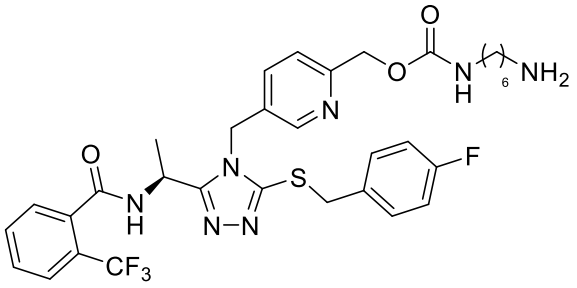

**$^1$H NMR** (400 MHz, MeOD) δ 8.22 (d, *J* = 1.9 Hz, 1H), 7.67 – 7.61 (m, 1H), 7.54 – 7.48 (m, 2H), 7.37 (dd, *J* = 8.2, 2.3 Hz, 1H), 7.30 (d, *J* = 8.1 Hz, 1H), 7.19 – 7.13 (m, 2H), 7.02 – 6.97 (m, 1H), 6.92 – 6.83 (m, 2H), 5.28 (q, *J* = 7.0 Hz, 1H), 5.23 – 5.15 (m, 2H), 5.06 (s, 2H), 4.23 (s, 2H), 3.03 (t, *J* = 7.0 Hz, 2H), 2.80 (t, *J* = 7.6 Hz, 2H), 1.57 – 1.49 (m, 5H), 1.46 – 1.36 (m, 2H), 1.28 (m, 4H).

**$^{13}$C NMR** (101 MHz, MeOD) δ 168.6, 163.6, 161.2, 160.7 (q, *J* = 35.9 Hz), 157.0, 156.9, 156.7, 151.1, 146.7, 136.0, 134.7 (q, *J* = 2.2 Hz), 132.8 (d, *J* = 3.2 Hz), 132.0, 130.7, 130.6 (d, *J* = 8.4 Hz), 129.9, 128.0, 126.8 (q, *J* = 32.0 Hz), 126.1 (q, *J* = 4.9 Hz), 121.6, 115.1 (d, *J* = 21.8 Hz), 65.4, 44.2, 40.7, 40.2, 39.2, 37.2, 29.2, 27.1, 25.8, 25.6, 17.3.

**HRMS** (ESI, pos. mode) m/z calc. for $C_{33}H_{37}N_7O_3F_4S^+$ 688.2687, found 688.2687 [M+H]

**Synthesis of 4.15**

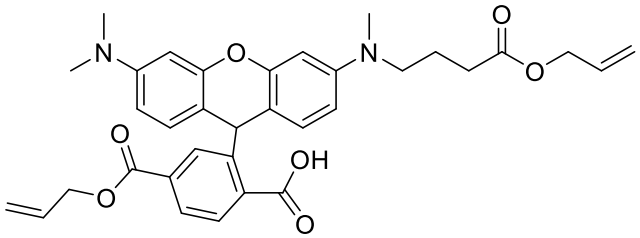

Tetramethyl rhodamine COOH (TMR-COOH **4.14** (61 mg, 0.12 mmol) and potassium carbonate (67 mg, 0.49 mmol) were dissolved in DMF (8 ml) and triethylamine (49 mg, 0.49 mmol) was added to the reaction mixture. Allyl bromide (44 mg, 0.37 mmol) was then added, and the reaction mixture was stirred at room temperature overnight. The reaction mixture was concentrated at reduced pressure and the residue dissolved in DCM (100 ml) and extracted with water (5 ml) three times. The organic phase was dried with $Na_2SO_4$ and concentrated *in vacuo* to yield a purple oil (70 mg, 99% yield). Identity of compound was confirmed by LC-MS.

**Synthesis of 4.16**

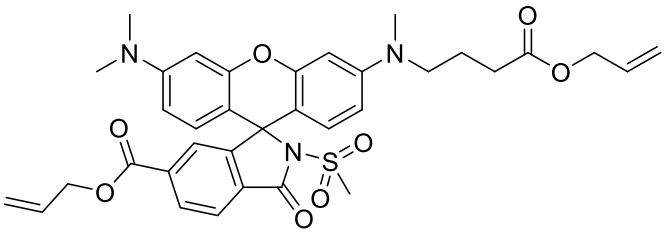

2-(3-((4-(Allyloxy)-4-oxobutyl)(methyl)amino)-6-(dimethylamino)-9H-xanthen-9-yl)-4-((allyloxy)carbonyl)benzoic acid **4.15** (30 mg, 0.05 mmol), methanesulfonamide (24 mg, 0.26 mmol) EDCI (39 mg, 0.21 mmol) and DMAP (25 mg, 0.21 mmol) were dissolved in DCM (2 ml) and heated up in a sealed vial at 60 °C overnight. Afterwards, the reaction mixture was diluted with DCM (40 ml) and washed with water (5 ml) 3 times. The organic phase was dried with $Na_2SO_4$ and concentrated at reduced

pressure. The residue was purified by RP HPLC ($H_2O$ (0.1% TFA) 10-90% MeCN) to give a purple solid (18 mg, 53% yield). Identity of compound was confirmed by LC-MS.

**Synthesis of 4.17**

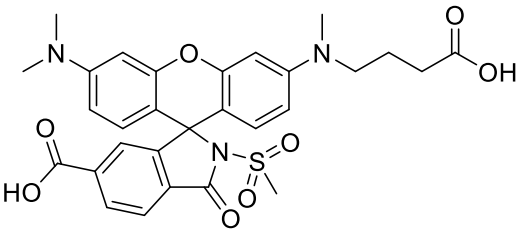

Allyl 3'-((4-(allyloxy)-4-oxobutyl)(methyl)amino)-6'-(dimethylamino)-2-(methylsulfonyl)-3-oxospiro[isoindoline-1,9'-xanthene]-6-carboxylate **4.16** (36 mg, 0.06 mmol), $Pd(PPh_3)_4$ (31 mg, 0.03 mmol) and 1,3 dimethyl barbituric acid (25 mg, 0.16 mmol) were dissolved in MeCN and stirred at room temperature for 2 hours. Subsequently, the reaction mixture was concentrated at reduced pressure and the residue was purified by RP-HPLC ($H_2O$ (0.1% TFA)/ 10-90% MeCN) to give a purple solid (31 mg, 98% yield). Identity of compound was confirmed by LC-MS.

**Synthesis of 4.18a**

3'-((3-Carboxypropyl)(methyl)amino)-6'-(dimethylamino)-2-(methylsulfonyl)-3-oxospiro[isoindoline-1,9'-xanthene]-6-carboxylic acid **4.17** (16 mg, 0.027 mmol) was dissolved in DMSO (1 ml) and DIPEA (71 mg, 0.55 mmol) and TSTU (8 mg, 0.027 mmol) were added and the reaction mixture was stirred at room temperature for 30 minutes, Subsequently, (S)-(5-((3-((4-fluorobenzyl)thio)-5-(1-(2-(trifluoromethyl)benzamido)ethyl)-4H-1,2,4-triazol-4-yl)methyl)pyridin-2-yl)methyl (6-aminohexyl) carbamate **4.13a** (19 mg, 0.027 mmol) was added and the reaction mixture was stirred at room temperature overnight. Then, TSTU (8 mg, 0.027 mmol) was added to the reaction mixture and stirred for 30 additional minutes. Then, 2-(2-((6-chlorohexyl)oxy)ethoxy)ethan-1-amine (6 mg, 0.027 mmol) was added to the reaction mixture and stirred for 2 hours. The reaction was concentrated at reduced pressure and purified by RP-HPLC ($H_2O$ (0.1% TFA)/ 10-90% MeCN (retention time: 34 minutes)) to give a purple solid (17 mg, 44% yield).

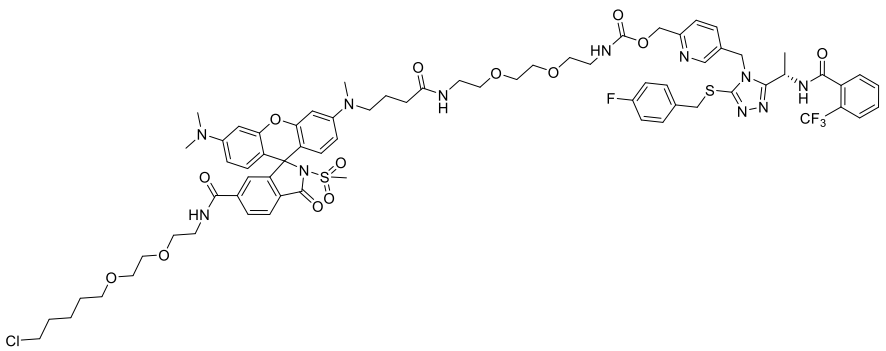

**$^1$H NMR** (400 MHz, MeOD) δ 8.32 (d, *J* = 2.3 Hz, 1H), 8.22 (ddd, *J* = 8.2, 1.7, 0.7 Hz, 1H), 8.09 (ddd, *J* = 8.2, 1.7, 0.6 Hz, 1H), 7.86 (d, *J* = 1.7 Hz, 1H), 7.74 (dd, *J* = 5.5, 3.8 Hz, 1H), 7.62 (ddd, *J* = 6.1, 3.2, 1.0 Hz, 2H), 7.47 (dd, *J* = 8.2, 2.3 Hz, 1H), 7.40 (d, *J* = 8.2 Hz, 1H), 7.29 – 7.23 (m, 2H), 7.09 (dd, *J* = 9.5, 3.6 Hz, 3H), 7.02 – 6.86 (m, 6H), 5.43 – 5.34 (m, 1H), 5.33 – 5.24 (m, 2H), 5.15 (s, 2H), 4.33 (s, 2H), 3.67 – 3.49 (m, 21H), 3.43 (t, *J* = 6.5 Hz, 2H), 3.36 (d, *J* = 5.4 Hz, 1H), 3.30 – 3.26 (m,

2H), 3.25 (s, 4H), 3.21 (s, 3H), 2.96 (s, 3H), 2.29 (t, *J* = 6.9 Hz, 2H), 2.02 – 1.92 (m, 2H), 1.76 – 1.67 (m, 2H), 1.62 (d, *J* = 6.9 Hz, 3H), 1.51 (p, *J* = 6.7 Hz, 2H), 1.45 – 1.29 (m, 8H).

**$^{13}$C NMR** (101 MHz, MeOD) δ 175.0, 169.9, 167.9, 167.7, 158.3, 148.2, 137.4, 136.2, 134.2, 133.4, 132.1, 132.0 (d, J = 8.3 Hz), 132.0, 131.5, 131.4, 131.3, 130.1, 129.4, 128.9, 127.6, 127.5 (q, J = 5.2 Hz), 123.0, , 116.5 (d, J = 21.9 Hz), 98.4, 72.1, 71.3, 71.3, 71.2, 71.1, 70.9, 70.5, 70.4, 67.0, 53.3, 45.7, 45.6, 42.1, 41.8, 41.4, 41.2, 41.0, 40.4, 39.4, 38.6, 33.7, 33.4, 30.4, 27.7, 26.4, 23.9, 18.7.

**HRMS** (ESI, pos. mode) m/z calc. for $C_{72}H_{84}N_{11}O_{13}ClF_4S_2^{2+}$ 743.7731, found 743. 7714 [M+2H]

**Synthesis of 4.18b**

3'-((3-Carboxypropyl)(methyl)amino)-6'-(dimethylamino)-2-(methylsulfonyl)-3-oxospiro[isoindoline-1,9'-xanthene]-6-carboxylic acid **4.17** (16 mg, 0.027 mmol) was dissolved in DMSO (1 ml) and DIPEA (71 mg, 0.55 mmol) and TSTU (8 mg, 0.027 mmol) were added and the reaction mixture was stirred at room temperature for 30 minutes,

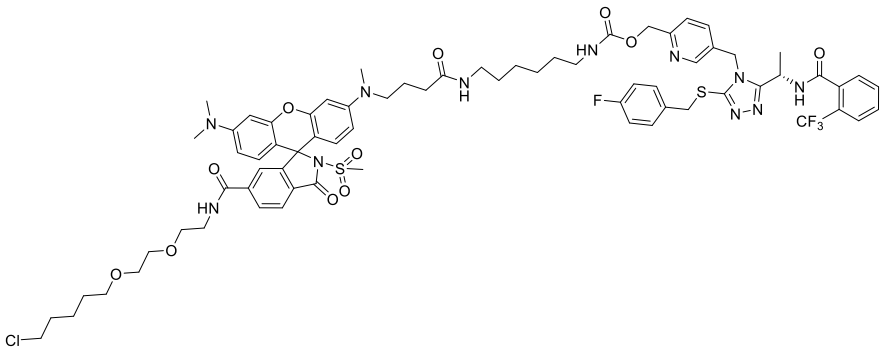

Subsequently, (S)-(5-((3-((4-fluorobenzyl)thio)-5-(1-(2-(trifluoromethyl)benzamido)ethyl)-4H-1,2,4-triazol-4-yl)methyl)pyridin-2-yl)methyl (2-(2-(2-aminoethoxy)ethoxy)ethyl)carbamate **4.13b** (20 mg, 0.027 mmol) was added and the reaction mixture was stirred at room temperature overnight. Then, TSTU (8 mg, 0.027 mmol) was added to the reaction mixture and stirred for 30 additional minutes. Then, 2-(2-((6-chlorohexyl)oxy)ethoxy)ethan-1-amine (6 mg, 0.027 mmol) was added to the reaction mixture and stirred for 2 hours. The reaction was concentrated at reduced pressure and purified by RP-HPLC ($H_2O$ (0.1% TFA)/ 10-90% MeCN (retention time: 32 minutes)) to give a purple solid (11 mg, 27% yield).

**$^{1}$H NMR** (400 MHz, MeOD) δ 8.36 (d, J = 2.3 Hz, 1H), 8.23 (dd, J = 8.2, 1.7 Hz, 1H), 8.08 (d, J = 8.1 Hz, 1H), 7.90 (d, J = 1.7 Hz, 1H), 7.76 – 7.69 (m, 1H), 7.65 – 7.58 (m, 2H), 7.54 (dd, J = 8.2, 2.3 Hz, 1H), 7.44 (d, J = 8.2 Hz, 1H), 7.27 – 7.22 (m, 2H), 7.17 (dd, J = 9.4, 2.6 Hz, 2H), 7.14 – 7.01 (m, 3H), 7.01 – 6.93 (m, 4H), 5.41 – 5.25 (m, 3H), 5.16 (s, 2H), 4.32 (s, 2H), 3.88 – 3.78 (m, 1H), 3.69 – 3.46 (m, 16H), 3.45 – 3.40 (m, 3H), 3.40 – 3.34 (m, 1H), 3.14 (t, J = 7.0 Hz, 2H), 3.08 (t, J = 7.0 Hz, 2H), 2.95 (s, 3H), 2.41 (t, J = 6.5 Hz, 1H), 2.27 (t, J = 6.9 Hz, 2H), 1.97 (t, J = 7.5 Hz, 2H), 1.73 (ddt, J = 25.0, 8.0, 6.7 Hz, 3H), 1.61 (d, J = 7.0 Hz, 4H), 1.53 – 1.28 (m, 18H), 1.24 (d, J = 6.8 Hz, 6H).

**$^{13}$C NMR** 13C NMR (101 MHz, MeOD) δ 174.7, 174.6, 169.9, 167.8, 167.6, 160.6, 159.2, 158.6, 158.5, 158.3, 157.9, 157.7, 152.5, 147.7, 139.5, 138.1, 136.9, 136.1, 134.1 (d, J = 3.1 Hz), 133.4, 132.3, 132.0 (d, J = 8.3 Hz), 131.8, 131.3, 130.2, 130.2, 129.7, 129.4, 128.2 (q, J = 32.0 Hz), 127.0 (q, J = 5.3 Hz), 126.5, 123.2, 116.5 (d, J = 21.3 Hz), 115.2, 114.3, 98.2, 98.1, 72.1, 71.3, 71.2, 71.2, 71.1, 70.5, 70.4, 66.5, 53.4, 46.8, 45.7, 45.7, 45.5, 42.1, 41.7, 41.2, 41.1, 40.4, 40.3, 39.5, 38.6, 38.1, 37.3, 33.7, 33.7, 33.2, 30.7, 30.5, 30.4, 30.3, 27.7, 27.7, 27.5, 27.3, 26.5, 26.4, 23.9, 21.5, 18.7.

**HRMS** (ESI, pos. mode) m/z calc. for $C_{72}H_{84}N_{11}O_{13}ClF_4S_2^{2+}$ 727.7782, found 727.7773 [M+2H].

## 5.0 References


(1) Rock, C. O.; Caldert, R. B.; Karim, M. A.; Jackowski, S. Pantothenate Kinase Regulation of the Intracellular Concentration of Coenzyme A. *J. Biol. Chem.* **2000**, *275* (2), 1377–1383. https://doi.org/10.1074/jbc.275.2.1377.

(2) Leonardi, R.; Zhang, Y. M.; Rock, C. O.; Jackowski, S. Coenzyme A: Back in Action. *Prog. Lipid Res.* **2005**, *44* (2–3), 125–153. https://doi.org/10.1016/j.plipres.2005.04.001.

(3) Chiarelli, L. R.; Mori, G.; Orena, B. S.; Esposito, M.; Lane, T.; De Jesus Lopes Ribeiro, A. L.; Degiacomi, G.; Zemanová, J.; Szádocka, S.; Huszár, S.; Palčeková, Z.; Manfredi, M.; Gosetti, F.; Lelièvre, J.; Ballell, L.; Kazakova, E.; Makarov, V.; Marengo, E.; Mikusova, K.; Cole, S. T.; Riccardi, G.; Ekins, S.; Pasca, M. R. A Multitarget Approach to Drug Discovery Inhibiting Mycobacterium Tuberculosis PyrG and PanK. *Sci. Rep.* **2018**, *8* (1), 1–10. https://doi.org/10.1038/s41598-018-21614-4.

(4) Leonardi, R.; Rock, C. O.; Jackowski, S. Pank1 Deletion in Leptin-Deficient Mice Reduces Hyperglycaemia and Hyperinsulinaemia and Modifies Global Metabolism without Affecting Insulin Resistance. *Diabetologia* **2014**, *57* (7), 1466–1475. https://doi.org/10.1007/s00125-014-3245-5.

(5) Sharma, L. K.; Subramanian, C.; Yun, M. K.; Frank, M. W.; White, S. W.; Rock, C. O.; Lee, R. E.; Jackowski, S. A Therapeutic Approach to Pantothenate Kinase Associated Neurodegeneration. *Nat. Commun.* **2018**, *9* (1). https://doi.org/10.1038/s41467-018-06703-2.

(6) Greenwald, E. C.; Mehta, S.; Zhang, J. Genetically Encoded Fluorescent Biosensors Illuminate the Spatiotemporal Regulation of Signaling Networks. *Chem. Rev.* **2018**, *118* (24), 11707–11794. https://doi.org/10.1021/acs.chemrev.8b00333.

(7) Tainaka, K.; Sakaguchi, R.; Hayashi, H.; Nakano, S.; Liew, F. F.; Morii, T. Design Strategies of Fluorescent Biosensors Based on Biological Macromolecular Receptors. *Sensors* **2010**, *10* (2), 1355–1376. https://doi.org/10.3390/s100201355.

(8) Brun, M. A.; Tan, K. T.; Nakata, E.; Hinner, M. J.; Johnsson, K. Semisynthetic Fluorescent Sensor Proteins Based on Self-Labeling Protein Tags. *J. Am. Chem. Soc.* **2009**, *131* (16), 5873–5884. https://doi.org/10.1021/ja900149e.

(9) Xue, L.; Prifti, E.; Johnsson, K. A General Strategy for the Semisynthesis of Ratiometric Fluorescent Sensor Proteins with Increased Dynamic Range. *J. Am. Chem. Soc.* **2016**, *138* (16), 5258–5261. https://doi.org/10.1021/jacs.6b03034.

(10) Sallin, O.; Reymond, L.; Gondrand, C.; Raith, F.; Koch, B.; Johnsson, K. Semisynthetic Biosensors for Mapping Cellular Concentrations of Nicotinamide Adenine Dinucleotides. *Elife* **2018**, *7*, 1–32. https://doi.org/10.7554/eLife.32638.

(11) Farrants, H.; Hiblot, J.; Griss, R.; Johnsson, K. *Rational Design and Applications of Semisynthetic Modular Biosensors: SNIFITs and LUCIDs*; Stein, V., Ed.; Methods in Molecular Biology; Springer New York: New York, NY, 2017; Vol. 1596. https://doi.org/10.1007/978-1-4939-6940-1.

(12) Masharina, A.; Reymond, L.; Maurel, D.; Umezawa, K.; Johnsson, K. A Fluorescent Sensor for GABA and Synthetic GABAB Receptor Ligands. *J. Am. Chem. Soc.* **2012**, *134* (46), 19026–19034. https://doi.org/10.1021/ja306320s.

(13) Mollwitz, B.; Brunk, E.; Schmitt, S.; Pojer, F.; Bannwarth, M.; Schiltz, M.; Rothlisberger, U.; Johnsson, K. Directed Evolution of the Suicide Protein O 6-Alkylguanine-DNA

Alkyltransferase for Increased Reactivity Results in an Alkylated Protein with Exceptional Stability. *Biochemistry* **2012**, *51* (5), 986–994. https://doi.org/10.1021/bi2016537.

(14) Hoehnel, S.; Lutolf, M. P. Capturing Cell-Cell Interactions via SNAP-Tag and CLIP-Tag Technology. *Bioconjug. Chem.* **2015**, *26* (8), 1678–1686. https://doi.org/10.1021/acs.bioconjchem.5b00268.

(15) England, C. G.; Luo, H.; Cai, W. HaloTag Technology: A Versatile Platform for Biomedical Applications. *Bioconjug. Chem.* **2015**, *26* (6), 975–986. https://doi.org/10.1021/acs.bioconjchem.5b00191.

(16) Wilhelm, J.; Kuhn, S.; Tarnawski, M.; Gotthard, G.; Tunnermann, J.; Tanzer, T.; Karpenko, J.; Mertes, N.; Xue, L.; Uhrig, U.; Reinstein, J.; Hiblot, J.; Johnsson, K. Kinetic and Structural Characterization of the Self-Labeling Protein Tags HaloTag7, SNAP-Tag, and CLIP-Tag. *Biochemistry* **2021**, *60* (33), 2560–2575. https://doi.org/10.1021/acs.biochem.1c00258.

(17) Hoelzel, C. A.; Zhang, X. Visualizing and Manipulating Biological Processes by Using HaloTag and SNAP-Tag Technologies. *ChemBioChem* **2020**, *21* (14), 1935–1946. https://doi.org/10.1002/cbic.202000037.

(18) Schnacke, P. L. Semisynthetic Protein Biosensors for Coenzyme A. **2021**, No. August.

(19) Brun, M. A.; Griss, R.; Reymond, L.; Tan, K. T.; Piguet, J.; Peters, R. J. R. W.; Vogel, H.; Johnsson, K. Semisynthesis of Fluorescent Metabolite Sensors on Cell Surfaces. *J. Am. Chem. Soc.* **2011**, *133* (40), 16235–16242. https://doi.org/10.1021/ja206915m.

(20) Brun, M. A.; Tan, K. T.; Griss, R.; Kielkowska, A.; Reymond, L.; Johnsson, K. A Semisynthetic Fluorescent Sensor Protein for Glutamate. *J. Am. Chem. Soc.* **2012**, *134* (18), 7676–7678. https://doi.org/10.1021/ja3002277.

(21) Reddy, B. K. K.; Landge, S.; Ravishankar, S.; Patil, V.; Shinde, V.; Tantry, S.; Kale, M.; Raichurkar, A.; Menasinakai, S.; Mudugal, N. V.; Ambady, A.; Ghosh, A.; Tunduguru, R.; Kaur, P.; Singh, R.; Kumar, N.; Bharath, S.; Sundaram, A.; Bhat, J.; Sambandamurthy, V. K.; Björkelid, C.; Jones, T. A.; Das, K.; Bandodkar, B.; Malolanarasimhan, K.; Mukherjee, K.; Ramachandran, V. Assessment of Mycobacterium Tuberculosis Pantothenate Kinase Vulnerability through Target Knockdown and Mechanistically Diverse Inhibitors. *Antimicrob. Agents Chemother.* **2014**, *58* (6), 3312–3326. https://doi.org/10.1128/AAC.00140-14.

(22) Lardon, N.; Wang, L.; Tschanz, A.; Hoess, P.; Tran, M.; D'Este, E.; Ries, J.; Johnsson, K. Systematic Tuning of Rhodamine Spirocyclization for Super-Resolution Microscopy. *J. Am. Chem. Soc.* **2021**, *143* (36), 14592–14600. https://doi.org/10.1021/jacs.1c05004.

# Chapter 7. Conclusions

## Conclusions

1. A family of multitarget drug ligands against Alzheimer´s disease based on a flavonoid scaffold was synthesised. Most of the compounds were found to be non-toxic and also to possess moderate antioxidant capabilities. The compounds that bear a tacrine fragment or a N-benzylpiperidine fragment inhibit AChE and BuChE some of them even in the low nanomolar range. Additionally, some hybrids have also proved to provide moderate protection against Aβ toxicity. Some of these hybrids are hits for future development against Alzheimer´s disease.

2. A multicomponent reaction involving a chalcone, a beta-ketoester and an amine was used to synthesise a family of m-diaryl dihydroanthranilates which were oxidised to their aromatic forms. This reaction was used to synthesise potential theragnostic systems, which consisted of dihydroanthranilates having a triphenylphosphonium group tethered by a carbon linker to its amine residue. Their aromatised derivatives showed promising optical properties and these compounds are to be tested in cell cultures to confirm their potential.

3. The dihydroanthranilate scaffolds synthesised were further derivatised into other structures such as acridones or m-terphenylamines. The latter had shown COX-1 selective inhibition in previous works and the family of compounds was amplified in order to obtain clearer SAR data. Additionally, potential multitarget drug ligands were synthesised by tethering a carbon-linked tacrine moiety to them. These compounds showed a good an AChE and BuChE inhibitory profile in the low-micromolar/high nanomolar range. COX-1/COX-2 inhibition assays will be performed to confirm their multitarget profile.

4. A general method for the mechanochemical synthesis of primary amides from their ester precursors has been developed. This method is robust as it tolerates different kinds of functional groups, such as aliphatic, aromatic heterocyclic, lactones, ketals and α-aminoesters and dipeptide esters. This method is fast, requires no solvent or gas influx and provides medium to high yields without the need for chromatography, creating a sustainable methodology for the synthesis of primary amides.

5. A one pot mechanochemical method for the synthesis of rufinamide has been developed. This method involves the use of readily available starting materials, is fast and requires no solvent or external heating, and also providing a good global yield. This method greatly improves green parameters in comparison to previously described methods for the synthesis of rufinamide.

6. Two different chemical ligands were synthesised for the determination of the activity of the enzyme panthotenate kinase and its real time visualization using confocal microscopy. The ligands were synthesised starting from readily available starting materials in a multi-step approach and were characterized. The ligands were then tested in cell cultures, and it was demonstrated that they were able to bind to the fusion protein and to exhibit FRET effect with it.

# Chapter 8. Representative spectra

## Representative spectra

## Chapter 3. Design, synthesis and study of a family of flavonoid-based multitarget drug ligands against Alzheimer's disease

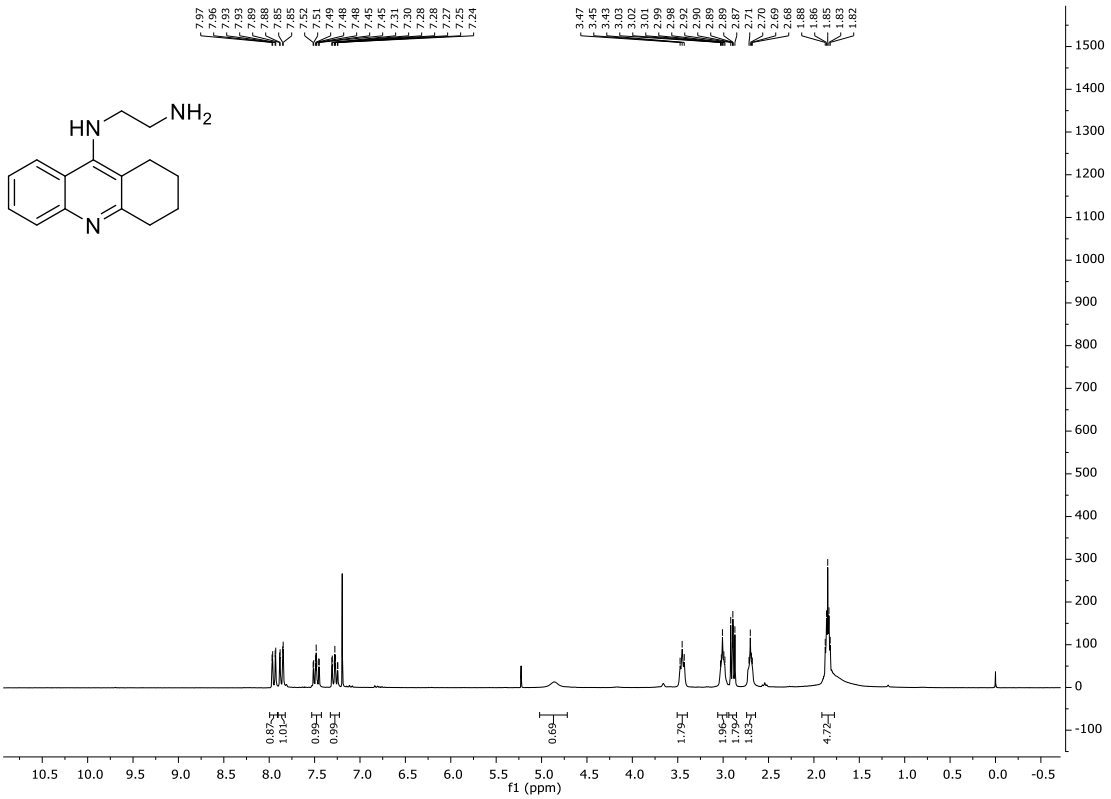


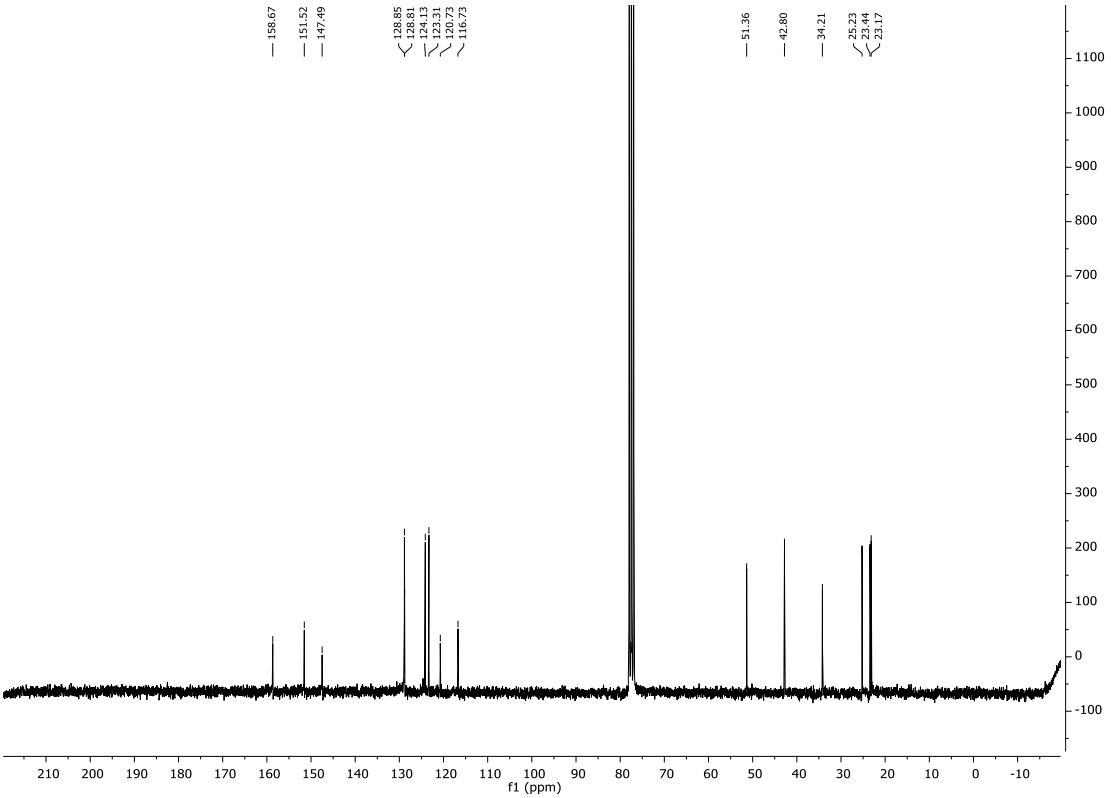

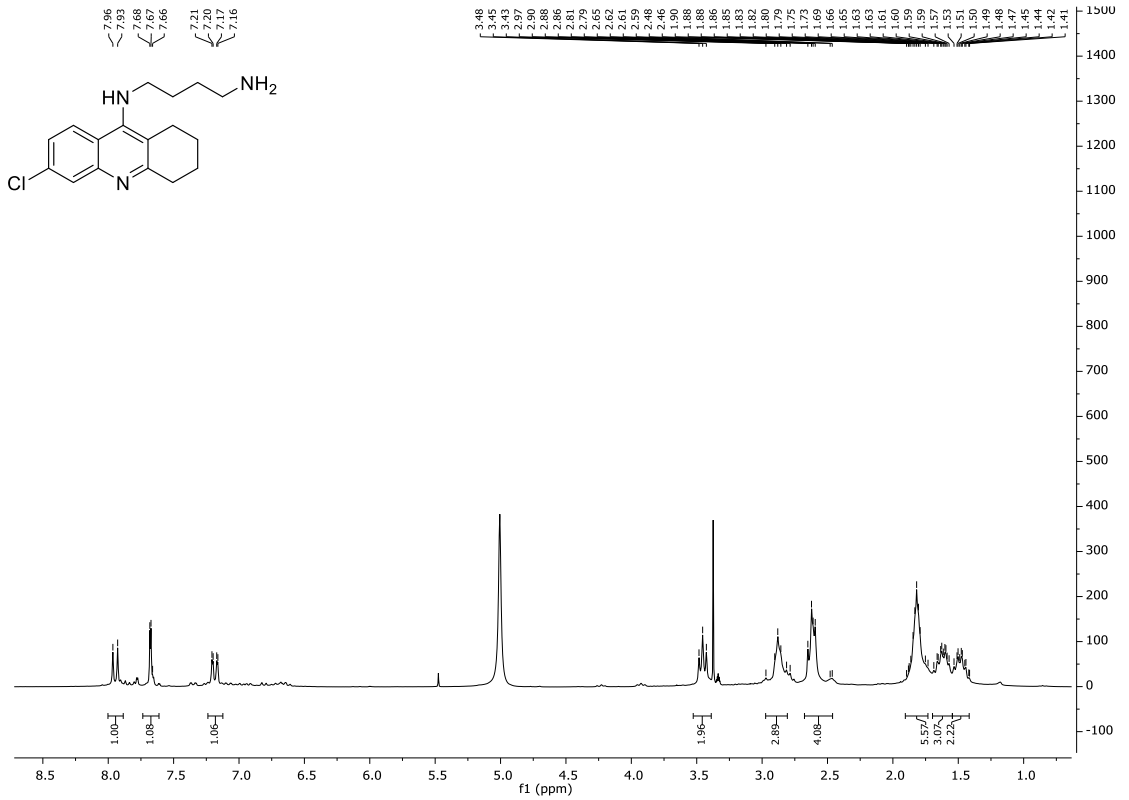
7.96
7.93
7.68
7.67
7.67
7.66
7.21
7.20
7.17
7.16
3.48
3.45
3.43
2.97
2.90
2.88
2.86
2.81
2.79
2.65
2.62
2.61
2.59
2.48
2.46
1.90
1.88
1.88
1.86
1.85
1.83
1.82
1.80
1.79
1.75
1.73
1.69
1.66
1.65
1.63
1.63
1.61
1.60
1.59
1.59
1.57
1.53
1.51
1.50
1.49
1.48
1.47
1.45
1.44
1.42
1.41
HN
NH2
Cl
N
1.00
1.08
1.06
1.96
2.89
4.08
5.57
3.07
2.22
f1 (ppm)

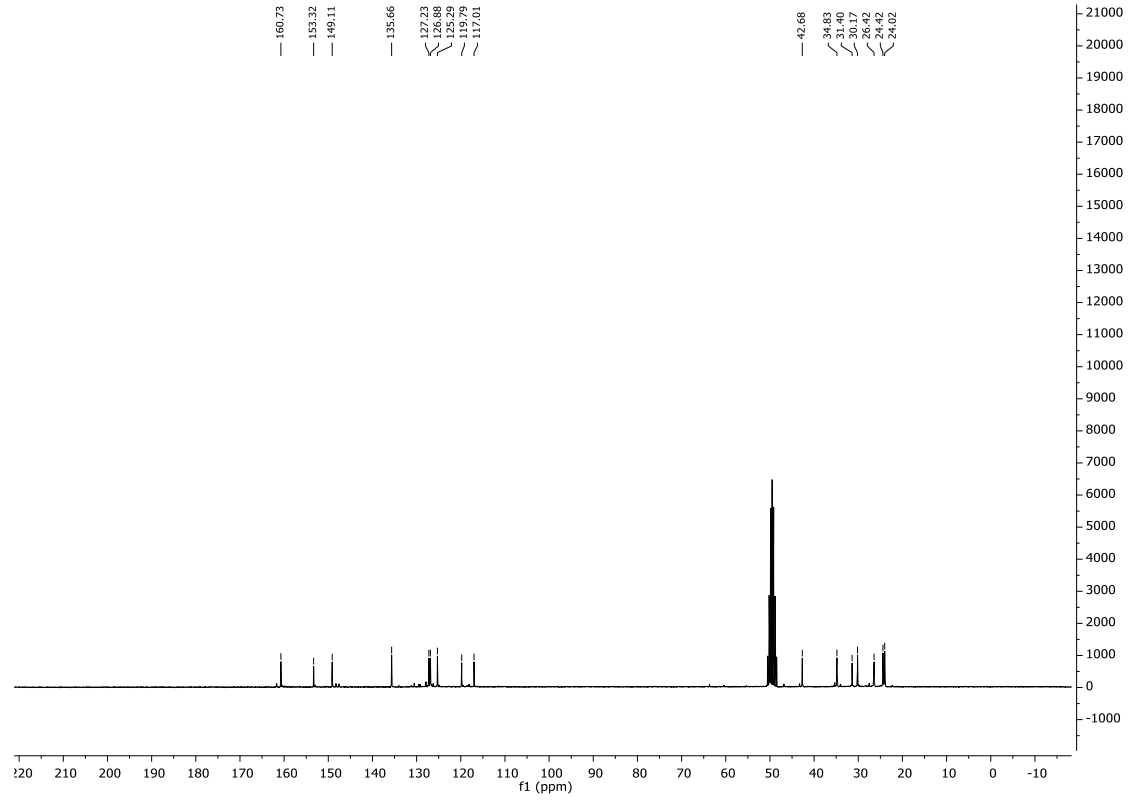
160.73
153.32
149.11
135.66
127.23
126.88
125.29
119.79
117.01
42.68
34.83
31.40
30.17
26.42
24.42
24.02
f1 (ppm)

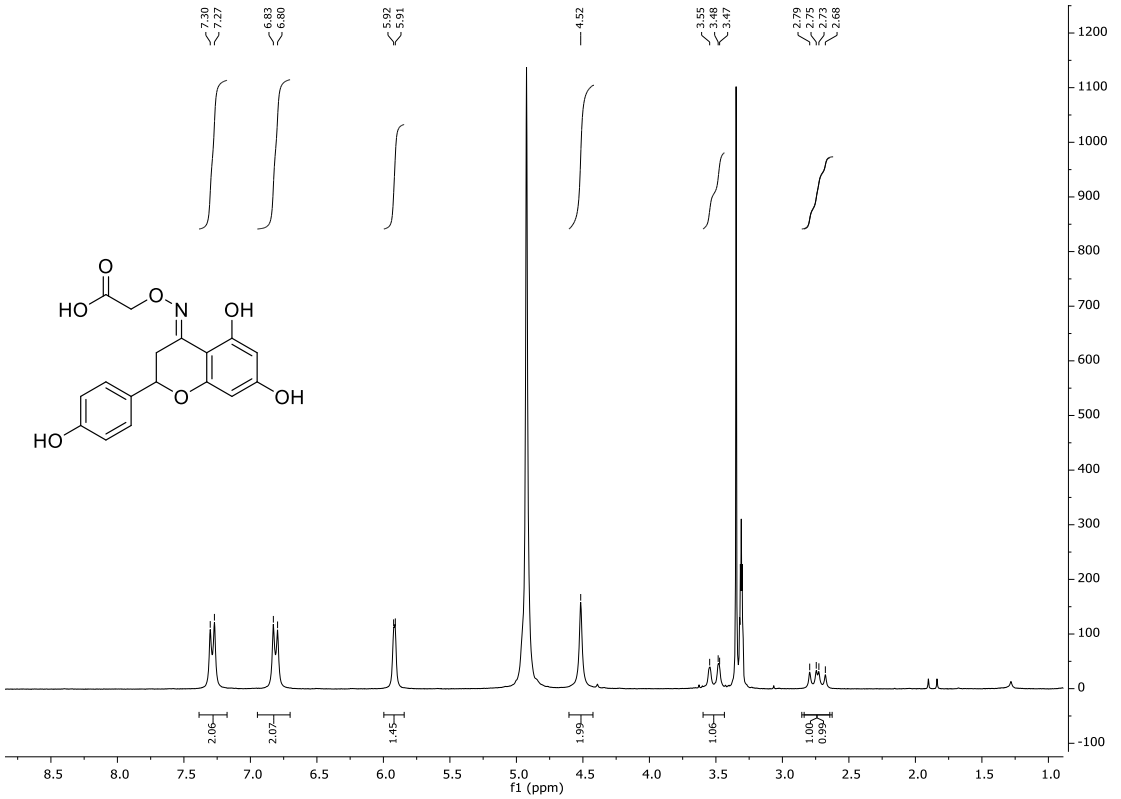
7.30
7.27
6.83
6.80
5.92
5.91
4.52
3.55
3.48
3.47
2.79
2.75
2.73
2.68
HO
O
O
N
OH
OH
HO
2.06
2.07
1.45
1.99
1.06
1.00
0.99
f1 (ppm)

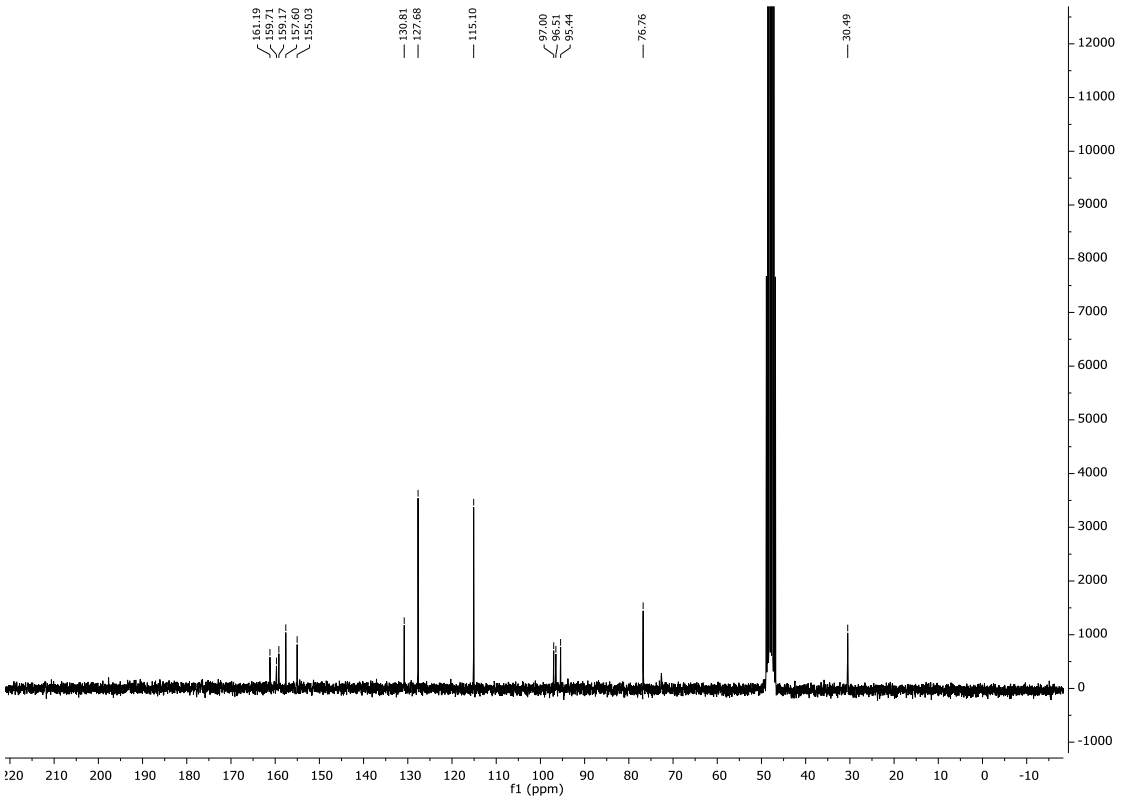
161.19
159.71
159.17
157.60
155.03
130.81
127.68
115.10
97.00
96.51
95.44
76.76
30.49
f1 (ppm)

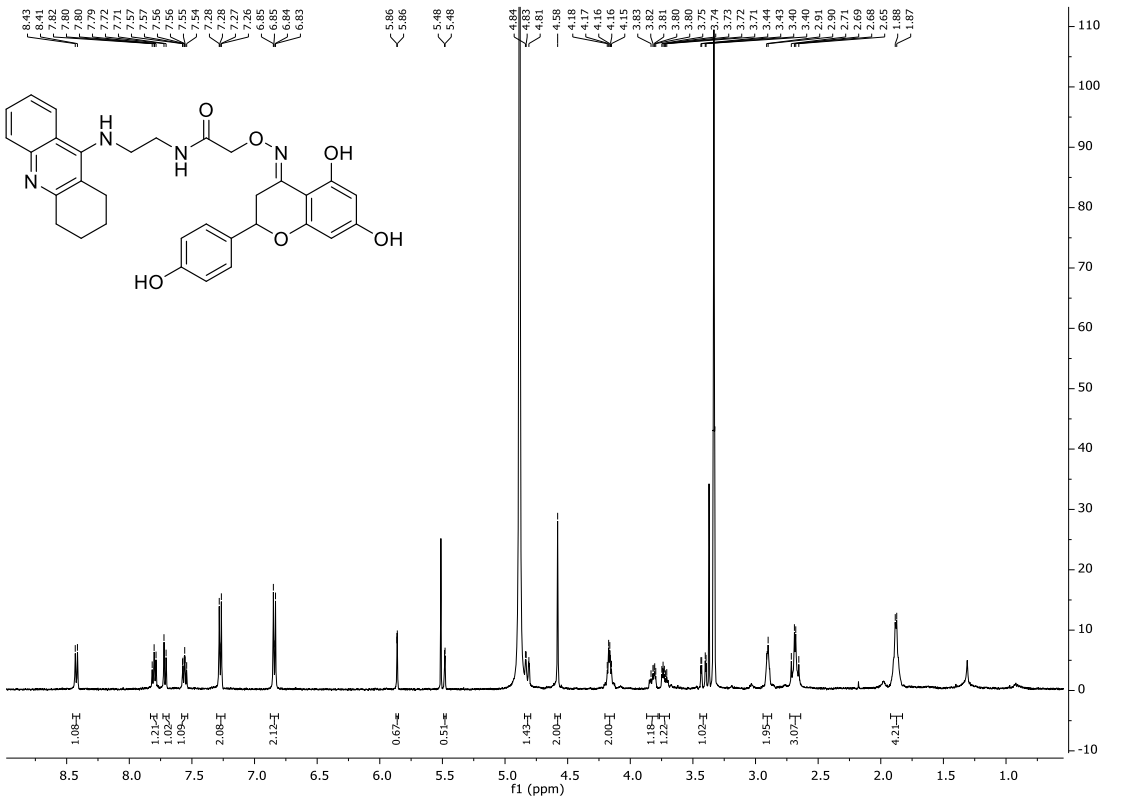
8.43 8.41 7.82 7.80 7.80 7.79 7.72 7.71 7.57 7.57 7.56 7.56 7.55 7.54 7.28 7.28 7.27 7.26 6.85 6.85 6.84 6.83 5.86 5.86 5.48 5.48 4.84 4.83 4.81 4.58 4.18 4.17 4.16 4.16 4.15 3.83 3.82 3.81 3.80 3.80 3.75 3.74 3.73 3.72 3.71 3.44 3.43 3.40 3.40 2.91 2.90 2.71 2.69 2.68 2.65 1.88 1.87
H N N H O O N OH N O OH HO
1.08 1.21 1.02 1.09 2.08 2.12 0.67 0.51 1.43 2.00 2.00 1.18 1.22 1.02 1.95 3.07 4.21
f1 (ppm)

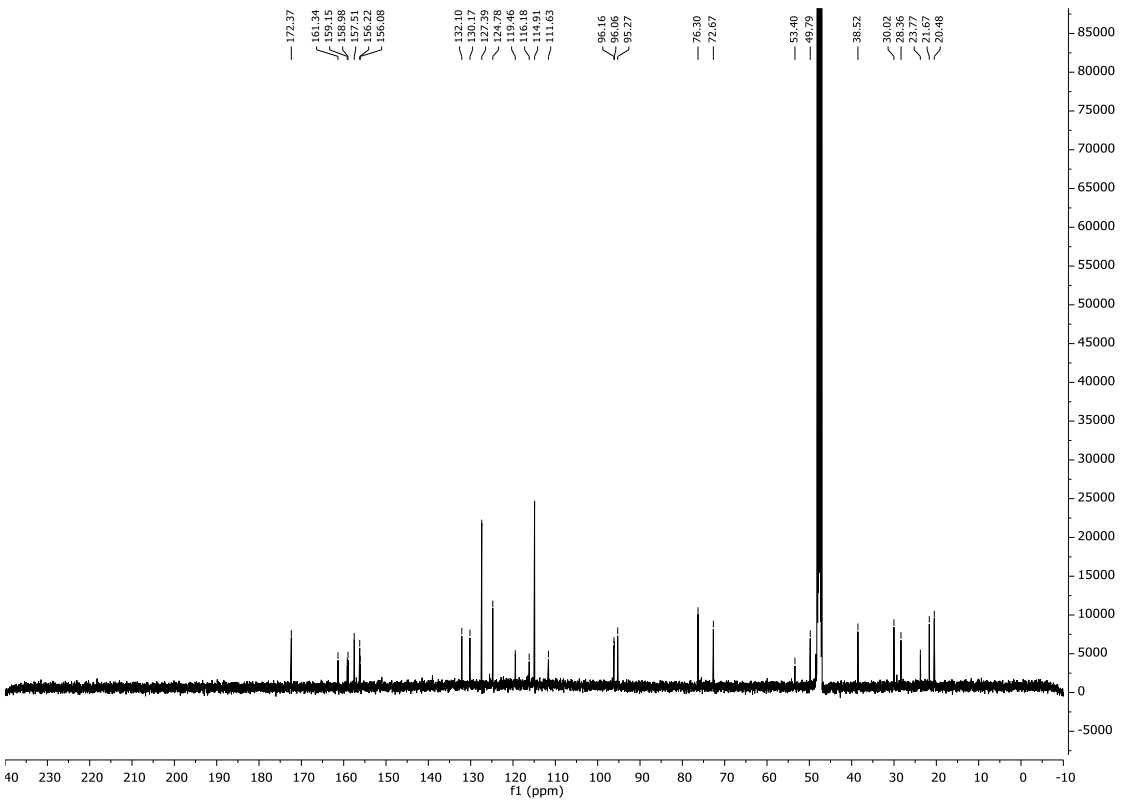
172.37 161.34 159.15 158.98 157.51 156.22 156.08 132.10 130.17 127.39 124.78 119.46 116.18 114.91 111.63 96.16 96.06 95.27 76.30 72.67 53.40 49.79 38.52 30.02 28.36 23.77 21.67 20.48
f1 (ppm)

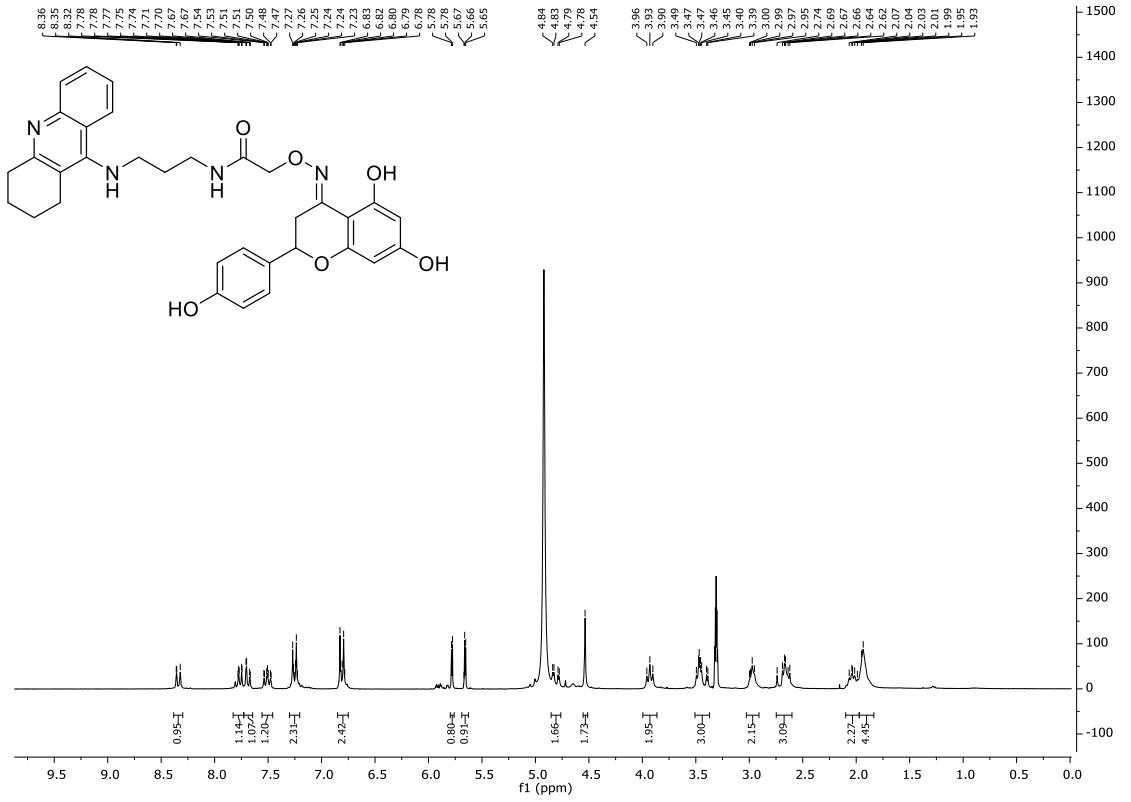
8.36 8.35 8.32 7.78 7.78 7.77 7.75 7.74 7.71 7.70 7.67 7.67 7.54 7.53 7.51 7.51 7.50 7.48 7.47 7.27 7.26 7.25 7.24 7.24 7.23 6.83 6.82 6.80 6.79 6.78 5.78 5.78 5.67 5.66 5.65
4.84 4.83 4.79 4.78 4.54
3.96 3.93 3.90 3.49 3.47 3.47 3.46 3.45 3.40 3.39 3.00 2.99 2.97 2.95 2.74 2.69 2.67 2.66 2.64 2.62 2.07 2.04 2.03 2.01 1.99 1.95 1.93
N
O
N
H
N
H
O
N
OH
OH
O
HO
0.95 1.14 1.07 1.20 2.31 2.42 0.80 0.91 1.66 1.73 1.95 3.00 2.15 3.09 2.22 4.45
f1 (ppm)

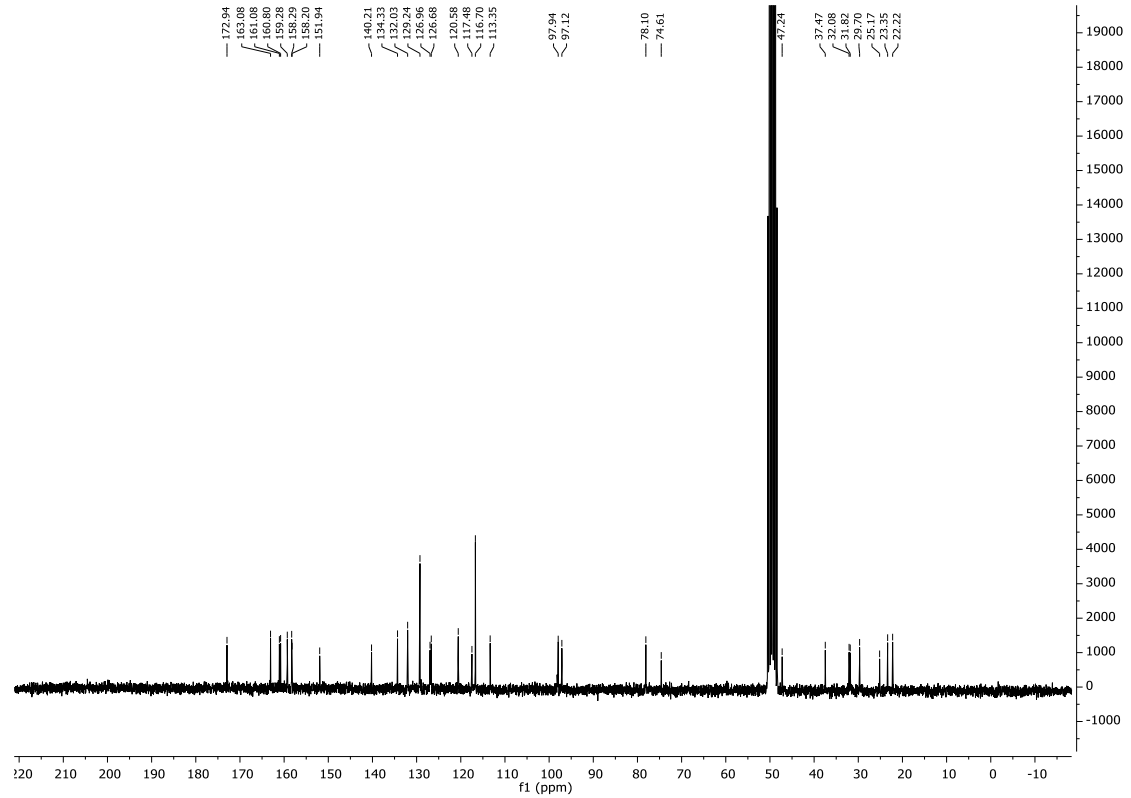
172.94 163.08 161.08 160.80 159.28 158.29 158.20 151.94
140.21 134.33 132.03 129.24 126.96 126.68 120.58 117.48 116.70 113.35
97.94 97.12
78.10 74.61
47.24
37.47 32.08 31.82 29.70 25.17 23.35 22.22
f1 (ppm)

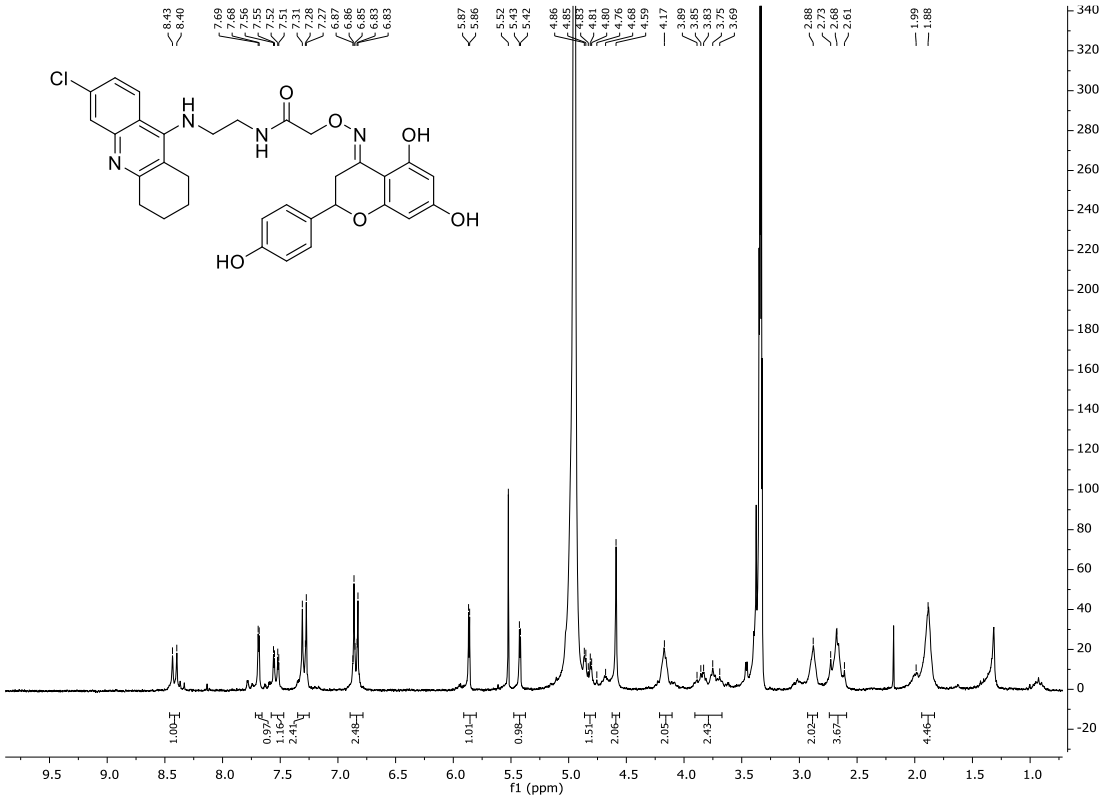
8.43
8.40
7.69
7.68
7.56
7.55
7.52
7.51
7.31
7.28
7.27
6.87
6.86
6.85
6.83
6.83
5.87
5.86
5.52
5.43
5.42
4.86
4.85
4.83
4.81
4.80
4.76
4.68
4.59
4.17
3.89
3.85
3.83
3.75
3.69
2.88
2.73
2.68
2.61
1.99
1.88
Cl
H
N
O
N
H
O
N
OH
N
OH
HO
1.00
0.97
1.16
2.41
2.48
1.01
0.98
1.51
2.06
2.05
2.43
2.02
3.67
4.46
f1 (ppm)

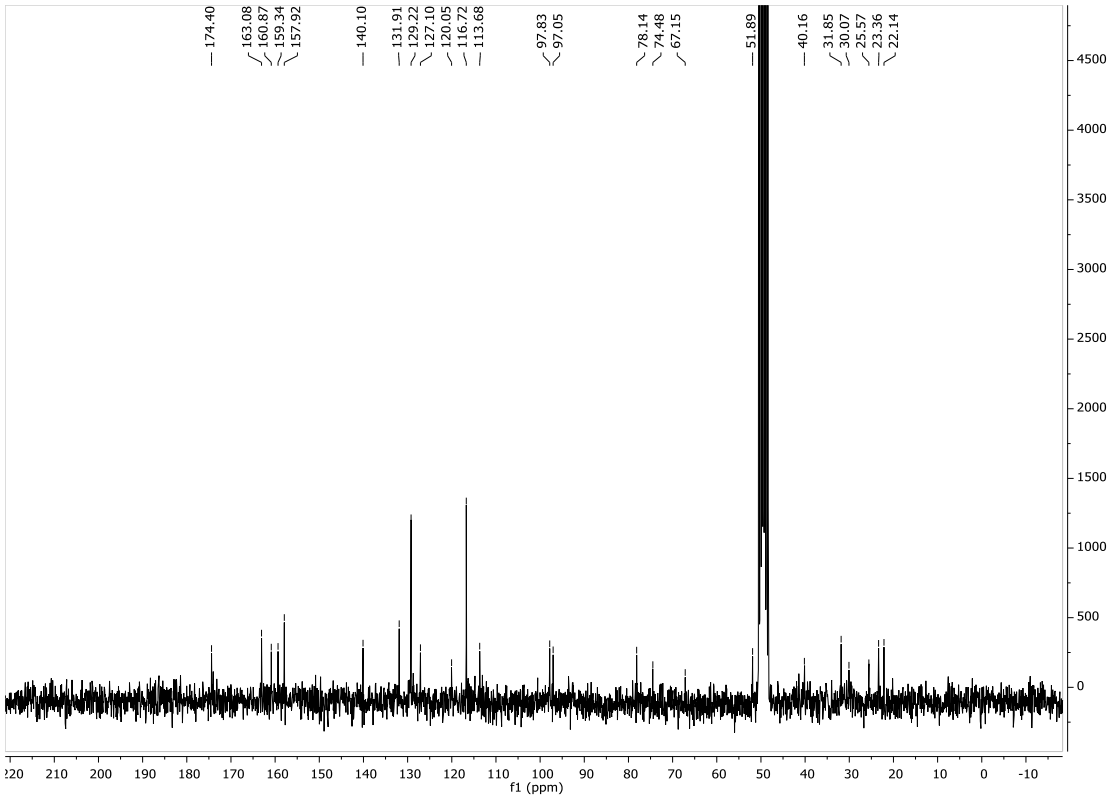
174.40
163.08
160.87
159.34
157.92
140.10
131.91
129.22
127.10
120.05
116.72
113.68
97.83
97.05
78.14
74.48
67.15
51.89
40.16
31.85
30.07
25.57
23.36
22.14
f1 (ppm)

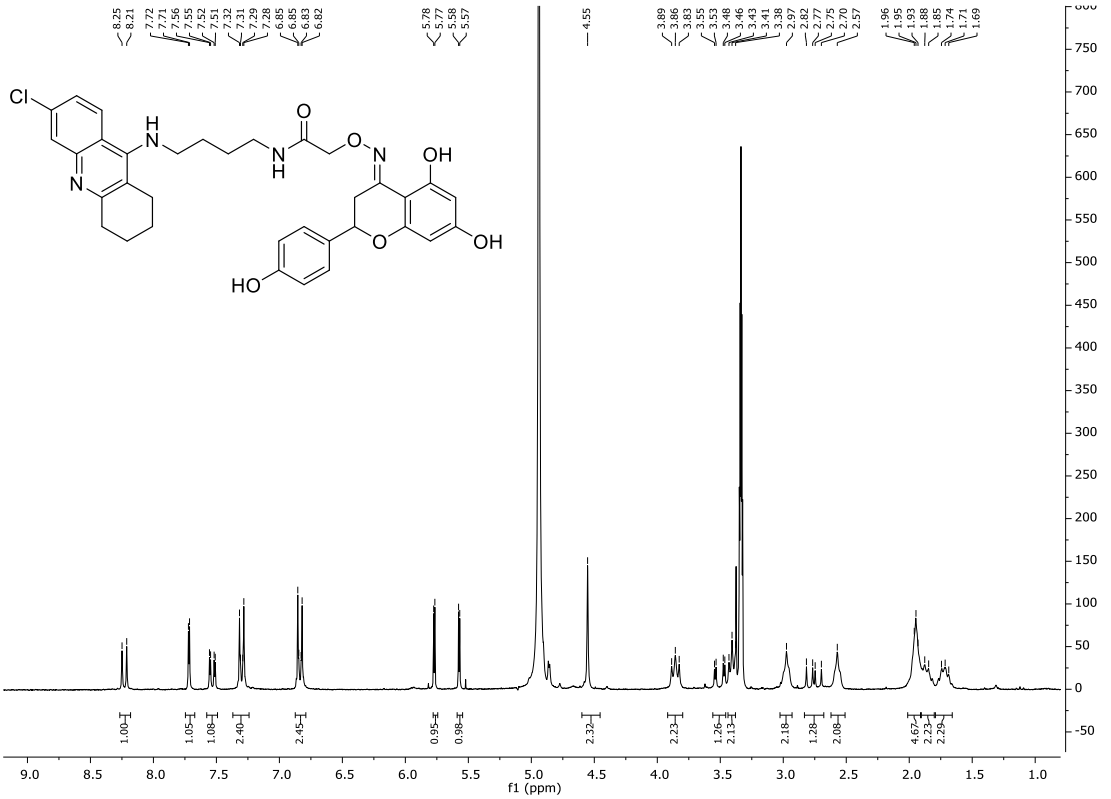
8.25
8.21
7.72
7.71
7.56
7.55
7.52
7.51
7.32
7.31
7.29
7.28
6.85
6.83
6.82
5.78
5.77
5.58
5.57
4.55
3.89
3.86
3.83
3.55
3.53
3.48
3.46
3.43
3.41
3.38
2.97
2.82
2.77
2.75
2.70
2.57
1.96
1.95
1.93
1.88
1.85
1.74
1.71
1.69
Cl
H
N
N
O
N
H
O
N
OH
OH
HO
O
1.00
1.05
1.08
2.40
2.45
0.95
0.98
2.32
2.23
1.26
2.13
2.18
1.28
2.08
4.67
2.23
2.29
f1 (ppm)

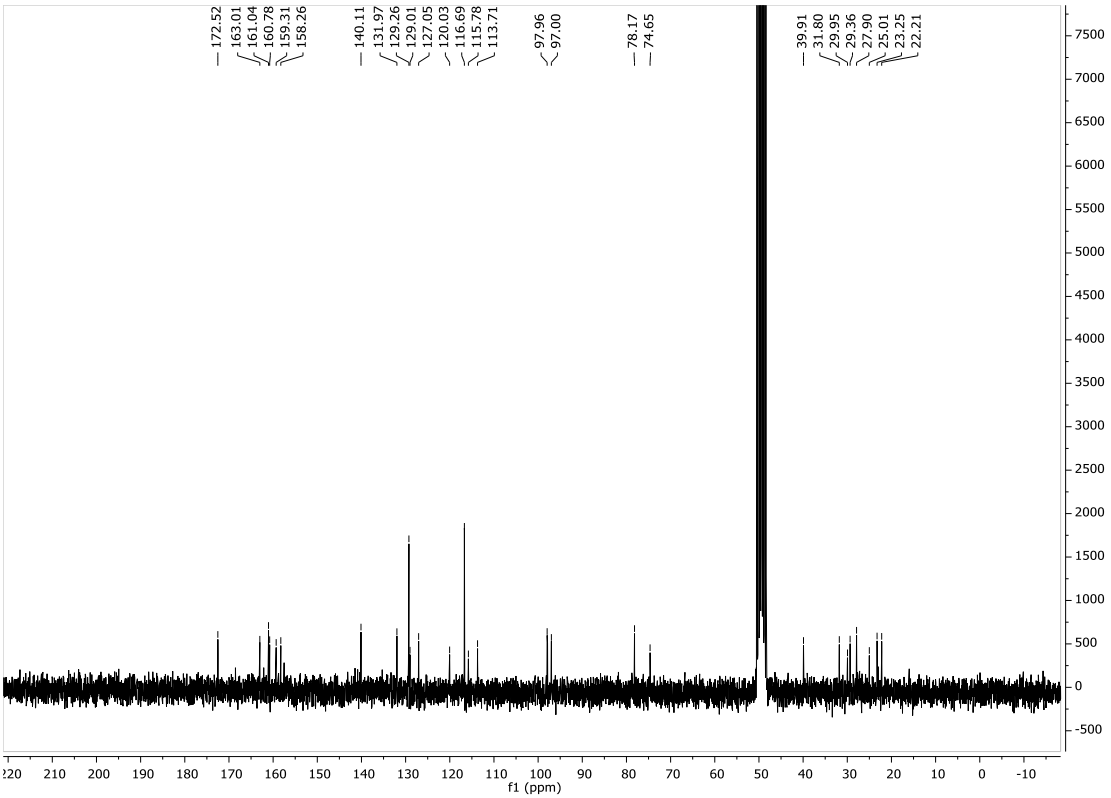
172.52
163.01
161.04
160.78
159.31
158.26
140.11
131.97
129.26
129.01
127.05
120.03
116.69
115.78
113.71
97.96
97.00
78.17
74.65
39.91
31.80
29.95
29.36
27.90
25.01
23.25
22.21
f1 (ppm)

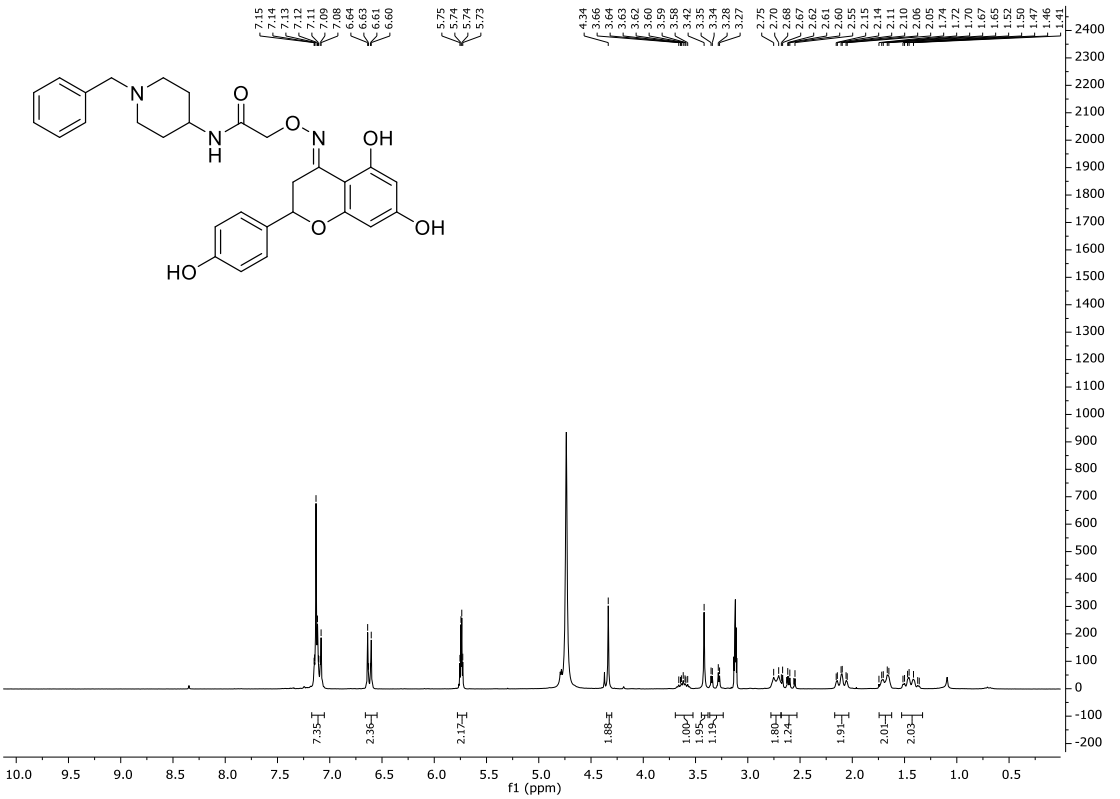
7.15
7.14
7.13
7.12
7.11
7.09
7.08
6.64
6.63
6.61
6.60
5.75
5.74
5.74
5.73
4.34
3.66
3.64
3.63
3.62
3.60
3.59
3.58
3.42
3.35
3.34
3.28
3.27
2.75
2.70
2.68
2.67
2.62
2.61
2.60
2.55
2.15
2.14
2.11
2.10
2.06
2.05
1.74
1.72
1.70
1.67
1.65
1.52
1.50
1.47
1.46
1.41
N
O
N
H
O
N
OH
O
OH
HO
7.35
2.36
2.17
1.88
1.00
1.95
1.19
1.80
1.24
1.91
2.01
2.03
f1 (ppm)

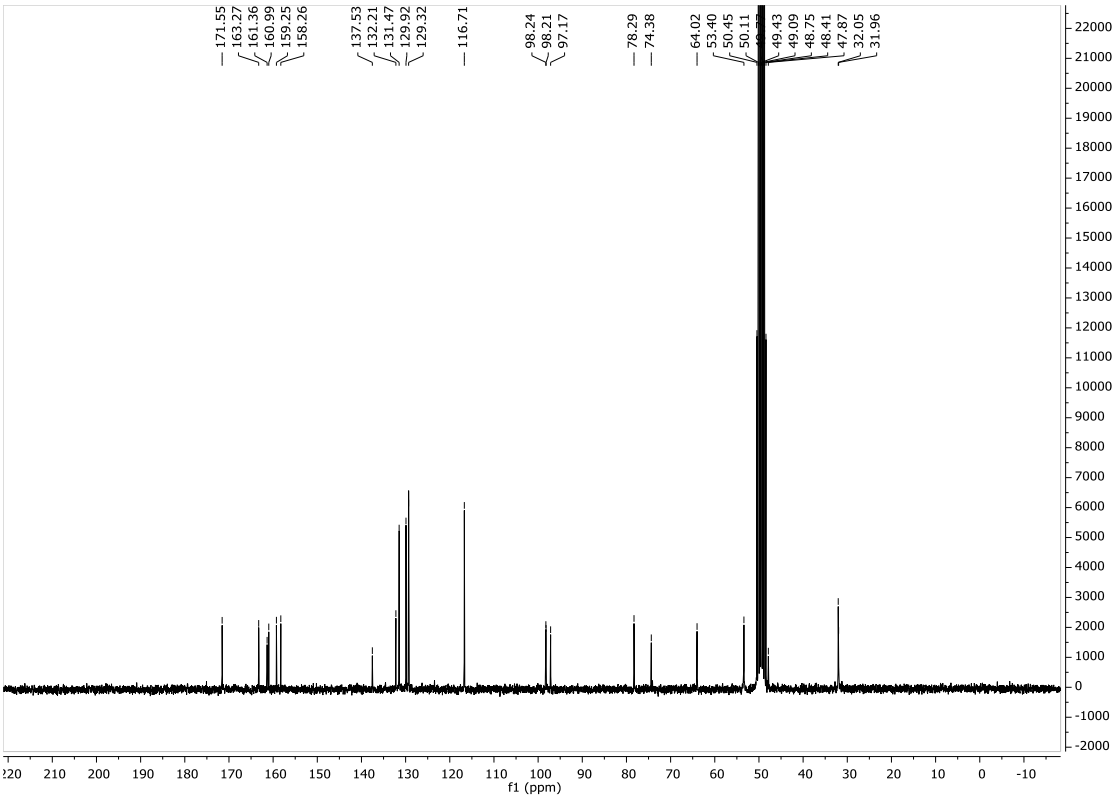
171.55
163.27
161.36
160.99
159.25
158.26
137.53
132.21
131.47
129.92
129.32
116.71
98.24
98.21
97.17
78.29
74.38
64.02
53.40
50.45
50.11
49.43
49.09
48.75
48.41
47.87
32.05
31.96
f1 (ppm)

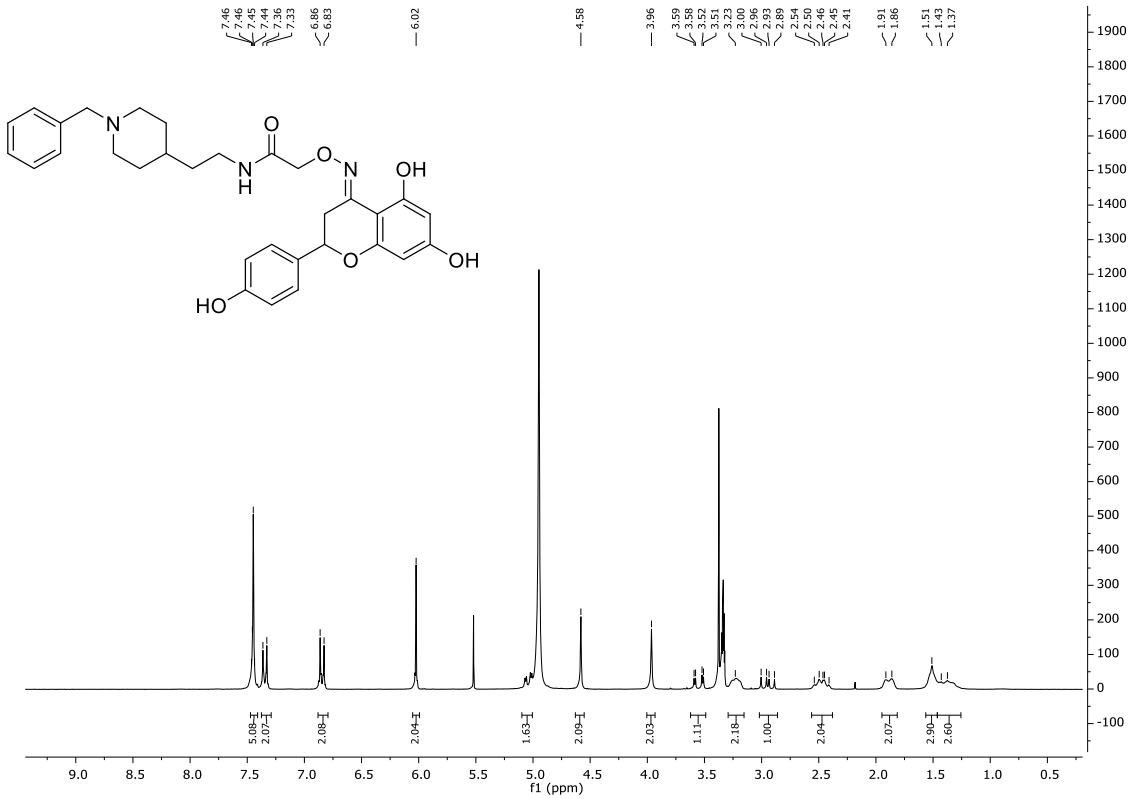
7.46
7.46
7.45
7.44
7.36
7.33
6.86
6.83
6.02
4.58
3.96
3.59
3.58
3.52
3.51
3.23
3.00
2.96
2.93
2.89
2.54
2.50
2.46
2.45
2.41
1.91
1.86
1.51
1.43
1.37
N
O
N
H
O
N
OH
OH
O
HO
5.08
2.07
2.08
2.04
1.63
2.09
2.03
1.11
2.18
1.00
2.04
2.07
2.90
2.60
f1 (ppm)

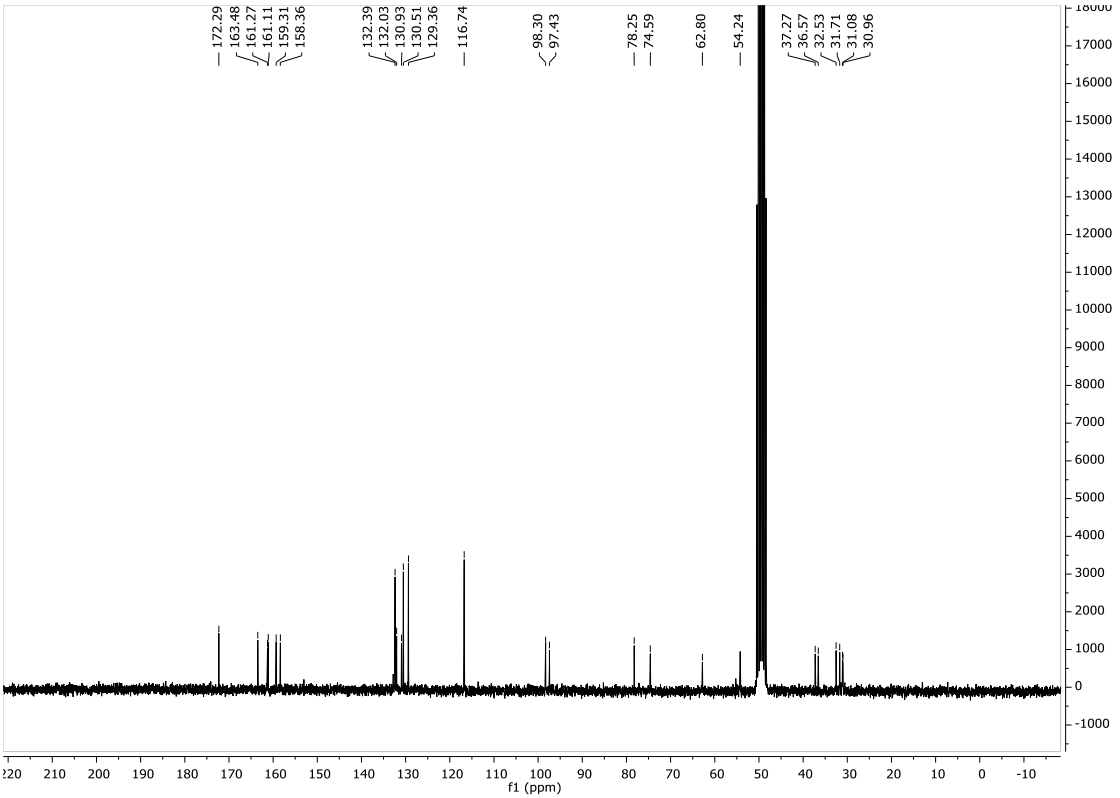
172.29
163.48
161.27
161.11
159.31
158.36
132.39
132.03
130.93
130.51
129.36
116.74
98.30
97.43
78.25
74.59
62.80
54.24
37.27
36.57
32.53
31.71
31.08
30.96
f1 (ppm)

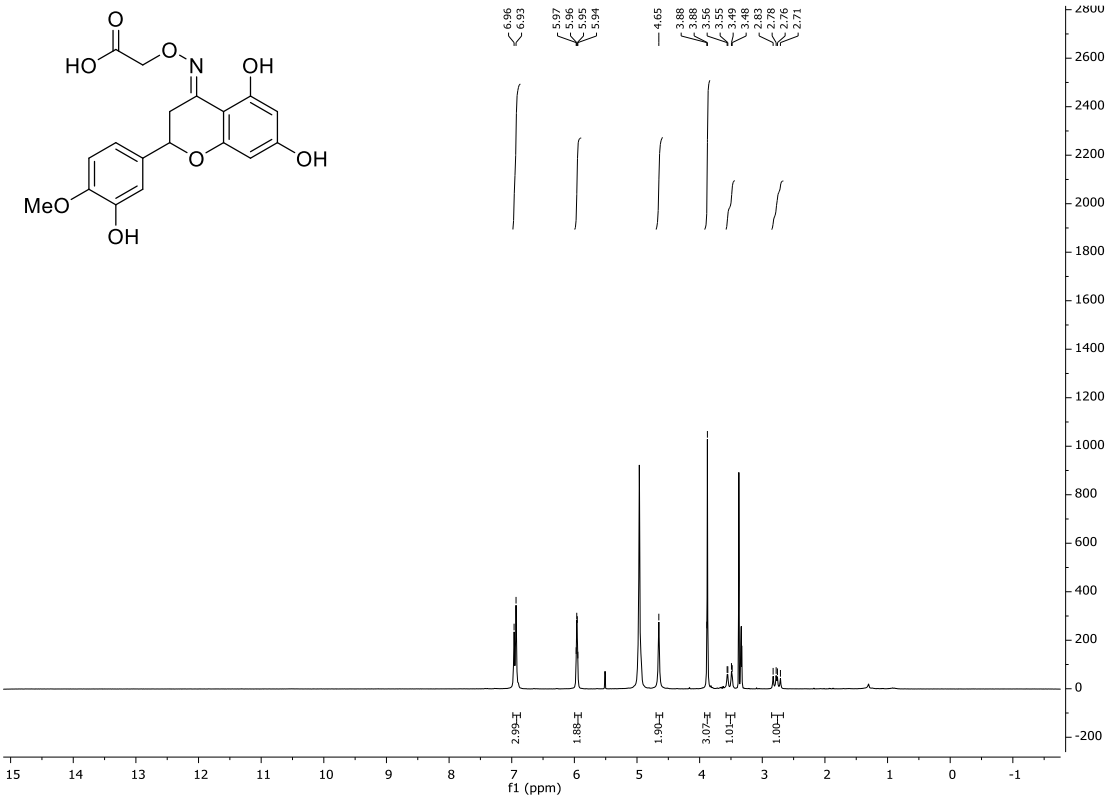
6.96
6.93
5.97
5.96
5.95
5.94
4.65
3.88
3.88
3.56
3.55
3.49
3.48
2.83
2.78
2.76
2.71
2.99
1.88
1.90
3.07
1.01
1.00
f1 (ppm)

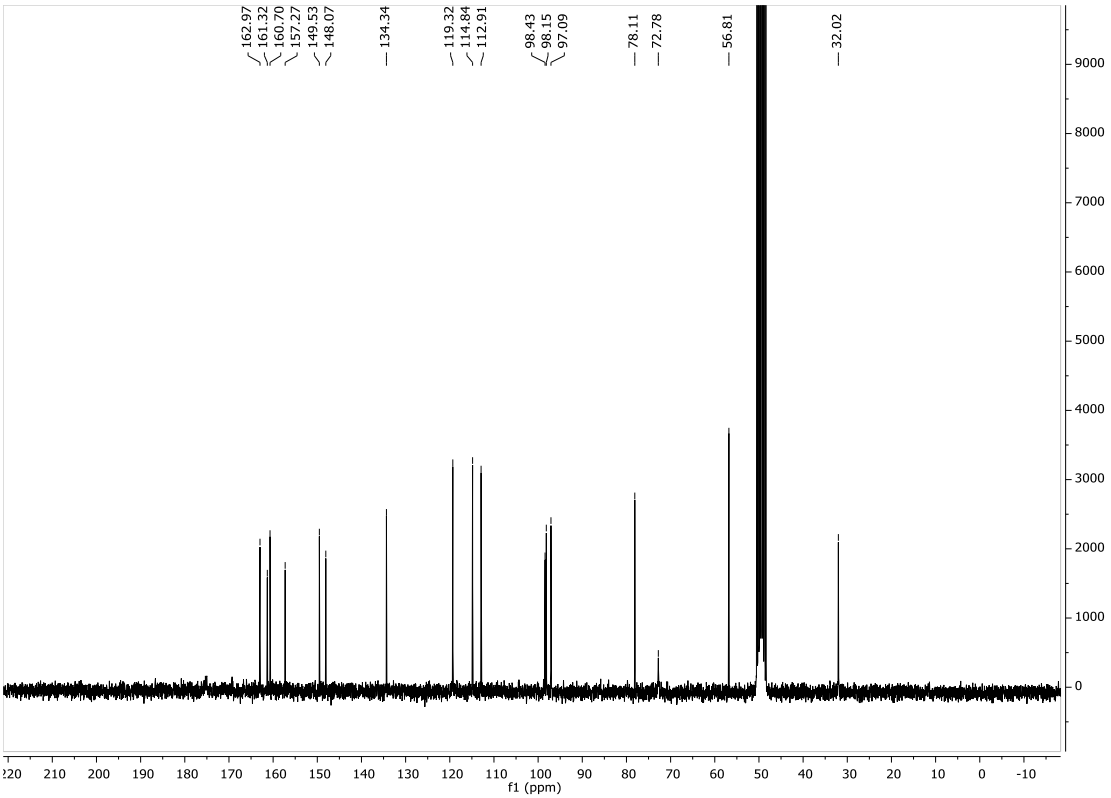
162.97
161.32
160.70
157.27
149.53
148.07
134.34
119.32
114.84
112.91
98.43
98.15
97.09
78.11
72.78
56.81
32.02
f1 (ppm)

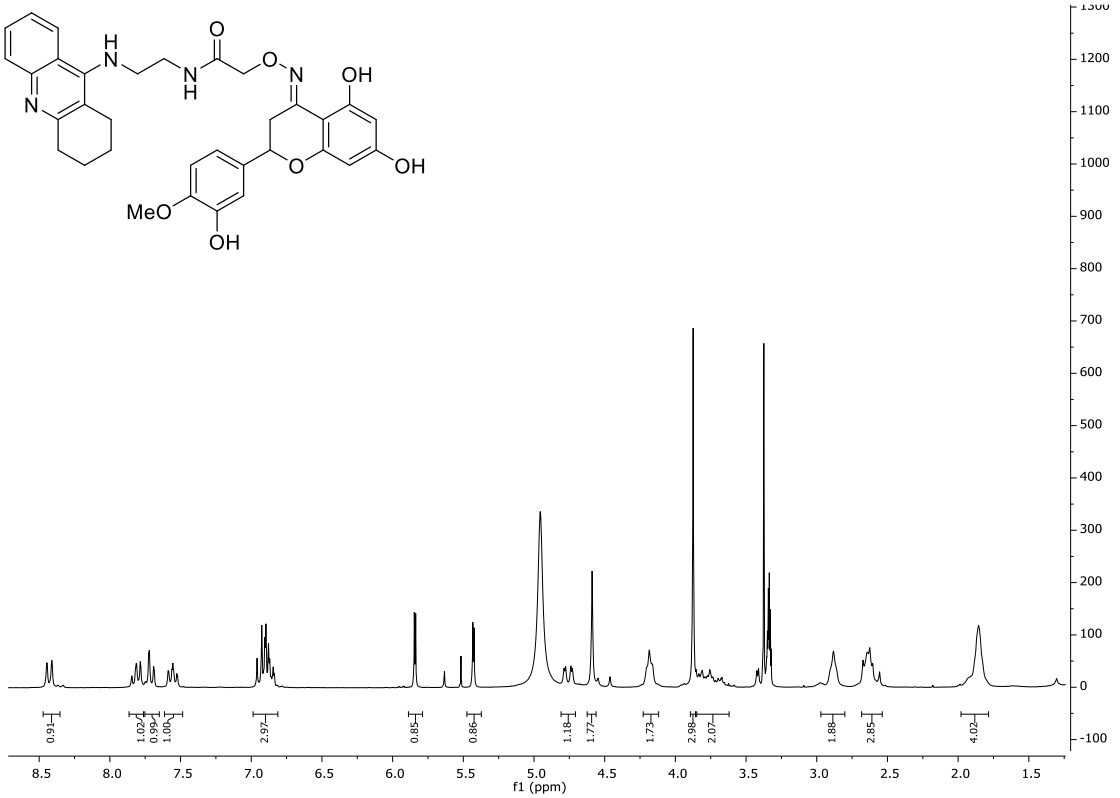
H
N
N
H
O
O
N
OH
OH
N
O
MeO
OH
0.91
1.02
0.99
1.00
2.97
0.85
0.86
1.18
1.77
1.73
2.98
2.07
1.88
2.85
4.02
f1 (ppm)

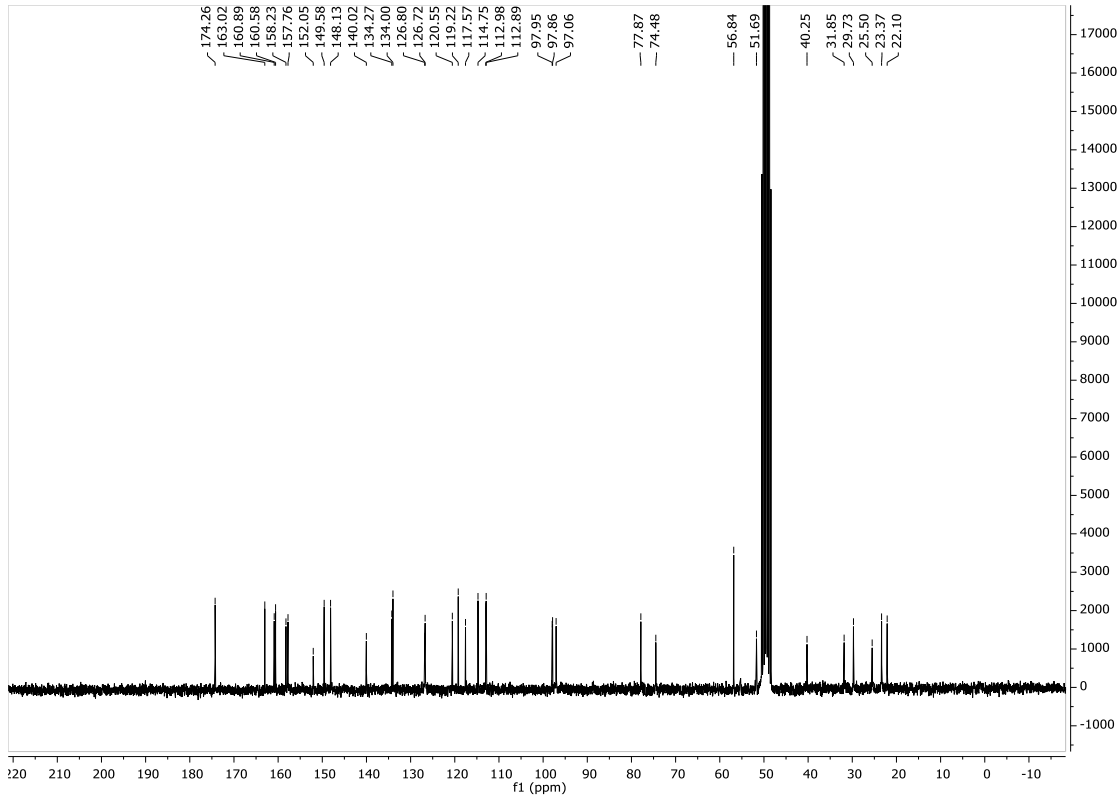
174.26
163.02
160.89
160.58
158.23
157.76
152.05
149.58
148.13
140.02
134.27
134.00
126.80
126.72
120.55
119.22
117.57
114.75
112.98
112.89
97.95
97.86
97.06
77.87
74.48
56.84
51.69
40.25
31.85
29.73
25.50
23.37
22.10
f1 (ppm)

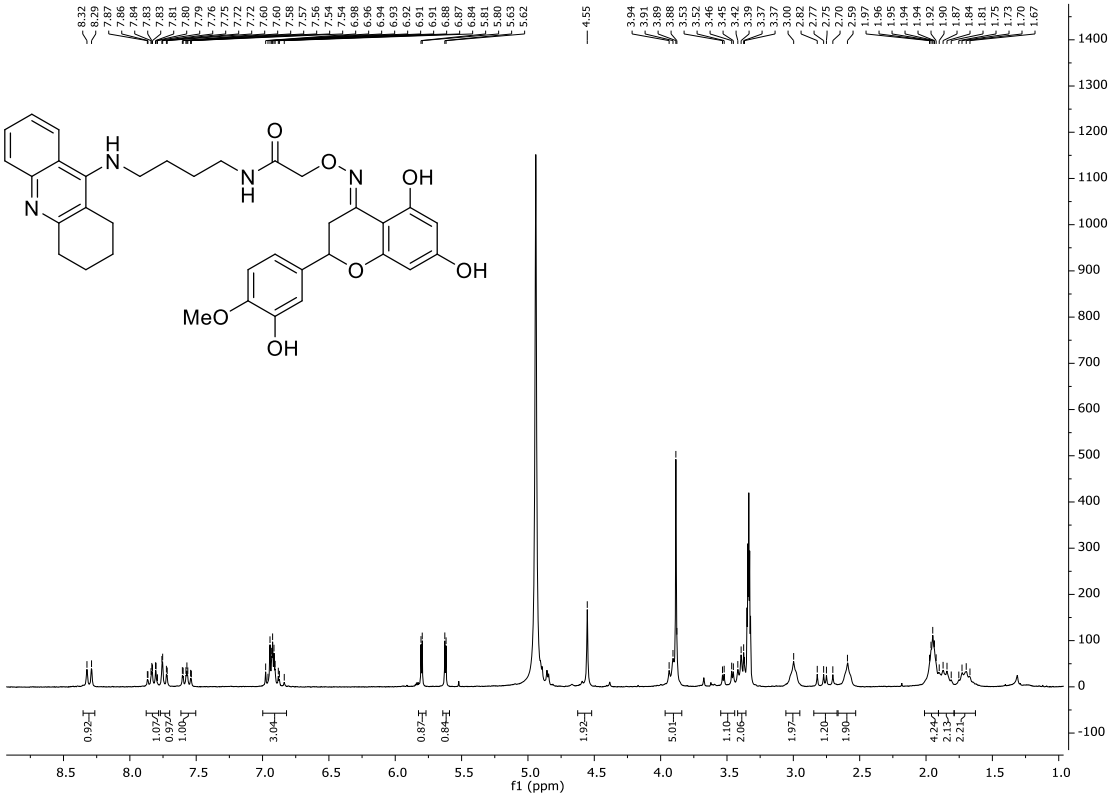
8.32 8.29 7.87 7.86 7.84 7.83 7.83 7.81 7.80 7.79 7.76 7.75 7.72 7.72 7.60 7.60 7.58 7.57 7.56 7.54 7.54 6.98 6.96 6.94 6.93 6.92 6.91 6.91 6.88 6.87 6.84 5.81 5.80 5.63 5.62 4.55 3.94 3.91 3.89 3.88 3.53 3.52 3.46 3.45 3.42 3.39 3.37 3.37 3.00 2.82 2.77 2.75 2.70 2.59 1.97 1.96 1.95 1.94 1.94 1.92 1.90 1.87 1.84 1.81 1.75 1.73 1.70 1.67
H N N H O O N OH N O OH MeO OH
0.92 1.07 0.97 1.00 3.04 0.87 0.84 1.92 5.01 1.10 2.06 1.97 1.20 1.90 4.24 2.13 2.21
f1 (ppm)

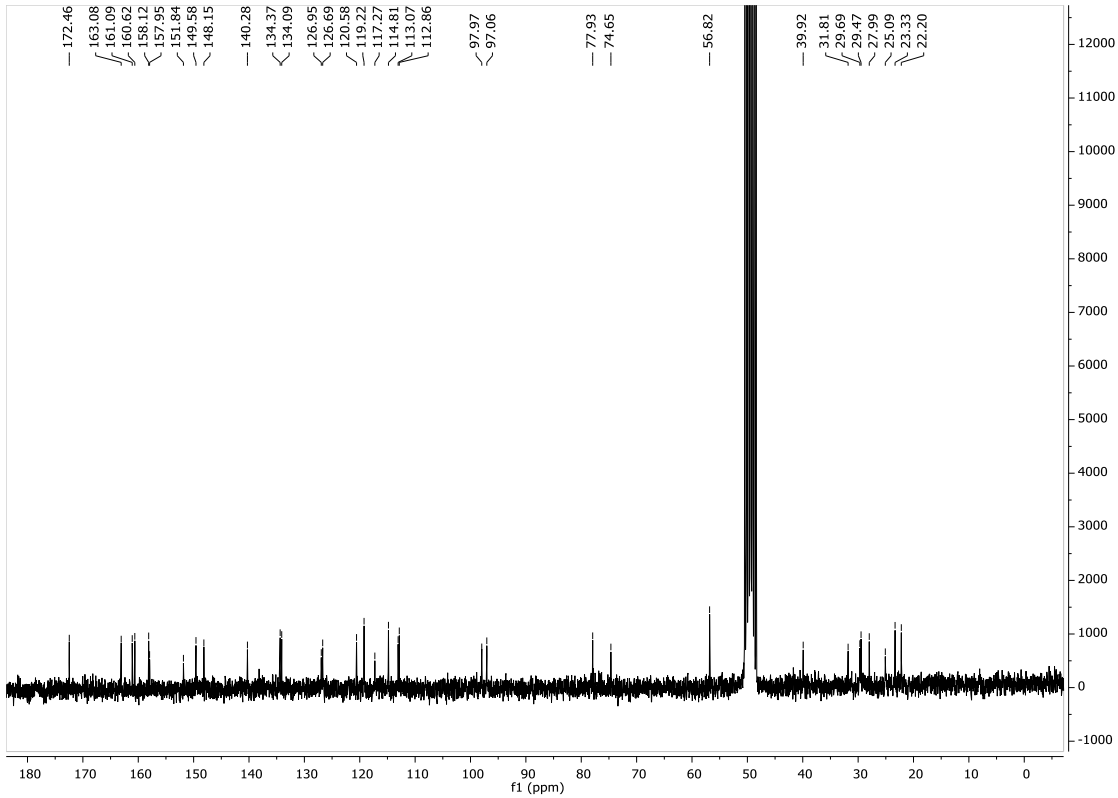
172.46 163.08 161.09 160.62 158.12 157.95 151.84 149.58 148.15 140.28 134.37 134.09 126.95 126.69 120.58 119.22 117.27 114.81 113.07 112.86 97.97 97.06 77.93 74.65 56.82 39.92 31.81 29.69 29.47 27.99 25.09 23.33 22.20
f1 (ppm)

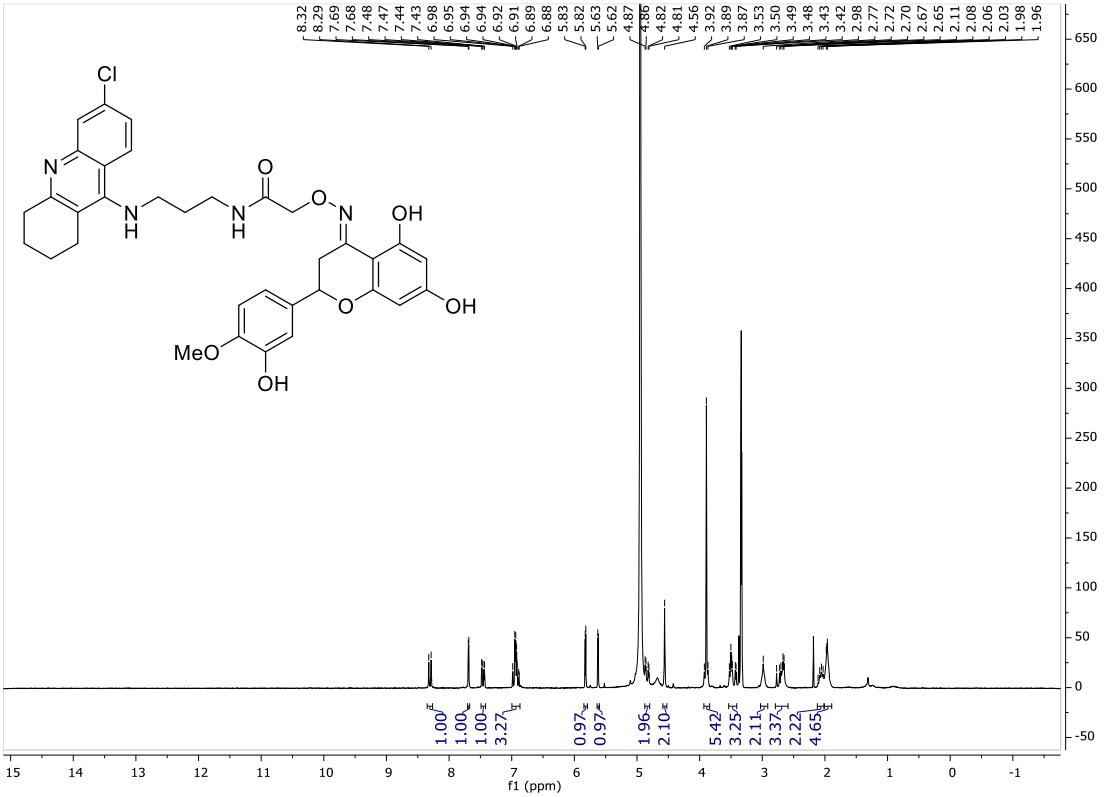
8.32
8.29
7.69
7.68
7.48
7.47
7.44
7.43
6.98
6.95
6.94
6.94
6.92
6.91
6.89
6.88
5.83
5.82
5.63
5.62
4.87
4.86
4.82
4.81
4.56
3.92
3.89
3.87
3.53
3.50
3.49
3.48
3.43
3.42
2.98
2.77
2.72
2.70
2.67
2.65
2.11
2.08
2.06
2.03
1.98
1.96
Cl
N
O
O
N
OH
N
H
N
H
OH
MeO
OH
1.00
1.00
1.00
3.27
0.97
0.97
1.96
2.10
5.42
3.25
2.11
3.37
2.22
4.65
f1 (ppm)

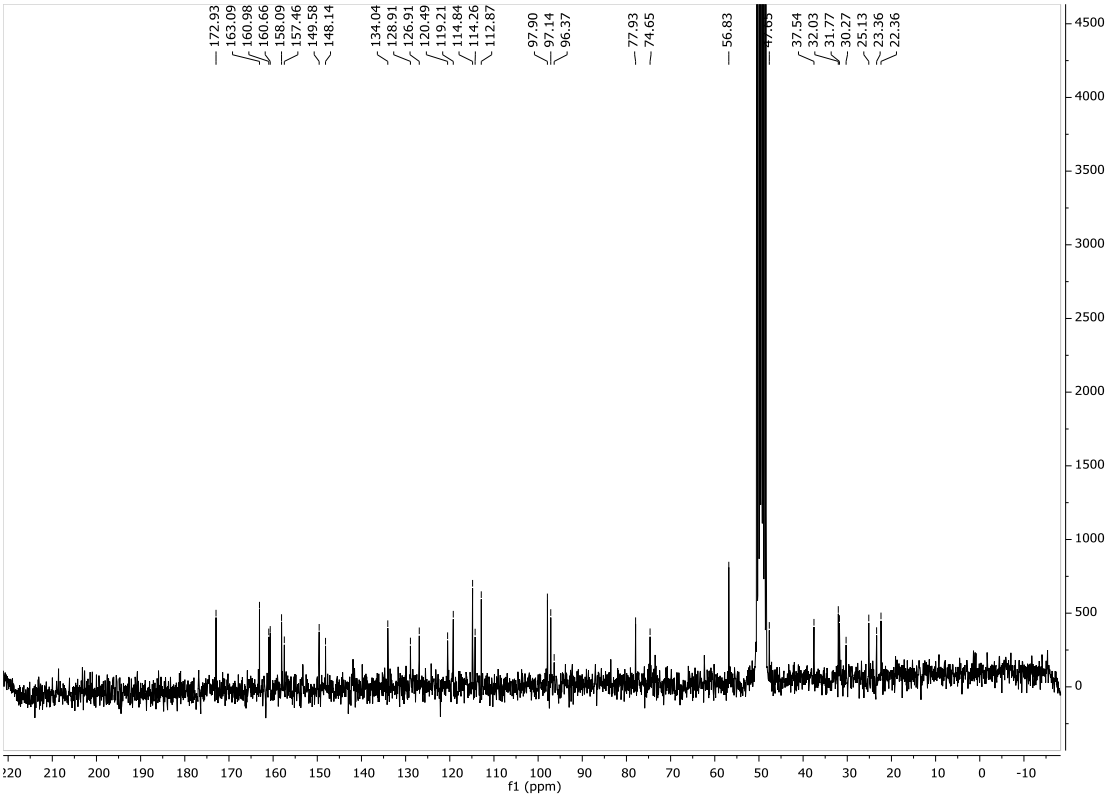
172.93
163.09
160.98
160.66
158.09
157.46
149.58
148.14
134.04
128.91
126.91
120.49
119.21
114.84
114.26
112.87
97.90
97.14
96.37
77.93
74.65
56.83
47.03
37.54
32.03
31.77
30.27
25.13
23.36
22.36
f1 (ppm)

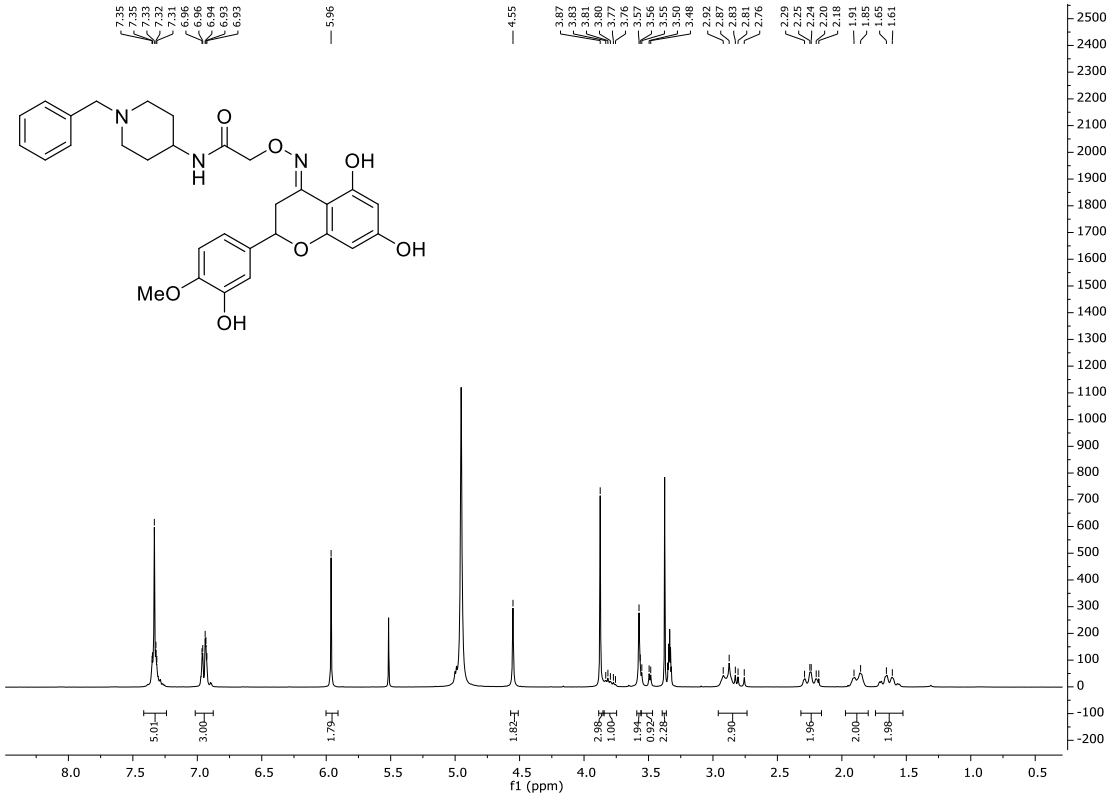
7.35
7.35
7.33
7.32
7.31
6.96
6.96
6.94
6.93
6.93
5.96
4.55
3.87
3.83
3.81
3.80
3.77
3.76
3.57
3.56
3.55
3.50
3.48
2.92
2.87
2.83
2.81
2.76
2.29
2.25
2.24
2.20
2.18
1.91
1.85
1.65
1.61
N
O
N
H
O
N
OH
OH
O
MeO
OH
5.01
3.00
1.79
1.82
2.98
1.00
1.94
0.92
2.28
2.90
1.96
2.00
1.98
f1 (ppm)

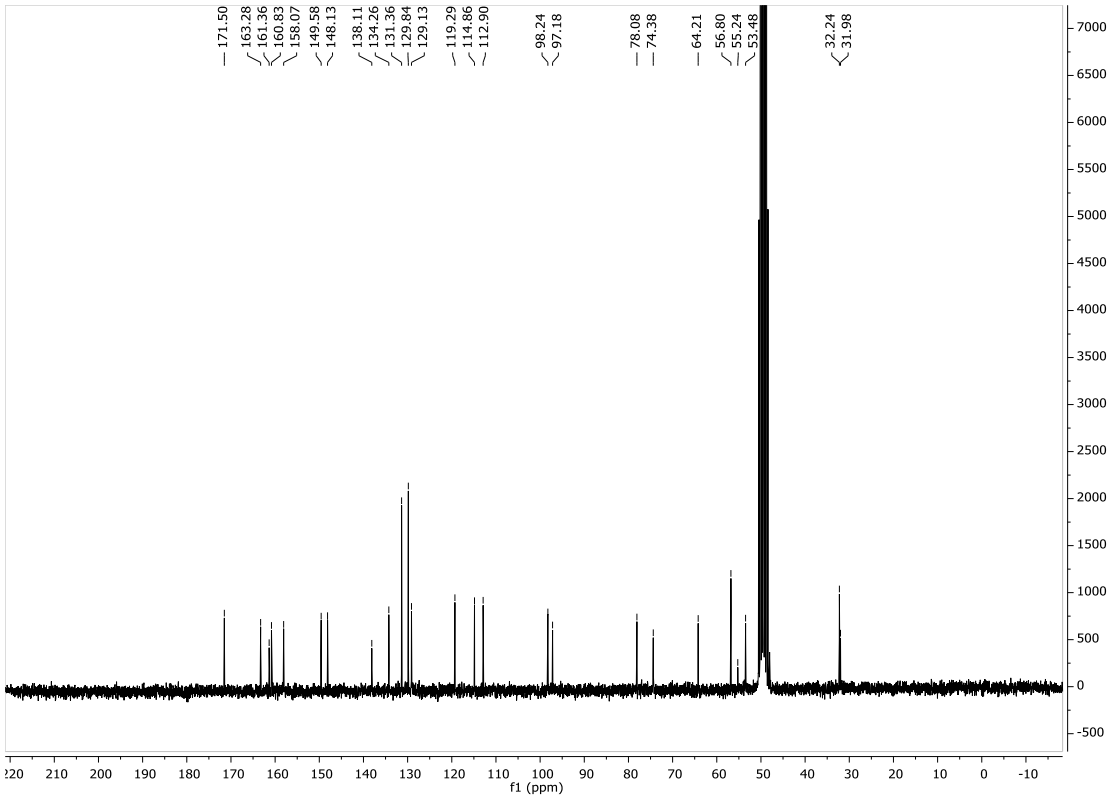
171.50
163.28
161.36
160.83
158.07
149.58
148.13
138.11
134.26
131.36
129.84
129.13
119.29
114.86
112.90
98.24
97.18
78.08
74.38
64.21
56.80
55.24
53.48
32.24
31.98
f1 (ppm)

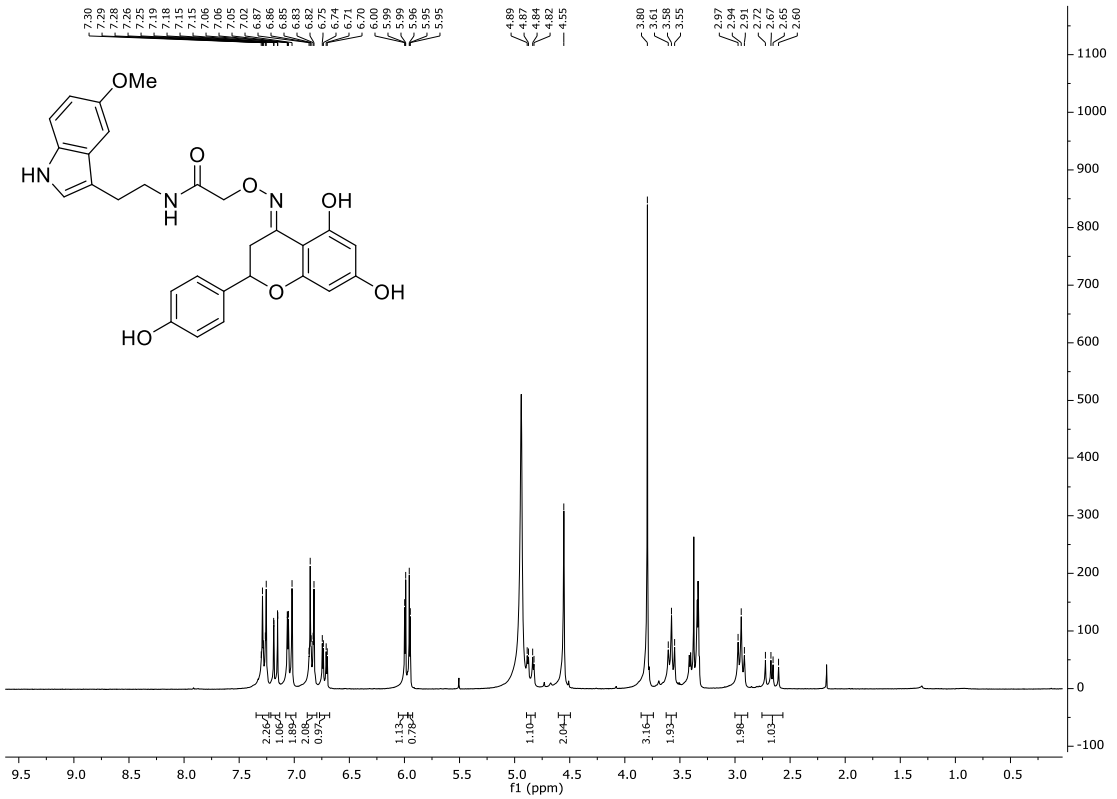
7.30
7.29
7.28
7.26
7.25
7.19
7.18
7.15
7.15
7.06
7.06
7.05
7.02
6.87
6.86
6.85
6.83
6.82
6.75
6.74
6.71
6.70
6.00
5.99
5.99
5.96
5.95
5.95
4.89
4.87
4.84
4.82
4.55
3.80
3.61
3.58
3.55
2.97
2.94
2.91
2.72
2.67
2.65
2.60
OMe
HN
O
N
H
O
N
OH
OH
O
HO
2.26
1.06
1.89
2.08
0.97
1.13
0.78
1.10
2.04
3.16
1.93
1.98
1.03
f1 (ppm)

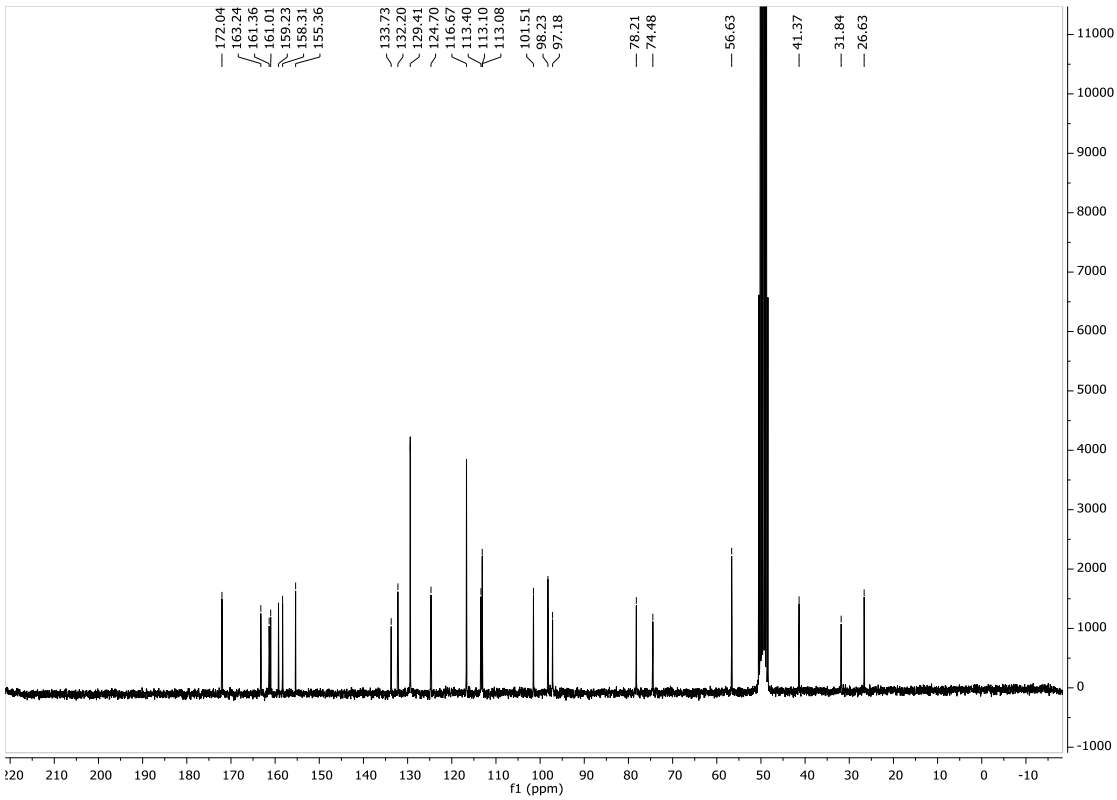
172.04
163.24
161.36
161.01
159.23
158.31
155.36
133.73
132.20
129.41
124.70
116.67
113.40
113.10
113.08
101.51
98.23
97.18
78.21
74.48
56.63
41.37
31.84
26.63
f1 (ppm)

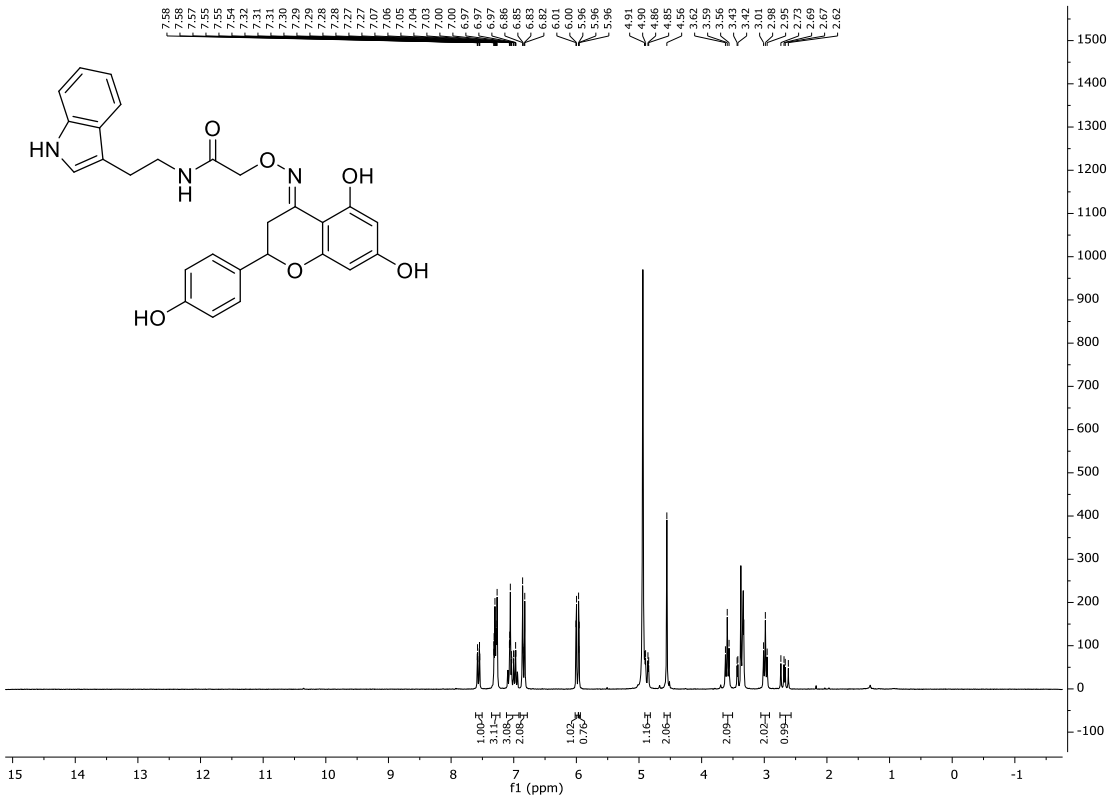
7.58
7.58
7.57
7.55
7.55
7.54
7.32
7.31
7.31
7.30
7.29
7.29
7.28
7.28
7.27
7.27
7.07
7.06
7.05
7.04
7.03
7.00
7.00
6.97
6.97
6.87
6.86
6.85
6.83
6.82
6.01
6.00
5.96
5.96
5.96
4.91
4.90
4.86
4.85
4.56
3.62
3.59
3.56
3.43
3.42
3.01
2.98
2.95
2.73
2.69
2.67
2.62
HN
O
N
H
O
N
OH
O
OH
HO
1.00
3.11
3.08
2.08
1.02
0.76
1.16
2.06
2.09
2.02
0.99
f1 (ppm)

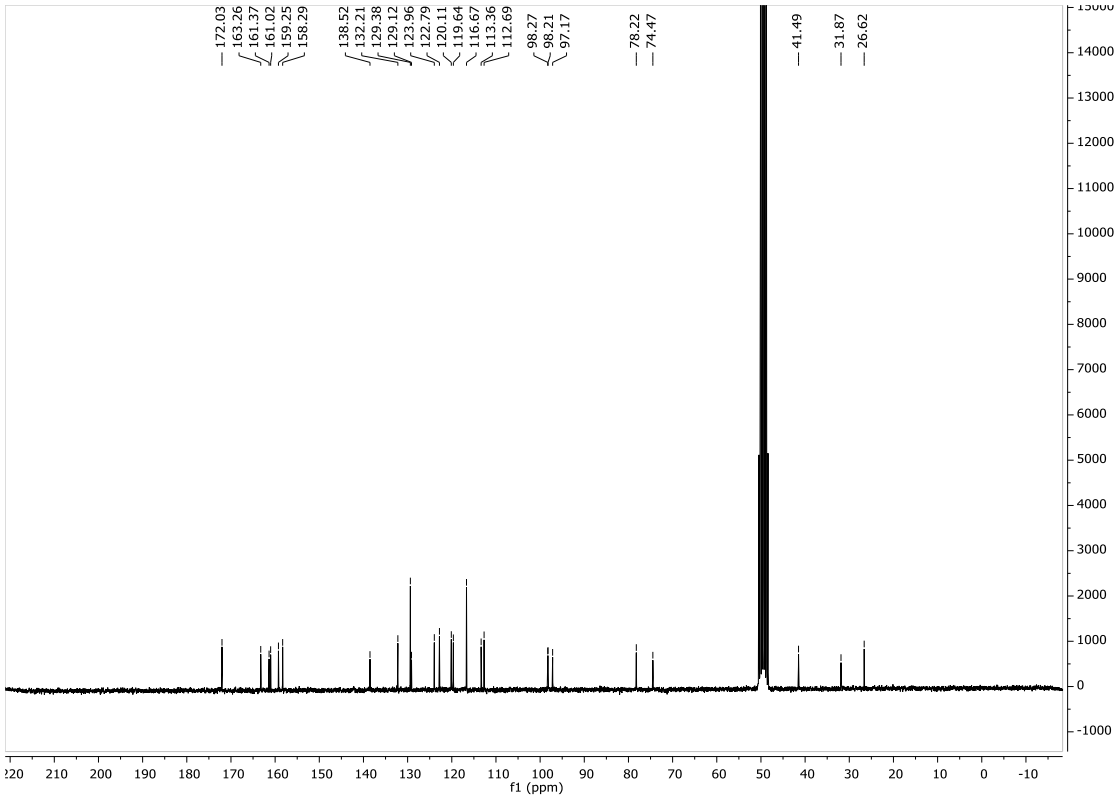
172.03
163.26
161.37
161.02
159.25
158.29
138.52
132.21
129.38
129.12
123.96
122.79
120.11
119.64
116.67
113.36
112.69
98.27
98.21
97.17
78.22
74.47
41.49
31.87
26.62
f1 (ppm)

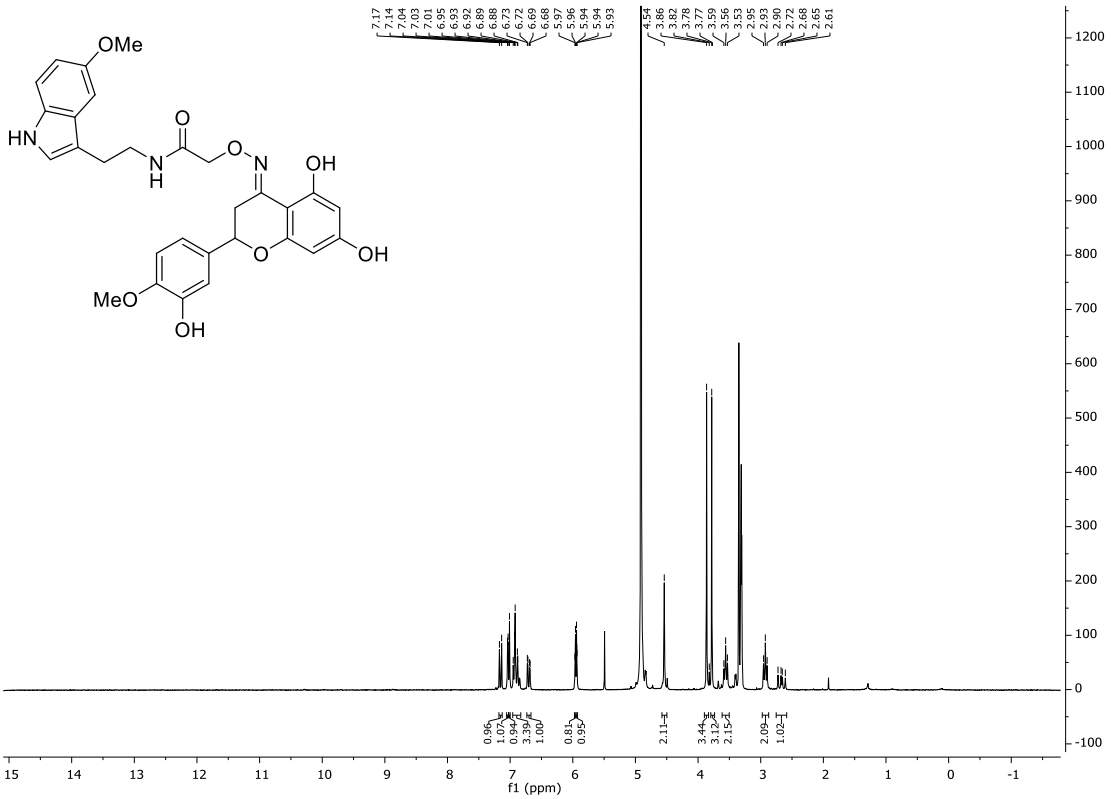
OMe
HN
O
N
H
O
N
OH
OH
O
MeO
OH
7.17
7.14
7.04
7.03
7.01
6.95
6.93
6.92
6.89
6.88
6.73
6.72
6.69
6.68
5.97
5.96
5.94
5.94
5.93
4.54
3.86
3.82
3.78
3.77
3.59
3.56
3.53
2.95
2.93
2.90
2.72
2.68
2.65
2.61
0.96
1.07
0.94
3.39
1.00
0.81
0.95
2.11
3.44
3.12
2.15
2.09
1.02
f1 (ppm)

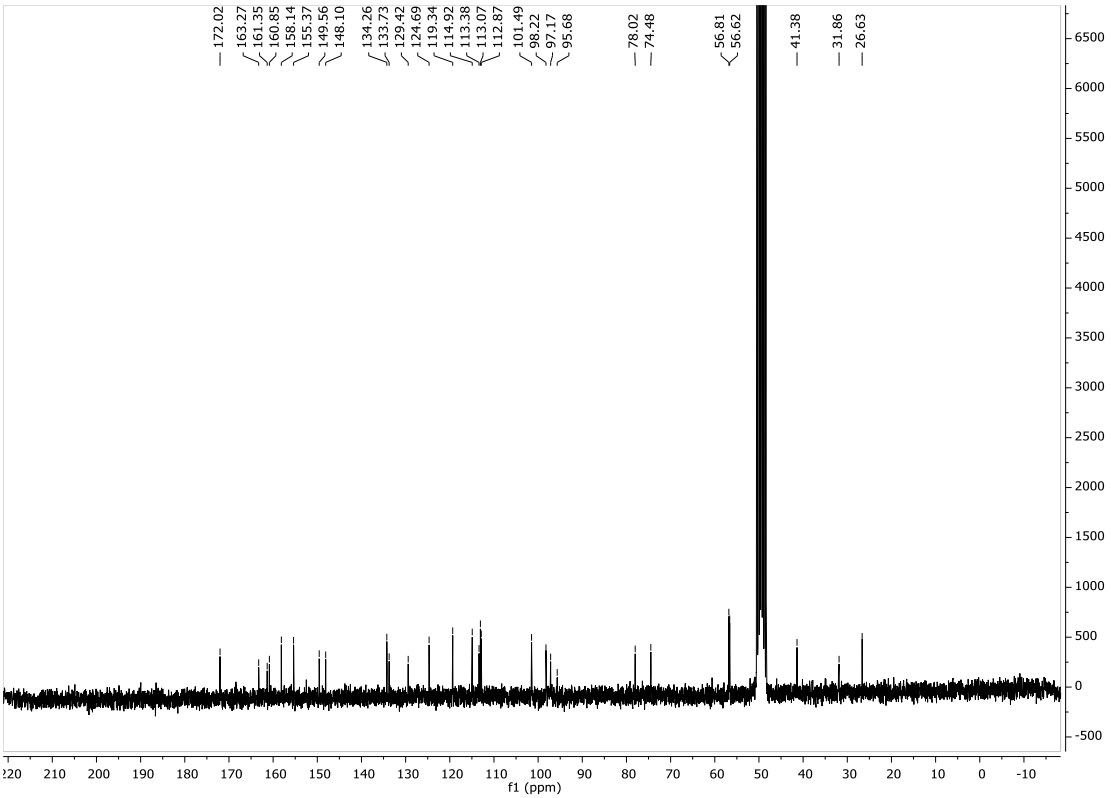
172.02
163.27
161.35
160.85
158.14
155.37
149.56
148.10
134.26
133.73
129.42
124.69
119.34
114.92
113.38
113.07
112.87
101.49
98.22
97.17
95.68
78.02
74.48
56.81
56.62
41.38
31.86
26.63
f1 (ppm)

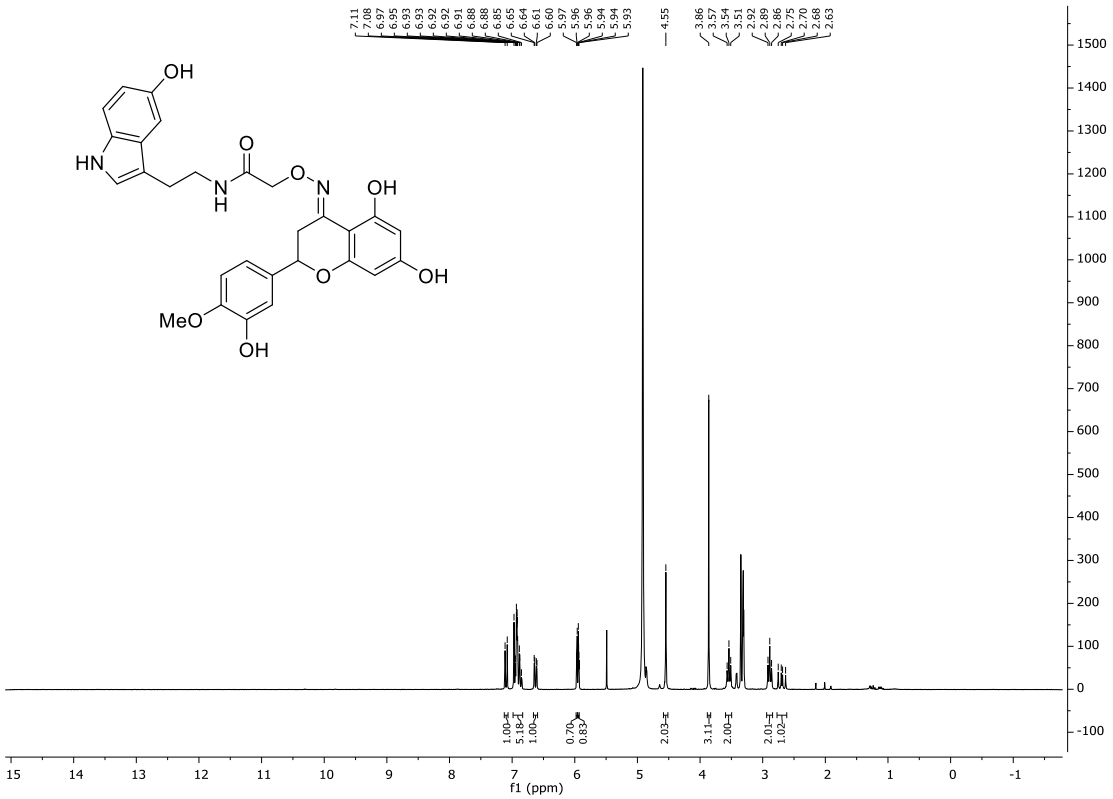
OH
HN
O
N
H
O
N
OH
OH
O
MeO
OH
7.11
7.08
6.97
6.95
6.93
6.92
6.92
6.91
6.88
6.88
6.85
6.65
6.64
6.61
6.60
5.97
5.96
5.96
5.94
5.94
5.93
4.55
3.86
3.57
3.54
3.51
2.92
2.89
2.86
2.75
2.70
2.68
2.63
1.00
5.18
1.00
0.70
0.83
2.03
3.11
2.00
2.01
1.02
f1 (ppm)

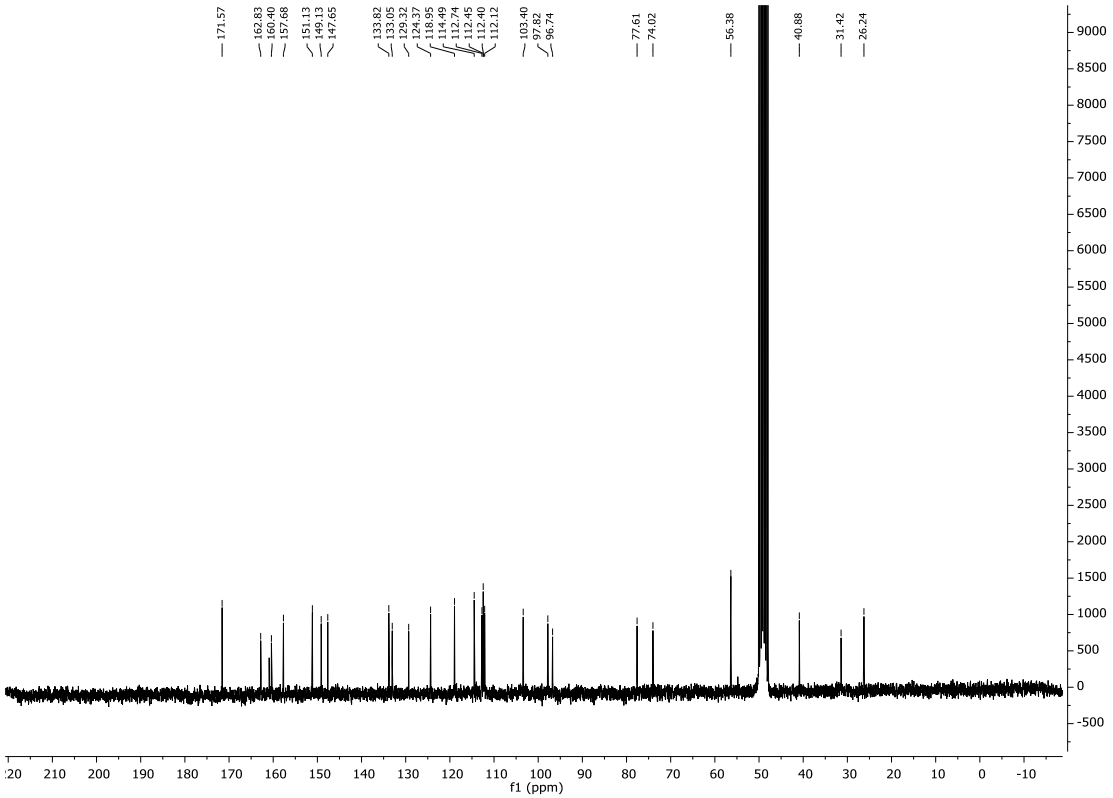
171.57
162.83
160.40
157.68
151.13
149.13
147.65
133.82
133.05
129.32
124.37
118.95
114.49
112.74
112.45
112.40
112.12
103.40
97.82
96.74
77.61
74.02
56.38
40.88
31.42
26.24
f1 (ppm)

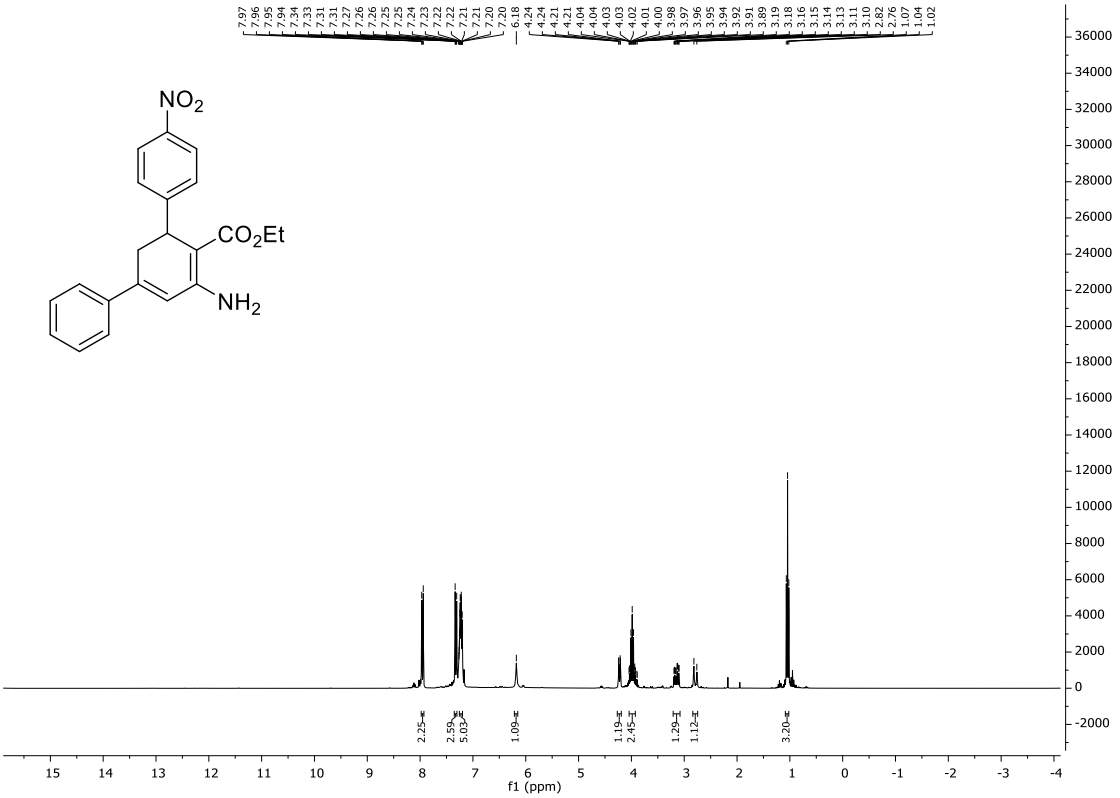
NO2
CO2Et
NH2
f1 (ppm)

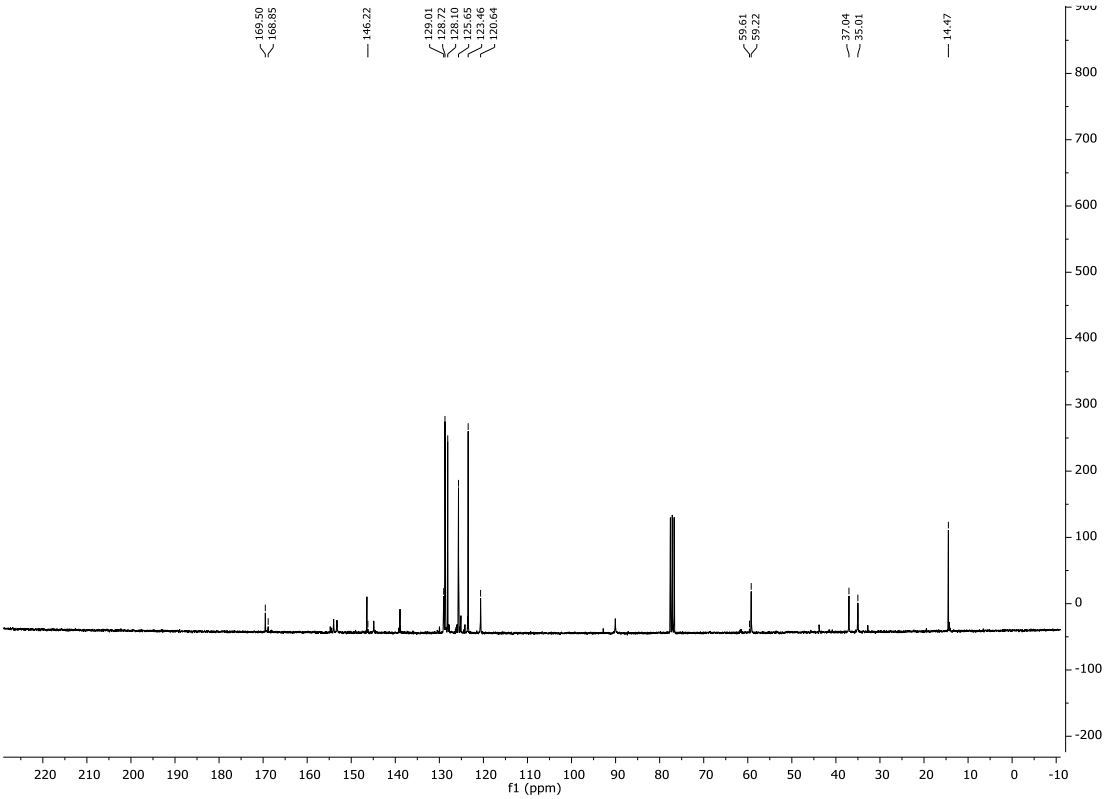
f1 (ppm)

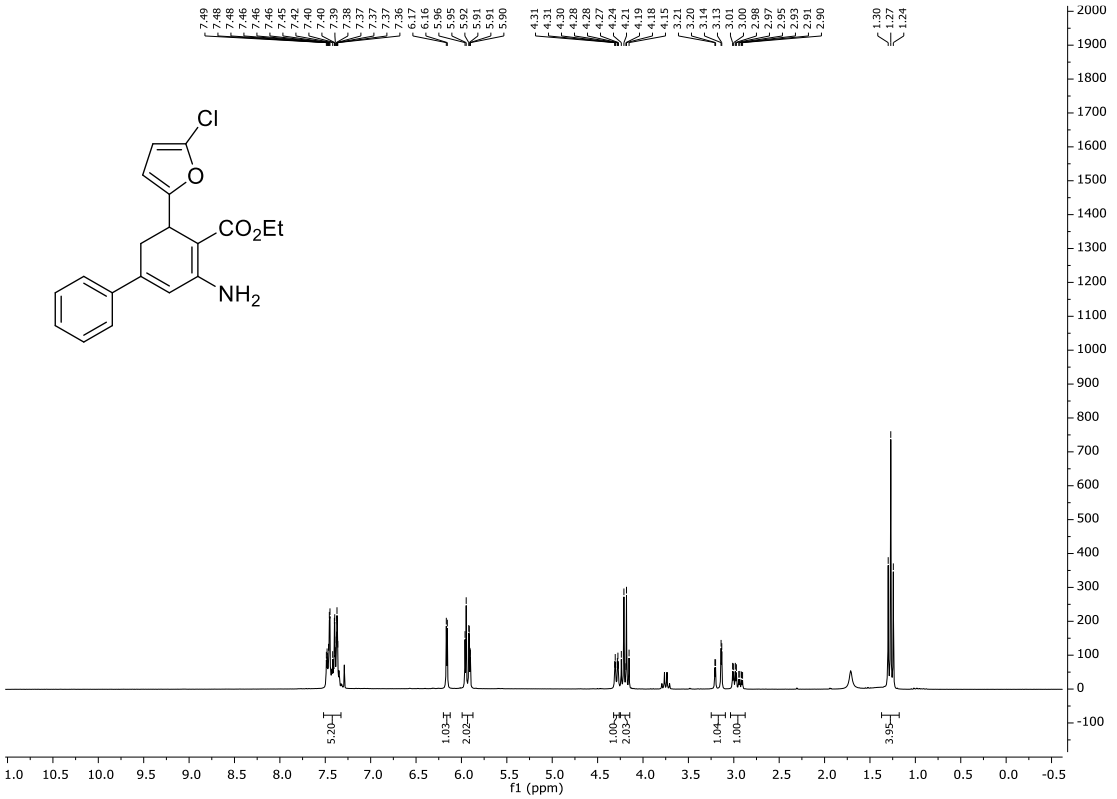
Cl
O
CO2Et
NH2
f1 (ppm)

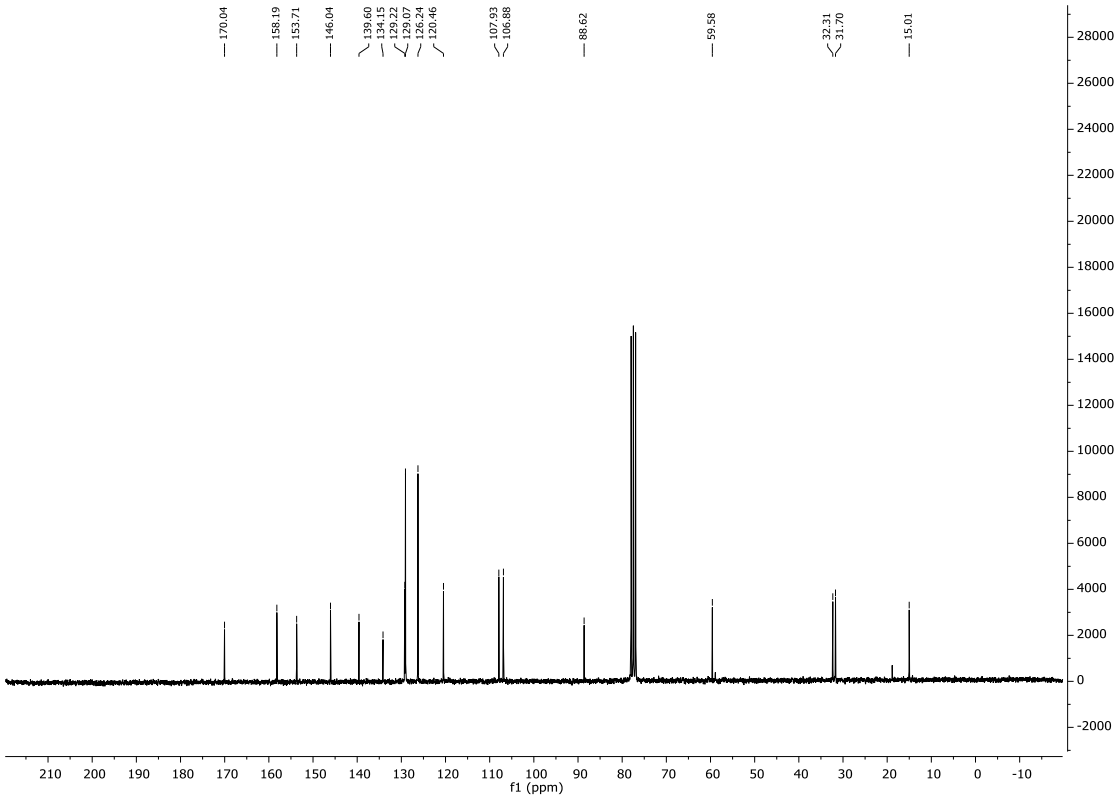
f1 (ppm)

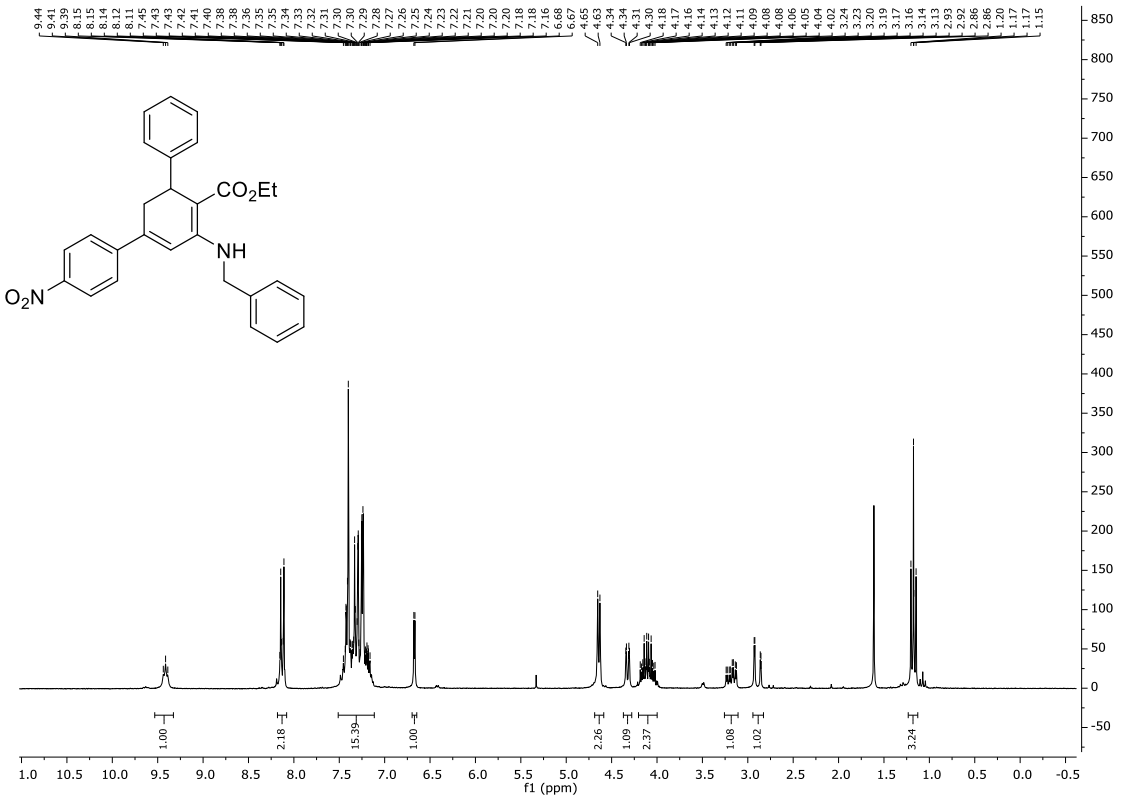
CO2Et
NH
O2N
f1 (ppm)

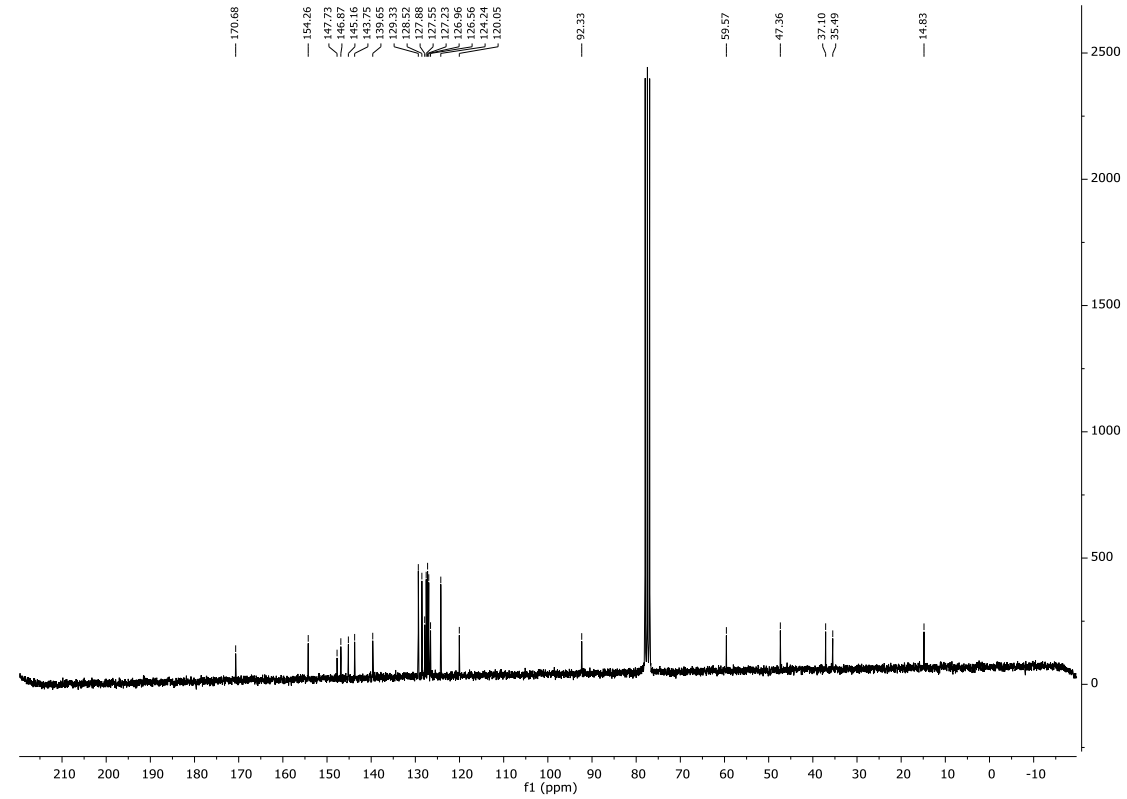
f1 (ppm)

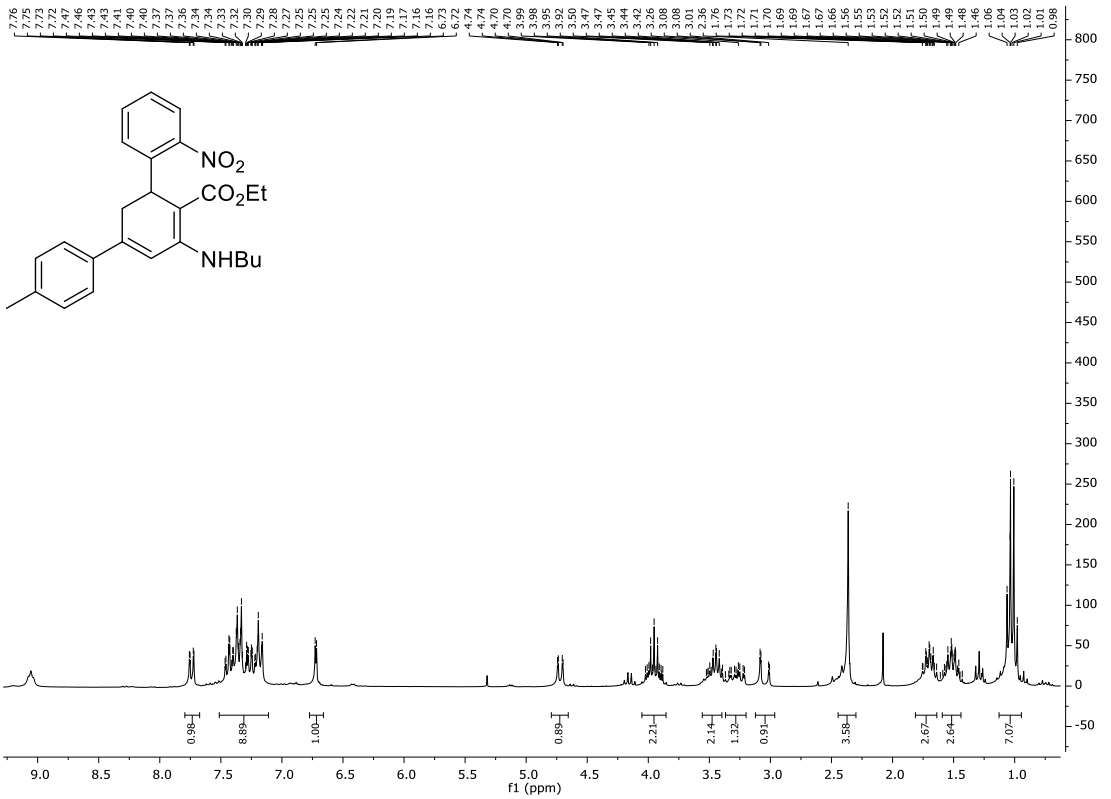
NO2
CO2Et
NHBu
f1 (ppm)

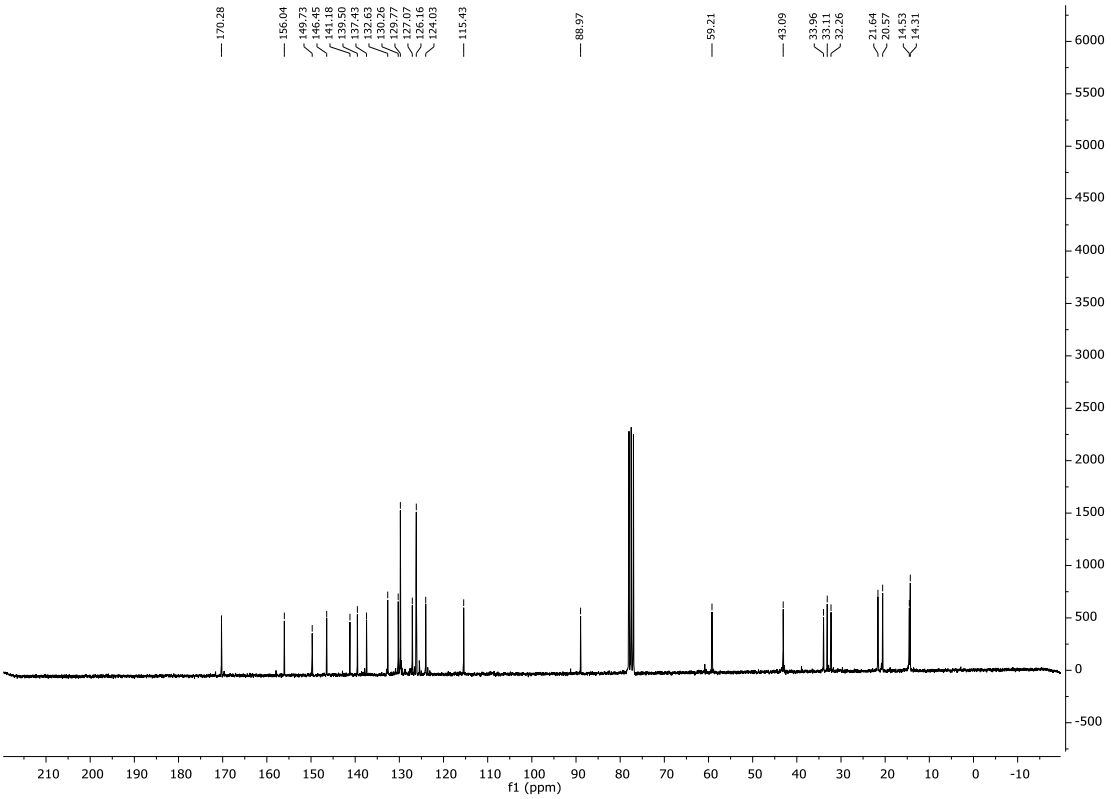
f1 (ppm)

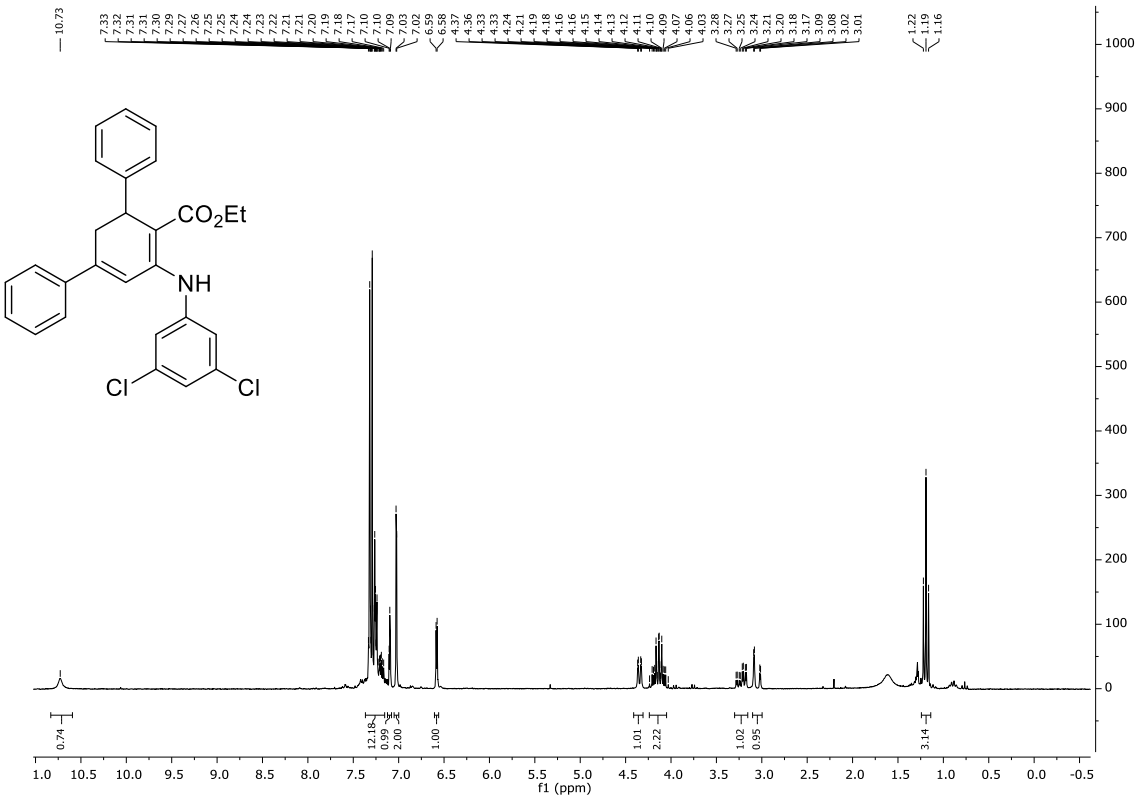
CO2Et
NH
Cl
Cl
f1 (ppm)

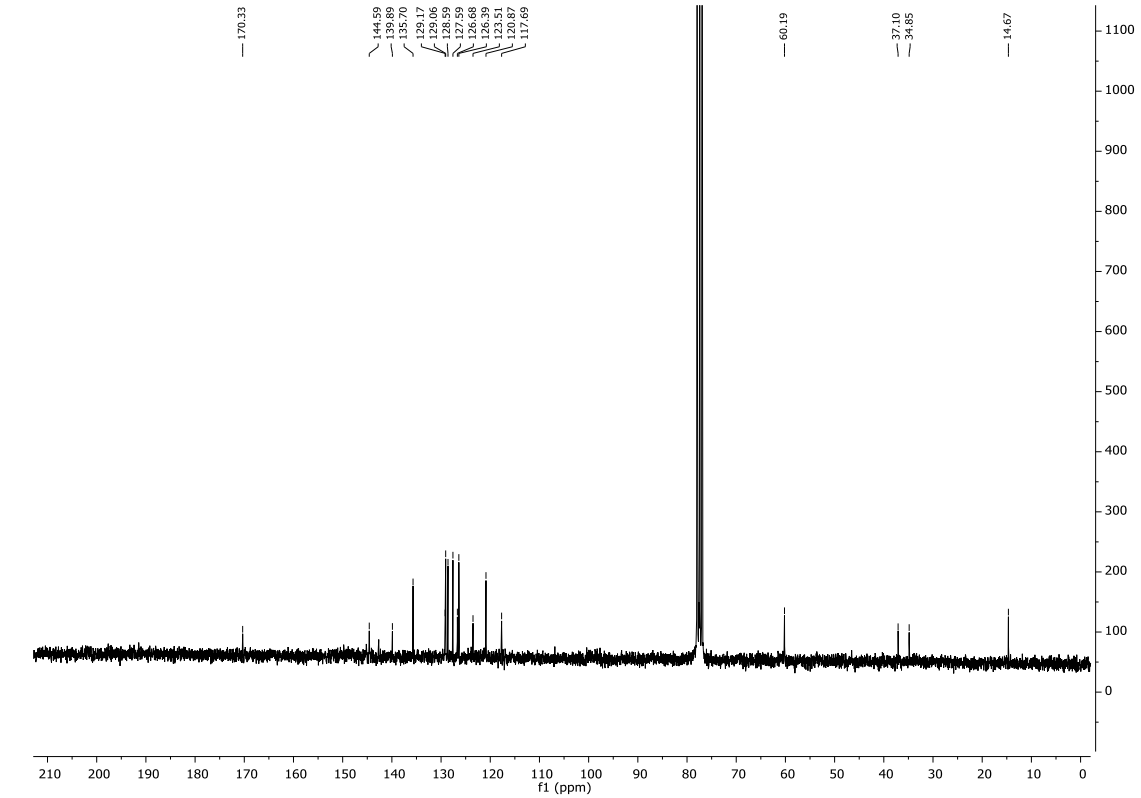
f1 (ppm)

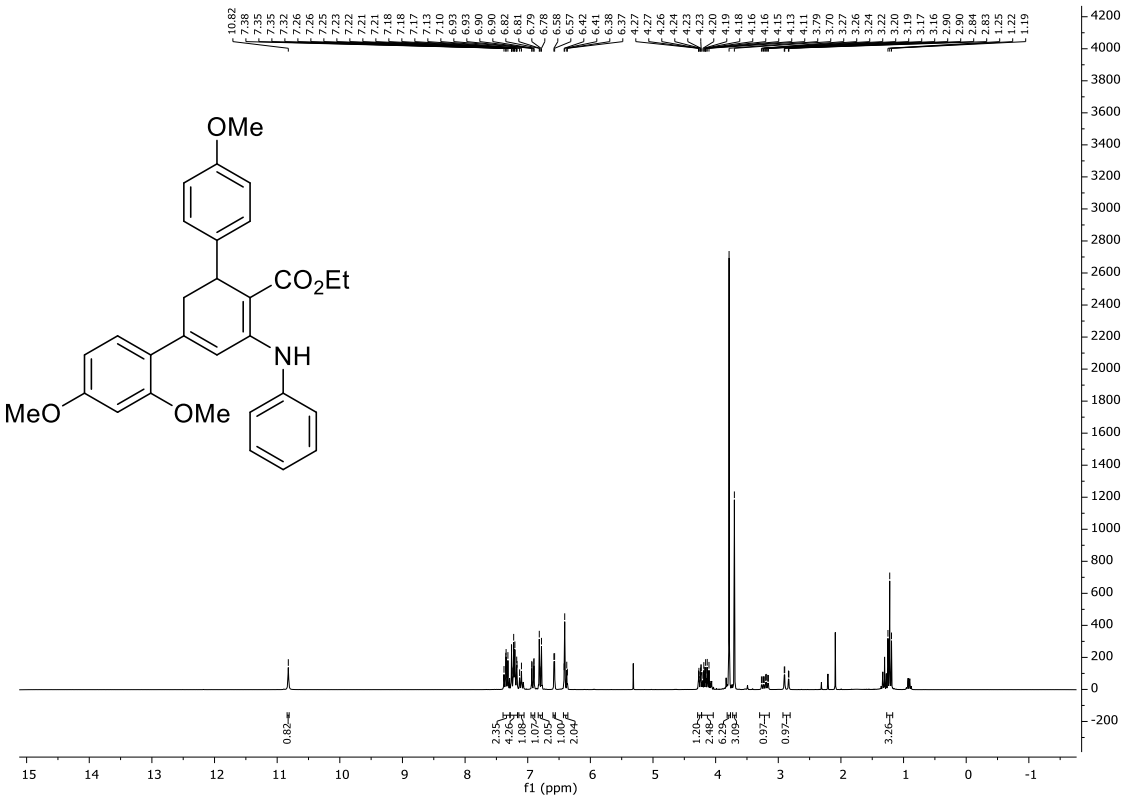
OMe
CO2Et
NH
MeO
OMe
f1 (ppm)

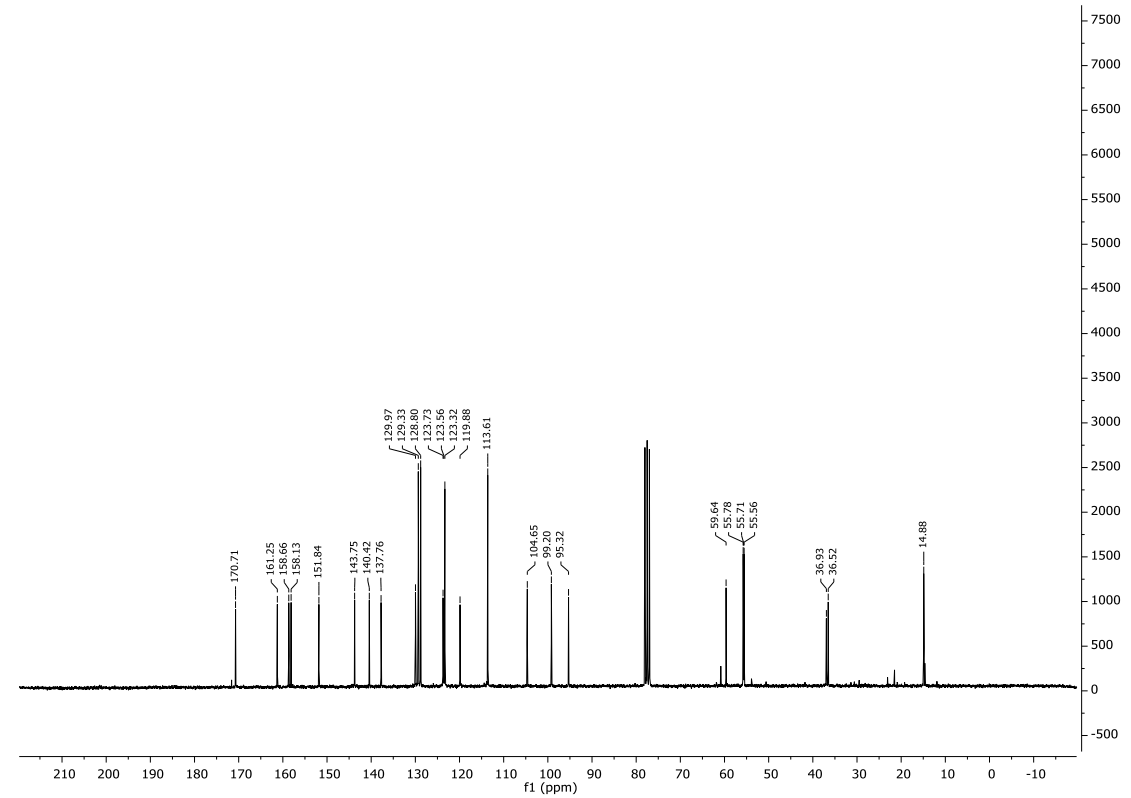
f1 (ppm)

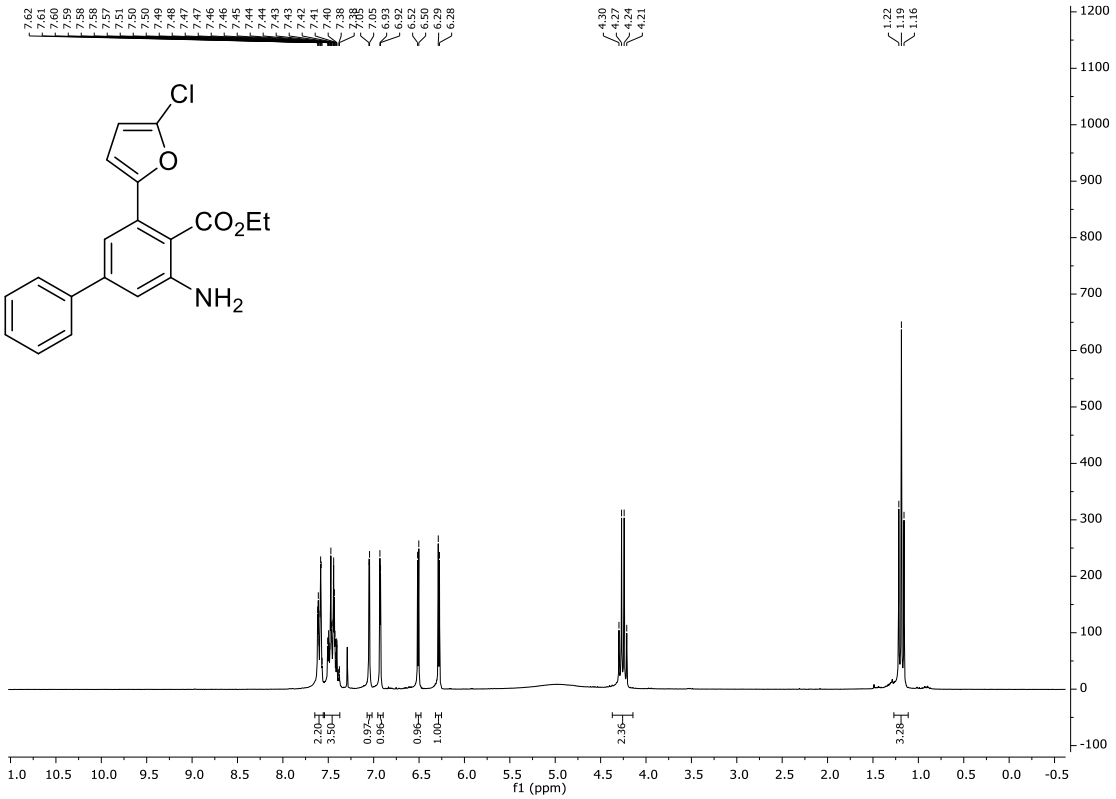
7.62
7.61
7.60
7.59
7.58
7.58
7.57
7.51
7.50
7.50
7.49
7.48
7.47
7.47
7.46
7.46
7.45
7.44
7.44
7.43
7.43
7.42
7.41
7.40
7.38
7.08
7.05
6.93
6.92
6.52
6.50
6.29
6.28
4.30
4.27
4.24
4.21
1.22
1.19
1.16
Cl
O
CO2Et
NH2
2.20
3.50
0.97
0.96
0.96
1.00
2.36
3.28
f1 (ppm)

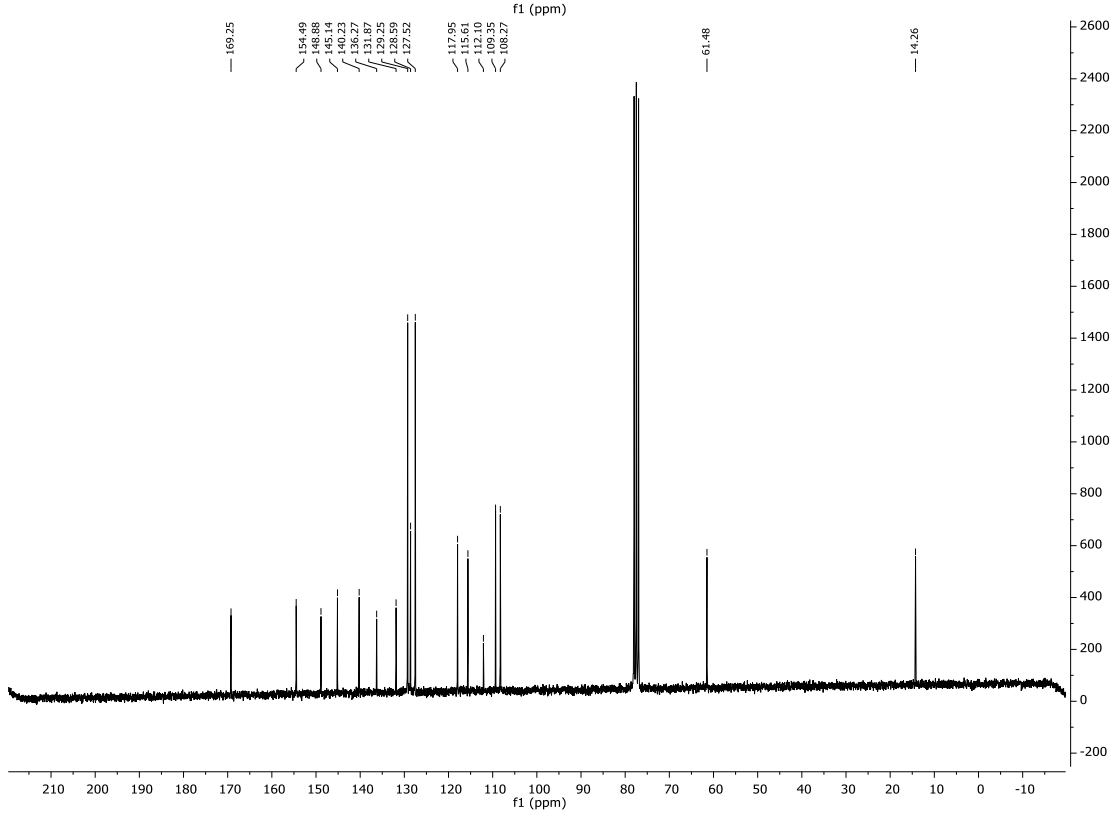
169.25
154.49
148.88
145.14
140.23
136.27
131.37
129.25
128.59
127.52
117.95
115.61
112.10
109.35
108.27
61.48
14.26
f1 (ppm)

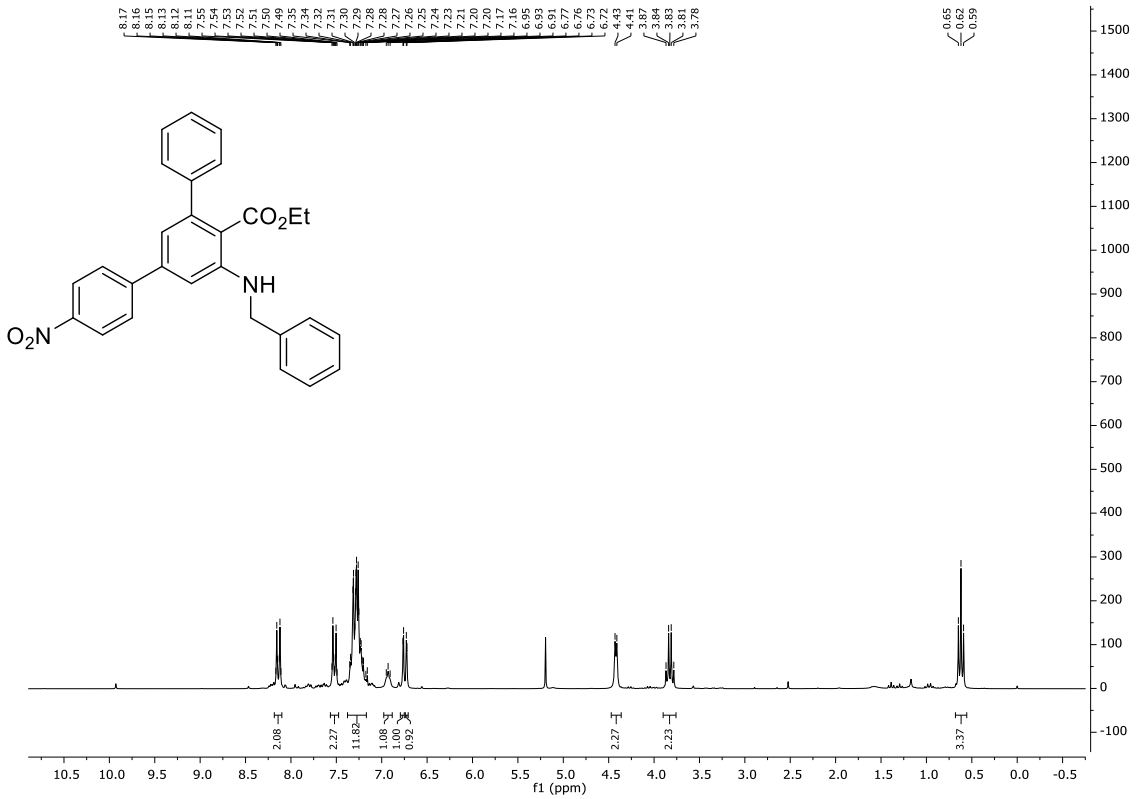
8.17
8.16
8.15
8.13
8.12
8.11
7.55
7.54
7.53
7.52
7.51
7.50
7.49
7.35
7.34
7.32
7.31
7.30
7.29
7.28
7.28
7.27
7.26
7.25
7.24
7.23
7.21
7.20
7.20
7.17
7.16
6.95
6.93
6.91
6.77
6.76
6.73
6.72
4.43
4.41
3.87
3.84
3.83
3.81
3.78
0.65
0.62
0.59
CO2Et
NH
O2N
2.08
2.27
11.82
1.08
1.00
0.92
2.27
2.23
3.37
f1 (ppm)

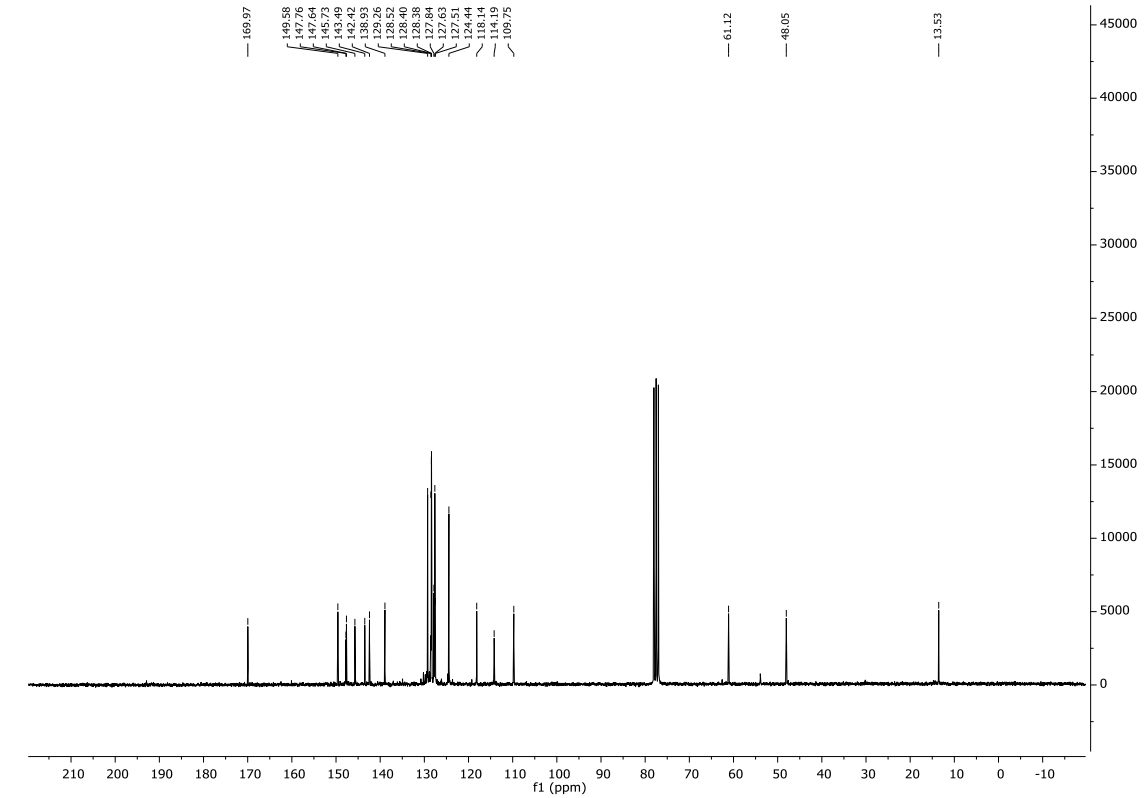
169.97
149.58
147.76
147.64
145.73
143.49
142.42
138.93
129.26
128.52
128.40
128.38
127.84
127.63
127.51
124.44
118.14
114.19
109.75
61.12
48.05
13.53
f1 (ppm)

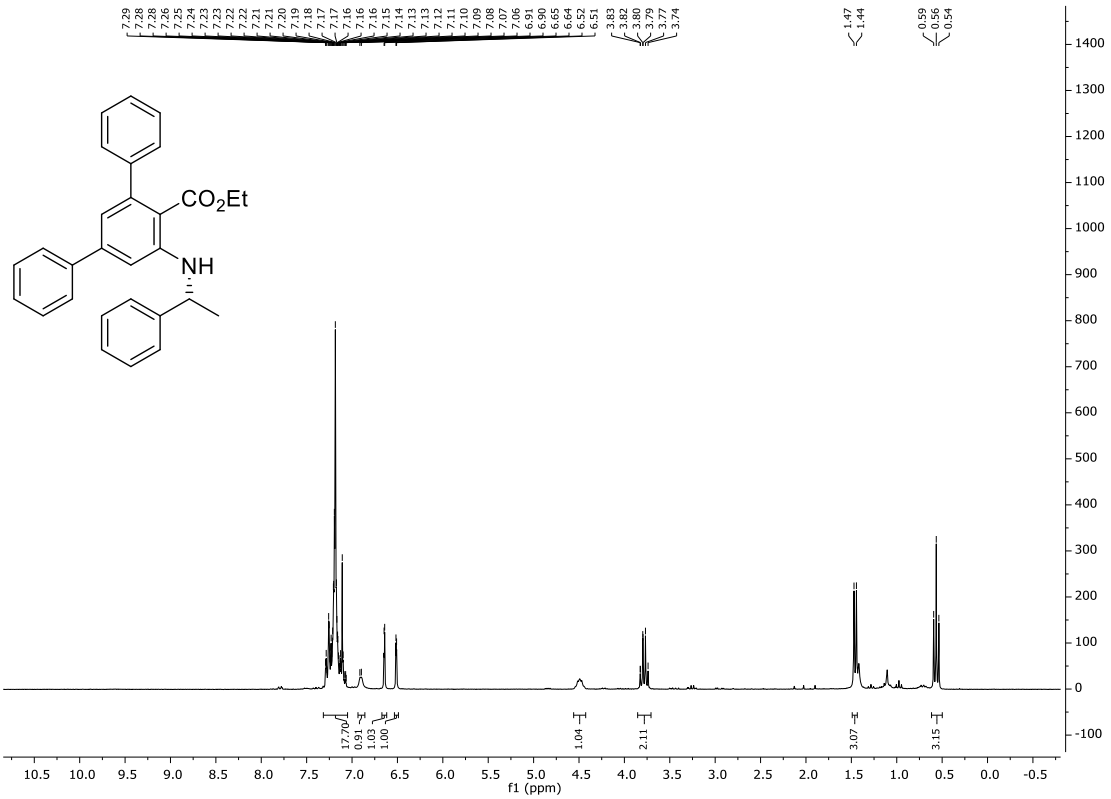
CO2Et
NH
f1 (ppm)

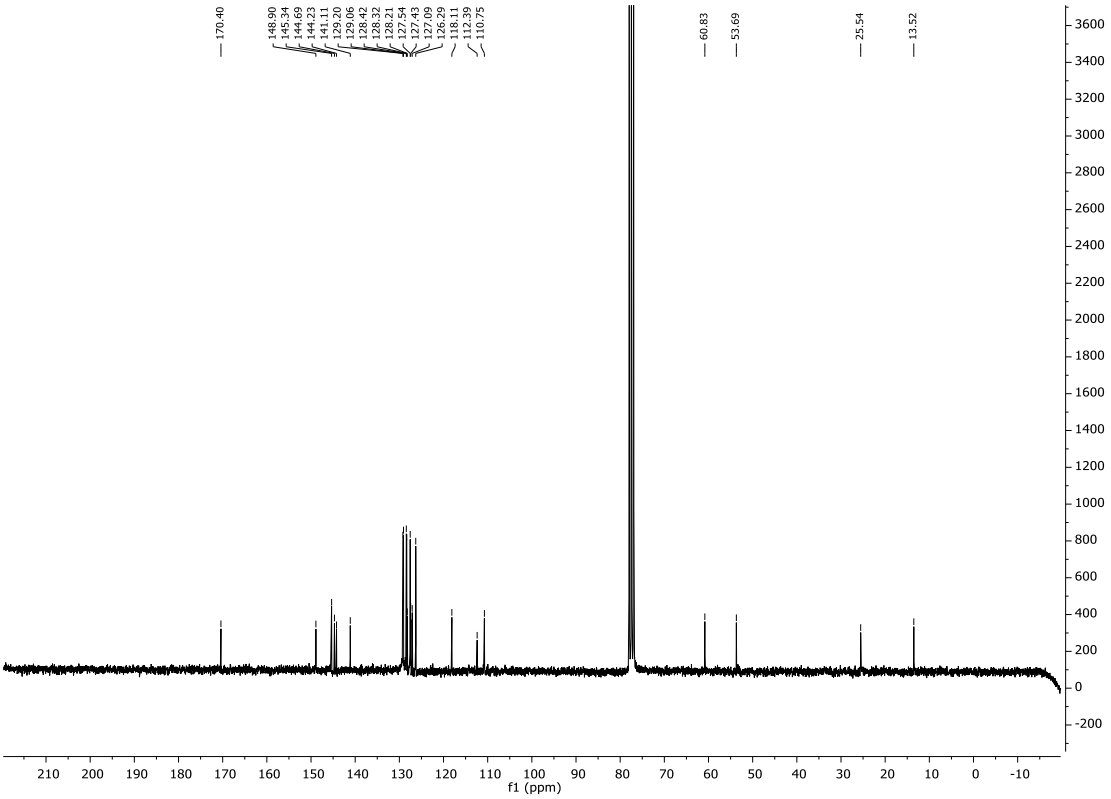
f1 (ppm)

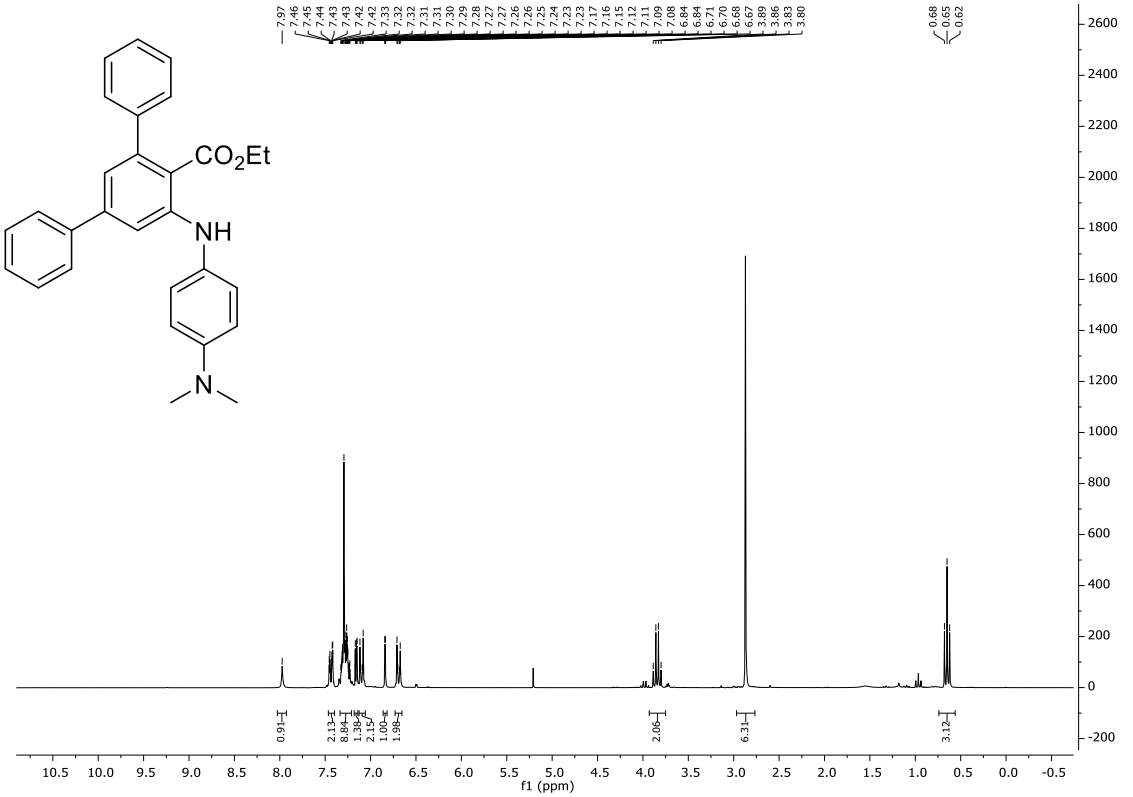
CO2Et
NH
N
f1 (ppm)

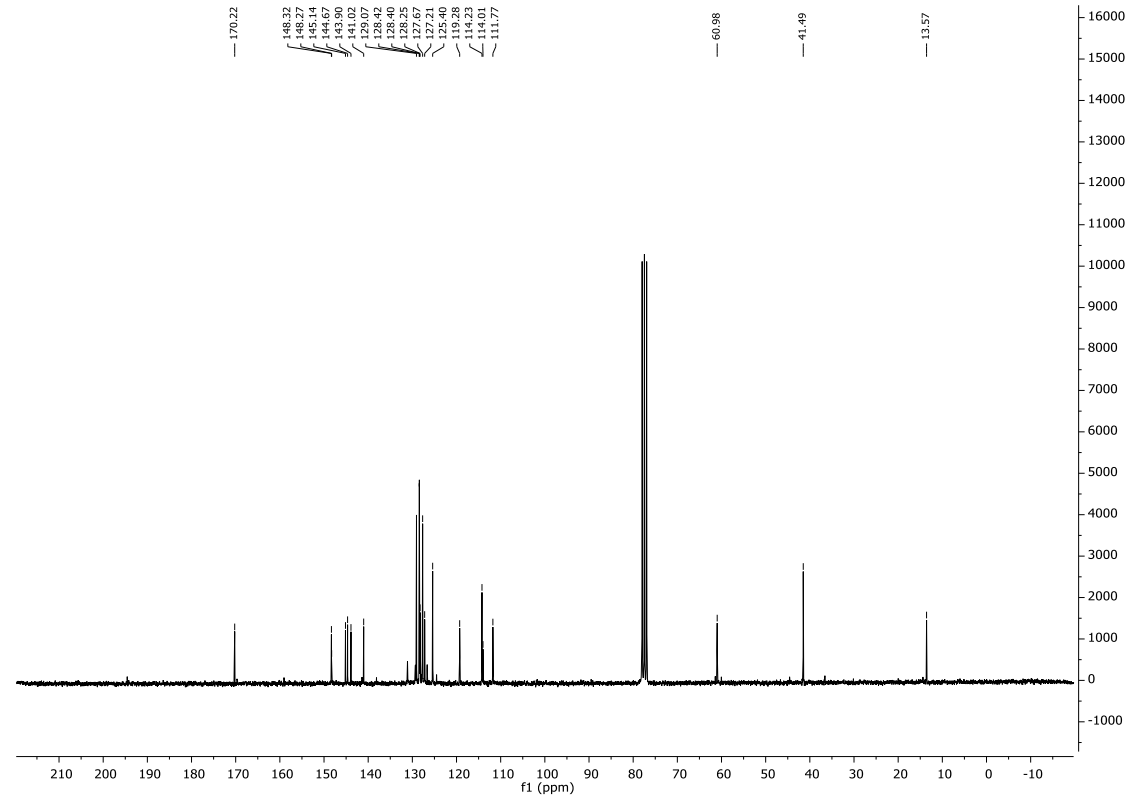
f1 (ppm)

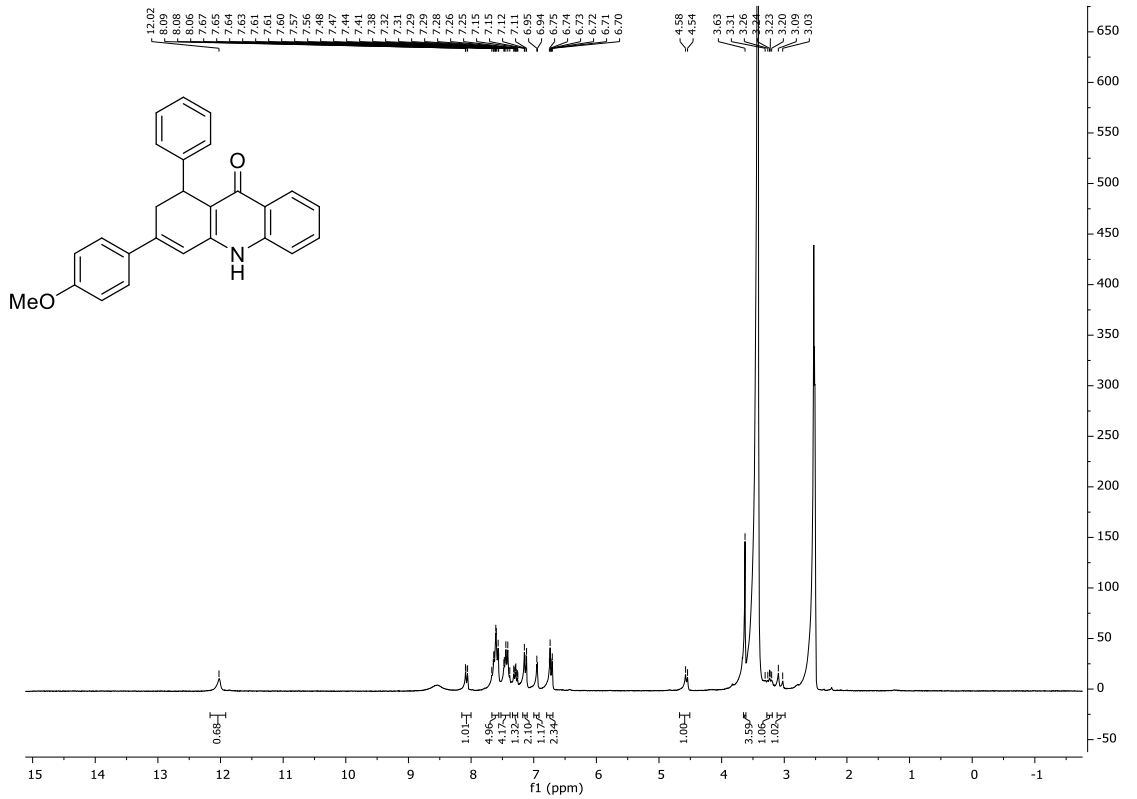
12.02
8.09
8.08
8.06
7.67
7.65
7.64
7.63
7.61
7.61
7.60
7.57
7.56
7.48
7.47
7.44
7.41
7.38
7.32
7.31
7.29
7.29
7.28
7.26
7.25
7.15
7.15
7.12
7.11
6.95
6.94
6.75
6.74
6.73
6.72
6.71
6.70
4.58
4.54
3.63
3.31
3.26
3.24
3.23
3.20
3.09
3.03
O
N
H
MeO
0.68
1.01
4.96
4.17
1.32
2.10
1.17
2.34
1.00
3.59
1.06
1.02
f1 (ppm)

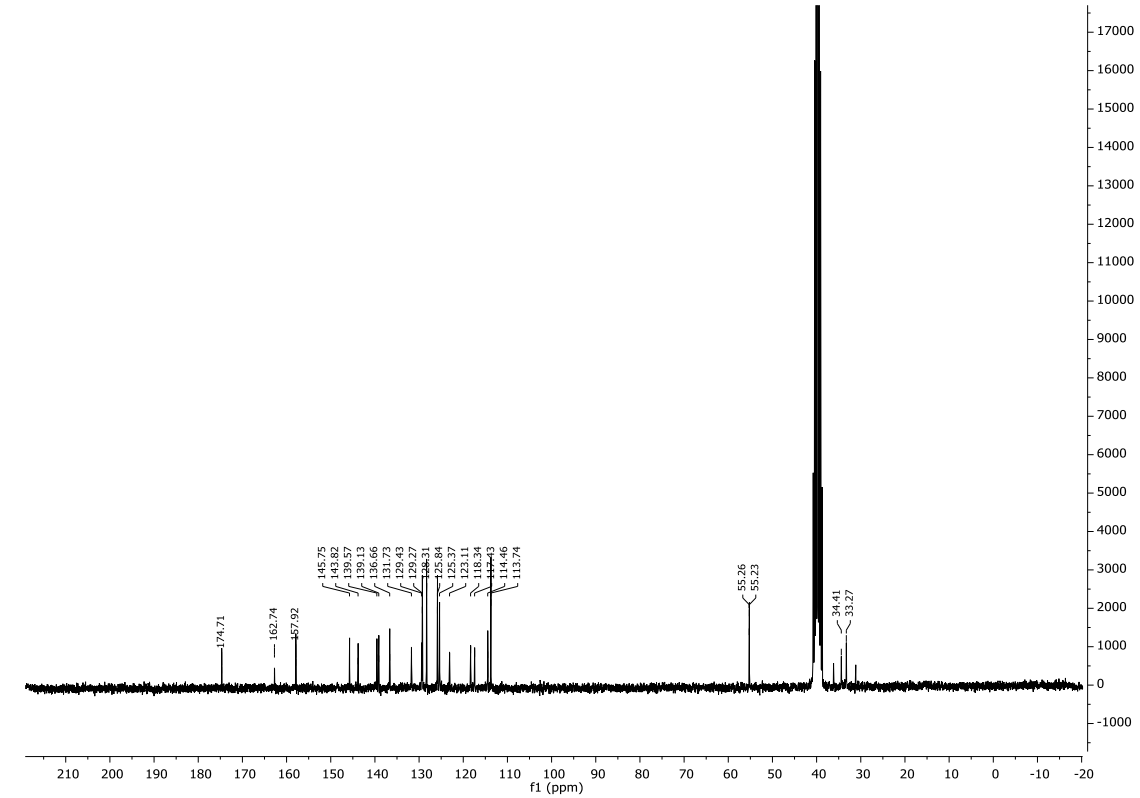
174.71
162.74
157.92
145.75
143.82
139.57
139.13
136.66
131.73
129.43
129.27
128.21
125.84
125.37
123.11
118.34
117.43
114.46
113.74
55.26
55.23
34.41
33.27
f1 (ppm)

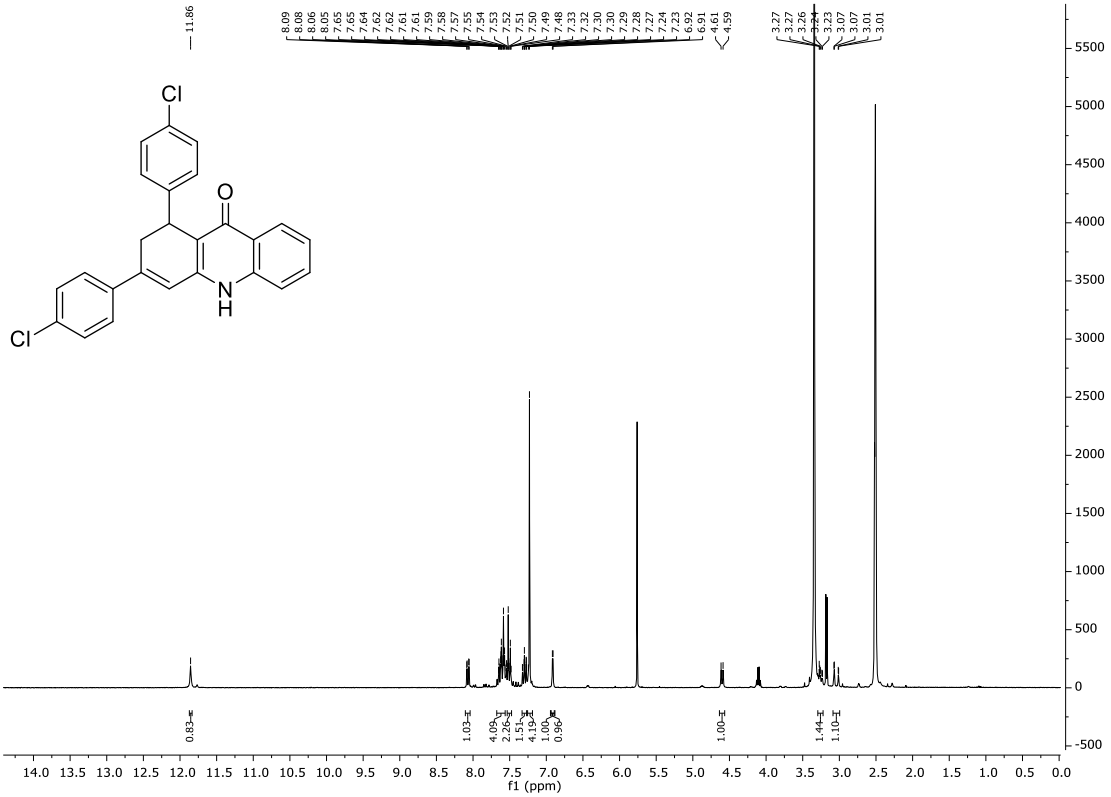
Cl
O
N
H
Cl
11.86
8.09
8.08
8.06
8.05
7.65
7.65
7.64
7.62
7.62
7.61
7.61
7.59
7.58
7.57
7.55
7.54
7.53
7.52
7.51
7.50
7.49
7.48
7.33
7.32
7.30
7.30
7.29
7.28
7.27
7.24
7.23
6.92
6.91
4.61
4.59
3.27
3.27
3.26
3.24
3.23
3.07
3.07
3.01
3.01
0.83
1.03
4.09
2.26
1.51
4.19
1.08
0.98
1.00
1.44
1.10
f1 (ppm)

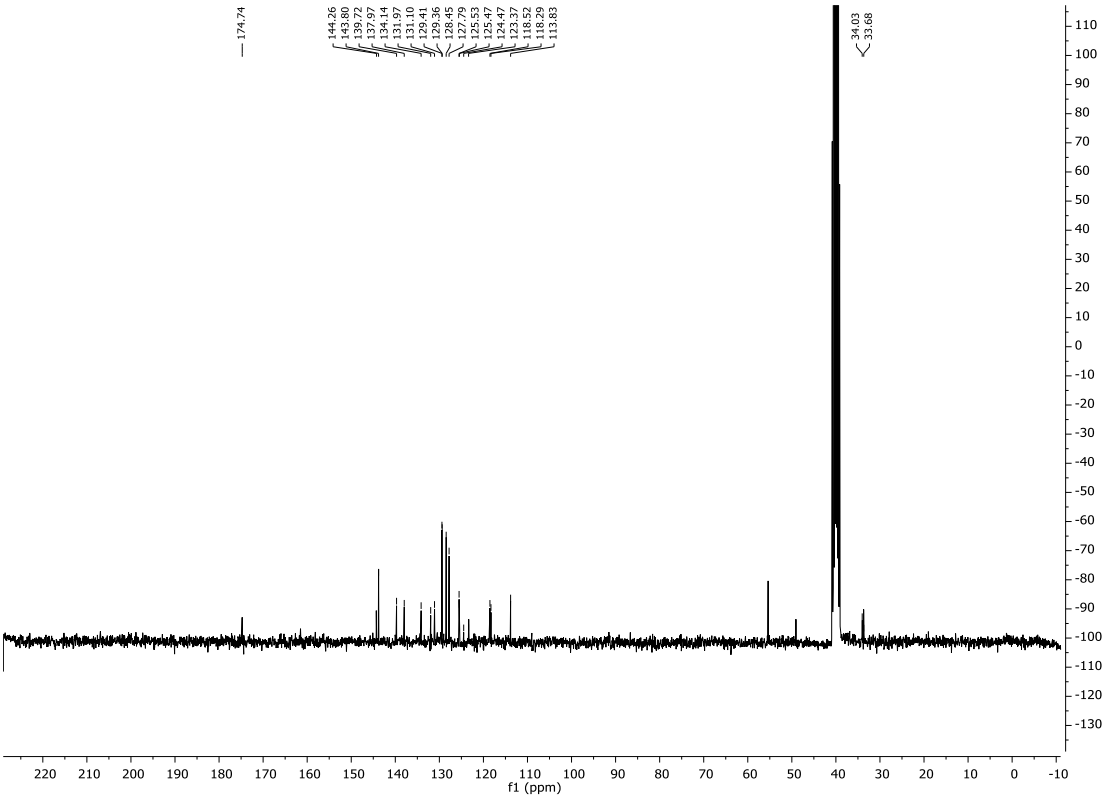
174.74
144.26
143.80
139.72
137.97
134.14
131.97
131.10
129.41
129.36
128.45
127.79
125.53
125.47
124.47
123.37
118.52
118.29
113.83
34.03
33.68
f1 (ppm)

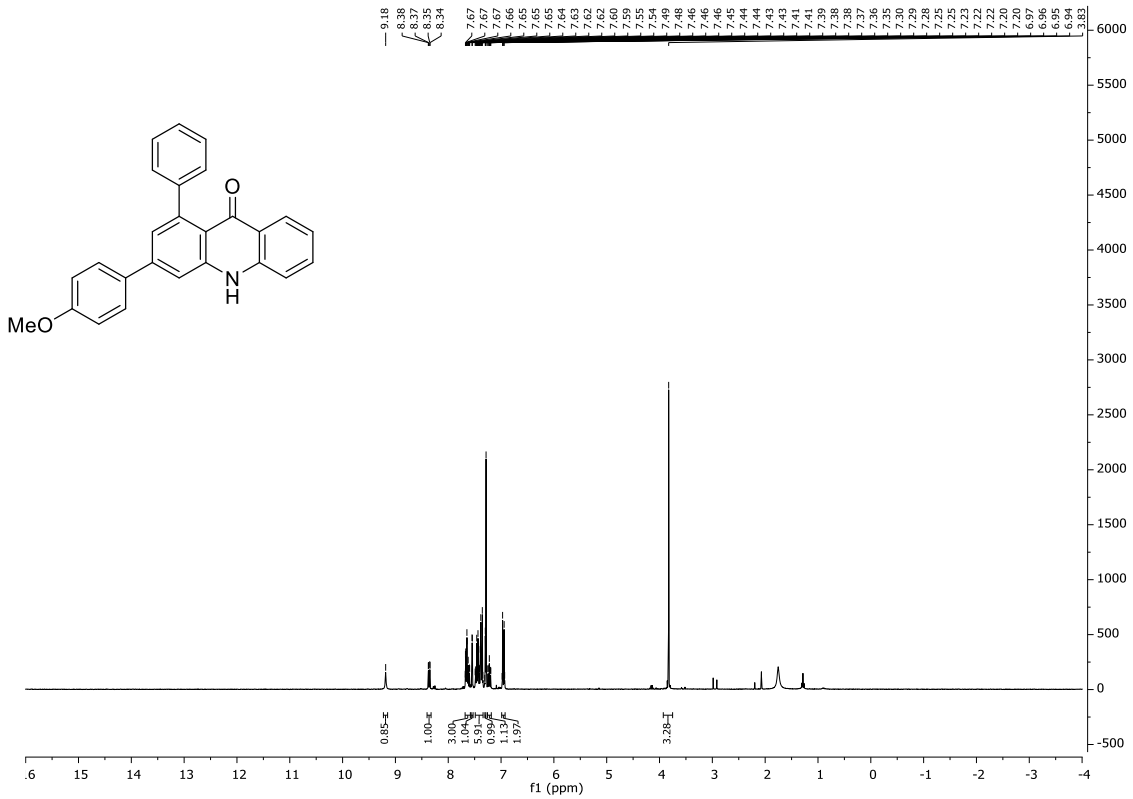
9.18
8.38
8.37
8.35
8.34
7.67
7.67
7.67
7.67
7.66
7.66
7.65
7.65
7.65
7.64
7.63
7.62
7.62
7.60
7.59
7.55
7.54
7.49
7.48
7.46
7.46
7.45
7.44
7.44
7.43
7.43
7.41
7.41
7.39
7.38
7.38
7.37
7.36
7.35
7.30
7.29
7.28
7.25
7.25
7.23
7.22
7.22
7.20
7.20
6.97
6.96
6.95
6.94
3.83
O
N
H
MeO
0.85
1.00
3.00
1.04
5.91
0.99
1.13
1.97
3.20
f1 (ppm)

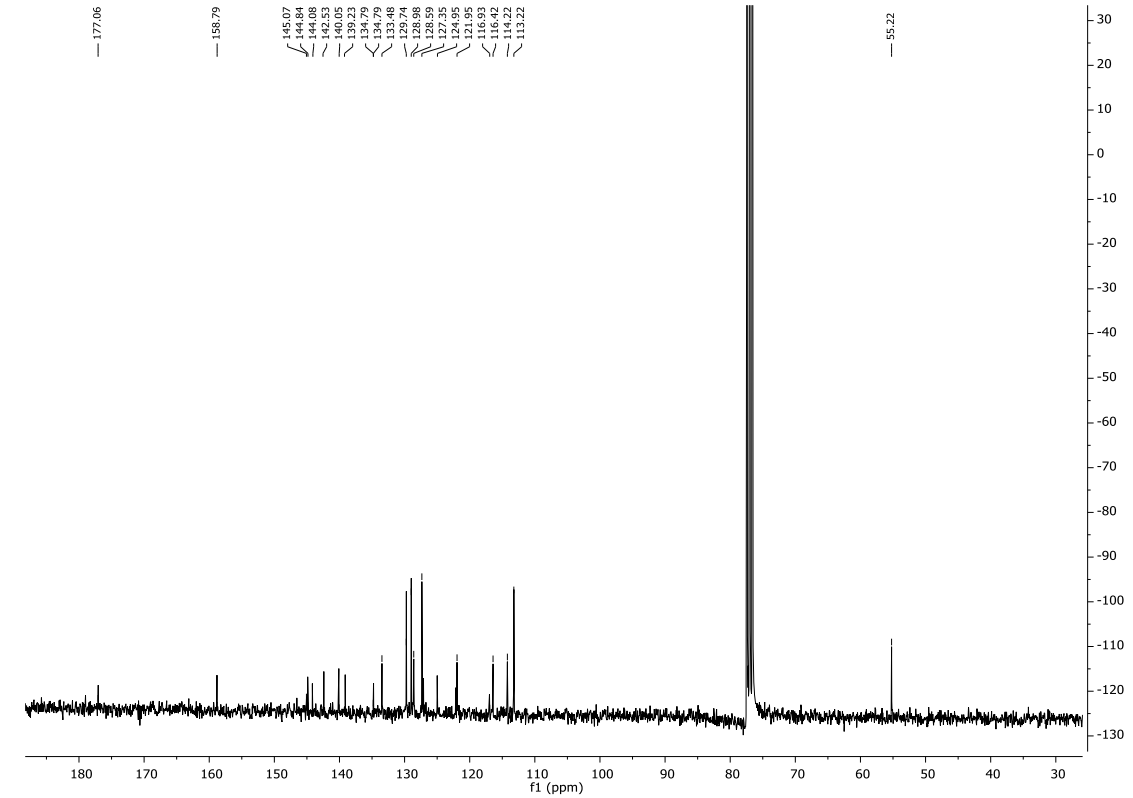
177.06
158.79
145.07
144.84
144.08
142.53
140.05
139.23
134.79
134.79
133.48
129.74
128.98
128.59
127.35
124.95
121.65
116.93
116.42
114.22
113.22
55.22
f1 (ppm)

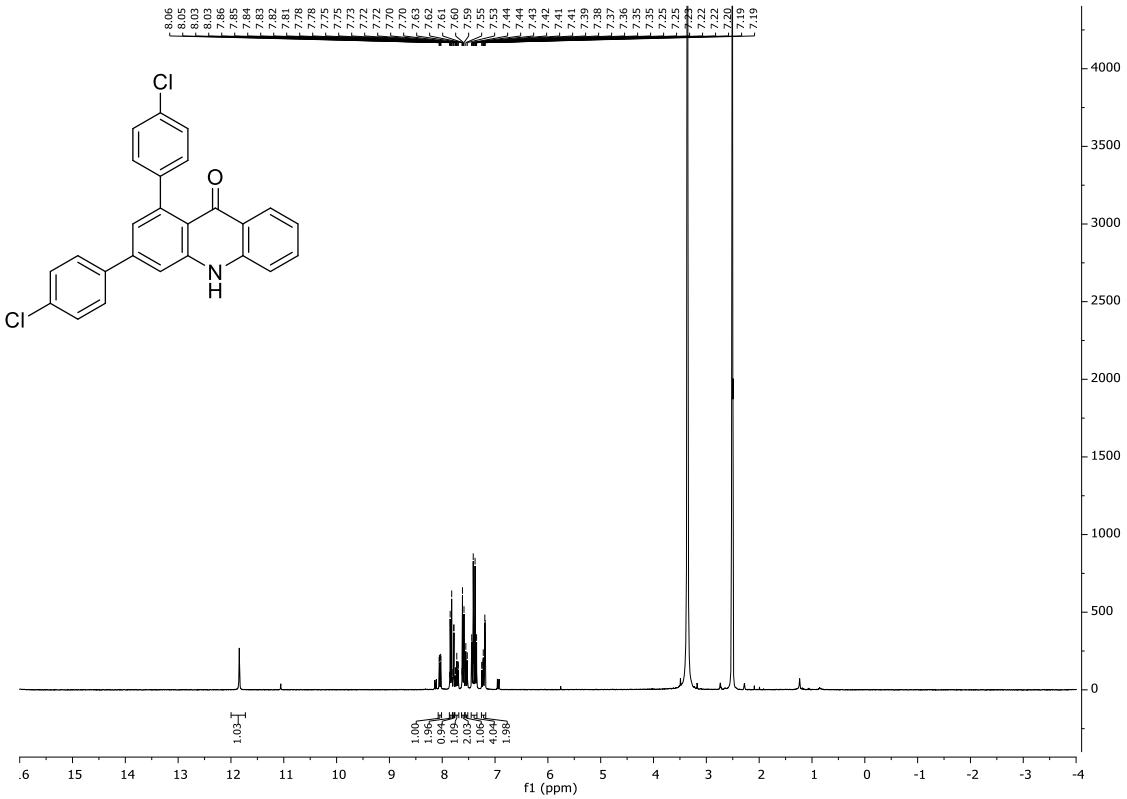
Cl
O
N
H
Cl
f1 (ppm)

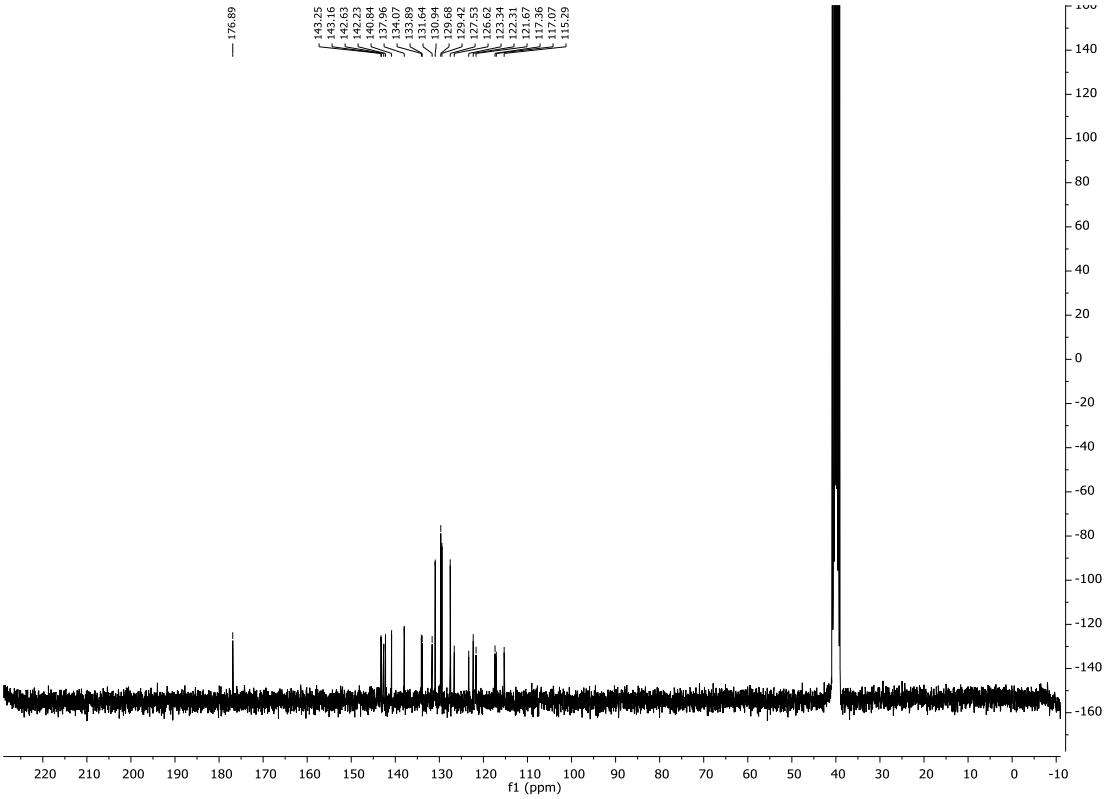
f1 (ppm)

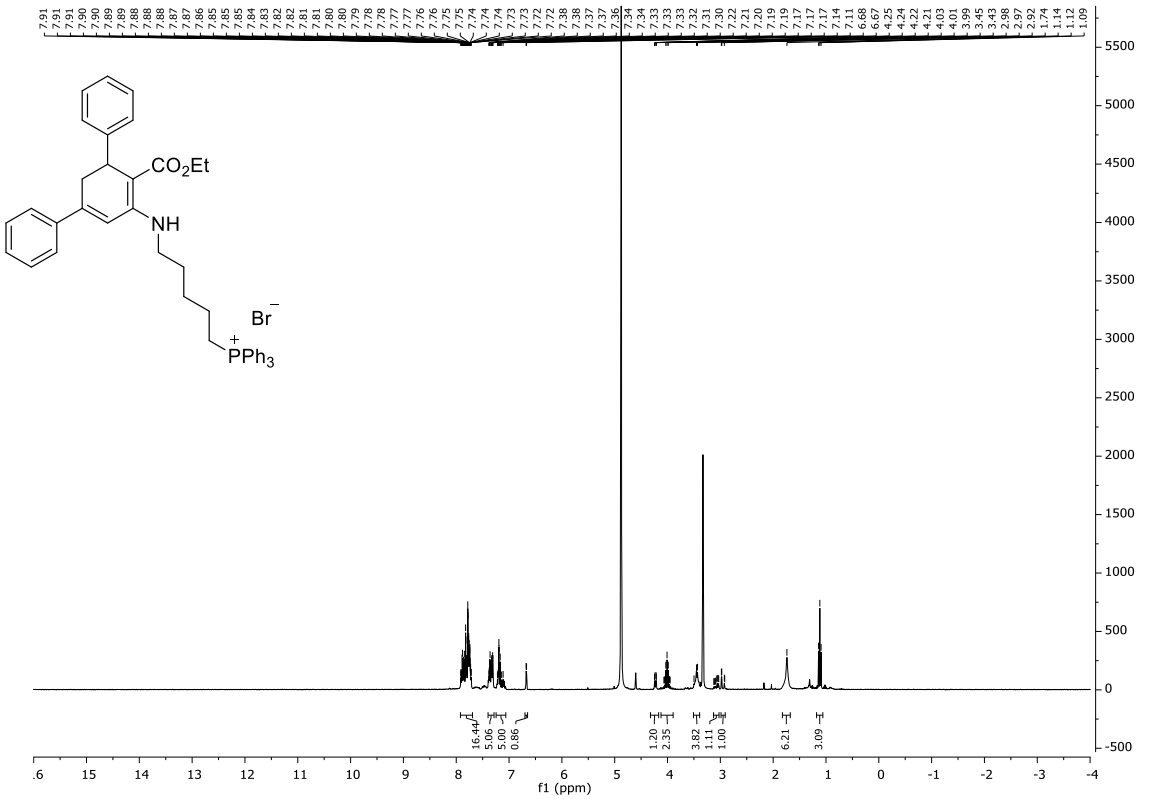
CO2Et
NH
Br−
+
PPh3
f1 (ppm)

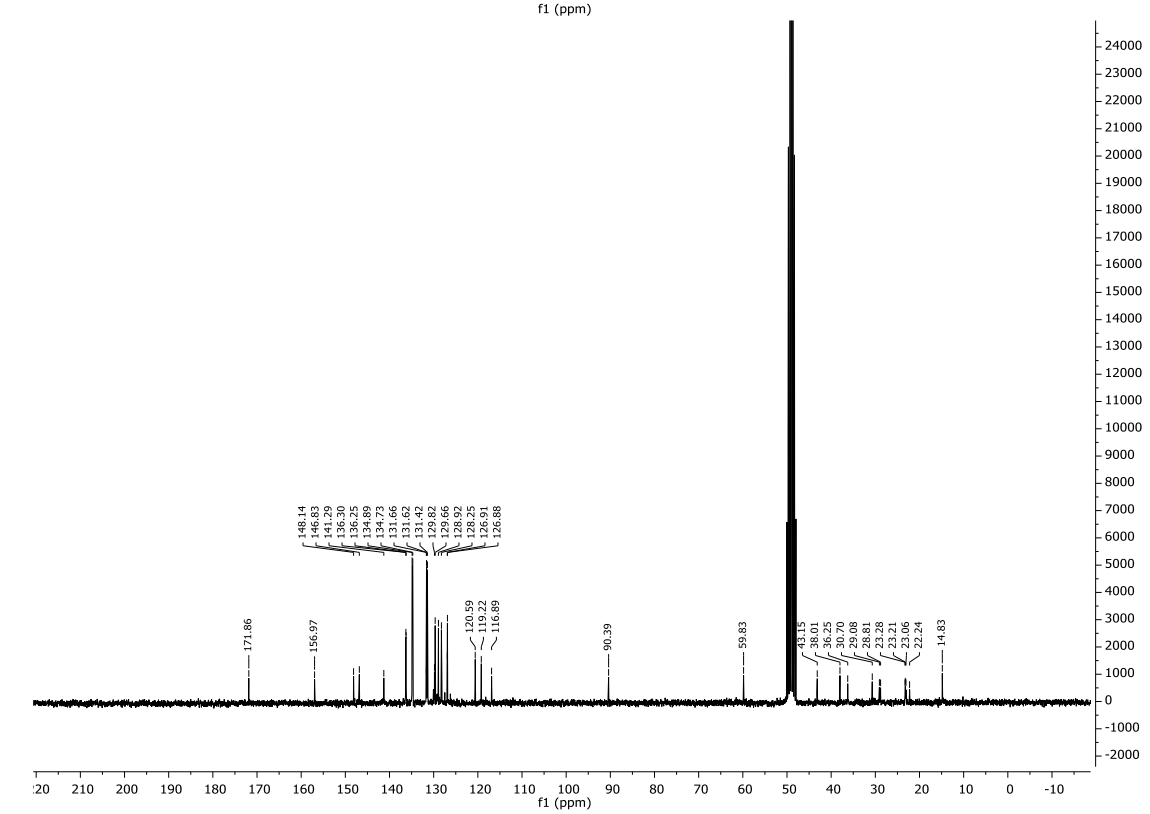
148.14
146.83
141.29
136.30
136.25
134.89
134.73
133.66
131.62
131.42
129.82
129.66
128.92
128.25
126.91
126.88
171.86
156.97
120.59
119.22
116.89
90.39
59.83
43.15
38.01
36.25
30.70
29.08
28.81
23.28
23.21
23.06
22.24
14.83
f1 (ppm)

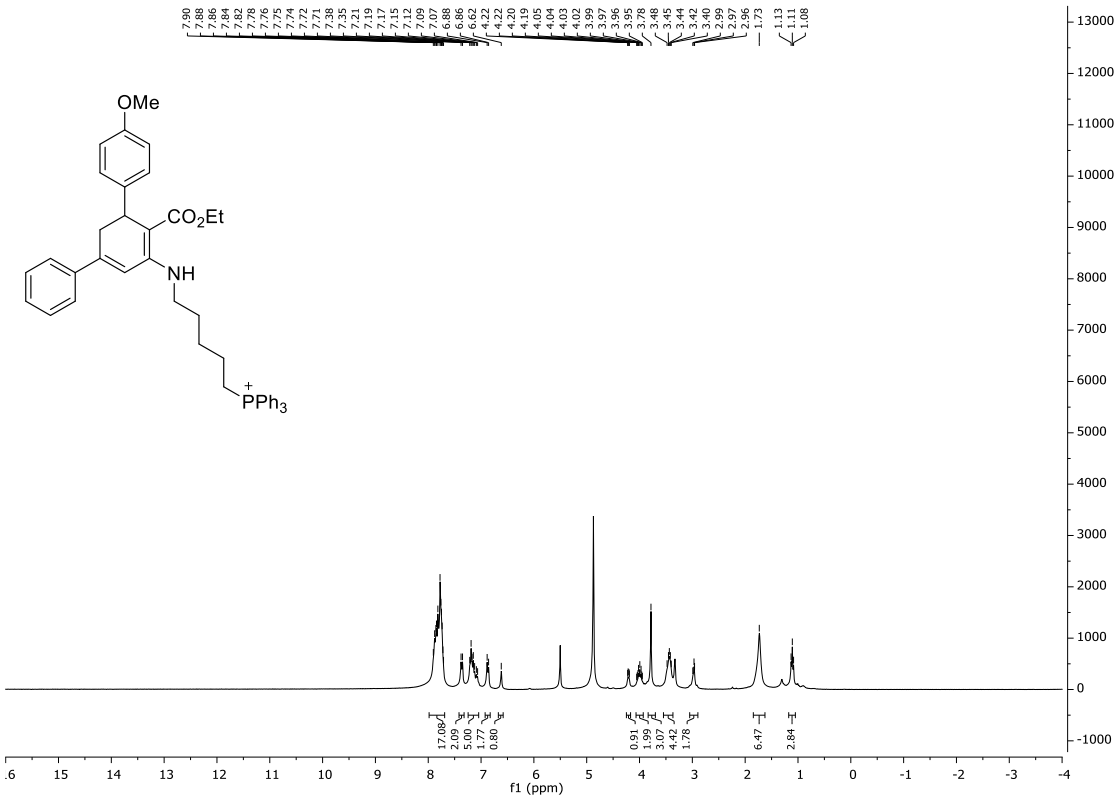
OMe
CO2Et
NH
PPh3
f1 (ppm)

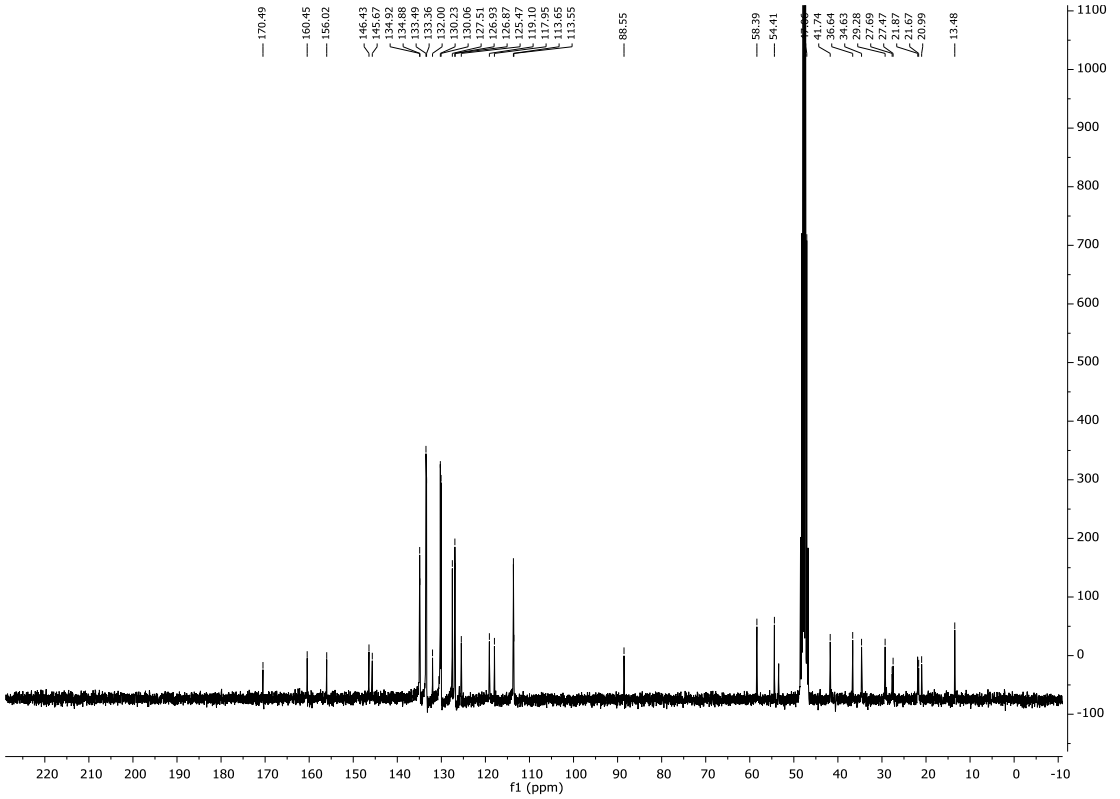
f1 (ppm)

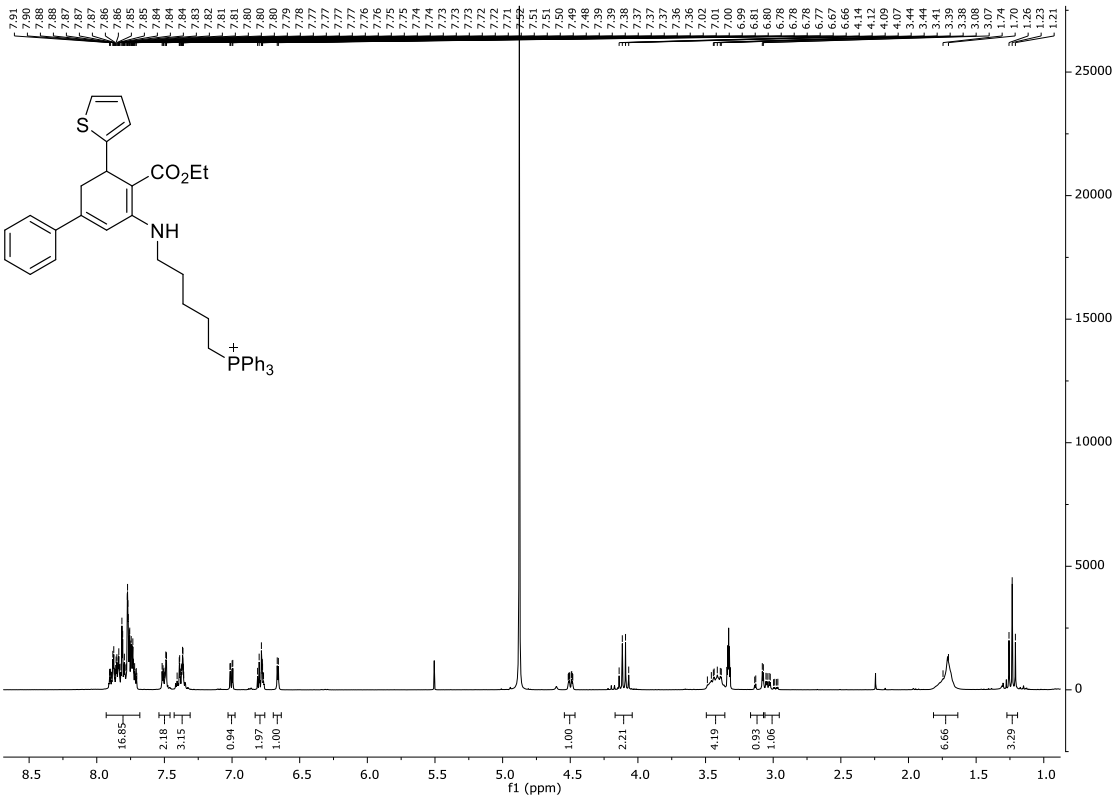
S
CO2Et
NH
PPh3
f1 (ppm)

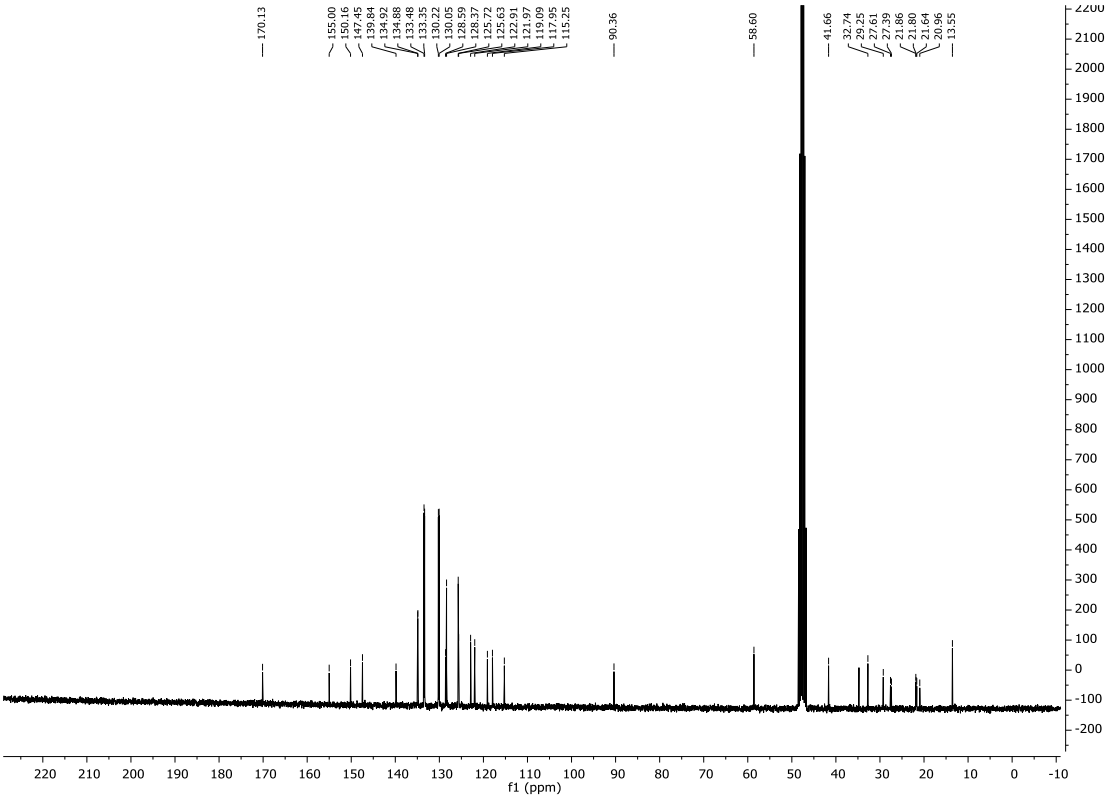
f1 (ppm)

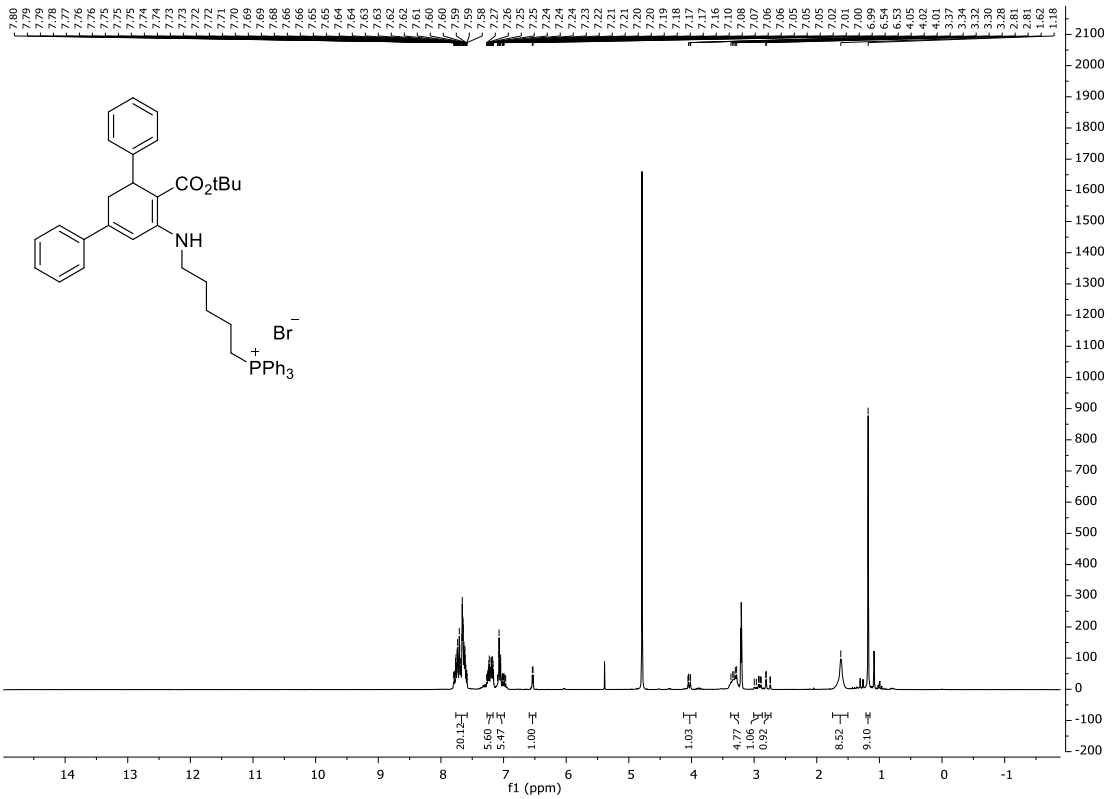
CO2tBu
NH
Br−
+
PPh3
f1 (ppm)

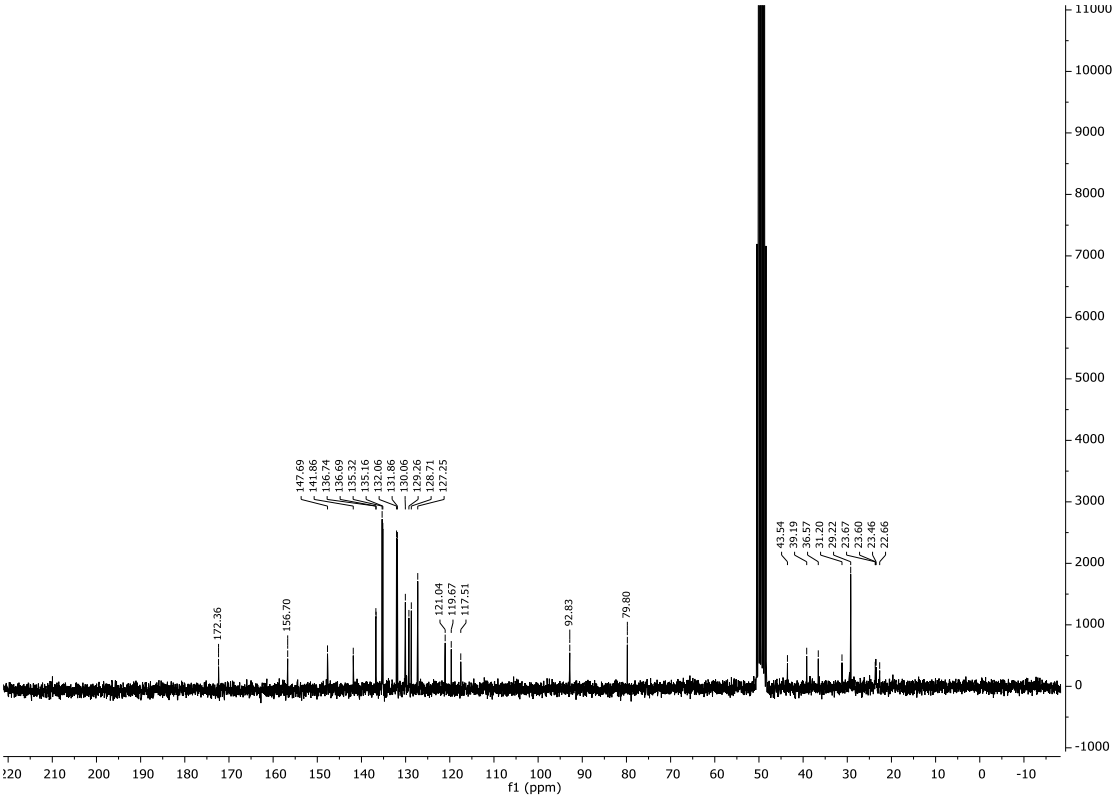
f1 (ppm)

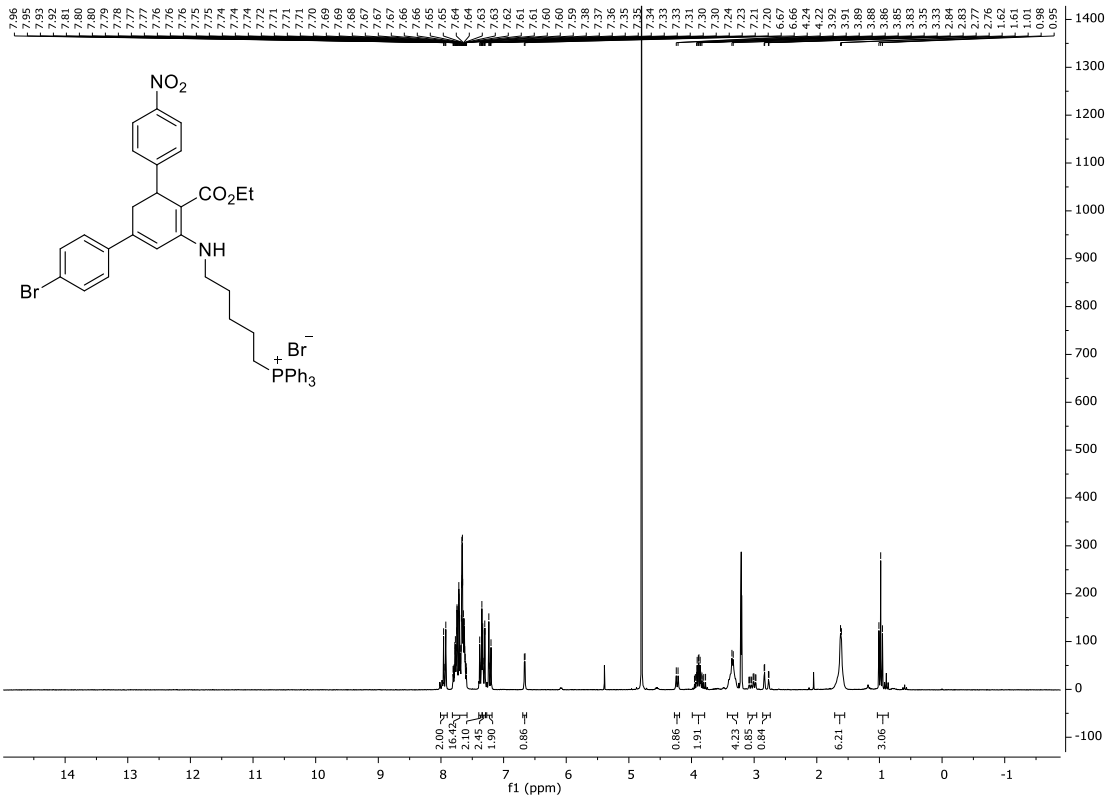
NO2
CO2Et
NH
Br
Br−
+PPh3
f1 (ppm)

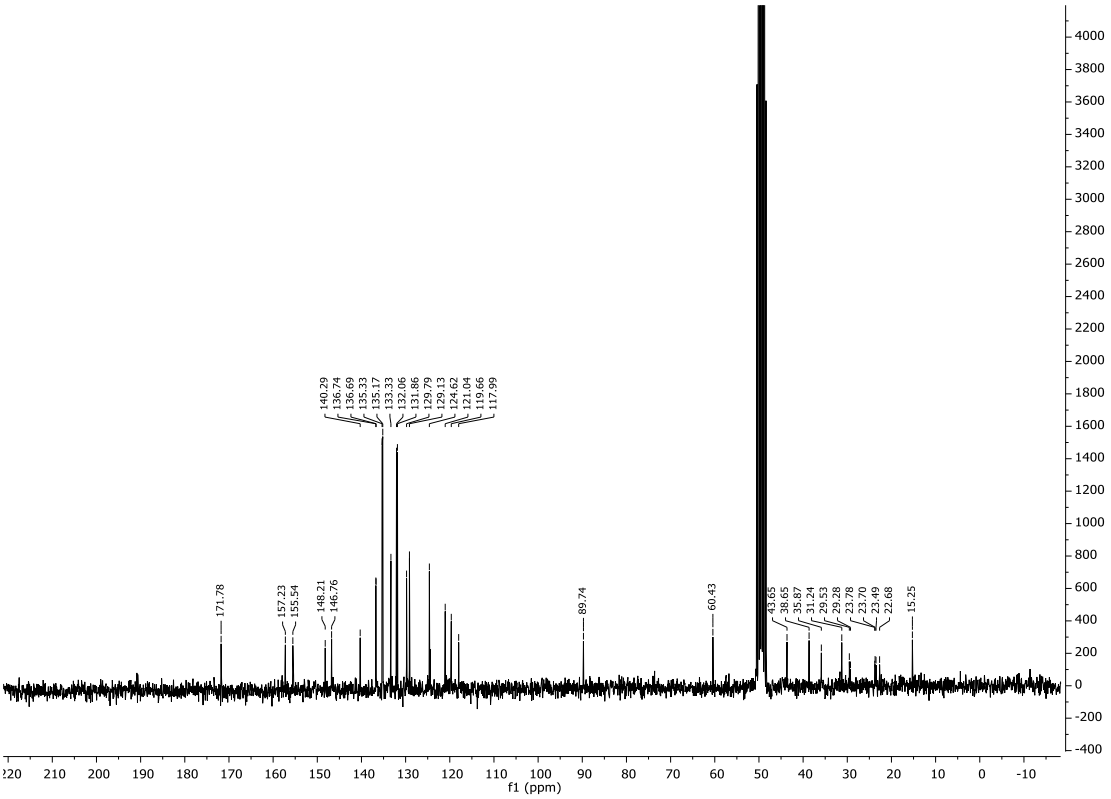
140.29
136.74
136.69
135.23
135.17
133.33
132.06
131.86
129.79
129.13
124.62
121.04
119.66
117.99
171.78
157.23
155.54
148.21
146.76
89.74
60.43
43.65
38.65
35.97
31.24
29.53
29.28
23.78
23.70
23.49
22.68
15.25
f1 (ppm)

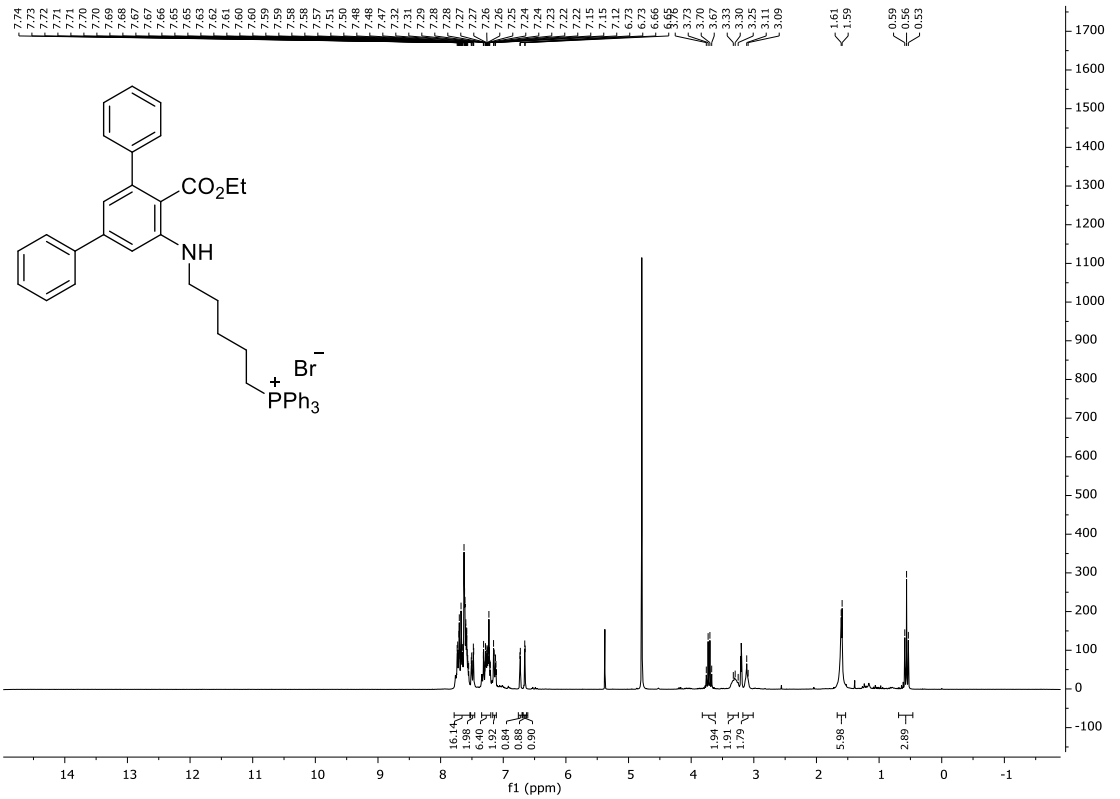
CO2Et
NH
Br
PPh3
f1 (ppm)

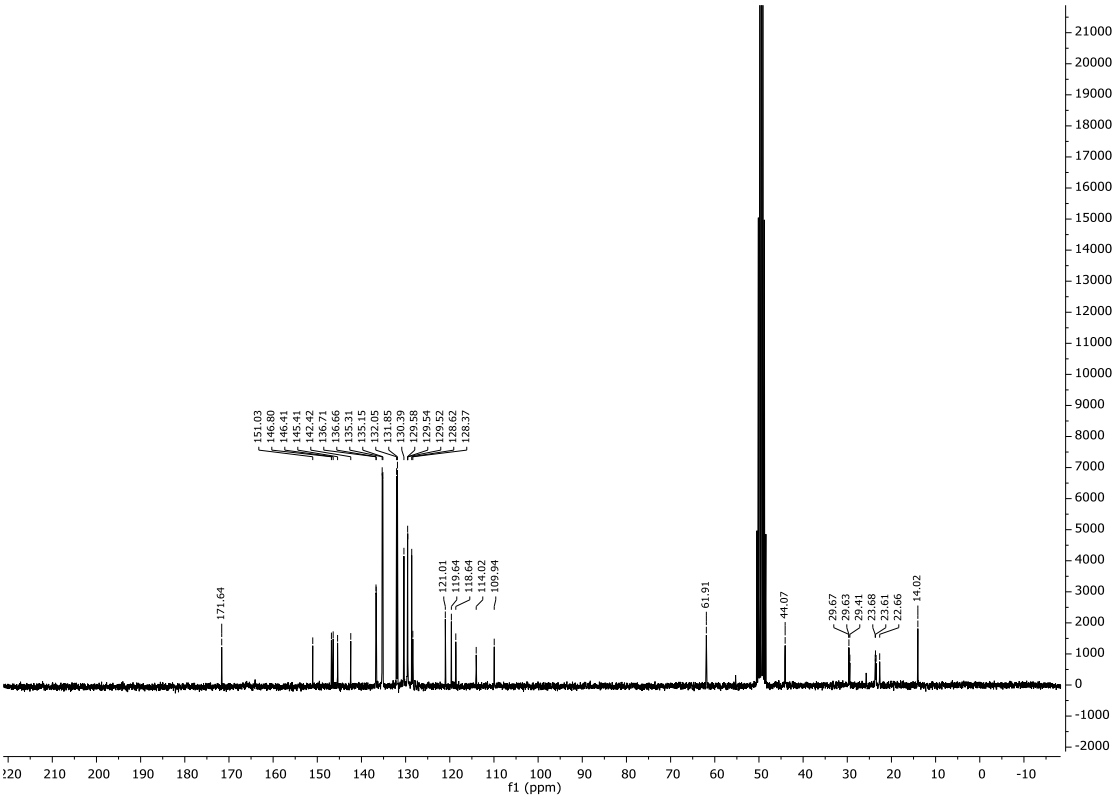
f1 (ppm)

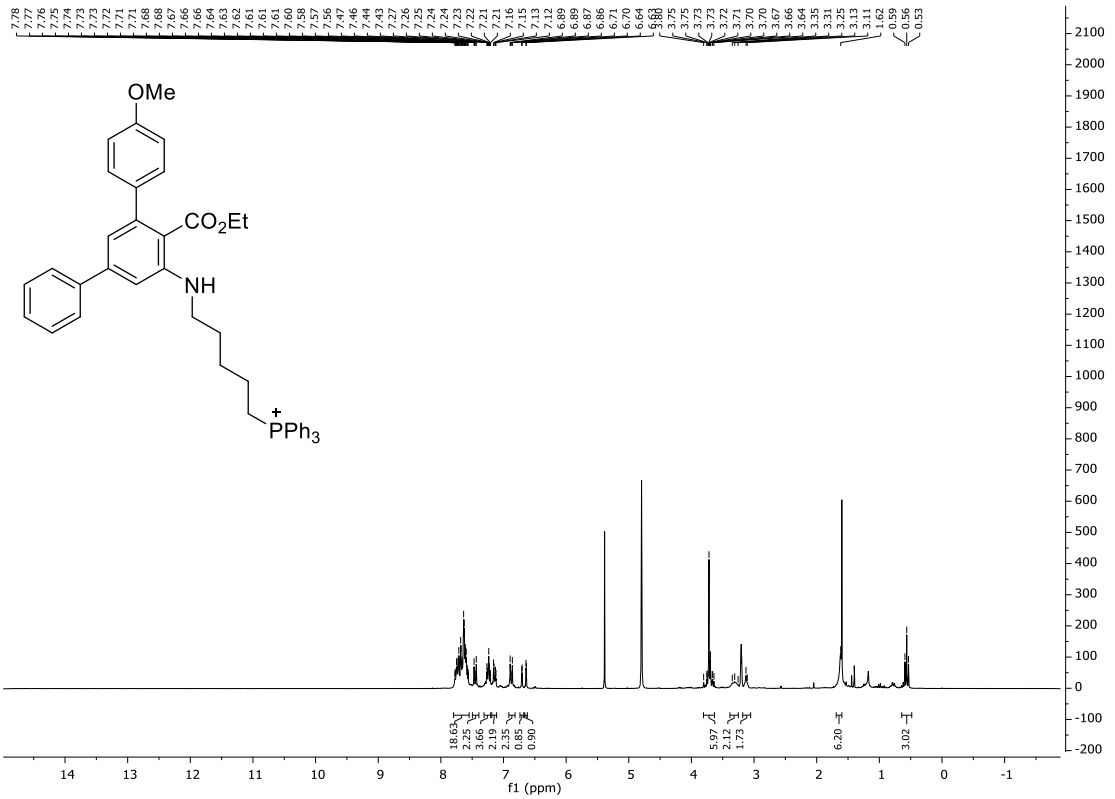
OMe
CO2Et
NH
PPh3
f1 (ppm)

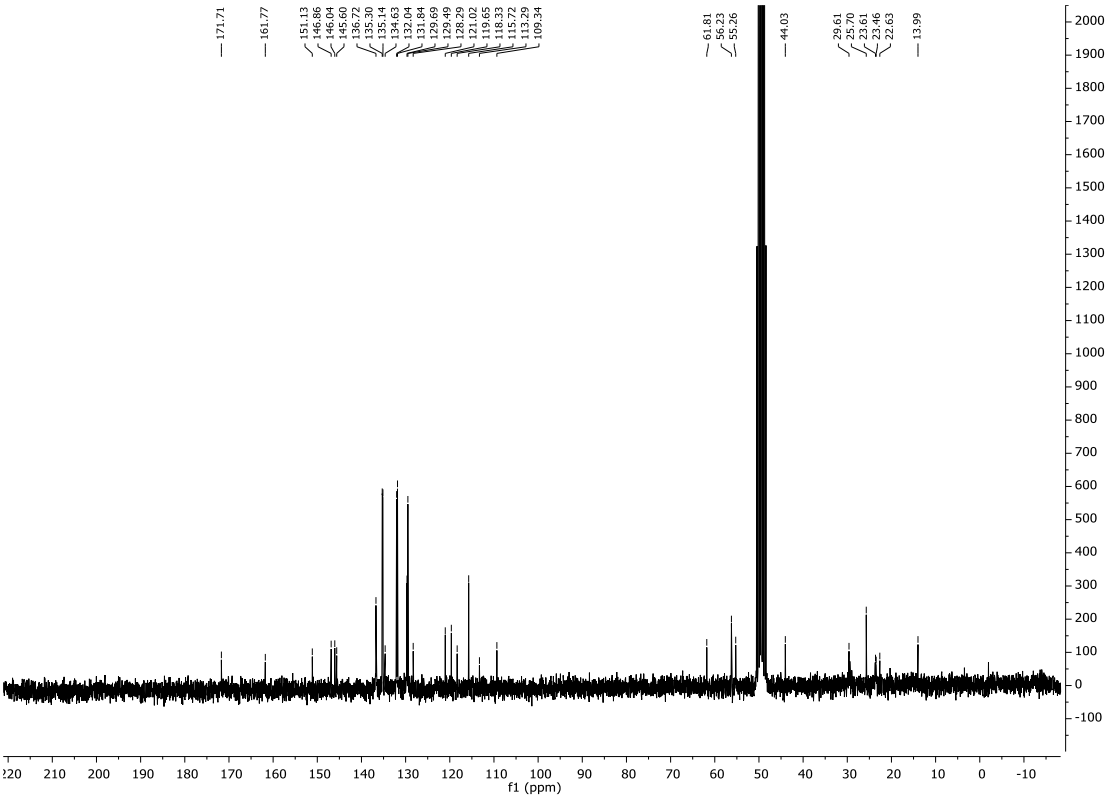
f1 (ppm)

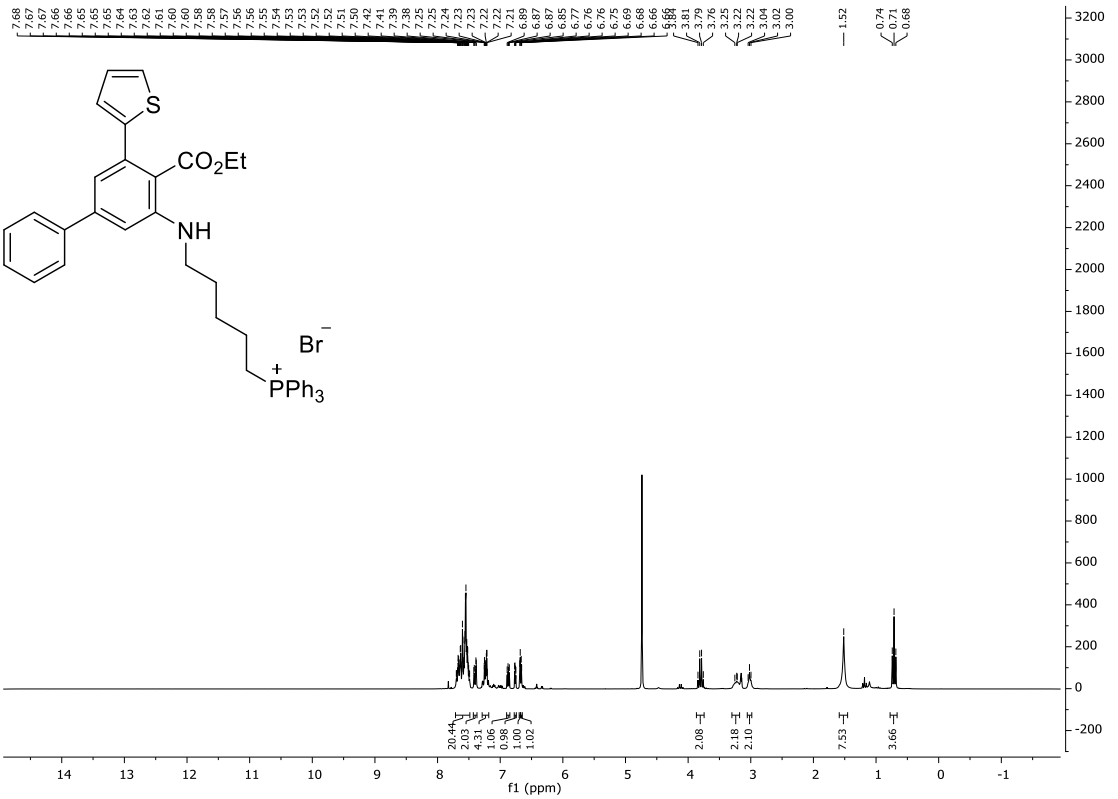
S
CO2Et
NH
Br
PPh3
f1 (ppm)

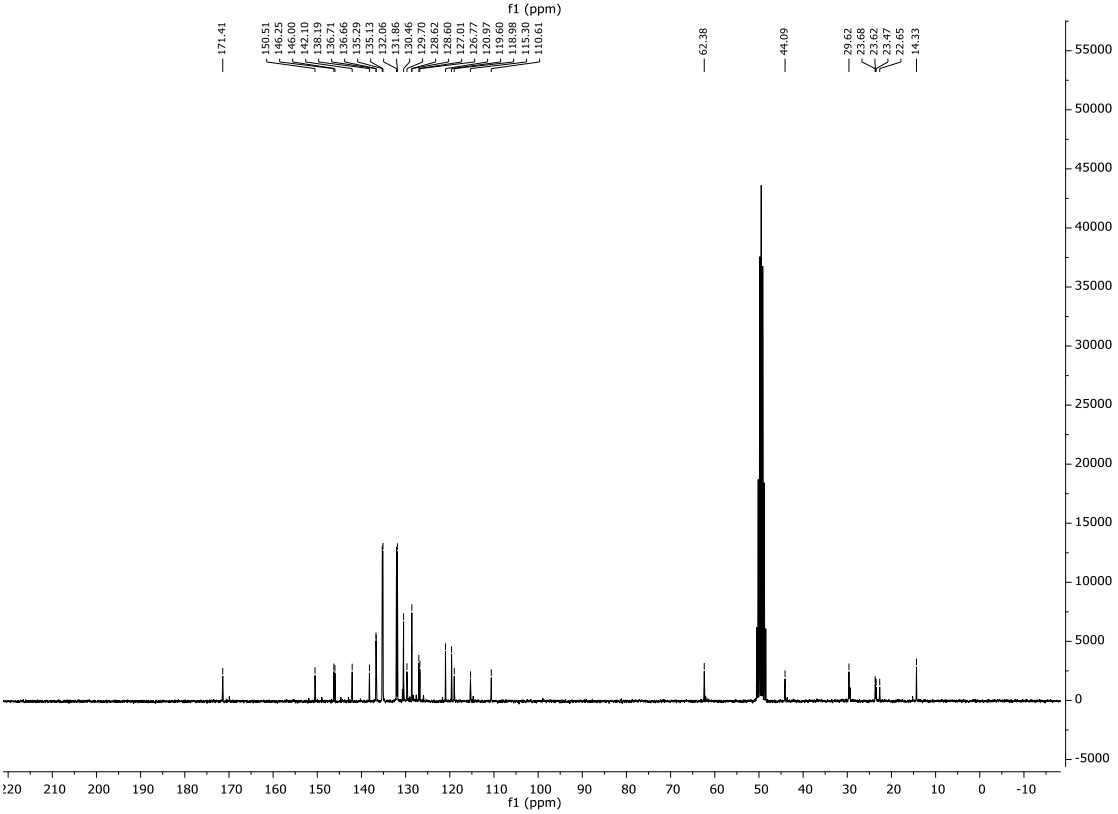
f1 (ppm)

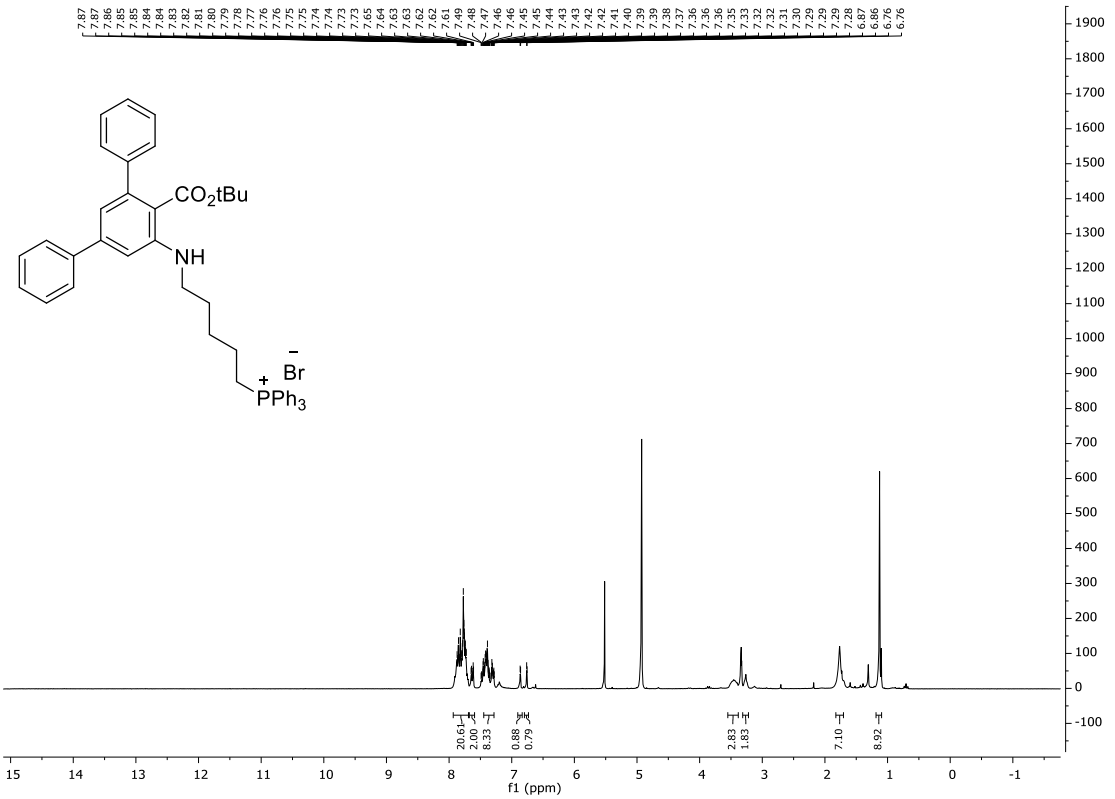
CO2tBu
NH
Br
PPh3
f1 (ppm)

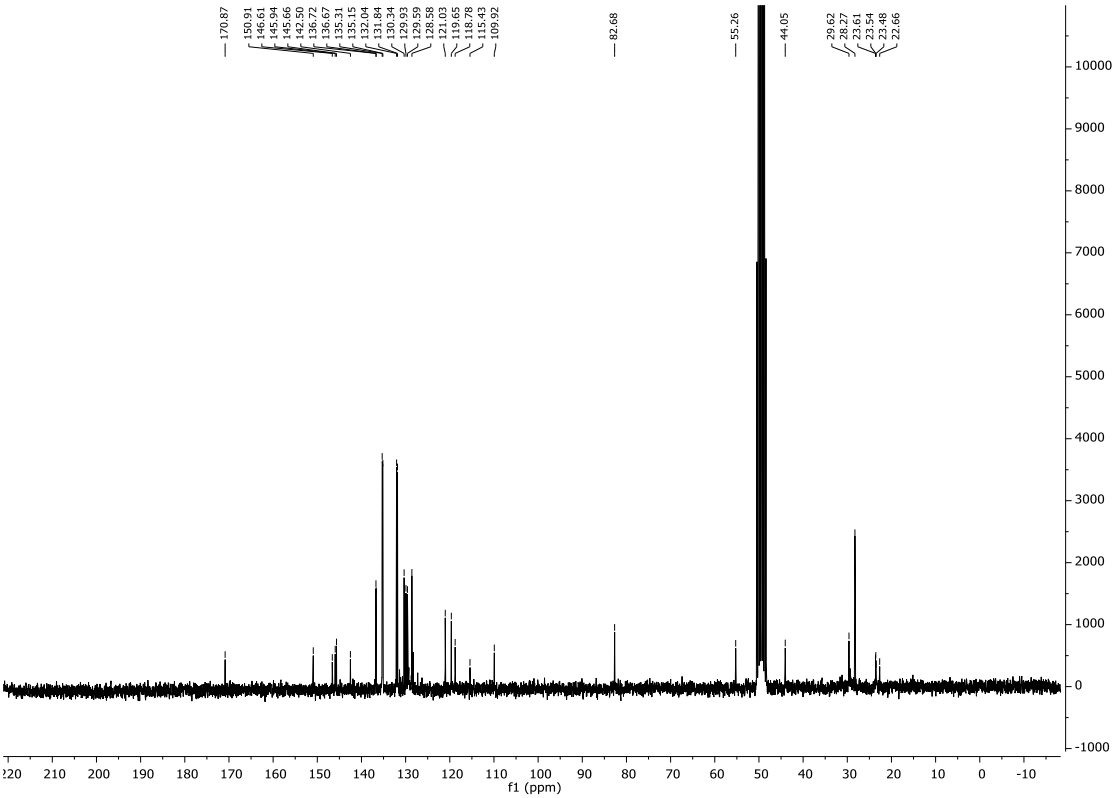
f1 (ppm)

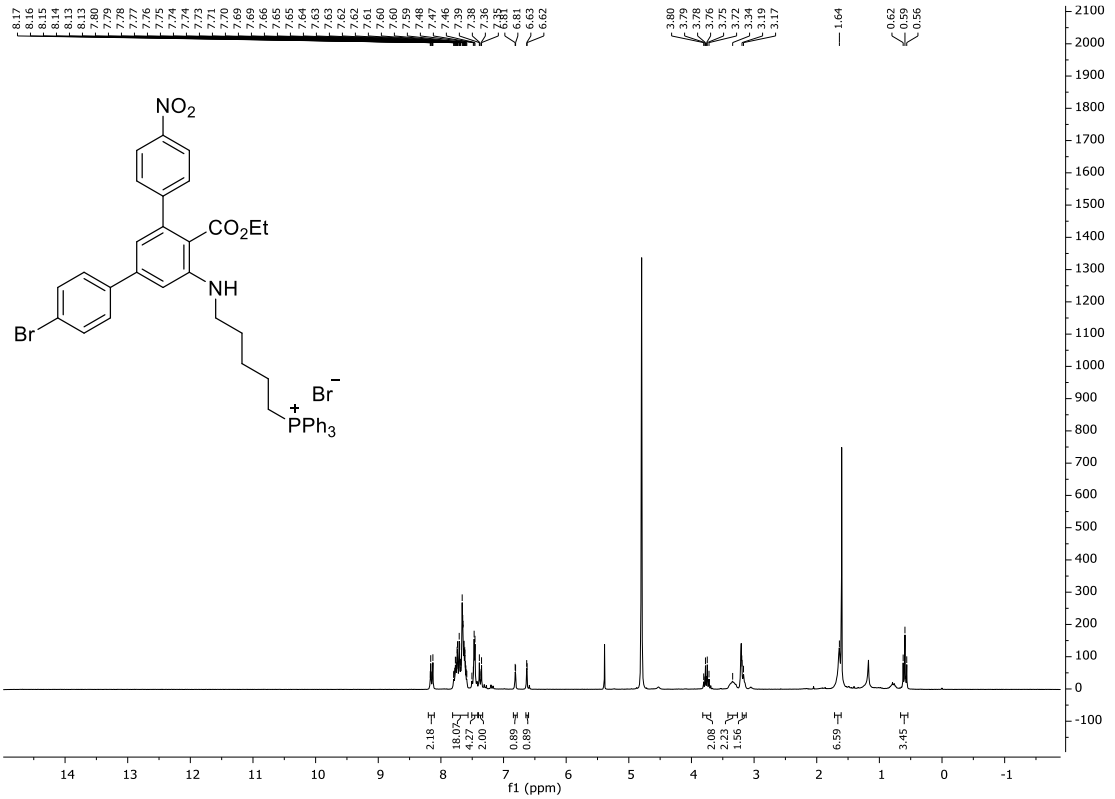
NO2
CO2Et
NH
Br
Br−
+
PPh3
f1 (ppm)

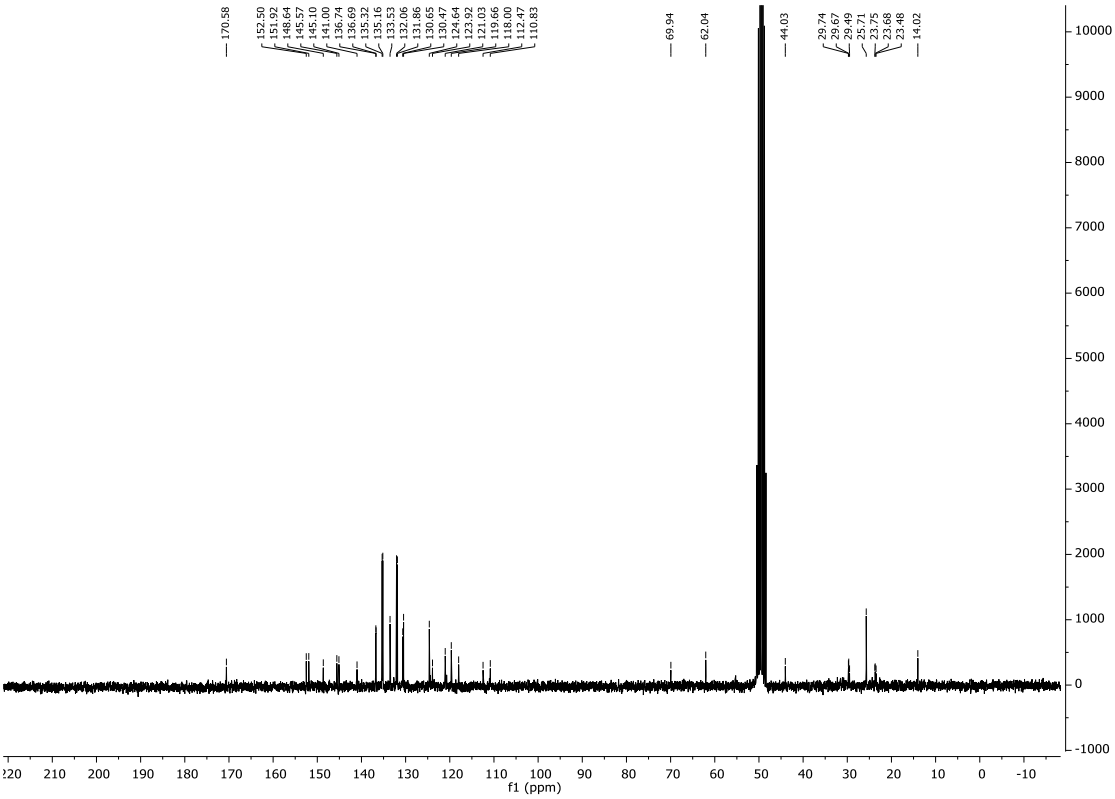
f1 (ppm)

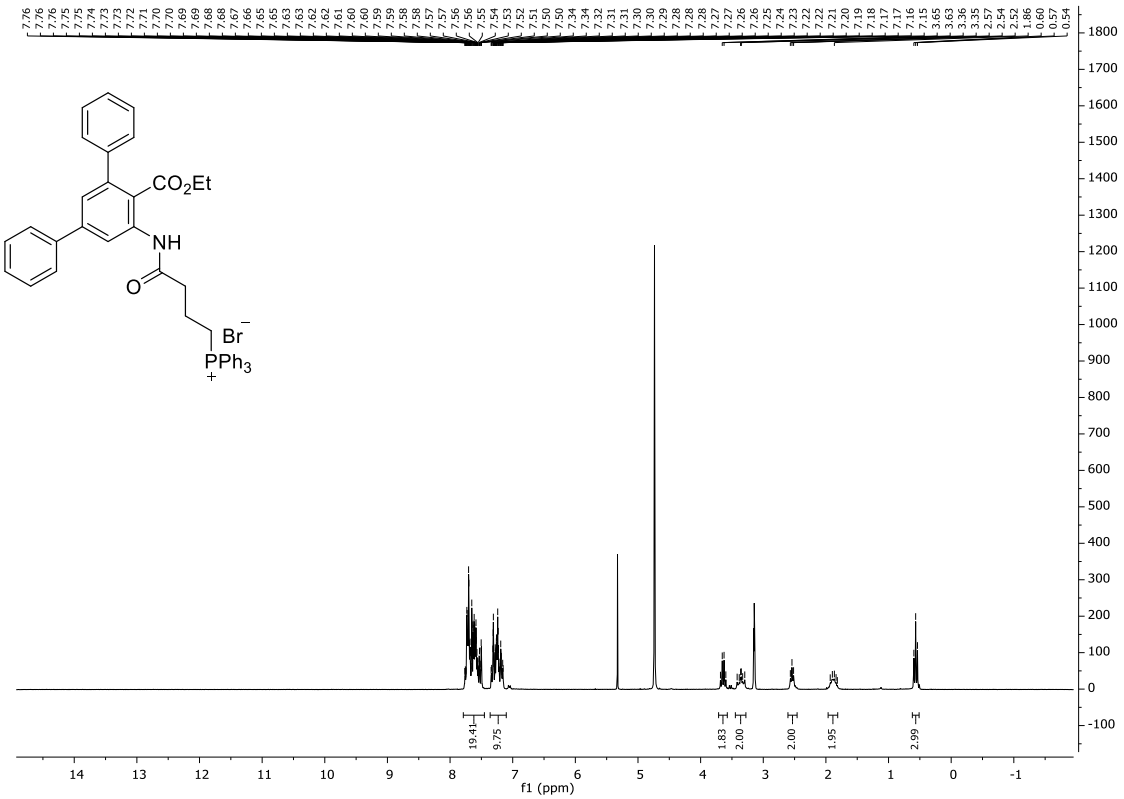
CO2Et
NH
O
Br−
PPh3+
f1 (ppm)

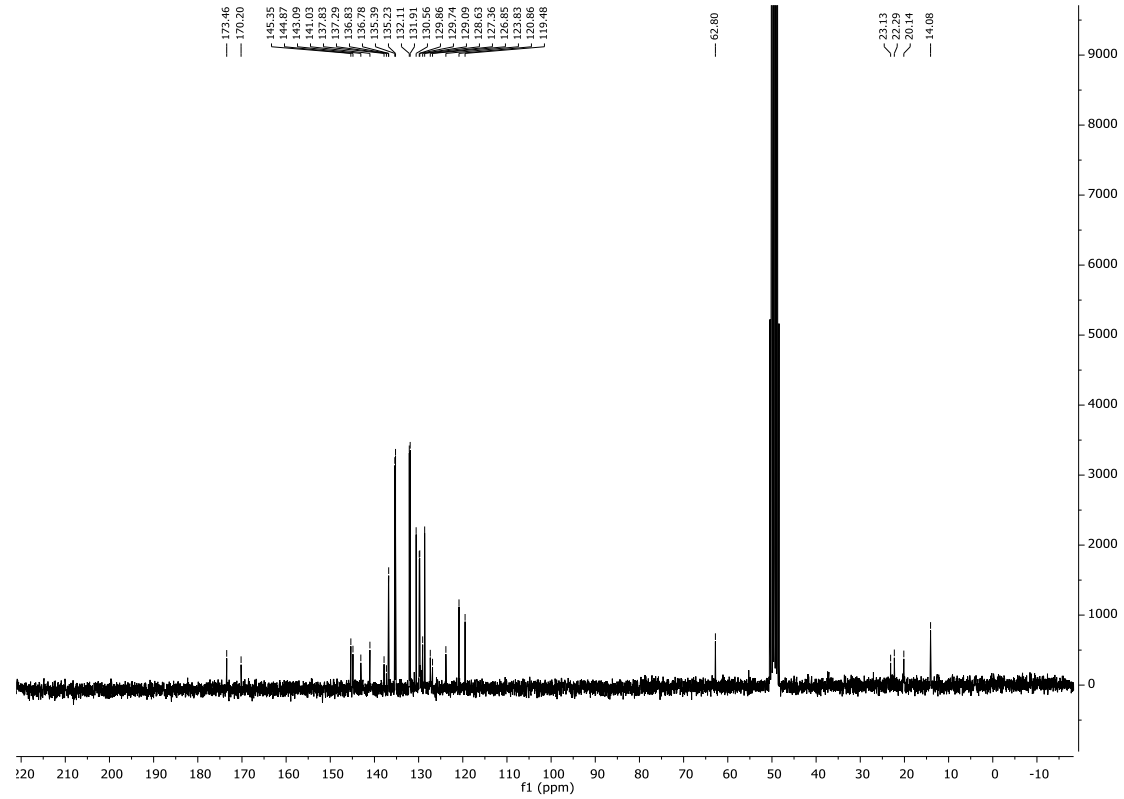
f1 (ppm)

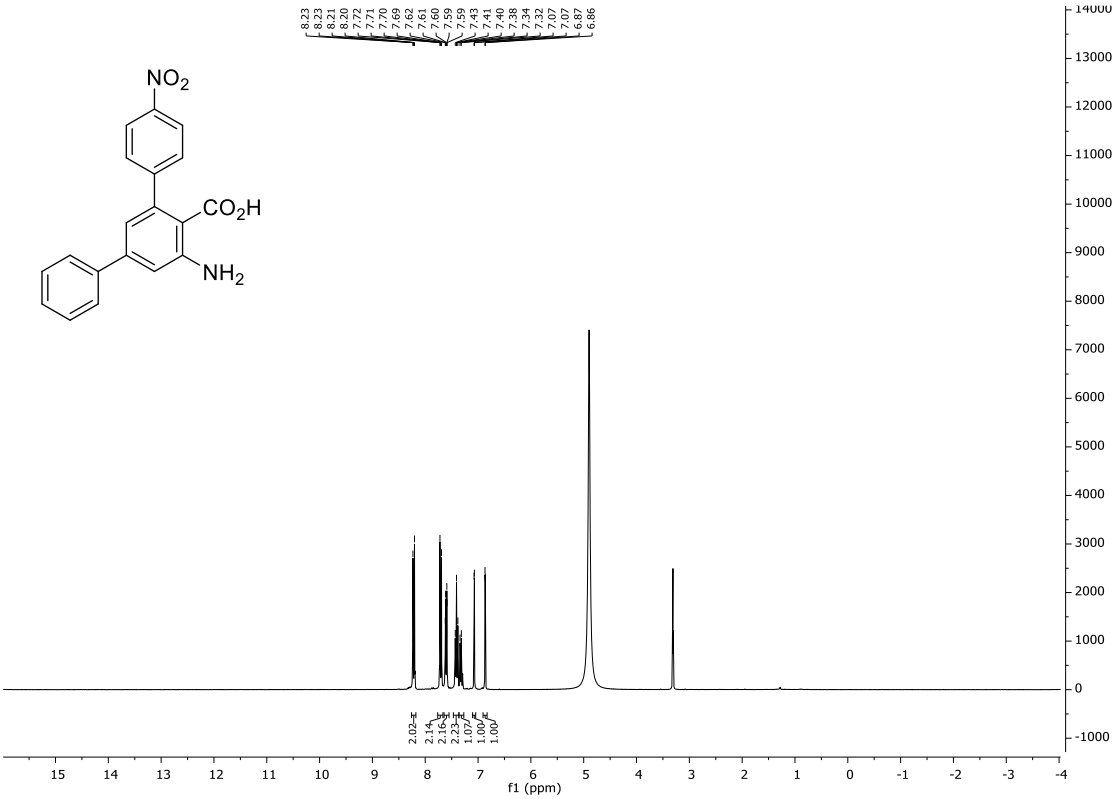
8.23
8.23
8.21
8.20
7.72
7.71
7.70
7.69
7.62
7.61
7.60
7.59
7.59
7.43
7.41
7.40
7.38
7.34
7.32
7.07
7.07
6.87
6.86
NO2
CO2H
NH2
2.02
2.14
2.16
2.23
1.07
1.00
1.00
f1 (ppm)

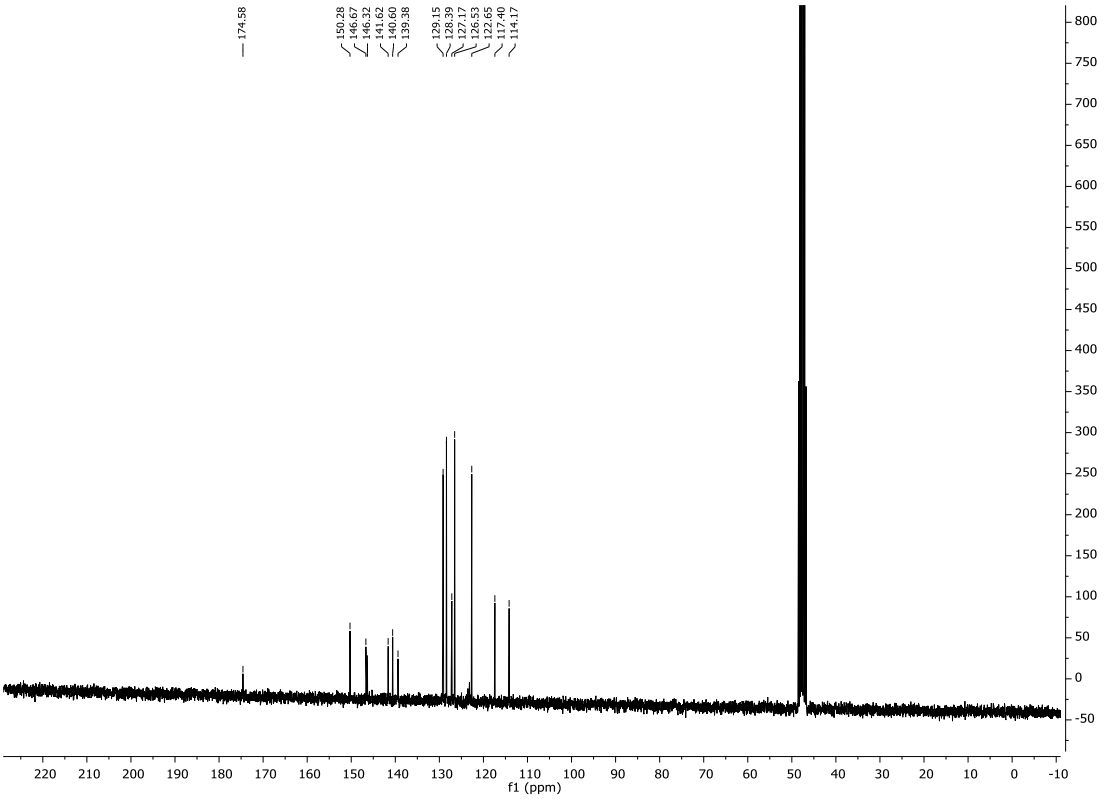
174.58
150.28
146.67
146.32
141.62
140.60
139.38
129.15
128.39
127.17
126.53
122.65
117.40
114.17
f1 (ppm)

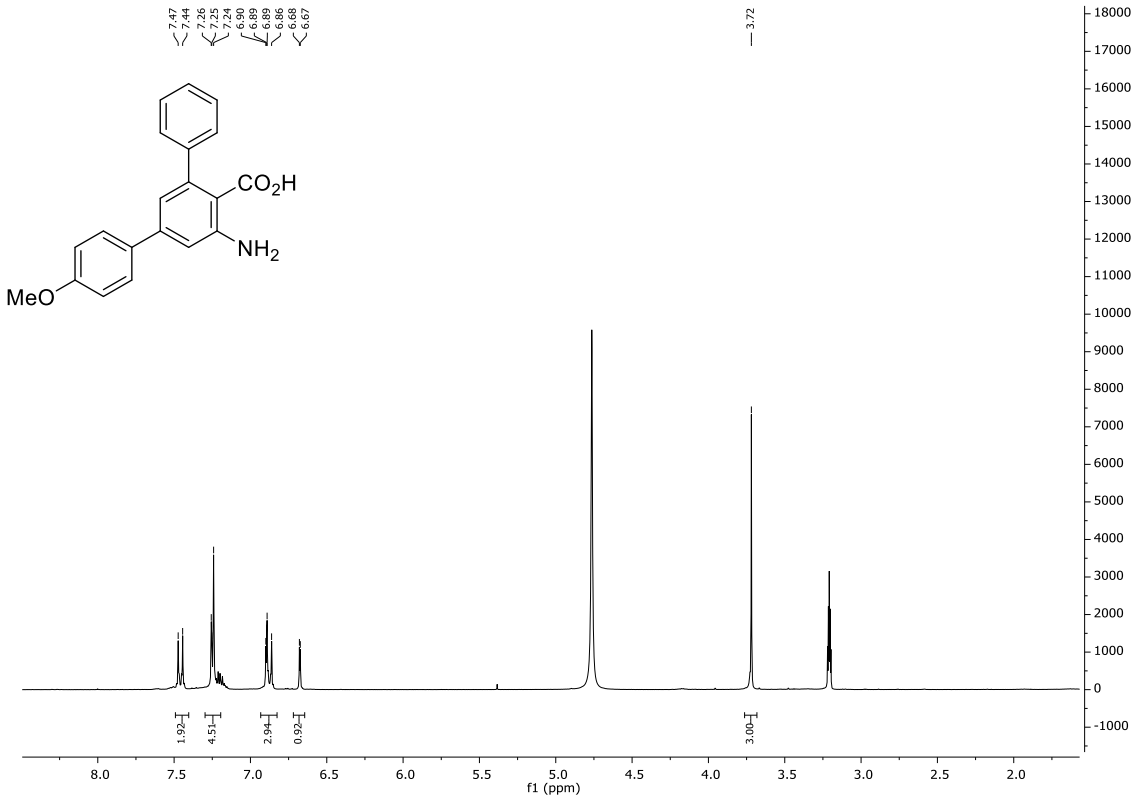
7.47
7.44
7.26
7.25
7.24
6.90
6.89
6.89
6.86
6.68
6.67
3.72
CO2H
NH2
MeO
1.92
4.51
2.94
0.92
3.00
f1 (ppm)

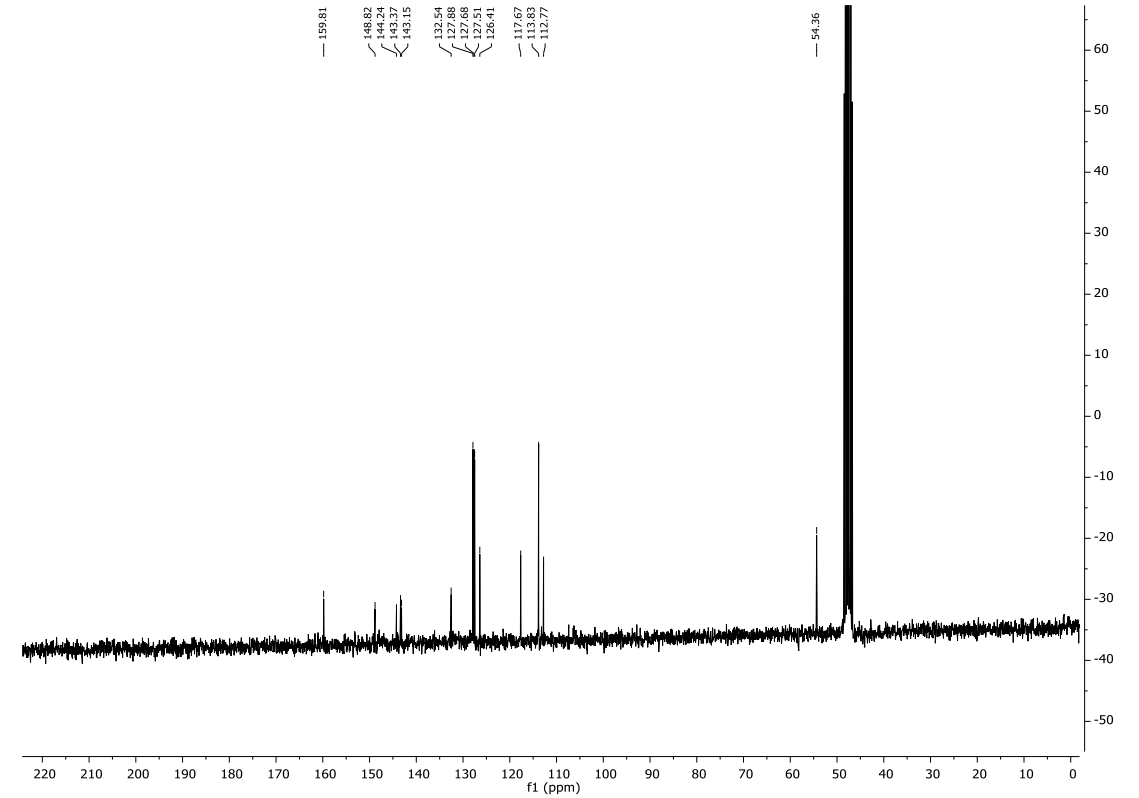
159.81
148.82
144.24
143.37
143.15
132.54
127.88
127.68
127.51
126.41
117.67
113.83
112.77
54.36
f1 (ppm)

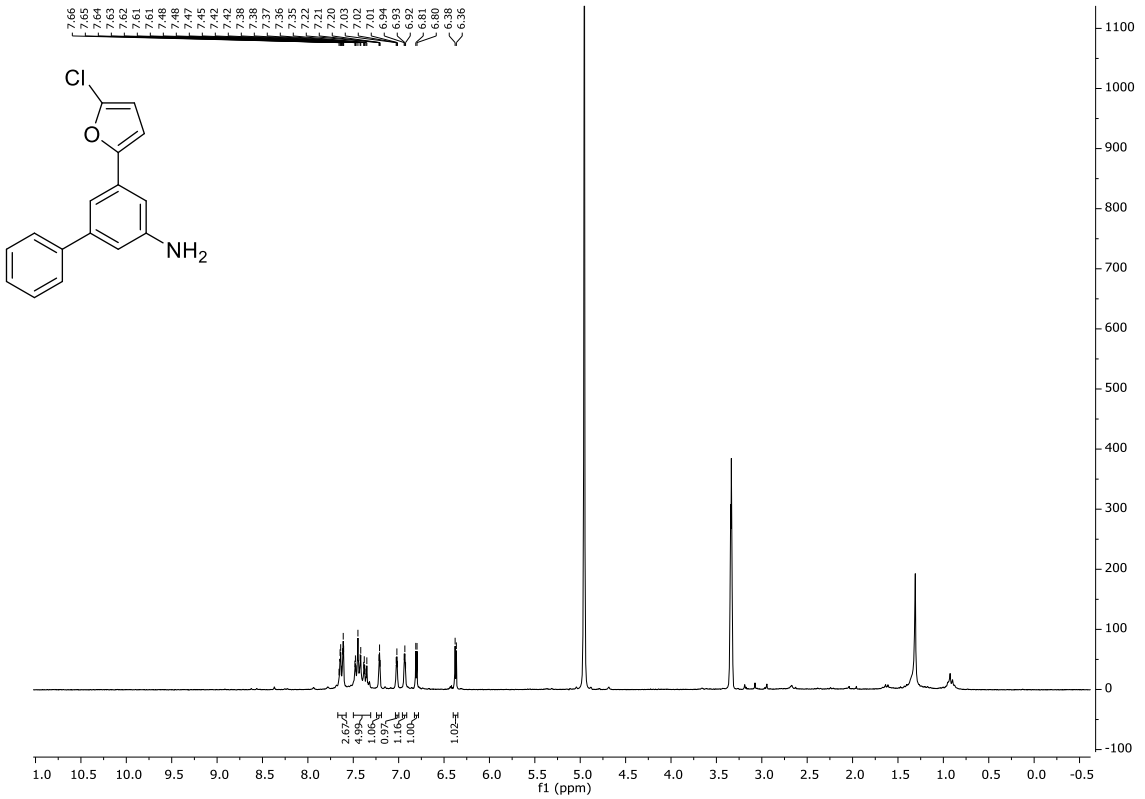
7.66
7.65
7.64
7.63
7.62
7.61
7.61
7.48
7.48
7.47
7.45
7.42
7.42
7.38
7.38
7.37
7.36
7.35
7.22
7.21
7.20
7.03
7.02
7.01
6.94
6.93
6.92
6.81
6.80
6.38
6.36
Cl
O
NH2
2.67
4.99
1.06
0.97
1.16
1.00
1.02
f1 (ppm)

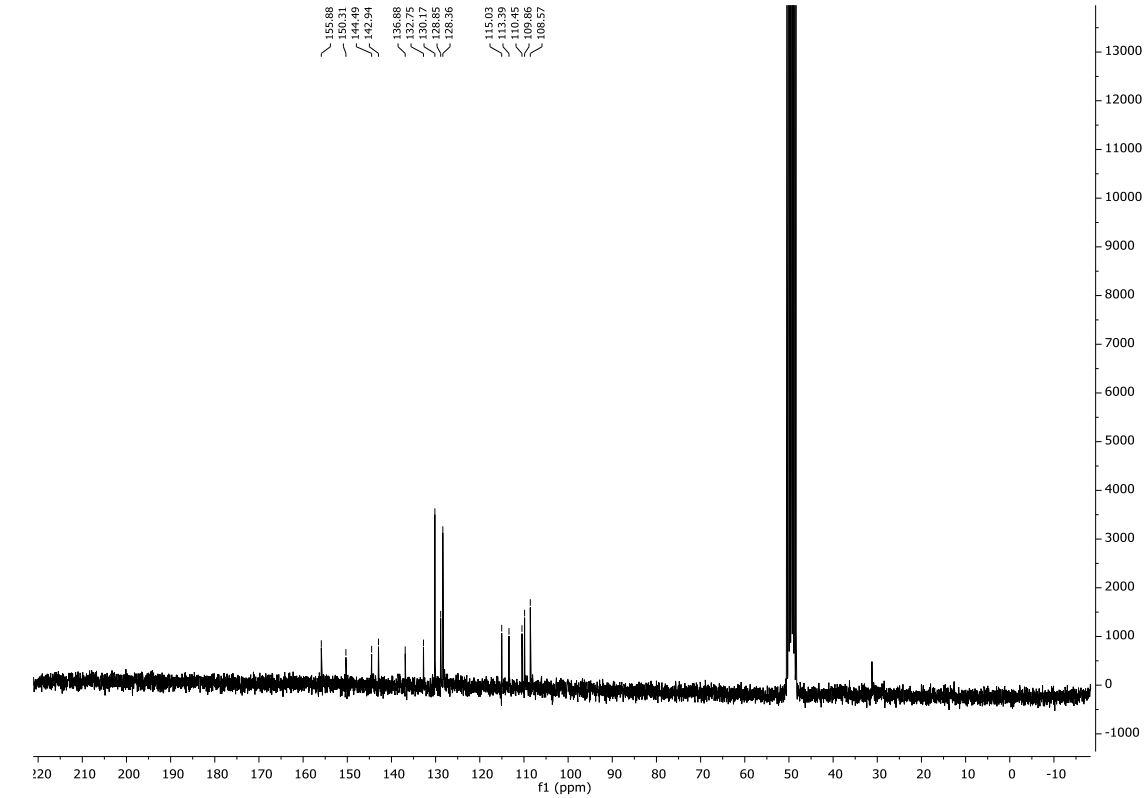
155.88
150.31
144.49
142.94
136.88
132.75
130.17
128.85
128.36
115.03
113.39
110.45
109.86
108.57
f1 (ppm)

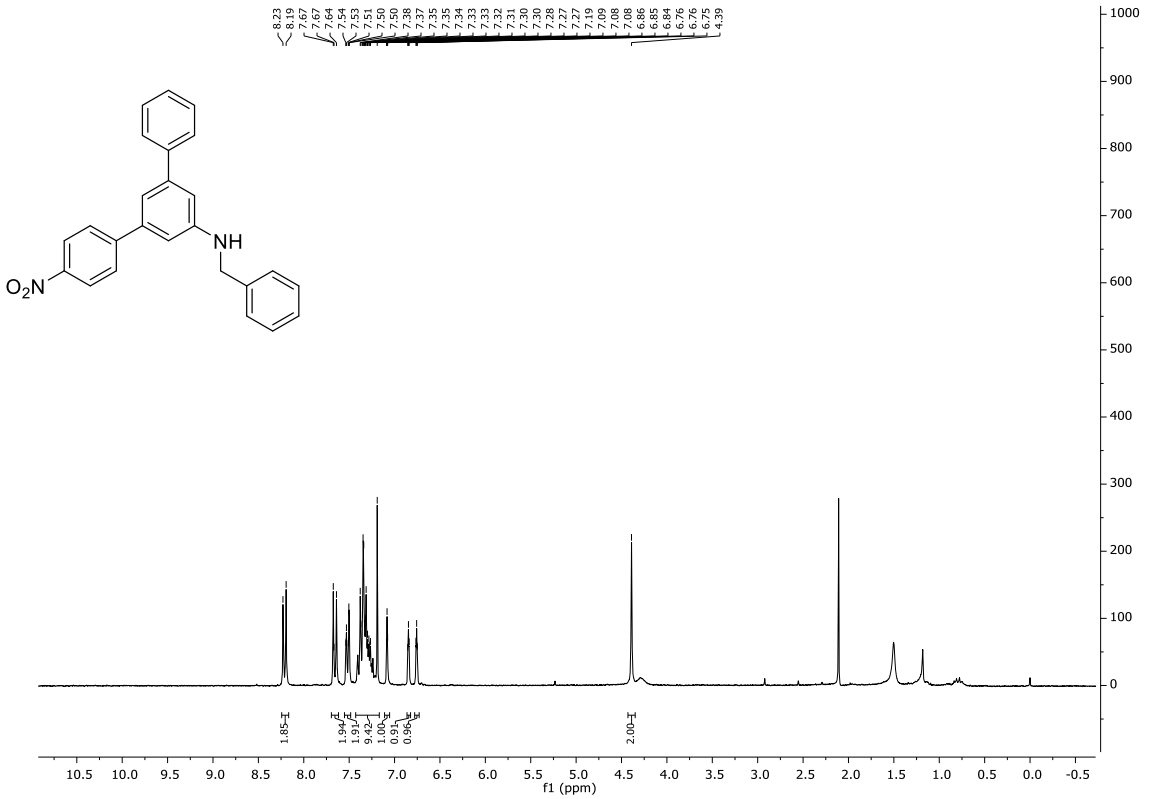
8.23
8.19
7.67
7.67
7.64
7.54
7.53
7.51
7.50
7.50
7.38
7.37
7.35
7.35
7.34
7.33
7.33
7.32
7.31
7.30
7.28
7.27
7.27
7.19
7.09
7.08
7.08
6.86
6.85
6.84
6.76
6.76
6.75
4.39
NH
O2N
1.85
1.94
1.91
9.42
1.00
0.91
0.96
2.00
f1 (ppm)

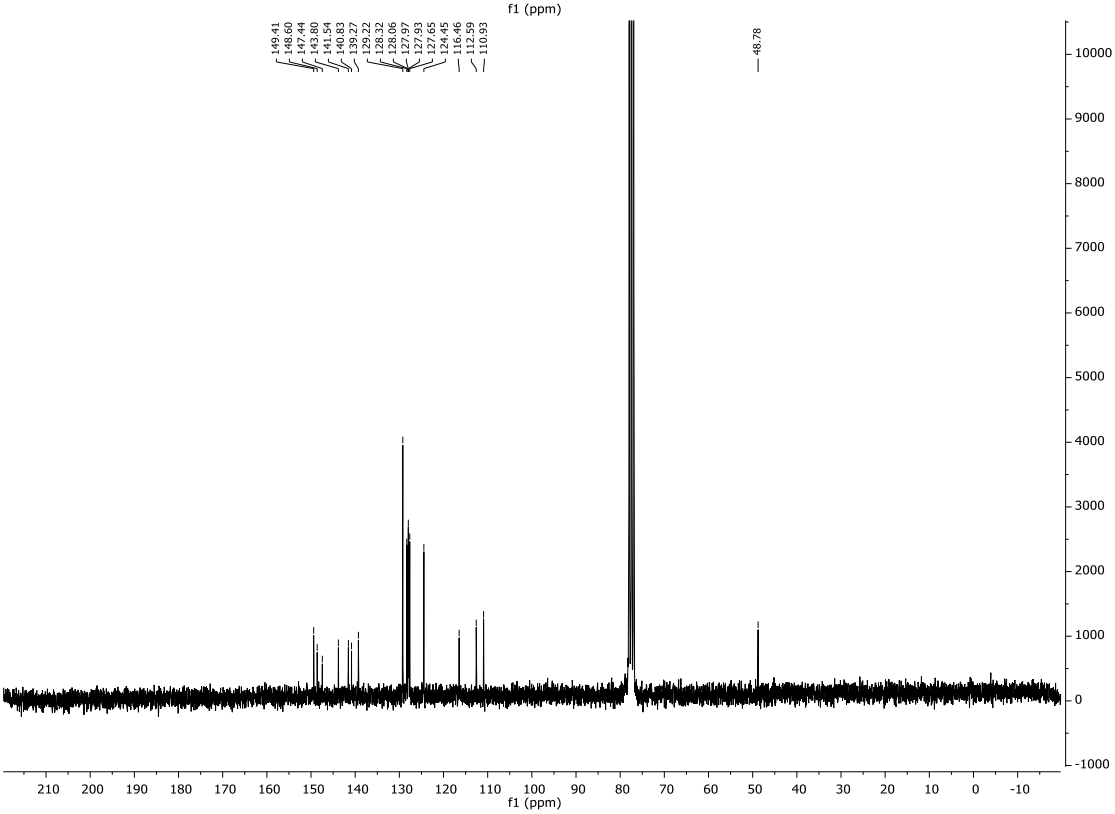
149.41
148.60
147.44
143.80
141.54
140.83
139.27
129.22
128.32
128.06
127.97
127.83
127.65
124.45
116.46
112.59
110.93
48.78
f1 (ppm)

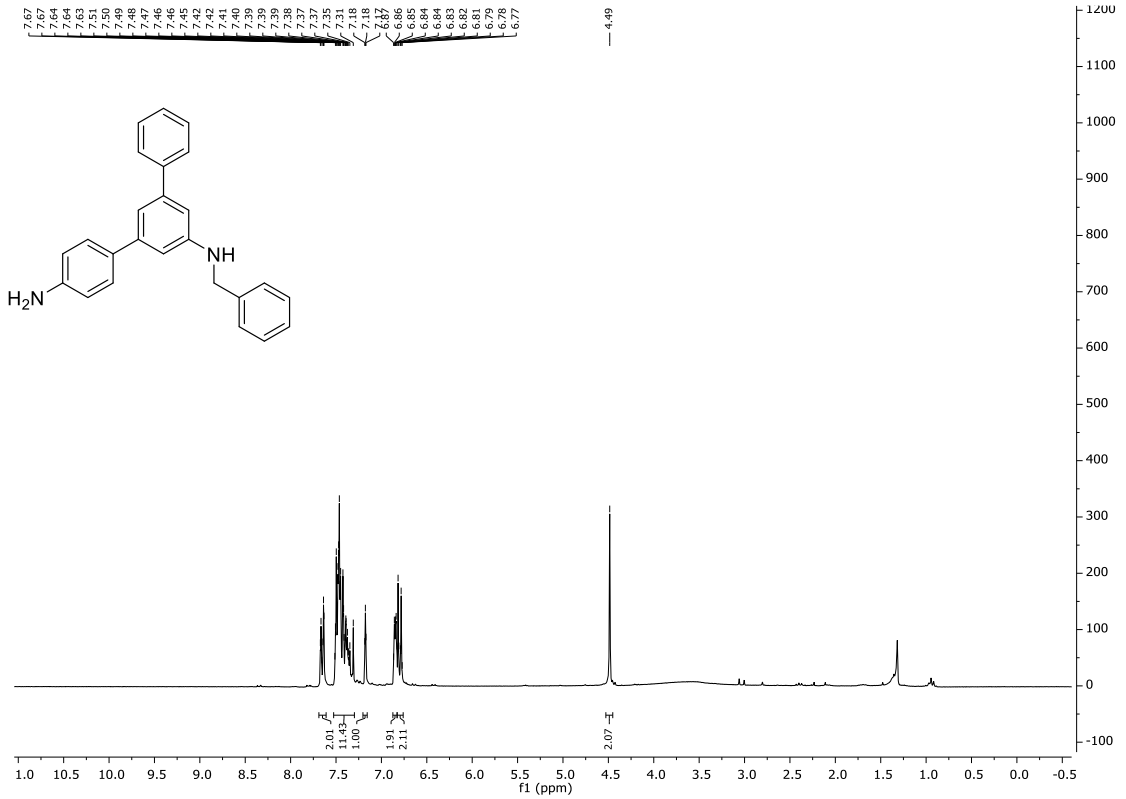
7.67
7.67
7.64
7.64
7.63
7.51
7.50
7.49
7.48
7.47
7.46
7.46
7.45
7.42
7.42
7.41
7.40
7.39
7.39
7.38
7.38
7.37
7.37
7.35
7.31
7.18
6.87
6.86
6.85
6.84
6.84
6.83
6.82
6.81
6.79
6.78
6.77
4.49
NH
$H_2N$
2.01
11.43
1.00
1.91
2.11
2.07
f1 (ppm)

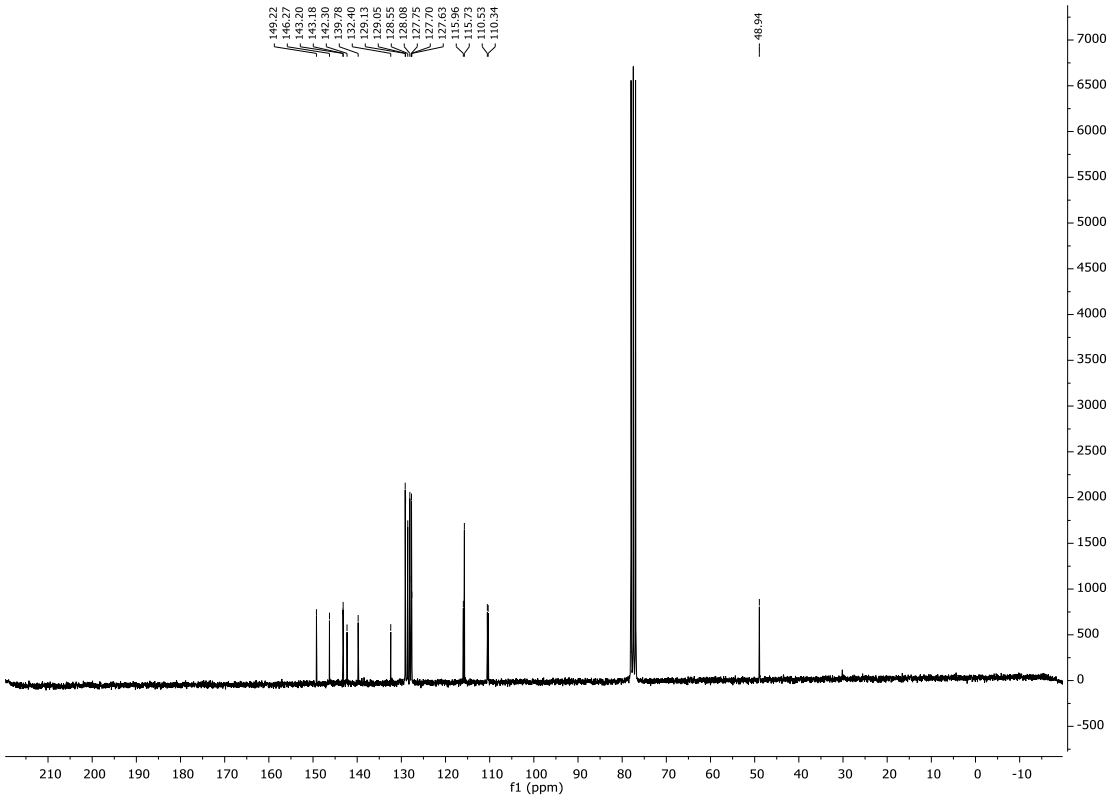
149.22
146.27
143.20
143.18
142.30
139.78
132.40
130.13
129.05
128.55
128.08
127.75
127.70
127.63
115.96
115.73
110.53
110.34
48.94
f1 (ppm)

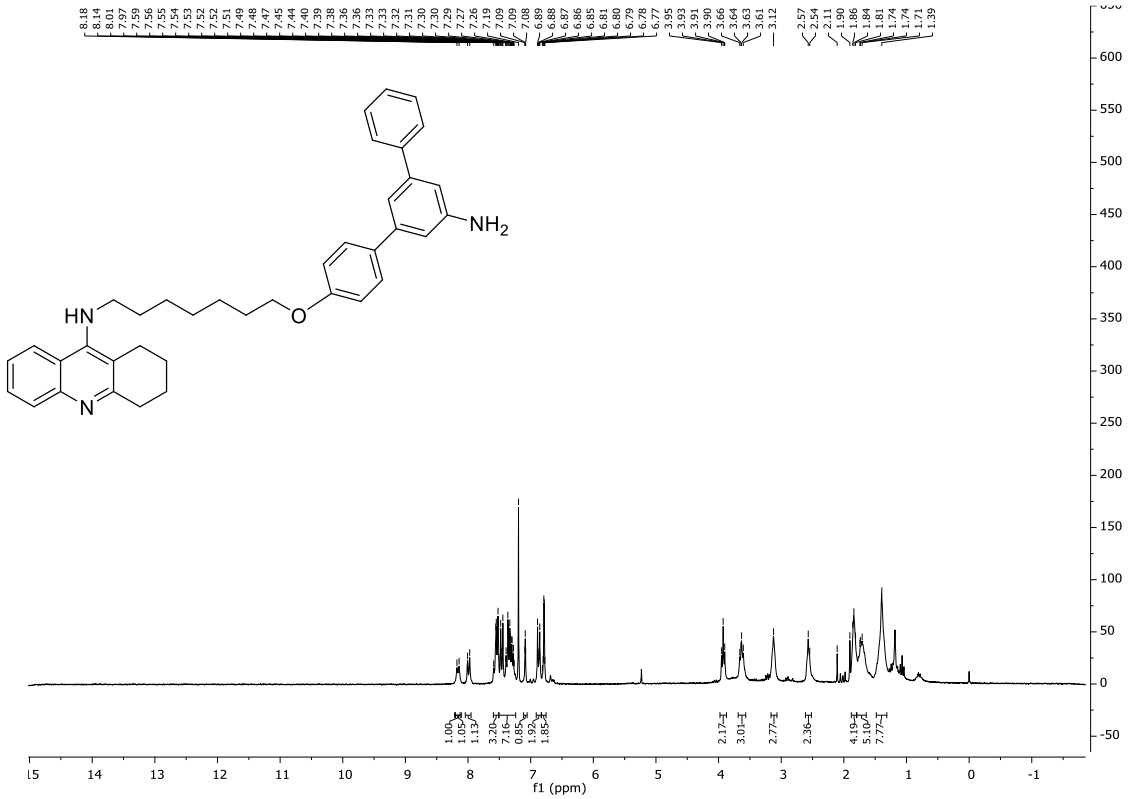
NH2
HN
O
N
f1 (ppm)

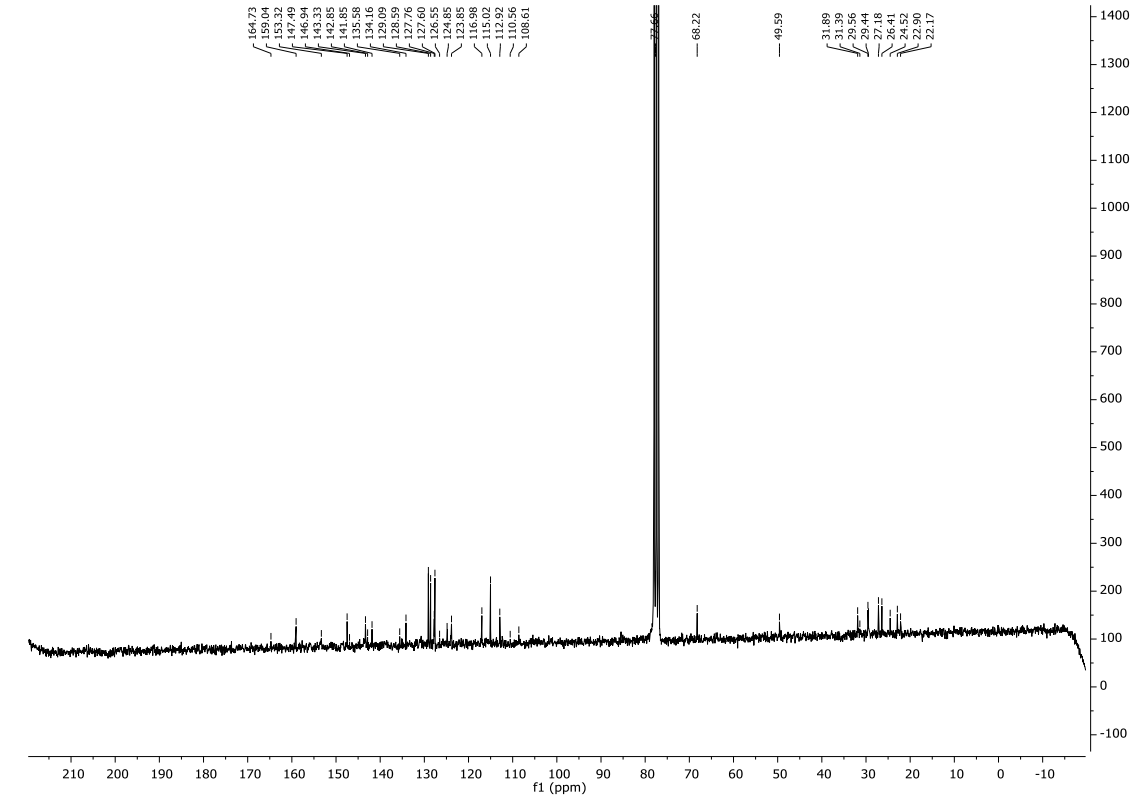
f1 (ppm)

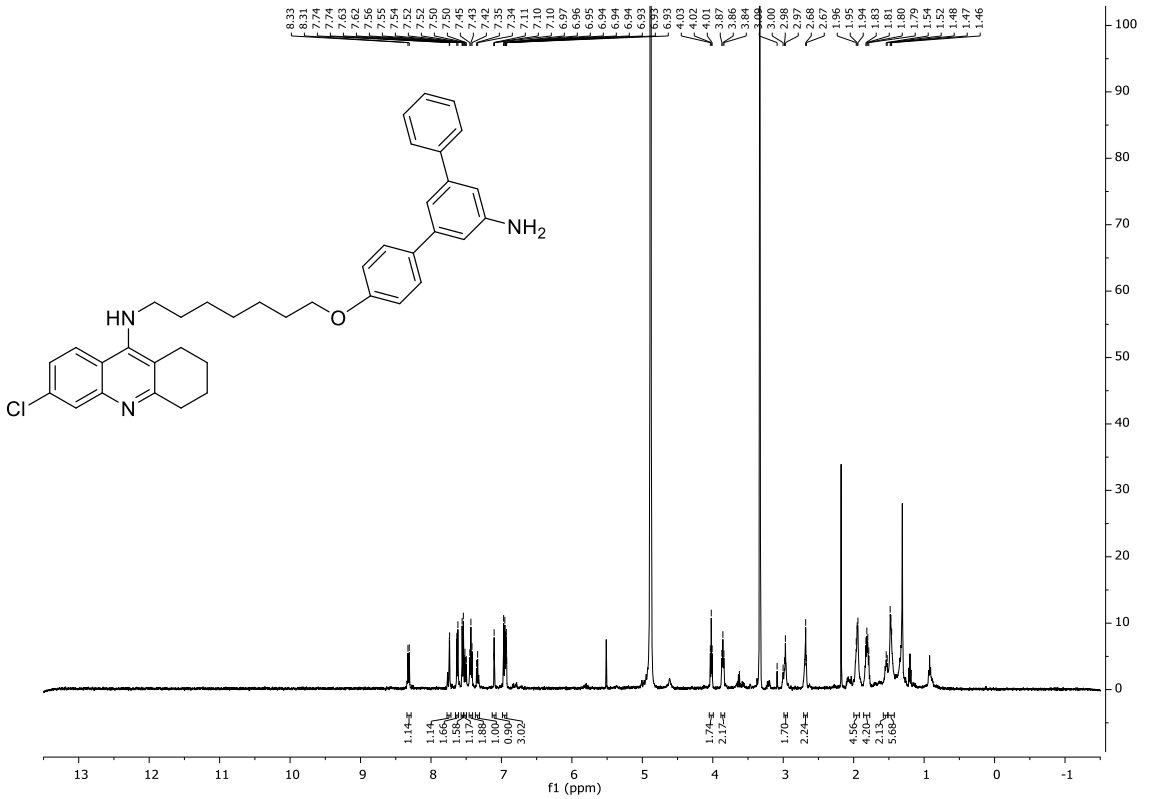
NH2
HN
O
Cl
N
f1 (ppm)

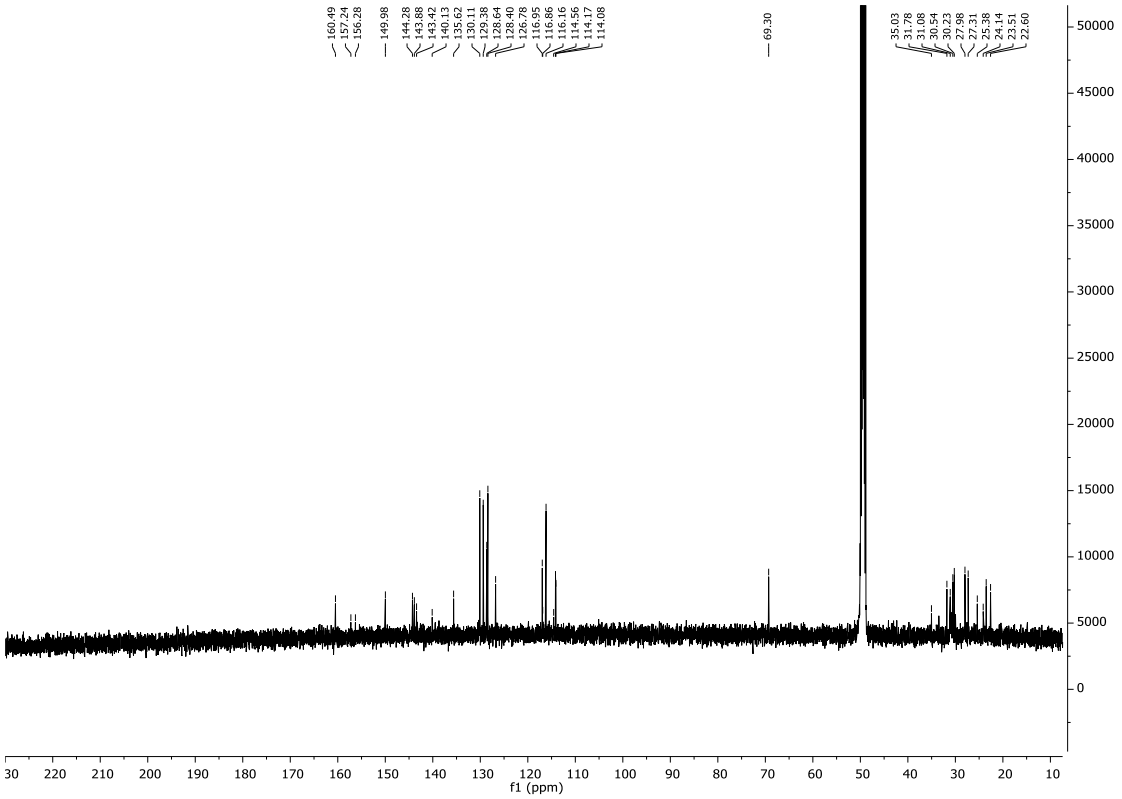
f1 (ppm)

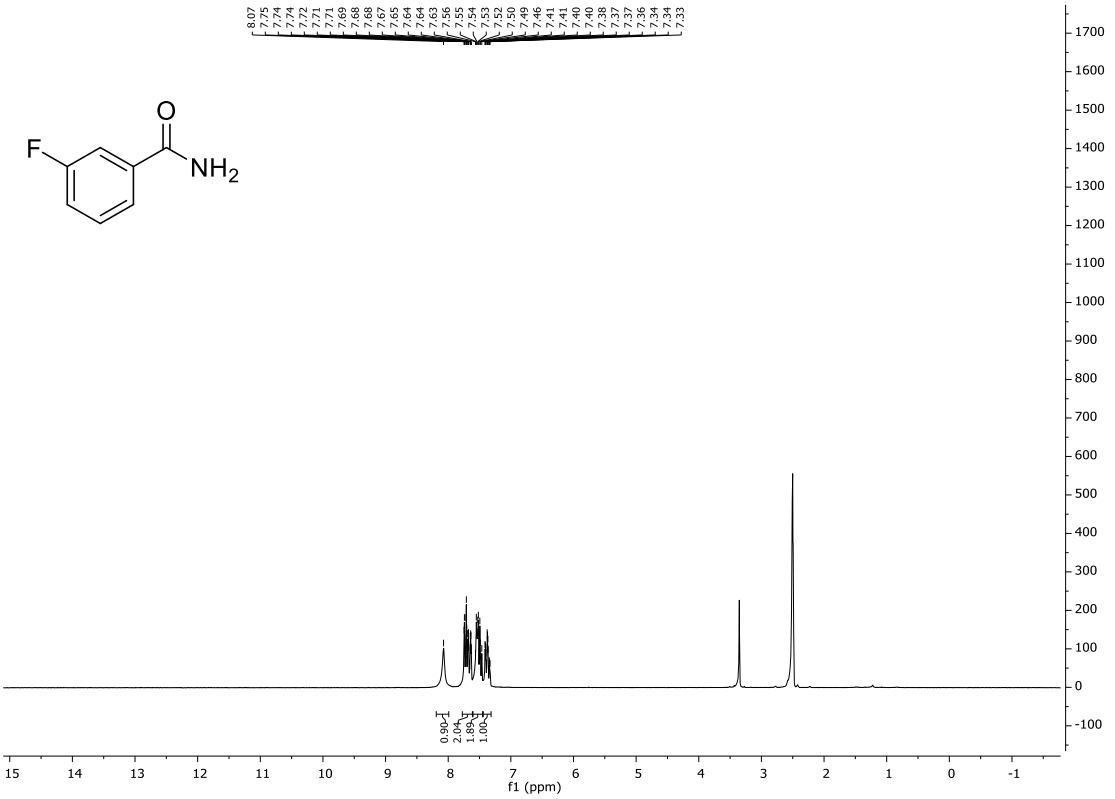
8.07
7.75
7.74
7.74
7.72
7.71
7.71
7.69
7.68
7.68
7.67
7.65
7.64
7.64
7.63
7.55
7.55
7.54
7.53
7.52
7.50
7.49
7.46
7.41
7.41
7.40
7.40
7.38
7.37
7.37
7.36
7.34
7.34
7.33
F
O
NH2
0.90
2.04
1.89
1.00
f1 (ppm)

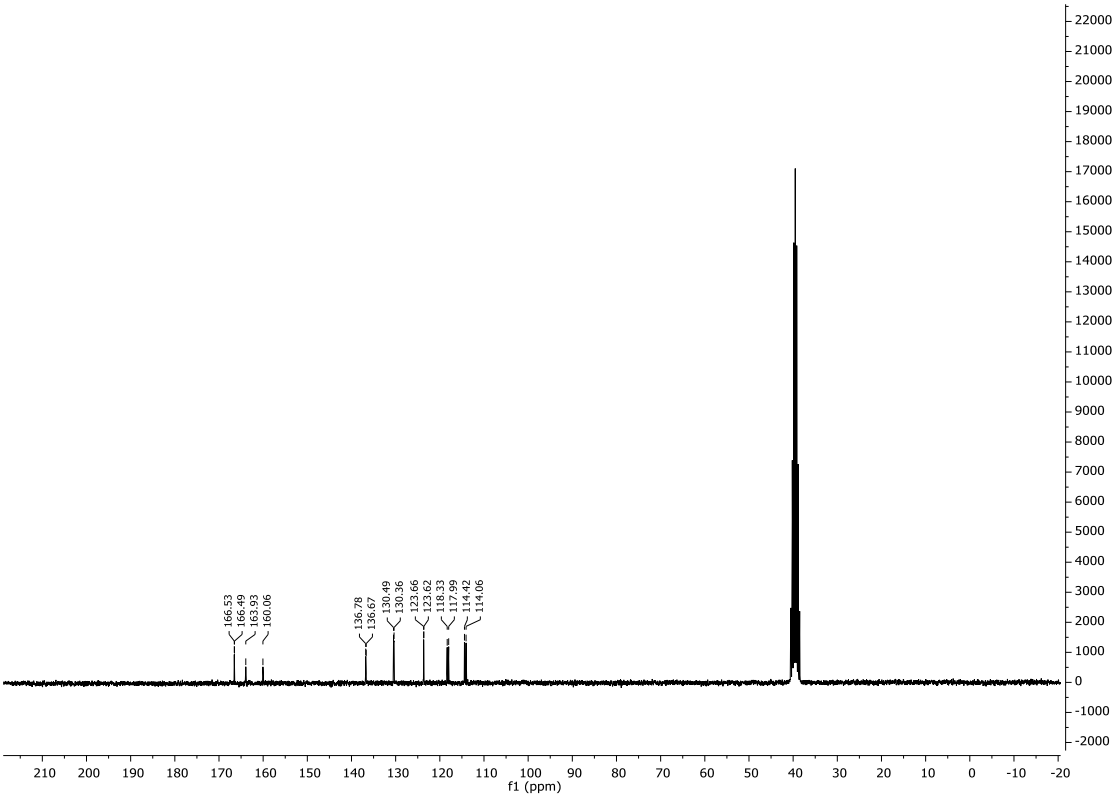
166.53
166.49
163.93
160.06
136.78
136.67
130.49
130.36
123.66
123.62
118.33
117.99
114.42
114.06
f1 (ppm)

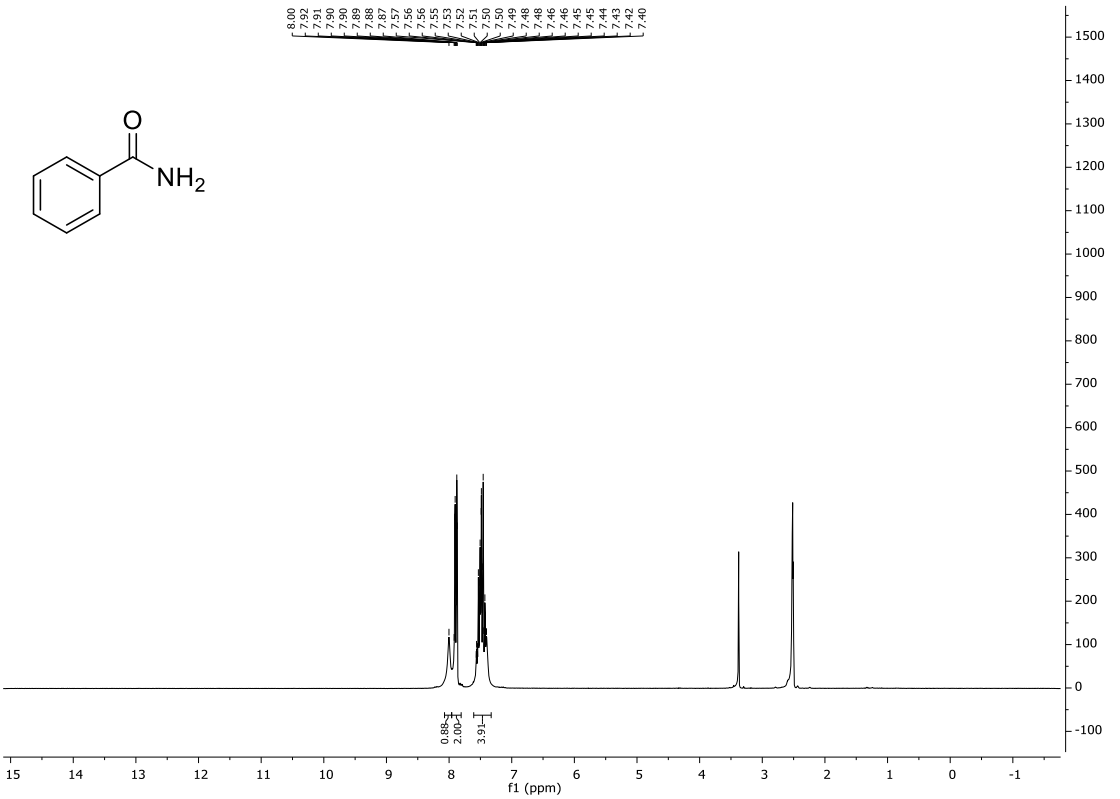
8.00
7.92
7.91
7.90
7.90
7.89
7.88
7.87
7.57
7.56
7.56
7.55
7.53
7.52
7.51
7.50
7.50
7.49
7.48
7.48
7.46
7.46
7.45
7.45
7.44
7.43
7.42
7.40
O
NH2
0.88
2.00
3.91
f1 (ppm)

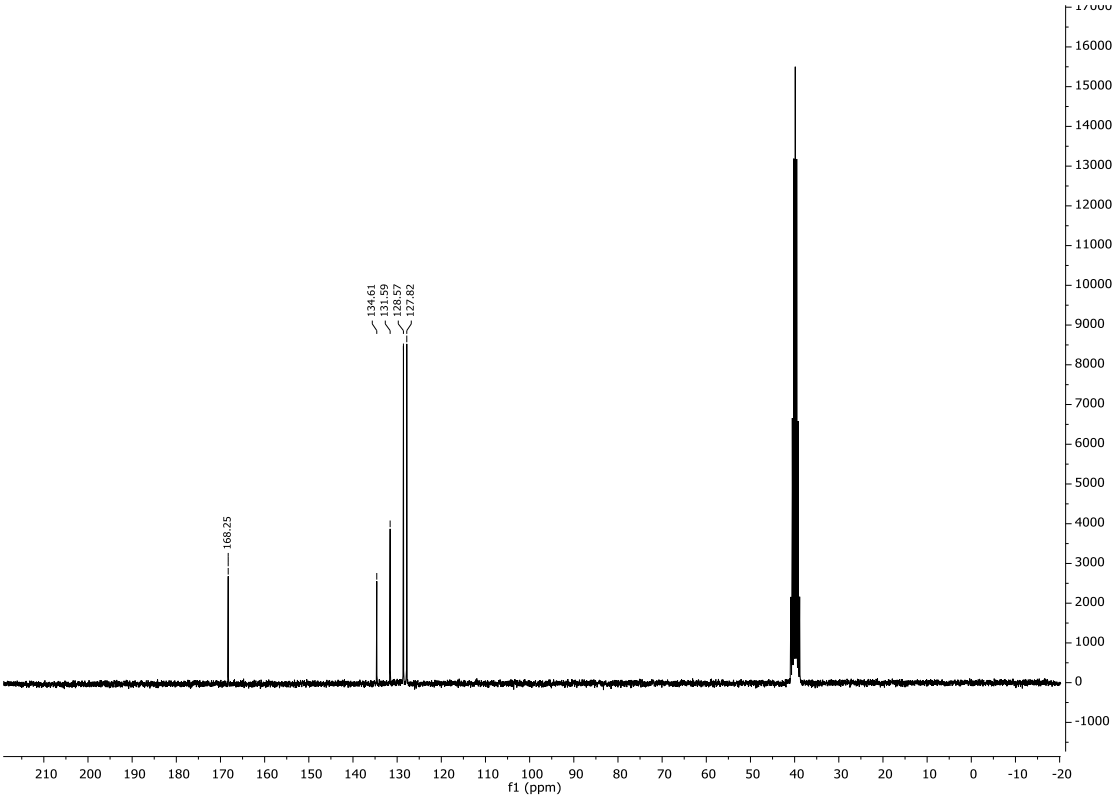
168.25
134.61
131.59
128.57
127.82
f1 (ppm)

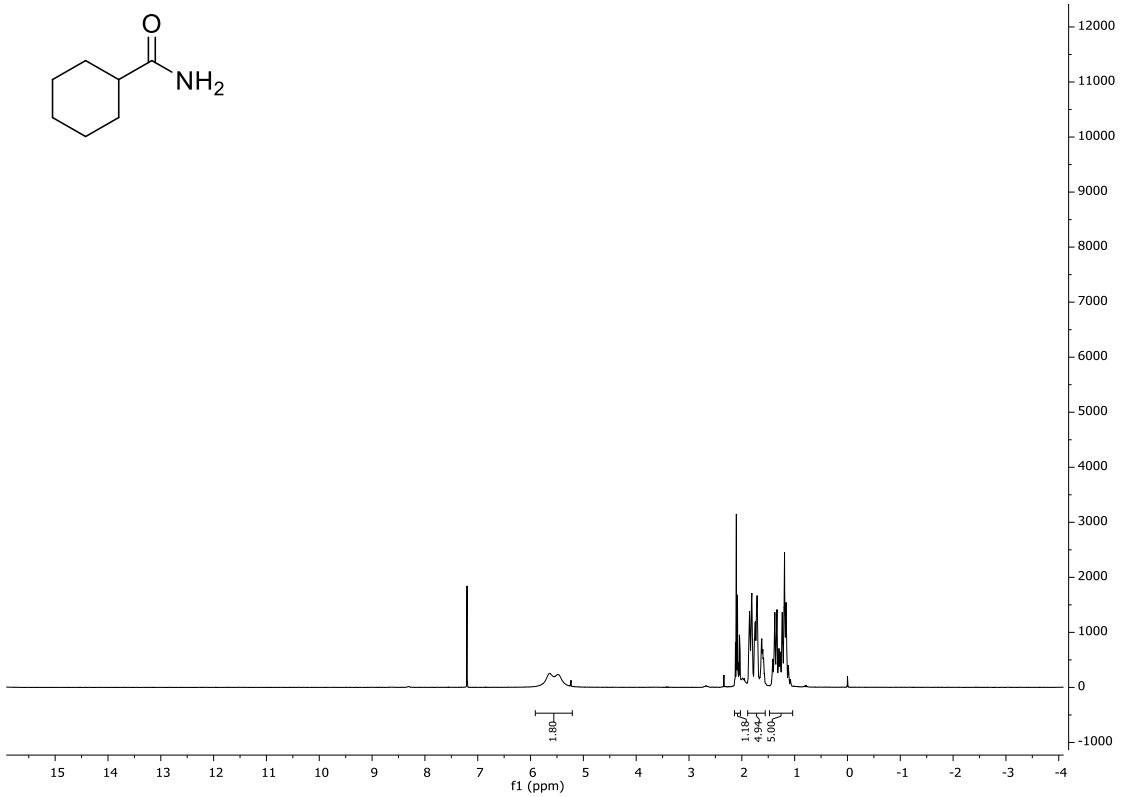
O
NH2
1.80
1.18
4.94
5.00
f1 (ppm)

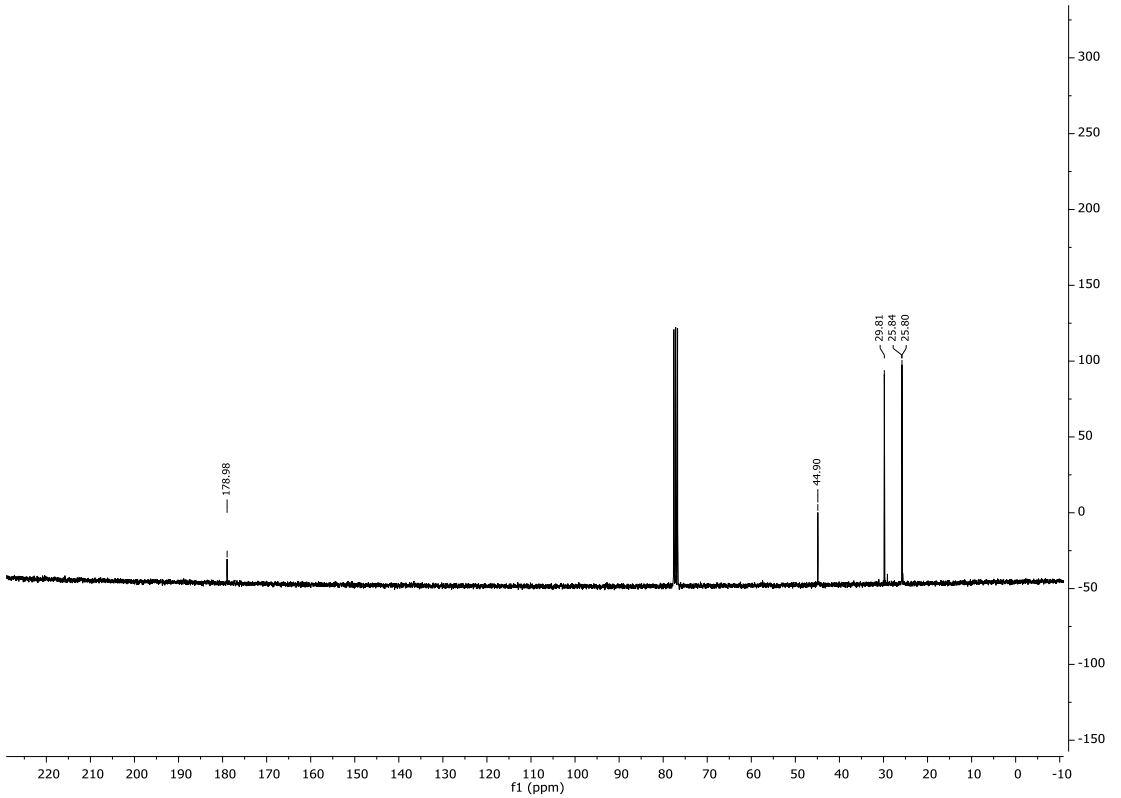
178.98
44.90
29.81
25.84
25.80
f1 (ppm)

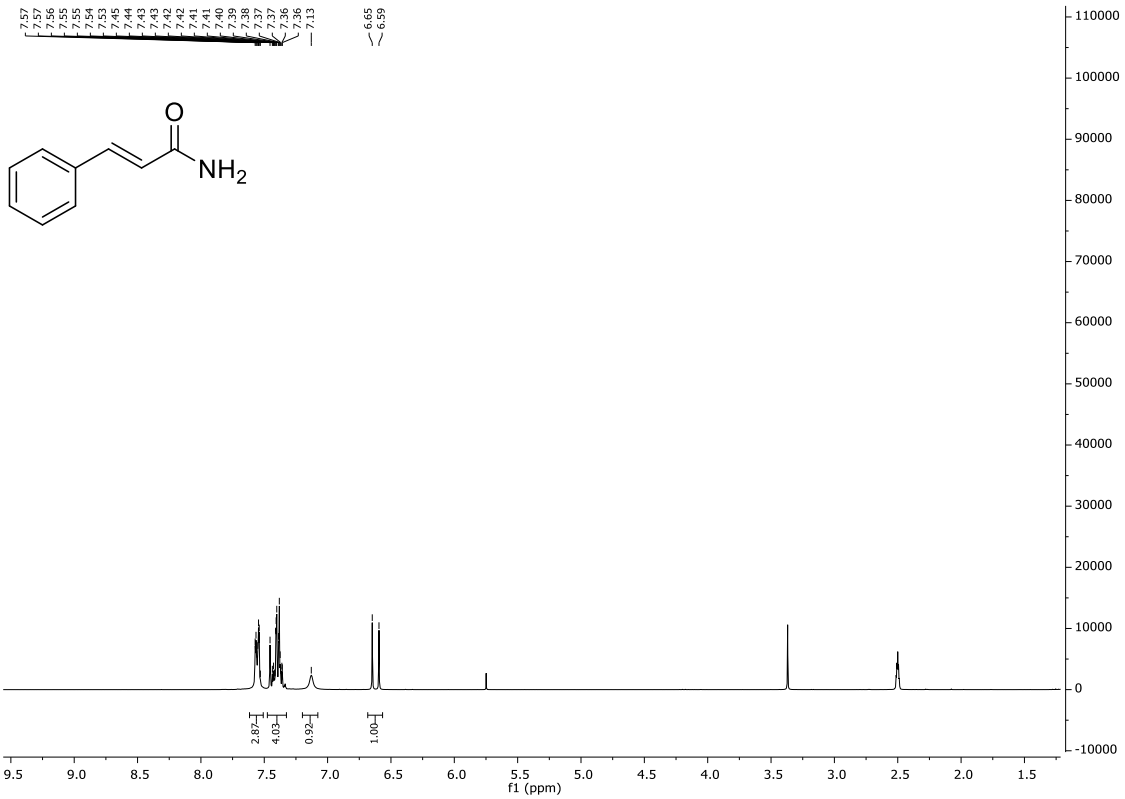
7.57
7.57
7.56
7.55
7.55
7.54
7.53
7.45
7.44
7.43
7.43
7.42
7.42
7.41
7.40
7.39
7.38
7.37
7.37
7.36
7.36
7.13
6.65
6.59
O
NH2
2.87
4.03
0.92
1.00
f1 (ppm)

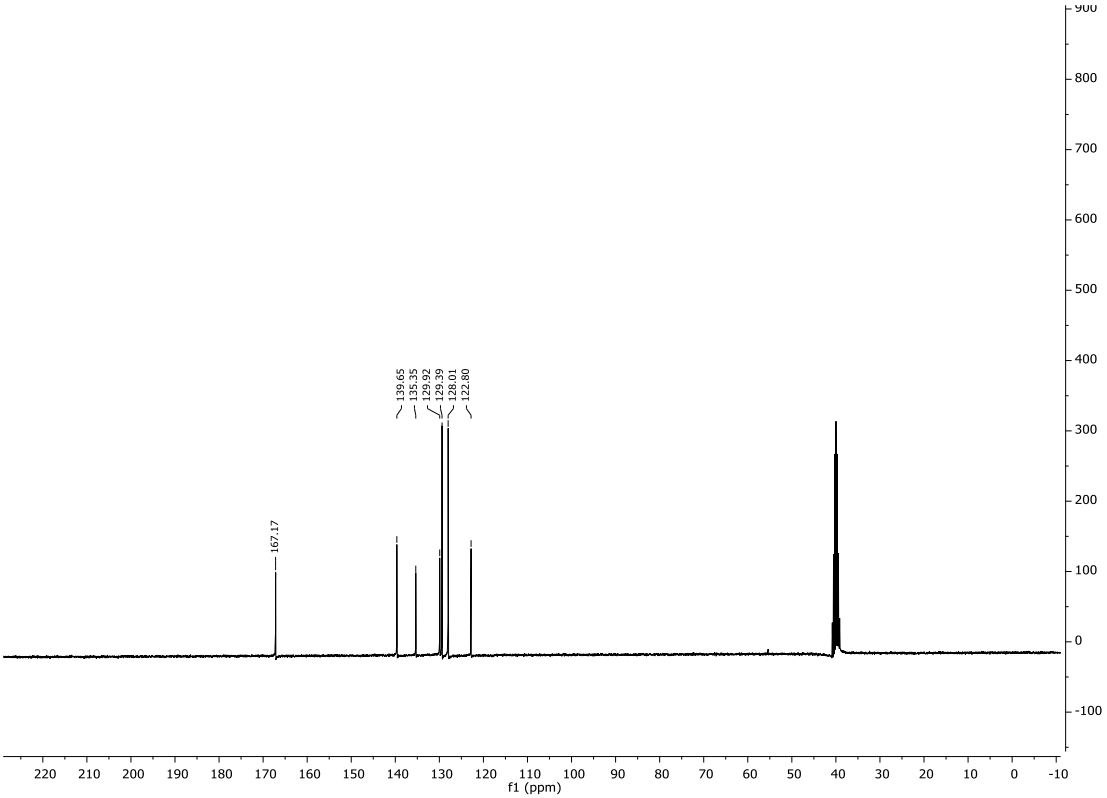
139.65
135.35
129.92
129.39
128.01
122.80
167.17
f1 (ppm)

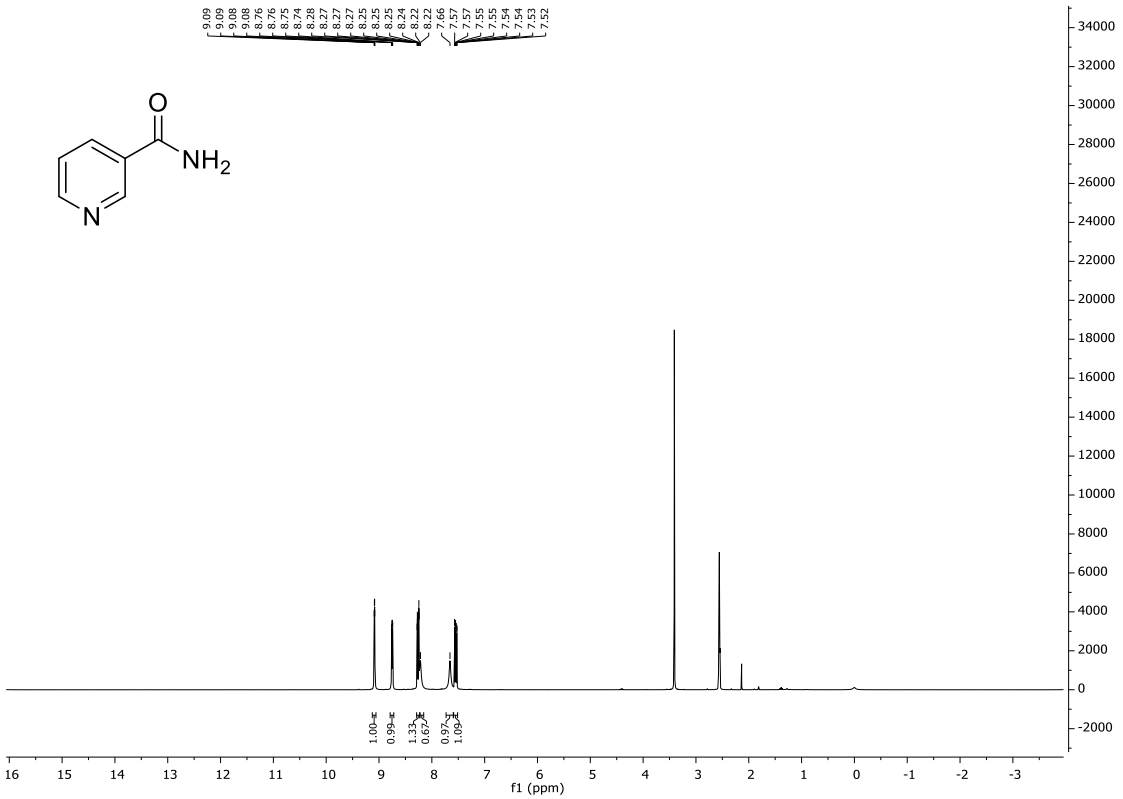
9.09
9.09
9.08
9.08
8.76
8.76
8.75
8.74
8.28
8.27
8.27
8.27
8.25
8.25
8.25
8.24
8.22
8.22
7.66
7.57
7.57
7.55
7.55
7.54
7.54
7.53
7.52
O
NH2
N
1.00
0.99
1.33
0.67
0.97
1.09
f1 (ppm)

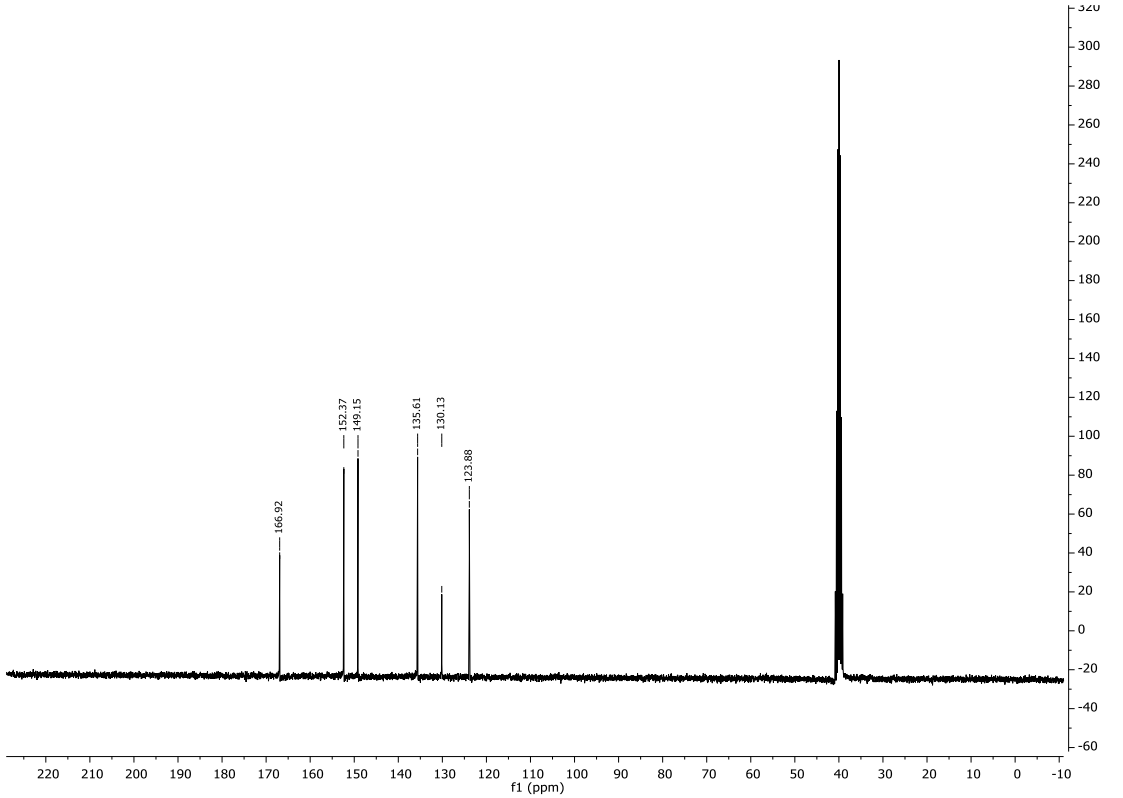
166.92
152.37
149.15
135.61
130.13
123.88
f1 (ppm)

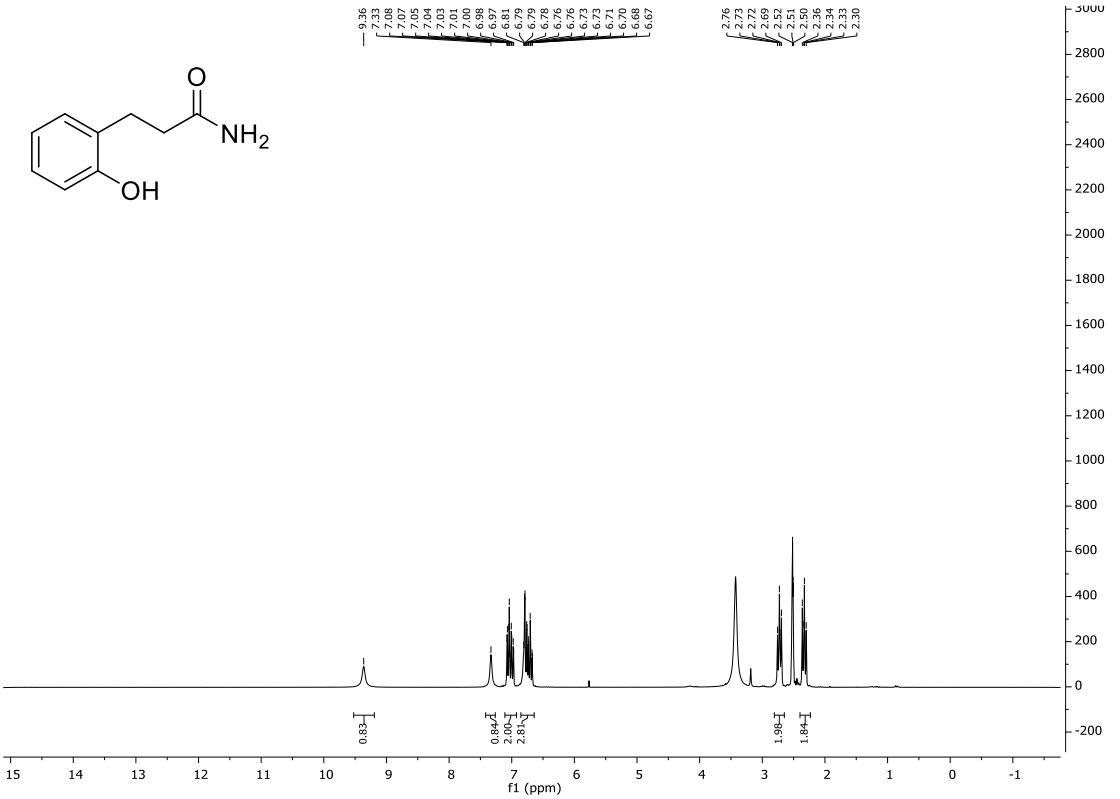
O
NH2
OH
9.36
7.33
7.08
7.07
7.05
7.04
7.03
7.01
7.00
6.98
6.97
6.81
6.79
6.78
6.76
6.73
6.71
6.70
6.68
6.67
2.76
2.73
2.72
2.69
2.52
2.51
2.50
2.36
2.34
2.33
2.30
0.83
0.84
2.00
2.81
1.98
1.84
f1 (ppm)

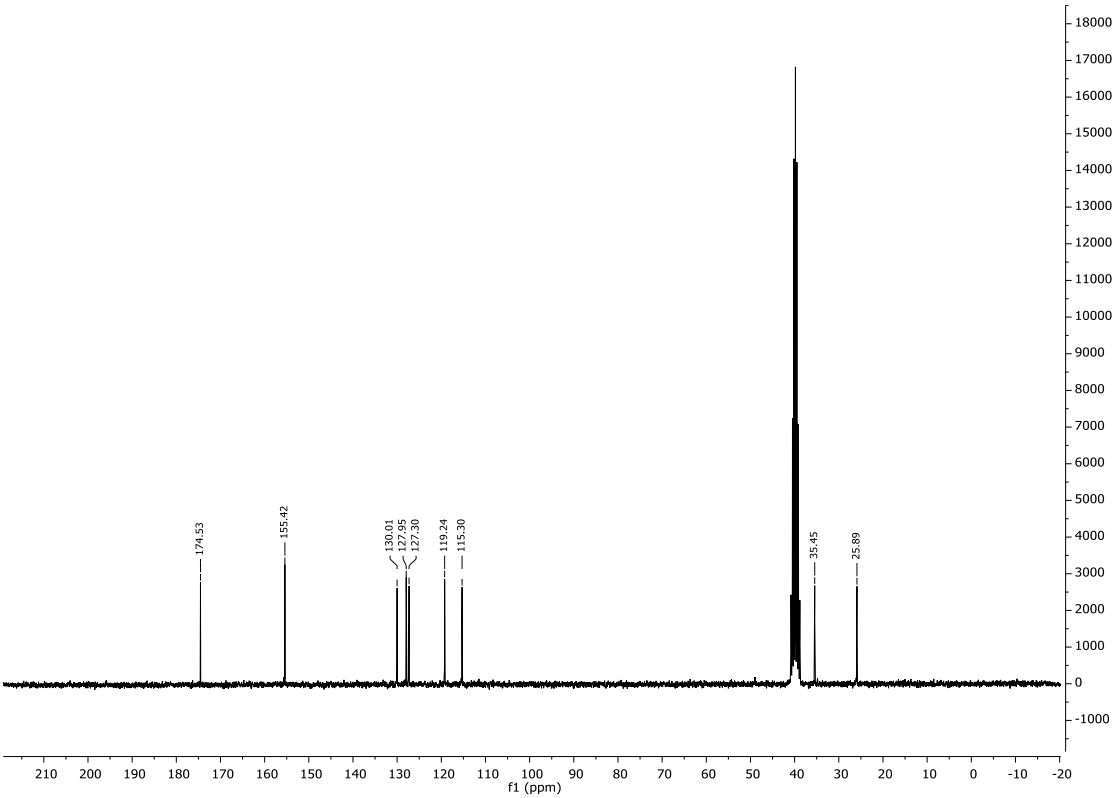
174.53
155.42
130.01
127.95
127.30
119.24
115.30
35.45
25.89
f1 (ppm)

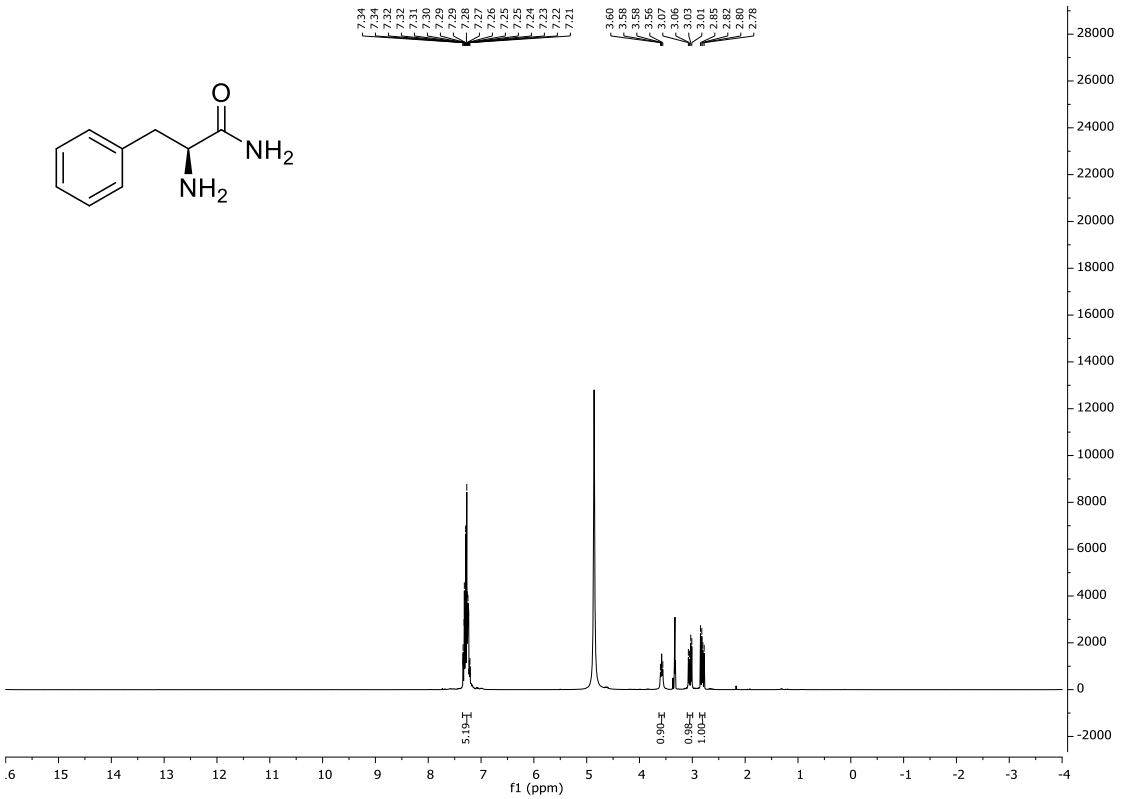
7.34
7.34
7.32
7.32
7.31
7.30
7.29
7.29
7.28
7.27
7.26
7.25
7.25
7.24
7.23
7.22
7.21
3.60
3.58
3.58
3.56
3.07
3.06
3.03
3.01
2.85
2.82
2.80
2.78
O
NH2
NH2
5.19
0.90
0.98
1.00
f1 (ppm)

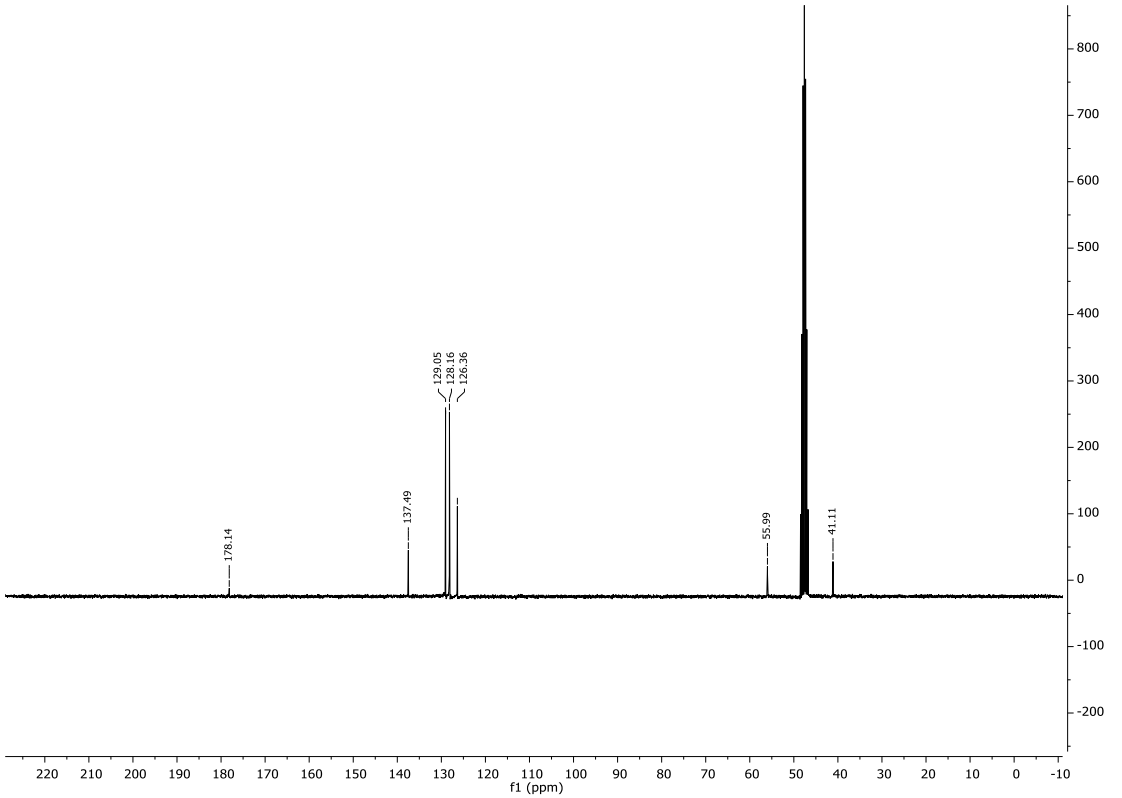
178.14
137.49
129.05
128.16
126.36
55.99
41.11
f1 (ppm)

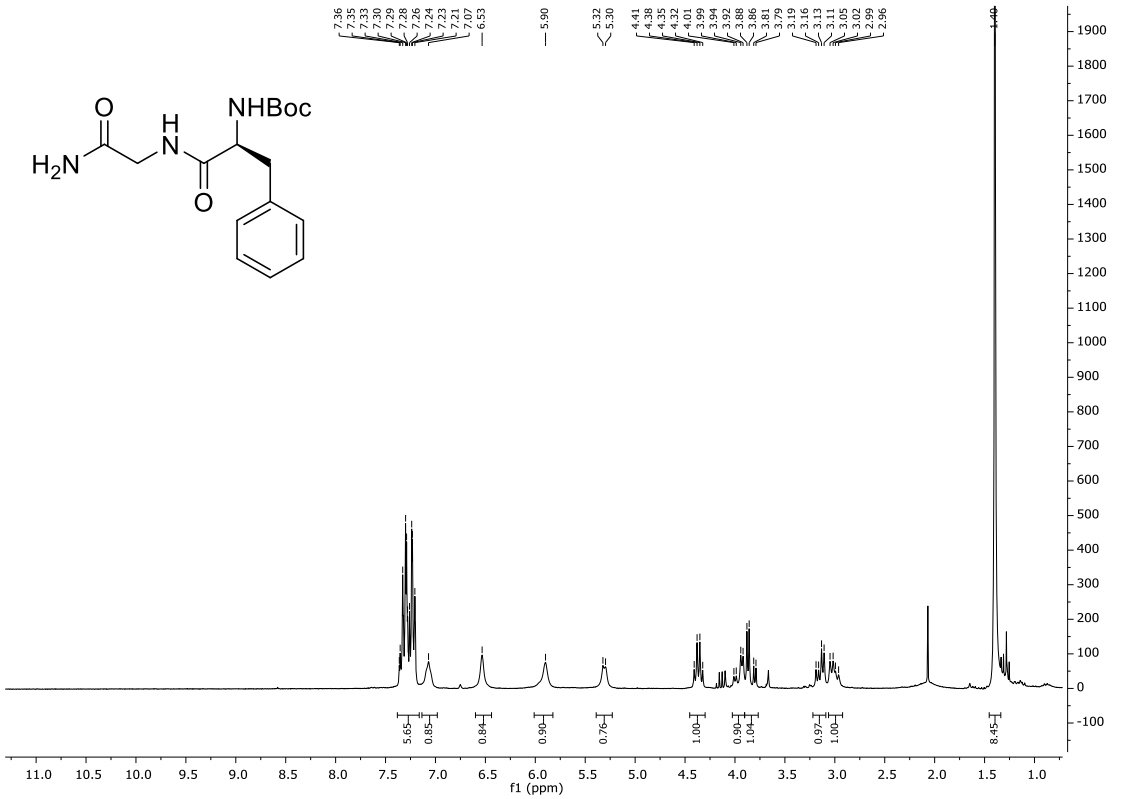
7.36
7.35
7.33
7.30
7.29
7.28
7.26
7.24
7.23
7.21
7.07
6.53
5.90
5.32
5.30
4.41
4.38
4.35
4.32
4.01
3.99
3.94
3.92
3.88
3.86
3.81
3.79
3.19
3.16
3.13
3.11
3.05
3.02
2.99
2.96
1.40
O
H
N
NHBoc
H2N
O
5.65
0.85
0.84
0.90
0.76
1.00
0.90
1.04
0.97
1.00
8.45
f1 (ppm)

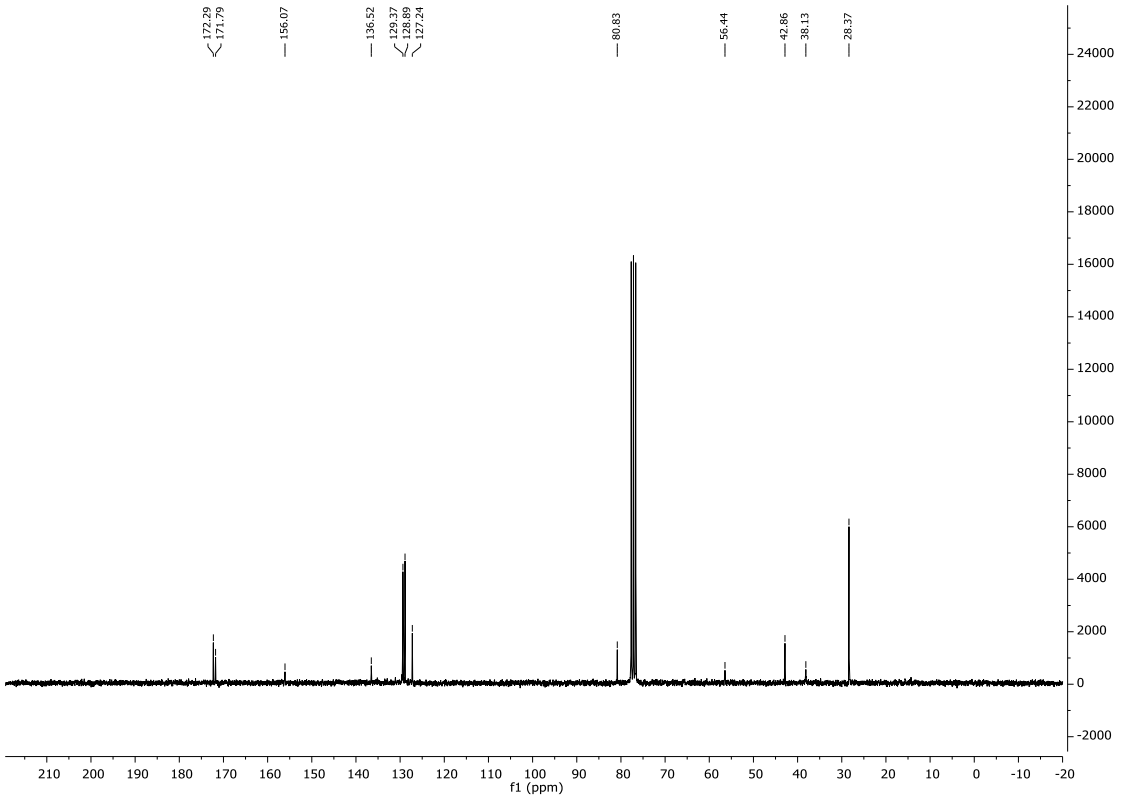
172.29
171.79
156.07
136.52
129.37
128.89
127.24
80.83
56.44
42.86
38.13
28.37
f1 (ppm)